Evolution of an Early Proterozoic Alluvially-Dominated Foreland Basin, Burnside Formation, Kilohigok Basin, N.W.T., Canada

by

David Speir McCormick

B.A. with High Honors in Geology, Dartmouth College (1984)
M.A. Geology, Columbia University (1987)

Submitted to the Department of Earth, Atmospheric, and Planetary Sciences in Partial Fulfillment of the Requirements for the Degree of

Doctor of Philosophy

at the

Massachusetts Institute of Technology

July 1992

© 1992 Massachusetts Institute of Technology
All rights reserved

Signature of Author _____
Department of Earth, Atmospheric, and Planetary Sciences
June 1992

Certified by _____
Professor John P. Grotzinger
Thesis Supervisor

Accepted by _____
Professor Thomas H. Jordan
Department Head

WITHDRAWN
MASSACHUSETTS INSTITUTE
FROM
MIT LIBRARIES
SEP 30 1992

Evolution of an Early Proterozoic Alluvially Dominated Foreland Basin, Burnside Formation, Kilohigok Basin, N.W.T., Canada

by

David Speir McCormick

Submitted to the Department of Earth, Atmospheric, and Planetary Sciences, July, 1992, in partial fulfillment of the requirements for the degree of
Doctor of Philosophy in Geology

Abstract

Kilohigok Basin is an Early Proterozoic sedimentary basin on the eastern margin of the Slave Province that records the collision and thrusting of the Rae Province over the Slave Province between 1.9-2.0 Ga. Kilohigok Basin developed as a continental foredeep during this collision, and Thelon Orogen, on the leading edge of the Rae Province, was the contemporaneous metamorphic-plutonic hinterland. A vast granulite gneiss terrane in the Rae Province, behind Thelon Orogen, called Queen Maud block, may be the deep crustal remnant of a large plateau uplifted in response to the collision. Thelon Orogen and Queen Maud block are probably the source of much of the detritus preserved in Kilohigok Basin.

In order to document the tectonic history sketched above, this study takes three complementary approaches to understanding the syn-orogenic siliciclastic deposits in Kilohigok Basin, with special emphasis placed on the thick, largely alluvial deposits that dominate the foreland basin fill. First, a sedimentological study differentiates marine from non-marine facies. Second, this facies scheme is used to identify unconformities within the largely alluvial succession in order to show the shifting of loads imposed on the Slave Province. Finally, the provenance of the sandstones within Kilohigok Basin is assessed through the use of sandstone and conglomerate petrography, paleocurrent data, and U-Pb dating of detrital zircons to improve intra- and interbasinal correlations and document changing composition and age of source areas contributing to Kilohigok Basin.

Physical sedimentologic criteria show that the alluvial system was a sandy braided stream and braid delta system that interfingered with low-energy, wave-influenced siliciclastic shelf facies on its distal margin. Based on the large lateral extent of sandy facies, lack of any muddy facies, low textural maturity, and the size and hierarchy of bedforms, we believe that the alluvial system was high energy and had high discharge probably caused by humid perennial or monsoonal climate in the source area.

The stratigraphic data show that initially the alluvial system drained longitudinally and was restricted to the proximal part of the basin between Thelon Orogen and a syn-depositional flexural arch that lay on the Slave craton. These initial foreland basin deposits have a highly tapered, wedge-shaped geometry. A distinct shift to transverse paleocurrent mode heralds the onset of the progradation of braided alluvial facies onto the craton. Alluvial facies abruptly shift 150 km across the entire Slave craton and shed detritus into the coeval passive margin in Wopmay Orogen. The transverse alluvial paleocurrent mode persisted throughout the rest of alluvial sedimentation. The geometry of the upper, mostly alluvial

part of the foredeep is much more tabular-shaped than the underlying initial foredeep deposits. The tabular geometry of the upper alluvial unit and the persistent transverse alluvial paleocurrents strongly suggest that subsidence was much more uniform across the foredeep during the main phase of alluvial sedimentation. Erosion of the hinterland supplied the voluminous siliciclastic detritus and subsequent isostatic rebound of the hinterland drove the extensive progradation. Humid climate, perhaps amplified by the topography of the Thelon mountain front, may have enhanced the erosion of the mountain belt, supplying more sediment to the basin, and leading to steep metamorphic gradients along the orogenic front.

Two independent flexural arches existed on the opposite margins of the Slave Province throughout most of the foreland basin phase. The arch closest to Thelon Orogen was caused by the loading of the margin of Slave Province by the over-riding Rae Province. The other flexural arch, on the western edge of the Kilohigok Basin, relates to the sediment load of a coeval passive margin in Wopmay Orogen with which the alluvial foreland basin deposits interfingered. During late alluvial sedimentation, the two previously independent flexural arches may have migrated and yoked together to form a single flexural arch in the middle of the Slave Province. This migration probably relates to imposition of the syn-orogenic sediment load and the cooling and strengthening of the passive margin lithosphere in Wopmay Orogen. An additional driving force is required to account for all the cratonic subsidence, perhaps related to dynamic effects of the collision of Slave and Rae Provinces.

Provenance information provides key constraints for correlations and models for the evolution of Kilohigok Basin and Thelon Orogen. Sandstone and conglomerate clast composition, paleocurrents, and the geochronology of detrital zircons document major source area shifts during the evolution of Kilohigok Basin. Passive margin sedimentary rocks underlying the foredeep deposits were derived from the interior of the Slave craton and had a Middle Archean (>3.3 Ga) detrital component. Initial marine and longitudinally-draining braid delta facies in the proximal foreland basin are subarkosic and were derived from Late Archean (2.6-2.7 Ga) plutonic and metamorphic sources along strike, probably within the Slave Province. The shift to transversely draining braided alluvial facies is accompanied by distinct changes to sublitharenite composition, an increasing component of metamorphic grains and clasts, and the introduction of detrital zircons of two distinct Early Proterozoic ages: one age synchronous with peak metamorphism and deformation in Thelon Orogen (1.97-1.99 Ga) and an older 2.3-2.4 Ga component. Zircon inheritance ages and our preliminary sampling from basement rocks in Queen Maud block suggest that these the older Proterozoic ages probably derive from Queen Maud block. This means that both Thelon Orogen and Queen Maud block provided the bulk of the detritus preserved in the main alluvial interval of Kilohigok Basin. Feldspar content increases markedly upward, probably indicating the input of more plutonic sources. The presence of Early Proterozoic zircons near the base of the alluvial succession in the distal foreland confirms correlations to the middle of the alluvial interval in the proximal part of the basin. Similar age Early Proterozoic detrital zircons in Wopmay Orogen confirm correlations between late alluvial sediments in Kilohigok Basin and initial foreland basin deposits in Wopmay Orogen.

Thesis Supervisor: John P. Grotzinger
Title: Professor of Geology

Table of Contents

Abstract 3
Acknowledgments 11
Biographical Sketch 13
Frontispiece 14
Dedication 15
Introduction 17
Advances in sedimentary basin analysis 17
The Early Proterozoic (1.9-2.0 Ga) Kilohigok Basin 19
Previous work 20
Kilohigok Basin–a part of the Canadian Shield: early reconnaissance studies 20
The fog descends: initial sedimentary basin studies and aulacogen models 21
The overwhelming weight of data: reinterpretation of Kilohigok Basin and Thelon Orogen as products of Slave-Rae collision 22
Impetus for this study 24
References Cited 25

Chapter 1: Distinction of Marine from Alluvial Facies in the Early Proterozoic (1.9 Ga) Burnside Formation, Kilohigok Basin, N.W.T., Canada 31
Abstract 31
Introduction 32
Geologic Setting 33
Sedimentology of the Burnside Formation 36
lithofacies and depositional environments 36
low-energy siltstone-dominated shallow marine shelf 37
description 37
interpretation 39
mixed siltstone-sandstone marine shelf and sandstone-dominated sand bars 40
description 40
interpretation 41
siltstone and sandstone with soft sediment deformation (delta front) 41
description 41
interpretation 42
tabular-bedded, planar-laminated sandstone (braid delta platform) 42
description 42
interpretation 43
small-scale trough cross-bedded sandstone (braid delta plain) 43
description 43
interpretation 43
single-storeyed trough cross-bedded sandstone (distal braid plain) 44
description 44
interpretation 44
multi-storeyed trough-cross-bedded sandstone (medial braid plain ± minor gravel) 44

description 45
interpretation 45
trough- and large-scale planar-tangential and cross-bedded sandstone (medial braid plain with gravel) 46
description 46
interpretation 46
sheet gravel and trough cross-bedded sandstone (gravelly medial braid plain) 47
description 47
interpretation 48
Burnside Dolomite 48
description 48
interpretation 49
regional relationships between lithofacies 50
Discussion 51
marine-alluvial transition 51
progradational case 52
retrogradational case 53
Burnside Formation braided alluvial system 55
Conclusions 58
References Cited 59
Table Caption 64
Table 65
Figure Captions 66
Figures 71

Chapter 2: Evolution and significance of an overfilled alluvial foreland basin: Burnside Formation (1.9 Ga), Kilohigok Basin, N.W.T., Canada 91
Abstract 91
Introduction 92
Geologic Setting 94
Sedimentary Facies of the Burnside Alluvial System 96
marine shelf facies 97
low-energy silty shallow marine shelf 97
mixed silty-sandy marine shelf and sand bars 97
sandy braid delta facies 98
delta front (rippled siltstone-sandstone) 99
braid delta platform (tabular bedded sandstone) 99
braid delta plain (trough bedded sandstone with mud clasts) 100
alluvial braid plain facies 100
distal braid plain (single-storeyed trough bedded sandstone) 100
medial braid plain without gravel (multi-storeyed trough bedded sandstone) 101
medial braid plain (trough- and tangentially cross-bedded sandstone) 101
gravelly medial braid plain (sheet gravel and trough cross-bedded sandstone) 102
Burnside Dolomite 102
Stratigraphic Architecture of the Burnside Alluvial System 103

distribution of unconformities during initial alluvial sedimentation 104
Burnside Dolomite and transgression of the alluvial system 110
end of Burnside alluvial sedimentation 112
Discussion 114
location and migration of flexural arches 115
significance of laterally extensive gravel sheets and transverse alluvial paleocurrents 118
impact of humid climate on the evolution of the Burnside alluvial system and Thelon Orogen 121
significance of preservation of thick cratonic alluvial sequence 124
Conclusions 126
References Cited 128
Table Caption 135
Table 136
Figure Captions 137
Figures 141

Chapter 3: Provenance and Detrital zircon geochronology of the 1.9-2.0 Ga Goulburn Supergroup, Kilohigok Basin, N.W.T., and its implications for the Early Proterozoic evolution of the northwest Canadian shield 155
Abstract 155
Introduction 158
Geologic Setting 159
Tectonic elements of the northwestern Canadian Shield 160
Slave Province (2.55-3.96 Ga) 160
Rae Province (2.2-2.4(?), 2.6-3.1? Ga) 161
Thelon Orogen-Taltson Magmatic Zone (1.90-2.02 Ga) 161
Setting and Architecture of Kilohigok Basin (1.88-2.0 Ga) 162
General Stratigraphy 163
Bear Creek foredeep 163
The Burnside Formation deltaic-alluvial molasse 164
proximal molasse sedimentation 165
distal molasse sedimentation 165
The upper Goulburn Supergroup 166
post-Goulburn Supergroup deformation 166
sedimentary petrography of the Goulburn Supergroup 167
petrographic methods 167
thin section petrography 167
conglomerate clast counts 171
petrographic results 171
vertical trends 172
Kimerot Group passive margin 172
lower Bear Creek Group marine foredeep 172
initial Burnside foredeep braid delta 173
Burnside braided alluvial foredeep 173
Burnside-Mara waning foredeep 175

upper Goulburn Supergroup rejuvenated foredeep 175
proximal to distal trends in the Burnside Formation 176
general petrographic observations and interpretations 177
paleocurrents of the Goulburn Supergroup 178
paleocurrent data 179
Kimerot Group passive margin 179
lower Bear Creek Group marine to deltaic foredeep 179
Burnside braided alluvial foredeep 179
upper Goulburn Supergroup tectonic quiescence 180
upper Goulburn Supergroup rejuvenated foredeep 181
implications of paleocurrents for provenance of the Goulburn Supergroup 181
detrital zircon geochronology of the Goulburn Supergroup 182
geochronologic methods 182
sampling and analytical problems in the analysis of detrital zircon 183
geochronologic results 184
Kimerot passive margin 184
lower Goulburn marine to deltaic foredeep 184
Burnside braided alluvial foredeep 185
proximal foredeep 185
distal foredeep 186
Bathurst Group rejuvenated foredeep 186
Coronation foredeep of Wopmay Orogen 187
preliminary basement ages from Queen Maud block 188
Discussion 188
provenance evolution of the Goulburn Supergroup 188
Kimerot passive margin: old Archean source on the Slave craton 190
early foredeep: lateral plutonic and metamorphic sources within the Slave Province 190
early Burnside deltaic foredeep: metamorphic sources from the Slave or Queen Maud? 191
early Burnside alluvial foredeep: metamorphic sources from Thelon Orogen and perhaps Queen Maud block 191
main Burnside alluvial foredeep: enigmatic Early Proterozoic and Thelon Orogen sources 193
rejuvenated foredeep: diverse immature sources 195
implications for correlations with Wopmay Orogen 195
implications of 2.2 to 2.4 Ga detrital zircons for the nature of Queen Maud block 196
Conclusions 196
References Cited 199
Table Captions 206
Tables 207
Figure Captions 213
Figures 218

Appendices 245
Appendix A: measured sections in the Burnside Formation 246
section 1: Bear Creek Hills 251
section 2: South TInney Hills & south Tinney Hills-upper section 274
section 3: north Tinney Hills 322
section 4: SE Folds 338
section 5: NW Folds 349
section 6: Rifle Lake 358
section 7: south Link Lake 362
section 8: middle Link Lake 365
section 9: north Link Lake 368
section 10: Hackett River 371
section 11: northwest Hackett River 374
section 12: Wolverine Canyon 377
section 13: Contwoyto Lake 406
section 14: Rockinghorse Lake 420
section 15: Buchan Bay 423
section 16: Wilberforce Hills 437
Appendix B: Petrographic data from the Goulburn Supergroup 472
BC-H 473
BC-R 475
STH-111 477
STH-116 479
STH-120 482
STH-126p 485
STH-127 489
STH-128 492
STH-130 495
STH-131 499
STH-132 503
STH-139 506
STH-142 509
STH-014 512
STH-021 516
WC-01A 518
WC-14 521
WC-27 524
WC-33 526
WC-58 528
WC-66 530
WC-68 532
WC-70 535
BSA-1 539
BSA-2 542
Appendix C: Zircon sample locations 546

Acknowledgments

This project would not have been possible without the generous logistical and technical support of the Geological Survey of Canada, Lithosphere and Canadian Shield division, particularly John McGlynn, Paul Hoffman, Janet King, Simon Hanmer, and the late, great Rein Tirrul. Shane Pelechaty, Alex Anastis, Sarah Bohan, Charley Gamba, Kurt Roggensack provided tireless field assistance and great companionship through long Arctic summers.

The long, tortuous journey began at Lamont-Doherty Geological Observatory where Marge Levy, Annie Holmes, Bernie Coakley, Ken and Dana Hudnut have been tremendous friends while in New York and across the years and miles since leaving L-DGO.

Many kind people made my stay at Washington University in St. Louis a pleasure. In particular, Greg Poole, Ben Rivard, Kevin Chamberlain, Ellen O'Leary, Laurel Shastri, and Megan Flanagan welcomed me into an unfamiliar city and university. Clark Isaksen and Todd Housh have been great companions both at Wash. U. and at MIT. In particular, Kevin, Todd, and Clark generously gave of their time to run my zircon samples and to try to explain to me the mysteries and wonders of U-Pb geochronology and isotope geology.

MIT-EAPS companions have been an inspiration, proving that you learn more from your peers than any other source. Julio Friedman, Caroline Ruppel, Peter Kaufman, Paula Washbusch, Cathy Summa, Dawn Sumner, Bev Saylor, Martha House, Dave Applegate, Allison Macfarlane, Dave Hawkins, and Meg Coleman have provided criticism, feedback, amusement, good advice, and all-around good cheer over the last few years. Nancy Dallaire and Pat Walsh provided great logistical support and good humor. Cathy, in particular, was a great office mate, confidante, and so much more. Peter Flemings, though only my office mate in the final few months, has been a good-humored sounding board over the years. He provided tremendous inspiration, continuous good words, and plain common sense through the last hard push, for which I am very grateful; better is the worst enemy of good enough.

I will be forever grateful to Margaret Ross for vital conversations and critical insight when I needed it the most.

I thank my parents and family for continual love and support, despite being a bit incredulous at how long this took to complete.

The late Noye Johnson was an initial inspiration to me and many others to become a geologist. To see why, just take a look at Journal of Geology, 1990, v.98, issue 4, especially p. 423-428. I miss greatly Noye's vigorous, creative mind and gentle, kind way with everyone.

Jeff Fox gave me my first taste of the excitement of research in the earth sciences and, despite my having forsaken marine geology, he and Janet have been enduring friends ever since.

Nick Christie-Blick, who initially took me on at Lamont-Doherty, has been a great source of feedback and papers bathed in red ink. I thank him for gracefully letting me pursue the Kilohigok Basin project when a young whipper-snapper of a post-doc lured me away from the Basin and Range.

Wiki Royden generously allowed me the means to come to MIT in the first place. She has greatly influenced my understanding of and thinking about geophysics. In addition, she has been tremendously supportive of me over the last 3 years.

Sam Bowring generously provided research opportunities and funding during the middle of the program and a lot of critical data at critical moments (like the final few weeks). His

interest in the project, creative ideas, and rigorous criticisms of results were essential to completing this project and greatly enhance the final outcome.

It's hard to properly acknowledge the contributions of John Grotzinger. No one else has so shaped my thinking about what geology is and can be. His voracious, tireless, omnivorous pursuit of understanding the earth is phenomenal to behold; his unfailing honesty and integrity are inspirational in a world of difficult choices. Through it all, it has been a pleasure to watch his career take root and flourish. Though sorely tested at times, he never gave up on me, providing support and insight at many critical times. He has been a tremendous friend as well as an inspirational advisor.

Finally, Ebit Speers has been a long-suffering companion through this long, circuitous trip. She bore the long separations and late nights with quiet grace. She has been an unshakable pillar of strength and encouragement when I have needed it most. She has taught me much about the power of faith, hope, and love. I hope I can repay her for these lessons over the next few decades. At long last we have the time to pursue our dreams together.

Biographical Sketch

I came to geology in college as I suspect many college undergraduates do: by being a disaffected pre-med student who absolutely detested my organic chemistry course and the attendant grade-grubbing students. Chuck Drake and Dick Bernie at Dartmouth College opened my eyes to the earth sciences through incredibly stimulating introductory courses. I immediately saw geology for what it is, mercenary travel, and signed on for the geology department's unparalleled semester-long off-campus geology program, affectionately known as the Rock Stretch.

My introduction to research came through a fortuitous summer job with Jeff Fox at University of Rhode Island Graduate School of Oceanography. Jeff, his graduate students, and colleagues provided an incredibly collegial, stimulating environment to see cutting-edge marine geology work in action. We made maps of mid-ocean ridges from Sea Beam bathymetric data Jeff et al. had collected on oceanographic cruises to decipher the tectonics processes of ridges of various spreading rates. Mapping by day and bike racing by night, I had the funnest summer of my life. Much to my great good fortune, when I had some free time between college and graduate school, Jeff let me tag along on an oceanographic cruise from Cape Town to Recife, Brazil. To this day, I'm not sure why I drifted away from marine geology.

My real introduction to geological research and field work came through the kindness of Gary Johnson and, in particular, Noye Johnson who included countless undergraduates in their research on the sedimentology and magnetostratigraphy of the Tertiary foreland basin fill of northern Pakistan. How else would I, as twenty-one-year-old who spoke not word one of Pushtu, have ended up on my own in northwestern Pakistan with a Land Rover, a native driver, and bag full of Rupee notes for 10 weeks during 1983-84? The field area lay within 50 miles of the Afganistan border while the Afgan War raged and the C.I.A. ran guns through the Northwest Frontier Province to supply the Mujahadeen. How ironic that my undergraduate thesis topic, the sedimentology and magnetostratigraphy of foreland basin deposits, would be so similar in scope to my Ph.D.

After college graduation in 1984, I was one of the fortunate few to land a temporary job at Union Texas Petroleum in Houston as the oil industry went bust. I worked half the time as an intern in an in-house stratigraphy and sedimentology lab and the other half in the seismic processing group. Tony Lomando provided a crash course in carbonate petrology and sedimentology and kept the work interesting in the stratigraphy lab. My experience at Union Texas reinforced my desire and need to go to graduate school.

After deciding to go to Lamont-Doherty for graduate school, Nick Christie-Blick let me go to the Basin and Range to do some pre-school field work in the Late Proterozoic siliciclastic sedimentary rocks in western Utah. There I was introduced to the thorny problems of distinguishing marine from non-marine sedimentary rocks and doing sequence stratigraphy in outcrop. These problems became integral to thesis topics with which I would wrestle.

In my first fall at Lamont, I met John Grotzinger, then a green post-doctoral fellow. John, with his inimitable gift for salesmanship, talked me into joining his field project in the Northwest Territories of Canada. Again, the possibilities of mercenary travel weighed heavily in my decision to work on John's project. Three field seasons and seven years later, a thesis was born.

Frontispiece

It differs remarkably from the main shore in being very rugged, rocky and sterile...

John Richardson's description, on Sat. 4 August 1821, of the Tinney Hills, Bathurst Inlet, N.W.T., Canada, which are held up by the sandstone of the Burnside Formation, the subject of much of this thesis. Quoted in C.S. Houston, 1984. **Arctic Ordeal: The journal of John Richardson, surgeon-naturalist with Franklin, 1820-1822.**

.....

In Precambrian rocks in which fauna is lacking and soils seem much less common, it may often be difficult to distinguish between fluvial and shallow marine deposits in thick sandstone formations.

J.D. Collinson, 1986. Alluvial Sediments, *in*, H.G. Reading (ed.), **Sedimentary Environments and Facies** (2nd Ed.), p. 44.

.....

One can learn much from a river. From the river I have learned too: everything comes back.

Herman Hesse, **Siddhartha**

Dedication

I dedicate this work to my father, Robert V. McCormick, who has always provided a model of pursuing life with vigor, boundless intellectual curiosity, healthy skepticism without cynicism, and, above all, a humanistic way solving problems.

Introduction

The study of sedimentary basins is a key element in order to understand of the long term evolution of the earth, because sedimentary basins are proxies for many of the processes that occur on the surface of and within the earth. For example, sedimentary rocks are the only record of climate change through time and the geometry of sedimentary basin fill reflects the dynamic processes that cause basins to subside. The understanding of sedimentary basins has been greatly enhanced during the past 20 years through that application of a combination of methods. These mainly have occurred through the advent of geodynamic models that seek to explain the physical processes that form the basins, new models for the formation of large scale stratigraphic packages, and the use of geochemical techniques to date strata and determine the chemical conditions that effect basins at various stages in their evolution.

In the following chapters sedimentologic, stratigraphic, petrographic, and isotopic techniques will be used to try to understand the history of an exceptionally well preserved Early Proterozoic foreland basin.

Advances in sedimentary basin analysis

The first big push in geodynamic models came from the study of the thermally controlled contractional subsidence of mid-ocean ridges. These models were subsequently extended to modern passive margins (Watts and Ryan, 1976; McKenzie, 1978) and later ancient passive margin deposits (Armin and Mayer, 1983; Bond and Kominz, 1984) to quantify the magnitude of the tectonic forces that drive basin subsidence and the timing of that subsidence.

Bally et al. (1966) first suggested that foreland basins were the product of thrust loading of the lithosphere in the adjacent mountain belt. Beaumont (1981) and Jordan (1981) first applied elastic plate flexure models to the explain the subsidence of foreland basins. These were the first studies to demonstrate the potential for relating basin fill geometry to the rheology of the lithosphere below the basin and the location and magnitude of orogenic loads. From the outset, though, the nature of the rheologic models have been a subject of debate. Beaumont (1981) required a viscous rheology to explain the stratigraphic evolution of the Canadian Rocky Mountain foreland basin, while Jordan (1981) was able to invoke a purely elastic one for the Idaho-Wyoming foreland. Subsequent geodynamic models that used observed modern orogenic loads and gravity anomalies could not account always account for preserved stratigraphic thicknesses in the adjacent foreland basins (Karner and Watts, 1983; Royden and Karner, 1984; Lyon-Caen and Molnar, 1985; Royden et al., 1987; Moretti and Royden, 1988). These studies demonstrated that additional cryptic or "hidden" tectonic loads, such as the weight of subducting

plate, can augment basin subsidence driven only partly by thrust loading in the orogenic belt.

More recent studies began to address the more subtle questions of what are the relations between a dynamically growing and eroding orogenic wedge and foreland basin filling (Schedl and Wiltschko, 1984; Karner, 1986; Flemings and Jordan, 1987; Flemings and Jordan, 1989; Beaumont et al., 1990; Beaumont and Hamilton, 1990; Beaumont et al., 1992). These workers have suggested that the architecture of basin fill and the distribution of unconformities within basins place important constraints on models for the evolution of foreland basins and their associated orogenic belts. By extension, comparing the architecture of foreland basin strata of various ages, it may be possible to gain insights into the long-term evolution of the continental lithosphere. Grotzinger and Royden (1990) undertook such a comparison. The most recently developed computer models employ three-dimensional, dynamically deforming orogenic wedges that are coupled to physically based precipitation and surface erosion models (Beaumont et al., 1990; Johnson and Beaumont, 1990; Beaumont et al., 1992). These models show the remarkable result that the evolution of orogenic belts may be greatly modified or entirely controlled by climatic effects imposed on or created by the growing orogenic wedge.

Looking to the sedimentary fill of basins, stratigraphy has been revolutionized by the development of sequence stratigraphic techniques (Sloss, 1963; Vail et al., 1977; Haq et al., 1987; Van Wagoner et al., 1988). Sequence stratigraphy divides basin fill into unconformity-bounded packages. This means that each sequence has chronostratigraphic significance in that all strata above a given sequence everywhere must be younger than the sequence below. The key element of this method is that it is a geometric method derived from the pattern of how strata terminate against one another. In other words, this method is independent of, but testable by, other geochronologic methods, such as biostratigraphy and isotope geochronology. It is the geometric nature of sequence stratigraphic principles that make them such a promising tool for time-stratigraphy, intrabasinal correlation, and the resolution of the geometry of stratal packages in Precambrian basins (Christie-Blick et al., 1988; Bowring and Grotzinger, 1992). The definition of depositional sequences in Precambrian foreland basins may make it possible to make qualitative and quantitative comparisons with Phanerozoic basins (Grotzinger and Royden, 1990). These sequences can be calibrated in absolute time where datable volcanic ash beds occur, often with precision rivaling that of Phanerozoic successions (Krogh, 1973; Krogh, 1982), so that absolute chronostratigraphy may be established (Bowring and Grotzinger, 1992). However, the relative chronostratigraphy established by sequence stratigraphy remains a useful framework, independent of geochronologic methods.

The developments in isotopic geochemical methods has been an absolutely critical element to the understanding of the evolution of orogenic belts and sedimentary basins. In particular, advances in the instrumentation and in U-Pb isotopic methods spearheaded by Krogh

(1973; 1982) have led to extremely high precision age determinations for rocks of any age. This has been especially critical to the study of Precambrian areas in two ways. First, this has allowed the dating of the crust that underlies or abuts the sedimentary basins, constraining the age of orogenic activity and bracketing the age of deposition in the sedimentary basins. Second, dating of volcanic material intercalated within sedimentary sequences provides absolute time control within the basins and can calibrate and test stratigraphic models for the basin. Finally, dating detrital minerals within siliciclastic successions can constrain the age and identity of source areas that contributed to the basin. This method of assessing provenance is a powerful complement to conventionally employed methods.

The Early Proterozoic (1.9-2.0 Ga) Kilohigok Basin

The Early Proterozoic Kilohigok Basin in the northwestern Canadian Shield provides a superb setting in which to employ these tools to assess basin evolution because of exceptionally complete exposure of sedimentary rocks, the ability to divide the stratigraphy into unconformity-bounded depositional sequences, and the presence of zircon-bearing tuff beds that allow U-Pb geochronolgy to place absolute age constraints on the depositional sequences (Bowring and Grotzinger, 1992). This paper investigates the implications of the architecture of alluvial facies within this foreland basin and the detritus contained within it for understanding the Slave-Rae collision that occurred at about 2.0 Ga. This study addresses three main issues. First, this study defines how to identify marine versus nonmarine siliciclastic facies. Using this information, unconformities can be identified within the unfossiliferous rocks. The second part of this study seeks to show how the distribution of large-scale unconformities in an alluvial sequence in foreland basins reflects fundamental shifts in subsidence and sedimentation patterns derived from the feedback between growth of the orogenic belt and climatically-modulated erosion, transport, and deposition of synorogenic detritus. Finally, the nature of the syn-orogenic detritus within the foreland basin provides critical information on the character and evolution of the sources areas that contributed clastic material. In particular, geochronologic data from detrital zircons test the validity of correlations within Kilohigok Basin, between Kilohigok Basin and the coeval Wopmay Orogen on the other side of the Slave Province, and helps test tectonic models for the collision between the Slave and Rae Provinces that created the Kilohigok Basin.

Previous work

Kilohigok Basin–a part of the Canadian Shield: early reconnaissance studies

The first geological description of the rocks in the Kilohigok Basin were by Richardson in 1823 (Houston, 1984), quoted in the frontispiece, who described the topographic expression of the hills held up by alluvial foreland basin fill. In addition, he described a distinctive conglomerate horizon that is now recognized within this alluvial sequence that contain abundant intraformational syn-orogenic clasts.

The Canadian Arctic Expedition of 1913-1918 was the first reconnaissance study that described the rocks of the area and, in particular, named the Precambrian sedimentary rocks (O'Neill, 1924). They described and named the "Goulburn Quartzite", but it appears from the description that Middle Proterozoic rocks that unconformably overlap the Goulburn Supergroup were lumped in the Goulburn Quartzite. A post-World War II expedition found quartzites on Victoria Island and assigned them to the Goulburn Quartzite in the sense used by O'Neill (Washburn, 1947). These quartzites are now recognized as correlatives of Goulburn Supergroup strata (Campbell and Cecile, 1979). In addition to geological information, the Candian Arctic Expedition collected geographic and cultural information, including Inuit names for places and objects. The name Kilohigok derives from the Inuit word Kilusiktok, that means the country about the western and southern side of Arctic Sound, literally, "the place that lies behind or inland".

The first modern geological studies of this area began with the massive helicopter "siege mapping" projects conducted by the Geological Survey of Canada in the 1950's and 1960's to inventory the geological resources of the vast *terra incognita* of northern Canada. These studies led to broad subdivisions of the northwestern Canadian shield (Fraser, 1964; Fraser and Tremblay, 1969; Fraser, 1978; Heywood and Schau, 1978). Stockwell (1964) first assigned the Goulburn strata to Aphebian (Early Proterozoic) age.

More focused studies at regional map-sheet scale led to the first gross lithologic subdivision of the stratigraphy of Kilohigok Basin (Bostock, 1965; Tremblay, 1967; Tremblay, 1968; Tremblay, 1971). The Goulburn sediments were raised to group status and correlated, fairly accurately, with their equivalents in what is now known as Wopmay Orogen (Fraser and Tremblay, 1969). The stratigraphic subdivisions established by Fraser and Tremblay are the basis for the current stratigraphic subdivision of the Goulburn Supergroup.

Tremblay made one key lithologic miscorrelation that led indirectly to the current project in Kilohigok Basin and this error was propagated by later investigators. He correlated dolomitic rocks on the westernmost end of Kilohigok Basin with the Kuuvik Formation

carbonate platform found farther to the east. The import of this miscorrelation is discussed below.

The fog descends: initial sedimentary basin studies and aulacogen models

The first sedimentological study of the Early Proterozoic basins that ring the Slave Province began in the late 1960's with the landmark study by Paul Hoffman of marvelously preserved strata in the East Arm of Great Slave Lake (Hoffman, 1969), now known as Athapuscow Basin. Not satisfied with having an entire sedimentary basin to himself, Hoffman proceeded to extend his studies into Wopmay Orogen, arguably one of the best exposed and best studied orogenic belts of any age. Based on the superb exposure of a wide range of crustal levels, he rightly comments that "there is no reason for shield geologists to suffer 'mountain envy' " (Hoffman et al., 1988).

In the mid 1970's, Campbell and Cecile began the first project specifically aimed at the Proterozoic strata in Kilohigok Basin (Campbell and Cecile, 1976; Cecile, 1976; Campbell, 1979; Campbell and Cecile, 1981). They conducted the first modern sedimentological studies in the basin and erected a much more detailed stratigraphic subdivision, but their formation boundaries remained identical to those established earlier. As alluded to above, they maintained the correlation of dolomitic rocks in the west to the Kuuvik carbonate platform proposed by Tremblay.

Hoffman (1973) interpreted the evolution of all three of the circum-Slave basins in terms of modern, actualistic tectonics, which he amplified upon later (Hoffman et al., 1974). In particular, he interpreted Kilohigok basin to be one of two aulacogens related to rifting in Wopmay Orogen (Hoffman, 1973; Hoffman, 1980). This interpretation was based on the linear trend of the basin, its association with a high-angle fault system, and thick succession of sediments recognized as correlatives to sequences in Athapuscow "Aulacogen" and Wopmay Orogen. However, citing the lack of evidence for extensive growth faulting and volcanism, Campbell and Cecile (1981) interpreted the basin as a northwest trending intracratonic trough, developed as a splay off of a hypothetical aulacogen to the north of Kilohigok basin, the Taktu aulacogen; Taktu is the Inuit word for fog, which seems appropriate given the cryptic nature of this inferred structure. The hypothetical aulacogen was believed to open westward into the passive margin of Wopmay Orogen. The splay (Kilohigok Basin) was believed to have formed during eastward propagation of the inferred aulacogen. The driving mechanism of splay subsidence was unspecified.

Paleomagnetic studies from all three circum-Slave basins suggest that in the Early Proterozoic these basins lay at tropical latitudes (Evans and Hoye, 1981; McGlynn and Irving,

1981). The data for all stratigraphic intervals sampled is relatively well clustered, except for one point in the lower part of the foreland basin strata of Kilohigok Basin. This suggests that a long time gap may lie between lower marine and upper alluvial foreland basin sediments in Kilohigok Basin and that they were deposited considerably before those in Wopmay Orogen or Athapuscow Basin. We now believe that the alluvial sediments correlate with the lowermost sediments in Wopmay Orogen.

The overwhelming weight of data: reinterpretation of Kilohigok Basin and Thelon Orogen as products of Slave-Rae collision

A combination of sedimentologic and stratigraphic, structural, geochronologic, and geophysical data showed that the original models for Kilohigok Basin were untenable and led directly to this project.

One key piece of evidence Campbell and Cecile (1981) appear to ignore in constructing their tectonic model is that the main alluvial sediments in Kilohigok Basin flow away from the zone of maximum subsidence. This is incompatible with extensional or strike-slip basin models. It is a common component of alluvial foreland basins, however.

The study of the sedimentary prism in the external zone of Wopmay Orogen that the passive margin carbonate platform is much narrower than those in Phanerozoic passive margin sequences (Grotzinger, 1985). Also, there is abundant siliciclastic detritus in lagoonal facies that coarsens and thickens towards the craton. Finally, there are some notable intervals within the carbonate platform that indicate relative sea level rises and backstepping of the carbonate facies towards the craton and towards Kilohigok Basin.

The incident that led to this project occurred when Hoffman and Grotzinger made a reconnaissance trip across Kilohigok Basin. In the outcrops closest to Wopmay Orogen they found dolomitic units that matched those found in the carbonate platform of Wopmay Orogen (Hoffman et al., 1984). Also, they noted that these carbonate units are sandwiched within the siliciclastic alluvial wedge that Campbell and Cecile (1981) showed drained to the west. Here lay the explanation for siliciclastic detritus in the passive margin of Wopmay Orogen. Furthermore, examination of Goulburn outcrops in the eastern side of the Slave Province led Hoffman and Grotzinger to speculate that the alluvial wedge represented foreland basin deposits caused by the unroofing of Thelon Orogen. At the time, Thelon Orogen was thought to be an Archean deformation zone that, at best, was reactivated in the Early Proterozoic; this was before any U-Pb geochronological data existed for the area. Hoffman then returned to the Geological Survey of Cananda in Ottawa, convinced John McGlynn to take funding from a graduate student from V.P.I. who had started a sedimentologic field study in Kilohigok Basin, and redirect the money

to Grotzinger. Independently, Rein Tirrul pointed out some unusual structural relations in the proximal part of Kilohigok Basin as mapped by Campbell and Cecile (1976) that he thought might be more characteristic of thrust faults that verged away from Thelon Orogen.

Based on these observations, two independent projects were begun in Kilohigok Basin: one structural geology project in southeastern tip by Tirrul, and a sedimentologic and stratigraphic project of the entire Kilohigok Basin by Grotzinger. The problem that motivated both these projects was to demonstrate whether there was a link between deformation in Thelon Orogen and the evolution of the sedimentary basins in the Slave Province. Tirrul discovered that the proximal 20 km of the basin was a foreland thrust-fold belt that experienced about 60% shortening (Tirrul, 1985; Tirrul and Grotzinger, 1990). The presence of a ductile sole thrust above the basement-cover contact in Kilohigok Basin and the existence of outliers of Goulburn Supergroup rocks between Kilohigok Basin and Thelon Orogen led Tirrul and Grotzinger (1990) to speculate that the thrusts probably root in the Thelon Orogen. Grotzinger found stratigraphic evidence for the Kilohigok Basin contained a short-lived passive margin sequence that was drowned on its outer margin and uparched and erosionally truncated to basement on the cratonic side (Grotzinger and Gall, 1986). These and other data led them to conclude that the bulk of Goulburn Supergroup strata represented foreland basin. Paleocurrents in the overlying alluvial strata indicate derivation from the direction of Thelon Orogen. U-Pb geochronologic work on volcanic ash beds and detrital zircons within Kilohigok Basin by Sam Bowring have provided an essential link between Thelon Orogen, Kilohigok Basin, and Wopmay Orogen (Bowring and Grotzinger, 1992).

Despite the contention by early workers that Thelon Orogen was largely an Archean feature (Thompson and Frey, 1984; Thompson et al., 1985; Thompson et al., 1986), U-Pb geochronology ultimately showed that all of the high grade metamorphism, deformation, and igneous activity occurred between 1.9-2.0 Ga (Culshaw, 1984; van Breemen et al., 1986; van Breemen et al., 1987a; van Breemen et al., 1987b; van Breemen et al., 1987c; van Breemen et al., 1987d; James et al., 1988; van Breeman et al., 1990; van Breeman and Henderson, 1991). A temporally equivalent continental magmatic arc lies south of the Slave Province, offset by a contemporaneous ductile transcurrent shear zone, and appears to be the lateral continuation of Thelon Orogen (Bostock et al., 1987a; Bostock et al., 1987b; Bostock and Loveridge, 1988; van Breemen et al., 1992).

Proterozoic collision and suturing between Slave and Rae Provinces was actually proposed in the 1970's by Gibb and his co-workers based on offsets in magnetic anomalies and paired gravity anomalies across the Thelon metamorphic front (Thomas et al., 1976; Gibb and Thomas, 1977; Gibb, 1978). Gibb (1978) interpreted the conjugate transcurrent Bathurst and McDonald fault systems to be analogous to the rigid indentor model proposed for the Himalayan

situation. Accumulated geochronological data showed that the transcurrent faulting actually postdates much of the collision along the southern and eastern margin of Slave Province. Hanmer and co-workers showed that earlier ductile transcurrent faulting existed along the Great Slave Lake shear zone that turns out to be coeval with Thelon Orogen and the Taltson Magmatic Zone (Hanmer and Lucas, 1985; van Breeman et al., 1990). Given the isotopic, structural, and geophysical data gathered in the 1980's, Hoffman (1987) resurrected the Himalayan analogy for Slave-Rae collision in order to explain the contemporaneous ductile deformation, high grade metamorphism, igneous activity, and, of course, the sedimentary basins preserved on the Slave Province. Part of this study tests this Himalayan model.

Based on recent syntheses of the plethora of recent geologic and geochronologic data from the Precambrian of North America and Canada, in particular, Hoffman (1988; Hoffman, 1989) has demonstrated that the Early Proterozoic witnessed the aggregation of myriad Archean continental nuclei into Laurentia over a relatively short span of time, 2.0 to 1.8 Ga. This appears to document the assembly of the oldest supercontinent in the Proterozoic. It appears that the Slave and Rae Provinces were the first such microcontinents to collide in this vast accretionary event.

Impetus for this study

This study of the alluvial elements of the foreland basin of Kilohigok Basin is important because it records the sedimentologic response to the Early Proterozoic collision between the Slave and Rae Provinces along the Thelon Orogen. The geometry of the alluvial fill reflects dynamic evolution of this orogenic belt and composition of the fill reflects the evolving drainage along and within Thelon Orogen and the adjacent Rae Province. These sedimentologic, stratigraphic, and provenance data provide key tests for geodynamic models for the evolution of Kilohigok Basin, Wopmay Orogen, and Thelon Orogen.

This study attempts an integrated approach to assess the history of the Kilohigok foreland basin. First, the detailed sedimentology of the shallow marine and alluvial facies of the Burnside Formation are described and interpreted. This environmental data is a key element in understanding the stratigraphic architecture of the alluvial wedge that derived from the adjacent orogen. This architecture allows interpretation of the how the basin and the adjacent orogen evolved. Finally, building on the sedimentologic and stratigraphic framework, the provenance of the foreland basin fill is assessed through the sandstone and gravel petrography, paleocurrents, and dating of detrital zircons within the sandstones. This shows how the drainage of the foreland basin evolved and what were the age and location of source areas that contributed to the extensive alluvial basin fill.

References Cited

Armin, R.A., and Mayer, L., 1983. Subsidence analysis of the Cordilleran miogeocline: implications for the timing of late Proterozoic rifting and amount of extension. Geology, v. 6, p. 702-705.

Bally, A.W., Gordy, P.L., and Stewart, G.A., 1966. Structure, seismic data, and orogenic evolution of southern Canadian Rockies. Bull. Can. Petrol. Geol., v. 14, p. 337-381.

Beaumont, C., 1981. Foreland basins. Geophys. J. Roy. Astron. Soc., v. 65, p. 471-498.

Beaumont, C., Fullsack, P., and Hamilton, J., 1992. Erosional control of active compressional orogens, in, K.R. McClay (ed.), Thrust Tectonics. Chapman and Hall (London), p. 1-18.

Beaumont, C., Fullsack, P., Willett, S., Hamilton, J., Johnson, D., Ellis, S., and Paton, M., 1990. Coupling of climate, surface processes and tectonics in orogens and their associated sedimentary basins, in, J. Hall (ed.), Lithoprobe: Lithoprobe East Transect, Report 13. Memorial University, St. John's, Newfoundland (St. John's, Newfoundland, Canada), p.

Beaumont, C., and Hamilton, J., 1990. Influence of surface erosional processes on the evolution of compressional orogens. Geol. Soc. America, N.E. Section, Abs. with Progs., v. 22, p. A4.

Bond, G.C., and Kominz, M.A., 1984. Construction of tectonic subsidence curves for the early Paleozoic miogeocline, southern Canadian Rocky Mountains: implications for subsidence mechanisms, age of breakup, and crustal thinning. Geol. Soc. America Bull., v. 95, p. 155-173.

Bostock, H.H., 1965. Point Lake east half (86H E1/2) map-area, District of Mackenzie, Report of Activities. Geological Survey of Canada, Paper 65-1 (Ottawa, Ontario), p. 22-26.

Bostock, H.H., and Loveridge, W.D., 1988. Geochronology of the Taltson Magmatic Zone and its eastern cratonic margin, District of Mackenzie, Radiogenic Age and Isotopic Studies: Report 2. Geological Survey of Canada, Paper 88-2 (Ottawa, Ontario), p. 59-65.

Bostock, H.H., van Breeman, O., and Loveridge, W.D., 1987a. Proterozoic geochronology in the Taltson Magmatic Zone, N.W.T, Radiogenic Age and Isotopic Studies: Report 1. Geological Survey of Canada Paper 87-2 (Ottawa, Ontario), p. 73-80.

Bostock, H.H., van Breemen, O., and Loveridge, W.D., 1987b. Proterozoic geochronology in the Taltson magmatic zone, N.W.T., Canada. Geological Survey of Canada, Paper 87-9. pp.

Bowring, S.A., and Grotzinger, J.P., 1992. Implications of new chronostratigraphy for tectonic evolution of Wopmay Orogen, northwest Canadian Shield. American Journal of Science, v. 292, p. 1-20.

Campbell, F.H.A., 1979. Stratigraphy and sedimentation in the Helikian Elu Basin and Hiukitak Platform, Bathurst Inlet-Melville Sound, Northwest Territories. Geological Survey of Canada, Paper 79-8 18 pp.

Campbell, F.H.A., and Cecile, M.P., 1976. Geology of the Kilohigok Basin. Geological Survey of Canada, Open File Map 332, 1:500 000 Scale.

Campbell, F.H.A., and Cecile, M.P., 1979. The northeastern margin of the Aphebian Kilohigok Basin, Melville Sound, Victoria Island, District of Franklin, Current Research, Part A. Geological Survey of Canada, Paper 79-1A p. 91-94.

Campbell, F.H.A., and Cecile, M.P., 1981. Evolution of the Early Proterozoic Kilohigok Basin, Bathurst Inlet-Victoria Island, Northwest Territories, in, F.H.A. Campbell (ed.), Proterozoic Basins of Canada. Geological Survey of Canada, Paper 81-10 p. 103-131.

Cecile, M.P., 1976. Stratigraphy and depositional history of the Upper Goulburn Group, Kilohigok Basin, N.W.T. Unpublished Ph.D. thesis, Carleton University (Ottawa, Canada).

Christie-Blick, N., Grotzinger, J.P., and von der Borch, C.C., 1988. Sequence stratigraphy in Proterozoic successions. Geology, v. 16, p. 100-104.

Culshaw, N.G., 1984. Rutledge Lake, Northwest Territories; a section across a shear belt within the Churchill Province, Current Research, Part A. Geological Survey of Canada, Paper 84 1-A p. 331-338.

Evans, M.E., and Hoye, G.S., 1981. Paleomagnetic results from the lower Proterozoic rocks of the Great Slave Lake and Bathurst Inlet areas, Northwest Territories, in, F.H.A. Campbell (ed.), Proterozoic Basins of Canada. Geological Survey of Canada, Paper 81-10 p. 191-202.

Flemings, P.B., and Jordan, T.E., 1987. Synthetic stratigraphy of foreland basins. Eos., Trans. Am. Geophys. Union, v. 68, p. 419.

Flemings, P.B., and Jordan, T.E., 1989. A synthetic stratigraphic model of foreland basin development. J. Geophys. Res., v. 94, No. B4, p. 3851-3866.

Fraser, J.A., 1964. Geological notes on the northeastern District of Mackenzie, N.W.T. Geological Survey of Canada, Paper 64-40 pp.

Fraser, J.A., 1978. Metamorphism in the Churchill Province, District of Mackenzie, Current Research, Part A. Geological Survey of Canada, Paper 78-1A p. 195-202.

Fraser, J.A., and Tremblay, L.P., 1969. Correlation of Proterozoic strata in the Northwestern Canadian Shield. Canadian Journal of Earth Sciences, v. 6, p. 1-9.

Gibb, R.A., 1978. Slave-Churchill collision tectonics. Nature, v. 271, p. 50-52.

Gibb, R.A., and Thomas, M.D., 1977. The Thelon front: a cryptic suture in the Canadian Shield. Tectonophys., v. 38, p. 211-222.

Grotzinger, J.P., 1985. Evolution of Early Proterozoic passive-margin carbonate platform, Rocknest Formation, Wopmay Orogen, N.W.T., Canada. Unpublished Ph.D. Thesis, Virginia Polytechnic Institute and State University (Blacksburg, VA).

Grotzinger, J.P., and Gall, Q., 1986. Preliminary investigations of Early Proterozoic Western River and Burnside River Formations: evidence for foredeep origin of Kilohigok Basin, N.W.T., Canada, Current Research, Part A. Geological Survey of Canada, Paper 86-1A p. 95-106.

Grotzinger, J.P., and Royden, L., 1990. Elastic strength of the Slave craton at 1.9 Gyr and implications for the thermal evolution of the continents. Nature, v. 347, p. 64-66.

Hanmer, S., and Lucas, S.B., 1985. Anatomy of a ductile transcurrent shear: The Great Slave Lake Shear Zone, District of Mackenzie, N.W.T. (preliminary report), Current Research. Geological Survey of Canada Paper 85-1B p. 7-22.

Haq, B.U., Hardenbol, J., and Vail, P.R., 1987. Chronology of fluctuating sea levels since the Triassic. Science, v. 235, p. 1156-1167.

Heywood, W.W., and Schau, M., 1978. A subdivision of the northern Churchill Structural Province, Current Research, Part A. Geological Survey of Canada, Paper 78-1A p. 139-143.

Hoffman, P.F., 1969. Proterozoic paleocurrents and depositional history of the East Arm fold belt, Great Slave Lake, Northwest Territories. Canadian Journal of Earth Sciences, v. 6, p. 441-462.

Hoffman, P.F., 1973. Evolution of an early Proterozoic continental margin: the Coronation geosyncline and associated aulacogens of the northwestern Canadian shield. Philosophical Transactions of the Royal Society of London, Series A, v. 273, p. 547-581.

Hoffman, P.F., 1980. Wopmay Orogen: A Wilson cycle of early Proterozoic age in the northwest of the Canadian Shield, in, D.W. Strangeway (ed.), The Continental Crust and its Mineral Deposits. Geological Association of Canada, Special Paper 20 (Ottawa, Ontario), p. 523-549.

Hoffman, P.F., 1987. Continental transform tectonics: Great Slave Lake shear zone (ca. 1.9 Ga), northwest Canada. Geology, v. 15, p. 785-788.

Hoffman, P.F., 1988. United plates of America, the birth of a craton: Early Proterozoic assembly and growth of Laurentia. Ann. Rev. Earth Planet. Sci., v. 16, p. 543-603.

Hoffman, P.F., 1989. Precambrian geology and tectonic history of North America, in, A.W. Bally, and A.R. Palmer (eds.), The geology of North America - An overview. Geological Society of America (Boulder, CO), p. 447-512.

Hoffman, P.F., Dewey, J.F., and Burke, K., 1974. Aulacogens and their genetic relation to geosynclines, with a Proterozoic example from Great Slave Lake, Canada, in, R.H. Dott Jr., and R.H. Shaver (eds.), Modern and Ancient geosynclinal Sedimentation. Society of Economic Paleontologists and Mineralogists, Special Publication 19 (Tulsa, OK), p.

Hoffman, P.F., Tirrul, R., Grotzinger, J.P., Lucas, S.B., and Eriksson, K.A., 1984. The Externides of Wopmay Orogen, Takijuk Lake and Kikerk Lake map areas, District of Mackenzie, Current Research, Part A. Geological Survey of Canada, Paper 84-1A p. 383-395.

Hoffman, P.F., Tirrul, R., King, J.E., St.-Onge, M.R., and Lucas, S.B., 1988. Axial projections and modes of crustal thickening, eastern Wopmay Orogen, northwest Canadian Shield, in, S.P. Clark, B.C. Burchfiel, and J. Suppe (eds.), Processes in Continental Lithospheric Deformation. Geological Society of America, Special Paper 218 (Denver, CO), p. 1-30.

Houston, C.S., 1984. Arctic Ordeal: The journal of John Richardson, surgeon-naturalist with Franklin, 1820-1822. McGill-Queen's University Press (Montreal and Kingston, Canada), 349 pp.

James, D.T., van Breeman, O., and Loveridge, W.D., 1988. Early Proterozoic U-Pb zircon ages for granitoid rocks from the Moraine Lake transect, District of Mackenzie, Radiogenic Age and Isotopic Studies: Report 2. Geological Survey of Canada, Paper 88-2 (Ottawa, Ontario), p. 67-72.

Johnson, D.D., and Beaumont, C., 1990. Surface processes and foreland basin stratigraphy. Geol. Soc. America, N.E. Section, Abs. with Progs., v. 22, p. A26.

Jordan, T.E., 1981. Thrust loads and foreland basin evolution, Cretaceous, western United States. Am. Assoc. Petrol. Geol. Bull., v. 65, p. 2506-2520.

Karner, G.D., 1986. On the relationships between foreland basin stratigraphy and thrust sheet migration and denudation. Eos, Trans. Am. Geophys. Union, v. 67, p. 1193.

Karner, G.D., and Watts, A.B., 1983. Gravity anomalies and flexure of the lithosphere at mountain ranges. Jour. Geophys. Res, v. 88, No. B12, p. 10449-10477.

Krogh, T.E., 1973. A low-contamination method for hydrothermal decomposition of zircon and extraction of U and Pb for isotopic age determinations. Geochim. Cosmochim. Acta, v. 37, p. 485-494.

Krogh, T.E., 1982. Improved accuracy of U-Pb zircon ages by creation of more concordant systems using an air abrasion technique. Geochim. Cosmochim. Acta, v. 45, p. 637-649.

Lyon-Caen, H., and Molnar, P., 1985. Gravity anomalies, flexure of the Indian plate, and the structure, support, and evolution of Himalaya and Ganga Basin. Tectonics, v. 4, p. 513-538.

McGlynn, J.C., and Irving, E., 1981. Horizontal motions and rotations of the Canadian Shield during the Early Proterozoic, in, F.H.A. Campbell (ed.), Proterozoic Basins of Canada. Geological Survey of Canada, Paper 81-10 p. 183-190.

McKenzie, D., 1978. Some remarks on the development of sedimentary basins. Earth and Planetary Science Letters, v. 40, p. 25-32.

Moretti, I., and Royden, L., 1988. Deflection, gravity anomalies and tectonics of doubly subducted continental lithosphere: Adriatic and Ionian Seas. Tectonics, v. 7, p. 875-893.

O'Neill, J.J., 1924. Report of the Canadian Arctic expedition 1913-18, Volume IX: Geology and Geography, Part A: The geology of the arctic coast of Canada, west of the Kent Peninsula. (Ottawa, ONT., Canada), 107 pp.

Royden, L., and Karner, G.D., 1984. Flexure of the lithosphere beneath Apennine and Carpathian foredeep basins: evidence for an insufficient topographic load. Am. Assoc. Petrol. Geol. Bull., v. 68, p. 704-712.

Royden, L., Patacca, E., and Scandone, P., 1987. Segmentation and configuration of subducted lithosphere in Italy: an important control on thrust belt and foredeep basin evolution. Geology, v. 15, p. 714-717.

Schedl, A., and Wiltschko, D.V., 1984. Sedimentological effects of a moving terrain. J. Geol., v. 92, p. 273-287.

Sloss, L.L., 1963. Sequences in the cratonic interior of North America. Geological Society of America Bulletin, v. 74, p. 93-114.

Stockwell, C.H., 1964. Fourth report on structural provinces, orogenies, and time-classification of rocks of the Canadian Precambrian Shield. Geological Survey of Canada, Paper 64-17, Part 2 (Ottawa, Ontario), 1-21 pp.

Thomas, M.D., Gibb, R.A., and Quince, J.R., 1976. New evidence from offset aeromagnetic anomalies for transcurrent faulting associated with the Bathurst and McDonald faults, Northwest Territories. Canadian Journal of Earth Sciences, v. 13, p. 1244-1250.

Thompson, P.H., Culshaw, N., Buchanan, J.R., and Manoljlovic, P., 1986. Geology of the Slave Province and Thelon Tectonic Zone in the Tinney Hills-Overby Lake (west half) map area, District of Mackenzie, Current Research, Part A. Geological Survey of Canada, Paper 86-1A p. 275-289.

Thompson, P.H., Culshaw, N., Thompson, D., and Buchanan, J.R., 1985. Geology across

the western boundary of the Thelon Tectonic Zone in the Tinney Hills-Overby Lake (west half) map area, District of Mackenzie, Current Research, Part A. Geological Survey of Canada, Paper 85-1A p. 555-572.

Thompson, P.H., and Frey, M., 1984. Illite "crystallinity" in the Western River Formation and its significance regarding the regional metamorphism of the early Proterozoic Goulburn Group, District of Mackenzie, Current Research, Part A. Geological Survey of Canada, Paper 84-1A p. 409-414.

Tirrul, R., 1985. Nappes in the Kilohigok Basin and their relationship to the Thelon Tectonic Zone, District of Mackenzie, Current Research, Part A. Geological Survey of Canada, Paper 85-1A p. 407-420.

Tirrul, R., and Grotzinger, J.P., 1990. Early Proterozoic collisional orogeny along the northern Thelon Tectonic Zone, Northwest Territories, Canada: Evidence from the foreland. Tectonics, v. 9, p. 1015-1036.

Tremblay, L.P., 1967. Contwoyto Lake map-area, District of Mackenzie (74 E/14). Geological Survey of Canada, Paper 66-28 (Ottawa, Ontario, Canada), pp.

Tremblay, L.P., 1968. Preliminary account of the Goulburn Group, N.W.T. Geological Survey of Canada, Paper 67-8 (Ottawa, Ontario, Canada), pp.

Tremblay, L.P., 1971. Geology of the Beechey Lake map-area, District of Mackenzie. Geological Survey of Canada, Memoir 365 (Ottawa, Ontario, Canada), pp.

Vail, P.R., Mitchum, R.M., and Thompson, S., III, 1977. Seismic stratigraphy and global changes of sea level, Part 3: Relative changes of sea level from coastal onlap, in, C. Payton (ed.), Seismic Stratigraphy - Applications to Hydrocarbon Exploration. American Association of Petroleum Geologists, Memoir 26 p. 63-81.

van Breeman, O., Hanmer, S.K., and Parrish, R.R., 1990. Archean and Proterozoic mylonites along the southeastern margin of the Slave Structural Province, Northwest Territories, Radiogenic Age and Isotopic Studies: Report 3. Geological Survey of Canada Paper 89-3 (Ottawa, Ontario), p. 55-62.

van Breeman, O., and Henderson, J.B., 1991. U-Pb zircon and monazite ages from the eastern Slave Province, Artillery Lake area, N.W.T., Radiogenic Age and Isotopic Studies: Report 2. Geological Survey of Canada Paper 88-2 (Ottawa, Ontario), p. 73-83.

van Breemen, O., Bostock, H.H., and Loveridge, W.D., 1992. Geochronology of granites along the margin of the northern Taltson Magmatic Zone and western Rae Province, Northwest Territories, Radiogenic Age and Isotopic Studies: Report 5. Geological Survey of Canada Paper 91-2 (Ottawa, Ontario), p. 17-24.

van Breemen, O., Henderson, J.B., Loveridge, W.D., and Thompson, P.H., 1986. Archean-Aphebian geochronology along the Thelon Tectonic Zone, Healey Lake area, N.W.T. Geol. Assoc. Canada, Prog. with Abs., v. 11, p. 139.

van Breemen, O., Henderson, J.B., Loveridge, W.D., and Thompson, P.H., 1987a. U-Pb zircon and monazite geochronology and zircon morphology of granulites and granite from the Thelon Tectonic Zone, Healey Lake and Artillery Lake map areas, N.W.T., Current Research, Part A. Geological Survey of Canada, Paper 87-1A p. 783-801.

van Breemen, O., Henderson, J.B., Sullivan, R.W., and Thompson, P.H., 1987b. U-Pb zircon and monazite ages from the eastern Slave Province, Healey Lake area, N.W.T., Radiogenic Age and Isotopic Studies: Report 1. Geological Survey of Canada Paper 87-2 (Ottawa, Ontario), p. 101-110.

van Breemen, O., Thompson, P.H., Bostock, H.H., and Loveridge, W.D., 1987c. Timing of plutonism in the northern Thelon Tectonic Zone and the Taltson Magmatic Zone. Geol. Assoc. Canada, Prog. with Abs., v. 12, p. 98.

van Breemen, O., Thompson, P.H., Hunt, P.A., and N., C., 1987d. U-Pb zircon and monazite geochronology from the northern Thelon Tectonic Zone, District of Mackenzie, Radiogenic Age and Isotopic Studies: Report 1. Geological Survey of Canada Paper 87-2 (Ottawa, Ontario), p. 81-93.

Van Wagoner, J.C., Posamentier, H.W., Mitchum, R.M., Jr., Vail, P.R., Sarg, J.F., Loutit, T.S., and Hardenbol, J., 1988. An overview of the fundamentals of sequence stratigraphy and key definitions, in, C.K. Wilgus, B.S. Hastings, C.G.S.C. Kendall, H.W. Posamentier, C.A. Ross, and J.C. Van Wagoner (eds.), Sea-level changes: an integrated approach. Soc. Econ. Paleontologists and Mineralogists, Spec. Pub. No. 42 p. 39-46.

Washburn, A.L., 1947. Reconnaisance geology of portions of Victoria Island and adjacent regions Arctic Canada. Geological Society of America, Memoir 22, 142 pp.

Watts, A.B., and Ryan, W.B.F., 1976. Flexure of the lithosphere and continental margin basins. Tectononphysics, v. 36, p. 25-44.

Chapter 1:
Distinction of Marine from Alluvial Facies in the Early Proterozoic (1.9 Ga) Burnside Formation, Kilohigok Basin, N.W.T., Canada

Abstract

The Burnside Formation records the shift from marine shelf to largely alluvial conditions in the Early Proterozoic (ca. 1.9 Ga) Kilohigok foreland basin in the northwest Canadian Shield. The Burnside Formation is a thick (up to 3.5 km), northwest-tapering siliciclastic wedge, representing a sandy braid delta and braided alluvial system that prograded northwest across the Archean Slave craton. Criteria have been developed to distinguish shallow marine from alluvial facies allowing construction of a stratigraphic framework for this unfossiliferous, alluvially dominated succession.

The sandy alluvial system prograded over a storm-influenced fine-grained siliciclastic shelf. Shelf associations can be divided into siltstone-dominated and mixed siltstone-sandstone. The siltstone-dominated association comprises facies ranging from mudstones deposited below storm wave influence to siltstones deposited under storm and fairweather wave conditions. Mixed siltstone-sandstone facies form coarsening-upwards sequences on the scale of several meters to a few ten's of meters that appear to represent prograding marine sand bars. Initial alluvial influence comprises associations of mixed siltstone and sandstone with shallow-water wave- and current-formed structures, abundant soft-sediment deformation, and isolated meter-size channels filled with trough cross bedded sandstone and associated rip-up clasts. Thick (10's to 100's of meters) of tabular bedded fine-grained sandstone represent delta platform environment between coarser-grained trough cross-bedded braid delta distributary channels. Unidirectional paleocurrents in the transitional alluvial facies indicate predominantly west to southwest transport.

The bulk of the Burnside formation comprises several associations representing sandy alluvial braid plain facies. Conglomeratic lithologies are subordinate to sandy ones and are restricted largely to the proximal (southeastern) part of the basin. Braid plain facies cover hundred's of meters of section and primarily consist of hierarchies of trough cross bedding on scales of a few to many tens of meters. Unidirectional paleocurrents from the main alluvial associations cluster with a single narrow west-northwest mode.

Associations of sedimentary facies and paleocurrents indicate that initially the alluvial system was restricted to the proximal part of the basin and drained longitudinally between

the orogenic hinterland and a syn-sedimentary flexural arch created by thrust loading. Contemporaneous shallow marine shelf facies existed to the northwest over and beyond the flexural arch. An abrupt shift to transverse drainage and the superposition of medial braid plain facies directly on marine shelf and deltaic facies in the foreland mark an abrupt, unconformable contact representing the progradation of the alluvial system over the cratonic foreland. The area where the maximum disparity between marine and non-marine facies coincides with the area of greatest stratigraphic thinning and erosion, and marks the crest of the flexural arch. Only the transverse paleocurrent mode is recorded over the flexural arch and in the distal foreland. Stratigraphic relations suggest that marginal marine and braid delta facies tracts in the distal foreland shifted abruptly over large distances and were sensitive to relative sea level changes. In contrast, braid plain facies tracts migrated very little and the shift of facies tracts appears to have been more gradual. The large lateral extent of alluvial facies suggests that humid or monsoonal climate conditions existed in the source area.

Introduction

The evolution of ancient alluvial sedimentary basins is generally approached by comparison with modern analogs, generally involving small to moderate size rivers (Miall, 1978; Ethridge and Flores, 1981; Collinson and Lewin, 1983; Walker and Cant, 1984; Ethridge et al., 1987). This presents a two-fold problem for the investigation of Precambrian sedimentary basins. First, the evolution of land plants since the Silurian has changed alluvial systems irrevocably by promoting bank stabilization and trapping of sediment, decreasing the effectiveness of aeolian processes, and by producing organic acids in soils that promote the formation of clays (Cotter, 1978; Long, 1978; Dalrymple et al., 1985). All of these effects favor meandering streams in the Phanerozoic. As a result, the braided stream, which is the ubiquitous model for Precambrian alluvial systems, has been restricted in the Phanerozoic to areas that experience extremes of climate or discharge. Therefore, actualistic analogs of Precambrian humid alluvial systems are very rare.

A second problem with deriving facies models from small to moderate sized modern alluvial systems is that subsidence rates commonly are low in the places where these rivers flow and therefore the deposits of these rivers have low preservation potential. Large alluvial systems must have existed in the past in rapidly subsiding, depositional settings that have created the preserved sedimentary record. An example of such a depositional setting is in a foreland basin where streams commonly drain high relief source areas and where high rates of basin subsidence exist for many tens of millions of years. Such settings promote the preservation of thick alluvial successions.

The distinction of marine from alluvial facies in Precambrian siliciclastic successions is a target of current research (Collinson, 1986). In Phanerozoic rocks, body and trace fossils are, in many cases, the definitive criterion for distinguishing between the two. Almost no such biogenic criteria exist for Precambrian successions, but physical sedimentological evidence, including associations of sedimentary structures and textures, bedding patterns, stratigraphic position, and comparison with Phanerozoic examples, provide useful starting points (Harris, 1987). Such criteria must be developed to aid the identification of unconformities and thus subdividing depositional sequences to allow time stratigraphic correlation in Precambrian basins (Christie-Blick et al., 1988). In this study, we develop paleo-environmental criteria for the Burnside Formation in order to identify unconformities in these Precambrian strata.

Both the temporal restriction of Precambrian alluvial systems and limited knowledge of large alluvial systems in modern settings prevents the application of extant facies models to Precambrian stream systems. We believe that a non-actualistic example of a large alluvial system deposited under humid perennial or monsoon discharge conditions exists in the Early Proterozoic Kilohigok Basin in the northwestern Canadian Shield. The Kilohigok Basin provides a superb setting to address some of these issues because of excellent exposures, the ability to identify regional unconformities to allow regional time correlation, and the presence of several zircon-bearing tuff beds that permit U-Pb geochronolgy to place absolute age constraints on the depositional sequences (Bowring and Grotzinger, 1992). The Burnside Formation of Kilohigok Basin affords an opportunity to assess several aspects of the evolution of an alluvial system in a foreland basin. This siliciclastic formation records the progradation of an alluvial system over 250 km across the Slave craton away from the source area (Grotzinger and McCormick, 1988). Issues addressed by this study of the Burnside Formation include the distinction between sandy marine and alluvial environments in Precambrian siliciclastic successions, the recognition of unconformities in the stratigraphic succession, and evidence for eustatic and tectonic controls on the alluvial system.

Geologic Setting

The Early Proterozoic (ca. 1.9 Ga) Kilohigok Basin is located in the northwestern corner of the Canadian Shield (Figures 1, 2). It is bounded to the west by Archean basement rocks of the Slave Province, largely composed of a complexly deformed Middle to Late Archean granitoids and Late Archean greywacke turbiditic successions with subordinate bimodal and felsic volcanics; the granite-greenstone assemblage is intruded by post-tectonic granitoids (Padgham, 1985). To the east, the basin abuts tectonically emplaced Archean

basement rocks and contemporaneous high grade rocks of the Early Proterozoic Thelon Orogen. The Thelon Orogen (2.02-1.92 Ga) is a collisional zone comprising regionally continuous high-grade metamorphic rocks and plutonic rocks of probable continental arc affinity associated with a major syn-plutonic dextral shear zone (Gibb and Thomas, 1977; Hanmer and Lucas, 1985; Thompson et al., 1985; van Breemen et al., 1986; Hoffman, 1987; Hoffman, 1988). Convergence along the Thelon Orogen and emplacement of northwest-directed thrust-nappes onto the eastern margin of the Slave Province likely drove the majority of subsidence of Kilohigok Basin (Grotzinger and McCormick, 1988; Tirrul and Grotzinger, 1990).

The Goulburn Supergroup of Kilohigok Basin comprises four tectono-stratigraphic units; only the lower two, the Kimerot and Bear Creek Groups, are considered here (Figure 3a) (Grotzinger and McCormick, 1988). The Kimerot Group (Figures 3a, 4) is a thin (0-500 m) southeast-facing prism consisting of a lower transgressive siliciclastic fluvial-to-marine shelf unit overlain by a peritidal carbonate platform. Grotzinger and McCormick (1988) interpret the Kimerot Group as a passive margin platform of brief duration (possibly <20 million years). The end of carbonate deposition is marked by drowning of the platform in response to initial convergence and thrust loading of the Slave margin along the Thelon Orogen (Figure 1) (Grotzinger and McCormick, 1988; Tirrul and Grotzinger, 1990). At the same time as drowning of the outer edge of platform occurred in the southeast, uplift and erosion of the inner shelf occurred to the northwest over a flexural arch (Figures 2, 4). The erosional cut-out of the Kimerot platform defines a northeast-trending line, called the Gordon Bay Arch (Figure 2); further toward the craton (northwest) of the cut-out, towards the craton, a regolith mantles the Archean basement only where the Kimerot platform sediments are absent. Grotzinger et al. (1988) interpret the regolith as an Early Proterozoic subaerial exposure surface related to flexurally induced uplift and erosion of Kimerot sedimentary rocks. The crest of the flexural arch lies about 75 km northwest of the platform cut-out where the maximum regolith development exists, where depositional sequences within the overlying marine units in the Bear Creek Group (Hackett, Rifle, Beechey, and Link Formations: Figure 3a) are thinnest, and where the maximum development of erosional unconformities exists within the Bear Creek Group (Figures 2, 3, 4) (Grotzinger et al., 1989).

The Bear Creek Group comprises a largely siliciclastic succession divisible into a lower mostly marine package and an upper mostly alluvial package (Figures 3a, 4). The lower Bear Creek Group is composed of unconformity-bounded depositional sequences (Figures 3a, 4: Hackett, Rifle, Beechey, and Link Formations) (Grotzinger and McCormick, 1988). These southeast-facing marine shelf onlap-offlap packages pass laterally abruptly into

correlative slope and basinal turbidite systems over a spatially restricted shelf edge. The turbidite units exist exclusively to the southeast of the Gordon Bay flexural arch, closest to the orogenic source area. Turbidite paleocurrents indicate southwest flow, parallel to the trends of the Gordon Bay Arch and the Thelon Orogen (Grotzinger and McCormick, 1988; Tirrul and Grotzinger, 1990).

The upper Bear Creek Group (Figures 3a&b, 4: Burnside, Mara, Quadyuk Formations) represents the change from marine to largely alluvial conditions caused by progradation of a northwest-directed braided alluvial system (Burnside Formation) followed by gradual waning of alluvial input and return to shallow marine conditions (Mara-Quadyuk Formations; Figures 3a&b, 4). Paleocurrents indicate remarkably uniform northwest transport across the Slave craton (Figure 5). Conglomerates include intraformational and intrabasinal clasts, as well as extrabasinal clasts derived from volcanic, plutonic, and metamorphic sources to the southeast.

On the basis of mapping of depositional sequences and lithostratigraphy, the Bear Creek Group correlates with sedimentary rocks in Wopmay Orogen (Hoffman et al., 1984; McCormick and Grotzinger, 1988; Grotzinger et al., 1989; Bowring and Grotzinger, 1992). The foredeep deposits of Hackett through middle Mara Formations correlate with the Wopmay passive margin. The upper Mara Formation and rocks of the Goulburn Supergroup overlying it correlate with foreland basin deposits in Wopmay Orogen.

The abrupt vertical shift from shallow marine platform (Kimerot Group) to deep marine basin that progressively shallows and passes upward into alluvial facies (Bear Creek Group) typifies many Phanerozoic foreland basins (Bally et al., 1966; Allen and Homewood, 1986). A tuff bed at the base the lower Bear Creek Group just above the contact with the Kimerot Group has yielded an U-Pb zircon date of 1.969 ± 0.001 Ga (Bowring and Grotzinger, 1992). This date closely constrains the drowning of the Kimerot platform and establishes a temporal link between deposition and flexural subsidence in Kilohigok Basin and magmatism and deformation in the Thelon Orogen. A tuff within the lower Bear Creek Group, between the Rifle and Beechey Formations, yield dates of 1.963 ± 0.006 Ga. A tuff bed within lowermost foreland basin sediments of Wopmay Orogen (Fontano Formation, Recluse Group: Figures 1, 2) correlates with the lower Mara Formation of Kilohigok Basin (Figure 3a&b, 4) and has been dated at 1.882 ± 0.0035 Ga (Bowring and Grotzinger, 1992). This constrains the duration of the main phase of Burnside Formation alluvial sedimentation to within about 80 million years, though it probably lasted less than that.

The Goulburn Supergroup was deformed by a series of structural events. The first event was northwest-directed thin-skinned thrusting that effected only the southeastern-most part of the basin (Figure 2) (Tirrul and Grotzinger, 1990). Thrust nappes and several

allochthonous thrust-bounded outliers of the Goulburn Supergroup root to the southeast in the Thelon Orogen. Subsequently two folding events occurred, shown by long-wavelength (ca. 50-75 km), northeast-trending, basement-involved folds, followed by transverse northwest-trending basement-involved folding of similar dimensions. The final phase of deformation involved approximately 115 km of sinistral offset along the Bathurst Fault (BFZ in Figure 1, 2) (Tirrul and Grotzinger, 1990). The present configuration of the "basin" results from selective structural preservation; the original shape of the basin was probably a prism trending parallel to the Thelon Orogen and tapering toward the northwest. The currently preserved geometry results largely from the basement-involved cross-folding events. Fortuitously, this folding produced an oblique cross-section of the original basin, that, when projected perpendicular to depositional strike, exposes nearly 250 km perpendicular to both facies belts and the original basin strike. Despite the age of the basin and the superimposition of several subsequent tectonic events, the metamorphic overprint on the Goulburn Supergroup sedimentary rocks has been slight: the highest metamorphic grade experienced by the Goulburn Supergroup is lowermost greenschist grade (Thompson and Frey, 1984), but nearly all of the Burnside Formation lies at much lower grade.

Sedimentology of the Burnside Formation

lithofacies and depositional environments

The Burnside Formation records the northwestward progradation of an alluvially dominated braided stream system over a southeast-facing siliciclastic marine shelf ramp. It must be emphasized from the outset that the Burnside Formation represents a sandy alluvial system. Conglomeratic facies, though common in the proximal (southeastern) part of the basin, do not extend to the marginal marine environments, although minor gravel is present locally. The term braid delta is used here to describe facies associations created by a *sandy* braided stream system debouching into and being modified by a shallow marine environment. We make this distinction because McPherson et al. (1987) have coined the term braid delta, but have used it to distinguish generally coarser-grained or conglomeratic deltaic deposits of braided stream systems. The important feature we wish to emphasize is how to distinguish marine-influenced alluvial facies from alluvial facies that experience no marine reworking.

The thickness and lateral extent of the Burnside Formation and its facies associations are vast. Currently preserved exposures of the Burnside Formation extend for 250 km projected across original depositional strike; the original alluvial system must have exceeded

350 km across depositional strike from the Thelon Orogen to the western edge of the Slave Province (Figure 1) where it influenced sedimentation in the contemporaneous passive margin of Wopmay Orogen. The alluvial succession attains 3500 m in the preserved part of the proximal (southeastern) foredeep, and by extrapolation towards the hinterland, the maximum thickness of the wedge must have been over 4000 m. In the cratonic foreland to the northwest, the maximum thickness of the Burnside Formation exceeds 2000 m. These thicknesses are comparable to Phanerozoic foreland basins. Paleocurrents indicate that the preserved Burnside Formation is not the product of a single alluvial fan such as the Kosi Fan of India (Wells and Dorr, 1987), but was a uniform west-northwest-draining braid plain or alluvial apron that lapped against the Thelon mountain belt to the east.

The Burnside Formation can be divided into facies associations described and interpreted below and summarized in Table 1. These facies associations are interpreted to represent four major environments: marine shelf, delta front and platform, braid delta plain, and braid plain. The origin and significance of a thin, stratigraphically restricted carbonate tongue, the Burnside Dolomite, is also discussed.

The braid delta plain and braid plain associations comprise the bulk of the Burnside Formation. Their facies motifs are remarkably simple and monotonous, vertically and laterally persistent, and facies associations change gradationally over hundreds of meters of stratigraphic section. These dominant associations signify long-term transverse drainage and aggradation of the alluvial system. In the distal foreland the alluvial system appear to have been sensitive to relative sea level changes with concomitant significant (10's to 100's of km) lateral shifts in the marginal marine facies tracts, while the proximal, highest-energy part of the system appears to have been less sensitive to relative sea level changes.

low-energy siltstone-dominated shallow marine shelf

Two facies associations contain siltstone. They are divided into siltstone-dominated and siltstone-sandstone associations. These associations are found largely in the Link Formation (Figures 3a, 8) that underlies the Burnside Formation and the distal sections of the Burnside Formation.

description

This association comprises six grayish-green facies. These facies are laminated mudstone, graded siltstone-mudstone couplets, wave-rippled siltstone in mudstone, hummocky or swaley cross-stratified coarse siltstone and very fine-grained sandstone, parallel- to wavy-laminated silt and sand with common silt- and sand-filled gutters, and

massive to parallel-laminated siltstone (Table 1; Figure 6a-c). In sections transitional from the Link Formation into the Burnside Formation these facies are commonly arranged in a vertical succession over a several meters to a few tens of meters in the order in which previously listed.

The laminated mudstone consists of bedding parallel layers <1 mm to a few mm's thick. No grading is apparent in hand lens, but bedding-parallel partings are distinct.

The graded siltstone-mudstone couplets are 1 to about 15 mm thick, though generally <10 mm; siltstone makes up the lower quarter to half of the couplets. Laminae are parallel to bedding. Contacts are sharp and bedding parallel in thinner layers, but can be slightly irregular, on the order of 1 mm, in thicker layers. Locally, especially as the couplet beds grow thicker, starved wave rippled siltstone is present. The starved ripple siltstone can make up 5 to 10% of the facies. Starved wave ripples are formed of coarser siltstone than the couplets themselves and have dimensions of 1 to 5 mm in height and wavelengths of 4 to 8 cm; the coarser siltstone laminae pass over mm's into the finer siltstone and mudstone that encase it. The thicker couplets are continuous on the scale of the outcrop (ten's of meters) with bed thickness changing by up to 25 to 50%.

The thicker bedded graded siltstone-mudstone couplets locally pass vertically into a wave-rippled siltstone in mudstone facies. This facies consists of 10 to 50 mm beds in which siltstone is sharply interlayered with mudstone. The siltstone is coarser than that in the graded couplets. The beds have sharp bases that are bedding-parallel to slightly wavy or erosive. Internally, the siltstones contain bedding-parallel to low-angle wavy laminae. The upper contacts of the siltstone layers have symmetrical wave ripple forms preserved with amplitudes of several mm's and wavelengths of several cm's. These beds are continuous over ten's of meters.

In thicker and coarser beds with grain size ranging up to very-fine sand, beds appear to be amalgamated. Beds are 15 to 30 cm thick with sharp, planar to slightly erosional bases and tops that are either planar where truncated by overlying beds of similar character or undulatory where overlain by finer siltstone or mudstone. Internally, these beds exhibit low-angle curved laminasets 5 to 20 mm thick (laminasets in the sense of (Campbell, 1966)). The curved, low-angle laminasets have wavelengths of 1 to 1.5 m and probably represent hummocky and swaley cross-stratification.

Another distinct siltstone facies contains parallel- to wavy-laminated coarse silt and very-fine sand with common silt- and sand-filled gutters (Figures 6c, 7). The wavy laminae are very common. Bed are much thinner (5-20 mm) than in the hummocky facies; bed-to-bed thickness varies greatly. Bottoms of beds are parallel to bedding; tops may be parallel to bedding or wavy, preserving ripple forms. Gutters are uniformly aligned ($111° \pm 13°$, n=12),

although locally their traces may be sinuous in plan view, meandering 10 to 20 cm laterally over wavelengths of 50 to 100 cm. They extend beyond the limit of bedding plane exposures (meters). Gutters vary in depth; they are generally 1 to 5 cm deep but a scour 30 cm deep was observed. This deeper scour contains siltstone with laminae that were traceable into the siltstone lateral to the scour; the laminae diverged and thickened into the scour. Material within gutters is generally unstratified; locally gutters contain clay chips mixed with silt and sand. Locally thin (1 to 2 cm) beds or laminae one to a few grains thick of the very-fine- to medium-grained sand can be traced laterally into gutters filled with material of the same caliber.

A final less common siltstone facies comprises massive to parallel-laminated coarse siltstone cm's to a few ten's of cm thick. There appears to be no grading in the beds. Most laminae, where distinct, appear to be bedding parallel, though locally, faint wavy laminae are seen.

Interpretation

The laminated mudstone facies is interpreted as the product of suspension fallout below wave base. Graded siltstone-mudstone couplets suggest rhythmic alternations of weak density flows; the thinner couplets lacking cross-lamination suggest deposition below storm wave base whereas the appearance of starved ripples suggest stronger flows imprinted by storm waves. The starved ripples further suggest that the conditions could form ripples but were limited by sediment supply. Wave rippled siltstone sharply interbedded with mudstone suggest deposition in alternating wave-influenced and quiet water conditions. The textures and sedimentary structures suggest conditions ranging from suspension fall-out and possibly weak density flows below storm wave-base (laminated mudstone, graded couplets) through storm-wave influenced structures of progressively higher energy and sediment supply (wave rippled siltstone, hummocky/swaley beds, gutter cast siltstones; Figure 6a-b).

Considered together, these siltstone facies suggest deposition on a storm-influenced muddy shelf. This succession is seen particularly well in one section just below the lower contact of the Burnside Formation (section 3, Figures 2, 7). In this section, interbedded wave-rippled siltstone and hummocky/swaley beds are overlain by thinner-bedded siltstone with gutters. We believe that the gutter cast facies represents a shallower water depth due to the predominance of wave formed structures in the siltstones that encase gutter layers. The transition from hummocky/swaley cross-stratified facies to gutter facies seen in the Burnside Formation does not match the succession of Dott and Bourgeois (1982) of storm-dominated progradational shelves where swaley facies are the shallowest facies with the thickest beds. In our study, the predominance of gutters isolated in wavy laminated siltstone and their

association with thin discontinuous siltstone or sandstone beds and deeper silt-sand filled scours (Figure 6c) suggest that storm conditions promoted erosion and bypassing in the shallowest water depths rather than deposition of amalgamated hummocky or swaley beds. Myrow (1987) and Myrow et al. (1988) describe a similar succession from the late Precambrian-early Cambrian of Newfoundland that they suggest may be more representative of fine-grained storm-influenced shelves.

Thick (cm to dm) massive to laminated beds of siltstone are interpreted as prodelta deposits of density currents under conditions of high sediment supply (Elliot, 1986a). This facies commonly passes up into the delta front siltstone association.

The fine grain size of facies in this association are consistent with a relatively high supply rate of material into the basin, both as suspended and as tractional load. These facies in this association grade vertically into transitional alluvial facies of the Burnside Formation proper.

mixed siltstone-sandstone marine shelf and sandstone-dominated sand bars

description

This association that is present in the Link Formation and in distal sections of the Burnside Formation, comprises two facies with coarser sandstone (Figures 3a&b, 4). The two facies are a mixed sandstone-siltstone facies and a sandstone-dominated facies; the two facies commonly grade vertically into one another over a few meters to ten's of meters.

In the mixed facies, fine- to medium-grained sandstones are sharply interbedded with mudstone-siltstone (Figure 9a&b). Sandstones commonly decrease in bed thickness with decreasing percentage of interbedded sandstone. Concomitant with decreasing bed thickness is a gradational change from high-amplitude (several cm) wave ripples to low-angle cross-laminae (Figure 9 b). Isolated thicker (10 to 20 cm) sandstone beds tend to exhibit massive bedding, parallel laminae, and locally low angle (hummocky?) cross-stratification at the base and wave reworked tops. No subaerial exposure features are seen, such as micritic carbonate replacement cement. Interbedded siltstones contain lower amplitude (<1 cm) wave ripples and parallel laminae; mudstones drape wave ripples or are parallel laminated. This mixed facies is present locally within siltstone-dominated association described above that contains abundant wave ripples.

The sandstone-dominated facies contains white, tabular-bedded, trough cross-bedded, medium grained sandstones that locally contain rounded grains of chlorite interpreted to have replaced primary glauconite. Trough cross beds are 20 to 50 cm thick.

Beds are commonly amalgamated and minor scouring is present between beds. Sandstones are present in packages several meters thick commonly marked by the presence of carbonate (micrite) cement that increases in abundance upwards. Sandstone bed thickness, grain size, and scale of cross-stratification all increase upwards on the scale of several meters. Coarse-grained sandstone is common in the uppermost bed or two in these coarsening-upwards sequences. The upper surfaces of these coarse sandstone beds locally appear to be scalloped with a few centimeters of erosional relief; very-coarse sand to granule size grains locally lie along this surface. Even in sequences that fine upwards over a few ten's of meters, smaller-scale coarsening-upwards sequences several meters thick are superimposed.

Interpretation

The mixed facies is interpreted as storm- and wave-dominated shelf sediments deposited near fairweather wave base. The lack of extensive wave-produced features suggests relatively minor wave influence between storm events. Low-angle cross-bedding in isolated fine- to medium-grained sandstones have been described by Nottvedt and Kreisa (1987) which they interpret as forming under combined-flow storm conditions like those forming hummocky cross-stratification in silt and very fine sand.

Such a progression suggests shallowing-upward marine sand bars units (de Raaf et al., 1977; Johnson, 1977) that may have been subaerially exposed and micrite-cemented in the vadose zone. Although, no compound cross-bedding, reactivation surfaces, tidal bundles, herringbone cross-bedding or bipolar paleocurrent trends were observed, tidal influence cannot be ruled out (Johnson and Beaumont, 1990). Similar facies are observed in other units in the lower Bear Creek Group (Grotzinger et al., 1987; Grotzinger et al., 1988).

Paradoxically, the medium-grained sandstone in this association is coarser than the very fine to fine-grained sandstone in transitional alluvial facies described below. This suggests that sand in this marine shelf association derive from another source. Grotzinger et al. (1989) suggest that the source of medium- to coarse-grained shallow marine and deltaic sandstone in the lower Bear Creek Group must have been derived from an exposed upland to the northeast, along strike of the Gordon Bay Arch (Figure 15a)

siltstone and sandstone with soft sediment deformation (delta front)

description

This association comprises several predominantly sandstone facies (Table 1, Figures 6d-e, 7). This association is marked by the first occurrence of red mudstone-siltstone beds

interbedded with wave rippled very fine-grained sandstone. Upward, siltstone beds (1-5 cm) appear with single-grain, planar to wavy-parallel laminae composed of fine to medium sand at the base of beds. The occurrence of this association is restricted to the lower few meters of the Transitional member of the Burnside Formation (Figure 7). There is an upward increase in bed thickness and grain size. Current, wave, and interference ripples are common. Locally, hummocky cross-stratified sandstone beds are interbedded. The most distinctive feature of this association, other than the red color, is the presence of common soft sediment deformation structures, such as flame, load, and ball-and-pillow structures, convolute laminae, and slumped beds (Figure 6d-e). Irregular, disconnected, three-armed cracks locally are present that may be syneresis cracks. Mud chips or curls are absent in beds overlying the disrupted beds.

Interpretation

The abundance of wave-formed structures, such as wave and interference ripples, the presence of possible syneresis cracks, and the lack of desiccation cracks or mud chips suggest deposition in a shallow subaqueous environment that was not subaerially exposed. Soft-sediment deformation and red color support high rate of terrestrial input causing slope over-steepening and promoting slumping. This association is most consistent with the platform of a prograding fluvial-dominated delta (Coleman et al., 1983; Elliot, 1986a; Martinsen, 1989). This interpretation is supported by vertical stratigraphic trends that place this association between prodelta shelf environment and delta platform-delta plain associations (Figure 7).

tabular-bedded, planar-laminated sandstone (braid delta platform)

description

This association consists of planar-laminated sandstone that is moderately- to well-sorted, very fine- to fine-grained, pink, and subarkosic. Beds are 10-60 cm, tabular, and laterally persistent over 10's to 100's of meters with abrupt, mostly planar, bases (Figure 9d). Locally, scours < 5 cm deep are present at the base of beds and within beds; layers or lenses of green mud clasts up to 5 cm thick commonly overlie scours. Scour depth increases with grain size of the sandstone. Internally, beds are mostly planar-laminated; several cm of current- and wave-rippled silty sandstone with mudstone and siltstone laminae cap most beds. Minor fining-upward is present in the upper few cm's of beds. Locally, isolated broad scours up to 10 m wide and 1 m deep contain fine- to medium-grained, trough cross-bedded sandstone (Figure 7). The scours and trough cross-bedded sandstone are enclosed entirely within the

planar laminated sandstone.

interpretation

The planar laminated sandstone association is similar to distributary mouth shoals and swash bars of a braid delta platform described by Vos (1981). This interpretation is on the basis of the lateral persistence of beds, textural maturity, fine grain size, and the common occurrence of planar laminae and ripples on bed tops. Individual beds are interpreted as the product of single flood events that supplied sand from braid delta distributary channels that were subsequently reworked by storm and wave action. The trough cross-bedded sandstone in broad scours are interpreted as braid delta distributary channels that cut across the delta platform during distributary channel avulsion and strong storm-induced flood events. It should be noted, however, that the channels are relatively shallow, suggesting that the deltaic system was not particularly high energy.

In coarsening-upward packages, especially in the Transitional member in the sections 2 and 3 (Figure 7, 8, 10), this association grades from underlying delta front and it is overlain by delta plain deposits. It tends to be overlain gradationally by delta plain association in the proximal end of the basin (Figure 7), whereas to the northwest (Figure 8) it is sharply overlain by medial to upper braid plain facies.

small-scale trough cross-bedded sandstone (braid delta plain)

description

This association comprises trough cross-bedded fine- to medium-grained sandstone with common clay chips (Figure 6f; 7: inset boxes at 80 m, 90 m, and 93 m). The presence of clay chips indicates scouring of mud-covered overbank areas or intertidal flats cannibalized during fluvial channel avulsion. Mudstone with associated sand-filled desiccation cracks has been observed in this facies, but is extremely uncommon (Figure 7: see inset box at 114 m).

interpretation

This is distinguished from trough cross-bedded sandstone in the delta platform association by the lateral persistence of beds; delta platform trough beds are restricted to channels cut into planar-laminated sandstone (Figure 7: compare inset box at 81 m with 111-117 m). The main distinction between the delta plain and the distal braid plain (described below) is that the delta plain association contains clay chips and is the stratigraphically set within asymmetric coarsening-upward packages (delta platform-delta

plain-distal braid plain), interpreted as deltaic units. These packages are present in the Transitional member of the Burnside Formation in the proximal (southeast) part of Kilohigok Basin (Figures 7, 8, 10). They are not recognized as a transitional associations in the distal part of the foreland.

single-storeyed trough cross-bedded sandstone (distal braid plain)

description

The single-storeyed trough cross-bedded sandstone association comprises the bulk of the Burnside Formation, especially to the west of Bathurst Inlet. This lithofacies consists of 50-120 cm beds of fine- to coarse-grained, pink sandstone with medium- and large-scale trough cross-bedding (10-30 cm and 30-80 cm, respectively) that decreases in scale upwards within beds. Lower contacts are undulatory 5-50 cm scours and are uncommonly overlain by a layer of mud clasts or gravel. Gravel along foresets is rare. Planar-laminated or ripple cross-laminated, very fine to fine grained sand may cap the upper 5-20 cm of beds, but beds are commonly scoured by overlying beds. Paleocurrents in this facies are commonly unimodal with low dispersion within and between beds. In the upper part of the section 3, troughs are commonly lined with heavy mineral laminae (Figure 9e).

interpretation

The upward decrease in grain size, the scale of trough cross-bedding, and unimodal low-dispersion paleocurrent directions suggest that this association represents vertical infilling of broad, shallow channels by migrating sinuous-crested subaqueous dunes in a sandy delta plain to lower braid plain environment subject to rapid channel switching and cannibalization (Campbell, 1976; Eriksson and Vos, 1979; Vos and Tankard, 1981; Walker and Cant, 1984). Near sections 2 and 3, the transition from the Gravelly Sandstone to Orange Sandstone member (Figures 4, 10) is characterized by upward-decreasing scale of cross-bedding, the appearance of common mud chip on scours, trough cross-beds with overturned foresets, and local massive sandstone scour fills. These features resemble ones found in the Proterozoic Skadduvarri Formation (Bergh and Torske, 1986) interpreted as resedimented braid delta distributary mouth deposits in a waning, transgressive setting.

multi-storeyed trough-cross-bedded sandstone (medial braid plain ± minor gravel)

The following two associations, both interpreted as medial braid plain environment, are distinguished from the distal braid plain facies by lateral continuity of cross-sets (Table

1). Stratigraphically, the multi-storeyed trough-cross-bedded sandstone association is present in the lower part of the Burnside Formation in the Buff Sandstone member; the gravel-bearing trough- and tangentially-cross-bedded sandstone is present in the Gravelly Sandstone member (Figures 3b, 4, 10).

description

This association comprises trough cross-bedded sandstone in bedsets 8 to 20 m thick. This association is restricted to the Buff Sandstone member (Figures 3, 8, 10) that pinches out southeast of the Gordon Bay Arch crest (Figures 8, 10). It is distinguished by a monotonous repetition of large-scale trough cross-bedding, with 5-10 cross-sets per bed. The association is composed of medium- to coarse-grained sandstone in beds 120-300 cm thick, bounded by low-relief surfaces, especially at the base of bedsets. Bedsets are composed of 5-10 beds. Within the Buff Sandstone member, minor quartz pebble layers and lenses a few cm thick line the base of beds; these are more common upward. Incompletely filled channel scours 1-3 m deep and 5-15 m wide are commonly seen in the lower half of bedsets (Figure 9f). Minor medium-scale trough cross-bedded, planar-laminated, and ripple cross-laminated sand appear only in the upper meter or two of a bedset. Individual beds are traceable over hundreds of meters laterally. Master bedset-bounding surfaces can be followed on aerial photographs for many kilometers between sections 2 and 3. Bedding surfaces could not be traced into larger-scale channel forms or proven to pinch out against master surfaces, but the presence of very large scale channels or lateral accretion surfaces cannot be rejected. Paleocurrents are unimodal low-dispersion toward the west-northwest (294° ± 27°, n=115).

interpretation

The repetition of trough cross-bedding, lateral persistence of master bedding surfaces, and the incomplete fining-upwards packages resemble the Westwater Canyon member of the Morrison Formation, a Jurassic braided alluvial sheet sandstone (Campbell, 1976). Large-scale (km) channel margins cannot be identified in the case of the Burnside Formation. This may be due the fact that outcrops between sections 2 and 3 are oriented nearly along the predominant transport direction in the Buff Sandstone member, whereas channels are best seen in sections perpendicular to transport. Very high width-to-depth ratios (100 to >1000) are expected in bedload-dominated, braided fluvial systems (Friend, 1983; Miall, 1988). This association is interpreted as the product of high-energy, laterally migrating, fluvial channels systems that were several meters to tens of meters deep. Incompletely filled nested channel scours suggest that frequent deep erosion occurred at lower topographic levels of the channel system, whereas vertical aggradation by sinuous crested dunes occurred at higher

topographic levels, probably on bars adjacent to major channels.

trough- and large-scale planar-tangential and cross-bedded sandstone (medial braid plain with gravel)

description

This association differs from the previous one in the presence of broad scours or channels 30-120 cm deep and 3-8 m wide that are infilled by planar-tangential cross-beds overlain by smaller scale trough cross-beds (Table 1, Figure 11). The planar tangential cross-bedding is commonly highly oblique (60°-90°) to both channel scours and trough cross-bedding that are unimodal with low dispersion (Figure 11; e.g., in the Gravelly Sandstone member between sections 2 and 3, planar tangential cross-beds: 178° ± 41°, n=9; trough cross-beds: 310° ± 29°, n=123). Sandstones are locally pebbly with gravel decreasing upwards within beds. Beds are 120-500 cm thick with a few cm of relief on beds. Scour infilling is commonly incomplete, leaving residual topography overlain by medium- or large-scale trough cross-bedding or planar laminae. This cross-bedding commonly decreases in scale upward. This facies is gradational with both trough cross-bedded sandstone and conglomeratic associations.

interpretation

The scale of bedding, larger scale of cross-bedding, and divergent paleocurrent patterns within beds suggest a combination of lateral or oblique accretion at lower topographic levels within fluvial channels and vertical accretion at higher levels during flood stage on a sandy braid plain. Planar cross-beds represent lateral infilling of scours off the margin of braid bars (compare with Proterozoic Waterberg Group (Eriksson and Vos, 1979) ; South Saskatchewan River and Battery Point models (Walker and Cant, 1984)).

The development of transverse braid bars in planar-and-trough cross-bedded association, as opposed to the exclusively trough cross-bedding found in the multi-storeyed trough association, suggests that larger size and range of bedload grain size in the planar-and-trough association preserved a more heterogeneous suite of bedforms. Rust (1984) indicates that gravelly planar cross-bedding is more common in ancient braid plain successions, especially under inferred humid conditions, due to deeper and more frequent floods that create greater topography within braided stream channels. The multiple scale and types of cross-bedding in this association suggest downstream migration of larger scale mesoforms within a large (meters to tens of meters) channel system having multiple active topographic levels (Jackson, 1975; Allen, 1983; Friend, 1983; Miall, 1988). Stratigraphic restriction this

association exclusively to the proximal part of the foreland suggests that this facies was deposited on a higher gradient and, therefore, experienced higher flow velocities than the multi-storeyed trough cross-bedded association that extends onto the craton.

sheet gravel and trough cross-bedded sandstone (gravelly medial braid plain)

description

Two facies comprise this association: clast-supported conglomerate and trough cross-bedded, medium- to coarse-grained and pebbly sandstone (Table 1). Conglomerates range from sheets that line scours a few meters deep and up to 20 meters wide, to beds up to 150 cm composed of clast-supported, crudely planar-stratified sheets (Figure 12a-b). The pebbly sandstone in this association is similar to multi-storeyed trough cross-bedded sandstone, except that the basal large-scale trough cross-sets contain gravelly, medium- to coarse-grained sand along cross-laminae. Beds are commonly 50-500 cm thick. The gravelly cross-beds are overlain by large-scale trough cross-sets lacking gravel that pass upward sharply into medium- (15-30 cm) and small-scale (5-10 cm) trough cross-bedding. The upper part of these fining-upward cycles is commonly truncated and incomplete. The preservation of complete cycles is more common upward, concomitant with decreasing gravel content.

Two closely spaced conglomerate units found at the top of the Gravelly Sandstone member between sections 2 and 3 are unusual in their bedding characteristics and clast composition (Figures 4, 10, 12b-d). These units have highly channeled contacts, are clast supported, and have sharp, planar tops. They are sharply interbedded with multi-storeyed and trough-tangentially cross-bedded sandstone associations. One of the horizons contains a dominant population of intraformational Burnside Formation clasts up to 100 cm (b-axis), much larger than any other conglomerate unit in the Burnside Formation (Figure 12c,d). The other horizon contains a large percentage of felsic volcanic and hypabyssal plutonic clasts. The clast composition of the two horizons are distinct (see Chapter 3), indicating that different source areas supplied them. In addition, the largest intraformational clasts are found at section 3, down inferred paleoslope from section 2 (Figure 2). This is anomalous compared to the well-developed downstream fining trend towards the northwest seen in all other conglomerate horizons (from sections 1 through 3, i.e., down paleo-slope; McCormick and Grotzinger (1988)).

Figure 8. Cross section of the transition from marine shelf to alluvial-dominated facies in the Bear Creek Group. The cross section from 3 to 12 lies approximately parallel to the dominant paleocurrent trend; sections 12 to 14 lie roughly perpendicular to the main alluvial

Interpretation

Basal scouring, lining of scours with gravel, clast support of conglomerates, planar stratification, occurrence with trough cross-bedded sandstone, and fining upward within beds indicate that this association was deposited on the base of deeply scoured channels in braided streams. Unstratified sandy, matrix-supported conglomerates or radial paleocurrents are not observed in this association, so these deposits do not represent debris flows on alluvial fans. These characteristics indicate that even this highest-energy facies of the Burnside Formation was deposited by stream flow on a braid plain still a significant distance from the orogenic source area. By comparison with published braided stream profiles (McPherson et al., 1987), the distance to the source area was probably more than 100 km from the most proximal outcrops in the southeast part of the basin (Figures 1, 2).

The intraformational conglomerate (Figure 12c,d) differs from the vast majority of conglomerates found in the Burnside Formation. The large clast size of the intraformational clasts, anomalous clast size fining and thickness trends, the abrupt contact with other facies, and highly channeled contacts suggest that the large intraformational conglomerate was probably derived from proximal uplift. The appearance of intraformational clasts high in the alluvial stratigraphic section supports an interpretation of a foreland basin setting because previously deposited syn-orogenic strata are commonly incorporated into the forward-propagating thrust-fold belt and are subject to re-erosion (Bally et al., 1966).

Burnside Dolomite

In the central and western part of the basin, a distinctive, areally restricted tongue of carbonate, the Burnside Dolomite, is sandwiched in the sandy siliciclastic Burnside wedge (Figures 4, 13-15). The Burnside Dolomite forms an eastward-tapering prism of cyclic peritidal dolomite and clastic dolomite mixed with siliciclastic detritus (Figure 9c). This stratigraphic geometry is the opposite of siliciclastic facies of the Burnside Formation. In Kilohigok Basin, the Burnside Dolomite interval is recognized from section 14 to as far east as sections 11 and 15, but a confident correlation cannot be made to the proximal end of the basin.

description

The Burnside Dolomite interval is 21 m thick at section 12. There it consists of cycles a few 10's of cm thick with basal intraclast lags of ripped-up dolarenite clasts overlain by wave-rippled dolosiltite grading up to dolarenite with common siliciclastic silt, sand, and rare granules. Cycles are capped by laminated dolomitic siltstone that may be brecciated. The

abundance of wave ripples, clastic-textured dolomite, upward-coarsening cycles, and evidence of brecciation suggest that this unit represents a subtidal to intertidal facies. The Burnside Dolomite unit at section 12 resembles the shallowing-upwards lagoonal facies of the Rocknest Formation (Grotzinger, 1986). Hoffman et al. (1984) and Grotzinger (1985) have correlated the Burnside Dolomite unit with an interval of the Rocknest Formation carbonate platform in Wopmay Orogen to the west.

At section 13, the Burnside section is incompletely preserved, but on the basis of comparison to section 12, the thick (ca. 85 m) dolomitic interval at correlates with the Burnside Dolomite member, as suggested by Hoffman et al. (1984) and Grotzinger (1985) (Figures 13, 14). The lower silty siliciclastic portion of this interval (ca. 25 m) contains tabular pink sandstone beds of the braid delta platform association. The upper carbonate portion of this interval (ca. 60 m) is characterized by cyclic alternation of laminated siliciclastic siltstone or mudstone passing up to clastic-textured dolomite with wave- and current-ripples, minor syneresis cracks, and abrupt upper contacts. Several cycles are capped by microbial laminites and domal stromatolites that increase in abundance upward.

The main difference between sections 12 and 13 is that from east to west the unit thickens, the grain size of siliciclastic material mixed with the carbonate decreases, microbial laminite units appear, and more deeper water sedimentary structures are present.

A thinner (13 m) dolomitic interval is present at section 16 at a similar stratigraphic level and they are believed to be correlative. This interval at section 16 is characterized by thin interbeds of quartz sand of the braid delta platform lithofacies and laminated dolomite interbeds that have been tectonically flattened and sheared sufficiently to obscure most sedimentary structures.

Interpretation

The Burnside Dolomite represents the most extensive and significant transgression of alluvial system (Hoffman et al., 1984; Grotzinger, 1985; McCormick and Grotzinger, 1988). Hoffman et al. (1984) interpreted the Burnside Dolomite as the probable correlative of the Rocknest Formation, a well-developed carbonate platform in Wopmay Orogen (Figure 2). Grotzinger (1985) and McCormick and Grotzinger (1988) have argued that the Burnside Dolomite correlates with an interval within the Rocknest Formation representing incipient drowning of the carbonate platform that caused back-stepping of all facies belts more than 100 km eastward toward the craton and into Kilohigok Basin. Grotzinger (1986) attributed this incipient drowning to a eustatic rise in sea level. Near section 11, coincident with the crest of the Gordon Bay flexural arch, the Burnside Dolomite is a thin (3 m) interval of cross-bedded intraclastic carbonate interpreted to be deposited in shallow water (Grotzinger

et al., 1987). Superimposed on the carbonate are diagenetic fabrics suggesting early peritidal marine cementation followed by subaerial exposure and vadose diagenesis. To the west, the Burnside Dolomite is characterized by an entirely subaqueous storm wave marine facies with no superimposed subaerial diagenetic fabrics.

The correlation between the Rocknest Formation and the Burnside Dolomite suggests that the development of the Rocknest lagoonal shelf impacted Burnside braid delta sedimentation. The Rocknest shelf comprised an outer reefal rim that buffered open marine waves (Grotzinger, 1986). The eastward increase in the caliber of siliciclastic detritus in Rocknest carbonate cycles and the lateral restriction of the Rocknest Formation (ca. 150 km) as compared to Phanerozoic passive margins (>250 km) led Hoffman et al. (1984) to conclude that the Rocknest platform was correlative with the Burnside alluvial system. Thus the Rocknest lagoon was the sink for fine-grained Burnside detritus. It is interesting to note the difference between facies transitions in two transgressive intervals at section 13 (Figure 13). The lower one probably correlates with the open marine siliciclastic shelf unit underlying the Rocknest platform (Odjick Formation). This lower package is characterized by upward transition into wave- and storm-dominated association. The upper package, culminating in the Burnside Dolomite unit gradually fines up through the delta front association. There are two possible explanations for the difference in the shallow marine facies. One explanation is that the rate of fluvially supplied sediment was higher below the Burnside Dolomite, due either to a lower rate of relative sea level rise or higher absolute fluvial sediment supply rates. A lower rate of sea level rise is discounted because the Burnside Dolomite was deposited over half of the Slave craton. The second possibility is that the Rocknest lagoon damped the storm energy so that in the transgressive interval the braid delta complex was less restricted by the impingement of storm waves.

The presence of the Burnside Dolomite in the three most distal sections (sections 12, 13, 14) provides a crude marker of the limit of marine transgression during and indicates that the paleoshoreline trended roughly north-northeast, nearly perpendicular to fluvial paleocurrent trends.

regional relationships between lithofacies

The most important observation is that the highest energy alluvial lithofacies, interpreted to represent medial braid plain environments, are largely restricted to the proximal, southeastern part of the basin (Figures 4, 8, 10, 15). The informal members of the Burnside Formation, which are easily subdivided in the between sections 1, 2, and 3, and mapped for ten's of kilometers, all pinch out or are cut out laterally to the northwest across

the Bathurst Fault zone and over the Gordon Bay Arch.

The Transitional member appears to be cut out over the Gordon Bay arch, but a distal equivalent reappears to the northwest that thickens in the vicinity of section 12 (Figures 3b, 4, 8). At section 12 the contact between underlying shelf siltstones and deltaic and braid plain facies appears to be gradational. The unconformable, erosional lower contact reappears to the west, until at sections 13 and 14 the Burnside Formation completely cuts through two underlying depositional sequences (Link and Beechey Formations; Figures 3b, 4).

The mixed sandstone-siltstone associations are present at two stratigraphic positions. The first position is at the base of the Link Formation, on top of a depositional sequence boundary (Grotzinger et al. 1988), near the crest of the Gordon Bay Arch (Figures 2, 8). This facies tends to pass upward into the mixed sandstone-siltstone facies.

The second stratigraphic position where these sandstones are present is within the Link Formation at the top of asymmetric, coarsening-upward, siltstone-to-sandstone packages several meters thick. These packages locally are capped by micrite-cemented surfaces. The local presence of glauconite, high textural and mineralogical maturity, uniformity of cross-bedding thickness, and occurrence with green siltstone facies suggest that these sandstones are products of shallow marine bars, like those described by Johnson (1977) and de Raaf et al. (1977).

Discussion

marine-alluvial transition

Two distinct facies motifs mark the marine to alluvial transition in the Burnside Formation, one during progradation and one during retrogradation. The progradational case is best illustrated in the at section 3 (Figures 2, 7), and the retrogradational case is exhibited well at section 13 (Figures 2, 13, 14). One characteristic of both of these cases is that beach deposits are not recognized. This may be explained by the dominance of the fluvial system where distributary channels tend to cut through and cannibalize topographically high beaches adjacent to channels, by the relatively minor influence of fairweather waves and tides demonstrated in this setting, and by the tendency for shoreface processes to erode beach facies (Elliot, 1986a; Elliot, 1986b; Johnson and Baldwin, 1986). Progradational systems, especially sandy alluvially dominated ones, rarely preserve intertidal facies, whereas retrogradational systems tend to preserve beach facies only in highly aggradational, wave- or tide-dominated settings (Johnson and Baldwin, 1986). All of these factors favoring erosion of

beach facies are likely to be enhanced in the case of the Burnside Formation by lower relative subsidence rates that existed on the craton, especially over the Gordon Bay Arch and near section 14.

progradational case

At section 3, the progradational interval is present at the base of the Burnside Formation (Figure 7). A common progression of facies defines the transition from storm-influenced shelf to braided stream environments in the proximal foreland: the order of associations is siltstone-dominated shelf to delta front to delta platform and delta plain to distal braid plain then sharply overlain by multi-storeyed medial braid plain.

Initial fluvial influence is probably recorded in gutter facies and thick massive siltstones. The strong correspondence between gutter orientations and trough cross-bedding in overlying braid delta facies at this location suggest that gutters may have been formed by erosive storm-surge ebb currents that were strengthened by alluvial flood discharge from the prograding braid delta (compare with Swift et al. (1987)). Initial deltaic influence is most evident in delta front siltstones and sandstones with current-formed structures and abundant soft-sediment deformation. Three distinctive asymmetric, coarsening-upward, delta front-to-delta plain packages are present in the Transitional member between section 1 and 3 and are arranged as alternations between delta platform and delta plain facies (Figure 10). There are relatively gradual transitions between delta platform and delta plain facies whereas they are sharp between delta plain and delta platform facies .

Coarsening-upward packages are common in alluvially dominated delta systems (Elliot, 1986a). Sequence stratigraphic models for deltaic environments portray the coarsening-upwards trends and the abrupt shift from delta plain to subaqueous delta front environment as common elements of the stacking patterns of parasequences (Van Wagoner et al., 1988; Van Wagoner et al., 1990). The cause for abrupt shift from delta plain to subaqueous delta platform environment is uncertain. The cause could be delta distributary lobe switching (an process intrinsic to deltaic sedimentary processes) (Elliot, 1986a), eustatic rise in sea level (an extrinsic cause) (Haq et al., 1987; Van Wagoner et al., 1988), or thrust loading in the hinterland (an extrinsic cause) (Jordan et al., 1988; Jordan and Flemings, 1990). An eustatic control is suspected due to the thickness of the parasequences (50-150 m), their facies similarity, the similarity of paleocurrent trends in each coarsening upwards sequence, their wide stratigraphic extent from the Bear Creek Hills to the edge of the craton (> 50 km across depositional strike; Figures 2, 10), and because eustatic controls have been suggested for depositional sequences of the lower Bear Creek Group that extend far beyond

the zones of tectonic influence (Grotzinger et al., 1988; Grotzinger et al., 1989).

In contrast to the well-developed deltaic units described above, the distal foreland west of section 8 (Figure 2, 8, 13) is characterized by a comparatively abrupt transition from marine shelf associations to medial braid plain associations. This is consistent with the interpretation that an erosional unconformity exists at the base of the Buff Sandstone member (multi-storeyed trough cross-bedded sandstone) and probably within the Conglomerate member. Gravel-bearing facies sit directly on Link Formation marine shelf facies over the crest of the Gordon Bay Arch (Figure 8). Beyond the arch, prograding deltaic facies motifs similar to those seen in the Transitional member near sections 2 and 3 are absent. This supports the inference that initially the deltaic system was restricted to the proximal part of the basin, but that starting at the time of Buff Sandstone member deposition, alluvial facies prograded towards the craton over areas of lower relative subsidence, like the Gordon Bay Arch. The net result is a relatively abrupt shift from shallow marine to alluvial facies, with poorly developed transitional facies.

Paleocurrent data (Figure 5) supports the contention that alluvial facies on the craton are at least as young as the Buff Sandstone member found in the proximal part of the basin (Figures 8, 10). In the southeast, paleocurrents in deltaic associations are southwest directed, whereas distal braid plain facies in the distal foreland are northwest directed. Therefore the initial alluvial facies on the craton must be no older than the Buff Sandstone member, the first facies to exhibit northwest paleocurrents (Figures 10, 13, 15). Gravel found in the basal parts of the Burnside Formation in the distal foreland must be no older than the Conglomerate member at sections 2 and 3 (Figures 10, 13-15). Subsidence rates have exerted a major influenced the location and style of alluvial facies (Alexander and Leeder, 1987).

retrogradational case

In the distal foreland several distinct coarsening- and fining-upward intervals are present representing the lateral migration of the paleo-shoreline between sections 12 and 13 (Figures 2, 13). Two types of alluvial-to-marine transitions are present. One represents the relatively abrupt shutting-off of the fluvial system and onset of storm-influenced sedimentation on a muddy shelf. The other represents a gradual transgression with wave reworking of fluvially supplied sand creating a sandy shelf. Both of these cases are well illustrated at section 13 (Figure 14).

In the first case (Figures 9 a-b, Figure 14: 210-320 m), the occurrence of white, texturally mature, medium-grained sandstones suggest that they are a product of background wave and storm processes when fluvial input was reduced. The coarse caliber and maturity of

the sandstones require winnowing of Burnside fluvial sands, probably from shoreface erosion of fluvial bars and spits (Elliot, 1986b; Johnson and Baldwin, 1986).

In the second case (Figure 14: 400-750 m), there is a gradational change from trough cross-bedded delta plain sandstone to planar-laminated delta platform sandstone, indicating that fluvial input to the shelf was continuous. Even when mud interbeds become common just below the Burnside Dolomite, pink tabular planar-laminated sandstone beds persist. This suggests that either the rate of relative sea level rise was lower than in the former case, or that the rate of sediment input from the Burnside alluvial system was much higher than before. The interpretation of higher sediment supply rate, and, therefore, alluvial dominance, is favored for the upper interval, because marine facies of the Burnside Dolomite extend much farther to the east (toward the hinterland) than the marine facies found at the base of the section and therefore represents a much more extensive transgression of the alluvial system. Marine facies at the base of the section are restricted to the area between sections 12 and 13 (Figures 2, 4), whereas marine facies of the Burnside Dolomite extend southeast of section 11 (Figures 2, 4, 8).

A comparison of these two intervals, section 12 versus section 13 (Figures 13, 14) suggests that in the Burnside Formation the imprint of relative sea level changes on sedimentary facies can only be demonstrated where marginal marine sedimentary facies are present. The lower half of the section 13 (Figure 14) contains several vertical intervals that can be interpreted as shifting of the paleo-shoreline across that area. The lower two-thirds of the section at section 12 (Figure 13) shows a general coarsening-upward then fining-upward trend. No marine facies are evident there, and lower braid plain conditions predominate. The effect of sediment supply appears to overwhelm that of any base-level control in the braid-plain. It is likely that the distal braid plain facies represents a large range of paleoslopes on the alluvial profile. If this is the case, then shifts in the position of the shoreline might not induce a change in alluvial facies in the subareal depositional system. Consequently, relative sea level changes may not be detectable by facies changes within the braid plain (compare Nummendal et al. (1987) and Swift et al. (1987) with Posamentier et al. (1988)). Rather, the only manifestation of such a shift and readjustment towards some characteristic alluvial profile may be subtle erosion surfaces detectable only in extensive outcrop. Given the simplicity and intergradation of braid plain associations in the Burnside Formation and discontinuous outcrop in the distal sections, it is not possible to demonstrate the existence of such erosional surfaces.

Burnside Formation braided alluvial system

The vertical and lateral persistence of facies and the tight clustering of paleocurrent trends (Figures 4, 5) indicate that the Burnside Formation represents a large alluvial apron with a uniform west-northwest to northwest paleoslope draining perpendicular out of the orogenic hinterland. The uniformity of paleoslope distinguishes the Burnside alluvial system from previously described braided alluvial systems. The present outcrop of the Burnside Formation across depositional strike exceeds 250 km; its original extent from the Thelon Orogen was at least 300 km. It is important to recognize that this configuration persisted for ten's of millions of years, resulting in up to 2.7 km of alluvial aggradation over the center of Slave Craton, well beyond the limit of flexurally driven subsidence. The simplicity of facies in the alluvial plain, the lack of any interbedded mud or silt, and the lack of any evidence of aeolian facies suggest steady high discharge conditions, perhaps due to humid climate and perennial flow or highly seasonal, high discharge monsoon conditions.

Such a sandy humid alluvial setting has no direct modern analog because post-Devonian sandy humid alluvial systems are commonly muddy and meandering. Land plants exert a fundamental control on Phanerozoic alluvial patterns by stabilizing channels and promoting preservation of muddy overbank areas (Cotter, 1978). The lack of fine material can be partially explained if the fine-grained component of sediment eroded from the source area was winnowed by aeolian processes in the source area and was transported directly to the marine environment, without passing through the alluvial system. Dalrymple et al. (1985) invoke such a scenario to explain the distribution of Cambrian shales in North America. Even the Kosi alluvial cone in India, which is cited commonly as a modern humid fan system, is dominated by muddy facies with channel systems anastamosing over most of its length (Wells and Dorr, 1987). Modern braided alluvial settings are characterized by climatic extremes, such as semi-arid basins or proglacial outwash plains (Boothroyd and Nummendal, 1978).

A Precambrian alluvial system of comparable vertical scale to the Burnside Formation is the Middle Proterozoic Missoula Group of the Belt basin (Winston, 1978; Winston, 1986), but the Belt differs in that sandy alluvial fan and braided fluvial facies were deposited over a much smaller lateral distance (<150 km). One of the reasons that the Belt alluvial facies are more spatially restricted is that the Belt was deposited in an extensional basin. The extensional faults that bounded the basin would not have created as much relief or drained as large and area as the Thelon mountain belt that formed the hinterland to the Kilohigok foreland basin. In the case of the Thelon mountains, erosional unroofing and isostatic rebound probably provided additional relief and source of sediment.

Another reason for the lateral restriction of the Belt sediments is that the Belt was deposited in a semi-arid climate with flashy, muddy discharge. One implication is that under semi-arid flash flood discharge, flow competence of streams may have decreased markedly by a combination loss of water into desiccated flood plains and unchannelized sheet flow on its alluvial apron. In contrast, the Burnside lithofacies are sand-dominated throughout and the alluvial facies are highly channelized. This is more consistent with humid, perennial flow conditions. The suggestion is that channelized flow and a high water table associated with humid conditions in the orogenic source area would reduce the tendency for flood water to be lost by sieving into underlying braid plain deposits. Consequently, it can be imagined that the channelized discharge could be maintained over a much longer downstream distance than in an arid setting. This may partly explain the great lateral extent of the Burnside Formation alluvial facies in comparison to other alluvial systems.

Alluvial systems of comparable lateral extent to the Burnside Formation are commonly found as relatively thin tabular units 10's to 100's of meters thick. This suggests that low subsidence rates promote extensive progradation of alluvial systems. The remarkable aspect of the Burnside Formation is that 1 to 2 km of alluvial sediments are preserved over the Slave craton. This requires a long-lived, continuously uplifting orogenic source area and a consistent alluvial profile to exhibit the stratigraphic patterns seen in the Burnside Formation. Some of this thickness can be attributed to alluvial aggradation, some to continued convergence and thrusting in the Thelon orogenic belt, and some is due to subsidence induced, in part, sediment loading of the Slave craton by the redistribution of mass from the uplifted Thelon orogenic belt into the Kilohigok Basin.

An alluvial succession of comparable vertical, and possibly lateral extent is the Middle Proterozoic Mbala Formation of Zambia (Andrews-Speed, 1986) and the middle Proterozoic Waterberg Group of South Africa (Eriksson and Vos, 1979). In these sand-dominated cases, however, coarse alluvial sediments are relatively laterally restricted, but alluvial facies resemble more closely those found in the Burnside Formation than the Belt Supergroup. The main similarities are the monotony of alluvial facies, uniform paleocurrents in the direction of downstream fining, and a lack of variability along depositional strike. The authors invoke a similar model of an alluvial apron of uniform paleoslope as the depositional setting, rather than radial alluvial fans.

A few examples of humid pre-Devonian alluvial systems have been inferred, but most are interpreted as alluvial fans (e.g., Precambrian Van Horn Sandstone of West Texas: McGowen (1971); Ordovician Mweelrea Group, Ireland: Pudsey (1984)). These appear to be of comparable vertical extent as the Burnside formation, but lateral facies changes are present over short distances. The major similarity between alluvial facies is that trough cross-

bedding dominates and channelization is low. However debris flow features are well developed in proximal areas and alluvial facies are laterally restricted to a few 10's of km at most from inferred basin margins (McPherson et al., 1987).

The preserved braid plain facies in the Burnside Formation consist of sand only and the braid plain facies extend more than 200 km before entering a marine environment on the west side of the Slave craton. If the climatic conditions on the braid plain were arid or semi-arid and the discharge that carried in these bedload-dominated streams were flashy or intermittent, one might expect that the water table over the braid plain would be relatively deep and that the stream-borne water would be lost by sieving into the sandy braid plain. If, however, discharge were either continuous or had large peaks of seasonal discharge that are characteristic of monsoon conditions, then one would predict a higher water table and a lower tendency for discharge to be lost by sieving into the alluvial plain. A high water table and a high rate of discharge in stream channels can be caused by high rates of precipitation in the source area alone, regardless of climate over the alluvial plain. Climatic conditions could be arid or humid over the alluvial plain, although humid conditions on the alluvial plain would be more conducive to long-distance flow.

Very little direct evidence can be offered for monsoon conditions in the case of the Burnside alluvial system. The present day monsoon of southern Asia is primarily a product of the latitudinal alignment of large land areas at low latitudes and the climatic effect is amplified by the presence of the Himalayan mountains and the Tibetan Plateau (J.T. Parrish, personal communication, 1992). Paleomagnetic data for Kilohigok Basin and Wopmay Orogen suggest that the Slave craton lay at low latitudes within the tradewind belt and that tradewinds should have flowed up the alluvial paleoslope toward the Thelon Orogen (Evans and Hoye, 1981; McGlynn and Irving, 1981; Hoffman and Grotzinger, in review). Accumulating geochronological evidence suggests that the Laurentia, perhaps Earth's first supercontinent, amalgamated due to the collision of numerous Archean continental nuclei between 2.0 and 1.8 Ga (Hoffman, 1988). This suggests that there may have been a large amount of land at low latitudes at the time that the Burnside Formation was deposited, but the longitudinal or latitudinal arrangement of the continental nuclei is unknown. Monsoon conditions are dominated by such high peaks of seasonal discharge that presumably monsoonal steam systems could create a high water table. In addition, high peak discharge would promote removal of the structures and deposits indicative of the intervening low-flow parts of the season that are commonly found on the topographically highest part of the channel systems that are most prone to erosion. However, soil forming processes should be active during the period between successive monsoons. No evidence for caliche or soils is found in the Burnside Formation. So alluvial deposits of highly seasonal monsoon conditions

might be quite similar to those produced under humid, continuous discharge conditions. We suggest monsoonal conditions as an alternative to humid perennial discharge conditions as a means of creating the observed widely distributed, sandy alluvial deposits.

Conclusions

The Burnside Formation represents an alluvial apron formed in response to long-lived orogenic activity on the margin of the Slave craton. It shares many features with braided stream-braid delta alluvial successions, but is distinguished by the large spatial and temporal scale of alluvial deposition transverse to its orogenic source area. Furthermore, a humid climate probably contributed to both alluvial dominance of depositional environments and the spatial scale of the alluvial system.

Sedimentological and stratigraphic studies of the Burnside Formation document the transition of the Early Proterozoic Kilohigok foreland basin from a southeast-facing marine shelf ramp with longitudinal transport to a northwest-directed alluvial apron that flowed transverse to the initial basin depocenter and across an inferred flexural arch. The abrupt superposition of braid plain associations on shelf and braid delta associations in the foreland suggest that progradation and shift of the paleo-shoreline was rapid and involved erosional truncation over the arch. The Burnside Formation intertongued with the evolving passive margin in Wopmay Orogen on the opposite side of the Slave Province. The contemporaneous development of the passive margin carbonate platform may have attenuated destructive marine processes that initially influenced the prograding braid delta, so that fluvial dominance was even more pronounced. The stratigraphic architecture of the Burnside Formation suggests initially longitudinal deltaic sedimentation occurred in the proximal foreland. The progradation of the Burnside alluvial wedge and deposition of over 2.5 km of alluvial sediments over the Slave craton probably was related to uplift of and mass redistribution from the orogenic hinterland.

References Cited

Alexander, J., and Leeder, M.R., 1987. Active tectonic controls on alluvial architecture, in, F.G. Ethridge, R.M. Flores, and M.D. Harvey (eds.), Recent Developments in Fluvial Sedimentology. Soc. Econ. Paleont. Mineral. (Tulsa, OK), p. 243-252.

Allen, J.R.L., 1983. Studies in fluviatile sedimentation: bars, bar-complexes and sandstone sheets (low sinuosity braided streams) in the Brownstones (L. Devonian), Welsh Borders. Sed. Geol., v. 33, p. 237-293.

Allen, P.A., and Homewood, P., 1986. Foreland Basins. Blackwell Scientific Publications (Oxford, UK), 453 pp.

Andrews-Speed, C.P., 1986. Gold-bearing fluvial and associated tidal marine sediments of Proterozoic age in the Mporokoso Basin, northern Zambia. Sed. Geol., v. 48, p. 193-222.

Bally, A.W., Gordy, P.L., and Stewart, G.A., 1966. Structure, seismic data, and orogenic evolution of southern Canadian Rockies. Bull. Can. Petrol. Geol., v. 14, p. 337-381.

Bergh, S.G., and Torske, T., 1986. The Proterozoic Skadduvarri Sandstone Formation, Alta, northern Norway: a tectonic fan-delta complex. Sed. Geol., v. 47, p. 1-25.

Boothroyd, J.C., and Nummendal, D., 1978. Proglacial braided outwash: a model for humid alluvial fan deposits, in, A.D. Miall (ed.), Fluvial Sedimentology. Canadian Soc. Petrol. Geol., Mem. 5, p. 641-668.

Bowring, S.A., and Grotzinger, J.P., 1992. Implications of new chronostratigraphy for tectonic evolution of Wopmay Orogen, northwest Canadian Shield. American Journal of Science, v. 292, p. 1-20.

Campbell, C.V., 1966. Lamina, laminaset, bed, and bedset. Sedimentology, v. 8, p. 825-828.

Campbell, C.V., 1976. Reservoir geometry of a fluvial sheet sandstone. Am. Assoc. Petrol. Geol. Bull., v. 60, p. 1009-1020.

Christie-Blick, N., Grotzinger, J.P., and von der Borch, C.C., 1988. Sequence stratigraphy in Proterozoic successions. Geology, v. 16, p. 100-104.

Coleman, J.M., Prior, D.B., and Lindsay, J.F., 1983. Deltaic influences on shelfedge instability processes, in, D.J. Stanley, and G.T. Moore (eds.), The Shelfbreak: Critical Interface on Continental Margins. Soc. Econ. Paleontol. Mineralogist, Spec. Pub. 33 (Tulsa, OK), p. 121-137.

Collinson, J.D., 1986. Alluvial sediments, in, H.G. Reading (ed.), Sedimentary Environments and Facies (2nd ed.). Blackwell Scientific Publications (Boston, MA), p. 20-62.

Collinson, J.D., and Lewin, J., 1983. Modern and ancient fluvial systems. Blackwell Scientific Publications (Oxford, UK), 575 pp.

Cotter, E., 1978. The evolution of fluvial style, with special reference to the central Appalachian Paleozoic, in, A.D. Miall (ed.), Fluvial Sedimentology. Canadian Soc. Petrol. Geol., Mem. 5, p. 361-384.

Dalrymple, R.W., Narbonne, G.M., and Smith, L., 1985. Eolian action and the distribution of Cambrian shales in North America. Geology, v. 13, p. 607-610.

de Raaf, J.F.M., Boersma, J.R., and van Gelder, A., 1977. Wave generated structures and sequences from a shallow marine succession, Lower Carboniferous, County Cork,

Ireland. Sedimentology, v. 24, p. 451-483.
Dott, R., Jr., and Bourgeois, J., 1982. Hummocky stratification: significance of its variable bedding sequences. Geol. Soc. America Bull., v. 93, p. 663-680.
Elliot, T., 1986a. Deltas, in, H.G. Reading (ed.), Sedimentary Environments and Facies (2nd ed.). Blackwell Scientific Publications (Boston, MA), p. 113-154.
Elliot, T., 1986b. Siliciclastic shorelines, in, H.G. Reading (ed.), Sedimentary Environments and Facies (2nd ed.). Blackwell Scientific Publications (Boston, MA), p. 155-188.
Eriksson, K.A., and Vos, R.G., 1979. A fluvial fan depositional model for Middle Proterozoic red beds from the Waterberg Group, South Africa. Precambrian Res., v. 9, p. 169-188.
Ethridge, F.G., and Flores, R.M., 1981. Recent and ancient nonmarine depositional environments: models for exploration. (Tulsa, OK), 347 pp.
Ethridge, F.G., Flores, R.M., and Harvey, M.D., 1987. Recent Developments in Fluvial Sedimentology. (Tulsa, OK), 389 pp.
Evans, M.E., and Hoye, G.S., 1981. Paleomagnetic results from the lower Proterozoic rocks of the Great Slave Lake and Bathurst Inlet areas, Northwest Territories, in, F.H.A. Campbell (ed.), Proterozoic Basins of Canada. Geological Survey of Canada, Paper 81-10, p. 191-202.
Friend, P.F., 1983. Toward an field classification of alluvial architecture or sequence, in, J.D. Collinson, and J. Lewin (eds.), Modern and Ancient Fluvial Systems. Blackwell Scientific Publications, Intern. Assoc. Sedimentologists, Spec. Pub. No. 6 (Oxford, UK), p. 345-354.
Gibb, R.A., and Thomas, M.D., 1977. The Thelon front: a cryptic suture in the Canadian Shield. Tectonophys., v. 38, p. 211-222.
Grotzinger, J.P., 1985. Evolution of Early Proterozoic passive-margin carbonate platform, Rocknest Formation, Wopmay Orogen, N.W.T., Canada. Unpublished Ph.D. Thesis, Virginia Polytechnic Institute and State University (Blacksburg, VA).
Grotzinger, J.P., 1986. Cyclicity and paleoenvironmental dynamics, Rocknest platform, northwest Canada. Geol. Soc. America Bull., v. 97, p. 1208-1231.
Grotzinger, J.P., Adams, R.D., McCormick, D.S., and Myrow, P., 1989. Sequence stratigraphy, correlations between Wopmay Orogen and Kilohigok Basin, and further investigations of the Bear Creek Group (Goulburn Supergroup), District of Mackenzie, Current Research, Part C. Geological Survey of Canada, Paper 89-1C, p. 107-120.
Grotzinger, J.P., Gamba, C., Pelechaty, S.M., and McCormick, D.S., 1988. Stratigraphy of a 1.9 Ga foreland basin shelf-to-slope transition: Bear Creek Group, Tinney Hills area of Kilohigok Basin, District of Mackenzie, Current Research, Part C. Geological Survey of Canada, Paper 88 1-C, p. 313-320.
Grotzinger, J.P., and McCormick, D.S., 1988. Flexure of the Early Proterozoic lithosphere and the evolution of the Kilohigok Basin (1.9 Ga), northwest Canadian shield, in, K. Kleinspehn, and C. Paola (eds.), New Perspectives in Basin Analysis. Springer-Verlag (New York), p. 405-430.
Grotzinger, J.P., McCormick, D.S., and Pelechaty, S.M., 1987. Progress report on the stratigraphy, sedimentology, and significance of the Kimerot and Bear Creek groups, Kilohigok Basin, District of Mackenzie, Current Research, Part A. Geological Survey of Canada, Paper 87 1-A, p. 219-238.

Hanmer, S., and Lucas, S.B., 1985. Anatomy of a ductile transcurrent shear: The Great Slave Lake Shear Zone, District of Mackenzie, N.W.T. (preliminary report), Current Research. Geological Survey of Canada Paper 85-1B, p. 7-22.

Haq, B.U., Hardenbol, J., and Vail, P.R., 1987. Chronology of fluctuating sea levels since the Triassic. Science, v. 235, p. 1156-1167.

Harris, C.W., 1987. Progradational sequences in the Early Proterozoic Uncompahgre Group, southwest Colorado: cyclic control on shallow marine sedimentation in a storm- and tide-dominated shelf. Unpublished Ph.D. dissertation (part 1), Virginia Polytechnic Institute and State University (Blacksburg, VA).

Hoffman, P.F., 1987. Continental transform tectonics: Great Slave Lake shear zone (ca. 1.9 Ga), northwest Canada. Geology, v. 15, p. 785-788.

Hoffman, P.F., 1988. United plates of America, the birth of a craton: Early Proterozoic assembly and growth of Laurentia. Ann. Rev. Earth Planet. Sci., v. 16, p. 543-603.

Hoffman, P.F., and Grotzinger, J.P., in review. Tradewind-controlled erosion and orogenic style. Geology.

Hoffman, P.F., Tirrul, R., Grotzinger, J.P., Lucas, S.B., and Eriksson, K.A., 1984. The Externides of Wopmay Orogen, Takijuk Lake and Kikerk Lake map areas, District of Mackenzie, Current Research, Part A. Geological Survey of Canada, Paper 84-1A, p. 383-395.

Jackson, R.G., II, 1975. Hierarchical attributes and a unifying model of bedforms composed of cohesionless material produced by shearing flow. Geol. Soc. America Bull., v. 86, p. 1523-1533.

Johnson, D.D., and Beaumont, C., 1990. Surface processes and foreland basin stratigraphy. Geol. Soc. America, N.E. Section, Abs. with Progs., v. 22, p. A26.

Johnson, H.D., 1977. Shallow-marine bar sequences: an example from the late Precambrian of north Norway. Sedimentology, v. 24, p. 245-270.

Johnson, H.D., and Baldwin, C.T., 1986. Shallow siliciclastic seas, in, H.G. Reading (ed.), Sedimentary Environments and Facies (2nd ed.). Blackwell Scientific Publications (Boston, MA), p. 229-282.

Jordan, T.E., and Flemings, P.B., 1990. From geodynamic models to basin fill - a stratigraphic perspective, in, T.A. Cross (ed.), Quantitative Dynamic Stratigraphy. Prentice-Hall (Englewood Cliffs, NJ), p. 149-164.

Jordan, T.E., Flemings, P.B., and Beer, J.A., 1988. Dating thrust activity by use of foreland basin strata, in, K. Kleinspehn, and C. Paola (eds.), New Perspectives in Basin Analysis. Springer-Verlag (New York), p. 307-330.

Long, D.G.F., 1978. Proterozoic stream deposits: some problems of recognition and interpretation of ancient sandy fluvial systems, in, A.D. Miall (ed.), Fluvial Sedimentology. Canadian Soc. Petrol. Geol., Mem. 5, p. 313-341.

Martinsen, O.J., 1989. Styles of soft-sediment deformation on a Namurian (Carboniferous) delta slope, Western Irish Namurian Basin, Ireland, in, M.K.G. Whateley, and K.T. Pickering (eds.), Deltas: Sites and Traps for Fossil Fuels. Geological Society Spec. Pub. 41, Blackwell Scientific (Oxford, UK), p. 167-177.

McCormick, D.S., and Grotzinger, J.P., 1988. Aspects of the Burnside Formation, Bear Creek Group, Kilohigok Basin, N.W.T., Current Research, Part A. Geological Survey of Canada, Paper 88 1-C, p. 321-339.

McGlynn, J.C., and Irving, E., 1981. Horizontal motions and rotations of the Canadian

Shield during the Early Proterozoic, in, F.H.A. Campbell (ed.), Proterozoic Basins of Canada. Geological Survey of Canada, Paper 81-10, p. 183-190.
McPherson, J.G., Shanmugam, G., and Moiola, R.J., 1987. Fan-deltas and braid deltas: varieties of coarse-grained deltas. Geol. Soc. America Bull., v. 99, p. 331-340.
Miall, A.D., 1978. Fluvial Sedimentology. Canadian Soc. Petrol. Geol., Mem. 5 859 pp.
Miall, A.D., 1988. Facies architecture in clastic sedimentary basins, in, K. Kleinspehn, and C. Paola (eds.), New Perspectives in Basin Analysis. Springer-Verlag (New York), p. 67-81.
Myrow, P.M., 1987. Sedimentology and depositional history of the Chapel Island Formation (Late Precambrian to Early Cambrian), southeast Newfoundland. Ph.D., Memorial University, St. John's, Newfoundland.
Myrow, P.M., Narbonne, G.M., and Hiscott, R.N., 1988. Storm-shelf and tidal deposits of the Chapel Island and Random Formations, Burin Peninsula: facies and trace fossils. Geological Association of Canada, Annual Meeting, Guidebook B6 108 pp.
Nottvedt, A., and Kreisa, R.D., 1987. Model for combined-flow origin of hummocky cross-stratification. Geology, v. 15, p. 357-361.
Nummendal, D., and Swift, D.J.P., 1987. Transgressive stratigraphy at sequence bounding unconformities: some principles derived from Holocene and Cretaceous examples, in, D. Nummendal, O.H. Pilkey, and J.D. Howard (eds.), Sea-Level Fluctuation and Coastal Evolution. Soc. Econ. Paleont. Mineral., Spec. Pub. No. 41, p. 241-260.
Padgham, W.A., 1985. Observations and speculations on supracrustal successions in the Slave Structural Province, in, L.D. Ayers, P.C. Thurston, K.D. Card, and W. Weber (eds.), Evolution of Archean Supracrustal Sequences. Geological Association of Canada, Special Paper 28, p. 133-152.
Posamentier, H.W., and Vail, P.R., 1988. Eustatic controls on clastic deposition II - sequence and systems tract models, in, C.K. Wilgus, B.S. Hastings, C.G.S.C. Kendall, H.W. Posamentier, C.A. Ross, and J.C. Van Wagoner (eds.), Sea-level changes: an integrated approach. Soc. Econ. Paleontologists and Mineralogists, Spec. Pub. No. 42, p. 125-154.
Pudsey, C.J., 1984. Fluvial to marine transition in the Ordovician of Ireland—A humid-region fan-delta? Geol. Jour., v. 19, p. 143-172.
Rust, B.R., 1984. Coarse alluvial deposits, in, R.G. Walker (ed.), Facies Models (2nd ed.). Geoscience Canada, Reprint Series 1, p. 53-70.
Swift, D.J.P., Hudelson, P.M., Brenner, R.L., and Thompson, P., 1987. Shelf construction in a foreland basin: storm beds, shelf sandbodies, and shelf-slope depositional sequences in the Upper Cretaceous Mesaverde Group, Book Cliffs, Utah. Sedimentology, v. 34, p. 423-457.
Thompson, P.H., Culshaw, N., Thompson, D., and Buchanan, J.R., 1985. Geology across the western boundary of the Thelon Tectonic Zone in the Tinney Hills-Overby Lake (west half) map area, District of Mackenzie, Current Research, Part A. Geological Survey of Canada, Paper 85-1A, p. 555-572.
Thompson, P.H., and Frey, M., 1984. Illite "crystallinity" in the Western River Formation and its significance regarding the regional metamorphism of the early Proterozoic Goulburn Group, District of Mackenzie, Current Research, Part A. Geological Survey of Canada, Paper 84-1A, p. 409-414.
Tirrul, R., and Grotzinger, J.P., 1990. Early Proterozoic collisional orogeny along the

northern Thelon Tectonic Zone, Northwest Territories, Canada: Evidence from the foreland. Tectonics, v. 9, p. 1015-1036.

van Breemen, O., Henderson, J.B., Loveridge, W.D., and Thompson, P.H., 1986. Archean-Aphebian geochronology along the Thelon Tectonic Zone, Healey Lake area, N.W.T. Geol. Assoc. Canada, Prog. with Abs., v. 11, p. 139.

Van Wagoner, J.C., Mitchum, R.M., Campion, K.M., and Rahmanian, V.D., 1990. Siliciclastic sequence stratigraphy in well logs, cores, and outcrops. American Association of Petroleum Geologists, Methods in Exploration Series, No. 7 (Tulsa, OK), 55 pp.

Van Wagoner, J.C., Posamentier, H.W., Mitchum, R.M., Jr., Vail, P.R., Sarg, J.F., Loutit, T.S., and Hardenbol, J., 1988. An overview of the fundamentals of sequence stratigraphy and key definitions, in, C.K. Wilgus, B.S. Hastings, C.G.S.C. Kendall, H.W. Posamentier, C.A. Ross, and J.C. Van Wagoner (eds.), Sea-level changes: an integrated approach. Soc. Econ. Paleontologists and Mineralogists, Spec. Pub. No. 42, p. 39-46.

Vos, R.G., 1981. Sedimentology of an Ordovician fan delta complex, western Libya. Sed. Geol., v. 29, p. 153-170.

Vos, R.G., and Tankard, A.J., 1981. Braided fluvial sedimentation in the Lower Paleozoic Cape Basin, South Africa. Sed. Geol., v. 29, p. 171-193.

Walker, R.G., and Cant, D.J., 1984. Sandy fluvial systems, in, R.G. Walker (ed.), Facies Models (2nd ed.). Geoscience Canada, Reprint Series 1, p. 71-89.

Wells, N.A., and Dorr, J.A., Jr., 1987. A reconnaissance of sedimentation on the Kosi alluvial fan of India, in, F.G. Ethridge, R.M. Flores, and M.D. Harvey (eds.), Recent Developments in Fluvial Sedimentology. Soc. Econ. Paleont. Mineral., Spec. Pub. No. 39, p. 51-61.

Winston, D., 1978. Fluvial systems of the Precambrian Belt Supergroup, Montana and Idaho, U.S.A., in, A.D. Miall (ed.), Fluvial Sedimentology. Canadian Soc. Petrol. Geol., Mem. 5, p. 343-359.

Winston, D., 1986. Sedimentology of the Ravelli Group, Middle Belt Carbonate, and Missoula Group, Middle Proterozoic Belt Supergroup, Montana, Idaho and Washington, in, S.M. Roberts (ed.), Belt Supergroup: A guide to Proterozoic rocks of western Montana and adjacent areas. Montana Bureau of Mines and Geology, Special Publication 94 (Butte, MT), p. 85-124.

Table Caption

Table 1: Lithofacies associations of the Burnside Formation, their distinguishing characteristics, their paleogeographic locations, and examples illustrated in the figures.

Association / Facies	Grain Size	Sedimentary Structures	Bedding Characteristics	Environmental Interpretation	Lateral Extent	Example (Member / Figures)
siltstone	green mud to (f) sand	even parallel laminae; graded laminae; wave ripples; hummocky/swaley cross-stratification; sand-filled gutters; massive beds	sub-mm to 10's of cm's; continuous	progradational storm-influenced muddy shelf	across entire basin	Link Fm., basal Transitional Mbr., sections 1-3; Figures 6, 7, 8, 10
mixed siltstone-sandstone	silt and white to green (f-c) sand	wave ripples and low-angle cross-laminae; low-angle cross-bedding, trough cross-bedding	5-50 cm; tabular to wavy, locally discontinuous	retrogradational storm-influenced mixed muddy-sandy shelf	across entire basin	Link Fm., distal Burnside Fm., sections 6-11, 13, 14; Figures 9, 13, 14
rippled siltstone-sandstone	red mud/silt to (vf) sand	streaky to ripple cross-laminae; common wave and oscillation ripples; common soft sediment deformation	1-15 cm; tabular, locally discontinuous	braid delta front	proximal foreland	basal Transitional Mbr., sections 1-3; Figures 6, 7, 8, 10
tabular bedded sandstone	pink (vf-f) sand	parallel and low-angle cross-laminae; internal scours with clay chips; isolated trough cross-beds in scours; current and wave ripples	10-50 cm; tabular (10-100's m)	braid delta platform	across entire basin	basal Transitional Mbr., sections 1-7, 12-14, 16; Figures 6, 7, 8, 9, 10
trough bedded sandstone with mud clasts	(f-m) sand	trough cross-beds (<25 cm); shallow scours and channels (dm); common clay chips	30-150 cm; lenticular to tabular; cross-bedding laterally-extensive	braid delta plain	across entire basin	Transitional Mbr., sections 1-3; Figures 6, 7, 8
single-storied trough cross-bedded sandstone	(f-m) sand	trough cross-beds (<50 cm); shallow scours and channels (dm); no clay chips	30-150 cm beds; 1-3 m bedsets; lenticular to tabular cross-bedding; laterally- and vertically-extensive	distal braid plain	across entire basin	Transitional Mbr., sections 1-16; Figures 8, 9, 10, 13, 14
multi-storied trough cross- bedded sandstone	(f-c) sand with sparse gravel	medium and large trough cross-beds (25-80 cm); upper plane laminae; medium trough cross-beds at bedset tops; basal master bedding surface laterally continuous over km's	50-300 cm beds; continuous; bedsets 8-20 m tracable over km's	medial braid plain with minor gravel	proximal foreland and craton	Buff Sandstone Mbr., sections 1-3; Figures 8, 9, 10
trough- and tangentially cross-bedded sandstone	(f-c) sand; locally pebbly	medium and large trough cross-beds; large planar-tangential cross-beds; deep scours (20-200 cm)	50-200 cm; continuous	medial braid plain	proximal foreland	Gravelly Sandstone Mbr., sections 1-3; Figures 10, 11
sheet gravel and trough cross-bedded sandstone	pebble to cobble conglomerate & (m-vc) sand	clast-supported lags and crudely-stratified gravel sheets; large trough cross-beds (dm), upper sets lack gravel; common large planar cross beds (m) at base	50-300 cm	gravelly medial braid plain	proximal foreland	Conglomerate Mbr., sections 1-3; Figures 8, 10, 12
Burnside Dolomite	mixed clastic carbonate and siliciclastic mud to sand, cyclic carbonates	graded laminae; wave ripples; small scale hummocky cross-stratification; parallel laminae (especially in siliciclastic sand; trough cross-bedding on craton	2-20 cm; tabular to wavy, locally discontinuous	mixed carbonate-siliciclastic lagoon and cyclic carbonates	distal foreland	Burnside Dolomite; Figures 9, 10 ,13

Table 1.

Figure Captions

Figure 1. Geologic and geographic elements of the northwestern Canadian Shield. Triangular ticks indicate zones of overthrusting with ticks on the overthrust plate; arrows indicate zones of strike slip displacement. Inset indicates the location of the map within North America. Figure modified from Hoffman (1987).

Figure 2. Geologic map of Kilohigok Basin. Circled numbers mark the locations of measured sections in the Burnside Formation that are shown in subsequent cross sections. The basin has been restored for approximately 115 km of left slip on the Bathurst fault zone as recommended by Tirrul and Grotzinger (1990). This displacement post-dates deposition of the Goulburn Supergroup. The Gordon Bay Arch was a flexural arch that was active during deposition of the Bear Creek Group (see Figures 3a&b, 4). A second independent flexural arch lay near Rockinghorse Lake and is termed the Rockinghorse Arch in subsequent cross sections.

Figure 3. A: Stratigraphic framework of the Goulburn Supergroup with an interpretation of the sedimentologic and tectonic evolution (Tirrul, 1985; Grotzinger and McCormick, 1988; Tirrul and Grotzinger, 1990). Volcanic ash bed ages are from Bowring and Grotzinger (1992). The upper ash bed age is on the basis of the correlation to a stratigraphic horizon in Wopmay Orogen; see text for explanation. B: Schematic cross section and correlation between members of the Burnside Formation and the Mara and Quadyuk Formations. Thick lines indicate inferred erosional, unconformable contacts; thin lines indicate gradational or inferred conformable lithological contacts. Thicknesses are diagrammatic and are not to scale.

Figure 4. Cross section of the Goulburn Supergroup from Kilohigok Basin to Wopmay Orogen (Figure 1). The line of section within Kilohigok Basin lies along the line from the Section 1 to Section 14 in Figure 2. The datum is a the top of the passive margin carbonate platform in Wopmay Orogen and its correlative within the Burnside Formation in Kilohigok Basin. Locations of lines of section in subsequent figures are indicated in Figure 2. The measured sections are projected onto a west-northwest line corresponding to the mean paleocurrent direction for the upper alluvial sandstone facies (Figure 5). The ages of ash beds are from Bowring and Grotzinger (1992).

Figure 5. Paleocurrent directions within the Burnside Formation on the basis of trough

cross-beds. The inset labeled "sections 2&3" are readings taken from roughly the same area as the rose with 883 measurements in Figure 2. This inset compares readings recorded in the Transitional member (lowermost one in Burnside Formation; Figures 3b, 7, 10) of inferred braid delta facies that have an anomalous southwest mode with paleocurrents recorded in overlying members of inferred braid plain facies that have the predominant northwest mode. Data from Campbell and Cecile (1981) are plotted with radius proportional to the number of paleocurrent measurements. Data from this study are plotted with area proportional to number of readings.

Figure 6. Transitional marine shelf to braid delta associations. A) Wave rippled siltstone-mudstone facies of the siltstone-dominated association. Coin for scale. B) Hummocky-swaley cross-stratified facies (marked as "s") of the siltstone-dominated association. Truncated swaley bed is interbedded with wave rippled and parallel-laminated siltstone. Pocketknife for scale. C) Gutter facies of the siltstone-dominated association. This 30 cm deep, 70 cm wide lenticular scour contains heterogeneous fill of siltstone and lenticular sandstone beds (marked as "s") 3 to 10 cm thick that exhibit gutters as well. Gutters are aligned parallel to this scour. The scour cut across wave-rippled siltstone-mudstone facies. D) Rippled red sandstone-siltstone facies of the delta front association. Arrow points to highly deformed horizon that is injected into overlying bed. The overlying bed is highly contorted and passes laterally into a slumped horizon (see next photo). Hammer for scale. E) Slumped bed (marked as "s") cuts out about 2.5 m of section. Bed dips at about 30° to regional bedding but parallel laminae remain internally coherent. Laterally this bed passes into contorted, massive sandstone that has been fluidized. Hammer for scale above slumped bed. F) Sandstones of delta platform and delta plain associations. Trough cross-bedded sandstone (marked as "t") with common mud chips are sharply interbedded tabular parallel-laminated sandstones. Pocketknife for scale at top of the lower trough cross-bedded sandstone.

Figure 7. Measured section of the upper Link and Transitional member of the Burnside Formation at section 3. This section exhibits the facies illustrated in Figure 6. The northwest to southwest mode of trough cross-beds suggest that northwest flow through gutters was down a prodelta slope.

Figure 8. Cross section of the transition from marine shelf to alluvial-dominated facies in the Bear Creek Group. The cross section from 3 to 12 lies approximately parallel to the dominant paleocurrent trend; sections 12 to 14 lie roughly perpendicular to the main alluvial paleocurrent trend. Sections locations are found in Figure 2. Note the pronounced thinning of all stratigraphic units over the crest of the Gordon Bay Arch and thickening into section

12, mimicking stratigraphic trends in the lower Bear Creek Group (Figure 4). Also note pinch-out of the Transitional and Buff Sandstone members of the Burnside Formation southeast of the arch crest. The Burnside Formation shown represents only the lower few tens of meters; the estimated thickness of the Burnside Formation in these areas is more than 1500 meters.

Figure 9. Common shallow marine to braid plain facies associations of the Burnside Formation. A) Mixed siltstone-sandstone association shelf facies with symmetrical wave ripples in upper bed interbedded with laminated mudstone (dark). Coin for scale. B) Mixed siltstone-sandstone association with low-angle cross-laminae and internal truncations. Coin for scale. C) Low-angle cross-laminae, internal truncations, and wave-rippled clastic dolarenite of Burnside Dolomite at section 12. Significant amounts of siliciclastic mud and sand are mixed with the carbonate silt and sand. Coin for scale. D) Delta platform sandstone with diffuse parallel laminae. Bed is capped by wavy-laminated green siltstone (arrow). Coin for scale. E) Multi-storeyed trough-crossbedded lithofacies with two scales of trough cross-bedding and bedding-parallel bounding surfaces between cross-sets. Staff is 1.5 m long. F) Multi-storeyed trough-crossbedded lithofacies seen at an oblique angle. Numerous internal scours are seen, and a master bedding surface with very low relief is seen at base. Scours are incompletely filled. Staff is 1.5 m long.

Figure 10. Cross section of the Burnside Formation in the proximal foredeep east of the Bathurst Fault Zone (see Figure 2 for location). Note that the vertical exaggeration is much less in this cross section than any other. Note also that the lateral thickening of all members increases between sections 2 and 1; section 2 was the approximate location of the shelf break in underlying lower Bear Creek Group stratigraphic sequences. The unpatterned space within the Orange Sandstone member labeled "section faulted out" is the location and interpreted stratigraphic separation on a fault that cuts through the section in the between sections 2 and 3. Stratigraphic separation of at least 800-1000 meters is inferred on the basis of extrapolation of thickness trends in the lower members from sections 1 to 10 (see Figure 8).

Figure 11. Gravelly tangential- and trough-crossbedded association at section 2. Large set of planar-tangential cross-beds carrying polymictic gravel in lower 30-50 cm of set. Scour at base of cross-set cuts down about 80 cm. Set is overlain by parallel-laminated sand. Planar tangential cross-beds are oriented about 240°, whereas the predominant trough cross-bed paleocurrent azimuth is directed into picture (about 300°). Staff is 1.5 m long.

Figure 12. Conglomeratic between sections 2 and 3. A) Base of Conglomerate member showing crudely bedded gravel with coarsest clasts at base of beds. Upper parts of beds are trough cross-bedded sandstone. Hammer for scale (circled). B) Uppermost conglomerate horizon at section 2 at the top of the Gravelly Sandstone member. Lower bed is volcanic clast horizon and upper bed is polymictic horizon with Burnside intraformational clasts. Note steep scour relief on channel margins and nearly bedding-parallel upper surface. Staff is 1.5 m long. C) Uppermost conglomerate horizon in the section 3. The largest dark clasts are Burnside lithofacies; they reach 50 to 100 cm and define deep channels. White clasts are vein quartz. Smallest clasts are the background polymictic population, similar to those in the previous photo. Staff is 1.5 m long. D) Fractured Burnside lithology clast. Vein quartz fracture filling that does not extent into the matrix sand. This clast must have been fractured and filled with quartz at depth before being re-incorporated into the Burnside fluvial system. Cannibalization of syn-orogenic sediments is common in foreland basins. Coin for scale (arrow).

Figure 13. Cross section of the Burnside Formation in the distal foredeep west of the Bathurst Fault Zone and the Gordon Bay Arch (see Figure 2 for location). Disconformities are those illustrated in Figures 8 and 9. The datum for this cross-section is the top of the Burnside Dolomite. This section is approximately perpendicular to the dominant paleocurrent trend.

Figure 14. Measured stratigraphic section 13. The lower part of the section shows an initial upward coarsening with fining-upward interval from delta platform sandstones to mixed sandstone-siltstone facies interpreted as a wave- and storm-influenced shelf facies. The second fining-upward interval to the Burnside Dolomite contains pink very fine grained sandstone of inferred fluvial origin interbedded in shallow shelf siltstone and mudstone. The Burnside Dolomite is a westward-thickening tongue of shallow marine carbonate extends eastward to the section 11 area (see Figures 2, 13, 15). It is believed to be correlative with the Rocknest carbonate platform in Wopmay Orogen (Figure 1). Patterns are as in Figure 9.

Figure 15. Interpretation of the paleogeography of the Burnside alluvial system. A: Time of horizontal datum in Figure 4. Note the emergent, southwestward plunging Gordon Bay arch that results from thrusting in the Thelon orogenic belt, southeast of Kilohigok Basin (Figure 1). Evidence for the plunging nature the Gordon Bay Arch comes from a section of the Burnside Formation at section 15 (Figure 2) that lies directly on granitic basement, suggesting that this area was probably emergent during deposition of the lower Bear Creek Group and part of the Burnside Formation. This may account for the high feldspar content

in the lower Bear Creek Group and lower deltaic Burnside Formation. The flexural arch indicated near the western boundary of the diagram is not related to the Gordon Bay flexural arch. Rather it results from sediment loading along the passive margin of Wopmay Orogen to the west. B: Time of the progradation of braid plain facies over the Gordon Bay flexural arch (this is the same as the datum in Figures 4, 8, and 9). This corresponds to the time of deposition of the Buff Sandstone member (Figures 3b, 9). The base of this member is largely marked by an erosional unconformity. C: Time of progradation of the Conglomerate member (Figure 3b). This marks the first time that alluvial facies prograde across the entire Slave Craton and interfinger with marine shelf facies in Wopmay Orogen. Paleocurrents indicate that transport was uniformly to the west-northwest or northwest (Figure 5). Gravel-bearing sandstones are present at sections 13 and 14. D: Time of transgression of the marine Burnside Dolomite over the alluvial system. The westward-thickening tongue of mixed siliciclastic-carbonate and cyclic carbonates are believed to correlate with the Rocknest Formation carbonate platform in Wopmay orogen that lies 20 km west of section 14 (Figures 1, 2). All alluvial facies appear to backstep at this time except in the most proximal part of the foredeep. E: Alluvial facies prograde back across the craton. Some gravel in braid plain facies is found as far west as section 12.F: End of alluvial sedimentation in the Bear Creek Group. A flexural arch may have existed over the section 12 area at the end of alluvial sedimentation. Quadyuk Formation shelf carbonate intertongues and passes laterally into deltaic Orange Sandstone member in the proximal foreland (Figures 3b, 4, 10). To the west on the craton, the Quadyuk is absent in section 12 . The exposed surface coincident with the single flexural arch represents an amalgamated exposure surface and a transgressive surface (Figure 10).

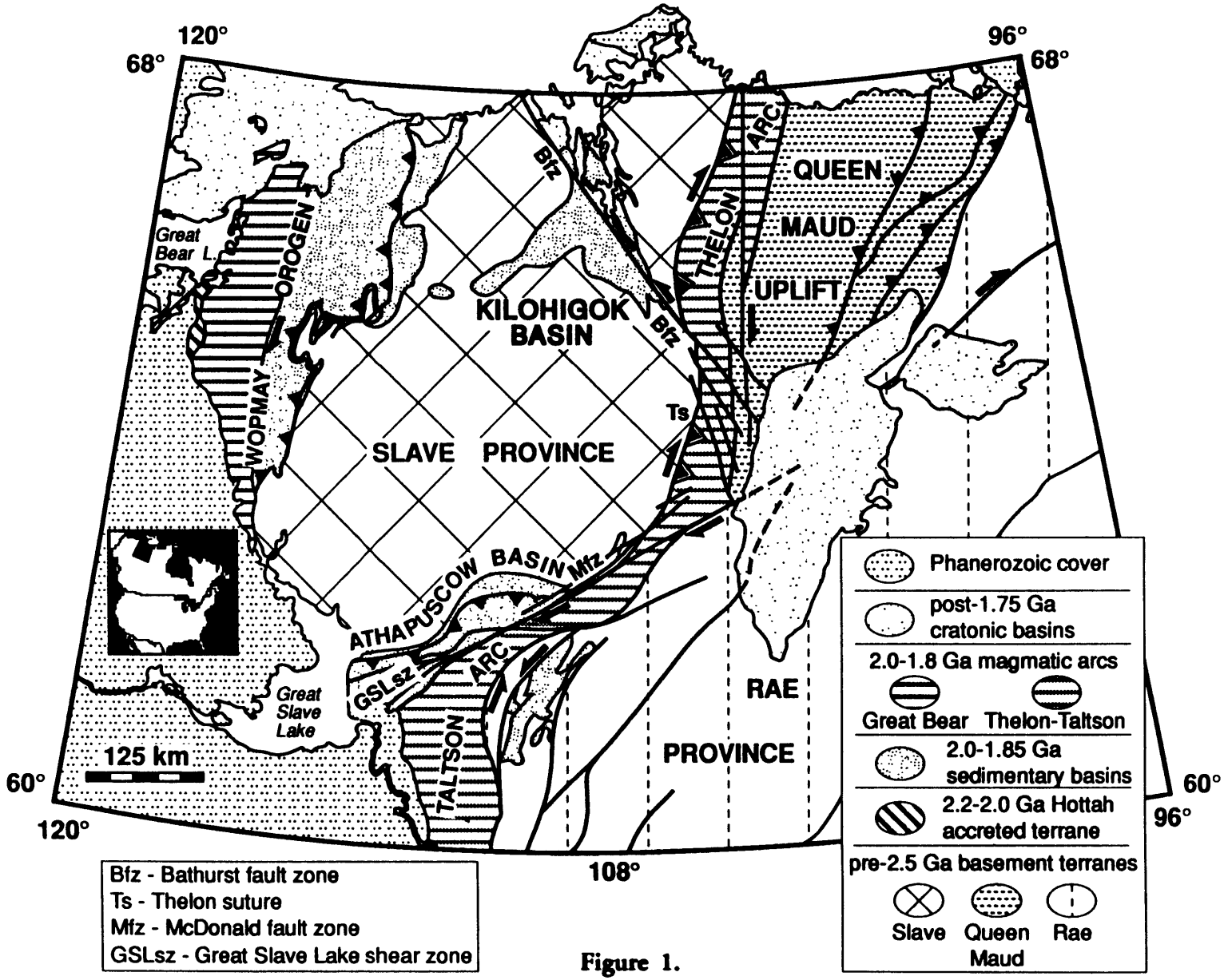
120°
68°
96°
68°
Great Bear L.
GREAT BEAR OROGEN
WOPMAY
Bfz
KILOHIGOK BASIN
THELON ARC
QUEEN MAUD UPLIFT
Bfz
Ts
SLAVE PROVINCE
ATHAPUSCOW BASIN
Mfz
GSLsz
ARC
Great Slave Lake
125 km
TALTSON
RAE PROVINCE
60°
120°
108°
60°
96°
Bfz - Bathurst fault zone
Ts - Thelon suture
Mfz - McDonald fault zone
GSLsz - Great Slave Lake shear zone
Phanerozoic cover
post-1.75 Ga cratonic basins
2.0-1.8 Ga magmatic arcs
Great Bear
Thelon-Taltson
2.0-1.85 Ga sedimentary basins
2.2-2.0 Ga Hottah accreted terrane
pre-2.5 Ga basement terranes
Slave
Queen Maud
Rae

Figure 1.

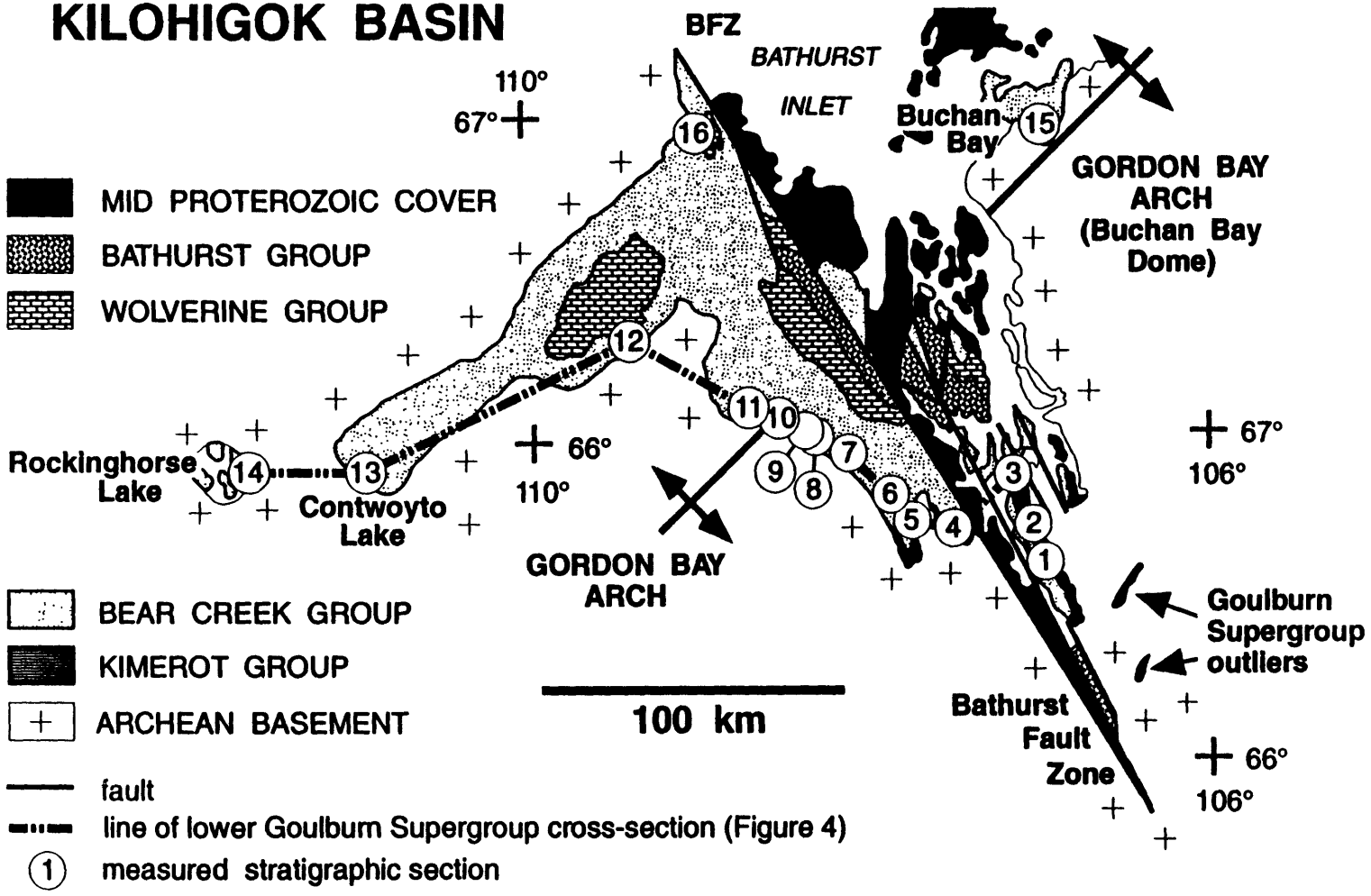
KILOHIGOK BASIN
BFZ
BATHURST INLET
110°
67°
Buchan Bay
GORDON BAY ARCH (Buchan Bay Dome)
MID PROTEROZOIC COVER
BATHURST GROUP
WOLVERINE GROUP
Rockinghorse Lake
Contwoyto Lake
66°
110°
67°
106°
GORDON BAY ARCH
BEAR CREEK GROUP
KIMEROT GROUP
ARCHEAN BASEMENT
100 km
Goulburn Supergroup outliers
Bathurst Fault Zone
66°
106°
fault
line of lower Goulburn Supergroup cross-section (Figure 4)
measured stratigraphic section

Figure 2.

Figure 3.

a

lower Goulburn Supergroup				
lithostratigraphy groups	lithostratigraphy formations	sedimentary environment	tectonic interpretation	volcanic ash age (Ma)
Upper Bear Creek Group	Quadyuk Mara Burnside	carbonate platform marine shelf braid delta / braided alluvial	hinterland unroofing & alluvial progradation over craton	1882 ± 2
Lower Bear Creek Group	Link Beechey Rifle Hackett	siliciclastic marine shelf / minor shelf carbonates / basinal turbidites	Bear Creek foredeep flexural subsidence and infilling of marine foredeep	1963 ± 6 1969 ± 1
Kimerot Group	Peg Kenyon	siliciclastic to carbonate platform	Kimerot passive margin	

b

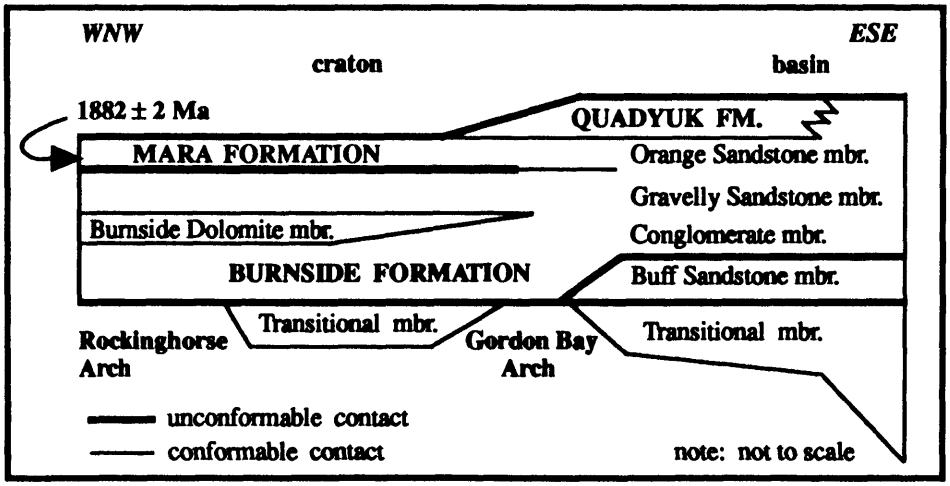

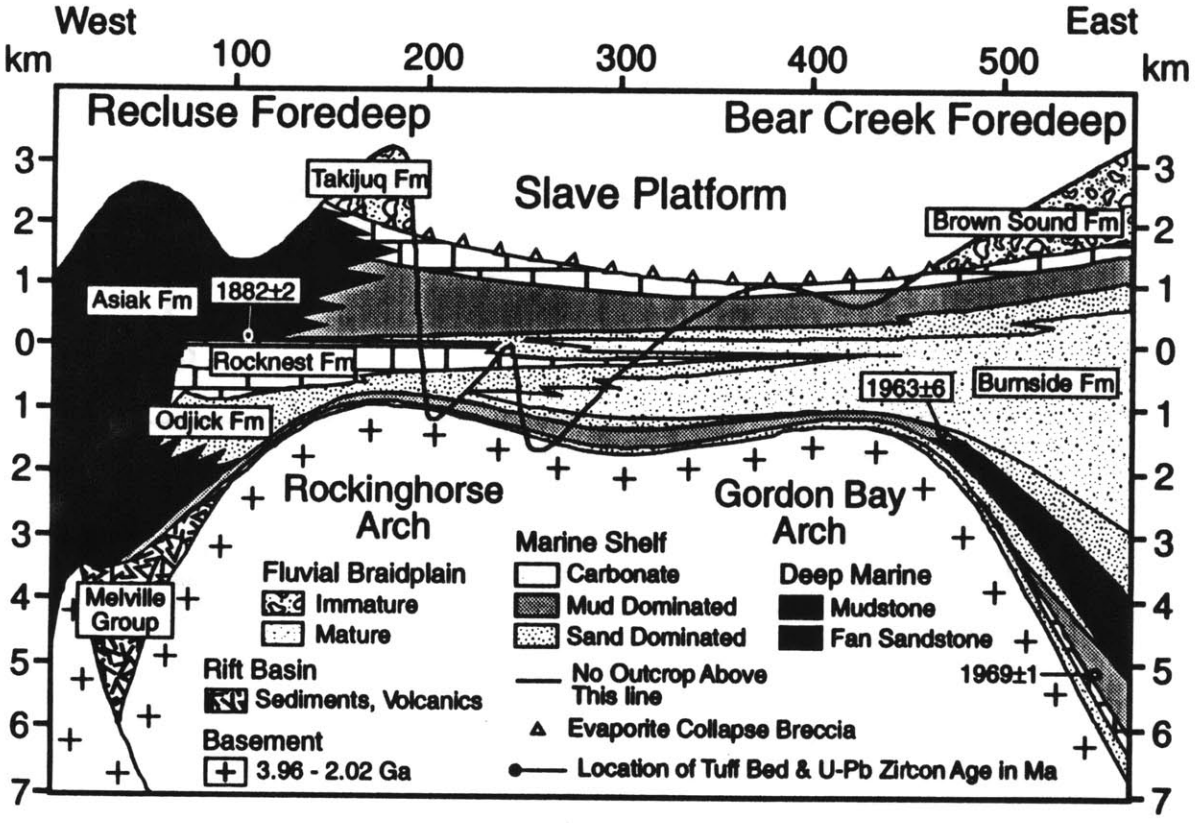
West
East
km
100
200
300
400
500
km
Recluse Foredeep
Bear Creek Foredeep
Slave Platform
Takijuq Fm
Brown Sound Fm
Asiak Fm
1882±2
Rocknest Fm
1963±6
Burnside Fm
Odjick Fm
Rockinghorse Arch
Gordon Bay Arch
Melville Group
Fluvial Braidplain
Immature
Mature
Rift Basin
Sediments, Volcanics
Basement
3.96 - 2.02 Ga
Marine Shelf
Carbonate
Mud Dominated
Sand Dominated
Deep Marine
Mudstone
Fan Sandstone
No Outcrop Above This line
1969±1
Evaporite Collapse Breccia
Location of Tuff Bed & U-Pb Zircon Age in Ma

Figure 4.

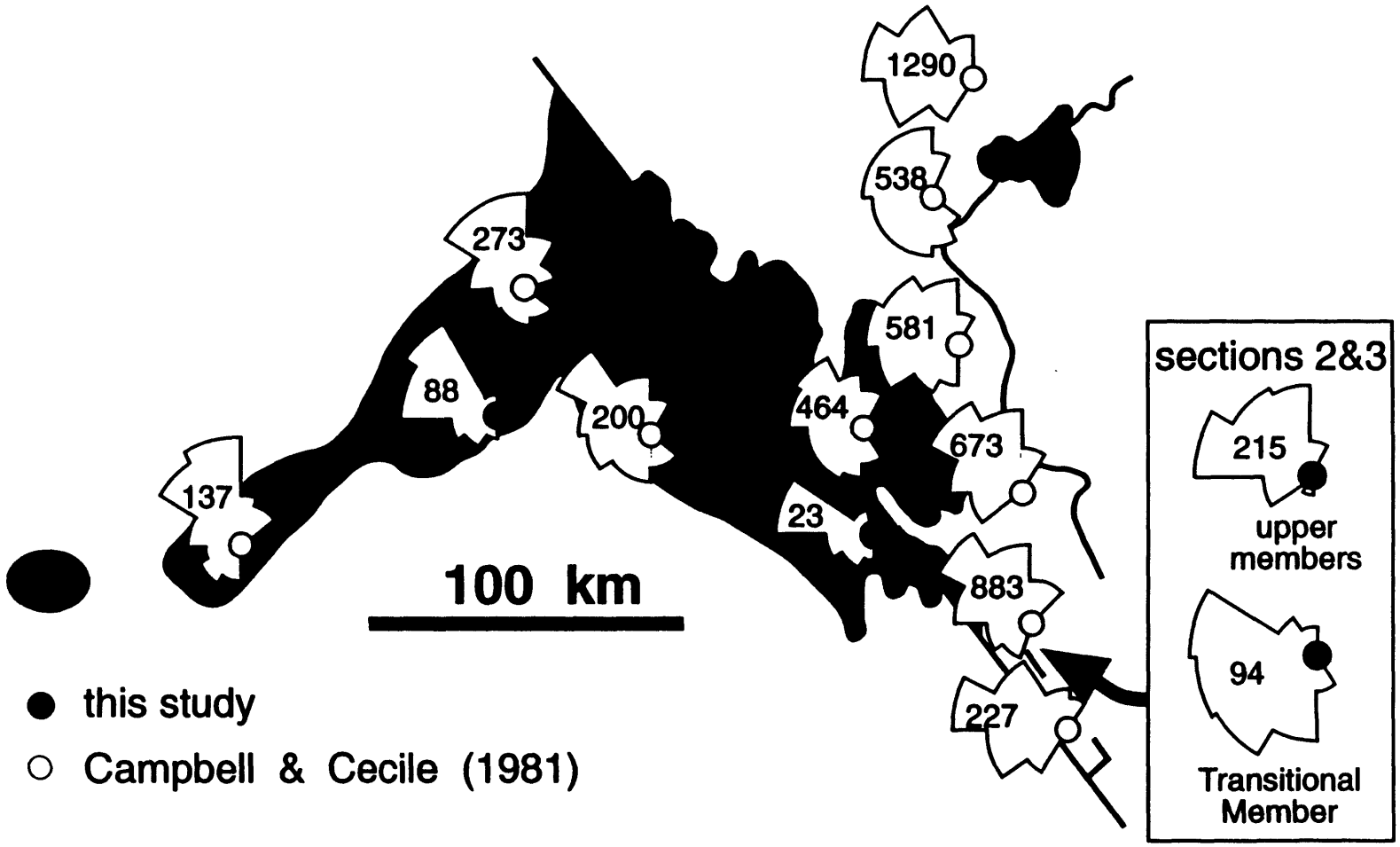
1290
538
273
581
88
200
464
673
137
23
883
227
100 km
this study
Campbell & Cecile (1981)
sections 2&3
215
upper members
94
Transitional Member

Figure 5.

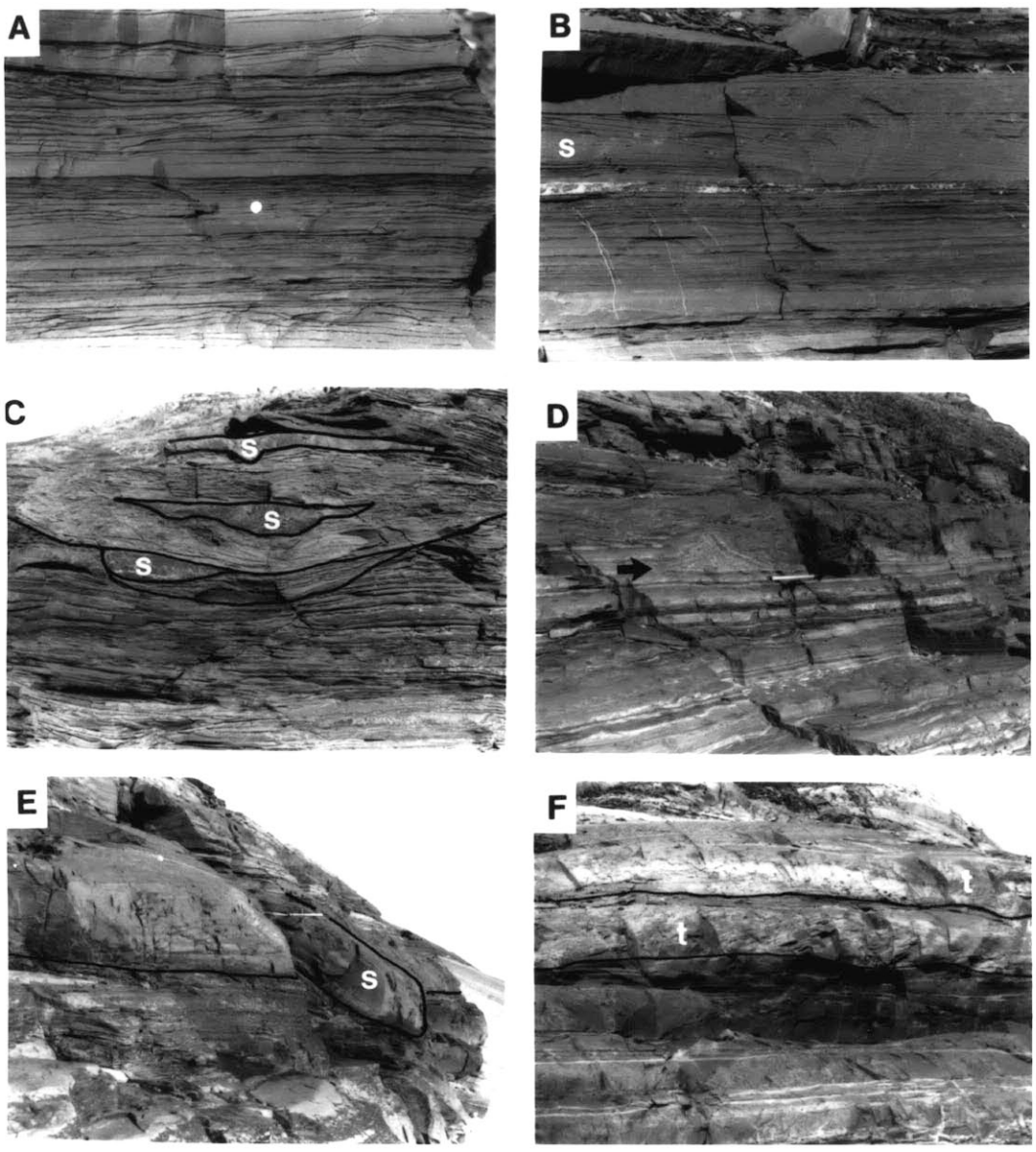

Figure 6.

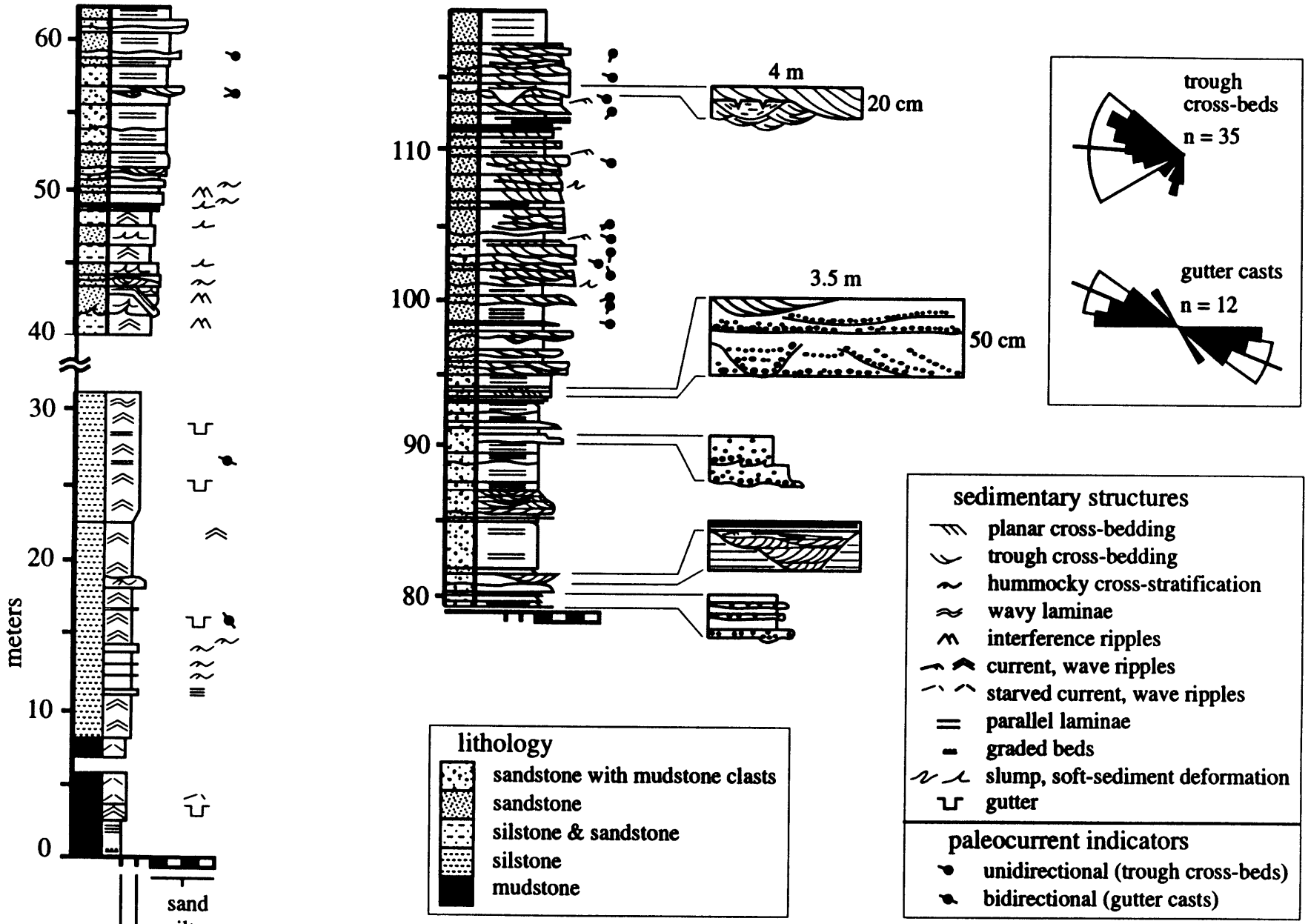
60
50
40
30
20
10
0
meters
sand
silt
mud
110
100
90
80
4 m
20 cm
3.5 m
50 cm
trough
cross-beds
n = 35
gutter casts
n = 12
lithology
sandstone with mudstone clasts
sandstone
silstone & sandstone
silstone
mudstone
sedimentary structures
planar cross-bedding
trough cross-bedding
hummocky cross-stratification
wavy laminae
interference ripples
current, wave ripples
starved current, wave ripples
parallel laminae
graded beds
slump, soft-sediment deformation
gutter
paleocurrent indicators
unidirectional (trough cross-beds)
bidirectional (gutter casts)

Figure 7.

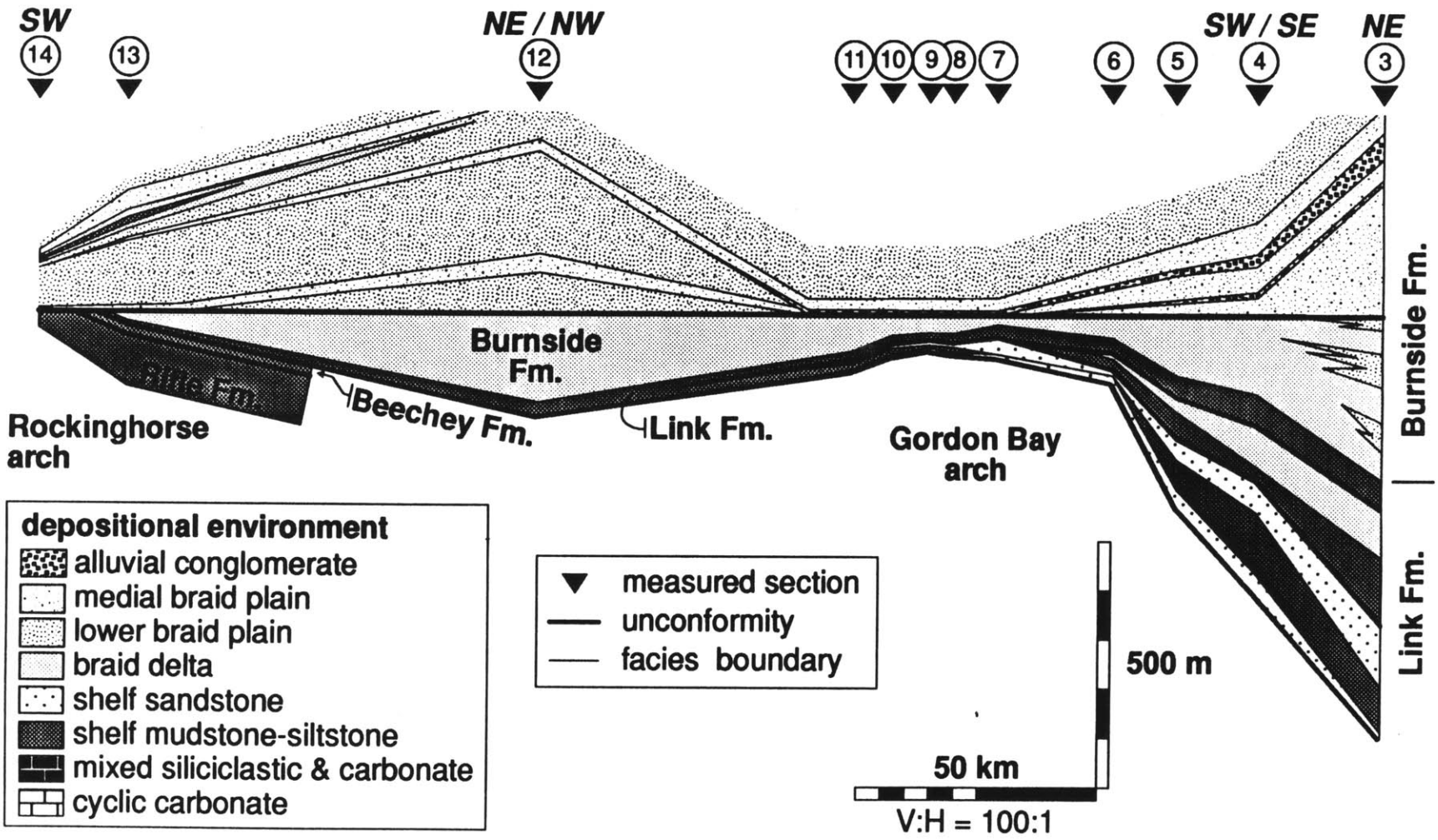
SW
NE / NW
SW / SE
NE
14
13
12
11
10
9
8
7
6
5
4
3
Burnside Fm.
Rockinghorse arch
Beechey Fm.
Link Fm.
Gordon Bay arch
Burnside Fm.
Link Fm.
depositional environment
alluvial conglomerate
medial braid plain
lower braid plain
braid delta
shelf sandstone
shelf mudstone-siltstone
mixed siliciclastic & carbonate
cyclic carbonate
measured section
unconformity
facies boundary
500 m
50 km
V:H = 100:1

Figure 8.

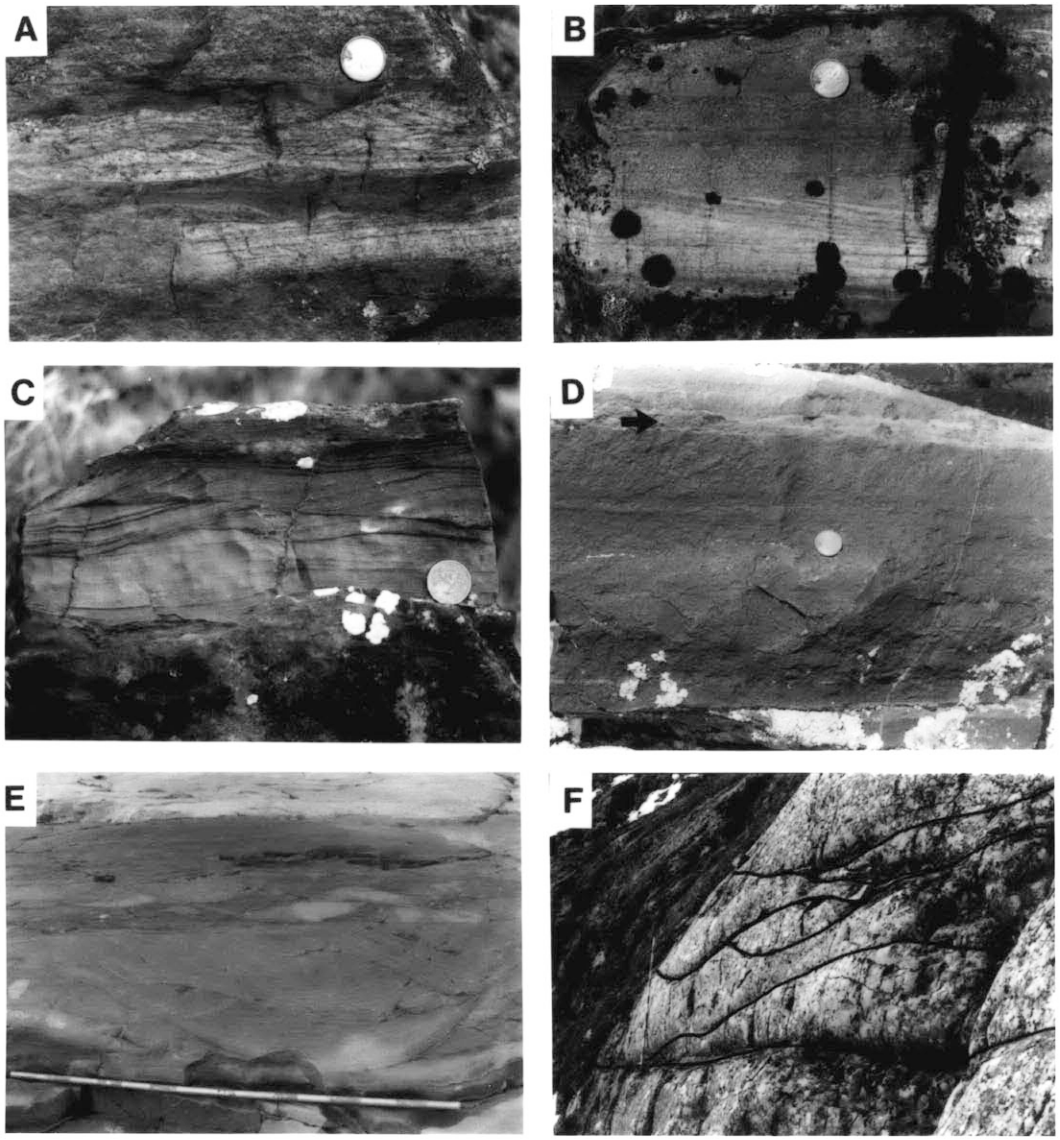

Figure 9.

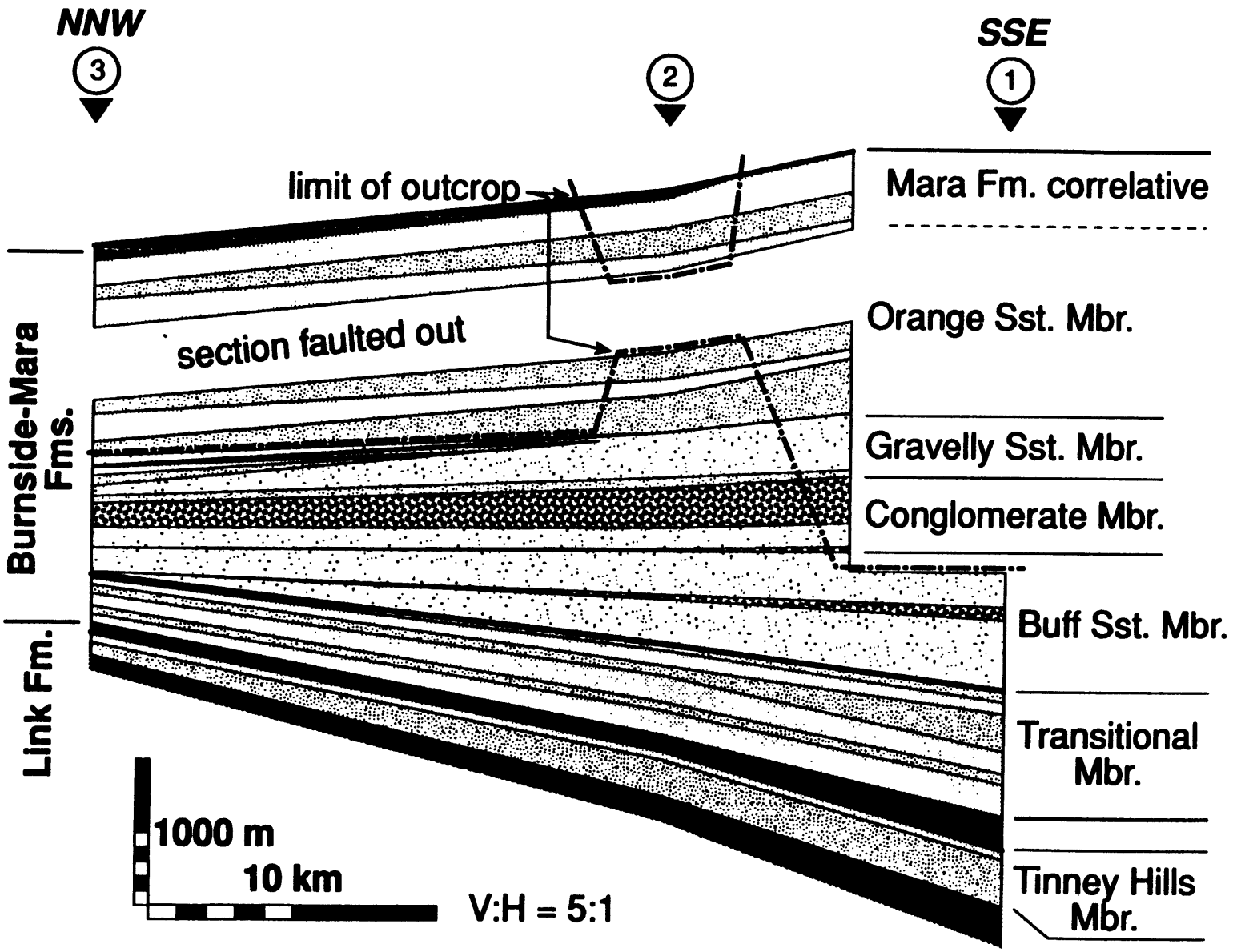
NNW
3
2
SSE
1
limit of outcrop
Mara Fm. correlative
section faulted out
Orange Sst. Mbr.
Burnside-Mara Fms.
Gravelly Sst. Mbr.
Conglomerate Mbr.
Buff Sst. Mbr.
Link Fm.
Transitional Mbr.
Tinney Hills Mbr.
1000 m
10 km
V:H = 5:1

Figure 10.

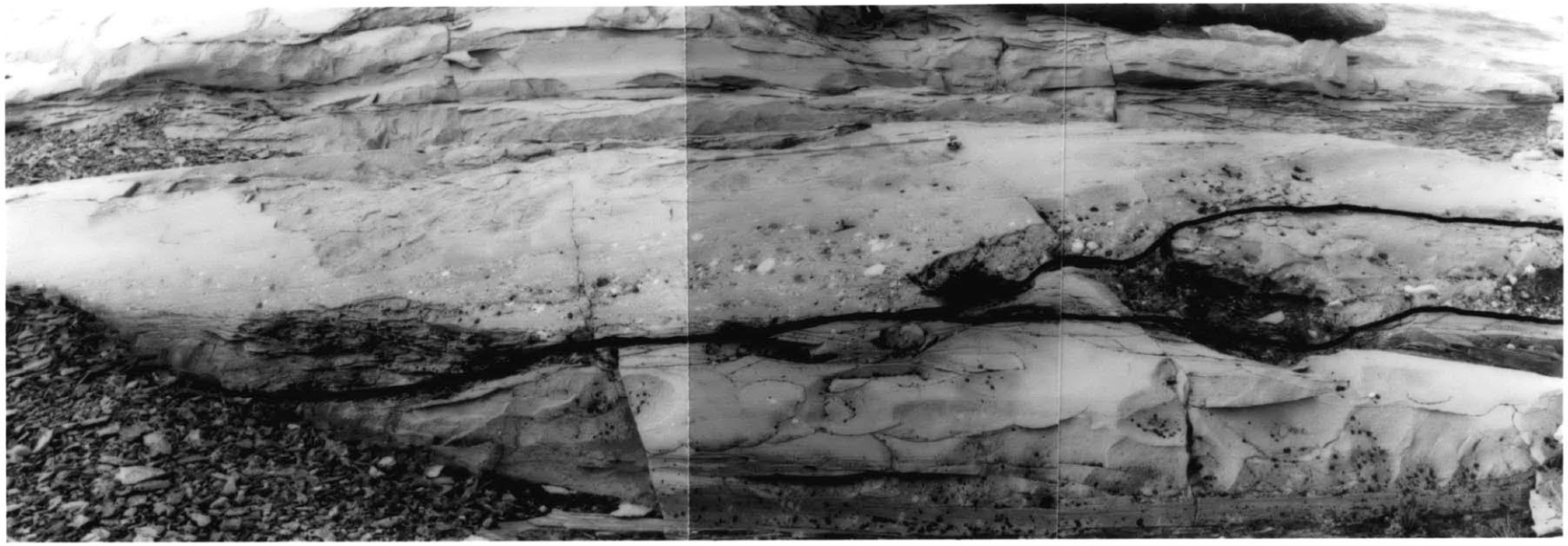

Figure 11.

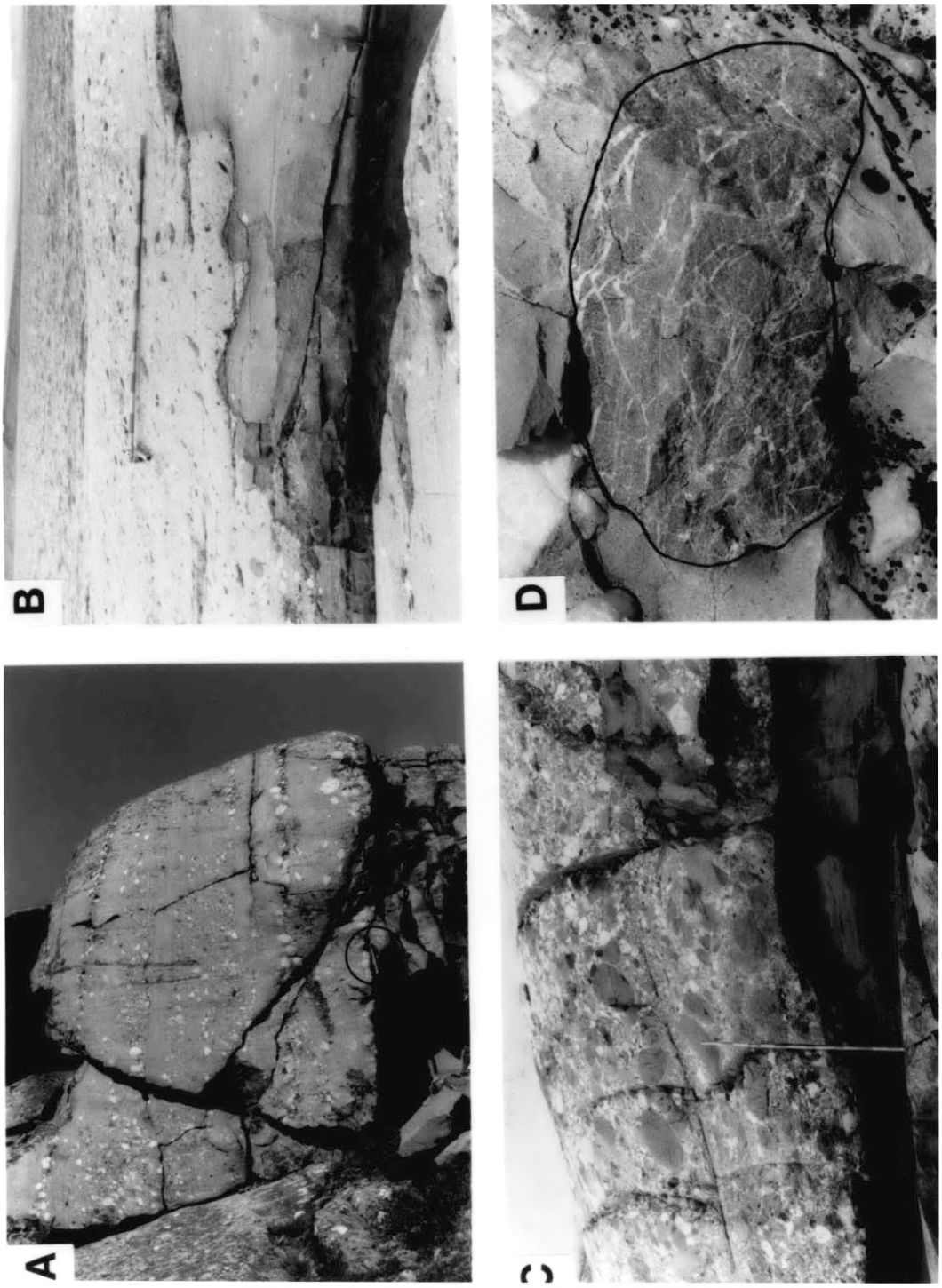

Figure 12.

Figure 13.

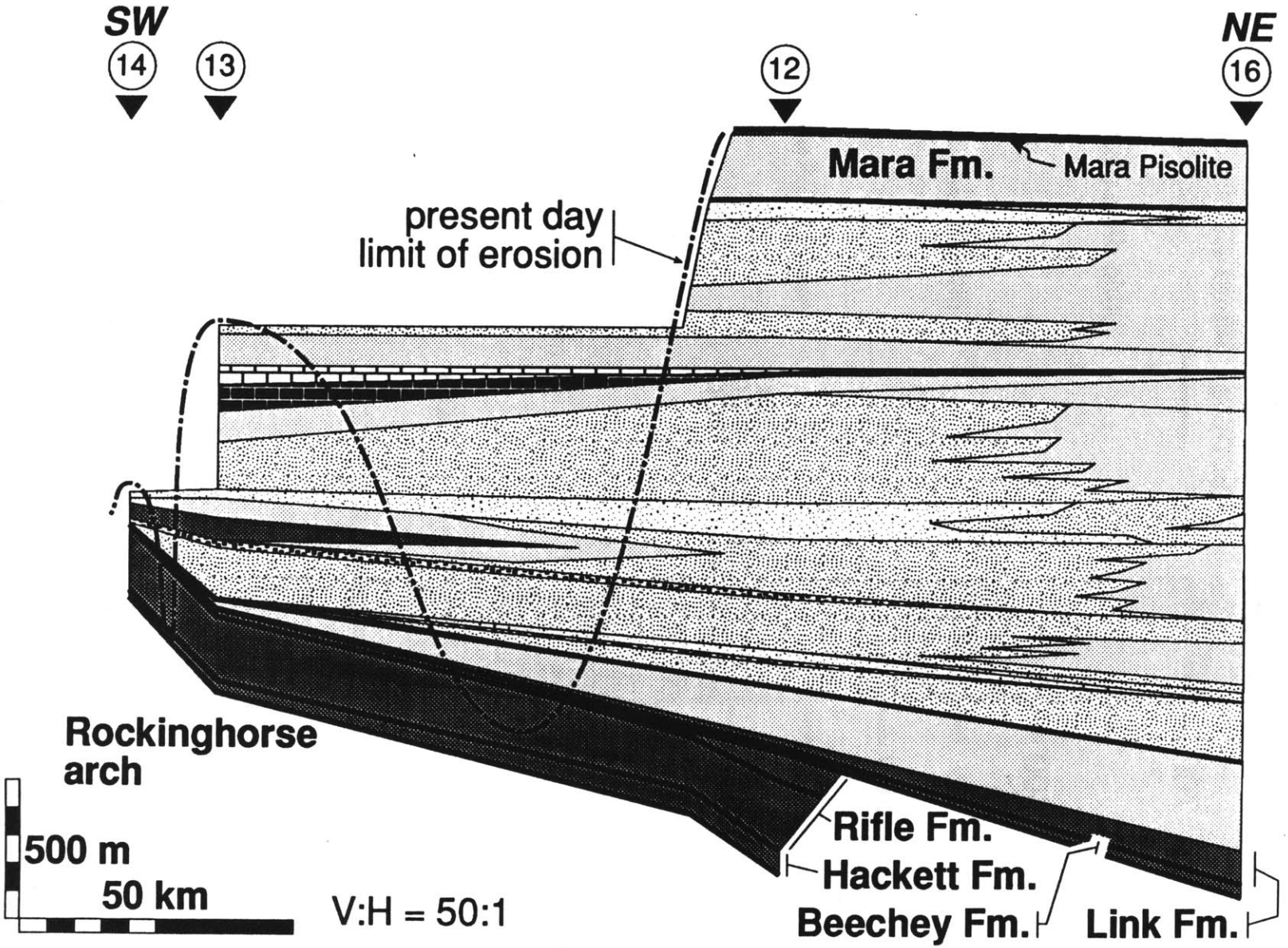
SW
14
13
12
NE
16
Mara Fm.
Mara Pisolite
present day
limit of erosion
Rockinghorse
arch
500 m
50 km
V:H = 50:1
Rifle Fm.
Hackett Fm.
Beechey Fm.
Link Fm.

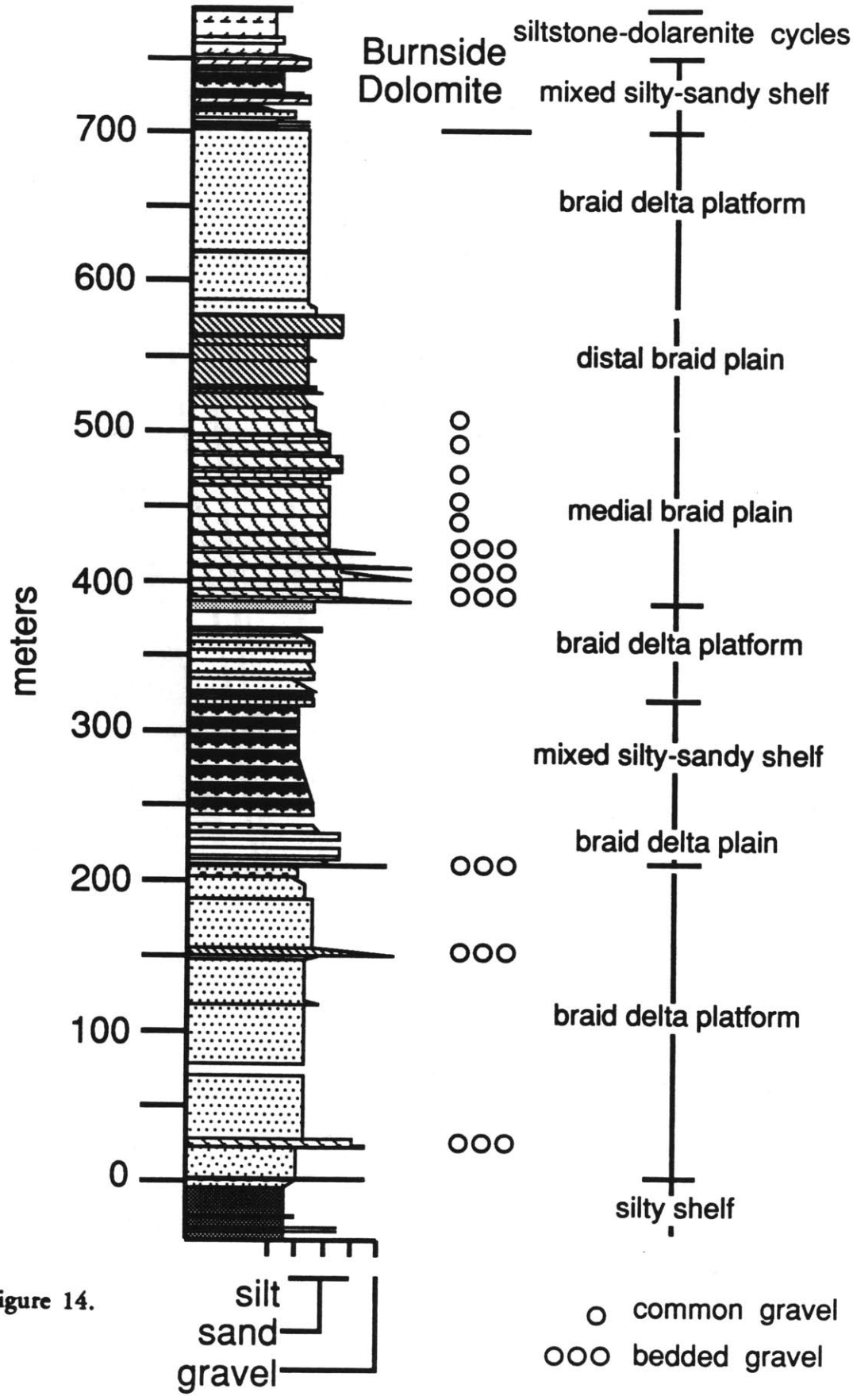
Burnside
Dolomite
siltstone-dolarenite cycles
mixed silty-sandy shelf
braid delta platform
distal braid plain
medial braid plain
braid delta platform
mixed silty-sandy shelf
braid delta plain
braid delta platform
silty shelf
meters
700
600
500
400
300
200
100
0
silt
sand
gravel
common gravel
bedded gravel

Figure 14.

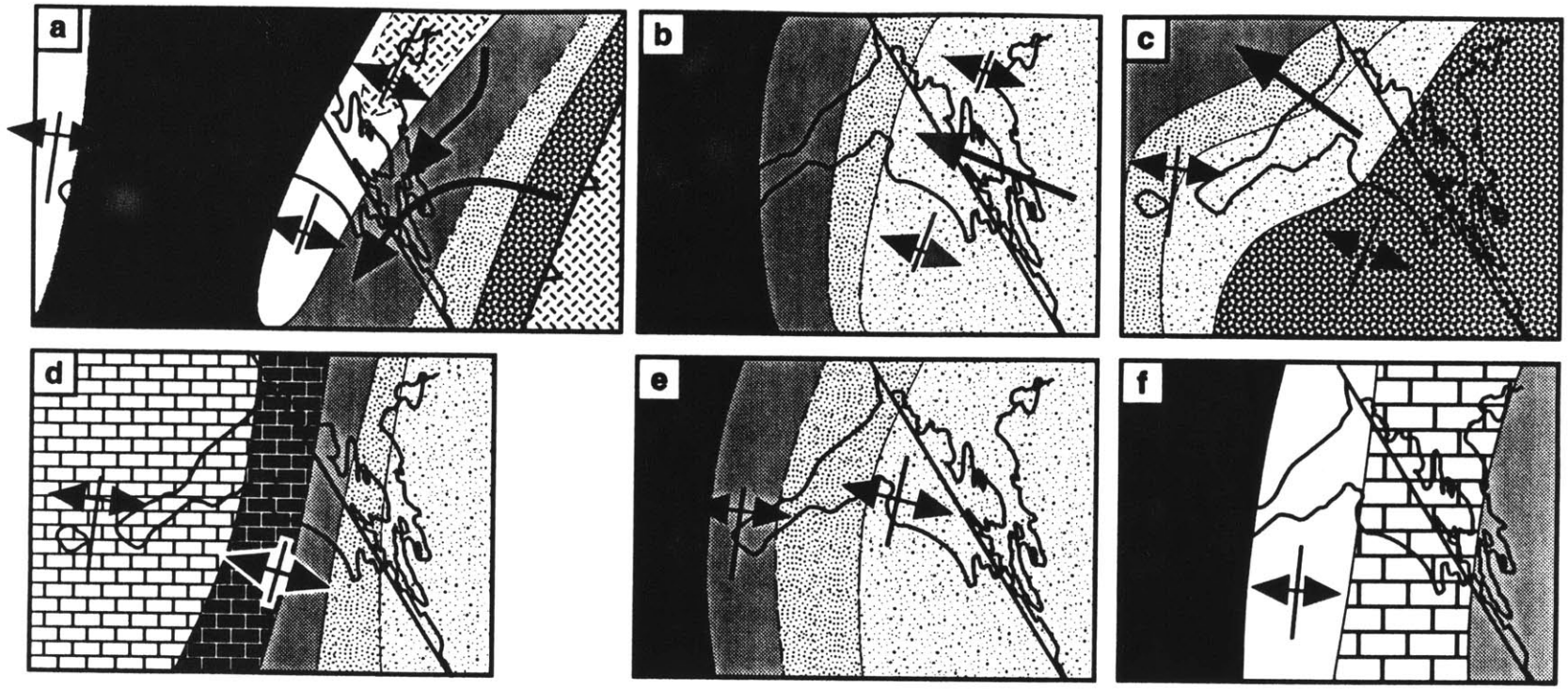
a
b
c
d
e
f
alluvial conglomerate
medial braid plain
lower braid plain
braid delta
shelf sandstone
shelf siltstone & mudstone
mixed siliciclastic/carbonate
cyclic carbonate
shelf carbonate
emergent on underlying Bear Creek Group sediments
emergent on crystalline basement
100 km
facies transition
approximate facies transition
paleocurrent trend
syn-sedimentary flexural arch
Thelon orogenic front

Figure 15.

Chapter 2:
Evolution and significance of an overfilled alluvial foreland basin: Burnside Formation (1.9 Ga), Kilohigok Basin, N.W.T., Canada

Abstract

The Burnside Formation records the transition from marine shelf to largely alluvial conditions in the Early Proterozoic (about 1.9 Ga) Kilohigok foreland basin in the Slave Province of the Canadian Shield. The Burnside Formation forms a thick (up to 3.5 km), northwest-tapering siliciclastic wedge, representing a braided alluvial system that prograded transversely across the Slave Province. The stratigraphic architecture of this unfossiliferous, predominantly alluvial succession documents the location and distribution of unconformities caused by lithospheric flexure in a Proterozoic foreland basin. The locations of these unconformities demonstrate the changing locations of tectonic and sedimentary loads on both sides of the Slave craton.

Associations of sedimentary facies and paleocurrents indicate that initially a braid delta system drained longitudinally, restricted to the proximal part of the basin between the Thelon Orogen, the orogenic hinterland, and a syn-sedimentary flexural arch. Paleocurrents for the lowermost braid delta facies in the proximal foreland were parallel to paleocurrents in underlying foreland basin turbidites, parallel to the flexural arch closest to the Thelon Orogen, parallel to the strike of the orogen, and perpendicular to the transport direction of thrust-nappes directed out of the orogenic belt. An abrupt shift to a transverse paleocurrent mode accompanied the onset of higher-gradient braided stream conditions across the entire foreland basin, showing that from this time, sediment supply exceeded subsidence in the proximal foreland. The long-lived, laterally extensive transverse dispersal and the presence of sedimentary facies lacking interbedded mud or sedimentary structures indicative of desiccation suggest that fluvial discharge was probably perennial.

The sharp superposition of medial braid plain facies directly on marine shelf and deltaic facies in the distal foreland indicates that the transition to non-marine conditions marks an erosional unconformity over two coeval flexural arches. The eastern flexural arch relates to convergence on the southeastern margin of the Slave Province and to thrust loading in the Thelon Orogen that created the Kilohigok foreland basin. The evolution of a passive margin on the western side of the Slave Province caused the other flexural arch. In the center of Kilohigok Basin a profound unconformity exists at the top of the Burnside alluvial

succession. This unconformity suggests that a single flexural arch existed at the end of alluvial sedimentation that may signify the migration and yoking together of the two previously independent flexural arches. This migration may have been caused by the combined mass of the thick alluvial sedimentary wedge over the eastern edge of the Slave craton, coupled with initial thrust loading and foreland basin development in Wopmay Orogen.

The transition within a foreland basin from largely marine to largely alluvial deposition reflects changing subsidence and sedimentation patterns across the basin due to mass redistribution from the orogenic hinterland into the foreland basin by erosion. This transition appears to separate two distinct phases in the evolution of the Kilohigok foreland basin. In the first phase, active thrust loading and asymmetric flexural subsidence restricted alluvial facies near the orogen. In the second phase, convergence slowed or ceased, and erosional unloading and uplift of the hinterland caused subsidence patterns to become more uniform across the foreland basin, promoting rapid progradation of alluvial facies across the basin. Paleomagnetic and sedimentological data indicate that the basin lay in the trade wind belt and that humid or monsoonal climatic conditions existed at the time. This suggests that moist trade winds blew onto the Thelon orogen on the side closest to the Kilohigok Basin. Such an orographic effect would have caused rapid erosion, localized the position of the Thelon orogenic front, increased the flux of material through the orogenic belt, and caused more extensive progradation of the alluvial system. In Kilohigok Basin, initially the alluvial system was restricted laterally and drained longitudinally. Eventually, however, the alluvial system prograded beyond the proximal flexural arch and drained transversely into the coeval passive margin of Wopmay Orogen on the opposite side of the Slave craton.

Introduction

Foreland basins have been studied intensively from a geological and geophysical perspective in the past decade to investigate the controls on the evolution of collisional orogens (Beaumont, 1981; Jordan, 1981; Karner and Watts, 1983; Allen and Homewood, 1986). In particular, numerical geophysical modeling studies have investigated the effects of the various large-scale factors such as the elastic thickness of the lithosphere, relaxation of lithospheric stresses, and the location and magnitude of orogenic loads (Beaumont, 1981; Jordan, 1981; Karner and Watts, 1983; Quinlan and Beaumont, 1984; Royden and Karner, 1984; Lyon-Caen and Molnar, 1985; Allen and Homewood, 1986; Kominz and Bond, 1986; Moretti and Royden, 1988). Recent studies have begun to address the stratigraphic and sedimentologic effects of the redistribution of mass resulting from erosion of the

orogenic belt (Schedl and Wiltschko, 1984; Karner, 1986; Flemings and Jordan, 1987; Flemings and Jordan, 1989; Beaumont et al., 1990; Beaumont and Hamilton, 1990; Beaumont et al., 1992). The architecture of the sedimentary fill and unconformities in foreland basins directly result from these factors. By comparing the architecture of foreland basin strata of various ages, it may be possible to gain insights into the long-term evolution of the continental lithosphere (Grotzinger and Royden, 1990).

It is difficult to extend such comparisons to Precambrian basins because of the lack of precise time constraints afforded by biostratigraphy, for example. Recently, however, advances have been made in geochronologic and stratigraphic methods which allow more precise resolution of time stratigraphy in Precambrian sedimentary basins. The principles of sequence stratigraphy, developed in Phanerozoic basins (Vail et al., 1977; Haq et al., 1987; Van Wagoner et al., 1988), have recently been applied to subdivide Precambrian strata into unconformity-bounded depositional sequences (Christie-Blick et al., 1988; Bowring and Grotzinger, 1992). These depositional sequences have chronostratigraphic significance and allow refined time-stratigraphy, intrabasinal correlation, and the resolution of the geometry of stratal packages in Precambrian basins. By defining depositional sequences in Precambrian foreland basins, it may be possible to make qualitative and quantitative comparisons with Phanerozoic basins (Grotzinger and Royden, 1990). These sequences can be calibrated in absolute time if datable volcanic ash beds can be found, often with precision rivaling that of Phanerozoic successions (Krogh, 1973; Krogh, 1982), so that absolute chronostratigraphy may be established (Bowring and Grotzinger, 1992). However, the relative chronostratigraphy established by sequence stratigraphy remains a useful framework, independent of geochronologic methods.

The Early Proterozoic Kilohigok Basin in the northwestern Canadian Shield provides a superb setting to address some of these issues because of excellent exposure of sedimentary rocks, the divisibility of the strata into unconformity-bounded depositional sequences, and the presence of several zircon-bearing tuff beds that allow U-Pb geochronolgy to place absolute age constraints on the depositional sequences (Bowring and Grotzinger, 1992). This paper investigates the implications of the architecture of alluvial facies within this foreland basin, and, particularly, the transition within the foreland basin from largely marine conditions with laterally restricted alluvial facies to largely alluvial conditions draining transversely across the Slave craton for ten's of millions of years (Grotzinger and McCormick, 1988; McCormick and Grotzinger, in review). The main issue addressed by this study concerns how the distribution of large-scale unconformities in an alluvial sequence in foreland basins reflects fundamental shifts in subsidence and sedimentation patterns derived from the feedback between growth of the orogenic belt and climatically modulated

erosion, transport, and deposition of synorogenic detritus.

Geologic Setting

The Early Proterozoic (about 1.9 Ga) Kilohigok Basin lies in the northwestern part of the Canadian Shield (Figures 1, 2). It is a structural inlier within the Slave Province. The Slave basement rocks consist of a complexly deformed greenstone assemblage of late Archean (2.66-2.70 Ga) greywacke turbidites with subordinate bimodal and felsic volcanic rocks, intruded by 2.58-2.63 Ga syn- to post-tectonic granitoid rocks (Padgham, 1985; Hoffman, 1988). About 50 km east of the basin lie tectonically emplaced rocks of Archean basement and the Early Proterozoic Thelon Orogen (Figures 1, 2). The Thelon Orogen (1.92-2.02 Ga) is a regionally continuous belt of high-grade metamorphic rocks and plutonic rocks of possible arc affinity that contains a major syn-plutonic dextral shear zone (Hanmer and Lucas, 1985; Thompson et al., 1985; Hoffman et al., 1986; van Breemen et al., 1986; Hoffman, 1987; Hoffman, 1988). The Thelon Orogen is a crustal-scale feature that probably represents a suture between the Slave and Rae Provinces (Gibb and Thomas, 1977; Gibb, 1978; Hoffman et al., 1986; Hoffman, 1987; Hoffman, 1988; Tirrul and Grotzinger, 1990), and is the likely root zone for several northwest-directed thrust-nappes that are present only in the part of Kilohigok Basin closest to Thelon Orogen (Tirrul and Grotzinger, 1990). Flexural subsidence of Kilohigok Basin most likely resulted from convergence along the Thelon Orogen and emplacement of related thrust-nappes (Grotzinger and McCormick, 1988; Tirrul and Grotzinger, 1990).

The lower Goulburn Supergroup of Kilohigok Basin comprises two tectono-stratigraphic units (Grotzinger and McCormick, 1988). The Kimerot Group (Figures 3, 4) is a thin (0-500 m) southeast-facing prism that onlaps unfaulted Archean basement and consists of a lower transgressive siliciclastic fluvial-to-marine shelf unit overlain by a peritidal carbonate platform. Grotzinger and McCormick (1988) interpreted the Kimerot Group to be a passive margin sequence deposited cratonward of the hinge zone; the sequence was probably relatively short-lived (<20 million years). The end of carbonate deposition is marked by synchronous drowning of the carbonate platform on its distal margin with subaerial exposure and progressive erosion down to basement towards the northwest onto the Slave craton (Figure 4). This represents flexural arching of the platform in response to initial convergence and thrust loading of the Slave margin along the Thelon Orogen (Grotzinger and McCormick, 1988). The locations of progressive cut-outs of the carbonate and siliciclastic units in the Kimerot platform define a northeast trend interpreted to lie parallel to the axis of a flexural arch, the Gordon Bay Arch (Figures 2, 4) (Grotzinger and Gall,

1986). The crest of the arch lies about 75 km northwest of this cut-out as defined by the development of a regolith on the Archean basement where the platform has been completely eroded (Grotzinger et al., 1987). This regolith coincides with the minimum thickness of several depositional sequences within the overlying lower Bear Creek Group (Bowring and Grotzinger, 1992).

The Bear Creek Group comprises a largely siliciclastic succession that is divisible into a lower mostly marine unit and an upper mostly alluvial unit (Figures 3, 4). The lower Bear Creek Group consists of unconformity-bounded depositional sequences (Figures 3, 4: Hackett, Rifle, Beechey, and Link formations) (Grotzinger et al., 1988; Grotzinger et al., 1989). These southeast-facing marine shelf sequences pass sharply into correlative deep-water turbidite complexes over a shelf edge, the position of which remains laterally restricted through the evolution of the lower Bear Creek Group. Turbidite paleocurrents indicate southwestward flow, parallel to the trend of the Gordon Bay Arch and the Thelon Orogen, and perpendicular to stretching lineations in post-depositional thrust nappes in the southeastern end of the basin (Grotzinger and McCormick, 1988; Tirrul and Grotzinger, 1990).

The upper Bear Creek Group (Figures 3, 4) represents the change from marine to largely alluvial setting caused by progradation of a northwest-directed braided alluvial system (Burnside Formation) followed by gradual waning of alluvial input and return to shallow marine conditions (Mara-Quadyuk formations; Figures 3, 4) (McCormick and Grotzinger, in review) . Paleocurrents indicate that the main phase of alluvial sedimentation had remarkably uniform northwest drainage across the Slave craton (Figure 5). Conglomerates include intrabasinal and intraformational clasts, as well as extrabasinal ones derived from metamorphic sources to the southeast.

The abrupt transition from shallow marine carbonate platform (Kimerot Group) to deep marine basin that progressively fills to provide alluvial conditions (Bear Creek Group) characterizes many Phanerozoic foreland basins (Bally et al., 1966; Allen and Homewood, 1986). A tuff bed at the base of the lower Bear Creek Group just above the contact with the Kimerot Group has yielded a U-Pb zircon age of about 1.969 ± 0.001 Ga (Bowring and Grotzinger, 1992). This age closely constrains the drowning of the Kimerot platform and establishes a temporal link between deposition and flexural subsidence in Kilohigok Basin and magmatism and deformation in the Thelon Orogen. Another tuff higher in the lower Bear Creek Group has yielded a U-Pb zircon age of 1.963 ± 0.006 Ga. An U-Pb zircon age of 1.882 ± 0.004 Ga from a tuff bed at the base of the Recluse Group, the foreland basin deposits of Wopmay Orogen (Figure 4), constrains the end of Burnside Formation sedimentation. The basal Recluse Group correlates to the Mara Formation that overlies the

Burnside Formation.

Several deformational events overprinted the Goulburn Supergroup beginning with northwest-directed thin-skinned thrusting that only effected the southeasternmost part of the basin (Tirrul and Grotzinger, 1990). Thrust nappes and several allochthonous thrust-bounded outliers of the Goulburn Supergroup root to the southeast in the Thelon Orogen. Subsequent folding occurred in long-wavelength (about 50-75 km), northeast-trending, basement-involved folds, followed by transverse northwest-trending basement-involved folding of similar dimensions. The final phase of deformation involved approximately 115 km of left-lateral strike-slip offset on the Bathurst Fault (Tirrul and Grotzinger, 1990). The present configuration of the "basin" derives from selective structural preservation of infolded or faulted remnants rather than its original basin shape, which was probably that of a prism trending parallel to the Thelon Orogen that thinned to the northwest. This preservation has resulted largely from the basement-involved cross-folding. Fortuitously, this selective preservation produced an oblique cross-section of the original basin, continuously exposed for nearly 350 km perpendicular to both facies belts and the original basin strike. The Goulburn Supergroup has been regionally metamorphosed to lower greenschist grade with temperatures in the range of 300°C to 375°C on the basis of illite crystallinity data (Thompson and Frey, 1984), but nearly all of the Goulburn Supergroup lies at much lower grade.

Sedimentary Facies of the Burnside Alluvial System

The Burnside Formation comprises a diverse suite of largely alluvial sandy siliciclastic facies. The facies associations of the Burnside Formation are interpreted to represent three major environments: low-energy marine shelf, near or above storm wave base; braid delta environments comprising delta front, delta platform, braid delta plain; and distal to medial alluvial braid plain. The origin and significance of a thin carbonate tongue, which is restricted to the distal (northwestern) part of the basin, are also discussed. The delta plain and braid plain associations comprise the bulk of the Burnside Formation. They are remarkable in the simplicity and monotony of their facies motifs, the vertical and lateral persistence of each facies, and the largely gradational change between facies over hundred's of meters of section vertically and ten's to hundred's of kilometers laterally. Most of the facies are sandy and are nearly devoid of interbedded siltstone and mudstone, except thin laminae at bed tops in deltaic facies. Gravel is a minor component that is most abundant in the proximal (southeastern) part of the basin. Overall, these facies document a long-lived and laterally extensive alluvial system. The facies associations of the Burnside Formation are

described and interpreted in detail in McCormick and Grotzinger (in review). We include only brief descriptions and interpretations here. Table 1 summarizes the features of each lithofacies illustrated in Figures 6 and 7.

marine shelf facies

Marine facies associations are present primarily at the lower and upper boundaries of the Burnside Formation and in the distal (northwest) part of the basin. Marine facies are almost entirely siliciclastic, although one stratigraphically important carbonate unit (Burnside Dolomite) exists and is discussed separately below. Two associations of shallow marine facies are distinguished (Table 1). The first represents progradational low-energy siltstone-dominated shallow marine shelf. The second represents retrogradational storm- and wave-influenced mixed silty-sandy shelf facies.

low-energy silty shallow marine shelf

The first shelf association is a siltstone-dominated facies which range from mm-scale laminated mudstone to hummocky- or swaley-cross-stratified green siltstone (Figure 6a). Hummocky- and swaley-stratified siltstone commonly contain gutter casts. In sections transitional from the Link Formation into the Burnside Formation, these facies are commonly arranged in a coarsening-upwards succession over several meters to a few ten's of meters, with upward increase in the scale of cross lamination, bed thickness, and grain size. All grains are coarse siltstone or below and all sedimentary structures are wave-formed.

Laminated mudstones and thick massive siltstone are interpreted as suspension fallout below wave-base. Increasing scale of wave-formed structures suggest decreasing water depth and increasing influence of wave and storm processes. Gutter casts suggest significant bypassing in shallow water. These facies are interpreted as a low-energy, progradational, storm-influenced muddy shelf (Johnson and Baldwin, 1986; Myrow, 1987; Myrow et al., 1988). This association grades upward into transitional braid delta front siltstone associations over a few meters to ten's of meters as part of an overall progradational succession.

mixed silty-sandy marine shelf and sand bars

The second marine shelf association comprises a mixed sandstone-siltstone facies and a sandstone-dominated facies that commonly intergrade. In the mixed facies, fine- to medium-grained sandstones a few cm's to 20 cm thick are sharply interbedded with mudstone-siltstone (Figure 6b). Sandstones are commonly wave-rippled or have low-angle cross-laminae. Interbedded siltstones contain wave ripples and parallel laminae.

The sandstone-dominated facies contains white, tabular-bedded, trough cross-bedded, medium- to coarse-grained sandstones that locally contain grains of rounded chlorite inferred to be after glauconite. These sandstone beds commonly cap asymmetric, coarsening-upwards parasequences several meters thick. Carbonate (micrite) cement is common in the upper few beds. The coarsest beds commonly have erosional lags on top and are abruptly overlain by mixed siltstone and sandstone. Even in sequences that fine upwards over ten's of meters, smaller-scale coarsening upwards sequences several meters thick are superimposed. No evidence for reactivation surfaces, herringbone cross-bedding, tidal bundling, or bipolar paleocurrent trends was observed in either the mixed or sandstone-dominated facies.

The mixed facies is interpreted as storm- and wave-influenced shelf sediments deposited near fairweather wave base under occasional storm-generated combined flow conditions (Nottvedt and Kreisa, 1987). The sandstone-dominated facies suggests shallowing-upward marine sand bars parasequences (de Raaf et al., 1977; Johnson, 1977), although tidal influence cannot be ruled out (Johnson and Baldwin, 1986; Nio and Yang, 1991). Micrite cements at the top of parasequences and scoured, lag-covered upper surfaces suggest subaerially exposure and vadose diagenesis, identical to features present in other units in the lower Bear Creek Group (Grotzinger et al., 1987; Grotzinger et al., 1988).

Paradoxically, the medium-grained sandstone in the sandstone-dominated association is coarser than the very fine to fine-grained sandstone in transitional alluvial facies described below. This suggests that sand in this marine shelf association is derived from another source. Grotzinger et al. (1989) suggested that the source of medium- to coarse-grained sand and relatively fresh, coarse feldspar in shallow marine facies in the lower Bear Creek Group must have been derived from an exposed upland to the northeast, probably along strike of the Gordon Bay Arch (Figure 2).

sandy braid delta facies

The term braid delta connotes coarse-grained siliciclastic sedimentary environments influenced by alluvial processes upon which the imprint of marine processes can be distinguished (McPherson et al., 1987). Braid delta facies, as defined by McPherson et al. (1987) and employed in recent studies, contain significant amounts of gravel. The bulk of the Burnside Formation represents a sandy alluvial system in which significant bedded conglomerates are restricted largely to the proximal end of the basin. We employ braid delta to mean sandy braided alluvial facies that show evidence of marine influence. The distinction of the deltaic environment from coastal plain and braid plain environments is important for paleogeographic reconstruction and in the stratigraphic interpretation of the effects of

relative sea level change on the alluvial system. Three associations identified in the Burnside Formation make up the braid delta setting: delta front, delta platform, and delta plain.

delta front (rippled siltstone-sandstone)

This association, comprising several facies (Table 1), is marked by the first occurrence of red mudstone-siltstone beds that are interbedded with wave rippled very fine-grained sandstone. Coarse siltstone to very-fine-grained sandstone beds coarsen and thicken upward. Parallel- and low-angle cross-laminae are abundant. Current, wave, and interference ripples are common as is extensive soft-sediment deformation. This association is present in the lower few meters to few ten's of meters of the Burnside Formation (Figures 6c,d).

The abundance of wave-formed structures, such as wave and interference ripples, suggests deposition in a shallow subaqueous environment, well above wave-base, but without subaerial exposure. Soft-sediment deformation supports a high rate of terrigenous input that caused slope oversteepening and promoted slumping. The red color of the alluvial-influenced facies underscores the idea of terrestrial source for this sediment. This association is most consistent with the front of a prograding fluvially dominated delta (Elliot, 1986).

braid delta platform (tabular bedded sandstone)

This association consists of tabular bedded, planar-laminated sandstone with minor wave and current ripples. The sandstone is well sorted, very fine- to fine-grained, pink, and subarkosic. Beds are tabular, have sharp bases, and are laterally persistent for ten's to hundred's of meters. Mud clasts commonly line sours at the base of and internal to beds. Locally, broad scours up to 10 m wide and 1 m deep contain fine- to medium-grained, trough cross-bedded sandstone. The trough cross-bedded sandstone within the scours is enclosed entirely within the planar laminated sandstone.

This association resembles distributary mouth shoals and swash bars of a braid delta platform described from the Ordovician of Libya by Vos (1981). Individual beds are interpreted as the product of single flood events that supplied sand from braid delta distributary channels that was subsequently reworked by storm and wave action. The trough cross-bedded sandstone in broad scours are interpreted as shallow braid delta distributary channels that cut across the delta platform.

In coarsening-upward sequences, this association grades from the underlying delta front facies and is overlain gradationally by braid delta plain facies in the proximal end of the basin, whereas in the distal foreland it is sharply overlain by braid plain facies.

braid delta plain (trough bedded sandstone with mud clasts)

This association comprises trough cross-bedded fine- to medium-grained sandstone with common clay chips. Cross-sets are 10 to 50 cm thick. Mudstone with associated sand-filled desiccation cracks is present very uncommonly in this facies.

This trough cross-bedded sandstone is distinguished from delta platform facies by the laterally extensive beds of predominantly trough cross-bedded sandstone. The presence of clay chips indicates scouring of mud-covered overbank areas or intertidal flats that were cannibalized during fluvial channel avulsion. The main distinction between the delta plain and the distal braid plain (described above) is that the delta plain facies contains clay chips. The delta plain facies lies within asymmetric coarsening-upward parasequences interpreted as deltaic cycles. These parasequences are present in the Transitional member of the Burnside Formation and the Tinney Hills member of the underlying Link Formation (Grotzinger et al., 1988) in the proximal (southeast) part of Kilohigok Basin (Figures 8, 9).

alluvial braid plain facies

The alluvial braid plain facies are those in which alluvial processes predominate with little or no evidence for marine reworking. The alluvial braid plain is divided into four associations: distal braid plain that comprises the bulk of the Burnside Formation across the entire outcrop belt, and three associations inferred to represent the medial braid plain environments. The medial braid plain environments are distinguished by the increasing scale of cross-bedding, the caliber of sand sized material, and, locally, the presence of gravel. These features suggest an increasing scale of alluvial channel systems operating. One alluvial association, restricted to the proximal part of the basin, carries a significant component of conglomerates.

distal braid plain (single-storeyed trough bedded sandstone)

This association comprises the bulk of the Burnside Formation, especially in the outcrop belt to the west of Bathurst Inlet (Figures 4, 8, 10). This lithofacies consists of repetitive 50-120 cm beds of fine- to medium-grained, pink subarkose with medium- and large-scale trough cross-bedding (10-30 cm and 30-80 cm, respectively) that decreases in scale upwards within beds. Minor parallel laminae and ripple cross-laminae are present near the tops of beds. Gravel and mud chips are uncommon. Paleocurrents in this facies are commonly unimodal with low dispersion.

The upward decrease in grain size, the scale of trough cross-bedding, and unimodal low-dispersion paleocurrent directions suggest that this association represents vertical

infilling of broad, shallow channels by migrating sinuous-crested subaqueous dunes in a sandy delta plain to lower braid plain environment subject to rapid channel switching and cannibalization (Campbell, 1976; Eriksson and Vos, 1979; Vos and Tankard, 1981; Walker and Cant, 1984).

medial braid plain without gravel (multi-storeyed trough bedded sandstone)

Two associations, both interpreted as medial braid plain environment, are distinguished from the distal braid plain facies described above by thicker cross-sets, greater lateral continuity of cross-sets and coarser grain size of sand. Stratigraphically, the first association, which largely lacks gravel, is present in the lower part of the Burnside Formation in the Buff Sandstone member (Figures 3b, 9); the other association is present in the Gravelly Sandstone member (Figures 3b, 9).

The first association contains medium- to coarse-grained trough cross-bedded subarkose in beds 120-300 cm thick. Beds show incomplete fining-upward sequences and crosscutting channel scours. Individual beds are traceable over hundred's of meters laterally. The repetition of trough cross-bedded sandstone is broken at intervals of 8 to 20 meters by a meter or two of planar-laminated or ripple cross-laminated sandstone that defines tops of bedsets. The surfaces at the base of bedsets can be traced for ten's of kilometers laterally between sections 2 and 3. Paleocurrents are unimodal with low-dispersion toward the west northwest ($294° \pm 27°$, n=115). This association is restricted to the Buff Sandstone member (Figures 3b, 9) which pinches out southeast of the crest of the Gordon Bay Arch (Figure 2, 4, 8).

The repetition of trough cross-bedding, lateral persistence of bedset-bounding surfaces, and the incomplete fining-upwards sequences resemble the Westwater Canyon member of the Morrison Formation, a Jurassic braided fluvial sheet sandstone with very high width-to-depth ratios (Campbell, 1976). Very high width-to-depth ratios (100 to >1000) typify bedload-dominated, braided fluvial systems (Friend, 1983; Miall, 1988). This association is interpreted as the product of perennially flowing, laterally migrating, fluvial channel systems that were many meters to ten's of meters deep with mostly longitudinal migration of bedforms within the channel system.

medial braid plain (trough- and tangentially cross-bedded sandstone)

This gravel-poor medial braid plain association differs from the previous association in the presence of broad scours or channels that are filled laterally by planar-tangential cross-beds then overlain by smaller scale trough cross-beds (Table 1). The planar tangential cross-

bedding is commonly highly oblique to both channel scours and trough cross-bedding that tends to be unimodal with low dispersion. Sandstones are locally pebbly with gravel decreasing upwards within beds. Beds are 120-500 cm thick with a few cm of relief on beds. Channels are incompletely filled by the tangential planar cross-sets. The remaining channel topography is commonly filled by smaller scale trough cross-sets that have paleoflow directions along parallel to channel scours.

The scale of bedding, larger scale of cross-bedding, and divergent paleocurrent patterns within beds suggest a combination of lateral or oblique accretion at different topographic levels within fluvial channels and vertical accretion at higher levels during flood stage on a sandy braid plain. Rust (1984) indicated that gravelly planar cross-bedding is more common in ancient braid plain successions. He interpreted this as a result of deeper and more frequent floods, which would be especially favored by especially humid conditions, which created greater topography within braided stream channels.

gravelly medial braid plain (sheet gravel and trough cross-bedded sandstone)

This association comprises clast-supported conglomerate and trough cross-bedded, medium- to coarse-grained and pebbly sandstone (Table 1). Beds in the conglomerates range from sheets that line scours a few meters deep and up to 20 meters wide, to crudely planar-stratified sheets. All the conglomerates are clast-supported. Beds are commonly 50-500 cm thick. The pebbly sandstone is similar to the multi-storey trough cross-bedded sandstone, except that cross-laminae contain gravel. Trough cross-sets lacking gravel overlie the gravelly cross-beds. The preservation of complete fining-upwards cycles is more common upward, concomitant with decreasing gravel content.

Basal scours, scours lined with gravel, clast support of conglomerates, crude planar stratification, association with trough cross-bedded sandstone, and fining-upwards trends within beds suggest that this association was deposited in deeply scoured channels of braided streams in the medial braid plain. These characteristics indicate that even this highest-energy facies of the Burnside Formation was deposited by stream flow on a braid plain at least 100 km from the source area (Figure 4, 8, 10). This association is present only in the proximal part of the basin east of the Gordon Bay Arch.

Burnside Dolomite

In the distal part of Kilohigok Basin, a unique, distinctive wedge of clastic dolomite mixed with siliciclastic detritus is present, called the Burnside Dolomite. The Burnside Dolomite is sandwiched between the otherwise sandy Burnside alluvial facies and forms an

eastward-tapering prism, a stratigraphic pattern opposite to those of the siliciclastic facies of the Burnside Formation (Figures 3b, Table 1). The Burnside Dolomite has been seen in outcrop from section 13 to as far east as sections 10 and 16 (Figures 2, 4, 10).

At section 13, the Burnside section is incompletely preserve, but contains a dolomitic interval about 100 m thick close to the top of the section. The carbonate contains cyclic alternations of laminated siliciclastic siltstone or mudstone passing upward into clastic-textured dolomite with wave- and current-ripples, minor syneresis cracks, and abrupt upper contacts. Microbial laminites and domal stromatolites cap several cycles and they increase in abundance upward. The cycles suggest that the carbonate facies represents subtidal to intertidal shallowing-upwards sequences in a mixed siliciclastic-carbonate system.

From west to east, the Burnside Dolomite thins, the laminites and stromatolites disappear, fewer sedimentary structures are present that suggest subtidal deposition, and siliciclastic detritus increases in abundance and grain size. The dolomitic interval becomes predominantly clastic textured dolarenite and dolosiltite mixed with siliciclastic material (Figure 6e).

Near section 10 (Figure 2), coincident with the crest of the Gordon Bay flexural arch, the Burnside Dolomite comprises a thin (3 m) interval of cross-bedded intraclastic carbonate, interpreted to have been deposited in shallow water, upon which is superimposed diagenetic fabrics suggesting early peritidal marine cementation followed by subaerial exposure and vadose diagenesis (Grotzinger et al., 1987). Outcrops west of this one represent entirely marine facies upon which no subaerial diagenetic fabrics are superimposed.

Hoffman et al. (1984) and Grotzinger (1985) first correlated dolomitic units at section 13 and section 12 (Figures 2, 10). Further, they pointed out that the Burnside Dolomite resembles shallowing-upwards, shale-based lagoonal facies of the Rocknest Formation of Wopmay Orogen (Grotzinger, 1986b) except that the siliciclastic material is coarser in Kilohigok Basin. The closest outcrop of the Rocknest Formation lies at the easternmost edge of Wopmay Orogen at Takijuk Lake, about 70 km beyond section 13 (Figure 1). The stratigraphic implications of the correlation between the Burnside Dolomite and the Rocknest Formation are discussed below.

Stratigraphic Architecture of the Burnside Alluvial System

The stratigraphic distribution of the facies associations of the Burnside Formation allows identification of both transitions from marine to alluvial environments, and unconformable contacts at these transitions (Figures 8, 9, 10). The stratigraphic distribution of these unconformities provides a powerful tool for assessing the evolution of the alluvial

system and the foreland basin. Figure 11 summarizes the paleogeographic evolution of the Burnside alluvial system.

Several key stratigraphic relationships emerge from the distribution of alluvial facies. The marine to alluvial transition at the base of the Burnside Formations is conformable in the proximal (southeastern) part of the basin, but significant intraformational unconformities lie above the transitional deltaic facies. To the northwest the intraformational unconformities cut down to the base of the formation and amalgamate, so that over the Gordon Bay Arch, braid plain facies directly overlie marine facies. To the northeast along strike of the Gordon Bay Arch, medial alluvial facies lie directly on crystalline basement (Figure 2, section 15). Beyond the arch in the distal foreland, the amalgamated unconformities separate, then merge again, into a profound erosional unconformity at the base of the Burnside Formation nearest to Wopmay Orogen. This distal unconformity and flexural bulge existed contemporaneously on the most distal margin of Kilohigok Basin, nearest to Wopmay Orogen.

A probable eustatic rise in sea level caused transgression of the Burnside Dolomite across at least half of the Slave craton and the Burnside alluvial plain. An abrupt facies change marks the end of alluvial sedimentation, and the upper contact of the Burnside Formation is locally an erosional unconformity. Finally, the locations of erosional unconformities recorded by the Burnside alluvial facies suggest that the two independent flexural arches in the foreland probably migrated several ten's of kilometers towards the center of the Slave craton by the end of alluvial sedimentation.

distribution of unconformities during initial alluvial sedimentation

Two major proximal-to-distal trends within the Burnside Formation are evident in cross-section. The first trend is that the lower transitional alluvial facies, present only in the proximal part of the foreland, southeast of the Gordon Bay Arch, forms a wedge that is highly tapered to the northwest (Figures 4, 8, 9). This contrasts sharply with the much more tabular, laterally extensive sheet of alluvial sediments represented by the upper part of the Burnside Formation; this upper sheet correlates with Burnside Formation sediments deposited on the cratonic foreland (Figures 4, 8, 10). These two major stratigraphic units within the Burnside Formation are separated locally by a profound erosional unconformity.

The stratigraphic geometry of the interval from the base of the Link Formation through the main conglomeratic unit in the Burnside Formation thins to the northwest over the Gordon Bay Arch, thickens towards section 12, then thins towards section 14 (Figures 4, 8). This geometry mimics the underlying marine facies of the lower Bear Creek Group. The increasing abundance of wave-influenced sandy shelf facies (Figures 4, 8) to the northwest in

the underlying foreland basin strata (Link Formation) suggests that the cratonic foreland experienced shallow water conditions more often than did the proximal, southeastern end of the basin (Grotzinger and McCormick, 1988; McCormick and Grotzinger, 1988; Bowring and Grotzinger, 1992). This is consistent with the foreland basin setting for the Bear Creek Group that predicts lower subsidence rates over the peripheral bulge and, therefore, more persistent shallow water conditions.

The Transitional member of the Burnside Formation, which is present only to the southeast of the Gordon Bay Arch, east of the Bathurst Fault, consists of up to 3 asymmetric coarsening-upwards sequences of braid delta facies (Figures 8, 9). These sequences are interpreted as a prograding braid delta system. Paleocurrents from trough cross beds in these sequences suggest that the braid delta prograded to the northwest, but show a distinct southwestern mode (Figure 5), more parallel to the trend of the Gordon Bay Arch. This suggests that the braid delta was restricted behind the Gordon Bay Arch, and that the initial alluvial system drained longitudinally to the southwest. Individual coarsening-upwards parasequences thin to the northwest and west of the Bathurst Fault, and the braid delta plain facies within the three parasequences pass laterally into tabular-bedded very-fine-grained sandstone representing the braid delta platform. The lateral correlation of braid delta facies to delta platform facies is underscored by the fact that in the proximal end of the basin, delta platform facies represent a few ten's of meters of the coarsening-upwards sequences, and trough cross-bedded sandstone with mud clasts predominate (braid delta plain). In contrast, west of the Bathurst Fault zone the Transitional member is over 200 m thick, but it consists entirely of delta platform facies (Figures 2, 8, sections 4 and 5). The paleocurrent trends and lateral facies changes indicate that the braid delta was restricted to the southeast of the Gordon Bay Arch during initial alluvial progradation.

In the proximal part of the basin, the coarsening-upwards braid delta parasequences of the Transitional member everywhere are overlain sharply by coarser multi-storeyed medial braid plain facies of the Buff Sandstone member (Figures 8, 9). The scale and organization of cross stratification, the lateral persistence of facies, and the grain size are very much greater in the Buff Sandstone member. This suggests that the contact between braid delta facies and braid plain facies represents an erosional unconformity that progressively cuts through more section to the northwest towards the Gordon Bay Arch (Figures 4, 8, 9). Judging by the sharp contact everywhere, the contact between the Transitional member and Buff Sandstone member is probably disconformable throughout the proximal part of the basin. This implies that there was a significant hiatus and erosion between the deposition of gradational braid delta and distal braid plain facies southeast of the Gordon Bay Arch and deposition of medial braid plain facies over and beyond the arch. The superposition of alluvial facies becomes

more abrupt to the northwest towards the Gordon Bay Arch where the same medial braid plain facies rest directly on facies of increasingly marine character. Braid delta plain facies and the coarsening-upward cycles within braid delta facies are not present west of the Bathurst Fault (Figures 2, 8); only the delta platform facies is preserved to the northwest on the craton (Figures 8, 10).

The contact between the Buff Sandstone and the Conglomerate members is equally abrupt, and probably also is an erosional unconformity that becomes more pronounced over the Gordon Bay Arch (Figures 4, 8, 9, 10). The basal alluvial facies of the Burnside Formation on the crest of the Gordon Bay Arch contains conglomerate resting directly on shelf facies sandstone and siltstone. The Buff Sandstone member contains minor amounts of gravel that consist solely of vein quartz. In contrast, the Conglomerate member contains a diverse polymictic population that includes abundant meta-greywacke and schist clasts. Metamorphic clasts are present in the basal Burnside Formation near the Gordon Bay Arch. This strongly suggests that the basal Burnside contact is an erosional unconformity over the arch and that disconformities within the main alluvial section amalgamate over the arch. Furthermore, the basal Burnside Formation on the craton is largely time equivalent to the Conglomerate member that is stratigraphically high within the section in the proximal part of the basin. This means that the basal Burnside contact on the craton represents a very large hiatus, especially over the Gordon Bay Arch and Rockinghorse arches.

Northwest of the Gordon Bay Arch, the transition from marine shelf facies of the Link Formation to alluvial braid plain facies of the Burnside Formation is gradational but the transition is much thinner. The reappearance of a transitional unit mimics thickening of marine shelf facies in underlying Lower Bear Creek Group sequences. The transitional marine-to-alluvial sequence is best exposed at section 12 and is 180 m thick (Figures 8, 10). The abrupt unconformable contact that is seen in sections over the flexural arch appears to be absent here, but there may be subtle, unrecognized surfaces of bypassing in this transitional interval. This suggests that the surface at the base of the Burnside Formation over the Gordon Bay Arch represents amalgamated unconformities and this single surface splits into two surfaces towards section 12. Regardless, the transitional interval at section 12 in the distal foreland represents the lateral correlative of the Transitional, Buff Sandstone, and Conglomerate members.

This transitional interval thins and disappears to the west of section 12 and a sharp, unconformable contact exists at section 14 (Figures 2, 4, 8, 10). At section 14, pebbly sandstone at the base of the Burnside Formation rests sharply on red mudstones of the Rifle Formation of the lower Bear Creek Group (Figure 8) that were deposited below wave base (Bowring and Grotzinger, 1992), indicating that two formations in the lower Bear Creek

Group and any transitional Burnside facies are cut out in this area (McCormick and Grotzinger, 1988; Grotzinger et al., 1989). This is the most profound erosional unconformity developed within the Burnside Formation along this cross section, because even over the Gordon Bay Arch all formations in the lower Bear Creek Group are present. Unlike the Gordon Bay Arch, the arch in this distal part of the foredeep probably does not relate to thrusting along the Thelon Orogen, but rather to the evolution of Wopmay Orogen on the west side of the Slave craton (Figures 1, 2). This is supported by flexural modeling of the lower Bear Creek Group that show that the effective elastic thickness of the Slave lithosphere was probably 8-16 km, implying a flexural wavelength of about the Slave craton lithosphere was on the order of 30-50 kilometers (Grotzinger and Royden, 1990). Simple plate flexure of an elastic beam of this range of flexural wavelengths would put the crest of a flexural arch at about 70-120 km from the plate end where a thrust load is applied (Turcotte and Schubert, 1982). The distal Rockinghorse flexural arch lies well beyond the flexural wavelength measured from the edge of the current eastern limit of Thelon Orogen. The significance of the distal Rockinghorse Arch is discussed below.

Stratigraphic trends and paleocurrents from the lower Burnside Formation suggest that the orientation of the Gordon Bay Arch may have changed between initiation of the foreland basin and deposition of the Burnside Formation. The trend of the Gordon Bay Arch is constrained by two sets of piercing points defined by the erosional cutout of the Kimerot Group before deposition of the lower Bear Creek Group (Figures 2, 3a, 4). This trend is southwest-northeast. The geologic base map (Figure 2) is restored for strike slip faulting on the basis of the Kimerot Group cutouts. However, if Burnside sections 3 and 4 are projected onto a northwest-trending line, perpendicular to the original Gordon Bay Arch trend, section 3 would lie down paleoslope from section 4, despite great thinning of all Burnside members from section 3 to section 4. This can be resolved by projecting sections 3 and 4 onto a section parallel to the fluvial paleocurrent trend. Paleocurrents from the Buff Sandstone member trend roughly 295°, or about 25° counterclockwise to the line normal to the original Gordon Bay Arch. Because the mean direction of fluvial paleocurrents from the deepest parts of the fluvial channels are sensitive indicators of paleoslope and gradients in subsidence (Alexander and Leeder, 1987), this 25 degree difference suggests the axis of the basin rotated counterclockwise between initiation of the flexural subsidence and the onset of major alluvial sedimentation. This further suggests that the direction of thrusting out of Thelon Orogen was more west-northwest-directed, which is consistent with the trends north-northeast trend of metamorphic rock bodies exposed today in Thelon Orogen (Thompson et al., 1985; Thompson et al., 1986).

The lower contact of the Burnside Formation in the northernmost section studied at

section 15 (Figures 1, 2) differs from all other locations. If the sinistral slip along the Bathurst Fault zone is removed (as in Figure 2), section 15 aligns with the original northeast trend of the Gordon Bay Arch. At section 15, facies interpreted as Burnside medial braid plain rest nonconformably on crystalline syenogranite basement; the entire Kimerot and lower Bear Creek Group is missing. Paleocurrents near section 15 are uniformly northwest-directed at all levels in the stratigraphic section (Figure 5). McCormick and Grotzinger (1988) have argued that the Gordon Bay Arch probably had a domal shape rather than a simple linear arch shape, and that section 15 may have been near the crest of the dome (Figure 2, 11). We call this feature the Buchan Bay dome. The domal shape is consistent with the along-strike variations in the location, width, and magnitude of orogenic loads reflected in the isopachs of Phanerozoic foredeeps (Jordan, 1981; Quinlan and Beaumont, 1984; Cross, 1986).

Two interpretations are possible for the depositional and erosional history near section 15. First, the lower Bear Creek Group could have been deposited near section 15 and subsequently eroded before Burnside alluvial deposition. Alternatively, the Buchan Bay dome could have been emergent throughout most of the deposition of the marine foredeep sequence, and was covered only when the alluvial system aggraded sufficiently to cover the bulge and to induce some subsidence through sediment loading. The latter case seems more likely for two reasons. Paleocurrent trends in the marine shelf sedimentary sequences of the lower Bear Creek Group are uniformly southwest-directed, pointing to a source near section 15 (Figure 2, 12). Also, the marine siliciclastic sediments contain common unaltered feldspar, which normally would not be expected for high-energy marine shelf environments associated with the lower part of the foreland basin. This is consistent with a proximal source area of areally extensive syenogranite basement located around section 15. Braid delta facies of the Burnside Formation with similar southwest-directed paleocurrent modes contain abundant fresh feldspar, whereas medial braid plain facies with northwest paleocurrent modes contain very little fresh feldspar and significant proportions of polycrystalline quartz indicative of derivation from metamorphic source areas (see chapter 3). All these data suggest that the area near section 15 was an emergent flexural dome (Figure 2, 12), and that the dome acted as the source of fresh felsic detritus to the lower Bear Creek Group until the Burnside Formation medial alluvial facies prograded across the craton.

The second major stratigraphic trend in the Burnside alluvial sequence is that the upper Burnside Formation does not display the extensive lateral changes in thickness that are present in the lower part (Transitional and Buff Sandstone members; compare Figures 2 and 9 with Figure 10). On the basis of the relationships discussed above, the Burnside Formation present on the craton must be correlative with the base of the Conglomerate member in the

proximal part of the basin. Paleocurrent data support this correlation. First, paleocurrents in the Transitional member in the Tinney Hills are largely southwest-directed, parallel to the Gordon Bay Arch, whereas they are northwest-directed in overlying members (Figure 5, see especially inset). On the craton west of the Bathurst Fault, paleocurrents are uniformly northwest-directed from the base of the formation, so transverse drainage always existed in the cratonic foreland. Also, the uniform paleoslope implied by paleocurrent data indicates that one alluvial system deposited the bulk of the Burnside Formation correlative with that part on the craton. The only departure from this tightly clustered paleocurrent grouping is at sections 13 and 14, the most distal sections, where a slightly more northerly pattern exists (Figure 2, 5). This is the only region where a different source area could be suggested, but paleocurrents there may have been deflected to the north by a gradient in subsidence that is implied by the northward thickening of correlative strata in Wopmay Orogen which is discussed below. The remarkable uniformity of paleocurrents across most of the basin implies that the alluvial system comprised a single large alluvial apron that lapped up against the Thelon mountain front. The slightly deflected distal paleocurrents suggest that perhaps a second large alluvial system to the south interfingered with the main west-northwest-flowing Burnside system. We prefer to interpret the deflected paleocurrent patterns as the result of a more northerly subsidence gradient related to the evolution of the passive margin of Wopmay Orogen.

If, as we believe, all the Burnside sedimentary rocks constituted a single alluvial system, conglomeratic sandstone that is present at or near the base of the Burnside Formation beyond the Gordon Bay Arch would correlate to proximal section no lower than the Conglomerate member (Figure 9). Thus most of the Burnside Formation over the craton is probably younger than the Buff Sandstone and perhaps the Conglomerate member in the proximal foredeep. This divides the Burnside Formation into two time-stratigraphic units. The lower unit, corresponding to the Transitional and Buff Sandstone members, forms a highly tapered wedge that thins to the northwest and is present only as thin strip in the depression between Gordon Bay and Rockinghorse arches. The upper unit of the Burnside Formation is much more tabular and comprises all the Burnside Formation that lies above the base of the Conglomerate member in the proximal foreland, and virtually all the Burnside Formation northwest of the Gordon Bay Arch. This correlation that splits the Burnside Formation into two gross units implies that the thickness, and therefore, the accumulation rates, of the upper Burnside Formation must have been much more uniform across the entire basin during upper Burnside time. This is not the highly asymmetric pattern of subsidence and sediment accumulation commonly associated with foreland basins. This implies that the pattern of subsidence across the basin changed markedly between the time of

initial progradation of the braid delta system, which was largely restricted southeast of the Gordon Bay Arch, and the time when braided alluvial facies prograded across the entire craton, over 350 km from the source area. McCormick and Grotzinger (in review) have suggested that the reason for the great lateral extent of the Burnside Formation may be due to humid climate and resulting perennial discharge or highly seasonal monsoon conditions. This interpretation is consistent with the lack of decelerating flow structures, the lack of fine detritus in any of the alluvial facies seen across the basin, the wide vertical and lateral extent of alluvial facies, and lack of aeolian facies. The implications of humid climate on the development of the foreland basin and Thelon Orogen are discussed below.

Burnside Dolomite and transgression of the alluvial system

The Burnside Dolomite represents the most extensive and significant transgression of the alluvial system, and it represents a crucial stratigraphic link between the foreland basin in Kilohigok Basin and the passive margin of Wopmay Orogen (McCormick and Grotzinger, 1988). The Burnside Dolomite forms an *eastward*-tapering wedge of mixed carbonate-siliciclastic and cyclic carbonate in an otherwise entirely sandy siliciclastic interval. Hoffman et al. (1984) interpreted the Burnside Dolomite as the probable correlative of the Rocknest Formation, a carbonate platform sequence in Wopmay orogen (Figures 2, 10). The Rocknest Formation consists of a well-developed shoal-complex and inner shelf cyclic facies that pass laterally westward into an outer-shelf reefal rim (Grotzinger, 1986a). Grotzinger (1985) and McCormick and Grotzinger (1988; in review) have argued that the Burnside Dolomite is equivalent to an interval within the Rocknest Formation that represents incipient drowning of the carbonate platform, which in turn caused back-stepping of all facies belts over 100 km eastward toward the Slave craton and Kilohigok Basin. Grotzinger (1986a) attributed this incipient drowning to a eustatic rise in sea level.

Two observations strengthen the correlation between the Burnside Formation and the passive margin in Wopmay Orogen. First, siliciclastic sediments that underlie the Rocknest carbonate platform (Odjick Formation) that outcrop about 70 km west of section 13 (Figures 1, 2) contain coarsening upwards parasequences of coarse, texturally submature, trough-cross-bedded sandstones that are identical to sandy distal facies of the Burnside Formation (McCormick and Grotzinger, 1988). Second, the correlation between the Rocknest Formation and the Burnside Dolomite is strengthened by the eastward increase in the amount and caliber of siliciclastic detritus in the Rocknest Formation that would be consistent if a the cyclic carbonate platform passed laterally into a braided alluvial system. This correlation suggests that the paleogeography of the Rocknest lagoonal shelf influenced

the character of Burnside braid delta sedimentation. The Rocknest shelf has an outer reefal rim that was an effective buffer of open marine waves (Grotzinger, 1986b). The eastward increase in the caliber of siliciclastic detritus in Rocknest carbonate cycles and the lateral restriction of the Rocknest Formation (about 150 km) as compared to Phanerozoic passive margins (>250 km) led Hoffman et al. (1984) to the conclusion that the Rocknest platform was correlative with the Burnside alluvial system. Thus the Rocknest lagoon was the sink for fine-grained Burnside detritus. In addition, the presence of the sediment load of the Burnside Formation on the Slave craton may have caused significant isostatic subsidence and allowed the Rocknest lagoon to expand farther eastward onto the Slave craton.

Near section 10 (Figures 2, 4, 8), where the easternmost outcrops of the Burnside Dolomite are seen, the Burnside Dolomite exhibits its most shallow water facies. The eastern facies of the Burnside Dolomite contain the coarsest siliciclastic material and diagenetic fabrics suggestive of subaerial exposure and vadose diagenesis are superimposed on the clastic dolomite. At section 12, fifty km to the west, the Burnside Dolomite is characterized by an entirely subaqueous marine facies in which no subaerial diagenetic fabrics are present. section 10 is near but slightly westward of the crest of the Gordon Bay flexural arch that was active during the early phases of the foredeep (lower Bear Creek Group) and during the previously described onset of Burnside alluvial sedimentation. These observations suggest that if the flexural arch migrated during Burnside alluvial sedimentation, it may have migrated westward a few ten's of kilometers from its position at the onset of alluvial sedimentation. This is consistent with the imposition of a significant sediment load on the western margin of the Slave Province related to infilling of the foreland basin and progradation of the alluvial system across the craton. This would cause the locus of the flexural bulge to migrate westward, regardless of any convergence along the Thelon Orogen.

Facies transitions in two transgressive sequences at section 13 differ in an interesting way (Figure 10). One represents relatively abrupt shutting-off of the fluvial system and onset of storm-influenced sedimentation on a muddy shelf. The other represents a gradual transgression with wave reworking of fluvially supplied sand creating a sandy shelf. In the first case, white, texturally mature, medium-grained sandstones are intercalated with mudstone suggesting that they are a product of background wave and storm processes when fluvial input was reduced. The coarse caliber and high maturity of the sandstones require winnowing of Burnside fluvial sands, probably from shoreface erosion of fluvial bars and spits. In the second case, transitional with the Burnside Dolomite, there is a gradational change from trough cross-bedded delta plain sandstone to planar-laminated delta platform sandstone indicating that fluvial input to the shelf was continuous. Even when mud interbeds become common just below the Burnside Dolomite, pink, tabular, planar-

laminated sandstone beds persist. This suggests that either the rate of relative sea level rise was lower than in the former case, or that the rate of sediment input from the Burnside alluvial system was much higher than before. The interpretation of higher sediment supply rate, and, therefore, alluvial dominance, is favored for the upper interval, because marine facies of the Burnside Dolomite extend much farther eastward than the marine facies found at the base of the section and therefore represents a much more extensive transgression of the alluvial system. Marine facies at the base of the section are restricted to the area between sections 12 and 13 (Figures 2, 8), whereas marine facies of the Burnside Dolomite extend southeast of section 11 (Figures 2, 8).

There are two possible explanations for the difference in transgressive shallow marine sequences. One explanation is that the rate of alluvially supplied sediment was higher below the Burnside Dolomite, due either to a lower rate of relative sea level rise or higher absolute fluvial sediment supply rates. A lower rate of sea level rise is discounted because the Burnside Dolomite was deposited over half of the Slave craton. The second possibility is that the Rocknest lagoon damped the storm energy so that in a transgressive sequence the braid delta complex was less effected by storm waves.

The presence, thickness, and facies of the Burnside Dolomite at sections 10, 12, 13, and 16 provide a crude marker of the limit of marine transgression during Burnside Dolomite sedimentation. These data indicate that the paleoshoreline trended roughly north-northeast, nearly perpendicular to fluvial paleocurrent trends and consistent with the interpretation that the Gordon Bay Arch rotated counterclockwise before deposition of the Burnside Formation.

end of Burnside alluvial sedimentation

Above the Burnside Dolomite and its lateral equivalents, the Burnside Formation returns to largely alluvial sedimentation across the entire craton (Figures 4, 9, 10, 11e). Minor gravel appears in trough cross-bedded facies in the upper part of section 12. Two distinctive polymictic conglomerate horizons outcrop in proximal sections in the Tinney Hills; one contains vein quartz clasts (up to 30 cm in diameter) and intraformational Burnside Formation clasts (up to 100 cm), whereas the other horizon contains undeformed rhyolite clasts (Figures 7d, 9) (McCormick and Grotzinger, in review). Sand-size grains of fresh potassium feldspar and strain-free monocrystalline quartz become more common as matrix higher in the alluvial section.

The end of alluvial sedimentation is represented by the siliciclastic braid delta shelf facies of the Mara Formation and the stromatolitic carbonate of the Quadyuk Formation.

There appears to be a nearly continuous record of sedimentation in the proximal sections (section 2), whereas on the craton (sections 12 and 16), there is evidence for the existence of erosional and starvation surfaces (Figures 9, 10). The Mara Formation shows an overall fining-upwards trend upon which is superimposed an abrupt deepening and then coarsening-upwards trend (Figures 9, 10).

At the proximal margin of the basin, the facies of the uppermost Burnside Formation (Orange Sandstone member; Figures 3b, 9, above an inferred fault) consists of a parallel-laminated feldspathic sandstone facies. Some siltstone interbeds are present at the bottom of the interval, but are less abundant higher in the section. Delta front sandstones coarsen and thicken upward and culminate in a few interbeds of peritidal stromatolitic dolomite. The sandstone-stromatolite units pass laterally northwest into a thicker (up to 60 m) stromatolitic carbonate platform, the Quadyuk Formation (Campbell and Cecile, 1981). This suggests that the Quadyuk Formation represents a transgression over the westward-deepening braid delta system where interbedded siliciclastic sand and stromatolitic carbonate pass laterally into extensive stromatolitic platform. The carbonate unit pinches out to the northwest, roughly coincident with the crest of the original Gordon Bay Arch.

In contrast, at section 12, the most distal complete section, the marked deepening of facies across the contact between the Burnside and Mara formations puts delta front sandstone and siltstone facies directly on lower braid plain facies (Figure 10). The contact between these two facies shows erosional relief of several ten's of cm that cuts across bedding. Micrite cement commonly replaces sandstone several ten's of cm below the contact. This cement gives the sandstone a vuggy-weathering character. The proportion of micrite cement is greatest just below the erosional surface. This sharp superposition of facies that were not laterally adjacent to one another and the presence of cement fabrics that suggest subaerial exposure below a distinct erosional surface, provide evidence for an erosional unconformity between the Burnside and Mara formations in the distal foreland.

The Mara Formation at section 12 coarsens up from delta front facies with common siltstone to tabular-bedded fine-grained sandstone, suggesting retrogradation of the waning alluvial system (Figures 4, 10). This coarsening-upward sequence capped by a sharp flooding surface mimics the overall trend seen in the proximal section at section 2 (Figure 9), where the coarser delta front sandstone association coarsens- and thickens-upward and culminates in a few interbeds of peritidal stromatolitic dolomite.

At the next closest section to the west, section 16 (Figures 2, 10, 11f), the carbonate unit of the Quadyuk Formation is completely missing and the upper few meters of the Mara Formation contain a replacement fabric of pelletal hematitic ironstone upon which a spherulitic dolomitic fabric is superimposed (the Mara Pisolite). The ironstone-pisolite unit

thickens from 5 m at section 16 to 13 m at section 12. Rather than a subaerial exposure fabric, these fabrics and lithologies suggest hematite and carbonate accumulation in a sediment-starved environment, below wave-base (Campbell and Cecile, 1981). The fabrics in the "pisolite" are concretionary or spherulitic, suggesting growth of large carbonate crystals that grew in phreatic or open marine conditions. In contrast, fabrics interpreted as vadose pisolites in the lower Bear Creek Group show growth of micritic carbonate coatings of grains with common, well-developed inverse grading and fitted fabrics (Grotzinger et al., 1989). The fabrics in the Mara Pisolite resemble fabrics within the lower Bear Creek Group that show abundant accretionary and concretionary hematite with superimposed dolomite precipitation and replacement. These fabrics are present along sequence boundaries in the lower Bear Creek Group, above which are facies associated with sediment starvation and rapid transgression. An example lies along the sub-Link Formation sequence boundary in the Tinney Hills where the sequence boundary and transgressive surfaces are amalgamated (Grotzinger et al., 1988). This suggests that the top of the Mara Formation was a major surface of sediment starvation before deposition of sub-wave base rhythmites of the Wolverine Group (Figure 3a).

The sandstone and carbonate units of the Burnside-Mara-Quadyuk Formations are abruptly overlain by sub-wave-base mudstones of the Wolverine Group across the entire craton, suggesting rapid, probably eustatic, drowning of the entire shallow marine shelf across the entire Slave craton and the proximal end of the Kilohigok Basin. This further suggests that the surface at the top of the Mara Formation in the distal foreland (sections 12 and 16) represents the amalgamation of three distinct surfaces: a lower subaerial exposure surface within the Mara Formation that is absent in the proximal foreland, a deep water transgressive starvation surface temporally equivalent to the Quadyuk Formation, and another starvation surface that marks the base of the Bathurst Group (base of the Peacock Hills Formation).

Discussion

The Burnside Formation represents the northwestward progradation of an alluvially dominated braided stream system over a southeast-facing siliciclastic marine shelf ramp. The thickness and lateral extent of the Burnside Formation and its facies associations are vast. Currently preserved exposures of the Burnside Formation extend for 250 km across depositional strike; the original alluvial system must have exceeded 350 km across depositional strike from the Thelon Orogen to the western edge of Wopmay Orogen (Figures 1, 2), where it influenced sedimentation patterns of the passive margin in Wopmay

Orogen. The alluvial sequence exceeds 3000 m in the preserved part of the proximal foredeep, and by extrapolation towards the hinterland, the maximum thickness of the wedge must have been more than 4000 m. In the cratonic foreland, the maximum thickness of the Burnside Formation exceeds 2700 m. These thicknesses are comparable to Phanerozoic foreland basins (Allen and Homewood, 1986), but the thickness and lateral extent of the alluvial section are large by any standard. Paleocurrents indicate that the preserved Burnside Formation is not the product of a single alluvial cone such as the Kosi Fan of India (Wells and Dorr, 1987), but was a uniform west-northwest-draining alluvial apron like a gigantic bajada system that lapped against the Thelon mountain belt to the southeast.

The stratigraphic data for the Bear Creek Group constrain several important elements of the evolution of Kilohigok Basin, Wopmay Orogen, and Thelon Orogen. First, the stratigraphic architecture constrains the location and migration of flexural arches within Kilohigok Basin that result from the evolution of the orogenic belts on the east and west of the Slave craton. Second, the tabular shape of the upper Burnside Formation, transverse paleocurrents, and laterally extensive gravel in the Burnside Formation suggest that there are two distinct phases of convergence and unroofing along the Thelon Orogen. Third, the sedimentological evidence for the compositional maturity of Burnside detritus and deposition of the Burnside Formation under humid conditions suggest that an orographic effect and the climate may have profoundly influenced the evolution of the Burnside alluvial system and the flux of material through the Thelon Orogen. Finally, the preservation of thick alluvial and marginal marine facies in the distal reaches of the Slave craton requires subsidence mechanisms, in addition to flexurally driven subsidence, that are probably a combination of long-term eustatic rise in sea level and dynamic effects exerted by collision along the eastern margin of the Slave craton, and passive margin subsidence on the western margin. Each of these issues is discussed below.

location and migration of flexural arches

The facies scheme and stratigraphic architecture discussed above allows identification of unconformities in this largely siliciclastic setting. The distribution of these unconformities suggests that two flexural arches existed on opposite sides of the Slave craton during early alluvial sedimentation due to the independent evolution of foreland basin in Kilohigok Basin and the passive margin in Wopmay Orogen. Sedimentary, stratigraphic, and geochronologic data provide a temporal link between both basins (Bowring and Grotzinger, 1992).

As has been shown, all stratigraphic units in the Bear Creek Group thin across depositional strike northwest towards the Gordon Bay Arch (Figures 2, 4, 8). This thinning

is accompanied by the development of increasingly profound and stratigraphically concentrated unconformable surfaces. Northwest of the arch, into the distal foreland basin, the transitional marine to alluvial units reappear and thicken into section 12 (Figures 2, 4, 8) then thin towards the sections 13 and 14, the area nearest to Wopmay Orogen. Again, the stratigraphic geometry of the transitional unit of the Burnside Formation mimics that of the lower Bear Creek Group marine units. At section 14 (Figures 2, 4, 8), the thinnest section in the entire basin, the Burnside Formation cuts out two underlying formations of the lower marine foredeep section on the craton (Beechey and Link Formations; Figure 3a, 4, 8, 10) so that it rests directly upon sub-wave base marine facies (Rifle Formation). Although the lower foredeep stratigraphy thins in this region, this appears to be the most profound erosional unconformity at the base of the Burnside Formation. Two sections measured in the easternmost part of Wopmay Orogen at the base of the siliciclastic part of the passive-margin sequence (Odjick Formation) (Hoffman et al., 1984) exhibit vertical facies and stratigraphic trends that suggest that they are the marine and deltaic lateral equivalents to the Burnside Formation (McCormick and Grotzinger, 1988). This explains the large volume of coarse siliciclastic detritus in the Wopmay passive margin and the lateral restriction of its carbonate platform (Rocknest Formation), as a result of significant alluvial input from the Burnside system (Grotzinger, 1986a). The persistence of siliciclastic input into and the lateral restriction of the carbonate platform in Wopmay Orogen contrast markedly with Phanerozoic passive margins for which the onset of carbonate sedimentation follows a reduction or cessation of siliciclastic sedimentation. In the case of the Burnside Formation and the passive margin of Wopmay Orogen, siliciclastic detritus continued to pump into the carbonate platform throughout its entire duration because a transversely draining foreland basin alluvial system interfingered with it from the opposite side of the craton (Grotzinger, 1985). Comparison of stratigraphic sections of the carbonate platform between the southern and northern ends of Wopmay Orogen indicates that subsidence increased markedly to the north along strike from the Rockinghorse Arch, suggesting that this flexural arch plunged to the north. This may partly explain the deflection of Burnside Formation alluvial paleocurrents towards the north at sections 13 and 14.

The stratigraphic evidence for the distribution of unconformities in the lower Bear Creek Group and Burnside Formation suggests that two flexural arches existed at the onset of Burnside sedimentation. The Gordon Bay Arch, the one nearer to the Thelon Orogen, resulted from flexural loading along the eastern Slave margin by collision along the Thelon Orogen. Alluvial paleocurrent trends (Figure 5) and the correlation of sections across the Bathurst Fault (Figure 8) suggests that the Gordon Bay Arch probably rotated about 25° counterclockwise between the beginning of deposition of the lower Bear Creek Group and

the onset of transversely draining alluvial sedimentation. The flexural arch on the western side of the Slave craton, the Rockinghorse Arch, most likely relates to the early evolution of the passive margin in Wopmay Orogen (Figures 1, 2, 4, 8). The thickening wedge of siliciclastic sedimentary rocks overlying the western margin of the Slave craton must have exerted an increasing sediment load on the cooling passive margin inducing flexural uplift to the east on the craton. The *magnitude* of the flexural strength of the lithosphere in evolving Phanerozoic passive margins is currently under debate (Steckler, 1989), but stratigraphic evidence for flexurally uplifted cratonic margins due to passive-margin sedimentation appears to be strong (Bond et al., 1989). Nunn et al. (1987) and Coakley and Watts (1991) suggest that flexure of the Mesozoic Colville trough and Barrow Arch in northern Alaska, produced largely by the northward emplacement of Brooks Range thrust sheets, was enhanced by sediment loading on the coeval Beaufort passive margin.

The pattern of subsidence and the location of unconformities appears to have changed markedly by the end of Burnside sedimentation. The thick wedge of siliciclastic detritus in the Burnside Formation, which reaches a thickness of up to 2700 m *on the craton*, suggests that a tremendous volume of detritus was eroded from Thelon Orogen and was deposited in the foreland basin. Such a redistribution of mass would have imposed an additional load much closer to the center of the craton, causing a statically located flexural bulge to migrate towards the foreland (northwest), independent of any additional convergence along the Thelon Orogen. Stratigraphic evidence at the contact in section 12 indicates that an erosional unconformity separates the Burnside and Mara Formation in the distal foreland. Previously, this was the locus of a depositional trough between the Rockinghorse and Gordon Bay arches. This suggests that a single coupled flexural arch existed in the center of the Slave craton in response to evolution of both Kilohigok Basin and Wopmay Orogen (Figure 11f).

Moretti and Royden (1988) have investigated conditions under which independent, though closely spaced, flexural bulges might interact in sedimentary basins, on the basis of both geologic examples and geophysical modeling. They show that if a lithospheric plate is subjected to two independent loads on opposite sides of the plate, such as subduction on both margins, the resulting pattern of flexurally created arches and troughs depends on a combination of the strength of the lithosphere and the distance between the loads. Their modeling suggests that, given a certain lithospheric strength, if the two orogenic loads are sufficiently separated, two independent flexural arches result. If the loads are sufficiently close, however, the arches yoke together to form a single enhanced flexural bulge. The stratigraphic pattern seen at the base of the Burnside Formation is consistent with independent flexural arches (Gordon Bay and Rockinghorse arches) separated by an

intervening trough (thick transitional section at section 12; Figures 8, 10, 11a-e).

On the western margin of the Slave craton, the abrupt termination of carbonate platform sedimentation is attributed to initiation of convergence and foreland basin sedimentation on the west side of the Slave Craton (Hoffman et al., 1984). This convergence created a flexural arch analogous to the earlier Gordon Bay Arch in Kilohigok Basin. Grotzinger (1986b) demonstrated the unconformity on top of the carbonate platform did *not* migrate across the entire carbonate platform, as is commonly assumed to occur during foreland basin evolution (Shanmugam, 1988), but rather that the outer part of the platform was drowned and the facies backstepped. Evidence for subaerial exposure of the platform exists only in the autochthonous, easternmost part of Wopmay (Grotzinger, 1985). Subaerial expression of the bulge, therefore, must have existed inboard (eastward) of the currently exposed limit of the carbonate platform in Wopmay Orogen. Similarly, erosional truncation, related to the uplift of the flexural bulge that existed at the onset of foreland basin sedimentation in Kilohigok Basin, also lies ten's of kilometers inboard of the shelf edge of the underlying Kimerot passive margin; the shelf edge is, in fact, synchronously drowned and mantled in deep shelf rhythmites (Grotzinger and McCormick, 1988). In addition, the margin of Wopmay Orogen had cooled for several ten's of millions of years since the onset of passive margin sedimentation (Bowring and Grotzinger, 1992) which would have meant that the strength of the lithosphere would have increased significantly. Bond et al. (1989) have shown that in Early Paleozoic passive margin platforms, a progressive cratonward migration of a flexural arch was caused by thermal subsidence, sediment loading, and time-dependent flexure cause. Thus the Rockinghorse arch should have migrated eastward, because the flexural strength and, therefore, the flexural wavelength would have increased with time and with cooling of the western Slave margin. Thus the coupled effects of erosion of the Thelon Orogen and the initiation of convergence in Wopmay Orogen appear to have produced a single, yoked flexural bulge centered near section 12 (Figures 8, 10, 11f). The position of the unconformity centered about section 12 implies that the Gordon Bay Arch migrated laterally approximately 50 km to the northwest over the duration of alluvial sedimentation.

significance of laterally extensive gravel sheets and transverse alluvial paleocurrents

The base of the main alluvial units of the Burnside Formation and the stratigraphic distribution of unconformities demonstrate a marked shift of the paleoshoreline from the Tinney Hills area to the area between sections 12 and 13. The transport of gravel across the entire Slave craton, more than 200 km, requires a fundamental change in the distribution of

subsidence across the basin. Two-dimensional modeling of gravel transport by Paola (1988) suggests that areally extensive conglomerates, especially in foreland basins, indicates reduced asymmetry of the cross-strike subsidence rate profile and probably reduced overall subsidence rates. Several authors have begun to address the stratigraphic effects of time-dependent erosion of foreland thrust-fold belts and to try to take into account the lag time in filling of basins and the depositional slopes that characterize different depositional environments (Karner, 1986; Flemings and Jordan, 1987; Heller et al., 1988; Flemings and Jordan, 1989; Heller and Paola, 1989; Beaumont et al., 1990; Flemings and Jordan, 1990; Johnson and Beaumont, 1990; Jordan and Flemings, 1990; Sinclair et al., 1991; Beaumont et al., 1992).

Some authors suggest that the coarsening-upward in foreland basins reflect a two stage history in the evolution of the basin and that the significance of the coarsening-upwards deposits depend on how far the deposit from the thrust front (Heller et al., 1988; Jordan et al., 1988; Flemings and Jordan, 1989; Heller and Paola, 1989; Flemings and Jordan, 1990). Proximal sections, generally within ten's of kilometers of the source area, tend to preserve areally restricted high gradient fan facies, such as alluvial fan facies, that pass laterally into relatively low-gradient distal facies (lacustrine or marine); a subaerial or marine erosion surface may be cut over or near the crest of the flexural bulge. The shape of the stratigraphic units deposited and preserved during the initial phase are highly asymmetric and taper away from the thrust load. In contrast, when thrusting slows or ceases, erosion unloads the orogenic wedge and the hinterland and proximal foreland basin rebound isostatically. Erosionally driven uplift may cut an erosional unconformity into the initially deposited foreland basin strata. The combination of increased sediment flux from erosion and reduced subsidence rates in the proximal part of the foreland basin promotes extensive progradation of the alluvial system towards the foreland. The shape of the deposits of this progradational phase are more tabular than the thrust driven, asymmetric phase. Proximal sections, therefore, should record coarsening-upwards due to progradation high-gradient facies during the initial, thrust driven asymmetric phase. Distal sections, in contrast, should record a coarsening upwards related to progradation during the second erosional phase.

Two aspects of the two-phase model have been called into question, based on the nature of the data that Heller et al. use to document their model. First, Burbank et al. (1988) suggest thrusting can be synchronous with extensive gravel progradation in foreland basins where the sediment supplied to the basin exceeds subsidence, such as when there are large, antecedent rivers, as in the Neogene Himalayan foreland basins. Burbank et al. point out that the Heller et al. model is two-dimensional and the model does not account for the longitudinal flux of sediment common to the foreland basins they consider (Mesozoic foreland of the western United States and the Neogene Indo-Gangetic foreland) (Heller et

al., 1989). DeCelles (1992) raises a second objection to the data Heller and Paola (1989) use to substantiate their model. DeCelles points out that the supposedly correlative and synchronously deposited gravel sheets of the Early Cretaceous Cloverly Formation in the western United States may represent numerous separate prograding parasequences and that within a single parasequence, the alluvial system transporting the gravel was draining longitudinally with respect to the mountain front.

Despite the above-stated reservations, Burbank (1992) uses a variation on the two-phase model to attempt to unravel the history uplift in the Himalayas. He demonstrates that the Ganges foredeep has been dominated by relatively tabular alluvial deposits and transversely draining rivers over the last 4 million years. He suggests that this has been due to the onset of extensive erosion of the Himalayas. The modern Indus foredeep and the Ganges foredeep prior to 4 Ma are relatively asymmetric and they are dominated by longitudinally flowing rivers and transverse rivers are restricted close to the mountain front.

The onset of the transverse paleocurrent trend in the Burnside Formation signals an important stage in the evolution of Kilohigok Basin and Thelon Orogen. Paleocurrent trends in the transitional units in the proximal (southeast) part of the basin are unimodal to the southwest, parallel to both the trend of the orogenic belt and the Gordon Bay flexural arch (Figure 5). Sharply superposed upon the transitional facies in the proximal part of the belt are medial braid plain facies with paleocurrent trends that are strongly unimodal to the northwest, perpendicular to the Gordon Bay Arch and to the trend of the axial foredeep, perpendicular to the Thelon Orogen, directed straight across the Slave craton towards Wopmay Orogen. This transverse trend of alluvial paleocurrents is not common in most foredeeps, especially beyond the flexural bulge of the basin. By comparison, most foredeeps, whether young with marine to alluvial sedimentation (e.g., Neogene Taiwan: Covey (1986)) or highly evolved with largely alluvial sedimentation (e.g., Neogene Alps: England (1981), Homewood et al. (1986); Neogene Indo-Gangetic trough Parkash et al. (1980)) exhibit predominant longitudinal drainage. This results largely from the tendency for depositional alluvial systems to track the maximum slope gradient and the gradient of maximum subsidence (Alexander and Leeder, 1987). The result is longitudinal filling and lateral dispersal into whatever open trough can accommodate the large volume of sediment derived from the subaerial phase of plate collision. Indeed in the case of Taiwan and the Himalayas, the bulk of the sediment ends up in marine fan systems or cones (England, 1981).

One of the signal aspects of the Burnside Formation is that transverse drainage predominates throughout the main phase of alluvial sedimentation and so we believe that the basin was largely overfilled during the latter part of its history. Significant conglomeratic deposits in the Burnside Formation are restricted largely to the proximal side of the syn-

sedimentary flexural arch. Within the proximal part of the basin, conglomeratic horizons can be walked out laterally, demonstrating the how they are correlative over many ten's of kilometers, and are not deposited in separate parasequences. The contrast between the highly tapered shape of the lower members and the more tabular-shaped upper members (Figures 4, 9, 10), combined with the uniformly northwest-directed paleocurrents (Figure 5) suggest that erosionally driven mass redistribution into the foreland during second phase of Burnside sedimentation may have been a prime mechanism driving subsidence over the craton.

Hoffman (1987) has suggested that the evolution of the eastern and southern margins of the Slave Province at this time would have been similar to the evolution of the Neogene Ingo-Gangetic system with a large marine trough on the southern margin of the Slave Province that opened to the west, although at a much smaller scale (Figure 1). This interpretation is consistent with the predominantly southeastern trend of paleocurrents in lower foredeep turbidites and the transitional alluvial sequence. A problem with this interpretation is that none of the currently preserved sediments in Athapuscow Basin is consistent with axially flowing marine turbidites sourced from Kilohigok Basin. It seems more likely that the apex of the Slave Province, at the intersection between Thelon Orogen and Great Slave Lake shear zone, was completely in contact with the Rae Province during foredeep sedimentation. This is the zone that preserves the greatest paired gravity and magnetic anomalies in this region, which are suggestive of flexural subsidence (Gibb and Thomas, 1977; Canada, 1987). Paleocurrent trends at sections 13 and 14 show a more northerly trend than anywhere else in the basin. In addition, the gravel size material at section 13 and especially section 14 is coarser than that seen at section 12, which is closer to the Thelon Orogen (Figures 1, 2). One way to explain this is to postulate a second alluvial system, farther south along Thelon Orogen close to the junction with the Great Slave Lake shear zone, that interfingered with the main alluvial system. that seems to account for the uniform west-northwest paleocurrents everywhere else in Kilohigok Basin. The other way to explain the northward deflection in paleocurrents is by invoking a more northerly gradient in subsidence in the passive margin of Wopmay Orogen. Thus, the onset of the major phase of alluvial sedimentation across the Slave Craton may have coincided with the closing of the connection between Kilohigok and Athapuscow basins.

impact of humid climate on the evolution of the Burnside alluvial system and Thelon Orogen

Recent advances in stratigraphic modeling show that both the climate and the erosion and redistribution of detritus from the orogen may exert profound, even dominant,

influences on the pattern of stratigraphy preserved in the foreland and the structural history of the orogenic belt from which the sediment is derived. Models that incorporate time-dependent erosion of orogenic topography show that the redistribution of mass from the orogen to the foreland greatly modifies the pattern of subsidence and the distribution of unconformities (Flemings and Jordan, 1987; Flemings and Jordan, 1989; Coakley and Watts, 1991; Sinclair et al., 1991). Other models that also attempt to mimic orographic effects, produced by the interaction of moisture-laden winds with growing orogenic topography, show that climate may exert a large and possibly controlling influence on both the evolution of the foreland basin and the orogen itself (Dahlen and Suppe, 1988; Beaumont et al., 1990; Beaumont et al., 1992). Essentially, if moisture-laden winds impinge on a subaerial mountain front of sufficient topographic relief, a critical feedback will be set up whereby orographic rain will induce rapid flux of material through the orogen that will be redistributed into the foreland. In addition, high rates of erosion will prevent lateral growth of the orogen, promoting extensive footwall reactivation and uplift, and will, essentially, pin the location of the frontal thrust and promote out-of-sequence thrusting within the orogenic wedge (Platt, 1986).

The preserved braid plain facies in the Burnside Formation consist of sand only and the braid plain facies extend more than 200 km before entering a marine environment on the west side of the Slave craton. If the climatic conditions on the braid plain were arid or semi-arid and the discharge that carried in these bedload-dominated streams were flashy or intermittent, one might expect that the water table over the braid plain would be relatively deep and that the stream-borne water would be lost by sieving into the sandy braid plain. If, however, discharge were either continuous or had large peaks of seasonal discharge that are characteristic of monsoon conditions, then one would predict a higher water table and a lower tendency for discharge to be lost by sieving into the alluvial plain. A high water table and a high rate of discharge in stream channels can be caused by high rates of precipitation in the source area alone, regardless of climate over the alluvial plain. Climatic conditions could be arid or humid over the alluvial plain, although humid conditions on the alluvial plain would be more conducive to long-distance flow.

Paleomagnetic and sedimentologic data imply that the Kilohigok Basin lay in the tropical trade wind belt (Evans and Hoye, 1981; McGlynn and Irving, 1981). Furthermore, shelf-edge stromatolites (analogous to spur-and-groove structures) from the Rocknest carbonate platform in Wopmay Orogen are strongly elongate southeast-northwest in present coordinates, and there is very little forereef debris. These observations led Grotzinger (1985) to propose that winds blew onto the Rocknest platform from the southwest. Stromatolites throughout the Goulburn Supergroup in the Kilohigok Basin show the same tight southeast-

northwest orientation (Campbell and Cecile, 1981; Grotzinger and McCormick, 1988). These observations require that the Slave craton lay in the northern hemisphere and that it was rotated 180° from its present configuration. The tropical trade winds therefore blew from the Wopmay Orogen towards Kilohigok Basin and the Thelon Orogen.

Very little direct evidence can be offered for monsoon conditions in the case of the Burnside alluvial system. The present day monsoon of southern Asia is primarily a product of the latitudinal alignment of large land areas at low latitudes and the climatic effect is amplified by the presence of the Himalayan mountains and the Tibetan Plateau (J.T. Parrish, personal communication, 1992). Accumulating geochronological evidence suggests that the Laurentia, perhaps Earth's first supercontinent, amalgamated due to the collision of numerous Archean continental nuclei between 2.0 and 1.8 Ga (Hoffman, 1988). This suggests that there may have been a large number of small continental plates at low latitudes at the time that the Burnside Formation was deposited, but the spatial arrangement of the continental plates is unknown. Monsoon conditions are dominated by such high peaks of seasonal discharge that presumably monsoonal steam systems could create a high water table. In addition, high peak discharge would promote removal of the structures and deposits indicative of the intervening low-flow parts of the season that are commonly found on the topographically highest part of the channel systems that are most prone to erosion. However, soil forming processes should be active during the period between successive monsoons. No evidence for caliche or soils is found in the Burnside Formation. So alluvial deposits of highly seasonal monsoon conditions might be quite similar to those produced under humid, continuous discharge conditions. We suggest monsoonal conditions as an alternative to humid perennial discharge conditions as a means of creating the observed widely distributed, sandy alluvial deposits.

The paleomagnetic data also suggest that the paleopoles for the Mara Formation coincide with those for correlative rocks in Wopmay Orogen and Athapuscow Basin. Interestingly, the only deviation from the common pole location is on in the lowermost foredeep deposits in Kilohigok Basin. This lower Bear Creek Group paleopole lies 80° from the average pole for all other units sampled. Evans and Hoye (1981) speculated that this could mean that there was a large time gap between the lower and upper Bear Creek Group. Given that there is an approximately 85 million year time span between the base of the foredeep and the Mara Formation (Bowring and Grotzinger, 1992), the big unconformity probably lies at the base of the Burnside Formation over the craton.

The composition of sandstones and conglomerates of the Burnside Formation suggests that a large component of Burnside detritus is derived from a metamorphic source area, probably Thelon Orogen and Queen Maud block. The Bear Creek Group through the

Transitional member of the Burnside Formation contains common fresh feldspar; paleocurrents indicate that the feldspar must be derived from the northeast, probably from the Buchan Bay Dome (Figures 2, 5). The Buff Sandstone and Conglomerate members of the Burnside Formation contain metagreywacke and schist clasts, common strained quartz and almost no feldspar. The only conglomerate lithologies that are found beyond the Gordon Bay Arch are duriclasts of vein quartz and jasper. Paleocurrents and detrital zircon U-Pb ages suggest that these probably are derived from Thelon Orogen and Queen Maud block (McCormick and Bowring, in preparation). Significant Early Proterozoic age detritus appears higher in the section in the Orange Sandstone member concomitant with increasing unstrained quartz, the reappearance and upward increase in feldspar, and the appearance of undeformed felsic volcanic clasts in the proximal part of the basin. Late Archean rocks are the source of basal Burnside Formation in the proximal foreland, but most of the formation probably contains syn-orogenic Early Proterozoic felsic detritus derived from Thelon Orogen and Queen Maud block.

The sedimentologic, stratigraphic, petrologic, and geochronologic data suggest that the Burnside Formation was deposited under humid, perennial flow conditions in a laterally extensive braided alluvial system. This alluvial system initially contained sediment derived from the eastern flank of the Slave Province, with much of the alluvial sequence preserved over the craton being derived from syn-orogenic rocks in Thelon Orogen. This supports the idea that humid climate and an orographic effect were responsible for the large lateral extent of the Burnside alluvial system, and for the large volume of detritus preserved in it. The shift in provenance to largely syn-orogenic volcanic, plutonic, and metamorphic rocks requires rapid exhumation of the orogenic belt, which would be promoted by humid climate on a windward orogen.

significance of preservation of thick cratonic alluvial sequence

Worthy of note are three important observations about the Goulburn Supergroup strata deposited beyond the Gordon Bay Arch in the distal foreland. First, lower Goulburn Supergroup strata over the craton are thin, relatively tabular, and the thickest preserved strata were deposited during a relative rise in sea level. Second, the Burnside Formation is tabular and very thick over the craton. Third, the Burnside alluvial facies interongue with marine facies in the distal foreland. All of these observations require long-term relative rise in sea level, plus external subsidence mechanisms in addition to sediment loading.

The Burnside Formation over the Slave craton commonly exceeds 2000 m in thickness (Figures 4, 10; sections 12 and 16). These strata lie well beyond the main flexural

arch and far exceed the thickness of strata that could be accommodated by any flexural subsidence beyond a peripheral bulge. In addition, the sedimentary facies in these areas represent lower braid plain to braid delta environments and interfinger with marine shelf facies and the Burnside Dolomite. So shallow water to non-marine conditions persisted through much of the deposition of the Burnside Formation in the distal foreland. These data suggest that continuous accommodation occurred in the distal foreland that cannot be explained solely by aggradation of a non-marine sequence. In addition, a 2 km sediment load could only induce no more than 1.5 km of isostatic subsidence. Another mechanism for the excess subsidence is required.

In the distal reaches of the Kilohigok Basin, for example near sections 13 and 14, the lower part of the Goulburn Supergroup are very thin, and most of the preserved strata reflect deposition during relative sea-level rise. The major component of strata there is the Red Siltstone member of the Rifle Formation that is present across the entire width of the Kilohigok Basin and which probably represents a eustatic rise in sea level (Grotzinger et al., 1987; Grotzinger and Royden, 1990). These data suggest that some accommodation could derive from long term sea level rise. Another important source of subsidence would have been thermal contraction and sediment loading of the passive margin of Wopmay Orogen. The problem with this mechanism, is that much of the Slave Craton is beyond the flexural wavelength for this to be an effective mechanism. The last potential source of extra subsidence is from the dynamic effects on the Slave craton of continent-continent collision on the east and extension on the west. Recent geophysical models suggest that tectonic forces exerted on the boundaries of plates may induce ten's to hundred's of meters subsidence in craton interiors (Mitrovica et al., 1989; Gurnis, 1990; Gurnis, 1992) and may explain significant craton-wide relative sea level rises during times of continental assembly (Kominz and Bond, 1991). This time of deposition of the Goulburn Supergroup coincides with assembly of what may be the first supercontinent in Earth history (Hoffman, 1988; Hoffman, 1989).

In summary, most of the subsidence on the Kilohigok foreland basin, especially in the proximal end of the basin, was caused by flexural subsidence due to the overriding Thelon Orogen. Extensive progradation of thick alluvial sediments across the craton probably occurred because of erosion of the Thelon Orogen under humid climatic conditions, perhaps due to an orographic effect caused by the growing mountain belt itself. The mass of this tabular sheet of sediment caused a large component of subsidence over the craton, beyond the syn-orogenic flexural arch. Possible long-term eustatic rise contributed to the some of the continuous aggradation over the craton. It seems likely, though, that some of the subsidence over the craton cannot be explained by the combination of these effects.

Therefore, some additional subsidence mechanism must have been at work, perhaps relating to the dynamic effects of continental collision and supercontinent aggregation.

Conclusions

Sedimentological and stratigraphic studies of the Burnside Formation document the transition of the Early Proterozoic Kilohigok foreland basin from a southeast-facing marine shelf, with longitudinal transport parallel to the Thelon Orogen, to an alluvially dominated system with transverse transport. Initial alluvial sedimentation took place in a prograding braid delta system restricted to the proximal end of the basin between the Thelon Orogen and the Gordon Bay Arch, believed to be related to foreland basin flexure. Sediment transport in these transitional units was largely longitudinal, parallel to the flexural arch. There was a major shift from areally restricted braid delta facies to the overlying areally extensive medial braid plain facies. The abrupt superposition of braid plain associations on marine shelf and braid delta associations in the foreland suggest that progradation and shift of the paleoshoreline was abrupt and involved erosional truncation over the proximal Gordon Bay Arch. The superposition of medial braid plain facies directly upon syenogranite basement to the north suggests that the flexural arch was more likely an emergent flexural dome or arch-and-dome system with its culmination to the north of the main part of the present outcrop belt.

Sedimentologic data from the most distal sections indicate that alluvial units cut down through two formations over a second flexural arch that existed on the west side of the Slave craton. Correlations suggest that the Burnside Formation intertongued with the evolving passive margin in Wopmay Orogen. The development of the Wopmay carbonate platform probably attenuated high-energy marine processes that initially influenced the prograding braid delta, so that later, alluvial dominance was even more pronounced.

The stratigraphic architecture of the Bear Creek Group suggests that the initial phase of foreland basin sedimentation was dominated by longitudinal infilling of the flexural moat. The presence of at least two unconformities in the lower Burnside Formation in the proximal foreland suggests that progradation of the Burnside alluvial wedge across the craton probably was related to reduced convergence and initial rebound in the orogenic hinterland due to erosion and mass redistribution. The stratigraphic architecture of the Burnside Formation indicates that two coeval flexural arches were active during alluvial sedimentation. One arch was caused by thrust loading due to convergence in the Thelon hinterland to the southeast. The other related to thermal subsidence and sediment loading of the passive margin in Wopmay Orogen on the opposite margin of the Slave craton. Initially, these two arches were

too far apart to be coupled. Coupling into a single flexural bulge occurred at the end of alluvial sedimentation and was probably due to two effects, the presence of a thick molasse sediment wedge over the craton well west of the Thelon orogenic hinterland and by the initiation of convergence and flexural subsidence in Wopmay Orogen.

Foreland basin sedimentary rocks through the initial, longitudinally draining alluvial facies (lower Burnside Formation) contain predominantly metamorphic detritus derived from the eastern margin of the Slave craton. The existence of laterally extensive conglomerate beds, compositionally mature sandstones, scarcity of fine-grained detritus, and the tabular shape of the transversely draining upper Burnside Formation suggests that most of alluvial sedimentation resulted from extensive unroofing of the Thelon Orogen and the adjacent Queen Maud block. All of these may relate to the existence of a humid rain shadow on the forward edge of the Thelon mountain front, and this climatic effect may have exerted a significant, or even dominant, control on the deep exhumation of the Thelon Orogen and Queen Maud block and the great thickness of alluvial detritus preserved in Kilohigok Basin.

Preservation of a great thickness of intertonguing marine and distal alluvial material over the craton end requires that subsidence was caused by more than the effects of sediment loading alone. An apparent long-term rise in sea level may have been caused by the dynamic effects of plate boundary forces related to collision along the eastern margin of the Slave Province, and the contemporaneous evolution of the passive margin along the western margin.

References Cited

Alexander, J., and Leeder, M.R., 1987. Active tectonic controls on alluvial architecture, in, F.G. Ethridge, R.M. Flores, and M.D. Harvey (eds.), Recent Developments in Fluvial Sedimentology. Soc. Econ. Paleont. Mineral. (Tulsa, OK), p. 243-252.

Allen, P.A., and Homewood, P., 1986. Foreland Basins. Blackwell Scientific Publications (Oxford, UK), 453 pp.

Bally, A.W., Gordy, P.L., and Stewart, G.A., 1966. Structure, seismic data, and orogenic evolution of southern Canadian Rockies. Bull. Can. Petrol. Geol., v. 14, p. 337-381.

Beaumont, C., 1981. Foreland basins. Geophys. J. Roy. Astron. Soc., v. 65, p. 471-498.

Beaumont, C., Fullsack, P., and Hamilton, J., 1992. Erosional control of active compressional orogens, in, K.R. McClay (ed.), Thrust Tectonics. Chapman and Hall (London), p. 1-18.

Beaumont, C., Fullsack, P., Willett, S., Hamilton, J., Johnson, D., Ellis, S., and Paton, M., 1990. Coupling of climate, surface processes and tectonics in orogens and their associated sedimentary basins, in, J. Hall (ed.), Lithoprobe: Lithoprobe East Transect, Report 13. Memorial University, St. John's, Newfoundland (St. John's, Newfoundland, Canada).

Beaumont, C., and Hamilton, J., 1990. Influence of surface erosional processes on the evolution of compressional orogens. Geol. Soc. America, N.E. Section, Abs. with Progs., v. 22, p. A4.

Bond, G.C., Kominz, M.A., Steckler, M.S., and Grotzinger, J.P., 1989. Role of thermal subsidence, flexure, and eustasy in the evolution of Early Paleozoic passive margin carbonate platforms, in, P.D. Crevello, J.L. Wilson, J.F. Sarg, and J.F. Read (eds.), Controls on Carbonate Platform and Basin Development. Soc. Econ. Paleont. Mineral. (Tulsa, OK), Spec. Pub. No. 44 (Tulsa, OK), p. 39-62.

Bowring, S.A., and Grotzinger, J.P., 1992. Implications of new chronostratigraphy for tectonic evolution of Wopmay Orogen, northwest Canadian Shield. American Journal of Science, v. 292, p. 1-20.

Burbank, D.W., 1992. Causes of recent Himalayan uplift deduced from deposited patterns in the Ganges basin. Nature, v. 357, p. 680-683.

Burbank, D.W., Beck, R.A., Raynolds, R.G.H., Hobbs, R., and Tahirkheli, R.A.K., 1988. Thrusting and gravel progradation in foreland basins: a test of post-thrusting gravel dispersal. Geology, v. 16, p. 1143-1146.

Campbell, C.V., 1976. Reservoir geometry of a fluvial sheet sandstone. Am. Assoc. Petrol. Geol. Bull., v. 60, p. 1009-1020.

Campbell, F.H.A., and Cecile, M.P., 1981. Evolution of the Early Proterozoic Kilohigok Basin, Bathurst Inlet-Victoria Island, Northwest Territories, in, F.H.A. Campbell (ed.), Proterozoic Basins of Canada. Geological Survey of Canada, Paper 81-10 p. 103-131.

Christie-Blick, N., Grotzinger, J.P., and von der Borch, C.C., 1988. Sequence stratigraphy in Proterozoic successions. Geology, v. 16, p. 100-104.

Coakley, B.J., and Watts, A.B., 1991. Tectonic controls on the development of unconformities: the North Slope, Alaska. Tectonics, v. 10, p. 101-130.

Covey, M., 1986. The evolution of foreland basins to steady state: evidence from the western Taiwan forland basin, in, P.A. Allen, and P. Homewood (eds.), Foreland Basins. Blackwell Scientific Publications (Oxford, UK), p. 77-90.

Cross, T.A., 1986. Tectonic controls of foreland basin subsidence and Laramide style deformation, western United States, in, P.A. Allen, and P. Homewood (eds.), Foreland Basins. Blackwell Scientific Publications (Oxford, UK), p. 15-40.

Dahlen, F.A., and Suppe, J., 1988. Mechanics, growth, and erosion of mountain belts, in, S.P. Clark, B.C. Burchfiel, and J. Suppe (eds.), Processes in Continental Lithospheric Deformation. Geological Society of America, Special Paper 218 (Denver, CO), p. 161-178.

de Raaf, J.F.M., Boersma, J.R., and van Gelder, A., 1977. Wave generated structures and sequences from a shallow marine succession, Lower Carboniferous, County Cork, Ireland. Sedimentology, v. 24, p. 451-483.

DeCelles, P.G., 1992. A field test of foreland-basin models in the overfilled, nonmarine part of the Jurassic-Cretaceous Cordilleran foreland basin, central Wyoming. Am. Assoc. Petrol. Geol., Prog. with Abs., v. p. 24.

Elliot, T., 1986. Deltas, in, H.G. Reading (ed.), Sedimentary Environments and Facies (2nd ed.). Blackwell Scientific Publications (Boston, MA), p. 113-154.

England, P., 1981. Metamorphic pressure estimates and sediment volumes for the Alpine orogeny: an independent control on geobarometers? Ear. Planet. Sci. Let., v. 56, p. 387-397.

Eriksson, K.A., and Vos, R.G., 1979. A fluvial fan depositional model for Middle Proterozoic red beds from the Waterberg Group, South Africa. Precambrian Res., v. 9, p. 169-188.

Evans, M.E., and Hoye, G.S., 1981. Paleomagnetic results from the lower Proterozoic rocks of the Great Slave Lake and Bathurst Inlet areas, Northwest Territories, in, F.H.A. Campbell (ed.), Proterozoic Basins of Canada. Geological Survey of Canada, Paper 81-10 p. 191-202.

Flemings, P.B., and Jordan, T.E., 1987. Synthetic stratigraphy of foreland basins. Eos., Trans. Am. Geophys. Union, v. 68, p. 419.

Flemings, P.B., and Jordan, T.E., 1989. A synthetic stratigraphic model of foreland basin development. J. Geophys. Res., v. 94, No. B4, p. 3851-3866.

Flemings, P.B., and Jordan, T.E., 1990. Stratigraphic modeling of foreland basins: interpreting thrust deformation and lithosphere rheology. Geology, v. 18, p. 430-434.

Friend, P.F., 1983. Toward an field classification of alluvial architecture or sequence, in, J.D. Collinson, and J. Lewin (eds.), Modern and Ancient Fluvial Systems. Blackwell Scientific Publications, Intern. Assoc. Sedimentologists, Spec. Pub. No. 6 (Oxford, UK), p. 345-354.

Geological Survey of Canada, 1987. Magnetic anomaly map of Thelon River, Northwest Territories (Map NQ 12-13-14 AM; 1:1000000 scale). Geological Survey of Canada, Magnetic anomaly map (residual total field).

Gibb, R.A., 1978. Slave-Churchill collision tectonics. Nature, v. 271, p. 50-52.

Gibb, R.A., and Thomas, M.D., 1977. The Thelon front: a cryptic suture in the Canadian Shield. Tectonophys., v. 38, p. 211-222.

Grotzinger, J.P., 1985. Evolution of Early Proterozoic passive-margin carbonate platform,

Rocknest Formation, Wopmay Orogen, N.W.T., Canada. Unpublished Ph.D. Thesis, Virginia Polytechnic Institute and State University (Blacksburg, VA).

Grotzinger, J.P., 1986a. Cyclicity and paleoenvironmental dynamics, Rocknest platform, northwest Canada. Geol. Soc. America Bull., v. 97, p. 1208-1231.

Grotzinger, J.P., 1986b. Evolution of early Proterozoic passive-margin carbonate platform: Rocknest Formation, Wopmay Orogen, N.W.T., Canada. J. Sed. Petrology, v. 56, p. 831-847.

Grotzinger, J.P., Adams, R.D., McCormick, D.S., and Myrow, P., 1989. Sequence stratigraphy, correlations between Wopmay Orogen and Kilohigok Basin, and further investigations of the Bear Creek Group (Goulburn Supergroup), District of Mackenzie, Current Research, Part C. Geological Survey of Canada, Paper 89-1C p. 107-120.

Grotzinger, J.P., and Gall, Q., 1986. Preliminary investigations of Early Proterozoic Western River and Burnside River Formations: evidence for foredeep origin of Kilohigok Basin, N.W.T., Canada, Current Research, Part A. Geological Survey of Canada, Paper 86-1A p. 95-106.

Grotzinger, J.P., Gamba, C., Pelechaty, S.M., and McCormick, D.S., 1988. Stratigraphy of a 1.9 Ga foreland basin shelf-to-slope transition: Bear Creek Group, Tinney Hills area of Kilohigok Basin, District of Mackenzie, Current Research, Part C. Geological Survey of Canada, Paper 88 1-C p. 313-320.

Grotzinger, J.P., and McCormick, D.S., 1988. Flexure of the Early Proterozoic lithosphere and the evolution of the Kilohigok Basin (1.9 Ga), northwest Canadian shield, in, K. Kleinspehn, and C. Paola (eds.), New Perspectives in Basin Analysis. Springer-Verlag (New York), p. 405-430.

Grotzinger, J.P., McCormick, D.S., and Pelechaty, S.M., 1987. Progress report on the stratigraphy, sedimentology, and significance of the Kimerot and Bear Creek groups, Kilohigok Basin, District of Mackenzie, Current Research, Part A. Geological Survey of Canada, Paper 87 1-A p. 219-238.

Grotzinger, J.P., and Royden, L., 1990. Elastic strength of the Slave craton at 1.9 Gyr and implications for the thermal evolution of the continents. Nature, v. 347, p. 64-66.

Gurnis, M., 1990. Plate-mantle coupling and continental flooding. Geophysical Research Letters, v. 17, p. 623-626.

Gurnis, M.G., 1992. Rapid continental subsidence following the initiation and evolution of subduction. Science, v. 255, p. 1556-1558.

Hanmer, S., and Lucas, S.B., 1985. Anatomy of a ductile transcurrent shear: The Great Slave Lake Shear Zone, District of Mackenzie, N.W.T. (preliminary report), Current Research. Geological Survey of Canada Paper 85-1B p. 7-22.

Haq, B.U., Hardenbol, J., and Vail, P.R., 1987. Chronology of fluctuating sea levels since the Triassic. Science, v. 235, p. 1156-1167.

Heller, P., and Paola, C., 1989. The paradox of Lower Cretaceous gravels and the initiation of thrusting in the Sevier orogenic belt, United States Western Interior. Geol. Soc. America Bull., v. 101, p. 864-875.

Heller, P.L., Angevine, C.L., Paola, C., Burbank, D.W., Beck, R.A., and Raynolds, R.G.H., 1989. Comment and reply on "Thrusting and gravel progradation in foreland basins: a test of post-thrusting gravel dispersal". Geology, v. 17, p. 959-961.

Heller, P.L., Angevine, C.L., Winslow, N.S., and Paola, C., 1988. Two-phase stratigraphic

model of foreland basin sequences. Geology, v. 16, p. 501-504.
Hoffman, P.F., 1987. Continental transform tectonics: Great Slave Lake shear zone (ca. 1.9 Ga), northwest Canada. Geology, v. 15, p. 785-788.
Hoffman, P.F., 1988. United plates of America, the birth of a craton: Early Proterozoic assembly and growth of Laurentia. Ann. Rev. Earth Planet. Sci., v. 16, p. 543-603.
Hoffman, P.F., 1989. Precambrian geology and tectonic history of North America, in, A.W. Bally, and A.R. Palmer (eds.), The geology of North America - An overview. Geological Society of America (Boulder, CO), p. 447-512.
Hoffman, P.F., Culshaw, N.G., Hanmer, S.K., LeCheminant, A.N., McGrath, P.H., Tirrul, R., Van Breeman, O., Bowring, S.A., and Grotzinger, J.P., 1986. Is the Thelon Front (NWT) a suture? Geol. Assoc. Canada, Prog. With Abs., v. 11, p. 82.
Hoffman, P.F., Tirrul, R., Grotzinger, J.P., Lucas, S.B., and Eriksson, K.A., 1984. The Externides of Wopmay Orogen, Takijuk Lake and Kikerk Lake map areas, District of Mackenzie, Current Research, Part A. Geological Survey of Canada, Paper 84-1A p. 383-395.
Homewood, P., Allen, P.A., and Williams, G.D., 1986. Dynamics of the Molasse Basin of western Switzerland, in, P.A. Allen, and P. Homewood (eds.), Foreland Basins. Blackwell Scientific Publications (Oxford, UK), p. 453.
Johnson, D.D., and Beaumont, C., 1990. Surface processes and foreland basin stratigraphy. Geol. Soc. America, N.E. Section, Abs. with Progs., v. 22, p. A26.
Johnson, H.D., 1977. Shallow-marine bar sequences: an example from the late Precambrian of north Norway. Sedimentology, v. 24, p. 245-270.
Johnson, H.D., and Baldwin, C.T., 1986. Shallow siliciclastic seas, in, H.G. Reading (ed.), Sedimentary Environments and Facies (2nd ed.). Blackwell Scientific Publications (Boston, MA), p. 229-282.
Jordan, T.E., 1981. Thrust loads and foreland basin evolution, Cretaceous, western United States. Am. Assoc. Petrol. Geol. Bull., v. 65, p. 2506-2520.
Jordan, T.E., and Flemings, P.B., 1990. From geodynamic models to basin fill - a stratigraphic perspective, in, T.A. Cross (ed.), Quantitative Dynamic Stratigraphy. Prentice-Hall (Englewood Cliffs, NJ), p. 149-164.
Jordan, T.E., Flemings, P.B., and Beer, J.A., 1988. Dating thrust activity by use of foreland basin strata, in, K. Kleinspehn, and C. Paola (eds.), New Perspectives in Basin Analysis. Springer-Verlag (New York), p. 307-330.
Karner, G.D., 1986. On the relationships between foreland basin stratigraphy and thrust sheet migration and denudation. Eos, Trans. Am. Geophys. Union, v. 67, p. 1193.
Karner, G.D., and Watts, A.B., 1983. Gravity anomalies and flexure of the lithosphere at mountain ranges. Jour. Geophys. Res, v. 88, No. B12, p. 10449-10477.
Kominz, M.A., and Bond, G.C., 1986. Geophysical modelling of the thermal history of foreland basins. Nature, v. 320, p. 252-256.
Kominz, M.A., and Bond, G.C., 1991. Unusually large subsidence and sea-level events during middle Paleozoic time: new evidence supporting mantle convection models for supercontinent assembly. Geology, v. 19, p. 56-60.
Krogh, T.E., 1973. A low-contamination method for hydrothermal decomposition of zircon and extraction of U and Pb for isotopic age determinations. Geochim. Cosmochim. Acta, v. 37, p. 485-494.
Krogh, T.E., 1982. Improved accuracy of U-Pb zircon ages by creation of more concordant

systems using an air abrasion technique. Geochim. Cosmochim. Acta, v. 45, p. 637-649.

Lyon-Caen, H., and Molnar, P., 1985. Gravity anomalies, flexure of the Indian plate, and the structure, support, and evolution of Himalaya and Ganga Basin. Tectonics, v. 4, p. 513-538.

McCormick, D.S., and Grotzinger, J.P., 1988. Aspects of the Burnside Formation, Bear Creek Group, Kilohigok Basin, N.W.T., Current Research, Part A. Geological Survey of Canada, Paper 88 1-C p. 321-339.

McCormick, D.S., and Grotzinger, J.P., in review. Distinction of marine from alluvial facies in an Early Proterozoic foreland basin: Burnside Formation (1.9 Ga), N.W.T., Canada. Sedimentology, v. p.

McGlynn, J.C., and Irving, E., 1981. Horizontal motions and rotations of the Canadian Shield during the Early Proterozoic, in, F.H.A. Campbell (ed.), Proterozoic Basins of Canada. Geological Survey of Canada, Paper 81-10 p. 183-190.

McPherson, J.G., Shanmugam, G., and Moiola, R.J., 1987. Fan-deltas and braid deltas: varieties of coarse-grained deltas. Geol. Soc. America Bull., v. 99, p. 331-340.

Miall, A.D., 1988. Facies architecture in clastic sedimentary basins, in, K. Kleinspehn, and C. Paola (eds.), New Perspectives in Basin Analysis. Springer-Verlag (New York), p. 67-81.

Mitrovica, J.X., Beaumont, C., and Jarvis, G.T., 1989. Tilting of continental interiors by the dynamical effects of subduction. Tectonics, v. 8, p. 1079-1094.

Moretti, I., and Royden, L., 1988. Deflection, gravity anomalies and tectonics of doubly subducted continental lithosphere: Adriatic and Ionian Seas. Tectonics, v. 7, p. 875-893.

Myrow, P.M., 1987. Sedimentology and depositional history of the Chapel Island Formation (Late Precambrian to Early Cambrian), southeast Newfoundland. Ph.D., Memorial University, St. John's, Newfoundland.

Myrow, P.M., Narbonne, G.M., and Hiscott, R.N., 1988. Storm-shelf and tidal deposits of the Chapel Island and Random Formations, Burin Peninsula: facies and trace fossils. Geological Association of Canada, Annual Meeting, Guidebook B6 108 pp.

Nio, S.D., and Yang, C., 1991. Diagnostic attributes of clastic tidal deposits: a review, in, D.G. Smith, G.E. Reinson, B.A. Zaitlin, and R.A. Rahmani (eds.), Clastic Tidal Sedimentology. Canadian Society of Petroleum Geologists, Special Publication 16 (Calgary, Alberta, Canada), p. 3-28.

Nottvedt, A., and Kreisa, R.D., 1987. Model for combined-flow origin of hummocky cross-stratification. Geology, v. 15, p. 357-361.

Nunn, J.A., Czerniak, M., and Pilger, R.H., Jr., 1987. Constraints on the structure of the Brooks Range and Colville Basin, northern Alaska, from flexure and gravity analysis. Tectonics, v. 6, p. 603-617.

Padgham, W.A., 1985. Observations and speculations on supracrustal successions in the Slave Structural Province, in, L.D. Ayers, P.C. Thurston, K.D. Card, and W. Weber (eds.), Evolution of Archean Supracrustal Sequences. Geological Association of Canada, Special Paper 28 p. 133-152.

Paola, C., 1988. Subsidence and gravel transport in alluvial basins, in, K. Kleinspehn, and C. Paola (eds.), New Perspectives in Basin Analysis. Springer-Verlag (New York), p. 231-244.

Parkash, B., Sharma, R.P., and Roy, A.K., 1980. The Siwalik Group (molasse) - sediments shed by the collision of continental plates. Sedim. Geol., v. 25, p. 127-159.

Platt, J.P., 1986. Dynamics of orogenic wedges and the uplift of high-pressure metamorphic rocks. Geol. Soc. America Bull., v. 97, p. 1037-1053.

Quinlan, G.M., and Beaumont, C., 1984. Appalachian thrusting, lithospheric flexure, and Paleozoic stratigraphy of eastern interior North America. Can. J. Ear. Sci., v. 21, p. 973-996.

Royden, L., and Karner, G.D., 1984. Flexure of the lithosphere beneath Apennine and Carpathian foredeep basins: evidence for an insufficient topographic load. Am. Assoc. Petrol. Geol. Bull., v. 68, p. 704-712.

Rust, B.R., 1984. Coarse alluvial deposits, in, R.G. Walker (ed.), Facies Models (2nd ed.). Geoscience Canada, Reprint Series 1 p. 53-70.

Schedl, A., and Wiltschko, D.V., 1984. Sedimentological effects of a moving terrain. J. Geol., v. 92, p. 273-287.

Shanmugam, G., 1988. Origin, recognition, and importance of erosional unconformities in sedimentary basins, in, K. Kleinspehn, and C. Paola (eds.), New Perspectives in Basin Analysis. Springer-Verlag (New York), p. 83-108.

Sinclair, H.D., Coakley, B.J., and Watts, A.B., 1991. Simulation of foreland basin stratigraphy using a diffusion model of mountain belt uplift and erosion: an example from the Central Alps, Switzerland. Tectonics, v. 10, p. 599-620.

Steckler, M.S., 1989. The role of the thermal-mechanical structure of the lithosphere in the formation of sedimentary basins, in, T.A. Cross (ed.), Quantitative Dynamic Stratigraphy. Prentice-Hall (Englewood Cliffs, NJ) p. 89-112.

Thompson, P.H., Culshaw, N., Buchanan, J.R., and Manoljlovic, P., 1986. Geology of the Slave Province and Thelon Tectonic Zone in the Tinney Hills-Overby Lake (west half) map area, District of Mackenzie, Current Research, Part A. Geological Survey of Canada, Paper 86-1A p. 275-289.

Thompson, P.H., Culshaw, N., Thompson, D., and Buchanan, J.R., 1985. Geology across the western boundary of the Thelon Tectonic Zone in the Tinney Hills-Overby Lake (west half) map area, District of Mackenzie, Current Research, Part A. Geological Survey of Canada, Paper 85-1A p. 555-572.

Thompson, P.H., and Frey, M., 1984. Illite "crystallinity" in the Western River Formation and its significance regarding the regional metamorphism of the early Proterozoic Goulburn Group, District of Mackenzie, Current Research, Part A. Geological Survey of Canada, Paper 84-1A p. 409-414.

Tirrul, R., 1985. Nappes in the Kilohigok Basin and their relationship to the Thelon Tectonic Zone, District of Mackenzie, Current Research, Part A. Geological Survey of Canada, Paper 85-1A p. 407-420.

Tirrul, R., and Grotzinger, J.P., 1990. Early Proterozoic collisional orogeny along the northern Thelon Tectonic Zone, Northwest Territories, Canada: Evidence from the foreland. Tectonics, v. 9, p. 1015-1036.

Turcotte, D.L., and Schubert, G., 1982. Geodynamics: Applications of continuum physics to geological problems. John Wiley & Sons, Inc. (New York), 450 pp.

Vail, P.R., Mitchum, R.M., and Thompson, S., III, 1977. Seismic stratigraphy and global changes of sea level, Part 3: Relative changes of sea level from coastal onlap, in, C. Payton (ed.), Seismic Stratigraphy - Applications to Hydrocarbon Exploration.

American Association of Petroleum Geologists, Memoir 26 p. 63-81.
van Breemen, O., Henderson, J.B., Loveridge, W.D., and Thompson, P.H., 1986. Archean-Aphebian geochronology along the Thelon Tectonic Zone, Healey Lake area, N.W.T. Geol. Assoc. Canada, Prog. with Abs., v. 11, p. 139.
Van Wagoner, J.C., Posamentier, H.W., Mitchum, R.M., Jr., Vail, P.R., Sarg, J.F., Loutit, T.S., and Hardenbol, J., 1988. An overview of the fundamentals of sequence stratigraphy and key definitions, in, C.K. Wilgus, B.S. Hastings, C.G.S.C. Kendall, H.W. Posamentier, C.A. Ross, and J.C. Van Wagoner (eds.), Sea-level changes: an integrated approach. Soc. Econ. Paleontologists and Mineralogists, Spec. Pub. No. 42 p. 39-46.
Vos, R.G., 1981. Sedimentology of an Ordovician fan delta complex, western Libya. Sed. Geol., v. 29, p. 153-170.
Vos, R.G., and Tankard, A.J., 1981. Braided fluvial sedimentation in the Lower Paleozoic Cape Basin, South Africa. Sed. Geol., v. 29, p. 171-193.
Walker, R.G., and Cant, D.J., 1984. Sandy fluvial systems, in, R.G. Walker (ed.), Facies Models (2nd ed.). Geoscience Canada, Reprint Series 1 p. 71-89.
Wells, N.A., and Dorr, J.A., Jr., 1987. A reconnaissance of sedimentation on the Kosi alluvial fan of India, in, F.G. Ethridge, R.M. Flores, and M.D. Harvey (eds.), Recent Developments in Fluvial Sedimentology. Soc. Econ. Paleont. Mineral., Spec. Pub. No. 39 p. 51-61.

Table Caption

Table 1: Lithofacies of the Burnside Formation.

Association / Facies	Grain Size	Sedimentary Structures	Bedding Characteristics	Environmental Interpretation	Lateral Extent	Example (Member / Figures)
siltstone	green mud to (f) sand	even parallel laminae; graded laminae; wave ripples; hummocky / swaley cross-stratification; sand-filled gutters; massive beds	sub-mm to 10's of cm's; continuous	progradational storm-influenced muddy shelf	across entire basin	Link Fm., basal Transitional Mbr., sections 1-3; Figures 6, 8, 9
mixed siltstone-sandstone	silt and white to green (f-c) sand	wave ripples and low-angle cross-laminae; low-angle cross-bedding, trough cross-bedding	5-50 cm; tabular to wavy, locally discontinuous	retrogradational storm-influenced mixed muddy-sandy shelf	across entire basin	Link Fm., distal Burnside Fm., sections 6-11, 13, 14; Figures 6, 8, 10
rippled siltstone-sandstone	red mud/silt to (vf) sand	streaky to ripple cross-laminae; common wave and oscillation ripples; common soft sediment deformation	1-15 cm; tabular, locally discontinuous	braid delta front	proximal foreland	basal Transitional Mbr., sections 1-3; Figures 6, 8, 9
tabular bedded sandstone	pink (vf-f) sand	parallel and low-angle cross-laminae; internal scours with clay chips; isolated trough cross-beds in scours; current and wave ripples	10-50 cm; tabular (10-100's m)	braid delta platform	across entire basin	basal Transitional Mbr., sections 1-7, 12-14, 16; Figures 6, 8, 9, 10
trough bedded sandstone with mud clasts	(f-m) sand	trough cross-beds (<25 cm); shallow scours and channels (dm); common clay chips	30-150 cm; lenticular to tabular; cross-bedding laterally-extensive	braid delta plain	across entire basin	Transitional Mbr., sections 1-3; Figures 6, 8, 9
single-storied trough cross-bedded sandstone	(f-m) sand	trough cross-beds (<50 cm); shallow scours and channels (dm); no clay chips	30-150 cm beds; 1-3 m bedsets; lenticular to tabular cross-bedding; laterally- and vertically-extensive	distal braid plain	across entire basin	Transitional Mbr., sections 1-3, 14, 16; Figures 8, 9, 10
multi-storied trough cross- bedded sandstone	(f-c) sand with sparse gravel	medium and large trough cross-beds (25-80 cm); upper plane laminae; medium trough cross-beds at bedset tops; basal master bedding surface laterally continuous over km's	50-300 cm beds; continuous; bedsets 8-20 m tracable over km's	medial braid plain with minor gravel	proximal foreland and craton	Buff Sandstone Mbr., sections 1-3; Figures 7, 8, 9
trough- and tangentially cross-bedded sandstone	(f-c) sand; locally pebbly	medium and large trough cross-beds; large planar-tangential cross-beds; deep scours (20-200 cm)	50-200 cm; continuous	medial braid plain	proximal foreland	Gravelly Sandstone Mbr., sections 1-3; Figures 7, 8, 9
sheet gravel and trough cross-bedded sandstone	pebble to cobble conglomerate & (m-vc) sand	clast-supported lags and crudely-stratified gravel sheets; large trough cross-beds (dm), upper sets lack gravel; common large planar cross beds (m) at base	50-300 cm	gravelly medial braid plain	proximal foreland	Conglomerate Mbr., sections 1-3; Figures 7, 8, 9
Burnside Dolomite	mixed clastic carbonate and siliciclastic mud to sand, cyclic carbonates	graded laminae; wave ripples; small scale hummocky cross-stratification; parallel laminae (especially in siliciclastic sand; trough cross-bedding on craton	2-20 cm; tabular to wavy, locally discontinuous	mixed carbonate-siliciclastic lagoon and cyclic carbonates	distal foreland	Burnside Dolomite; Figures 6, 10

Table 1.

Figure Captions

Figure 1. Geologic and geographic elements of the northwestern Canadian Shield. Triangular ticks indicate zones of overthrusting, with ticks on the overthrust plate; arrows indicate zones of strike slip displacement. Inset indicates the location of the map within North America. Figure modified from Hoffman (1987).

Figure 2. Geologic map of Kilohigok Basin. Circled numbers mark the locations of measured sections in the Burnside Formation that are shown in subsequent cross sections. The basin has been restored by removing approximately 115 km of left slip on the Bathurst fault zone as recommended by Tirrul and Grotzinger (1990). This displacement post-dates deposition of the Goulburn Supergroup. The Gordon Bay Arch was a flexural arch that was active during deposition of the Bear Creek Group (see Figures 3a&b, 4). A second independent flexural arch lay near Rockinghorse Lake and is termed the Rockinghorse Arch in subsequent cross sections. Thrust nappes described by Tirrul and Grotzinger (1990) are restricted to the part of the basin most proximal to Thelon Orogen to the south section 1.

Figure 3. A: Stratigraphic framework of the Goulburn Supergroup with an interpretation of the sedimentologic and tectonic evolution (Tirrul, 1985; Grotzinger and McCormick, 1988; Tirrul and Grotzinger, 1990). Volcanic ash bed ages are from Bowring and Grotzinger (1992). The upper ash bed age is on the basis of correlation to a stratigraphic horizon in Wopmay Orogen (see text for explanation). B: Schematic cross section and correlation between members of the Burnside Formation and the Mara and Quadyuk Formations. Thick lines indicate inferred erosional, unconformable contacts; thin lines indicate gradational or inferred conformable lithological contacts. Thicknesses are diagrammatic and not to scale.

Figure 4. Cross section of the Goulburn Supergroup from Kilohigok Basin to Wopmay Orogen (Figure 1). The line of section within Kilohigok Basin lies along the line from the section 1 to section 14 in Figure 2. The datum is the top of the passive margin carbonate platform in Wopmay Orogen and its correlative within the Burnside Formation in Kilohigok Basin. Locations of lines of section in subsequent figures are indicated in Figure 2. The measured sections are projected onto a west-northwest line corresponding to the mean paleocurrent direction for the upper alluvial sandstone facies (Figure 5). The ages of ash beds are from Bowring and Grotzinger (1992).

Figure 5. Paleocurrent directions within the Burnside Formation on the basis of the azimuth of trough cross-bed axes. The inset labeled "sections 2&3" are readings taken from between sections 2 and 3 in Figure 2, roughly the same area as the rose with 883 measurements. This inset compares readings recorded in the Transitional member (lowermost one in Burnside Formation; Figures 3b, 8, 9) of inferred braid delta facies that have a distinct and statistically significant SW mode with paleocurrents recorded in overlying members of inferred braid plain facies that have the predominant NW mode. Data from Campbell and Cecile (1981) are plotted with radius proportional to the number of paleocurrent measurements. Data from this study are plotted with area proportional to number of readings.

Figure 6. Photographs of siliciclastic shelf to braid delta facies in the Burnside Formation. A: Swaley cross-stratified siltstone from the silty marine shelf facies (marked "s"). Truncated swaley bed is interbedded with wave-rippled and parallel-laminated siltstone. Pocketknife for scale. B: Mixed silty-sandy shelf facies with symmetrical wave ripples in upper bed interbedded with laminated mudstone (dark). Coin for scale. C: Trough cross-bedded sandstone (marked "t") with common mud chips of braid delta distributary facies. Tabular parallel-laminated sandstones are sharply interbedded with trough cross-bedded sandstone. Pocketknife for scale at top of the lower trough cross-bedded sandstone. D: Low-angle cross-laminae, internal truncations, and wave-rippled clastic dolarenite of Burnside Dolomite at section 12 (Figures 2, 4, 10). Significant amounts of siliciclastic mud and sand are mixed with the carbonate silt and sand. Coin for scale.

Figure 7. Photographs of medial braided alluvial facies in the Burnside Formation from the proximal part of the basin (sections 1-3; Figures 2, 3). A: Lateral view of the contact of the Transitional member (braid delta and distal braid plain; to the left of the slanted line, labeled "T") with Buff Sandstone member (medial braid plain; to the right of the slanted line, labeled "B") at section 2. Beds dip to the right at about 45°. Note the laterally continuous surfaces in the Buff Sandstone member that bound bedsets approximately 8-12 m thick. Field of view represents about 200 m of section vertically and 500-600 m laterally. B: Base of Conglomerate member showing crudely bedded gravel with coarsest clasts at base of beds. Upper parts of beds are trough cross-bedded sandstone. Hammer for scale (circled). C: Uppermost conglomerate horizon at section 2 at the top of the Gravelly Sandstone member. Lower bed is volcanic clast horizon and upper bed is polymictic horizon with Burnside intraformational clasts. Note steep scour relief on channel margins and nearly bedding-parallel upper surface. Staff is 1.5 m long. D: Fractured clast derived from Burnside Formation alluvial facies. Note vein quartz fracture filling that does not extent into the

matrix sand. This clast must have been cemented, then fractured and filled with quartz at depth before being re-incorporated into the Burnside fluvial system. Cannibalization of syn-orogenic sediments is common in foreland basins. Coin for scale (arrow).

Figure 8. Cross section of the transition from marine shelf to alluvial-dominated facies in the Bear Creek Group. The cross section from 3 to 12 lies approximately parallel to the dominant paleocurrent trend; sections 12 to 14 lie roughly perpendicular to the main alluvial paleocurrent trend. Sections locations are found in Figure 2.

Figure 9. Cross section of the Burnside Formation in the proximal foredeep east of the Bathurst Fault Zone (see Figure 2 for location). Note that the vertical exaggeration is much less in this cross section than in any other. Note also that the lateral thickening of all members increases between sections 2 and 1; section 2 was the approximate location of the shelf break in the underlying lower Bear Creek Group stratigraphic sequences. The unpatterned space within the Orange Sandstone member labeled "section faulted out" is the location and interpreted stratigraphic separation on a fault that cuts through the section between sections 2 and 3. Stratigraphic separation of at least 800-1000 meters is inferred on the basis of extrapolation of thickness trends in the lower members from sections 1 to 10 (see Figure 8).

Figure 10. Cross section of the Burnside Formation in the distal foredeep west of the Bathurst Fault Zone and the Gordon Bay Arch (see Figure 2 for location). Disconformities are those illustrated in Figures 8 and 9. The datum for this cross-section is the top of the Burnside Dolomite. This section is approximately perpendicular to the dominant paleocurrent trend.

Figure 11. Interpretation of the paleogeography of the Burnside alluvial system. A: Time of horizontal datum in Figure 4. Note the emergent, southwestward plunging Gordon Bay arch that results from thrusting in the Thelon orogenic belt, southeast of Kilohigok Basin (Figure 1). Evidence for the plunging nature the Gordon Bay Arch comes from a section of the Burnside Formation at section 15 (Figure 2) that lies directly on granitic basement, suggesting that this area was probably emergent during deposition of the lower Bear Creek Group and part of the Burnside Formation. This may account for the high feldspar content in the lower Bear Creek Group and lower deltaic Burnside Formation. The flexural arch indicated near the western boundary of the diagram is not related to the Gordon Bay flexural arch. Rather it results from sediment loading along the passive margin of Wopmay Orogen to the west. B: Time of the progradation of braid plain facies over the Gordon Bay flexural

arch (this is the same as the datum in Figures 4, 8, and 9). This corresponds to the time of deposition of the Buff Sandstone member (Figures 3b, 9). The base of this member is largely marked by an erosional unconformity. C: Time of progradation of the Conglomerate member (Figure 3b). This marks the first time that alluvial facies prograde across the entire Slave Craton and interfinger with marine shelf facies in Wopmay Orogen. Paleocurrents indicate that transport was uniformly to the west-northwest or northwest (Figure 5). Gravel-bearing sandstones are present at sections 13 and 14. D: Time of transgression of the marine Burnside Dolomite over the alluvial system. The westward-thickening tongue of mixed siliciclastic-carbonate and cyclic carbonates are believed to correlate with the Rocknest Formation carbonate platform in Wopmay orogen that lies 20 km west of section 14 (Figures 1, 2). All alluvial facies appear to backstep at this time except in the most proximal part of the foredeep. E: Alluvial facies prograde back across the craton. Some gravel in braid plain facies is found as far west as section 12.F: End of alluvial sedimentation in the Bear Creek Group. A flexural arch may have existed over the section 12 area at the end of alluvial sedimentation. Quadyuk Formation shelf carbonate intertongues and passes laterally into deltaic Orange Sandstone member in the proximal foreland (Figures 3b, 4, 10). To the west on the craton, the Quadyuk is absent in section 12 . The exposed surface coincident with the single flexural arch represents an amalgamated exposure surface and a transgressive surface (Figure 10).

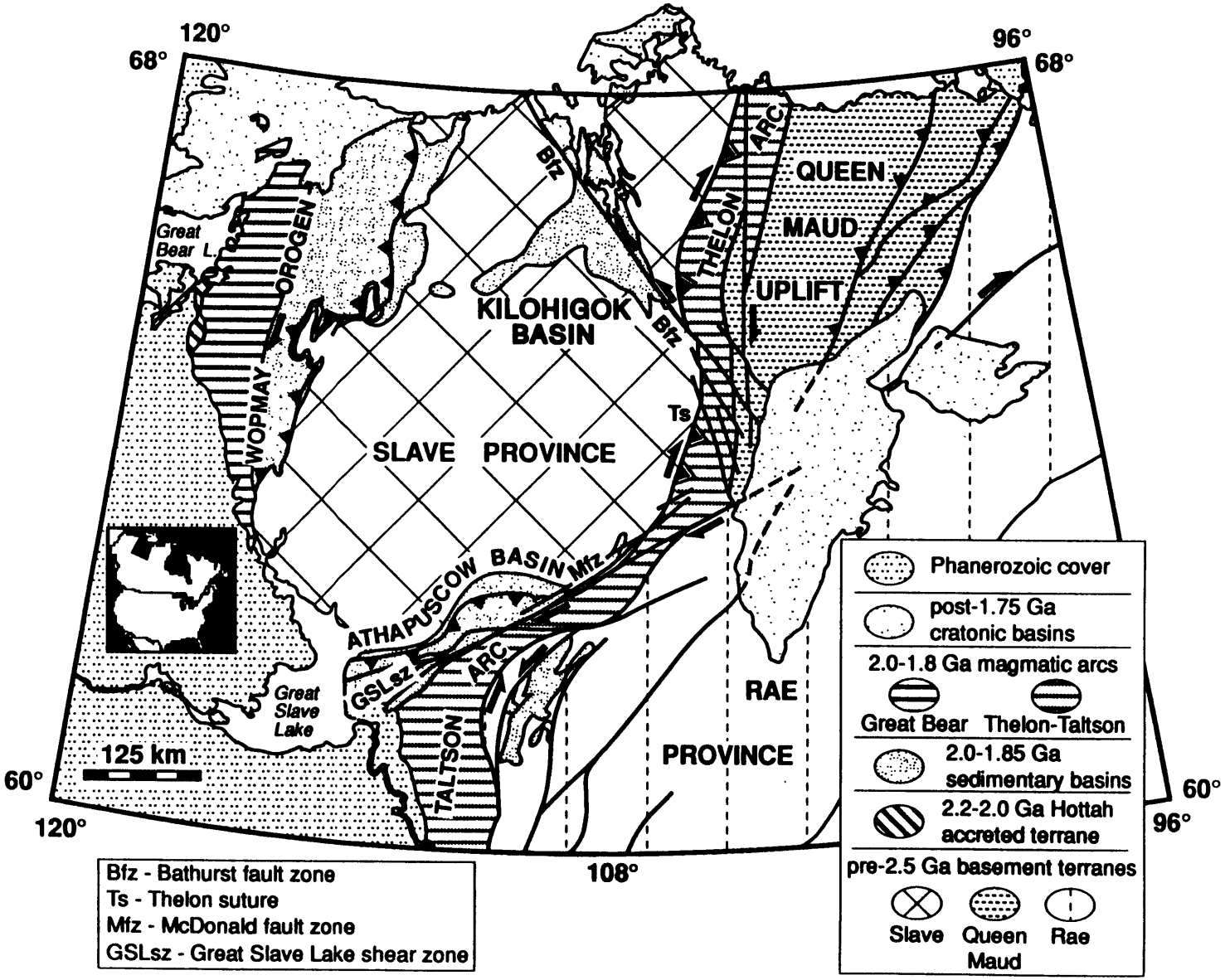
120°
68°
96°
68°
Great Bear L.
WOPMAY OROGEN
Bfz
THELON ARC
QUEEN
MAUD
UPLIFT
KILOHIGOK BASIN
Bfz
Ts
SLAVE PROVINCE
ATHAPUSCOW BASIN
Mfz
GSLsz
ARC
Great Slave Lake
TALTSON
RAE
PROVINCE
125 km
60°
120°
108°
96°
60°
Bfz - Bathurst fault zone
Ts - Thelon suture
Mfz - McDonald fault zone
GSLsz - Great Slave Lake shear zone
Phanerozoic cover
post-1.75 Ga cratonic basins
2.0-1.8 Ga magmatic arcs
Great Bear
Thelon-Taltson
2.0-1.85 Ga sedimentary basins
2.2-2.0 Ga Hottah accreted terrane
pre-2.5 Ga basement terranes
Slave
Queen Maud
Rae

Figure 1.

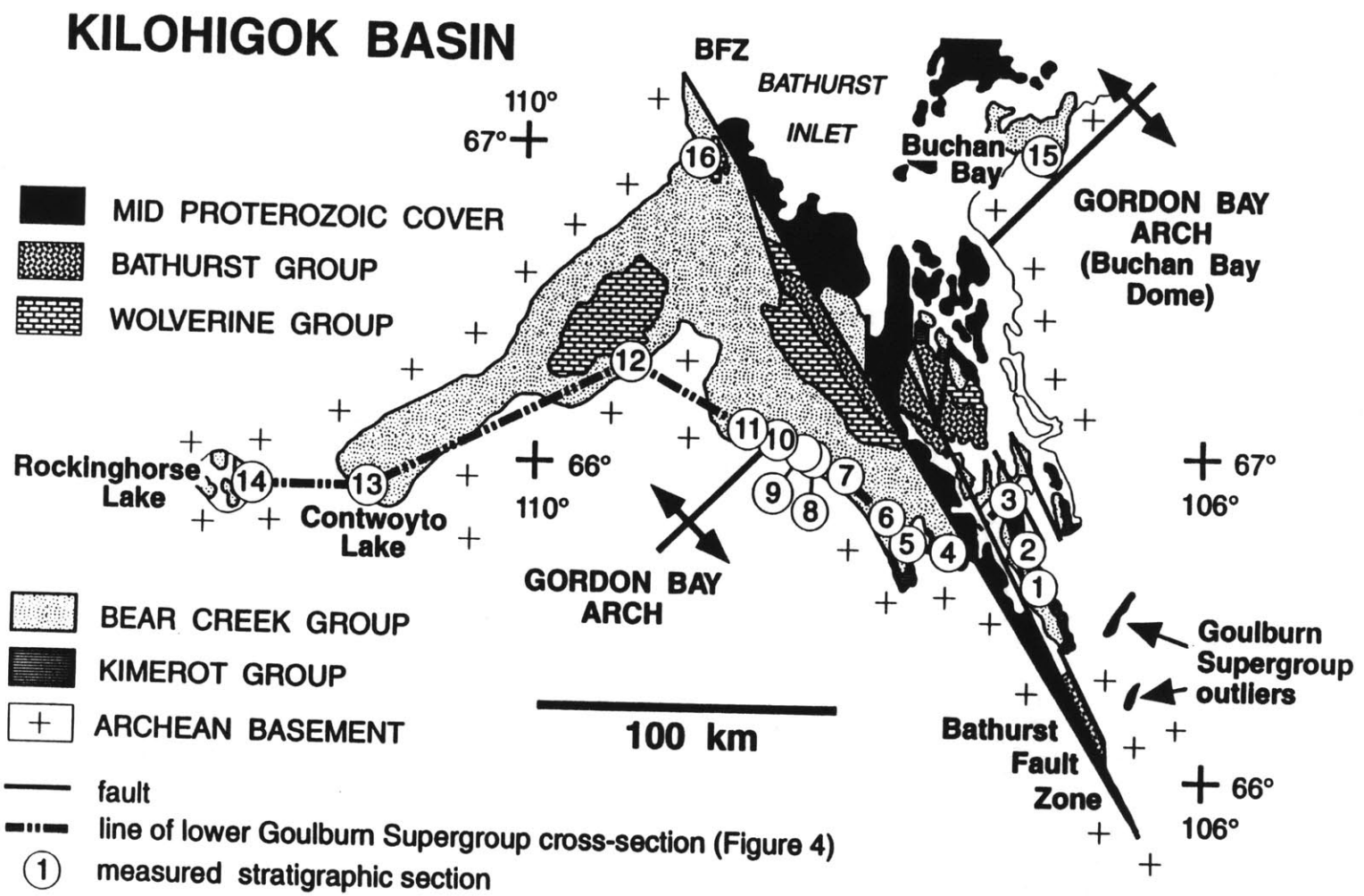
KILOHIGOK BASIN
BFZ
BATHURST
INLET
110°
67°
Buchan Bay
GORDON BAY ARCH (Buchan Bay Dome)
MID PROTEROZOIC COVER
BATHURST GROUP
WOLVERINE GROUP
Rockinghorse Lake
Contwoyto Lake
66°
110°
67°
106°
GORDON BAY ARCH
BEAR CREEK GROUP
KIMEROT GROUP
ARCHEAN BASEMENT
100 km
Goulburn Supergroup outliers
Bathurst Fault Zone
66°
106°
fault
line of lower Goulburn Supergroup cross-section (Figure 4)
measured stratigraphic section

Figure 2.

a

lower Goulburn Supergroup				
lithostratigraphy groups	lithostratigraphy formations	sedimentary environment	tectonic interpretation	volcanic ash age (Ma)
Upper Bear Creek Group	Quadyuk Mara Burnside	carbonate platform marine shelf braid delta / braided alluvial	hinterland unroofing & alluvial progradation over craton	1882 ± 2
Lower Bear Creek Group	Link Beechey Rifle Hackett	siliciclastic marine shelf / minor shelf carbonates / basinal turbidites	Bear Creek foredeep: flexural subsidence and infilling of marine foredeep	1963 ± 6 1969 ± 1
Kimerot Group	Peg Kenyon	siliciclastic to carbonate platform	Kimerot passive margin	

b

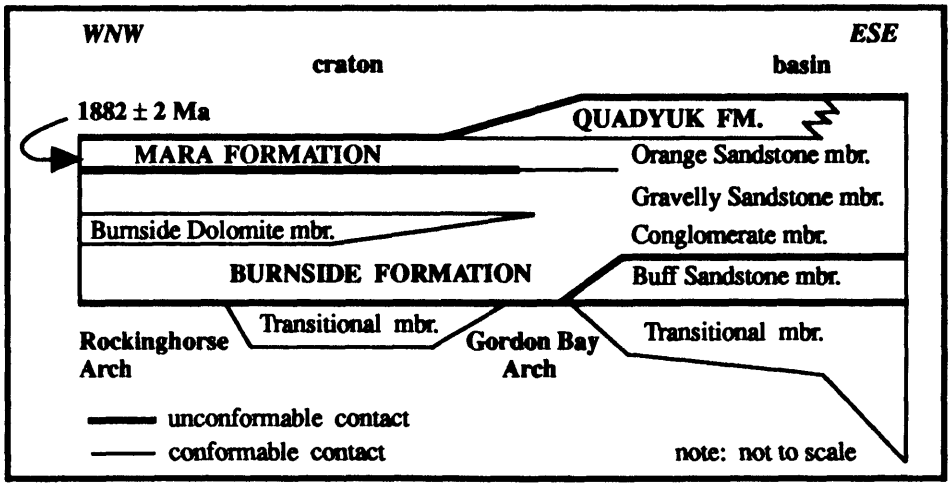

Figure 3.

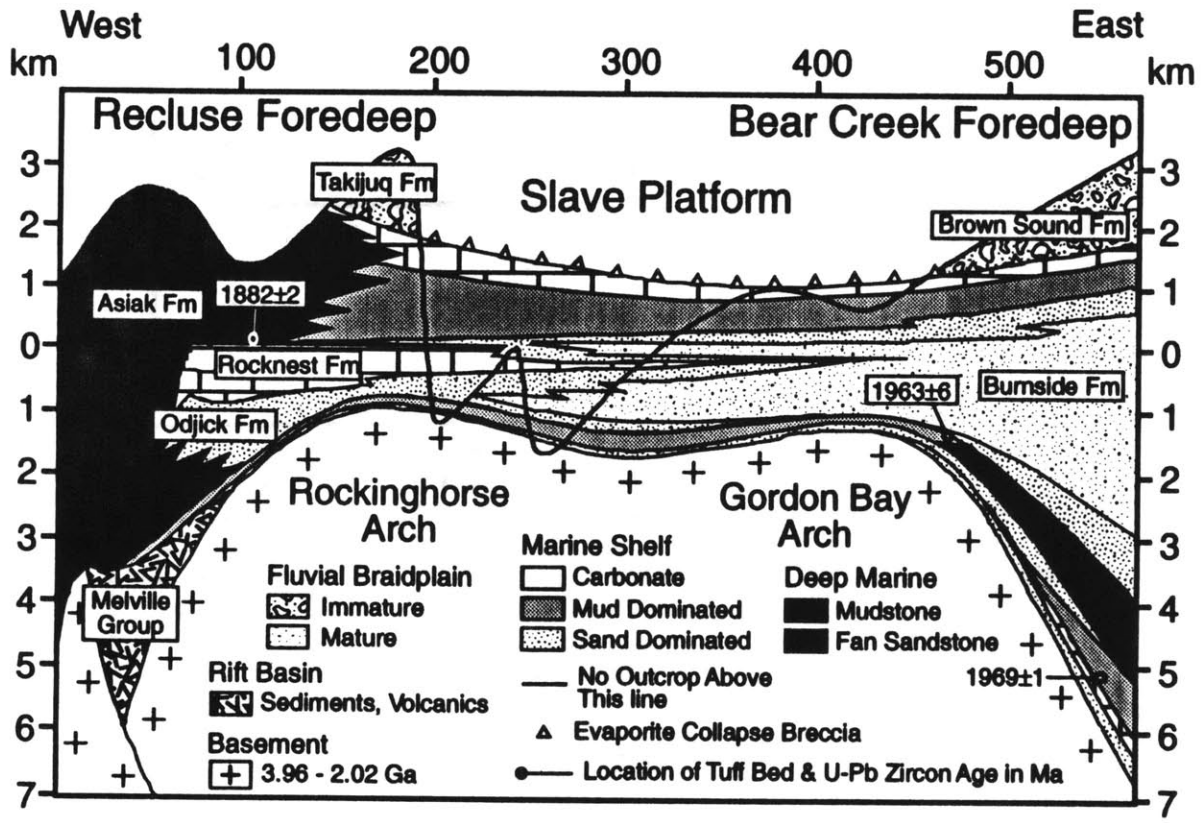
West
East
km
100
200
300
400
500
km
Recluse Foredeep
Bear Creek Foredeep
Slave Platform
Takijuq Fm
Brown Sound Fm
Asiak Fm
1882±2
Rocknest Fm
1963±6
Burnside Fm
Odjick Fm
Rockinghorse Arch
Gordon Bay Arch
Melville Group
Fluvial Braidplain
Immature
Mature
Rift Basin
Sediments, Volcanics
Basement
3.96 - 2.02 Ga
Marine Shelf
Carbonate
Mud Dominated
Sand Dominated
Deep Marine
Mudstone
Fan Sandstone
No Outcrop Above This line
1969±1
Evaporite Collapse Breccia
Location of Tuff Bed & U-Pb Zircon Age in Ma

Figure 4.

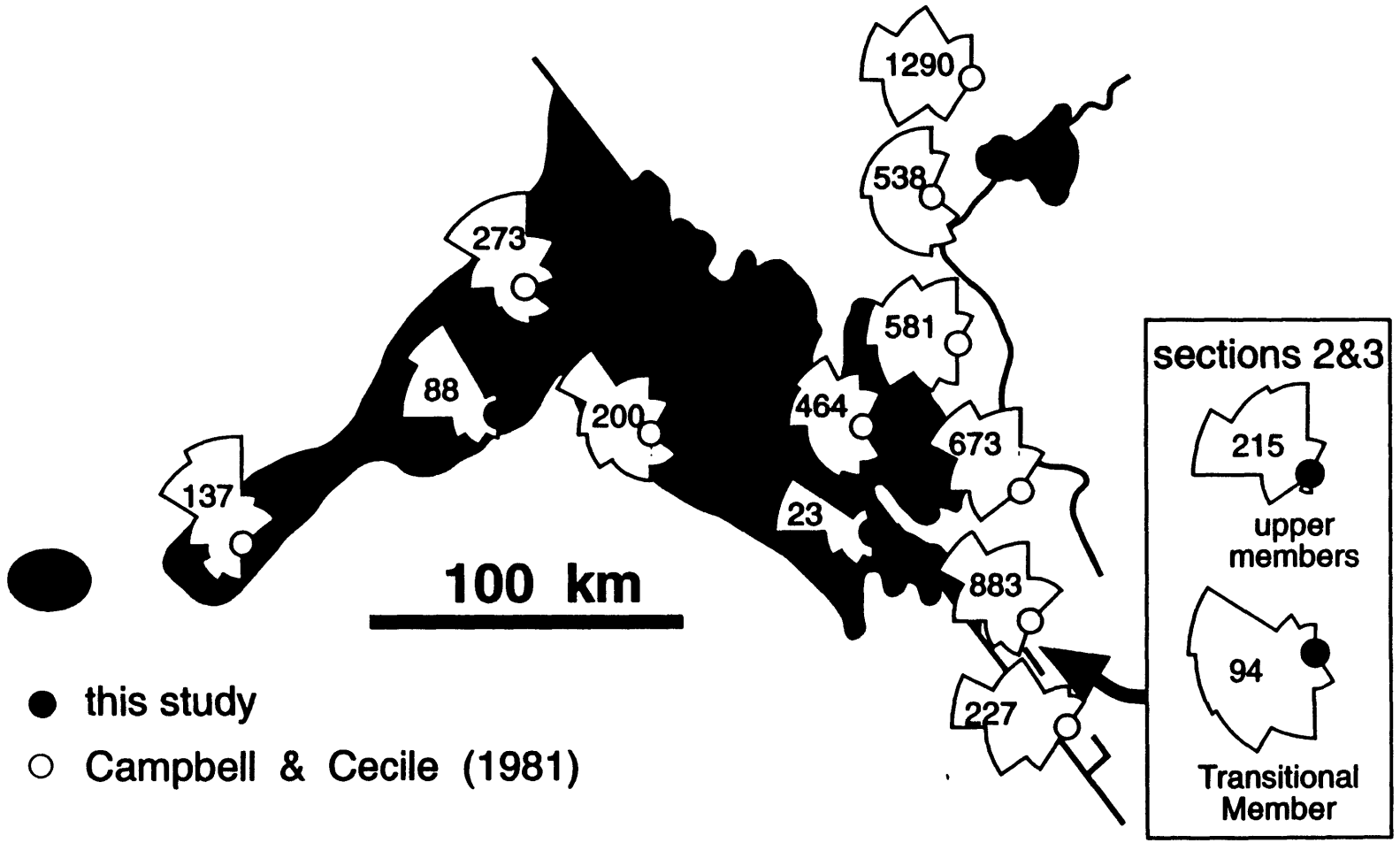
1290
538
273
581
88
200
464
673
137
23
883
227
100 km
this study
Campbell & Cecile (1981)
sections 2&3
215
upper members
94
Transitional Member

Figure 5.

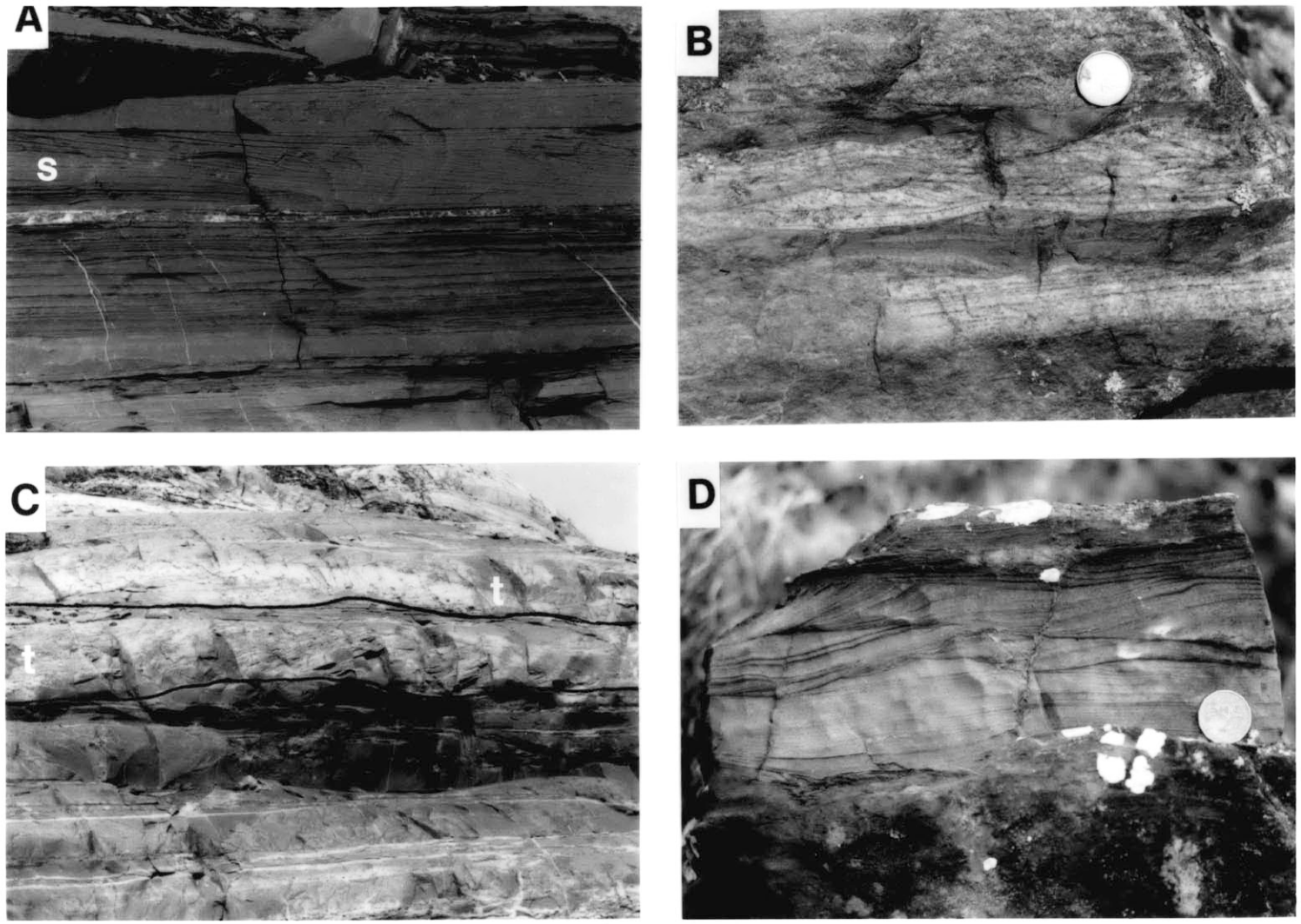

Figure 6.

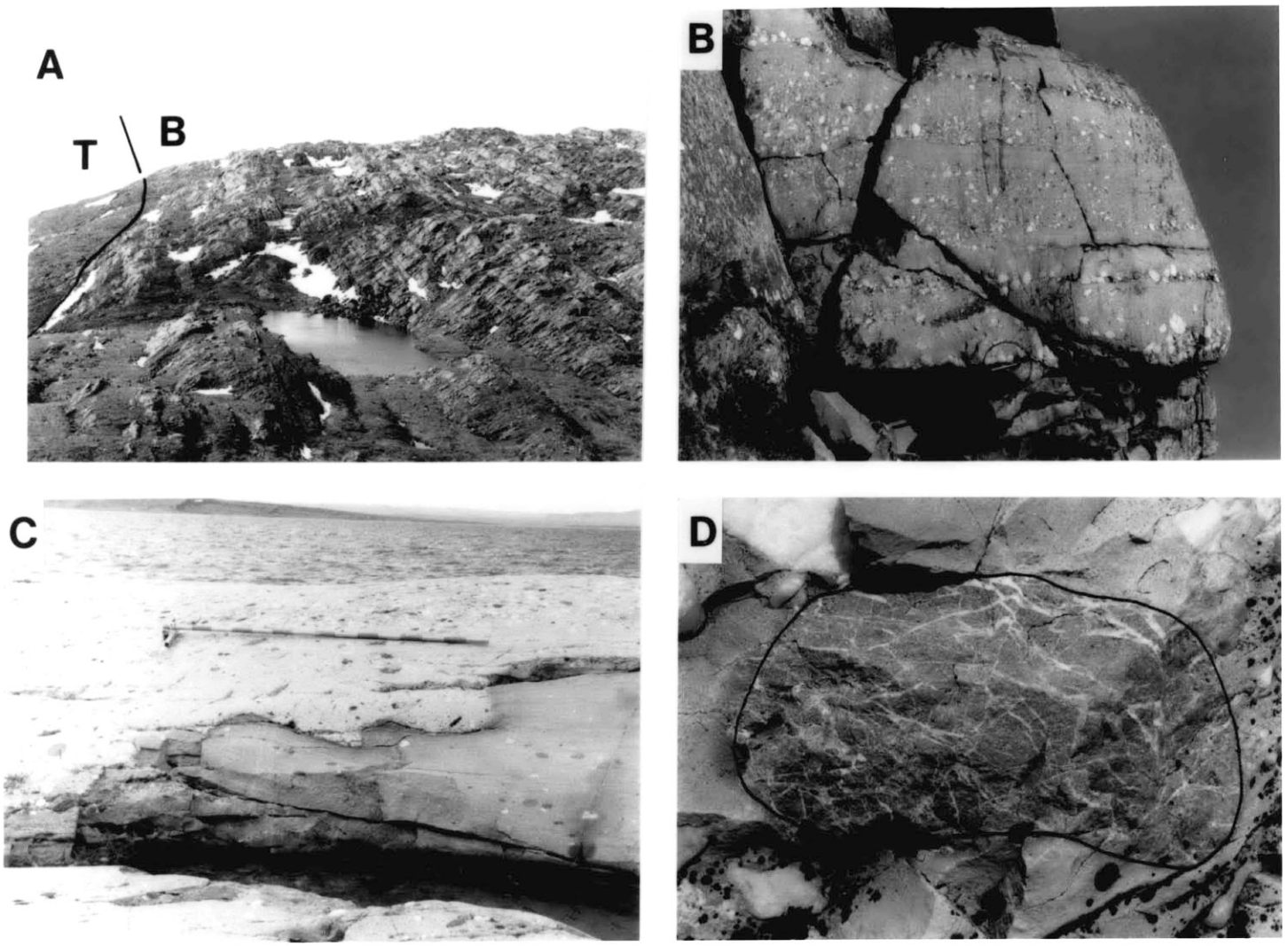

Figure 7.

NE / NW
SW / SE
13
12
11
10
9
8
7
6
5
4
Burnside Fm.
Rifle Fm.
Beechey Fm.
Link Fm.
Gordon Bay arch
itional environment
ıvial conglomerate
dial braid plain
er braid plain
id delta
lf sandstone
lf mudstone-siltstone
ed siliciclastic & carbonate
lic carbonate
measured section
unconformity
facies boundary
500 m
50 km
V:H = 100:1
Burnside Fm.
Link Fm.

Figure 8.

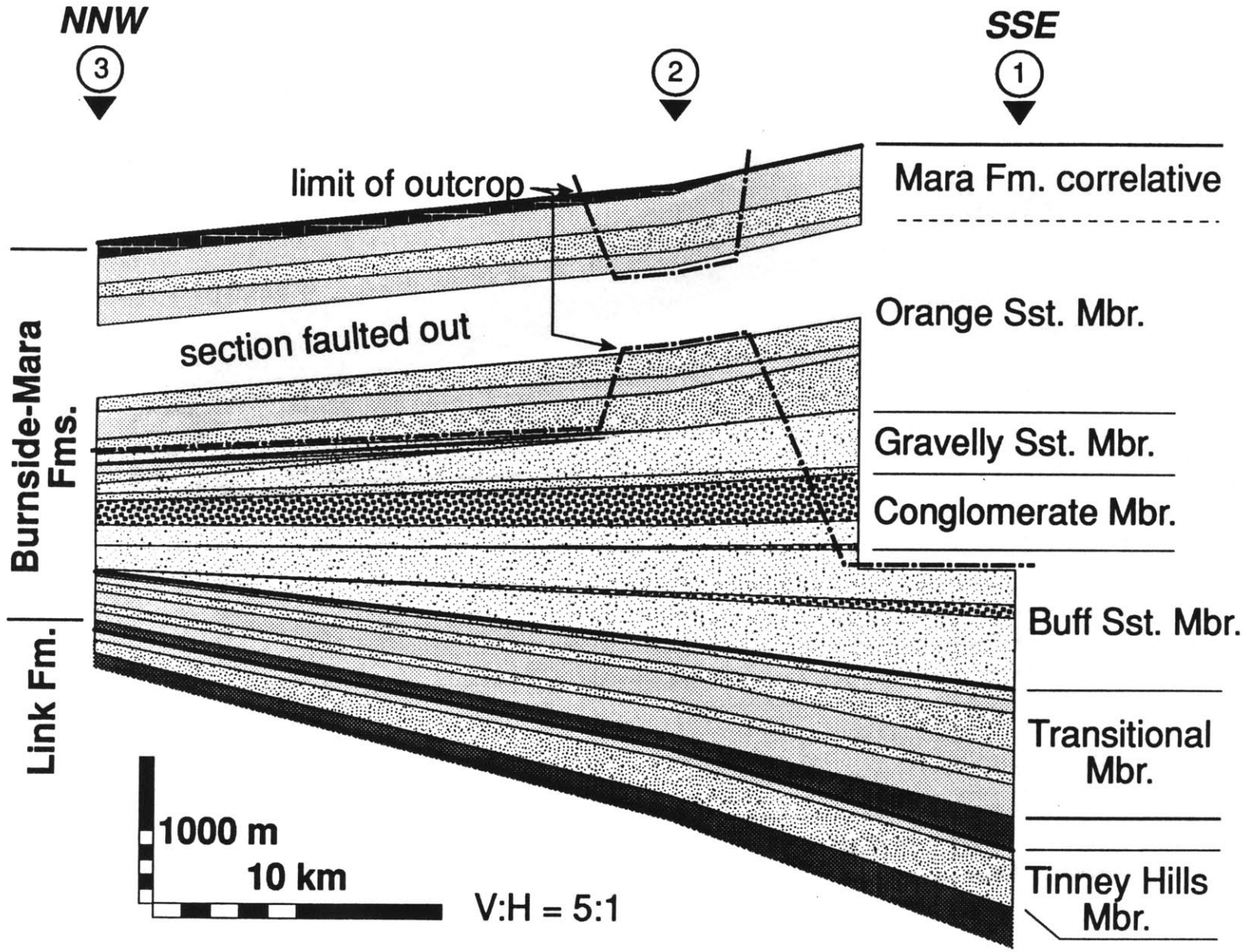
NNW
3
2
SSE
1
limit of outcrop
Mara Fm. correlative
Orange Sst. Mbr.
section faulted out
Burnside-Mara Fms.
Gravelly Sst. Mbr.
Conglomerate Mbr.
Buff Sst. Mbr.
Link Fm.
Transitional Mbr.
Tinney Hills Mbr.
1000 m
10 km
V:H = 5:1

Figure 9.

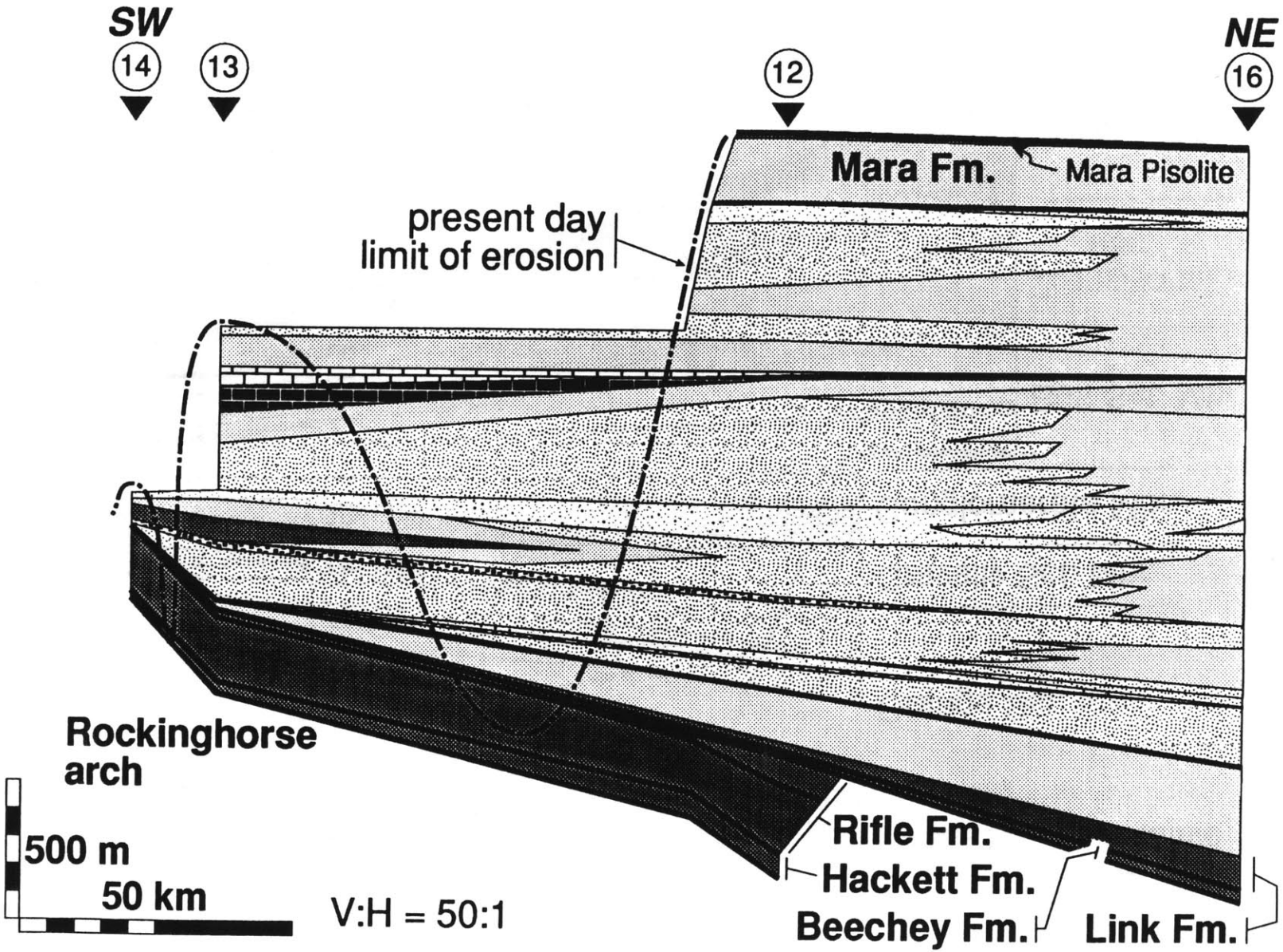
SW
14
13
12
NE
16
Mara Fm.
Mara Pisolite
present day
limit of erosion
Rockinghorse
arch
500 m
50 km
V:H = 50:1
Rifle Fm.
Hackett Fm.
Beechey Fm.
Link Fm.

Figure 10.

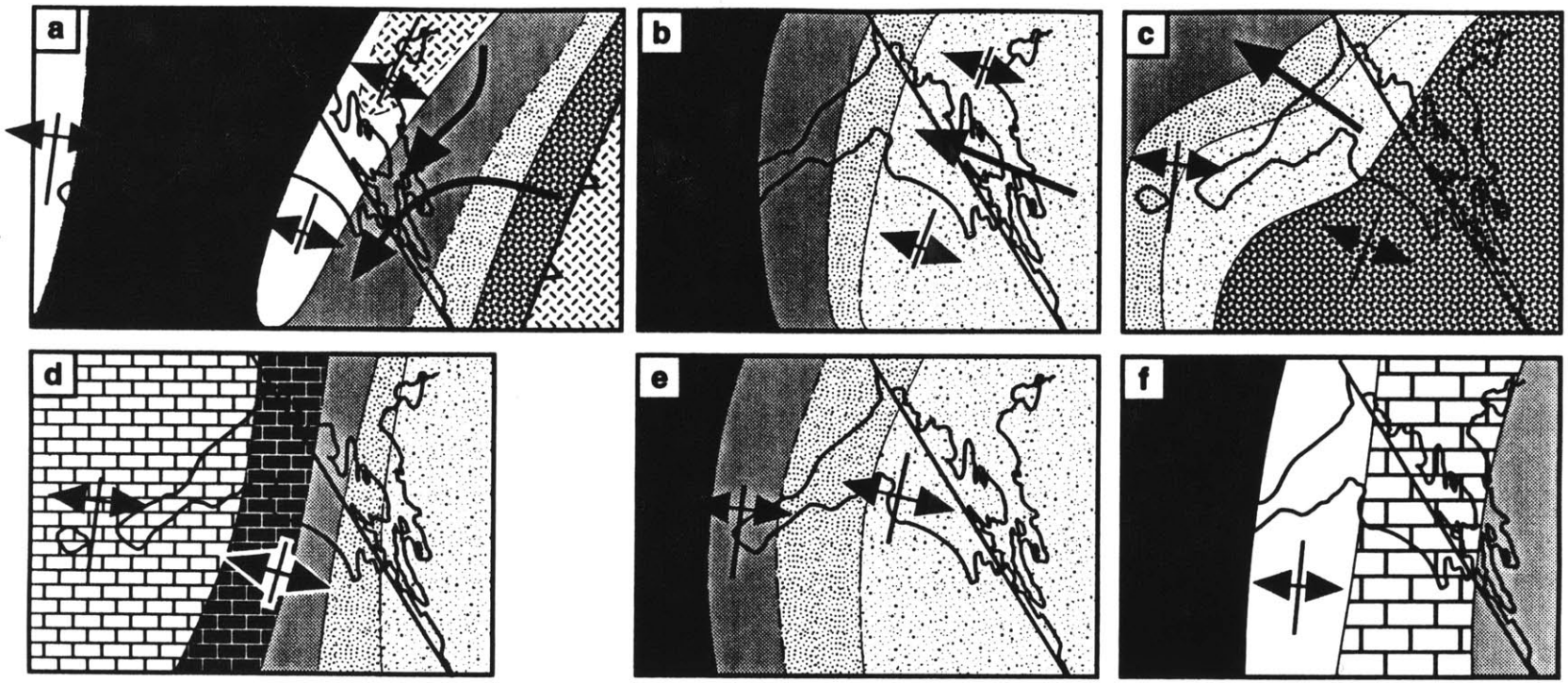

alluvial conglomerate
medial braid plain
lower braid plain
braid delta
shelf sandstone
shelf siltstone & mudstone
mixed siliciclastic/carbonate
cyclic carbonate
shelf carbonate
emergent on underlying Bear Creek Group sediments
emergent on crystalline basement

100 km

facies transition
approximate facies transition
paleocurrent trend
syn-sedimentary flexural arch
Thelon orogenic front

Figure 11.

Chapter 3:
Provenance and Detrital zircon geochronology of the 1.9-2.0 Ga Goulburn Supergroup, Kilohigok Basin, N.W.T., and its implications for the Early Proterozoic evolution of the northwest Canadian shield

Abstract

Sedimentary rocks of the Goulburn Supergroup in Kilohigok Basin on the eastern margin of the Archean Slave Province record a protracted history of collision and hinterland unroofing as the Archean (-Proterozoic?) Rae Province was thrust westward over the Archean Slave Province. The Thelon Orogen (1.92-2.02 Ga) is the orogenic belt formed on the leading edge of the Rae Province during this collision. An extensive granulite gneiss terrane within the western Rae Province, called the Queen Maud block, abuts Thelon Orogen. It has been proposed that Queen Maud block is the deep crustal remnant of a Tibetan-type uplift caused by the Slave-Rae collision. Sandstones of the Goulburn Supergroup record the varying exposure of basement rock type, location, and age through the combined use of sandstone petrography, paleocurrents, and detrital zircon geochronology. These data complement existing sedimentologic and stratigraphic data and provide critical tests of the tectonic models for Kilohigok Basin, Thelon Orogen, and Queen Maud block. In addition, we have dated detrital zircons from basal foreland basin strata in the coeval Wopmay Orogen on the western margin of the Slave Province in order to test predictions made through previous stratigraphic and geochronologic work. Finally, reconnaissance samples from the largely unknown Queen Maud block within Rae Province were collected in an attempt to characterize the age of basement rocks that may have contributed to the foreland basin detritus in Kilohigok Basin.

Alluvial sandstones at the base of the Goulburn Supergroup that represent deposits of a short-lived passive margin were derived from the interior of the Slave craton and contain Middle Archean (ca. 3.38 Ga) detrital zircons. These may either be derived from cryptic Middle Archean basement or from second-cycle erosion of Late Archean metasediments.

A distinct shift to axial, longitudinal drainage to the southwest accompanies the onset of flexural foreland basin subsidence and sedimentation. Shelf and turbidite sandstones are subarkosic and display a remarkably uniform Late Archean (2.61-2.62) detrital zircon signature. This age range is typical for basement rocks of the eastern Slave Province.

Stratigraphic evidence suggests that a large granitic terrane along strike from the syn-depositional flexural arch was emergent at this time and provided both fresh feldspar and the appropriate aged zircons. On the basis of similar Late Archean detrital zircon ages, the foreland basin turbidites appear to be sourced from the cratonic side of the basin, rather than the Thelon Orogen.

Initial prograding braid delta facies drained longitudinally and were restricted to the proximal part of the basin between Thelon Orogen and the syn-depositional flexural arch. These sandstones are petrographically similar to those in the underlying shelf facies, but are more feldspathic. Detrital zircons have ages indistinguishable to the underlying foreland basin shelf and turbidite sandstones. This probably means that braid delta sandstones are derived from the same Late Archean areas on the edge of the Slave Province. However, preliminary dates from the basement sample in Queen Maud block closest to Thelon Orogen has nearly identical ages (2.62 Ga), making this interpretation ambiguous. The lack of syn-Thelon age detritus in the samples dated so far suggest that the rocks were most likely derived from the Slave Province.

The sharpest break in petrographic, paleocurrent, and geochronologic character is present between deltaic and alluvial facies of the Burnside Formation in the proximal foredeep. Transverse paleocurrents herald the main phase of unroofing of Thelon Orogen. This transverse mode persists throughout the rest of alluvial sedimentation and is the only mode recorded in the distal foredeep on the craton. The lowest braid plain facies lack feldspar and contain increasing amounts of quartz grains, lithic fragments, and conglomerate clasts that suggest erosion of metamorphic sources. The lowest detrital zircon samples yet dated from within the main conglomeratic interval contain 1.97 Ga zircons that match ash bed ages at the base of the foredeep and peak metamorphic and igneous ages within Thelon Orogen. The pronounced downslope reduction in conglomerate clast size and preferential destruction of less resistant lithologies suggest that the high-energy braided alluvial system rapidly abraded less-resistant clasts. This may relate to humid climatic conditions in the source area that could have promoted extensive weathering of source rocks before transport. A humid climate may explain the lack of obvious arc detritus despite the presence of syn-orogenic detrital zircons.

At the top of the main conglomeratic interval significant amounts of intrabasinal clasts appear suggesting that foreland propagating thrusts uplifted the earlier deposited syn-orogenic detritus. At the same stratigraphic level, 2.3.-2.4 Ga detrital zircons appear. This is significant because basement rocks of this age do not exist within either the Slave Province or Thelon Orogen. Such ages have been reported from the westernmost edge of the Rae Province that borders the Taltson Magmatic Zone, a continental magmatic arc that is

temporal and tectonic equivalent of Thelon Orogen south of the Slave Province. One of the samples from the middle of Queen Maud block has a nearly concordant U-Pb age of 2.40 Ga. This suggests that the source of the enigmatic earliest Proterozoic detritus in the Goulburn Supergroup lay within Queen Maud block.

The sublitharenite composition of the lower alluvial sandstones of the Burnside Formation implies that they are not correlative with subarkosic alluvial sandstones in the distal foreland, despite the fact that both sandstone units have northwest paleocurrent trends. Rather, more feldspathic sandstones lie higher in the proximal alluvial section. Concomitant with the increase in feldspar is the appearance of felsic volcanic detritus. Detrital zircons dated so far from the upper part of the Burnside alluvial package exhibit two Pb-Pb age ranges, 1.97-1.99 Ga (Thelon Orogen peak metamorphism), and 2.2-2.4 Ga (the enigmatic age suggesting a source within Queen Maud block). Detrital zircons at the base of the distal alluvial section show ages of both Late Archean (2.61-2.63 Ga) and Early Proterozoic ca. 2.41-2.43 Ga. The younger age confirms the correlation to braided alluvial facies in the middle of the Burnside Formation in the proximal foreland. The upper samples from in the distal foreland have detrital zircons with Pb-Pb ages of 2.16-2.18 Ga. Such an age range has been demonstrated from cores of metamorphic zircons within Thelon Orogen. The detrital zircon samples from the base of the foredeep of Wopmay Orogen have nearly identical Early Proterozoic Pb-Pb ages of 2.10 and 2.18 Ga confirming the correlation to the top of the Burnside Formation. This allow the correlation of a volcanic ash bed within the basal foredeep of Wopmay Orogen to place an upper limit on the age Burnside Formation sedimentation at about 1.88 Ga.

Arkosic sandstones at the top of the Goulburn Supergroup probably also are derived from Thelon Orogen and Queen Maud block and record the rejuvenation of the Kilohigok foreland basin. They are broadly similar in composition to the arkoses at the top of the Burnside Formation, but the proportion of plutonic and metamorphic lithic material increases upwards. The detrital zircons in these strata display both Early Proterozoic (2.36-2.40 Ga) and older Late Archean (ca. 2.80 Ga) Pb-Pb ages. The latter age broadly matches an U-Pb age of ca. 2.86 Ga from one of the Queen Maud block samples.

These provenance data suggest that the Queen Maud block must have contributed significant detritus to the Kilohigok foreland basin. Furthermore, the preponderance of Early Proterozoic Pb-Pb ages in detrital zircons that do not appear to be derived from either Slave Province or Thelon Orogen and from our reconnaissance samples of basement rocks within Queen Maud block suggest that Queen Maud block and the Rae Province in general may have experienced a protracted Early Proterozoic history before collision with the Slave Province.

Introduction

The determination of provenance has long been a central aim of stratigraphy and sedimentary petrology in order to assess the paleogeography and tectonic environments of sedimentary basins and the source material from which they were derived. Toward this goal of reconstructing provenance, many petrographic techniques have been developed (Basu et al., 1975; Dickinson and Suczek, 1979; Matter and Ramseyer, 1985; Morton, 1985). Each technique has its limitations of applicability, for example, due to the effects of climate, transport processes, the mixing of detritus derived from several sources, and diagenetic modification (Mack, 1984).

This chapter presents an attempt at an integrated provenance study of the Early Proterozoic (ca. 1.9 Ga) Kilohigok Basin. We augment the previously presented sedimentological and stratigraphic data by using sandstone and conglomerate clast petrography, paleocurrent data, and the U-Pb geochronology of detrital zircons from well-constrained stratigraphic horizons within the Goulburn Supergroup across the basin with emphasis on the evolution of the Burnside Formation alluvial system. These data provide a critical test of tectonic models for the evolution of Kilohigok Basin wherein the basin resulted largely from the collision and thrusting of the Archean Slave Province under the Rae Province to the east (Grotzinger and McCormick, 1988). On the basis of magnetic anomaly patterns and U-Pb geochronological data, Hoffman (1987) has proposed a Himalayan-type tectonic model for this area. East of the suture zone in the Rae Province, a wide zone of granulite-grade gneisses, called the Queen Maud block, is interpreted as a deep crustal remnant of a Tibetan-type uplift which was thrust westward over the Slave Province during collision. The age information derived from U-Pb dating tests whether the orogenic highlands and the proposed Tibetan-type uplift contributed detritus to the foreland basin.

U-Pb geochronology of detrital zircons, which are common in siliciclastic sequences, provides a powerful method of assessing provenance that complements traditional petrographic methods. Zircon is highly resistant to abrasion and dissolution. The main virtue of this method is that the geochronologic data can distinguish between the age of sources in sandstones of mixed or uncertain provenance. Such uncertainties can arise when the sedimentary sequence is deformed or metamorphosed. Similarly, potential source areas may be eroded, covered by later successions, or the source areas may be separated from the coeval sedimentary basin by rifting or tectonostratigraphic terrane dispersal. In foreland basins in particular, a changing spectrum of detrital zircon ages may be present within a stratigraphic section where distinct horizons of clastic material appear; such changing zircon populations can provide a correlation tool as well as a means of assessing the unroofing history and

drainage evolution of the orogenic hinterland. These uses of detrital zircons are especially promising for Precambrian basins which lack fossils for correlation, and commonly are composed almost entirely of sandstones lacking distinctive marker beds. Detrital zircon data can also be used to establish the timing of terrane linkage through the appearance of unique zircon populations from juxtaposed crustal blocks. Thus detrital zircon stratigraphy can be an important technique that can complement and be integrated with more commonly used methods used in a comprehensive basin analysis program.

Detrital zircon geochronology of Goulburn Supergroup sandstones can address two questions. First, it will constrain whether foredeep sediments were derived solely from an Early Proterozoic continental magmatic arc near the suture zone or whether the granulite terrane farther to the east was uplifted at that time and providing detritus to the Kilohigok foreland basin. Second, the systematic sampling of suites of detrital zircons tied to a well established regional stratigraphic and sedimentologic framework, integrated with a comprehensive paleocurrent and petrographic study, can help evaluate of the controls of the drainage area and conditions within the alluvial-deltaic system on zircon dispersal patterns.

The Goulburn Supergroup is well suited to this detrital zircon stratigraphic study for several reasons. First, the Goulburn Supergroup sandstones are texturally- and mineralogically-submature, sublitharenites to arkoses, so they are likely to contain a component of first-cycle detrital zircons. Second, a well understood regional stratigraphic and sedimentologic framework of the Goulburn Supergroup has already been established. Third, several distinct pulses of clastic material, marked by unique lithologies, suggest progressive unroofing of the hinterland and introduction of unique detrital zircon populations at several horizons. Fourth, most of the Goulburn Supergroup is continuously exposed with little structural disruption for over 250 km across depositional strike. Fifth, sedimentary rocks of this basin have been metamorphosed only to lower greenschist grade. Last, the potential source terranes are well-exposed to the east and a growing body of geochronologic data exists for these areas.

The results of this study show the general applicability of the U-Pb detrital zircon technique to foreland basins of any age for assessing the source area unroofing history and paleogeography, as a complement to conventional stratigraphic and provenance methods.

Geologic Setting

The Early Proterozoic (ca. 1.9 Ga) Kilohigok Basin is located in the northwestern corner of the Canadian Shield (Figures 1, 2). It is bounded to the west by Archean basement rocks of the Slave Province, largely composed of complexly deformed Late Archean

greywacke turbidites with subordinate bimodal and felsic volcanics, intruded by syn- to post-tectonic granitoids. In the western Slave Province, enclaves of older gneissic basement have been found. To the east, the basin is bounded by tectonically emplaced Archean basement rocks and contemporaneous high grade rocks of the Early Proterozoic Thelon Orogen (Figure 1). The Thelon Orogen is a regionally continuous belt of high grade metamorphic rocks and plutonic rocks of probable arc affinity. The Taltson Magmatic Zone, a calc-alkaline continental magmatic arc contemporaneous with the Thelon Orogen, is offset from Thelon Orogen along a major syn-plutonic dextral shear zone along the southern margin of the Slave Province, the Great Slave Lake shear zone (Figure 1). The Thelon Orogen is a crustal-scale feature that likely represents a suture between the Slave and the western Rae provinces, and is the probable root zone for several northwest-directed thrust-nappes that are present in the southeastern corner of Kilohigok Basin (Figure 2). Flexural subsidence of Kilohigok Basin resulted from convergence along the Thelon Orogen and emplacement of related thrust-nappes. The Rae Province and the high grade granulite gniess terrane of Queen Maud block in particular are poorly known, but are assumed to be Late Archean in age.

Tectonic elements of the northwestern Canadian Shield

Slave Province (2.55-3.96 Ga)

The northwestern Canadian Shield is composed largely of Archean "granite-greenstone" terranes with Early Proterozoic sedimentary fold belts and magmatic arcs on their margins (Figure 1). The Slave Province largely comprises a complexly deformed greenstone assemblage of greywacke turbidite and subordinate bimodal and felsic volcanic suites (Padgham, 1985). These rocks were deformed and regionally metamorphosed at greenschist to upper amphibolite grade, then later intruded by granites and tonalite-granodiorite suites (Frith and Loveridge, 1982; Thompson et al., 1985). Supracrustal rocks are 2.71 to 2.67 Ga, while post-tectonic granitoids range from 2.63 to 2.58 Ga (Krogh and Gibbins, 1978; Frith and Loveridge, 1982; Frith et al., 1986; van Breemen et al., 1987b; van Breemen et al., 1987d; Isachsen et al., 1991). In the Slave Province, older rocks exist in the western portion of the province and are dated at 2.80 to 3.96 Ga (Easton, 1985; Bowring and Grotzinger, 1992). The eastern part of the Slave Province lacks evidence of the older crust and consists of high proportion of metasediments and subordinate metavolcanic material (Padgham, 1985; van Breemen et al., 1987b).

Rae Province (2.2-2.4(?), 2.6-3.1? Ga)

The northwestern Churchill Province, or Rae Province of Hoffman (1988; Hoffman, 1989), is a broad gneiss terrane of whose age is poorly constrained but is inferred to be Archean age. The Rae Province is divisible into several smaller blocks (Fraser, 1978; Heywood and Schau, 1978). The westernmost terrane is the granulite-grade terrane, the Queen Maud block, that abuts the east side of the Thelon Orogen. The Queen Maud block is juxtaposed on its eastern side against a greenschist- to amphibolite-grade greenstone block composed of bimodal metavolcanic rocks dated at 2.8 to 2.9 Ga and older granite plutons and felsic metavolcanic rocks at 2.58 to 2.61 Ga (Lecheminant et al., 1987) with relics of older gneiss (2.9 to 3.1 Ga) reported (Hoffman, 1989). Recently, some paragneisses with ages of 2.2-2.4 Ga ages have been reported from the western margin of the Rae Province that borders the Taltson Magmatic Zone (Bostock and Loveridge, 1988; van Breemen et al., 1992). The Queen Maud block may have been thrust over the eastern lower-grade block of the Rae Province with an oblique dextral sense in Early Proterozoic time. The eastern block preserves small remnants of Early Proterozoic sediments in the Amer Basin (Patterson, 1986).

This study will show that detrital zircons from alluvial foreland basin sediments in Kilohigok Basin yield Pb-Pb ages of 2.2-2.4 Ga that do not represent a mixture of Archean and younger Proterozoic material. Also reconnaissance samples from Queen Maud block yield a similar earliest Proterozoic age. This strongly suggests that much of the alluvial foreland basin was derived from Thelon Orogen and Queen Maud block and that Queen Maud block probably contained as yet unrecognized crust of earliest Proterozoic age, 2.2-2.4 Ga. This age range is poorly represented in the Canadian Shield and the world in general, but new isotopic studies suggest that it may be an important component of Precambrian belts, for example, in the subsurface of western Canada (Bowring and Podosek, 1989; Ross et al., 1991).

Thelon Orogen-Taltson Magmatic Zone (1.90-2.02 Ga)

A distinct break in lithology, geophysical properties, and age delineates a north-south trending belt marking the boundary between the Slave and Rae Provinces. This belt is spectacularly manifested on the magnetic anomaly map of the area (see Hoffman, 1987). Geologically, the western boundary of the Thelon Orogen is marked by the eastern limit of Archean rocks cut by Proterozoic mafic dikes and the western limit of the Early Proterozoic granitoids and granulite gneisses (Thompson et al., 1986; Henderson et al., 1987). The Thelon Orogen consists of a suite of older (1.95 to 2.02 Ga) granodioritic plutons that

underwent coeval granulite metamorphism, and a younger suite of peraluminous granites emplaced during uplift (van Breemen et al., 1987c). The rocks in the Thelon Orogen have been deformed by dextral and subsequent dip-parallel shear zones with mostly reverse fault sense. Although cores of some metamorphic zircons have an older component, their upper intercept ages lie between 2.2 and 2.4 Ga (Henderson and van Breemen, 1992); no Archean component has been demonstrated north of the McDonald fault zone. This precludes the possibility that Thelon represents reworked Archean supracrustal material of Slave Province basement (van Breemen et al., 1987a; van Breemen et al., 1987c). Henderson and Loveridge (1990) report evidence for an inherited Archean (2.55 Ga) component in a deformed 1.9 Ga granitic batholith south of the McDonald fault zone. The eastward extent of this belt and its relation with the Queen Maud block is largely unknown. Within the western Thelon Orogen, metamorphic mineral assemblages (kyanite-staurolite) indicate 12-15 km of syn- to post-collisional uplift (Thompson et al., 1985).

Although offset by over 200 km from the Thelon Orogen, the Taltson Magmatic Zone exposes a petrologically similar, temporally equivalent zone of granite to diorite plutons. U-Pb zircon and monazite ages are 1.99 to 1.92 Ga (van Breemen et al., 1987b; Bostock et al. 1987). The Great Slave Lake shear zone (Hanmer and Lucas, 1985), that offsets Thelon and Taltson, was a synchronously active dextral transcurrent shear zone (2.02-1.95 Ga: van Breeman et al., 1990), that Hoffman (1987) has interpreted as a continental transform. North trending sinistral shear zones exist on the eastern boundary of the Taltson magmatic zone (Culshaw, 1984; Bostock et al., 1987a; Bostock et al., 1987b; Bostock and Loveridge, 1988). The metamorphic grade of the Rae Province in this area is much lower than that in the Queen Maud block (Bostock et al., 1987b). Significantly, some igneous rock that intrude basement gneisses on the eastern edge the Taltson Magmatic Zone have been dated as earliest Proterozoic at 2.27 to 2.44 Ga (van Breemen et al., 1987d; Bostock and Loveridge, 1988; van Breemen et al., 1992).

Setting and Architecture of Kilohigok Basin (1.88-2.0 Ga)

The Kilohigok Basin is one of three roughly coeval Early Proterozoic sedimentary basins on the edge of the Slave Province. Kilohigok Basin lies within 50 km of the edge of the Thelon Orogen (Figures 1,2). The areal extent of the Goulburn Supergroup was previously much greater. Its present outcrop pattern results from broad, basement involved folding which post-dates deposition of the pre- and syn-orogenic sedimentary rocks of the Goulburn Supergroup. The lower Goulburn Supergroup is continuously exposed for 250 km across depositional strike, except for the thrust deformation in the proximal end of the basin

and the late strike-slip deformation restricted to the Bathurst fault zone (Figure 2). All units in the lower Goulburn Supergroup have been mapped at 1:50,000 scale.

General Stratigraphy

The Goulburn Supergroup can be divided into four tectono-stratigraphic sequences (Figures 3, 4) (Grotzinger and McCormick, 1988). These represent an initial short-lived thermal subsidence stage (Kimerot Group) with a lower transgressive siliciclastic alluvial to shelf sequence overlain by a carbonate platform; a foredeep stage (Bear Creek Group), divisible into a deep-water flysch (lower Bear Creek Group) grading to shallow-water to alluvial molasse (Burnside Fm.); a thin shale-carbonate sheet (Wolverine Group); and a final shallow-marine to alluvial siliciclastic wedge (Bathurst Group) probably indicating foredeep reactivation. The Goulburn Supergroup is mildly deformed and metamorphosed to lower greenschist grade (Thompson and Frey, 1984). It is unconformably overlain by syn-strike-slip sedimentary rocks related to movement on the Bathurst fault system, and overlapped by gently dipping Middle Proterozoic sedimentary and volcanic rocks (Campbell, 1979; Campbell and Cecile, 1981). Detailed accounts of the lithofacies and the stratigraphy of the Kimerot and Bear Creek Groups are given by Grotzinger and McCormick (1988) and McCormick and Grotzinger (in review a); the Wolverine and Bathurst Groups are described by Campbell and Cecile (1981).

Bear Creek foredeep

Several lines of evidence that are discussed more fully by Grotzinger and McCormick (1988) support a foredeep origin of the Bear Creek Group resulting from overthrusting in the Thelon Orogen. These include the presence of a northeast trending flexural arch (Gordon Bay Arch, Figure 2) developed on top of the passive-margin platform which was synchronously drowned in the proximal part of the basin while being up-arched and erosionally truncated in the foreland; axially directed paleocurrents in lower Bear Creek Group basinal turbidites; transversely directed paleocurrents in the alluvial molasse (Burnside Formation); and northwest-vergent thin-skinned thrust nappes in the proximal end of the basin.

Ash beds near the base of the lower Bear Creek Group pin the age of initial foredeep subsidence at about 1.967 ± 0.001 Ga, on the basis of an U-Pb zircon age (Bowring and Grotzinger, 1992). Another ash within the lower Bear Creek Group yields an age of 1.963 ± 0.006 Ga (Bowring and Grotzinger, 1992).

The lower Bear Creek Group consists of four shallow-marine shelf sequences that

pass basinward (southeast) into deeper marine turbidites (Grotzinger and McCormick, 1988). The sequences are separated by regional unconformities that can be correlated continuously across the entire Kilohigok Basin (Bowring and Grotzinger, 1992).

The Burnside Formation deltaic-alluvial molasse

The lower Bear Creek Group grades up to the Burnside Formation (Figures 3,4), a thick (up to 3.5 km), northwest-tapering wedge of predominantly alluvial subarkose that dominates the upper Bear Creek Group. Recent stratigraphic and sedimentologic studies have shown that the Burnside Formation represents a braid delta-braided alluvial system which prograded to the northwest across the Slave Province and interfingered with marine shelf sedimentary rocks in the distal foreland (McCormick and Grotzinger, in review a).

Lithofacies and paleocurrents indicate that initially the deltaic system was restricted to the proximal part of the basin, southeast of the flexural arch. Paleocurrent measurements indicate initial paleoslope was to the southwest, parallel to lower Bear Creek Group turbidite paleocurrents and parallel to the flexural arch (Figures 2,5). A sharp shift to a low-dispersion, northwestern paleocurrent mode, transverse to the arch, accompanies the onset of braided stream conditions (Figure 5). In the foreland, over and beyond the flexural arch, all paleocurrents are northwest-directed and the transition between underlying shallow-shelf facies and the braided alluvial facies is much thinner ($\leq$ 200 m). The consistent pattern of northwest paleocurrents throughout the basin indicates that the Burnside alluvial system formed a broad alluvial apron which blanketed the northern Slave craton.

Preliminary ^{40}Ar-^{39}Ar studies suggest that the allochthons of the eastern Thelon Orogen were uplifted through blocking isotherms around 1.99 Ga (D. Thompson, personal communication, 1987), the time of peak metamorphism and structural deformation in Thelon Orogen (van Breemen et al., 1986; van Breemen et al., 1987a; van Breemen et al., 1987b; van Breemen et al., 1987d; Henderson and Loveridge, 1990; van Breeman and Henderson, 1991; Henderson and van Breemen, 1992), possibly bracketing the beginning of overthrusting. Allochthonous Slave Province on the west probably began uplift around 1.93 Ga (D. Thompson, personal communication, 1987), putting a possible lower limit on the start of post-collisional isostatic unloading of the Thelon Orogen. These data indicate that flexural subsidence in Kilohigok Basin were contemporaneous with deformation, igneous activity, and metamorphism in the Thelon Orogen.

If isostatic unloading in the hinterland due to erosion was roughly synchronous with the onset of the main phase of Burnside sedimentation in the foreland, this would explain the predominant northwestern, or transverse, mode of alluvial paleocurrents. Unlike the

Tertiary Ganges foredeep which bypasses the majority of sediment longitudinally into the Bengal Fan, the Burnside alluvial system shed most of its detritus directly across the foreland of the Slave craton into the passive margin of Wopmay Orogen. The trans-craton dispersal is more analogous to the Cretaceous-Tertiary Colville foredeep in northern Alaska (Grantz and May, 1982). In this situation, north-prograding alluvial-deltaic systems, carrying material from uplifted Brooks Range thrust sheets, filled the Colville trough, overtopped the Barrow Arch, and shed detritus into the Beaufort passive margin. This suggests that alluvial dispersal in Kilohigok Basin across the foreland may have been controlled by isostatic uplift in Thelon Orogen and the small size of the Slave craton (about 350 km across).

proximal molasse sedimentation

The proximal Burnside Formation sections (Figure 6) show an upward increase in conglomerate, once the northwestern paleocurrent mode is established. Initially clasts are predominantly vein quartz with minor chert, jasper, and quartzite. Higher in the section, clast populations become more polymictic and metamorphic rock fragments appear, such as metasiltstone and schist. Intraformational Burnside Formation clasts appear indicating reworking of the foredeep sediments.

Another important question is the extent of contribution of the Queen Maud block to the Burnside Formation. McCormick and Grotzinger (in review a) argue that on the basis of high quartz content (≥ 80%), apron-like geometry, and the great thickness (≥ 2 km) and lateral extent (> 200 km), the Burnside Formation could not be derived solely from the Thelon Orogen. They suggest that the Queen Maud block must have contributed to the Burnside Formation and therefore must have been uplifted and Thelon Orogen must have been breached during Bear Creek Group time to provide the volume of material in both the foredeep and that which was bypassed across the Slave craton. Detrital zircon age data, presented below, support this idea.

distal molasse sedimentation

The distal northwestern sections of the Burnside Formation (Figures 2,7) record the progradation of the braid delta-braided alluvial system across the Kilohigok Basin and intertonguing with siliciclastic marine shelf lithofacies (McCormick and Grotzinger, in review a).Paleocurrents in all sections are uniformly northwest-directed throughout alluvial sedimentation (Figure 5). Coarse siliciclastic facies of the distal Burnside Formation resemble those in the lower siliciclastic portion of the passive margin of Wopmay Orogen and we believe that they are correlative. A thin but distinct eastward thinning tongue of carbonate in the upper half of the Burnside Formation in distal sections correlates to the passive margin

carbonate platform in Wopmay Orogen (Hoffman et al., 1984; Grotzinger, 1985). These correlations provides a temporal link between the foreland basin of Kilohigok Basin on the eastern margin of Slave Province with the passive margin of Wopmay Orogen on the western margin. Waning alluvial to braid delta facies at the top of the Burnside and Mara formations have been correlated with similar facies at the base of the foredeep of Wopmay Orogen. This puts an upper bound of Burnside alluvial sedimentation roughly at the onset of foredeep sedimentation in Wopmay Orogen.

The upper Goulburn Supergroup

The upper Burnside Formation fines-upward and passes into marine shelf sedimentary rocks (Mara-Quadyuk-Peacock Hills Formations), then into a widespread stromatolite reef carbonate platform (Kuuvik Fm., Wolverine Group) which interfingered with and transgressed over the waning Burnside alluvial-deltaic system (McCormick and Grotzinger, in review a; McCormick and Grotzinger, in review b).

The siliciclastic Bathurst Group records probable reactivation of the foredeep with a regressive phase of shallow-marine to alluvial sub-arkosic to arkosic sandstones. Conglomerates near the top contain felsic volcanic clasts (Campbell and Cecile, 1981) that resemble those found in the upper Burnside Formation .

post-Goulburn Supergroup deformation

The Goulburn Supergroup is deformed in a progressive thin- and thick-skinned thrusting event that affects only the southeastern-most 30 km of the basin end of the basin closest to Thelon Orogen (Tirrul and Grotzinger, 1990). Northwest-directed thrusting and long-wavelength (50-75 km) basement-involved folds predate brittle transcurrent faulting on the Bathurst Fault system. Several fault-bounded outliers of the lower Goulburn Supergroup lie between the southeastern end of Kilohigok Basin and the leading western edge of the Thelon Orogen (Figure 2) (Thompson et al., 1985; Thompson et al., 1986; Tirrul and Grotzinger, 1990). Stretching lineations support northwest transport and suggest that the basal detachment of the thrust-fold belt roots in the Thelon Orogen (Tirrul and Grotzinger, 1990).

In summary, the sedimentary rocks of the Goulburn Supergroup record short-lived thermal subsidence rapidly followed by flexural foredeep subsidence and sedimentation in Kilohigok Basin caused by underthrusting of the eastern margin of the Slave Province under the Rae Province. The sedimentary record of the foredeep can be tied to igneous and metamorphic events in the Thelon Orogen in the hinterland via the U-Pb geochronology of

ash beds and detrital zircons in the Goulburn Supergroup. Stratigraphic and geochronologic data indicate that the foreland basin in Kilohigok Basin evolved synchronously with the passive margin of Wopmay Orogen.

sedimentary petrography of the Goulburn Supergroup

petrographic methods

thin section petrography

Twenty-five (25) thin sections of siliciclastic sandstones were selected in order to interpret the petrographic and provenance evolution of the Goulburn Supergroup. Samples in the proximal foredeep ranged from shelf sandstones of the lower Bear Creek Group to deltaic and braid plain sandstones of the Bathurst Group. A thin section was chosen for each stratigraphic horizon at which a detrital zircon sample was taken. Additional samples were selected from within the Burnside Formation to characterize more fully the petrography of each member and facies of the formation in both the proximal (section 2) and distal (section 12) parts of the basin. The comparison of proximal to distal petrographic data is used to identify downstream changes in petrographic character and to support previously proposed stratigraphic correlations. At least 400 framework grains were counted per thin section in order to insure reasonable statistics for grain data; 400 grains gives approximately ± 2% reliability for modal abundances of 2-5% or 95-98%, ± 4% for modal abundance 20% or 80%, and ± 5% for 50% modal abundance (van der Plas and Tobi, 1965).

Two approaches were used to maximize the amount of petrographic data gleaned from point counting. The first was to use the so-called Gazzi-Dickinson method for framework grain identification in order to constrain the tectonic setting of the source area (Dickinson and Suczek, 1979; Dickinson et al., 1983; Ingersoll et al., 1984; Dickinson, 1985). The Gazzi-Dickinson method classifies any sand size mineral grain as the mineralogical type of the grain regardless of whether the mineral is present as a monomineralic grain or within a lithic fragment. A grain is classified as a particular lithic fragment only if the cross hairs of the microscope falls on material within a lithic fragment that is less than sand size (<62.5 microns). Although this would seem to reduce information from petrographically important lithic fragments (Suttner et al., 1985), separate note is made of their lithology and other relevant data. Furthermore, by recasting the data in several forms, similar information is largely recaptured (Dickinson and Suczek, 1979; Dickinson et al., 1983; Dickinson, 1985). The Gazzi-Dickinson method leads to the greatest consistency

of resulting data from samples of variable grain size. In other words, when using other methods large shifts in position on ternary diagrams, such as QFL or QmFLt diagrams, occur when different sand size fractions are compared. All methods suggest using medium- to coarse-grained sands to facilitate lithic fragment identification. Some intervals of interest in the Goulburn Supergroup are very fine to fine grained, so the Gazzi-Dickinson method seemed the most likely to yield consistent results across grain sizes. The grain type parameters counted are shown in Table 1. Separate notes were made of varieties of lithic fragments, cement, and matrix as well as diagenetic effects, although they do not directly impact the recalculated point count data (Table 2) that was subsequently plotted according to the method of Dickinson and Suczek (1979) and Dickinson et al. (1983) (Figures 9 and 10).

The second approach to point counting discriminates between different varieties of quartz grains. This additional set of criteria was used because the Goulburn Supergroup sandstones are mostly subarkoses to sublitharenites to quartz arenites, so additional provenance information was sought from the grains that dominate the framework grain population. Four types of quartz were distinguished on the basis of the criteria of Basu et al. (1975) and Young (1976): monocrystalline non-undulose (Qmnu), monocrystalline undulose (Qmu), polycrystalline with 2 to 3 subgrains (Qpq2-3), and polycrystalline with more than 3 subgrains (Qpq>3). These categories, when applied to similar sized sand samples, can yield much information about whether the source area had quartz-bearing rocks that had undergone strain and at what temperature the strain occurred. Figure 8 shows how quartz grain type varies with lithology and grain size data from Holocene stream sands in Spain (Tortosa et al., 1991). The most useful and reliable petrographic criteria appears to be that low grade metamorphic rocks (schists) yield abundant polycrystalline quartz with more than 3 subgrains. Granitic and medium- to high-grade quartzose metamorphic rocks both tend to yield polycrystalline quartz with larger (and fewer) subgrains that have undergone temperature-dependent annealing with growth of strain free subgrains with intergrain boundaries joining at 120° angles. Undulose monocrystalline quartz is common in both granitic and medium- to high-grade quartzose metamorphic rocks. This four-fold classification of quartz grain type is useful to distinguish qualitatively between sandstones derived from largely low grade metamorphic versus plutonic and high grade metamorphic sources. The stratigraphic trends in quartz grain type are shown in Figures 11 and 12.

Several important complicating factors have to be addressed before interpreting the provenance of the Goulburn Supergroup sandstones. These complications are the effect of grain-size changes on sample classification, proper distinction of aphanitic rock fragments, the impact of diagenetic alteration of framework grains, the distinction of plagioclase from K-feldspar, and the effect of post depositional strain on the classification of quartz grains.

The grain-size-dependence of the grain classification methods is intrinsic to sandstone petrographic studies; as grain size decreases, diagnostic provenance information is lost in two ways. First, lithic fragments break down to constituent monomineralic grains that are less diagnostic and aphanitic grains that are less identifiable. Second, polycrystalline quartz breaks down to monocrystalline quartz. This is further dependent on the size of subgrains, skewing data towards less diagnostic monocrystalline quartz varieties (Figure 8). This problem of information loss through grain size reduction is intrinsic to the petrographic study of sandstones so, when possible, is best avoided by studying medium- to coarse-grained sand fractions. As stated above, the Gazzi-Dickinson method for grain classification minimizes, but does not eliminate, biases due to grain size changes between samples. Most Goulburn Supergroup samples are medium- to very coarse-sandstones, but some distal facies are very fine to fine grained.

One of the most severe problems for this study is the correct classification of aphanitic lithic fragments. The Goulburn Supergroup has undergone variable amounts of diagenesis so that some framework grains are not easily identified. For instance, many feldspars have undergone variable alteration to white micas or, locally, have been replaced by dolomite. Some polycrystalline quartz grains and chert are preferentially altered to chert plus mica. Definite felsic volcanic rock clasts are found at certain horizons but the microscopic identification of these volcanic lithic fragments is very difficult, especially as grain size decreases, because some look like chert with or without flow banding or polycrystalline quartz that has been variably altered. Given the difficulty of properly identifying volcanic lithics known to exist in the section, these petrographic data almost certainly under-represent the contribution of silicic volcanic detritus to the Goulburn Supergroup. Therefore no attempt has been made to use ternary diagrams that discriminate on the basis of specific lithic type. The importance of ambiguous identification of aphanitic lithic grains will be addressed when interpreting the tectonic significance of these sandstones.

The diagenetic alteration of framework grains variably affects different components of these sandstones. The alteration of feldspar, polycrystalline quartz and chert, and fine grained lithic fragments makes proper modal identification difficult. The only way to make a reasonable classification of highly altered grains is to search with a given thin section and a suite of samples to find less altered grains. Feldspars are often distinguished on the basis of relief against quartz grains, cleavage, and the presence of a spectrum of alteration textures and mineralogies within a single sample. Higher degrees of alteration makes distinction between plagioclase and K-feldspar more difficult. Often ghost twins are present when dolomite replaces plagioclase, but when polysynthetic twinning is lacking, the distinction is ambiguous. Although the thin sections were stained for both K-feldspar and plagioclase, the

staining was of highly variable quality and I suspect that some plagioclase was altered to albite. The most useful criteria for plagioclase was the presence of polysynthetic twins. As a result of these factors, these data probably accurately reflect the amount of total feldspar in a sample, although the data under-represent the amount of plagioclase in these sandstones. Therefore, no attempt has been made to plot the petrographic data on ternary diagrams that distinguish between K-feldspar and plagioclase.

Finally, the post-depositional strain imparted on the Goulburn Supergroup sandstones complicates the quartz type classification. In general, the Goulburn Supergroup has been subjected to very little strain and have attained at most lower greenschist metamorphic grade (Thompson and Frey, 1984). The samples studied were part of homoclinally dipping or broadly folded stratigraphic panels locally cut by minor late transcurrent faults. The only exception is at section 12 (Figure 2) where rock cleavage and mica growth occurred in finer grained rocks. The main complication arising from the relatively low strain conditions to which these rocks were subjected is that compactional strain causes undulose extinction in monocrystalline quartz grains. The method outlined above for classifying quartz grains distinguishes non-undulose from undulose monocrystalline quartz on the basis of extinction within 5° rotation of the flat microscope stage (Basu et al., 1975; Young, 1976). With enough point strain, there is the potential to misclassify non-undulose grains as undulose. There are several ways to avoid this problem. First, in samples with more intergranular matrix, the matrix absorbs more of the compactional strain and less is imparted on the quartz. Second, undulosity caused by point-to-point contact gives distinct patterns of undulosity that radiate from the point contacts that represent a photoelastic effect of plastically strained materials. The relatively low strain conditions imposed on the Goulburn Supergroup sandstones create a mild undulosity that radiates from point contacts, that goes extinct within 5-10°, and that does not create polygonized subgrains with distinct extinction domains. When such features were seen in quartz grains, the grains were classified as non-undulose. The potential remains that undulose monocrystalline quartz grains were overcounted relative to non-undulose monocrystalline quartz grains, but this shift would be systematically greater in matrix-poor and more highly strained rocks. On the whole, however, undulosity is not used here as a definitive criteria for judging the provenance of quartz grains, rather it is used as secondary data to back up interpretations on the basis of the types of polycrystalline quartz present.

Appendix B contains the complete description, tabulation of grain types counted, and calculated parameters for the point counted thin sections of the 25 Goulburn Supergroup sandstones.

conglomerate clast counts

Significant conglomerate horizons in the Burnside Formation are restricted to the southeastern, proximal part of the basin, between the Thelon Orogen and the Gordon Bay flexural arch (Figure 2). A series of conglomerate clast counts were performed along the line of measured sections 2 and 3 (Figures 2, 6). The main horizons counted were conglomerate beds in the conglomeratic facies of the Buff Sandstone member, the base and top of the Conglomerate member, and two horizons at the top of the Gravelly Sandstone member (Figures 3b, 6), one of which contains distinctive undeformed felsic volcanic clasts and another that contains abundant Burnside Formation lithology intraclasts. The lithology and size of apparent a- and b-axes of the clasts of 100 to 275 clasts were measured at each of the horizons. Figure 13 shows the vertical variation in significant conglomerate clast types at sections 2 (a) and section 3 (b). Location of the conglomerate count sites and total count data are presented in Appendix B.

petrographic results

Sandstones in the Goulburn Supergroup range from quartz arenites to sublitharenites to arkoses. In the proximal part of the basin there are distinct and significant vertical petrographic trends in sandstone composition, quartz grain type, and conglomerate clast composition (within the Burnside Formation) and reflect distinct shifts in the type of source area lithology. Proximal to distal petrographic trends within the Burnside Formation result from both the mechanical abrasion of unstable grains in a high energy braided stream system over several hundred kilometers of transport that may have been augmented by wind abrasion and sorting. In addition, the Burnside alluvial and deltaic facies deposited on the craton correlate with the upper half of the Burnside Formation deposited in the proximal foredeep so much of the variability seen in the proximal part of the basin has no lateral equivalent on the craton.

Table 1 explains the point counting parameters and their associated symbols, and how data were recast to conform to the method of Dickinson and Suczek (1979) and Basu et al. (1975). Table 2 summarizes petrographic data for the point counted thin sections. Figure 9 shows two sets of ternary diagrams (QFL and QmFLt) for all samples in the Goulburn Supergroup broken out by lithotectonic unit (see Figure 3a); Figure 10 presents similar diagrams for only Burnside Formation sandstones from the proximal foredeep broken out by member and facies. Figures 11 and 12 show vertical variations of quartz grain type in the proximal and distal Burnside Formation, respectively. Figure 13 shows the vertical and downstream changes in conglomerate clasts in the proximal part of the foredeep.

Paleocurrent data, stratigraphic correlations, and detrital zircon geochronology all serve to strengthen the interpretations of these results and will be considered together in the discussion that follows.

vertical trends

Kimoret Group passive margin

No thin section of sandstones from the Kenyon Formation was point counted, but the sandstones are described from outcrop and hand sample by Grotzinger and McCormick (1988). The sandstones of the Kenyon Formation (Figure 3a) are medium- to very coarse-grained, locally pebbly, with grains subrounded to well rounded, and contain 10-15% feldspar. Paleocurrents indicate that the basal alluvial sandstones are derived from the northwest on the Slave craton. Hummocky cross stratified marine sandstones in the upper Kenyon Formation exhibit finer grain size and higher textural maturity, but have roughly the same amount of feldspar as the alluvial sandstones.

lower Bear Creek Group marine foredeep

Similar to the Kenyon Formation sandstones, all of the shallow marine shelf sandstones deposited in the lower Bear Creek Group marine foredeep exhibit a significant component of fresh to variably altered feldspar (Figures 14a, 9; Table 2). No thin sections were made of the lower Bear Creek Group turbidites, but outcrop and hand sample observations suggest they are compositionally and texturally similar and contain similar amounts of feldspar (5-15%). Stratigraphic correlations and the presence of carbonate slump blocks suggest that they are derived largely from material on the cratonic side of the basin (Grotzinger et al., 1988; Grotzinger and McCormick, 1988). Thin sections do exist for shelf facies sandstones and they were point counted (samples BC-H and BC-R). The lower sample (BC-H; Hackett Fm.) from the lowermost unit in the Bear Creek Group contains significantly more Qmnu and Qpq>3 than the overlying sample (BC-R; Rifle Fm.), but both contain similar amounts of feldspar and are coarse grained (Figure 11, Table 2). Most of the polycrystalline quartz contains strain free subgrains indicative of plutonic or higher grade metamorphic source area. A plutonic source is consistent with the presence of sand-sized granitic rock fragments and relatively fresh feldspar in shelf facies that are commonly the most energetic and prone to mechanical destruction of rock fragments and feldspar through reworking. Some polycrystalline grains with serrate subgrain boundaries are present so some lower grade metamorphic source areas probably contributed to the shelf sandstones. The

higher percentage of polycrystalline quartz grains that are recast as part of the Lt category pushes the Hackett Formation sample from the "cratonic interior" field to the "quartzose recycled" field of the "recycled orogen" domain in the plots of Dickinson and Suczek (1979) (Figure 9b).

Initial Burnside foredeep braid delta

Well developed coarsening-up braid delta cycles exist only in the Transitional member of the Burnside Formation in the proximal foredeep to the southeast of the Gordon Bay Arch. These sandstones are enriched in feldspar and especially plagioclase compared with those in the marine facies in the underlying lower Bear Creek Group (samples STH-111 and STH-136; Figures 9a&b, 14b, Table 2). This may reflect a difference in the rate of reworking and destruction of labile grains in alluvial versus marine shelf settings (Potter, 1978). Schistose quartz (foliated quartz plus mica) lithic fragments are present. Quartz grains with bubble inclusion trails are common and a few quartz grains contain inclusions of vermiculitic chlorite after other clays that have been interpreted as indicating a low temperature hydrothermal origin . They plot between the "cratonic interior" and "quartzose recycled" fields on the QmFLt diagram by virtue of polycrystalline quartz content and minor lithic fragments (Figure 10b, 11).

Burnside braided alluvial foredeep

The first major petrographic shift in the proximal foredeep is present at the base of the Buff Sandstone member that marks the onset of the main braided alluvial sedimentation with west-northwest paleoflow that onlaps the craton. The sandstones within the Buff Sandstone and Conglomerate members almost completely lack feldspar and all the sandstones plot along the quartz-lithic fragment legs of the ternary diagrams in the "quartzose recycled" field (samples 120-132; Figures 10, 14c&d, Table 2). Polycrystalline quartz with >3 subgrains increases markedly upward through these two members (Figure 11). Lithic fragments show predominantly metamorphic sources such as schistose quartz, schist, and ferruginous cherts, jasper, and cherty "banded iron formation" (Figure 15a&b). The increasing proportion of polycrystalline quartz (most notably Qpq>3) cannot be attributed entirely to increasing grain size of the sandstone samples because, for example, samples 127-131 are of comparable coarse to very coarse grain size (compare with Figure 8).

These observations on the increasing contribution of metamorphic detritus to the Buff Sandstone and Conglomerate members are complemented by conglomerate clast counts (Figure 13). Clast counts within the Buff Sandstone show vein quartz predominates with subordinate quartzite. The proportion of quartzite relative to vein quartz appears to decreases

down paleoslope on the basis of projection onto a line parallel with the predominant west-northwest paleocurrent direction for the main Burnside Formation sandstones. It is important to note that these outcrops are not aligned along the paleoslope vector; the north Tinney Hills location (section 3) lies about 10 km to the north. Within the conglomeratic upper part of the Buff Sandstone member distinct metamorphic clasts appear, such as a hard black metasiltstone, foliated micaceous quartzites, schists, jasper, and banded iron formation. The proportions of all of these decrease down paleoslope relative to vein quartz.

Significantly, a very coarse conglomerate horizon that marks the top of the Conglomerate member shows two marked departures from the petrographic trends of the Buff Sandstone through the Conglomerate member. First, there is a sharp decrease in the proportion of polycrystalline quartz (sample STH-132; Figures 11, 14e; Table 2). Feldspar is still absent from the sandstones. From this level upward the proportion of Qpq>3 stays between 15-19% of total quartz. Second, conglomerates show the first appearance of significant proportions of what appear to be intrabasinal sandstone clasts that resemble the Burnside Formation (Figure 13). Note particularly that the proportion of Burnside Formation clasts is higher (49% vs. 8%) relative to vein quartz in the area inferred to lie further down paleoslope. This differs from the trend for most clast lithologies. A similar anomalously coarse conglomerate appears at the top of the Gravelly Sandstone member. This distinctive highly channelized conglomerate horizon displays very large Burnside Formation clasts up to 1 meter and vein quartz up to 25 cm superimposed on a background of polymictic metamorphic and intrabasinal clasts ≤10 cm. In the coarse Burnside clast horizons, intraformational clasts comprise up to 27% of total clasts. In the background polymictic horizons, Burnside Formation clasts are about 6-9%. The coarsest area for this conglomerate lies in section 3; horizons farther up paleoslope lack the large clasts and have a lower proportion of Burnside Formation intraformational clasts (Figure 13). This anomalous coarseness and high proportion of intraformational clast conglomerates in the down paleoslope location suggests a much more proximal source area for these conglomerates and that source area was located to the north. This suggests the existence a of single alluvial channel system that carried the anomalously coarser detritus that interfingered with the relatively uniformly west-northwest flowing alluvial systems that characterize the majority of Burnside alluvial sedimentation. We suggest that this anomalous intrabasinal source was caused by intrabasinal thrusting, a feature common in the foreland propagating deformation seen in Phanerozoic foreland thrust-fold belts (Bally et al., 1966; Price, 1981). Despite the presence of common intraformational clast in these conglomerate horizons, sedimentary lithic fragments were not commonly seen in thin section, suggesting that they were readily disaggregated when they reached fine gravel size.

Another distinctive conglomerate horizon is present near the coarse Burnside clast conglomerate that contains abundant undeformed felsic volcanic clasts (Figure 13, 15c). The proportion of volcanic clasts ranges from about 24% to 44% in some horizons. Concomitant with the increase in felsic volcanic and granitic clasts seen at the top of the Gravelly Sandstone member is a distinctive increase in feldspar content while the proportion of polycrystalline quartz remains relatively stable (samples STH-139 and STH-142; Figures 10, 11, 15c). These are the first samples in the upper Burnside Formation to shift away from the QF leg of the ternary diagrams. The petrographic and clast data show that these sandstones derive from diverse volcanic, plutonic, and metamorphic sources.

Burnside-Mara waning foredeep

The end of Burnside alluvial sedimentation in the proximal foredeep is marked by a general waning to braid delta and finally mixed carbonate-siliciclastic prodelta shelf (Orange Sandstone member that is equivalent to the Mara and Quadyuk formations; Figure 3a&b). On the basis of correlations with the thick (up to 2.7 km) Burnside sections on the craton, McCormick and Grotzinger (in review b) believe that the proximal section of the Burnside Formation is not complete and a fault that cuts out at least 800 m of the Burnside Formation section must lie between the Gravelly Sandstone and Orange Sandstone members. The Orange Sandstone member contains abundant feldspar that increases upward. The samples point counted actually classify as arkoses with 23% and 54% feldspar (samples STH-014 and STH-021; Figures 10, 16a; Table 2). Minor felsic volcanic fragments are present. The low percentage of polycrystalline quartz in the uppermost Burnside sample may be an artifact of the fine grain size of the sandstone. Iron oxide grain coatings and cement are common. Ferruginous sandstones are the hallmark of the Mara Formation across the basin.

In the ternary diagrams, the samples from the Gravelly Sandstone member appear to lie along a mixing line between the litharenites of the Buff Sandstone and Conglomerate members and those of the Orange Sandstone. This suggests the upper Burnside alluvial system records increasing input from granitic source terrane. Detrital zircon data presented below supports this suggestion.

upper Goulburn Supergroup rejuvenated foredeep

After the tectonic quiescence recorded in the sub-wavebase carbonate-siliciclastic and carbonate platform sedimentation of the Wolverine Group, renewed influx of arkosic siliciclastic sandstone is present in the Bathurst Group. The composition lower sample (BSA-1) of braid delta facies closely matches that of the uppermost sample of the Orange

Sandstone member of the Burnside Formation except that the Bathurst Group sample has a much lower proportion of plagioclase relative to K-feldspar than in the Orange Sandstone member(Figures 9, 10; Table 2). The upper sample of braid plain facies (BSA-2) shows a decrease in the amount of total feldspar, plagioclase decreases by half, and a polycrystalline quartz increases sharply. The amount of polycrystalline quartz, especially Qpq>3, is as high as that in the Conglomerate member of the Burnside Formation. The upper sample contains foliated quartz-mica metamorphic clasts, felsic volcanic clasts, and granitic plutonic clasts. The top of the Goulburn Supergroup appears to record a mixed plutonic-metamorphic source provenance.

proximal to distal trends in the Burnside Formation

The samples from the distal foredeep that were point counted lie solely within the Burnside Formation. They do not record the widely varying petrographic signatures that are expressed in the Burnside Formation in the proximal foredeep, such as in feldspar and polycrystalline quartz (compare Figures 9 vs. 10 and 11 vs. 12; Table 2). The main trends are a gradual decrease in polycrystalline quartz content upward, an increase in feldspar content to a plateau of about 30%, and decreasing or effectively absent lithic fragments. All the samples plot close to the Q–F and Qm–F legs of the ternary diagrams (Figure 9). Sample WC-33 is the notable departure from the overall trend. This sample contains a very high proportion of feldspar and a low proportion of polycrystalline quartz.

It is important to note that the sandstone compositions of the distal samples cannot be produced by grain size reduction from lithic rich sandstone in the proximal foredeep. First, the proximal sandstones in the Buff Sandstone and Conglomerate members are not very rich in lithic fragments and the lithic fragments are not dominantly plutonic clasts. It is only in the Gravelly Sandstone and Orange Sandstone members that the feldspar and volcano-plutonic lithic fragment content reaches proportions that could yield compositions seen in the distal foredeep. On the basis of sedimentologic, stratigraphic, and paleocurrent data, we have argued that the base of the Burnside Formation in the distal foredeep must be correlative to the Conglomerate member or higher in the proximal foredeep. Barring an out of plane source for the feldspar, which seems unlikely given the predominance of west-northwest paleocurrents as discussed below, these petrographic data strongly suggest that the base of the Burnside Formation in the distal foredeep correlates with the Gravelly Sandstone member in the proximal foredeep. The samples with higher feldspar content (19-35% in samples WC-33 and above) probably correlate with the Orange Sandstone member, including the interval in the Orange Sandstone member that has been cut out by faulting the

proximal foredeep section. Detrital zircon data bear out this correlation.

general petrographic observations and interpretations

One of the notable aspects of the Goulburn Supergroup sandstones is the paucity of lithic fragments. Most of the lithic fragments observed consist of polycrystalline quartz, granitic-plutonic rock fragments composed mostly of quartz, and chert ± iron oxide. In other words, these lithic fragments are ones expected to survive transport in a high energy braided stream system. The decrease in conglomerate content from the proximal to distal part of the basin and the exclusive presence of duriclasts in distal conglomerates suggests high levels of mechanical abrasion in the main Burnside alluvial system. Although intrabasinal clasts of the Burnside-type sandstones do appear in proximal conglomerates, they appear to be almost absent west of the Gordon Bay Arch. The source of these clasts probably was foreland propagating thrust sheets that uplift the upper veneer of syn-orogenic strata. Clearly, though, labile grains were efficiently broken down in the Burnside alluvial system.

Another minor observation is that none of the plagioclase seen in thin section exhibits any zoning that is thought to be diagnostic of volcanic origin (Pittman, 1963; Pittman, 1970). Most of the feldspar seen in felsic volcanic clasts appear to be highly altered to phyllosilicates. The fresh feldspar present, especially K-feldspar, and the common occurrence of microcline suggest that much of the feldspar derives from plutonic or high grade metamorphic sources.

Although it is tempting to attribute the lack of labile grains in Goulburn Supergroup sandstones to the effects of humid or monsoonal climate on the production of quartz sands in the source area, it is difficult to document such a causal relationship (compare, for example, Mack and Suttner (1977) with Walker (1978)). The relationship between climate and sandstone composition continues to be a thorny and contentious area of research, fraught with ambiguities and unconstrained variables (Basu, 1976; James et al., 1981; Suttner et al., 1981; Franzenienelli and Potter, 1983; Suttner and Basu, 1986b; Johnsson et al., 1988; Johnsson et al., 1991). The effects of transport abrasion and post-depositional diagenetic destruction of labile grains are not easily isolated from source area weathering. The best possible conditions under which to isolate climatic effects on framework mineralogy are to derive the sandstones from phaneritic crystalline rocks in mature extensional settings on continental plates, transport them less than 100 km in low order streams, cement them early to seal the rocks from further diagenesis, and to bury the sandstones shallowly (Suttner and Basu, 1986a; Vebel and Saad, 1991). The compressional tectonic setting, long transport distance, and moderate to high gradient stream or marine reworking characterize the

Goulburn Supergroup in general, and the Burnside Formation sandstones in particular. All sandstones in the Goulburn Supergroup have been transported at least 50 km from the Slave Province or the Thelon Orogen, in most cases much farther. For Burnside Formation and Bathurst Group alluvial sandstones derivation from Thelon Orogen and probably Queen Maud block suggest much longer transport distances (>100 km) and sedimentary facies suggest transport in moderate to high gradient braided stream systems. Diagenetic modification, especially late diagenesis, has been of moderate but variable intensity, but generally a range of feldspar alteration suggests source area weathering has variably imprinted different grains. Different diagenetic susceptibility due to varying mineral composition cannot be ruled out, however.

On the basis of the long distance of transport, lack of interbedded mudstones and siltstones, and the scale of stratification in the Burnside Formation, McCormick and Grotzinger (in review a) interpret the main part of Burnside Formation to have formed under humid perennial or monsoonal conditions. The presence of halite casts and solution collapse breccias in the Bathurst Group (Campbell and Cecile, 1981) strongly suggest that climate became drier toward the end of Goulburn sedimentation. Such indicators of desiccation are absent in lower Goulburn Supergroup sediments. Similar arid sedimentary facies are found in Wopmay Orogen and Athapuscow Basin (Hoffman, 1969; Hoffman, 1973; Hoffman et al., 1984) that we believe are stratigraphically correlative. This suggests that the surface of the entire Slave craton desiccated, perhaps in response to the orographic barriers caused by mountain belts that ringed the entire craton (Hoffman and Grotzinger, in review). The most feldspathic sandstones in the Goulburn Supergroup are present in the uppermost Burnside and Mara formations and the Bathurst Group when the climate is inferred to have changed. It is not possible, however, definitely to attribute this shift to a change from humid to arid climate, especially since the sedimentologic evidence for drier climate is recorded in the basin and may bear little relation to conditions in the source area.

paleocurrents of the Goulburn Supergroup

Paleocurrent data provide some of the most critical constraints on the interpretation of tectonic setting and provenance of the Goulburn Supergroup. There are well-defined changes in the mode and dispersion of paleocurrents between each of tectono-stratigraphic units (Figure 5). These data are taken from Campbell and Cecile (1981), Grotzinger and McCormick (1988), and McCormick and Grotzinger (in review b). Where angular dispersion of paleocurrent data is reported, the angular dispersion represents one circular standard deviation of the data.

paleocurrent data

Kimerot Group passive margin

Paleocurrents indicate that initial passive margin alluvial strata were derived from the Slave Province and flowed to southeast with low dispersion (122° ± 38°, n = 61). Alluvial paleocurrent patterns pointing away from the craton interior are common to passive margins. Shallow marine cyclic carbonate-siliciclastic strata in the passive margin that onlap the alluvial strata show two weak modes: one to the south-southeast and one to the west-northwest. The mean direction is southwest mode with very high dispersion (232° ± 103°, n = 270).

lower Bear Creek Group marine to deltaic foredeep

An abrupt shift in paleoflow is present in the lower Bear Creek Group foreland basin strata. Turbidites in the lower Bear Creek Group flowed uniformly with low dispersion to the southwest (223° ± 30°, n = 134) in a longitudinal, axial direction, parallel to the trend of the Thelon Orogen and the syn-depositional Gordon Bay flexural arch, toward Athapuscow Basin.

Partly coeval shallow marine shelf sandstones in the lower Bear Creek Group show a west-southwestern mode with moderate to high dispersion (262° ± 60°, n = 252) with minor modes to the west-northwest and southwest. One notable characteristic of lower Bear Creek Group shelf sandstones is the presence of 10-25% fresh angular feldspar grains. Although this is discussed more fully below, these data suggest that much of the sand in the lower Bear Creek Group was eroded from a granitic terrane along strike of the basin. A significant tract of syenogranite upon which the Burnside Formation alluvial foreland basin sediments are deposited, without intervening lower Bear Creek Group marine rocks, suggests that the area near Buchan Bay was a topographic dome and supplied granitic detritus to the foredeep (McCormick and Grotzinger, in review b).

Burnside braided alluvial foredeep

There are two important transport modes in the Burnside alluvial system: an initial southwestern mode in a transitional braid delta facies and a northwestern mode that dominates braid plain facies across the entire craton (Figure 5). The braid delta facies is stratigraphically restricted to the proximal part of the basin between the Thelon Orogen and the Gordon Bay flexural arch. The paleocurrent mode from trough cross beds in braid delta facies is southwest with low dispersion (238° ± 29°, n = 59). This mode is axial and

longitudinal like the lower Bear Creek Group turbidites. This suggests that initial deltaic progradation was laterally restricted by the Gordon Bay Arch.

An abrupt shift is present between deltaic and braid plain facies in the proximal foredeep (Figure 5). The first high energy braid plain facies have trough cross bed paleocurrents that indicate flow to the west-northwest (294° ± 27°, n = 115) with low dispersion. All paleocurrents recorded in the Burnside Formation in the distal foredeep have a similar west-northwestern mode (Figure 5). McCormick and Grotzinger (in review b) indicate that all of the Burnside Formation found on the craton correlates with the Conglomerate member or higher in the proximal foredeep on the basis of the stratigraphic thinning and cutouts of the Transitional and Buff Sandstone members as one approaches the Gordon Bay Arch. Over the crest of the arch, the base of the Burnside Formation is characterized by conglomeratic braid plain facies sitting directly on marine shelf facies (McCormick and Grotzinger, in review a). One remarkable aspect of the Burnside Formation is that this west-northwest mode persists throughout Burnside sedimentation and that it is nearly uniform across the basin. One important observation about the paleocurrent trend in the high energy braid plain facies of the Burnside Formation is that the paleocurrent mode is not orthogonal to the Gordon Bay Arch or to turbidite paleocurrent trends in the lower Bear Creek Group. Rather the mean paleocurrent direction (about 295°) is about 20-30° counterclockwise to the line normal to the Gordon Bay Arch (trending about 045°). Given the low dispersion of paleocurrents, this rotation is statistically significant. It suggests that initial thrusting and loading that created the foredeep was probably northwest directed, but by the time of main Burnside sedimentation, the direction of thrusting in the Thelon Orogen was more west-northwesterly directed.

upper Goulburn Supergroup tectonic quiescence

The mixed siliciclastic braid delta-carbonate shelf of the uppermost Bear Creek are sharply overlain by shelf sediments of the Wolverine Group deposited below wavebase (Figure 3a). Mixed carbonate rhythmites and siliciclastic mudstones contain climbing ripples with a dominant paleocurrent trend of west-northwest with a weaker mode to the south-southwest (Campbell and Cecile, 1981). This suggests a carbonate shelf with west-northwest paleoslope lay to the east and may have backstepped in response to an interval of tectonic quiescence and possibly a relative sea level rise over the basin. The mudstone-rhythmite facies is gradationally overlain by a carbonate platform containing stromatolites elongated in a south-southwest direction with low dispersion (Campbell and Cecile, 1981).

upper Goulburn Supergroup rejuvenated foredeep

Renewed influx of upward-coarsening siliciclastic sandstones gradationally overlying the Wolverine carbonate platform marks the Bathurst Group (Figure 3a). Lower very fine to fine-grained braid delta to lower braid plain sandstones of the Brown Sound Formation have a pattern of high dispersion paleocurrents that range from east-southeast to west-southwest with the mean lying somewhere near south or west-southwest (Campbell and Cecile, 1981). Overlying braid plain sandstones of the Amagok Formation have a tighter clustering of trough cross bed paleocurrents that have a mean direction of west or west-southwest (Campbell and Cecile, 1981). Grotzinger and McCormick (1988) interpret the Bathurst Group to represent the rejuvenation of the Kilohigok foreland basin. This is supported by the fact that paleocurrent trends are similar in the Burnside Formation and Bathurst Group and the composition of sandstones are similar to the upper Burnside-Mara Formations. Detrital zircons ages from these units are also similar as will be reported below.

implications of paleocurrents for provenance of the Goulburn Supergroup

The paleocurrent data from the Goulburn Supergroup are key elements of the model for the tectonic evolution of the Kilohigok Basin. In addition, paleocurrent data provide essential constraints on the interpretation of the detrital zircon geochronolgy that follows by pointing to the source areas from which the sandstone were probably derived. The data suggest that the basal alluvial sediments of the Kimerot passive margin were derived from the interior of the Slave craton. In contrast, turbidites and shelf sandstones of the lower Bear Creek Group foreland basin were derived from the areas to the northeast along strike from the basin probably on the eastern edge of the Slave Craton. The transitional braid delta facies of the Burnside alluvial system appear to derive from the east-northeast, either from the easternmost edge of the Slave Province or from the leading edge of Thelon Orogen. The main phase of Burnside alluvial sedimentation and all alluvial sediments over the Slave craton were derived from the east-southeast from the Thelon Orogen and perhaps from the interior of the Queen Maud block further to the east. The braid delta and alluvial sediments of the Bathurst Group also appear to mark renewed progradation of syn-orogenic sediments into Kilohigok Basin after a quiescent period. The Bathurst Group braid delta sediments probably experienced marine modification and longshore transport to the south, while braid plain sediments derive from the east-northeast, probably from Thelon Orogen, as did the majority of the Burnside alluvial sediments.

detrital zircon geochronology of the Goulburn Supergroup

geochronologic methods

Twenty to thirty (20-30) kilogram bulk samples from the Goulburn Supergroup sandstones were collected from horizons that contained medium- to coarse-grained sandstones; some contained conglomerate. The bulk samples were crushed, sieved, and the sand size fraction was concentrated on a Wilfley table. After drying, magnetic minerals and metal filings were removed by pouring the concentrate through a tube that was subjected to a large external magnetic field; the material caught by the magnet was discarded. The remaining concentrate was gravimetrically separated with bromoform and then methyl iodide. The dense mineral concentrate, those grains that settled through both heavy liquid phases, had remaining magnetic, Fe-oxide-coated, or Fe-oxide-rich material removed with a hand magnet. The remainder was split into progressively less magnetic fractions with a Franz isodynamic magnetic separator that very efficiently segregates grains of subtly different magnetic properties. The most diamagnetic and least magnetic fractions that, in general, yield the most concordant U-Pb dates were selected for hand picking under binocular microscope. Populations of visually similar zircons were segregated on the basis of morphology, size, color, degree of abrasion, presence of inclusions, presence of cores, and zoning. Small numbers of grains per population (≤ 10; most ≤ 5) were chosen. The most euhedral, clear, and delicate populations were chosen for these initial analyses in order to maximize the chance of getting the youngest possible samples, rather than the dark, well rounded zircons that suggest older and perhaps second cycle detrital origin. In order to improve the concordance of individual samples, most of the samples were air abraded with pyrite after the method of Krogh (1982) to remove grain surface coatings and metamict outer rinds of the zircons. The air abraded samples were dissolved in HF in teflon microbombs. Samples analyzed at Washington University in St. Louis were spiked with a mixed $^{208}Pb/^{235}U$ tracer; samples analyzed at the Massachusetts Institute of Technology had a $^{205}Pb/^{235}U$ tracer. Following anion exchange column separation, the Pb was loaded onto rhenium filaments using a standard silica gel-phosphoric acid technique, and the U was loaded on rhenium filaments with graphite. About half the isotopic measurements were made with a VG-354E mass spectrometer at Washington University, while the other half were made on a VG Sector 54 mass spectrometer at the Massachusetts Institute of Technology. Procedural blanks for the samples run at Washington University were between 20 to 30 picograms for Pb and less than 5 picograms for U. Procedural blanks for the

samples run at the Massachusetts Institute of Technology were between 5 to 10 picograms for Pb and less than 3 picograms for U. The standard errors associated with the measurement of the $^{206}Pb/^{238}U$ and $^{207}Pb/^{235}U$ ratios are ±0.4% (2 standard deviations) and the error in the $^{207}Pb/^{206}Pb$ ratio are about ±0.1% (2 standard deviations).

sampling and analytical problems in the analysis of detrital zircon

Even with a few grains from visually homogeneous populations, there still remains the possibility that reported isotopic data and calculated Pb-Pb ages reflect a mixture of different age zircons. Only if the analysis plotted on concordia, could the Pb-Pb age be viewed potentially as the crystallization age of a single population. In addition, statistical regression, such as that normally performed on igneous or metamorphic U-Pb analyses (Ludwig, 1980), requires analyses of several different magnetic fractions of grains of identical population. The data presented here are initial results from analyses of small numbers of grains (≤6) from visually homogeneous populations; 1 to at most 3 magnetic fractions from each sample have been analyzed. There are practical limitations for detrital zircon studies due to the large amount of time to prepare and run samples. One could never analyze all the populations in a single sample, let alone for multiple samples. To feel confident that one had characterized all the ages of the rocks contributing zircons to the detrital sample, one would have to run at least twice as many zircons as there are potentially contributing source areas.

Only by using several single grain analyses could one feel confident that the "Pb-Pb age" calculated and reported here represents the true crystallization age of a single population of zircons. Single grain analyses are intended for the near future to refine the interpretation of ages that are reported below. As the age of source areas potentially contributing to the Goulburn Supergroup vary by several hundred million years, even this reconnaissance study dating a few populations from each sample yields distinct and widely separated age determinations.

A practical approach that is a trade-off between single-and multiple-grain analyses could be approached along the following lines. If one were to use multi-grain samples of an homogeneous population for initial dating, you could test whether the Pb-Pb age obtained was a mix of different ages by dating 1 to 3 single grains segregated from the same population. If the Pb-Pb ages of the single grains were all identical to the multi-grain populations, then one could feel confident that the population probably had a single crystallization age. If the Pb-Pb ages of the single grain samples were spread over some range the bounded the Pb-Pb of the multi-grain sample, one would suspect that the multi-grain Pb-Pb was a mixture of different-aged minerals. So two to four analyses per population, one

multi-grain and the others single grain, could be used as a good test of the age of homogeneous detrital zircon populations.

geochronologic results

Despite the use of multiple grain fractions and the limited number of fractions per sample, the age of contributing source terranes are of sufficiently large age difference that large shifts in Pb-Pb ages of detrital zircons are seen at stratigraphically restricted horizons and point to large changes in drainage during the evolution of the Goulburn Supergroup. The results from detrital zircon U-Pb isotope analyses from the Goulburn Supergroup in the proximal part of Kilohigok Basin are summarized in concordia plots in Figure 17. Results from the distal foredeep and Coronation Supergroup in Wopmay Orogen are summarized in Figure 18. The results of U-Pb dating of four basement samples from Queen Maud block are presented in Figure 19. All U-Pb data are tabulated in Table 3.

Kimerot passive margin

The detrital zircons from the basal alluvial sandstones of the Kimerot Group contain zircons yielding Pb-Pb ages of Middle Archean age (about 3.38 Ga; S. Bowring, personal communication). This is the oldest detrital zircon age for the Goulburn Supergroup yet recorded. Paleocurrents indicate that these sandstones were derived from the northwest in the interior of the Slave Province (Figure 16). The Slave Province is dominated by Late Archean (2.58-2.7) metavolcanic, metasedimentary, and plutonic rocks, but older Middle to Early Archean enclaves of gneissic basement have been reported in the western part of the Slave Province.

lower Goulburn marine to deltaic foredeep

The entire lower Bear Creek Group in the proximal foredeep up through the deltaic Transitional member of the Burnside Formation shows a very uniform Late Archean Pb-Pb ages. Figure 17 shows that although these sample come from a wide stratigraphic distribution over 3-4 km of stratigraphic section vertically, the samples from the turbidites, Hackett shelf sandstones and the Transitional member all fall on a chord that intercepts concordia at between 2.61-2.62 Ga. This is not a regression line; one cannot properly regress U-Pb data from detrital zircons within a single sample as it is uncertain whether they truly derive from the same source. But it is remarkable that they are roughly collinear and suggests that they do derive from a source terrane of consistent 2.61-2.62 Ga age. The sample from the Rifle shelf sandstone (sample 6 in Table 3) has an older Late Archean Pb-Pb age of 2.71 Ga. This age

falls at the upper end of the spectrum of ages common to the metavolcanic rocks of the granite-greenstone assemblages that dominate the Slave Province (Isachsen et al., 1991). One sample from the Transitional member of the Burnside Formation has an older Pb-Pb age of 2.64 Ga (sample 7 in Table 3) that is within the range of plutonic rocks of the eastern Slave Province.

Burnside braided alluvial foredeep

proximal foredeep

Detrital zircon ages record a sharp shift in source area Pb-Pb ages at the break between the deltaic Transitional member and the Buff Sandstone members of the Burnside Formation in the proximal foredeep. This break matches the contrast in sedimentology, stratigraphy, paleocurrents, and petrography recorded at this stratigraphic level and the U-Pb data serve to strengthen the interpretation that this marks a fundamental shift in the evolution of the Goulburn Supergroup and the Kilohigok Basin-Thelon Orogen system.

The lowest sample within the main alluvial interval that has been dated lies at the base of the Conglomerate member (sample 9 in Table 3). The single fraction dated yields the youngest detrital sample yet dated, 1.97 Ga, and is nearly concordant. This date overlaps igneous and metamorphic ages for the Thelon Orogen and overlaps with volcanic ash bed ages in the lower Goulburn Supergroup (Bowring and Grotzinger, 1992). The top of the Conglomerate member exhibits a Pb-Pb age of 2.33 Ga (sample 10 in Table 3), the first in a series of earliest Proterozoic detrital zircon ages that are unrepresented by rocks that have been reported for Slave Province or Thelon Orogen. We present evidence below that material of this age may indeed be an important component of the Queen Maud block.

The remaining samples from within the Burnside Formation exhibit the two Early Proterozoic ages ranges that appear in the Conglomerate member. The top of the Gravelly Sandstone member contains nearly concordant 1.99 Ga detrital zircons (sample 11 in Table 3). This age overlaps with ages from Thelon Orogen as noted above. At this stratigraphic level, one of the prominent conglomerate horizons includes undeformed felsic volcanic clasts. Preliminary dates from zircons in these clasts yield Pb-Pb ages of 2.23 and 2.25 Ga (samples 14 and 15 in Table 3; Figure 17) and detrital zircons in the matrix sand yielded a 2.24 Ga Pb-Pb age (S.A. Bowring, personal communication).

The uppermost samples from the Orange Sandstone member, which should correlate with the Mara Formation, have zircons with ages of 2.41 and 2.50 Ga. These dates are older than most of the earliest Proterozoic detrital zircon ages by 40-50 m.y., but they overlap with

those at the base of the distal foredeep and with overlying Bathurst Group sandstones at the top of the Goulburn Supergroup. Alternatively, they could be a mixture of Archean and Proterozoic zircons.

distal foredeep

The distal foredeep displays an array of dates that differ from those found in the proximal foredeep (Figure 18). The lowermost sample (samples 16 and 17 in Table 3) shows two distinct ages: one Late Archean at 2.63 Ga and one earliest Proterozoic at 2.44 Ga. The Late Archean age falls just about on the line that characterized detrital zircons in the lower Bear Creek Group in the proximal foredeep. The presence of Late Archean zircons is not taken to be particularly significant as the ages of the areas beyond the Thelon Orogen are not well characterized and ages of this range are recorded in many of the Archean blocks of the Canadian Shield (Hoffman, 1989). Some preliminary data presented below suggest that material of this age may exist to the east of Thelon Orogen in Queen Maud block. The absence of a particular age spectrum in datable detrital minerals from the samples discussed here does not indicate that material of that age is absent from the sample; we have not exhaustively analyzed our samples. What is significant is the presence of Proterozoic age zircon samples in these basal samples. The distal sections appear to contain Proterozoic zircons from the onset of significant alluvial-influenced sedimentation.

The lone sample from the most distal Burnside Formation sample (section 13 in Figure 2; sample 21 in Table 3) has a similar earliest Proterozoic Pb-Pb age of 2.41 Ga and is relatively concordant. The similarity of ages at sections 12 and 13 supports the correlation between them and implies similar age material will be found in the passive margin of Wopmay Orogen to the west.

The upper three samples from section 12 (Figure 2; samples 16-18 in Table 3) display a narrow range of younger Early Proterozoic zircons (2.16-2.18 Ga). The upper two samples are relatively concordant. These are relatively young ages that have not been noted either in proximal Burnside Formation detrital zircons or in the eastern Slave Province or Thelon Orogen.

Bathurst Group rejuvenated foredeep

The uppermost detrital zircon samples from the Goulburn Supergroup lie in the Bathurst Group in the proximal end of the foredeep (Figure 17; samples 22-24 in Table 3). The three fractions analyzed in alluvial facies show two distinct Pb-Pb age populations: 2.36-2.40 and 2.8 Ga. The younger ages overlap with those found in the Orange Sandstone

member. The older age is distinctly older than the Late Archean basement found in the eastern Slave Province and unrepresented by ages reported from Thelon Orogen, but older ages in this range have been reported from farther west in the Slave Province. Paleocurrent evidence precludes the western Slave Province being the source of these zircons, though. Our preliminary data from basement rock samples from Queen Maud block suggests that rocks of this age may also exist there.

Coronation foredeep of Wopmay Orogen

Several detrital zircon samples were taken from the passive margin and foreland basin strata of the Coronation Supergroup in Wopmay Orogen in order to test some of the correlations proposed on the basis of previous stratigraphic and geochronologic work (Bowring and Grotzinger, 1992; McCormick and Grotzinger, in review a).The two detrital zircon ages that we report both lie in the foreland basin strata (Recluse Group) in the easternmost part of Wopmay Orogen that is nearest to Kilohigok Basin (Figures 1, 4). These samples are located in the Tree River and Asiak formations. The Tree River Formation is the lowermost foreland basin strata on the cratonic side of Wopmay Orogen. It is a ferruginous, very fine grained sandstone and siltstone that is capped by a spherulitic ironstone. It thins from east to west, pinching out landward of the edge of the carbonate platform in the passive margin. The lithology and stratigraphic trends led Hoffman et al. (1984) and Grotzinger (1985) to correlate the Tree River Formation with the Mara Formation. The Pb-Pb ages of detrital zircons from the Tree River Formation are 2.10 and 2.18 Ga, apparently overlapping ages of the upper Burnside Formation just below the Burnside-Mara contact in the distal foreland (Figures 4, 7, 18).

The final detrital zircon age is from the Asiak greywacke turbidites that overlap the Tree River Formation in the foreland basin succession. The detrital zircons have ages of 1.96 Ga and are nearly concordant. These sediments definitely thin from west to east (Hoffman, 1973; Hoffman et al., 1984). Their age suggests that they derive from an exotic arc terrane (Hottah arc) that lies on the outer western margin of Wopmay Orogen (Bowring and Grotzinger, 1992). Bowring and Grotzinger (1992) report an U-Pb zircon age of 1.882 ± 0.004 Ga from a volcanic ash at a similar stratigraphic level. The correlation between the Tree River Formation and the Mara Formation means that the ash bed age puts an upper bound on Burnside-Mara alluvial sedimentation at about 1.88 Ga.

preliminary basement ages from Queen Maud block

The Queen Maud block is largely unexplored and has only been studied in the reconnaissance geology projects of the 1960's and 1970's (Fraser, 1964; Heywood and Schau, 1978). The age of basement rocks the Rae Province east of Thelon Orogen is largely unknown and no dates have been reported from the Queen Maud block. Given the proposed Tibetan uplift model for this area, it is important to have some data about the ages represented in this vast terra incognita. During a thirty-six hour reconnaissance trip, we collected four widely spaced samples from basement rocks in Queen Maud block (Figure 19). Single fractions from each sample have been analyzed so far.

The sample nearest to Thelon Orogen, a quartzo-feldspathic gniess, came from east of where Hoffman (1987) speculated the eastern limit of Thelon Orogen lay on the basis of magnetic anomaly patterns (Canada, 1987). The sample comes from an area that is a magnetic low. The sample is nearly concordant and has a Pb-Pb age of 2.62 Ga (sample 26 in Table 3). This age overlaps with the ages of plutonic rocks in the eastern Slave Province. The second sample from a quartzo-feldspathic gniess in a area of a broad magnetic high with curving anomaly patterns yields a mildly discordant Pb-Pb age of 2.86 Ga (sample 27 in Table 3). This is older than ages reported from the eastern Slave Province and Thelon Orogen. The third sample is a garnet granite that yields a virtually concordant age of 2.40 Ga (sample 28 in Table 3). Rocks of this age have not bee reported from anywhere in either the Slave Province or Thelon Orogen, but have been reported from the eastern margin of Taltson Magmatic arc the western edge of the Rae Province south of the McDonald-Wilson fault zone (Figure 1). The final sample yields a highly discordant age of 2.43 Ga (sample 29 in Table 3). These preliminary data suggest that the Queen Maud block is a heterogeneous terrane that contains both Late Archean and earliest Proterozoic elements. The implications of these data are discussed below.

Discussion

provenance evolution of the Goulburn Supergroup

The evidence from petrography, paleocurrents, and dating of detrital zircons all strengthen observations on and interpretations of the coupled evolution of the Kilohigok foreland basin and Thelon Orogen. Figure 20 summarizes the major paleocurrent modes associated with the different lithotectonic elements of the Goulburn Supergroup and the associated ages of detrital zircons from that stratigraphic interval. Major changes in the

content of feldspar, polycrystalline quartz, and lithic fragments, paleocurrent direction, and detrital zircon age are present at the boundaries between the Kimerot passive margin and Bear Creek foredeep and at the contact between the Transitional and Buff Sandstone members of the Burnside Formation. A more gradual transition exists between the Conglomerate and Gravelly Sandstone members as litharenites give way vertically to subarkoses and finally arkoses in the Orange Sandstone member.

The U-Pb dating of detrital zircons in Kilohigok Basin and Wopmay Orogen show three broad age spectra (Figures 17, 18). First, Kimerot sandstones show an Middle Archean component (ca. 3.38 Ga) that was derived from the interior of the Slave Province. In the proximal foredeep, the lower Bear Creek Group up through the deltaic Transitional member of the Burnside Formation show a very uniform Late Archean source (2.6-2.7 Ga) that was probably derived from exposed Slave Province along strike from the basin. A distinct shift to sublitharenite sandstone composition and detrital zircon ages to Early Proterozoic (1.97-1.99 and 2.32-2.50) is present within the Buff Sandstone and Conglomerate members. Although distal alluvial sandstones have a consistent northwestern paleocurrent mode and contain Early Proterozoic detrital zircons in the lowest samples, the distal sandstones are subarkosic. This suggests that the distal sandstones must correlate with the stratigraphically higher, more feldspathic sandstones in the Gravelly Sandstone and Orange Sandstone members. This northwest drainage persisted for the rest of Burnside alluvial sedimentation. The distal Burnside alluvial samples all show Early Proterozoic components (2.10-2.18, 2.44 Ga). Finally, a virtually identical Early Proterozoic detrital zircon signature is recorded in the basal foreland basin shelf sandstones of Wopmay Orogen that we believe are the distal equivalent of the upper Burnside and Mara Formations. Early Proterozoic (2.36-2.40 Ga) and Late Archean (ca. 2.80 Ga) detrital zircons mark the late alluvial, immature arkoses in the Bathurst Group. In light of the Late Archean and Early Proterozoic ages we report from Queen Maud block, it appears that both the Thelon Orogen and Queen Maud block may be the source of much of the Burnside Formation detritus and that Queen Maud block may have a large component of Early Proterozoic (2.3-2.4 Ga) material within it. The source of 2.1-2.2 Ga zircons is enigmatic.

It must be emphasized that these geochronologic results are on the basis of the analysis of small numbers of grains from homogeneous populations of zircons and derive from the analysis of one to at most three populations per sample. Only through the analysis of single grains will we feel confident in having potentially determined the age of the source area that contributed the zircons. Even then, the possibility of having multiple stages of zircon growth and complex Pb loss histories could complicate further the interpretation of the detrital zircon ages. Only through the analysis of multiple populations per sample will we

feel confident in having characterized the spectrum of ages of source terranes that have contributed to the Goulburn Supergroup through its history.

Kimerot passive margin: old Archean source on the Slave craton

Two potential sources for the Middle Archean (ca. 3.38 Ga) zircons can be envisioned. First, they could derive from Middle Archean basement. Paleocurrents indicate a source to the northwest within the Slave Province. Gneissic basement outcrops with older Archean ages exist in the western Slave Province (Bowring et al., 1989), but have not been reported from the eastern Slave Province (Hoffman, 1989). Alternatively, they could be second cycle detrital zircons from the Late Archean metasediments derived from older sources. These remain the oldest detrital zircons yet dated in the Goulburn Supergroup. Derivation from gneissic basement would explain the feldspar content in these alluvial sandstones. These data suggest that a belt of older basement rocks, similar to the old gneisses exposed just east of Wopmay Orogen, continue to the north towards the Arctic coast. Gneisses older than 3.30 Ga exist in areas near the Tree River and the Anialak River (S.A. Bowring, personal communication).

early foredeep: lateral plutonic and metamorphic sources within the Slave Province

The Slave Province is dominated by a "granite-greenstone" assemblage of older metavolcanic rocks and greywacke metaturbidites with younger plutonic rocks. The 2.61-2.62 Ga ages seen in several of the lower Bear Creek Group sandstones are consistent with the 2.63 to 2.58 Ga ages common for the younger plutonic rocks in the Slave Province. Derivation from granitic rocks would explain the common feldspar content of the lower Bear Creek Group sandstones. The slightly older detrital zircon Pb-Pb age in the Rifle sandstone (2.71 Ga) overlaps with metavolcanic ages common to the Slave Province (2.67-2.70 Ga), but this age could reflect a mixture of the 2.6 Ga material with older Archean material. Paleocurrents for the lower Bear Creek Group consistently point to a source area in the northeast, roughly along strike of the Thelon Orogen and the Gordon Bay flexural arch. Grotzinger et al. (1989) and Tirrul and Grotzinger (1990) have shown that the turbidite fan channel complexes exposed in the proximal part of the basin were mostly derived from slumping from temporally equivalent shallow marine shelf material. This interpretation is underscored by the 2.61-2.62 Ga Pb-Pb ages of their detrital zircons that are collinear with shelf and deltaic sandstones of the Bear Creek Group (Figure 17).

McCormick and Grotzinger (in review a) show that to the northeast along strike

from the Gordon Bay Arch high energy braided alluvial facies of the Burnside Formation, identical to the Buff Sandstone and Conglomerate members, lie directly on a large tract of syenogranite basement with no intervening Kimerot Group or lower Bear Creek Group (location 15 in Figure 2). They have argued that the Gordon Bay Arch was probably an emergent dome that was exposed to the northwest during lower Bear Creek time. This could account for the feldspar content of lower Bear Creek Group and its derivation from late plutons yielding the younger Late Archean ages. Several attempts by us to date the syenogranite underlying the Burnside Formation at location 15 failed.

early Burnside deltaic foredeep: metamorphic sources from the Slave or Queen Maud?

Petrographic evidence indicates that the Transitional member of the Burnside Formation was similar to but more feldspathic than the underlying shelf sandstones of the lower Bear Creek Group. Paleocurrents remain nearly parallel to the Gordon Bay Arch, although they are rotated clockwise 10° to 15°. The detrital zircons suggest that the Transitional member braid delta sandstones may have been derived from identical age areas as the underlying Bear Creek shelf sandstones and turbidites.

Our preliminary U-Pb zircon data from Queen Maud block complicates this interpretation. The sample that came from the area closest to Thelon Orogen yields a Pb-Pb age of 2.62 that overlaps Late Archean basement ages common to the eastern Slave Province and detrital zircon ages in the lower Bear Creek Group. This means that it is possible that this initial deltaic lobe could have been sourced from within Queen Maud block and one would not be able to distinguish between Slave and Queen Maud sources, *a priori*. One argument against this interpretation is that one would expect to see Thelon age detritus at least at the same time as, if not before, material derived from behind the orogenic belt. Again, the absence of an age range is not proof of its nonexistence in the foredeep at this stratigraphic level. The fact that we have not identified it so far suggests that the deltaic sediments were derived from the Slave Province rather than Queen Maud block at this time.

early Burnside alluvial foredeep: metamorphic sources from Thelon Orogen and perhaps Queen Maud block

Paleocurrent modes shift markedly from southwest to west-northwest between the Transitional and Buff Sandstone members. Feldspar disappears from the sandstones, strained quartz becomes more common, and metamorphic lithic fragments appear. The nearly concordant 1.97 Ga detrital zircon from the base of the Conglomerate member matches volcanic ash bed ages for the base of the lower Goulburn Supergroup (Bowring and

Grotzinger, 1992) that lies 4-5 kilometers of section below this stratigraphic horizon. This suggests that the leading edge of Thelon Orogen was the source of metamorphic detritus. Thelon Orogen today exposes high-grade granite gneisses, migmatites, and mylonites that have U-Pb zircon and monazite ages that indicate the main phase of convergence, deformation, and magmatic activity in Thelon Orogen occurred from 1.97 to 2.0 Ga (van Breemen et al., 1987a; van Breemen et al., 1987b; van Breemen et al., 1987c; van Breemen et al., 1987d; James et al., 1988; van Breeman and Henderson, 1991; Henderson and van Breemen, 1992). The lack of feldspar combined with the presence of metamorphic rock fragments and strained quartz is consistent with derivation from metasedimentary sources. The detrital zircon age that overlaps Thelon metamorphism and plutonism suggests reworking of syn-orogenic magmatic material. However, as pointed out before, the lack of significant arc detritus from the putative continental magmatic arc in Thelon Orogen is vexing. Part of the explanation may lie in the destructive energy of transport processes that characterize the high gradient braided stream facies of the Burnside Formation that appear to efficiently destroy more labile lithic fragments and conglomerate clasts. Perhaps, also, the "arc" was breached early by antecedent river system as the Thelon mountains began to isostatically uplift when the main phase of convergence slowed or ceased and erosional uplift began. Erosion induced uplift is consistent with the present steep metamorphic gradient at the leading edge of Thelon Orogen (Beaumont et al., 1990; Beaumont et al., 1992; Hoffman and Grotzinger, in review).

The presence of detrital zircons with ages of 2.3-2.4 Ga at the top of the Conglomerate member marks a significant new source area age spectrum that is not easily explained in the context of most of the published geochronological data. Paleocurrents require that these conglomerates and sandstones were derived from the direction of Thelon Orogen. As stated above, all basement ages from the eastern Slave Province have been reported as approximately lying between 2.6 and 2.7 Ga. Thelon Orogen is dominated by syn-metamorphic ages of 1.97-2.02 Ga and younger igneous activity between 1.90-1.95 Ma.

Henderson and van Breeman (1992) have recently reported cores of zircons in metasedimentary rocks that yield mildly discordant ages between 2.17 to 2.21 Ga. Even allowing for metamorphic overgrowths at about 2.0 Ga as recorded by the tips of the zircons, the age of the cores of these zircons could not be older than 2.4 Ga (Henderson and van Breemen, 1992). More direct evidence for the existence of 2.3-2.4 Ga rocks lies on the western margin of the Rae Province immediately adjacent to the Taltson Magmatic Zone, the temporal equivalent of Thelon Orogen south of the McDonald-Wilson fault zone. Bostock and Loveridge (1988) and van Breemen et al. (1992) have dated several gneissic bodies that border Taltson and find that orthogneisses ranging in age from 2.39 to 2.44 Ga

while younger paragneisses range from 2.27 to 2.34 Ga. Taken together, these data show that crust of ca. 2.3-2.4 Ga exists within the Rae Province. Our preliminary data suggest that similar age material probably exists within Queen Maud block (Figure 19).

Stratigraphic evidence indicates that the initial high energy braided alluvial facies in the Buff Sandstone and Conglomerate members thin to the northwest towards the crest of the Gordon Bay Arch (McCormick and Grotzinger, in review a). The Buff Sandstone member cuts out the thinning Transitional member and the Conglomerate member cuts out much of the Buff Sandstone member. Over the Gordon Bay Arch, conglomeratic sandstone sits directly on marine shelf rocks. The conglomerates are entirely composed of duriclasts of vein quartz, with subordinate jasper, quartzite, chert, and banded iron formation. The presence of metamorphic clasts support the correlation of Conglomerate member or higher with the base of the Burnside Formation over the craton. The presence of these duriclasts also underscores the role of transport abrasion of gravel in the high energy Burnside alluvial system.

main Burnside alluvial foredeep: enigmatic Early Proterozoic and Thelon Orogen sources

The Gravelly Sandstone member in the proximal foredeep contains increasing amounts of feldspar and zircons with at least two Early Proterozoic age groups: 1.97-1.99 (syn-Thelon metamorphism) and 2.23-2.30 Ga (seen in felsic volcanic clasts). Paleocurrents require derivation of these sands and conglomerates from the area of Thelon and Queen Maud block. As suggested above, the source of the earliest Proterozoic zircons probably lies within Queen Maud block given the initial dates reported here. The mixing of Thelon age detritus and the older Proterozoic suggests that the Thelon Orogen was breached and Queen Maud block contributed significant amounts of detritus at least from the time of the top of the Conglomerate member. These Early Proterozoic ages persist through the Orange Sandstone member (2.41 and 2.50 Ga).

One important petrographic observation that bears on the correlations and stratigraphic evolution of the Burnside Formation is that the entire distal section contains significant proportions of feldspar. This feldspar cannot be derived from clasts commonly observed in the Buff Sandstone or Conglomerate members because they are dominated by lithologies that would yield mostly mono- and polycrystalline quartz or chert. The feldspar in the distal samples is of comparable size to that of co-deposited quartz grains, suggesting that they are not a wind-borne component selectively winnowed from different sources, but rather derive from the same source rocks (Dalrymple et al., 1985). As significant feldspar reappears in the Gravelly Sandstone member in the proximal foredeep, this suggest this

middle member correlates with the base of the foredeep in the distal section. Detrital zircons at the base of the Burnside Formation in the distal foreland have both Late Archean (2.63 Ga) and earliest Proterozoic ages (2.44 Ga). The presence of Early Proterozoic detritus confirms that base of Burnside Formation in the distal foreland correlates with the top of the Conglomerate member, with its 2.33 Ga zircons, or higher. Again, the Conglomerate member lacks feldspar, so the correlative horizon probably lies higher, within the Gravelly Sandstone member.

The sample from the most distal Burnside Formation sample (section 13, Figure 2) also yields an earliest Proterozoic age of 2.41 Ga. Previous sedimentologic and stratigraphic work (McCormick and Grotzinger, 1988; Bowring and Grotzinger, 1992; McCormick and Grotzinger, in review a) has shown that the coarse lower Burnside Formation correlates lithostratigraphically with the siliciclastic lower portion of the passive margin prism in Wopmay Orogen (Odjick Formation, Epworth Group). We predict that the age of the samples from the siliciclastic lower portion of the passive margin prism in Wopmay Orogen (Odjick Formation, Epworth Group) will contain detrital zircons of about 2.41-2.44 Ga on the basis of the correlation of base of the Burnside Formation in the distal foredeep with the middle member of the Odjick Formation.

The ages recorded in the middle to upper part of the distal section (section 12) are Early Proterozoic but appear to lie in a distinct age bracket between the syn-Thelon and 2.3-2.4 Ga ages seen so far in the proximal foredeep. These distal samples show a narrow range of Pb-Pb ages from 2.16 to 2.18 Ga. The data from the upper two samples (samples 17 and 18 in Table 3) are relatively concordant. If these are crystallization ages, then sources of this age have not been identified as yet. The only rocks of this age yet dated anywhere in the area are the 2.18 Ga alkaline granite phase of the Blachford Intrusive Suite, an alkaline-peralkaline complex of plutons, that lies on the southern boundary of the Slave Province (Bowring et al., 1984). A younger peralkaline phase of the Blachford has been dated at 2.09 Ga. Another alkaline complex in the Slave Province is the Big Spruce Complex near southern Wopmay Orogen (2.19 Ga) (Cavell and Baadsgaard, 1986).These alkaline complexes, and especially the Big Spruce complex, are not likely sources of young the detrital zircons because paleocurrents point to derivation from a southeast or east-southeasterly source. Other than these areas, though, the 2.1-2.2 interval is not recognized in the potential source areas for the Burnside Formation. The zircons from the felsic volcanic clasts in the Gravelly Sandstone member yield ages that are about 40 to 50 m.y. older. These 2.16-2.18 Ga ages match those found in the base of the foreland basin phase of Wopmay Orogen. The significance of this is discussed below.

rejuvenated foredeep: diverse immature sources

The samples from the Bathurst Group in the proximal foreland basin matches the Orange Sandstone member of the Burnside Formation petrographically with its high feldspar content. The uppermost sample, from where the detrital zircon sample was taken, has higher proportions of metamorphic derived lithic fragments and polycrystalline quartz. The paleocurrents for these sandstones are more southerly than most of the Burnside Formation, but still point to a source toward the Thelon Orogen. The detrital zircon ages show a mix of Early Proterozoic (2.36, 2.40 Ga) and older Late Archean (ca. 2.80 Ga). The older age is interesting, because no rocks of that age have been dated in the eastern Slave Province. One of the samples from the western half of Queen Maud block has a somewhat discordant Pb-Pb of 2.68 Ga (sample 27 in Table 3; Figure 19). Both sets of ages would appear to be consistent with rejuvenation of the Goulburn foredeep with continued influx dominantly from Queen Maud block.

implications for correlations with Wopmay Orogen

The correlations between the Goulburn Supergroup and the Coronation Supergroup of Wopmay Orogen appear to be strong on the basis of sequence stratigraphy and augmented by U-Pb geochronology on zircons from volcanic ash beds (Bowring and Grotzinger, 1992). One of the correlations suggested is between the Mara Formation and the Tree River Formation siliciclastic rocks at the base of the foredeep of Wopmay Orogen. This correlation is greatly strengthened now by the occurrence of detrital zircons of nearly identical Pb-Pb ages of 2.18 Ga in the upper Burnside Formation vs. 2.10 and 2.18 Ga in Tree River Formation from outcrops nearest to Kilohigok Basin. This detrital link confirms the temporal link between the waning stages of Burnside alluvial sedimentation and the initiation of foreland basin sedimentation in Wopmay Orogen. Given this detrital link, the age of a volcanic ash bed, dated at 1.882 ± 0.004 Ga, at a horizon just above the Tree River Formation provides an upper bound on the age of deposition of the Burnside and Mara Formations.

As indicated above, the correlations at the base of the Burnside Formation to the siliciclastic strata in the lower part of the passive margin of Wopmay Orogen can also be tested by dating detrital zircons. We predict that the middle member of the Odjick Formation will have detrital zircons of age 2.4-2.44 Ga, as does the base of the Burnside Formation in the distal foredeep.

implications of 2.2 to 2.4 Ga detrital zircons for the nature of Queen Maud block

The detrital zircons from the Goulburn Supergroup and the preliminary dates from basement rocks in Queen Maud block presented here provide the first strong evidence for the existence of both Late Archean (2.6-2.7, plus >2.8 Ga) and earliest Proterozoic (2.2-2.4 Ga) material in Queen Maud block. As indicated above, rocks of 2.3-24 Ga have been reported on the westernmost edge of the Rae Province directly adjacent to the Taltson Magmatic Zone (Bostock and Loveridge, 1988; van Breemen et al., 1992). This suggests that the Rae Province, and the Queen Maud block in particular, may be a composite of diverse Archean and Proterozoic terranes part of which assembled in the Early Proterozoic before collision with the Slave Province.

The Early Proterozoic ages, in particular, are important because crust of this age has not been recognized in the Canadian Shield until recently. Exposed shield rocks are biased towards Late Archean (2.6-2.7 Ga) and Early Proterozoic (1.8-2.0 Ga) ages. The lack of crystallization ages in this 2.0-2.4 Ga range have led some to believe that there was a temporal gap in which no crust of that age was generated (Patchett and Arndt, 1986; Bennett and DePaolo, 1987). A growing body of evidence suggests that much of the Precambrian basement rocks, which lie west of the Canadian Shield beneath Phanerozoic cover, are composed of juvenile Early Proterozoic crust formed between 2.1-2.4 Ga (Bowring and Podosek, 1989; Ross et al., 1991). These data from the detrital zircon and preliminary basement age dates suggest that more earliest Proterozoic crust may lie within Queen Maud block, further showing that crustal formation between the Late Archean and Early Proterozoic was more continuous than currently recognized.

Conclusions

Evidence from sandstone petrography, paleocurrents, and detrital zircon geochronology of the 2.00 to 1.88 Ga Goulburn Supergroup documents marked changes in provenance as the Kilohigok Basin evolved. Initial passive margin sandstones show an old Middle Archean (ca. 3.38 Ga) signature from within the Slave Province. The marine to deltaic lower Bear Creek foreland sediments show a remarkably uniform Late Archean (2.6-2.7 Ga) source. This phase shows distinctly subarkosic sandstones that were probably derived from exposed basement within the Slave Province that lay to the northeast along strike of the basin.

A sharp shift to sublitharenitic sandstone accompanies a switch to transverse

northwestern drainage that marks the onset of the main phase of alluvial sedimentation in the Burnside Formation. This transverse mode, flowing from Thelon Orogen, persists throughout alluvial sedimentation demonstrating that the basin was perennially overfilled. Conglomerate clasts show predominantly a metamorphic source similar to those of the metagreywacke-metavolcanic assemblages that are common in the Late Archean granite-greenstone terranes. Two age spectra of Early Proterozoic detrital zircons first appear in these transversely draining braid plain facies, 1.97-1.99 and 2.2-2.4 Ga. The 1.97-1.99 Ga detrital zircons are the same age as volcanic ash beds that date onset of foreland basin sedimentation and the age of the main phase of metamorphism and structural evolution of Thelon Orogen, the hinterland to Kilohigok foreland basin. Preliminary ages from basement rocks suggest that Queen Maud block contains rocks of 2.3-2.4, 2.6-2.7, and 2.8-2.9 Ga. The youngest of these age ranges, ages not seen in Slave Province or Thelon Orogen, suggest that Queen Maud block was a significant source of the Early Proterozoic detritus recorded in the Burnside alluvial sediments.

Similar earliest Proterozoic ages are recorded at the base of the Burnside Formation in the distal foredeep. The distal sands contain significant amounts of feldspar and thus must correlate with units higher than the main conglomerate interval that lacks feldspar. The upper sandstones in the distal foredeep appear to have detrital zircons of about 2.1-2.2 Ga, an age range that is not represented by ages currently reported for Thelon Orogen or the Rae Province. These ages are present in sandstones at the base of the foreland basin strata in Wopmay Orogen that are the lateral equivalent of and are sourced by the Burnside-Mara alluvial system. This correlation allows a tie between a volcanic ash bed near the base of the foreland basin sediments of Wopmay Orogen to bracket the waning Burnside-Mara alluvial system to older than about 1.88 Ga.

Rejuvenated foreland alluvial sedimentation in the proximal part of Kilohigok Basin contains arkosic sandstones with mixed plutonic and metamorphic provenance, similar to, but with more metamorphic detritus than, sandstones at the top of the Burnside Formation. Paleocurrents indicate derivation from Thelon Orogen and maybe Queen Maud block. Detrital zircons show a mix of Early Proterozoic (2.36, 2.4 Ga) and an older Late Archean (ca. 2.86 Ga) ages. Both of these age ranges are similar to preliminary basement ages from within Queen Maud block.

The common component of 2.1-2.4 Ga detrital zircons in the alluvial foredeep of Kilohigok Basin and the presence of rocks of this age in Queen Maud block suggest that Queen Maud block contributed substantial detritus to the foreland basin of Kilohigok Basin. This would appear to lend credence to a Tibetan Plateau analogy for the Queen Maud block within a Himalayan-type collision between Slave and Rae Province at 2.0 Ga. Furthermore,

Queen Maud block may contain substantial areas of Early Proterozoic material that must have accreted to the Rae Province before it collided with the Slave Province. A growing inventory of 2.0-2.4 Ga basement ages within and on the margins of the Canadian shield suggests that crust formation across the Archean-Proterozoic boundary may have been more continuous than previously believed.

References Cited

Bally, A.W., Gordy, P.L., and Stewart, G.A., 1966. Structure, seismic data, and orogenic evolution of southern Canadian Rockies. Bull. Can. Petrol. Geol., v. 14, p. 337-381.

Basu, A., 1976. Petrology of Holocene fluvial sand derived from plutonic source rocks: implications to paleoclimatic interpretation. v. 46, p. 694-709.

Basu, A., Young, S.W., Suttner, L.J., James, W.C., and Mack, G.H., 1975. Re-evaluation of the use of undulatory extinction and polycrystallinity in detrital quartz for provenance interpretation. Journal of Sedimentary Petrology, v. 45, p. 873-882.

Beaumont, C., Fullsack, P., and Hamilton, J., 1992. Erosional control of active compressional orogens, in, K.R. McClay (ed.), Thrust Tectonics. Chapman and Hall (London), p. 1-18.

Beaumont, C., Fullsack, P., Willett, S., Hamilton, J., Johnson, D., Ellis, S., and Paton, M., 1990. Coupling of climate, surface processes and tectonics in orogens and their associated sedimentary basins, in, J. Hall (ed.), Lithoprobe: Lithoprobe East Transect, Report 13. Memorial University, St. John's, Newfoundland (St. John's, Newfoundland, Canada).

Bennett, V.C., and DePaolo, D.J., 1987. Proterozoic crustal history of the western United States as determined by neodymium isotopic mapping. v. 99, p. 674-685.

Bostock, H.H., and Loveridge, W.D., 1988. Geochronology of the Taltson Magmatic Zone and its eastern cratonic margin, District of Mackenzie, Radiogenic Age and Isotopic Studies: Report 2. Geological Survey of Canada, Paper 88-2 (Ottawa, Ontario), p. 59-65.

Bostock, H.H., van Breeman, O., and Loveridge, W.D., 1987a. Proterozoic geochronology in the Taltson Magmatic Zone, N.W.T, Radiogenic Age and Isotopic Studies: Report 1. Geological Survey of Canada Paper 87-2 (Ottawa, Ontario), p. 73-80.

Bostock, H.H., van Breemen, O., and Loveridge, W.D., 1987b. Proterozoic geochronology in the Taltson magmatic zone, N.W.T., Canada. Geological Survey of Canada, Paper 87-9. pp.

Bowring, S.A., and Grotzinger, J.P., 1992. Implications of new chronostratigraphy for tectonic evolution of Wopmay Orogen, northwest Canadian Shield. American Journal of Science, v. 292, p. 1-20.

Bowring, S.A., and Podosek, F.A., 1989. Nd isotopic evidence from Wopmay orogen for 2.0-2.4 Ga crust in western North America. Earth and Planetary Science Letters, v. 94, p. 217-230.

Bowring, S.A., Van Schmus, W.R., and Hoffman, P.F., 1984. U-Pb zircon ages from Athapuscow aulacogen, East Arm of Great Slave Lake, N.W.T., Canada. Can. J. Ear. Sci., v. 21, p. 1315-1324.

Bowring, S.A., Williams, I.S., and Compston, W., 1989. 3.96 Ga gneisses from the Slave Province, Northwest Territories. Geology, v. 17, p. 971-975.

Campbell, F.H.A., 1979. Stratigraphy and sedimentation in the Helikian Elu Basin and Hiukitak Platform, Bathurst Inlet-Melville Sound, Northwest Territories. Geological Survey of Canada, Paper 79-8 18 pp.

Campbell, F.H.A., and Cecile, M.P., 1981. Evolution of the Early Proterozoic Kilohigok Basin, Bathurst Inlet-Victoria Island, Northwest Territories, in, F.H.A. Campbell

(ed.), Proterozoic Basins of Canada. Geological Survey of Canada, Paper 81-10, p. 103-131.

Cavell, P.A., and Baadsgaard, H., 1986. Geochronology of the Big Spruce alkaline intrusion. Canadian Journal of Earth Sciences, v. 23, p. 1-10.

Culshaw, N.G., 1984. Rutledge Lake, Northwest Territories; a section across a shear belt within the Churchill Province, Current Research, Part A. Geological Survey of Canada, Paper 84 1-A, p. 331-338.

Dalrymple, R.W., Narbonne, G.M., and Smith, L., 1985. Eolian action and the distribution of Cambrian shales in North America. Geology, v. 13, p. 607-610.

DeCelles, P.G., and Hertel, F., 1989. Petrology of fluvial sands from the Amazonian foreland basin, Peru and Bolivia. Geological Society of America Bulletin, v. 101, p. 1552-1562.

Dickinson, W.R., 1985. Interpreting provenance relations from detrital modes of sandstones, in, G.G. Zuffa (ed.), Provenance of Arenites. D. Reidel Publishing Co. (Boston, MA), p. 333-361.

Dickinson, W.R., Beard, L.S., Brakenridge, G.R., Erjavec, J.L., Ferguson, R.C., Inman, K.F., Knepp, R.A., Lindberg, F.A., and Ryberg, P.T., 1983. Provenance of North American Phanerozoic sandstones in relation to tectonic setting. v. 94, p. 222-235.

Dickinson, W.R., and Suczek, C.A., 1979. Plate tectonics and sandstone compositions. American Association of Petroleum Geologists Bulletin, v. 63, p. 2164-2182.

Easton, R.M., 1985. The nature and significance of pre-Yellowknife Supergroup rocks in the Point Lake area, Slave Structural Province, Canada, in, L.D. Ayers, P.C. Thurston, K.D. Card, and W. Weber (eds.), Evolution of Archean Supracrustal Sequences. Geological Association of Canada, Special Paper 28, p. 153-168.

Franzenienelli, E., and Potter, P.E., 1983. Petrology, chemistry, and texture of modern river sands, Amazon River system. Journal of Geology, v. 91, p. 23-39.

Fraser, J.A., 1964. Geological notes on the northeastern District of Mackenzie, N.W.T. Geological Survey of Canada, Paper 64-40 pp.

Fraser, J.A., 1978. Metamorphism in the Churchill Province, District of Mackenzie, Current Research, Part A. Geological Survey of Canada, Paper 78-1A, p. 195-202.

Frith, R.A., and Loveridge, W.D., 1982. Ages of Yellowknife Supergroup volcanic rocks, granitoid intrusive rocks and regional metamorphism in the northeastern Slave Province, Current Research, Part A. Geological Survey of Canada, Paper 82-1A, p. 225-237.

Frith, R.A., Loveridge, W.D., and van Breemen, O., 1986. U-Pb ages on zircon from basement granitoids of the western Slave Structural Province, northwest Canadian Shield, Current Research, Part A. Geological Survey of Canada, Paper 86-1A, p. 113-119.

Geological Survey of Canada, 1987. Magnetic anomaly map of Thelon River, Northwest Territories (Map NQ 12-13-14 AM; 1:1000000 scale). Geological Survey of Canada, Magnetic anomaly map (residual total field).

Grantz, A., and May, S.D., 1982. Rifting history and structural development of the continental margin north of Alaska, in, J.S. Watkins, and C.L. Drake (eds.), Studies in Continental Margin Geology. Am. Assoc. Petrol. Geol., Memoir 34 (Tulsa, OK), p. 77-100.

Grotzinger, J.P., 1985. Evolution of Early Proterozoic passive-margin carbonate platform,

Rocknest Formation, Wopmay Orogen, N.W.T., Canada. Unpublished Ph.D. Thesis, Virginia Polytechnic Institute and State University (Blacksburg, VA).

Grotzinger, J.P., Adams, R.D., McCormick, D.S., and Myrow, P., 1989. Sequence stratigraphy, correlations between Wopmay Orogen and Kilohigok Basin, and further investigations of the Bear Creek Group (Goulburn Supergroup), District of Mackenzie, Current Research, Part C. Geological Survey of Canada, Paper 89-1C, p. 107-120.

Grotzinger, J.P., Gamba, C., Pelechaty, S.M., and McCormick, D.S., 1988. Stratigraphy of a 1.9 Ga foreland basin shelf-to-slope transition: Bear Creek Group, Tinney Hills area of Kilohigok Basin, District of Mackenzie, Current Research, Part C. Geological Survey of Canada, Paper 88 1-C, p. 313-320.

Grotzinger, J.P., and McCormick, D.S., 1988. Flexure of the Early Proterozoic lithosphere and the evolution of the Kilohigok Basin (1.9 Ga), northwest Canadian shield, in, K. Kleinspehn, and C. Paola (eds.), New Perspectives in Basin Analysis. Springer-Verlag (New York), p. 405-430.

Hanmer, S., and Lucas, S.B., 1985. Anatomy of a ductile transcurrent shear: The Great Slave Lake Shear Zone, District of Mackenzie, N.W.T. (preliminary report), Current Research. Geological Survey of Canada Paper 85-1B, p. 7-22.

Henderson, J.B., and Loveridge, J.B., 1990. Inherited Archean zircon in the Proterozoic Thelon Tectonic Zone: U-Pb geochronology of the Campbell granite, south of McDonald fault, District of Mackenzie, Northwest Territories, Radiogenic Age and Isotope Studies: Report 3. Geological Survey of Canada, Paper 89-2 (Ottawa, Ontario), p. 63-70.

Henderson, J.B., McGrath, P.H., James, D.T., and Macfie, R.I., 1987. An integrated geological, gravity and magnetic study of the Artillery Lake area and the Thelon Tectonic Zone, District of Mackenzie, Current Research, Part A. Geological Survey of Canada, Paper 87-1A, p. 803-814.

Henderson, J.B., and van Breemen, O., 1992. U-Pb zircon ages from an Archean orthogneiss and a Proterozoic metasedimentary gneiss of the Thelon Tectonic Zone, District of Mackenzie, N.W.T., Radiogenic Age and Isotope Studies: Report 5. Geological Survey of Canada, Paper 91-2 (Ottawa, Ontario), p. 25-33.

Heywood, W.W., and Schau, M., 1978. A subdivision of the northern Churchill Structural Province, Current Research, Part A. Geological Survey of Canada, Paper 78-1A, p. 139-143.

Hoffman, P.F., 1969. Proterozoic paleocurrents and depositional history of the East Arm fold belt, Great Slave Lake, Northwest Territories. Canadian Journal of Earth Sciences, v. 6, p. 441-462.

Hoffman, P.F., 1973. Evolution of an early Proterozoic continental margin: the Coronation geosyncline and associated aulacogens of the northwestern Canadian shield. Philosophical Transactions of the Royal Society of London, Series A, v. 273, p. 547-581.

Hoffman, P.F., 1987. Continental transform tectonics: Great Slave Lake shear zone (ca. 1.9 Ga), northwest Canada. Geology, v. 15, p. 785-788.

Hoffman, P.F., 1988. United plates of America, the birth of a craton: Early Proterozoic assembly and growth of Laurentia. Ann. Rev. Earth Planet. Sci., v. 16, p. 543-603.

Hoffman, P.F., 1989. Precambrian geology and tectonic history of North America, in, A.W.

Bally, and A.R. Palmer (eds.), The geology of North America - An overview. Geological Society of America (Boulder, CO), p. 447-512.

Hoffman, P.F., and Grotzinger, J.P., in review. Tradewind-controlled erosion and orogenic style. Geology.

Hoffman, P.F., Tirrul, R., Grotzinger, J.P., Lucas, S.B., and Eriksson, K.A., 1984. The Externides of Wopmay Orogen, Takijuk Lake and Kikerk Lake map areas, District of Mackenzie, Current Research, Part A. Geological Survey of Canada, Paper 84-1A, p. 383-395.

Ingersoll, R.V., Bullard, T.F., Ford, R.L., Grimm, J.P., Pickle, J.D., and Sares, S.W., 1984. The effect of grain size on detrital modes: a test of the Gazzi-Dickinson point-counting method. Journal of Sedimentary Petrology, v. 54, p. 103-116.

Isachsen, C.E., Bowring, S.A., and Padgham, W.A., 1991. U-Pb zircon geochronology of the Yellowknife volcanic belt, NWT, Canada: new constraints on the timing and duration of greenstone belt magmatism. J. Geol., v. 99, p. 55-67.

James, D.T., van Breeman, O., and Loveridge, W.D., 1988. Early Proterozoic U-Pb zircon ages for granitoid rocks from the Moraine Lake transect, District of Mackenzie, Radiogenic Age and Isotopic Studies: Report 2. Geological Survey of Canada, Paper 88-2 (Ottawa, Ontario), p. 67-72.

James, W.C., Mack, G.H., and Suttner, L.J., 1981. Relative alteration of microcline and sodic plagioclase in semi-arid and humid climates. Journal of Sedimentary Petrology, v. 51, p. 151-164.

Johnsson, M.J., Stallard, R.F., and Lundberg, N., 1991. Controls on the composition of fluvial sands from a tropical weathering environment: sands of the Orinoco River drainage basin, Venezuela and Columbia. Geological Society of America Bulletin, v. 103, p. 1622-1647.

Johnsson, M.J., Stallard, R.F., and Meade, R.H., 1988. First-cycle quartz arenites in the Orinoco River basin, Venezuela and Columbia. Journal of Geology, v. 96, p. 263-277.

Krogh, T.E., 1982. Improved accuracy of U-Pb zircon ages by creation of more concordant systems using an air abrasion technique. Geochim. Cosmochim. Acta, v. 45, p. 637-649.

Krogh, T.E., and Gibbins, W., 1978. U-Pb isotopic ages of basement and supracrustal rocks in the Point Lake area of the Slave Structual Province, Canada. Geol. Assoc. Canada, Prog. with Abs., v. 7, p. 61.

Lecheminant, A.N., Roddick, J.C., and Henderson, J.R., 1987. Geochronology of Archean and Early Proterozoic magmatism in the Baker Lake-Wager Bay region, N.W.T. Geol. Assoc. Canada, Prog. with Abs., v. 12, p. 66.

Ludwig, K.R., 1980. Calculations of uncertainties of U-Pb data. Earth and Planetary Science Letters, v. 46, p. 212-220.

Mack, G.H., 1984. Exceptions to the relationship between plate tectonics and sandstone composition. Journal of Sedimentary Petrology, v. 54, p. 212-220.

Mack, G.H., and Suttner, L.J., 1977. Paleoclimate interpretation from a petrographic comparison of Holocene sands and the Fountain Formation (Pennsylvanian) in the Colorado Front Range. Journal of Sedimentary Petrology, v. 47, p. 89-100.

Matter, A., and Ramseyer, K., 1985. Cathodoluminescence microscopy as a tool for provenance studies of sandstones, in, G.G. Zuffa (ed.), The Provenance of Arenites.

D. Reidel Publishing Co. (Dordrecht, Holland), p. 191-211.
McCormick, D.S., and Grotzinger, J.P., 1988. Aspects of the Burnside Formation, Bear Creek Group, Kilohigok Basin, N.W.T., Current Research, Part A. Geological Survey of Canada, Paper 88 1-C, p. 321-339.
McCormick, D.S., and Grotzinger, J.P., in review a. Distinction of marine from alluvial facies in an Early Proterozoic foreland basin: Burnside Formation (1.9 Ga), N.W.T., Canada. Sedimentology.
McCormick, D.S., and Grotzinger, J.P., in review b. Evolution and significance of an overfilled alluvial foreland basin: Burnside Formation (1.9 Ga), Kilohigok Basin, N.W.T., Canada. Basin Research.
Morton, A.C., 1985. Heavy minerals in provenance studies, in, G.G. Zuffa (ed.), The Provenance of Arenites. D. Reidel Publishing Co. (Dordrecht, Holland), p. 249-277.
Padgham, W.A., 1985. Observations and speculations on supracrustal successions in the Slave Structural Province, in, L.D. Ayers, P.C. Thurston, K.D. Card, and W. Weber (eds.), Evolution of Archean Supracrustal Sequences. Geological Association of Canada, Special Paper 28, p. 133-152.
Patchett, P.J., and Arndt, N.T., 1986. Nd isotopes and tectonics of 1.9-1.7 crustal genesis. Earth and Planetary Science Letters, v. 78, p. 329-338.
Patterson, J.G., 1986. The Amer Belt: remnant of an Aphebian foreland fold and thrust belt. Canadian Journal of Earth Sciences, v. 23, p. 2012-2023.
Pittman, E.D., 1963. Use of zoned plagioclase feldspar as an indicator of provenance. Journal of Sedimentary Petrology, v. 33, p. 380-386.
Pittman, E.D., 1970. Plagioclase feldspar as an indicator of provenance of sedimentary rocks. Journal of Sedimentary Petrology, v. 40, p. 591-598.
Potter, P.E., 1978. Petrology and chemistry of big river sands. Journal of Geology, v. 86, p. 423-449.
Price, R.A., 1981. The Cordilleran foreland thrust and fold belt in southern Canadian Rocky Mountains, in, K.R. McClay, and N.J. Price (eds.), Thrust and Nappe Tectonics. Geological Society of London, Special Paper 9 (London), p. 427-448.
Ross, G.M., Parrish, R.R., Villeneuve, M.E., and Bowring, S.A., 1991. Geophysics and geochronology of the crystalline basement of the Alberta Basin, western Canada. Canadian Journal of Earth Sciences, v. 28, p. 512-522.
Suttner, L.J., and Basu, A., 1986a. Alluvial sandstone composition and paleoclimate, I. Framework mineralogy. Journal of Sedimentary Petrology, v. 56, p. 329-345.
Suttner, L.J., and Basu, A., 1986b. Alluvial sandstone composition and paleoclimate, II. Authigenic mineralogy. Journal of Sedimentary Petrology, v. 56, p. 346-358.
Suttner, L.J., Basu, A., Decker, J., Helmold, K.P., Ingersoll, R.V., Bullard, T.F., Ford, R.L., and Pickle, J.D., 1985. The effect of grain size on detrital modes: a test of the Gazzi-Dickinson point-counting method-dissussion and reply. Journal of Sedimentary Petrology, v. 55, p. 616-627.
Suttner, L.J., Basu, A., and Mack, G.H., 1981. Climate and the origin of quartz arenites. Journal of Sedimentary Petrology, v. 51, p. 346-358.
Thompson, P.H., Culshaw, N., Buchanan, J.R., and Manoljlovic, P., 1986. Geology of the Slave Province and Thelon Tectonic Zone in the Tinney Hills-Overby Lake (west half) map area, District of Mackenzie, Current Research, Part A. Geological Survey of Canada, Paper 86-1A, p. 275-289.

Thompson, P.H., Culshaw, N., Thompson, D., and Buchanan, J.R., 1985. Geology across the western boundary of the Thelon Tectonic Zone in the Tinney Hills-Overby Lake (west half) map area, District of Mackenzie, Current Research, Part A. Geological Survey of Canada, Paper 85-1A, p. 555-572.

Thompson, P.H., and Frey, M., 1984. Illite "crystallinity" in the Western River Formation and its significance regarding the regional metamorphism of the early Proterozoic Goulburn Group, District of Mackenzie, Current Research, Part A. Geological Survey of Canada, Paper 84-1A, p. 409-414.

Tirrul, R., 1985. Nappes in the Kilohigok Basin and their relationship to the Thelon Tectonic Zone, District of Mackenzie, Current Research, Part A. Geological Survey of Canada, Paper 85-1A, p. 407-420.

Tirrul, R., and Grotzinger, J.P., 1990. Early Proterozoic collisional orogeny along the northern Thelon Tectonic Zone, Northwest Territories, Canada: Evidence from the foreland. Tectonics, v. 9, p. 1015-1036.

Tortosa, A., Palomares, M., and Arribas, J., 1991. Quartz grain typed in Holocene deposits from the Spanish Central System: some problems in provenance analysis, in, A.C. Morton, S.P. Todd, and P.D.W. Haughton (eds.), Developments in Sedimentary Provenance Studies. Geological Society Special Publication No. 57 (London), p. 47-54.

van Breeman, O., and Henderson, J.B., 1991. U-Pb zircon and monazite ages from the eastern Slave Province, Artillery Lake area, N.W.T., Radiogenic Age and Isotopic Studies: Report 2. Geological Survey of Canada Paper 88-2 (Ottawa, Ontario), p. 73-83.

van Breemen, O., Bostock, H.H., and Loveridge, W.D., 1992. Geochronology of granites along the margin of the northern Taltson Magmatic Zone and western Rae Province, Northwest Territories, Radiogenic Age and Isotopic Studies: Report 5. Geological Survey of Canada Paper 91-2 (Ottawa, Ontario), p. 17-24.

van Breemen, O., Henderson, J.B., Loveridge, W.D., and Thompson, P.H., 1986. Archean-Aphebian geochronology along the Thelon Tectonic Zone, Healey Lake area, N.W.T. Geol. Assoc. Canada, Prog. with Abs., v. 11, p. 139.

van Breemen, O., Henderson, J.B., Loveridge, W.D., and Thompson, P.H., 1987a. U-Pb zircon and monazite geochronology and zircon morphology of granulites and granite from the Thelon Tectonic Zone, Healey Lake and Artillery Lake map areas, N.W.T., Current Research, Part A. Geological Survey of Canada, Paper 87-1A, p. 783-801.

van Breemen, O., Henderson, J.B., Sullivan, R.W., and Thompson, P.H., 1987b. U-Pb zircon and monazite ages from the eastern Slave Province, Healey Lake area, N.W.T., Radiogenic Age and Isotopic Studies: Report 1. Geological Survey of Canada Paper 87-2 (Ottawa, Ontario), p. 101-110.

van Breemen, O., Thompson, P.H., Bostock, H.H., and Loveridge, W.D., 1987c. Timing of plutonism in the northern Thelon Tectonic Zone and the Taltson Magmatic Zone. Geol. Assoc. Canada, Prog. with Abs., v. 12,, p. 98.

van Breemen, O., Thompson, P.H., Hunt, P.A., and N., C., 1987d. U-Pb zircon and monazite geochronology from the northern Thelon Tectonic Zone, District of Mackenzie, Radiogenic Age and Isotopic Studies: Report 1. Geological Survey of Canada Paper 87-2 (Ottawa, Ontario), p. 81-93.

van der Plas, L., and Tobi, A.C., 1965. A chart for judging the reliability of point counting

results. American Journal of Science, v. 263, p. 87-90.
Vebel, M.A., and Saad, M.K., 1991. Paleoweathering or diagenesis as the principle modifier of sandstone framework composition? A case study from some Triassic rift-valley redbeds of eastern North America, in, A.C. Morton, S.P. Todd, and P.D.W. Haughton (eds.), Developments in Sedimentary Provenance Studies. Geological Society Special Publication No. 57 (London), p. 91-99.
Walker, T.R., 1978. Discussion: Paleoclimate interpretation from a petrographic comparison of Holocene sands and the Fountain Formation (Pennsylvanian) in the Colorado Front Range. Journal of Sedimentary Petrology, v. 48, p. 1011-1013.
Young, S.W., 1976. Petrographic textures of detrital polycrystalline quartz as an aid to interpreting crystalline source rocks. Journal of Sedimentary Petrology, v. 46, p. 596-603.

Table Captions

Table 1. Point counting parameters modified after Dickinson and Suczek (1979) and DeCelles and Hertel (1989) for framework and lithic fragment types and Basu et al. (1975) for quartz grain types.

Table 2. Summary of Goulburn Supergroup sandstone point count data and recalculated count parameters. See Table 1 for description of symbols. Note that the first tabulation of Q, F, and L (columns 3-5) are expressed as a percentage of total framework grains, whereas the second tabulation (columns 11-13) is a ternary recalculation to percentage of total Q+F+L .

Table 3. Summary of Goulburn Supergroup zircon U-Pb data. Samples from the Kimerot, lower Bear Creek Group, and the Burnside Formation in the proximal foredeep (south Tinney Hills) were collected at or near sections 1 and 2 in Figure 2. Samples of the Burnside Formation from the distal foredeep (Wolverine Canyon and Contwoyto Lake) were collected at sections 12 and 13 respectively. Samples from Wopmay Orogen were collected near Takijuk Lake in the easternmost part of Wopmay Orogen closest to Rockinghorse Lake (Figures 1, 2). Sample locations for Queen Maud block basement are shown on Figure 19.

Table 1
point counting parameters

symbol	definition
Qmnu	non-undulatory monocrystalline quartz
Qmu	undulatory monocrystalline quartz
Qpq2-3	polycrystalline quartz with 2-3 subgrains
Qpq>3	polycrystalline quartz with >3 subgrains
P	plagioclase feldspar
K	potassium feldspar
Lv	microlitic volcanic-hypabyssal lithic fragments
Lm	metasedimentary lithic fragments
Ls	mudstone-siltstone, sandstone lithic fragments
Cht	chert (cryptocrystalline quartz)
M	phyllosilicates
D	dense minerals
U	unidentifiable grains
	calculated parameters
Qm	total monocrystalline quartz grains (= Qmnu + Qmu)
Qpq	total polycrystalline quartz grains (= Qpq2-3 + Qpq>3)
Q	total quartzose grains (= Qmnu + Qmu + Qpq2-3 + Qpq>3 + Cht)
F	total feldspar grains (= P + K)
L	total unstable lithic grains (= Lv + Lm + Ls)
Lm	metamorphic lithic grains (= Lm)
Lv	volcanic-hypabyssal grains
Ls	sedimentary lithic grains
Qp	total polycrystalline quartzose grains (= Qpq2-3 + Qpq>3 + Cht)
Lvm	volcanic-hypabyssal and metavolcanic grains (= Lv)
Lsm	sedimentary and metasedimentary grains (= Ls + Lm)
Lt	total lithic grains (= Qp + Lm + Lv + Ls)
	normalized modes
QFL%Q	100 * Q / (Q + F + L)
QFL%F	100 * F / (Q + F + L)
QFL%L	100 * L / (Q + F + L)
LmLvLs%Lm	100 * Lm / (Lm + Lv + Ls)
LmLvLs%Lv	100 * Lv / (Lm + Lv + Ls)
LmLvLs%Ls	100 * Ls / (Lm + Lv + Ls)
QpLvmLsm%Qp	100 * Qp / (Qp + Lvm + Lsm)
QpLvmLsm%Lvm	100 * Lvm / (Qp + Lvm + Lsm)
QpLvmLsm%Lsm	100 * Lsm / (Qp + Lvm + Lsm)
QmFLt%Qm	100 * Qm / (Qm + F + Lt)
QmFLt%F	100 * F / (Qm + F + Lt)
QmFLt%Lt	100 * Lt / (Qm + F + Lt)
QmPK%Qm	100 * Qm / (Qm + P + K)
QmPK%P	100 * P / (Qm + P + K)
QmPK%K	100 * K / (Qm + P + K)
QmQp%Qmnu	100 * Qmnu / (Qmnu + Qmu + Qpq2-3 + Qpq>3)
QmQp%Qmu	100 * Qmu / (Qmnu + Qmu + Qpq2-3 + Qpq>3)
QmQp%Qpq2-3	100 * Qpq2-3 / (Qmnu + Qmu + Qpq2-3 + Qpq>3)
QmQp%Qpq>3	100 * Qpq>3/ (Qmnu + Qmu + Qpq2-3 + Qpq>3)

Table 2.

		% total framwork grains											
N	Sample	Qm	Qpg	Q	F	L	Lm	Lv	Ls	Qp	Lvm	Lsm	Lt
1	BC-H	74.1	17.1	91.6	8.4	0.0	0.0	0.0	0.0	17.5	0.0	0.0	17.5
2	BC-R	80.3	10.2	90.5	6.8	0.7	0.7	0.0	0.0	10.2	0.0	0.7	10.9
3	STH-111	70.4	11.0	82.9	15.0	0.2	0.0	0.0	0.2	12.4	0.0	0.2	12.7
4	STH-116	71.3	9.3	81.9	13.1	0.5	0.5	0.0	0.0	10.6	0.0	0.5	11.1
5	STH-120	73.3	23.3	97.8	1.7	0.0	0.0	0.0	0.0	24.5	0.0	0.0	24.5
6	STH-126p	61.9	17.3	96.8	1.7	1.1	1.1	0.0	0.0	34.8	0.0	1.1	35.9
7	STH-127	71.6	24.1	98.6	0.2	0.2	0.2	0.0	0.0	27.0	0.0	0.2	27.2
8	STH-128	74.3	20.8	95.2	0.4	1.5	1.5	0.0	0.0	20.8	0.0	1.5	22.4
9	STH-130	60.3	30.3	91.1	0.0	8.4	8.4	0.0	0.0	30.8	0.0	8.4	39.2
10	STH-131	49.4	37.8	87.7	0.0	11.8	11.3	0.0	0.5	38.3	0.0	11.8	50.1
11	STH-132	69.6	23.1	95.1	0.0	0.0	0.0	0.0	0.0	25.5	0.0	0.0	25.5
12	STH-139	63.0	24.2	89.4	6.4	4.2	2.6	0.2	1.4	26.4	0.2	4.0	30.6
13	STH-142	59.1	20.4	81.1	9.4	8.7	1.5	6.2	1.1	21.9	6.2	2.6	30.6
14	STH-014	56.8	15.6	74.4	23.3	2.2	0.7	0.0	1.5	17.6	0.0	2.2	19.8
15	STH-021	37.2	4.6	42.0	51.3	2.2	0.0	1.7	0.4	4.8	1.7	0.4	7.0
16	WC-01A	64.4	13.8	79.1	0.2	1.8	1.8	0.0	0.0	14.6	0.0	1.8	16.4
17	WC-14	64.8	22.5	88.7	8.8	1.6	1.4	0.0	0.2	23.8	0.0	1.6	25.5
18	WC-27	76.4	17.7	94.3	4.2	0.7	0.7	0.0	0.0	17.9	0.0	0.7	18.6
19	WC-33	61.1	3.2	64.5	35.0	0.0	0.0	0.0	0.0	3.4	0.0	0.0	3.4
20	WC-58	69.4	10.4	79.9	18.9	0.0	0.0	0.0	0.0	10.4	0.0	0.0	10.4
21	WC-66	62.2	5.4	68.9	29.1	0.9	0.9	0.0	0.0	6.7	0.0	0.9	7.6
22	WC-68	61.7	8.8	70.9	28.2	0.0	0.0	0.0	0.0	9.2	0.0	0.0	9.2
23	WC-70	58.5	5.4	66.2	29.9	0.0	0.0	0.0	0.0	7.7	0.0	0.0	7.7
24	BSA-1	40.1	5.4	45.9	47.4	3.9	3.9	0.0	0.0	5.8	0.0	3.9	9.7
25	BSA-2	38.0	22.8	60.8	33.8	4.8	2.3	0.8	1.7	22.8	0.8	4.1	27.6

Table 2.

	QFL			QmFLt			QmPK		
Sample	Q	F	L	Qm	F	Lt	Qm	P	K
BC-H	91.6	8.4	0.0	74.1	8.4	17.5	89.8	4.8	5.4
BC-R	92.4	6.9	0.7	82.0	6.9	11.1	92.2	2.9	4.9
STH-111	84.4	15.3	0.2	71.8	15.3	12.9	82.4	4.9	12.6
STH-116	85.8	13.7	0.5	74.6	13.7	11.6	84.5	0.0	15.5
STH-120	98.3	1.7	0.0	73.7	1.7	24.6	97.8	0.3	1.9
STH-126p	97.2	1.7	1.1	62.2	1.7	36.1	97.3	0.0	2.7
STH-127	99.5	0.2	0.2	72.3	0.2	27.5	99.7	0.3	0.0
STH-128	98.0	0.5	1.6	76.5	0.5	23.0	99.4	0.0	0.6
STH-130	91.5	0.0	8.5	60.6	0.0	39.4	100.0	0.0	0.0
STH-131	88.1	0.0	11.9	49.6	0.0	50.4	100.0	0.0	0.0
STH-132	100.0	0.0	0.0	73.2	0.0	26.8	100.0	0.0	0.0
STH-139	89.4	6.4	4.2	63.0	6.4	30.6	90.8	0.0	9.2
STH-142	81.8	9.4	8.8	59.7	9.4	30.9	86.3	1.6	12.1
STH-014	74.4	23.3	2.2	56.8	23.3	19.8	70.9	3.6	25.5
STH-021	44.0	53.8	2.3	39.0	53.8	7.3	42.0	27.8	30.2
WC-01A	97.6	0.2	2.2	79.5	0.2	20.2	99.7	0.0	0.3
WC-14	89.5	8.9	1.6	65.4	8.9	25.7	88.1	0.6	11.3
WC-27	95.0	4.3	0.7	77.0	4.3	18.8	94.7	0.0	5.3
WC-33	64.9	35.1	0.0	61.4	35.1	3.5	63.6	7.4	29.0
WC-58	80.8	19.2	0.0	70.3	19.2	10.6	78.6	0.5	20.9
WC-66	69.7	29.4	0.9	62.9	29.4	7.7	68.1	3.4	28.4
WC-68	71.6	28.4	0.0	62.3	28.4	9.3	68.7	2.0	29.3
WC-70	68.9	31.1	0.0	60.8	31.1	8.0	66.2	2.1	31.8
BSA-1	47.2	48.8	4.0	41.3	48.8	9.9	45.8	8.3	45.8
BSA-2	61.2	34.0	4.9	38.3	34.0	27.8	53.0	4.3	42.7

Table 2.

	LmLvLs			QpLvmLsm			QmQpq			
Sample	Lm	Lv	Ls	Qp	Lvm	Lsm	Qmnu	Qmu	Qpq2-3	Qpq>3
BC-H	0.0	0.0	0.0	100.0	0.0	0.0	46.4	34.9	4.6	14.1
BC-R	100.0	0.0	0.0	93.8	0.0	6.3	75.0	13.8	7.0	4.3
STH-111	0.0	0.0	100.0	98.1	0.0	1.9	62.5	23.9	9.5	4.0
STH-116	100.0	0.0	0.0	95.9	0.0	4.1	74.4	14.0	5.9	5.6
STH-120	0.0	0.0	0.0	100.0	0.0	0.0	62.4	13.4	13.2	10.9
STH-126p	100.0	0.0	0.0	97.0	0.0	3.0	64.8	13.4	8.5	13.4
STH-127	100.0	0.0	0.0	99.1	0.0	0.9	61.3	13.5	7.7	17.5
STH-128	100.0	0.0	0.0	93.1	0.0	6.9	72.4	5.8	3.9	18.0
STH-130	100.0	0.0	0.0	78.5	0.0	21.5	58.4	8.2	11.8	21.6
STH-131	95.7	0.0	4.3	76.4	0.0	23.6	48.3	8.4	10.7	32.7
STH-132	0.0	0.0	0.0	100.0	0.0	0.0	66.8	8.3	9.1	15.9
STH-139	61.9	4.8	33.3	86.3	0.7	13.1	56.7	15.6	9.2	18.6
STH-142	17.1	70.7	12.2	71.5	20.1	8.3	51.6	22.7	9.1	16.6
STH-014	30.0	0.0	70.0	88.9	0.0	11.1	67.2	11.2	7.0	14.6
STH-021	0.0	80.0	20.0	68.8	25.0	6.3	72.4	16.7	5.2	5.7
WC-01A	100.0	0.0	0.0	89.2	0.0	10.8	58.3	24.0	7.1	10.6
WC-14	85.7	0.0	14.3	93.6	0.0	6.4	62.1	12.2	11.7	14.1
WC-27	100.0	0.0	0.0	96.2	0.0	3.8	63.4	17.8	6.5	12.3
WC-33	0.0	0.0	0.0	100.0	0.0	0.0	82.0	13.0	0.8	4.2
WC-58	0.0	0.0	0.0	100.0	0.0	0.0	65.0	21.9	6.4	6.7
WC-66	100.0	0.0	0.0	88.2	0.0	11.8	80.1	11.9	3.0	5.0
WC-68	0.0	0.0	0.0	100.0	0.0	0.0	74.8	12.8	5.1	7.3
WC-70	0.0	0.0	0.0	100.0	0.0	0.0	72.7	18.8	3.2	5.3
BSA-1	100.0	0.0	0.0	60.0	0.0	40.0	78.3	9.9	5.2	6.6
BSA-2	48.0	16.0	36.0	82.5	2.8	14.7	55.2	7.3	12.1	25.4

Table 3

Sample	Fraction	Weight (mg)	Concentrations U (ppm)	Pb (ppm)	Ratios corrected for blank and common Pb 206Pb/ 204Pb	206Pb/ 238U	207Pb/ 235U	207*Pb/ 206*Pb	206/207 Age (Ma)	spike	analysis location
	detrital zircons from Goulburn Supergroup, Kilohigok Basin										
	Kenyon Fm. (Kimerot Group) alluvial sandstone										
1	WR1a (Starvin Lake)								3381.0	208Pb/235U	WU
	lower Bear Creek Group										
2	WR2e turbidites nd2 lg rdd	0.107				0.32329	7.78864		2603.5	208Pb/235U	WU
	Hackett Fm. (lower Bear Creek Group) shelf sandstone										
3	BCH d2 med rd pink	0.080	147.7	62.7	3026.7	0.36287	8.80465	0.17598	2615.3	208Pb/235U	WU
4	BCH d2 large rd pink	0.063	105.9	33.6	988.9	0.26812	6.49288	0.17564	2612.1	208Pb/235U	WU
5	BCH d1 med rd pink	0.412	136.2	55.0	1517.9	0.33329	8.06185	0.17544	2610.2	208Pb/235U	WU
	Rifle Fm. (lower Bear Creek Group) shelf sandstone										
6	BCR nm5 lg rd	0.028				0.35099	9.00134		2707.0	208Pb/235U	WU
	Burnside Formation in proximal foredeep (section 2)										
7	STH-1 nm2 dark pink rdd	0.154				0.38275	9.42888		2640.6	208Pb/235U	WU
8	STH-1 nm2 lg rd	0.107				0.39789	9.64353		2613.5	205Pb/235U	MIT
9	STH-4 nm+2 long clear	0.009	647.0	239.6	1742.0	0.34651	5.78462	0.12108	1972.2	205Pb/235U	MIT
10	STH-5 d2 large rd	0.059	76.0	34.1	751.0	0.38019	7.78517	0.14851	2328.9	208Pb/235U	WU
11	STH-6 d2 large rd	0.031	694.0	250.3	6242.5	0.34134	5.75696	0.12232	1990.4	208Pb/235U	WU
12	STH-8 d1 clear euhedral	0.002	394.5	178.9	1090.9	0.39506	8.94397	0.16420	2499.4	205Pb/235U	MIT
13	STH-8 d1 lg pink long	0.011	302.6	140.6	4020.0	0.43162	9.28156	0.15596	2412.4	205Pb/235U	MIT
	felsic volcanic clasts in Gravelly Sst. Mbr. of Burnside Fm. (= STH-6)										
14	Ryolite g-1 mag2					0.37938	7.39122		ca. 2245	208Pb/235U	WU
15	Ryolite g-1 nm-2	1.600	239.1	105.7	10416.7	0.37849	7.29117	0.13971	2223.8	208Pb/235U	WU
	Burnside Formation in distal foredeep (section 12)										
16	WC-1 d1 lg rd clear	0.080	126.6	52.4	774.3	0.33379	7.29116	0.15843	2438.9	208Pb/235U	WU
17	WC-1 d2 single grain	0.047	48.7	27.9	486.9	0.42494	10.39590	0.17743	2629.0	208Pb/235U	WU
18	WC-2 d2 med clear elong	0.046	209.6	62.2	1203.4	0.25422	4.75642	0.13570	2173.0	208Pb/235U	WU
19	WC-3 d1 short clear	0.042	69.1	30.4	3828.0	0.37743	6.99074	0.13433	2155.4	205Pb/235U	MIT
20	WC-4 d1 elongate rdd	0.082	44.8	16.8	10839.5	0.36347	6.59913	0.13168	2176.3	205Pb/235U	MIT
	Burnside Fm. in distal foredeep (section 13)										
21	BC-CL nm+2 large euhed	0.013	324.2	143.0	3383.2	0.42437	9.12967	0.15603	2413.1	205Pb/235U	MIT

Table 3

Sample	Fraction	Weight (mg)	Concentrations U (ppm)	Pb (ppm)	Ratios corrected for blank and common Pb 206Pb/ 204Pb	206Pb/ 238U	207Pb/ 235U	207*Pb/ 206*Pb	206/207 Age (Ma)	spike	analysis location
	Brown Sound Fm. (Bathurst Group)										
22	BSA-2 d1 lg rd	0.079	122.6	52.8	1997.6	0.36755	7.85298	0.15496	2401.4	208Pb/235U	WU
23	BSA-2 d1 lg dark euhedral	0.107	320.4	128.9	2628.4	0.36378	7.57541	0.15103	2357.6	208Pb/235U	WU
24	BSA-2 equant faceted	0.012	103.0	59.8	734.4	0.47810	12.97180	0.19678	2799.7	208Pb/235U	WU
	detrital zircons from Coronation Supergroup, Wopmay Orogen										
	Tree River Fm. (Recluse Group)										
25	CS-Rtr nm4 short clear	0.007	482.7	181.1	12464.7	0.33772	6.06348	0.13021	2100.9	205Pb/235U	MIT
26	CS-Rtr d1 long clear	0.006	333.3	124.6	19758.0	0.33554	6.28995	0.13596	2176.3	205Pb/235U	MIT
	Asiak Fm. greywacke (Recluse Group)										
27	greywacke d-3	1.389	177.5	68.8	3215.4	0.34263	5.67478	0.12012	1958.0	208Pb/235U	WU
	zircons from Queen Maud basement rocks (Queen Maud block)										
28	QM1 d1	0.890	758.0	385.1	5586.6	0.46024	11.18290	0.17623	2617.6	208Pb/235U	WU
29	QM2 d1	0.533	475.8	272.6	41666.7	0.50052	14.12905	0.20473	2864.5	208Pb/235U	WU
30	QM3 d3	0.877	368.8	173.2	4761.9	0.44471	9.48606	0.15471	2398.4	208Pb/235U	WU
31	QM4 d2	0.513	438.3	97.7	4672.9	0.21117	4.57532	0.15714	2425.1	208Pb/235U	WU

Note on location of analyses:
WU = analysis done at Washington University in St. Louis
MIT = analysis done at Massachusetts Institute of Technology

Figure Captions

Figure 1. Geologic and geographic elements of the northwestern Canadian Shield. Triangular ticks indicate zones of overthrusting with ticks on the overthrust plate; arrows indicate zones of strike slip displacement. Inset indicates the location of the map within North America. Figure modified from Hoffman (1987).

Figure 2. Geologic map of Kilohigok Basin. Circled numbers mark the locations of measured sections in the Burnside Formation that are shown in subsequent cross sections. The basin has been restored by removing approximately 115 km of left slip on the Bathurst fault zone as recommended by Tirrul and Grotzinger (1990). This displacement post-dates deposition of the Goulburn Supergroup. The Gordon Bay Arch was a flexural arch that was active during deposition of the Bear Creek Group (see Figures 3a&b, 4). A second independent flexural arch lay near Rockinghorse Lake and is termed the Rockinghorse Arch in subsequent cross sections.

Figure 3. A: Stratigraphic framework of the Goulburn Supergroup with an interpretation of the sedimentologic and tectonic evolution (Tirrul, 1985; Grotzinger and McCormick, 1988; Tirrul and Grotzinger, 1990). Volcanic ash bed ages are from Bowring and Grotzinger (1992). The upper ash bed age is on the basis of the correlation to a stratigraphic horizon in Wopmay Orogen (see text for explanation). B: Schematic cross section and correlation between members of the Burnside Formation and the Mara and Quadyuk Formations. Thick lines indicate inferred erosional, unconformable contacts; thin lines indicate gradational or inferred conformable lithological contacts. Thicknesses are diagrammatic and are not to scale.

Figure 4. Cross section of the Goulburn Supergroup from Kilohigok Basin to Wopmay Orogen (Figure 1). The line of section within Kilohigok Basin lies along the line from the Section 1 to Section 14 in Figure 2. The datum is a the top of the passive margin carbonate platform in Wopmay Orogen and its correlative within the Burnside Formation in Kilohigok Basin. Locations of lines of section in subsequent figures are indicated in Figure 2. The measured sections are projected onto a west-northwest line corresponding to the mean paleocurrent direction for the upper alluvial sandstone facies (Figure 5). The ages of ash beds are from Bowring and Grotzinger (1992).

Figure 5. Paleocurrents trends within siliciclastic units of the Goulburn Supergroup. Arcs are

circular standard deviation of paleocurrent measurements. Note derivation of basal Kimerot alluvial sandstones from the interior of the Slave Province. There is a dominant southwestern mode in the lower Bear Creek Group turbidite, shelf, and early deltaic sandstones. A pronounced shift to northwestern mode marks the main phase of Burnside alluvial sedimentation. Data from Campbell and Cecile (1981) and Grotzinger and McCormick (1988).

Figure 6. Stratigraphic cross section of the Burnside Formation in the proximal part of the basin. See Figure 2 for section location. Sample numbers (in square boxes) refer to sample numbers in Table 3).

Figure 7. Stratigraphic cross section of the Burnside Formation in the distal part of the basin part of the basin. See Figure 2 for section location. Sample numbers (in square boxes) refer to sample numbers in Table 3).

Figure 8. The distribution of quartz types by size fraction derived from different basement lithologies in Holocene stream sands in Spain from the study by Tortosa et al. (1991). All sands are from first-order streams. Quartz types are those defined by Basu et al. (1975) and Young (1976). Note the strong primary lithology dependence of quartz type and the marked secondary decrease in polycrystalline quartz with decreasing grain size. The high proportions of polycrystalline quartz (Qpq>3) in schists means low-grade metamorphic quartz is readily distinguished from granitic and high-grade metamorphic sources. The large variation in undulose monocrystalline quartz in granites prevents unambiguous discrimination of granitic from high-grade metamorphic sources.

Figure 9. Ternary plots of Goulburn Supergroup point count data broken out by lithotectonic unit (Figure 3a). Plots and "tectonic province" fields are after Dickinson and Suczek (1979). The tectonic province fields are included for comparative purposes, not necessarily for pinpointing tectonic setting as explained in the text. A: Q-F-L plot. B: Qm-F-Lt plot. Data in Table 1 and Appendix B.

Figure 10. Ternary plots of Burnside Formation point count data from the proximal foredeep only broken out by members (Figure 3b) and sedimentary facies. Diagrams and data are exactly as in previous diagram. A: Q-F-L plot. B: Qm-F-Lt plot.

Figure 11. Vertical trends in quartz type in the Goulburn Supergroup in the proximal part of the Kilohigok Basin and the associated stratigraphic unit and facies of the sample. Quartz types are those defined by Basu et al. (1975) and Young (1976). Symbols defined in Table 1.

Compare with Figure 8 and the next figure.

Figure 12. Vertical trends in quartz type in the Goulburn Supergroup in the distal part of the Kilohigok Basin. Symbols as in previous figure. Compare with Figure 8 and the previous figure.

Figure 13. Burnside Formation conglomerate clast counts from the proximal (southeastern) part of Kilohigok Basin. The stratigraphic sections, labeled south Tinney Hills (a; section 2 in Figure 2) and north Tinney Hills (b; section 3), are located about 10 km apart; north Tinney Hills is farther down paleoslope.

Figure 14. Photomicrographs of Goulburn Supergroup sandstones in the proximal foredeep. Field of view of all photomicrographs is approximately 1.0118 x 1.54 mm. All photomicrographs are viewed with cross polars. A: Lower Bear Creek Group shelf sandstone (sample BC-H). Note fresh rounded microcline feldspar. B: Braid delta facies in the Transitional member of the Burnside Formation (sample STH-111). Note fresh rounded feldspar and poor sorting. C: High energy braid plain facies in the Buff Sandstone member of the Burnside Formation (sample STH-120). Note lack of feldspar. D: Matrix sandstone in high energy conglomeratic braid plain facies at the base of the Conglomerate member (sample STH-130). Note polycrystalline quartz (P), chert (C), and sericitic matrix (bright flecks between grains) E: Matrix sandstone in high energy conglomeratic braid plain facies at the top of the Conglomerate member (sample STH-132). Note common polycrystalline quartz with both 2-3 subgrains and >3 subgrains with serrate grain boundaries. F: High energy braid plain facies of the Gravelly Sandstone member at the level of the volcanic clast conglomerate horizon (sample STH-142). Note quartz with microcline inclusion, microcline grains, and polycrystalline quartz with low strain subgrain boundaries.

Figure 15. Photomicrographs of Burnside Formation conglomerate clasts. A: Clast of highly strained schistose quartz from the Conglomerate member of the Burnside Formation in the proximal foredeep. Clast contains mostly quartz of variable grain size and with irregular, serrate subgrain boundaries plus subordinate muscovite. B: Quartz-biotite schist with annealed strain free quartz from the Conglomerate member of the Burnside Formation in the proximal foredeep. C: Undeformed felsic volcanic clast from the Gravelly Sandstone member of the Burnside Formation in the proximal foredeep (from the stratigraphic horizon equivalent to sample STH-142). Clast consists of beta quartz (gray and black), feldspars that have been completely altered to phyllosilicates (large speckled grain on left center), and a groundmass of chalcedony and chert plus phyllosilicates.

Figure 16. More photomicrographs of Goulburn Supergroup sandstones. A: Braid delta facies of the Orange Sandstone member of the Burnside Formation (sample STH-014), the stratigraphic equivalent of the Mara Formation (compare with photo F). Note microcline, partly altered plagioclase, monocrystalline and polycrystalline quartz. B: Braid delta facies in lower Bathurst Group (sample BSA-1). Note abundant microcline and plagioclase of variable rounding. C: Marine shelf-prodelta sandstone of the basal Burnside Formation in the distal foredeep (sample WC-01A). Large grain on lower left is an intrabasinal silty mudstone clast. Note strain-free polycrystalline quartz. D: Lower braid plain facies near the base of the Burnside Formation in the distal foredeep (sample WC-14). Note microcline and plutonic lithic fragment; texturally immature. E: Lower braid plain facies of at the top of the Burnside Formation in the distal foredeep (sample WC-68). Plane polarized light. Darker, high relief, relatively euhedral patches are dolomite replacing intragranular pore fill and grain edges. Lighter high relief grains are feldspar. F: Iron rich braid delta facies of the basal Mara Formation in the distal foredeep (sample WC-70). Plane polarized light. The sample lies 2 meters above and erosional unconformity at the top of the Burnside Formation. Black iron oxide grain coatings are common. Common mica that defines cleavage in other parts of the sample.

Figure 17. U-Pb concordia diagram of detrital zircons from the Goulburn Supergroup in the proximal foredeep. The line that intersects concordia between 2.61-2.62 Ga is not a regression line, but rather a hand-fit line included to illustrate the suggestion that the detrital zircons from lower Bear Creek Group sediments in the proximal foredeep are derived from a source area that yields zircons with remarkably similar Pb-Pb ages (Table 3). As yet no Early Proterozoic ages have been found in detrital zircon samples from this interval. Samples above the Transitional member of the Burnside Formation all have detrital zircons with ages that contain Early Proterozoic zircons in two age ranges, 1.97-199 (Thelon Orogen), and 2.1-2.4 Ga (unreported from Thelon Orogen). Compare this with Early Proterozoic ages seen throughout Burnside Formation samples in the distal foreland (Figure 18). See Figure 19 for zircon ages from basement rocks in Queen Maud block. Inset labeled "2 sigma error" represents the size of error ellipses for each data point; this ellipse shows two standard deviation error in both U-Pb ratios (± 0.4%) and the uncertainty associated with the $^{207}Pb/^{206}Pb$ ratio (± 0.1%).

Figure 18. U-Pb concordia diagram of detrital zircon isotope data from the Goulburn Supergroup in the distal foredeep and from the foreland basin sediments of Wopmay Orogen. The line intersecting concordia at about 2.61-2.62 Ga is the same one as in Figure

17 and is included for comparison as explained in the text. Inset labeled "2 sigma error" represents the size of error ellipses for each data point; this ellipse shows two standard deviation error in both U-Pb ratios (± 0.4%) and the uncertainty associated with the $^{207}Pb/^{206}Pb$ ratio (± 0.1%).

Figure 19. U-Pb concordia diagram of Queen Maud block zircon geochronologic data. Inset is a map of the zircon sample locations within the Queen Maud block and is the same as the map in Figure 1. Note nearly concordant sample Queen Maud 3 at ca. 2.40 Ga. Inset labeled "2 sigma error" represents the size of error ellipses for each data point; this ellipse shows two standard deviation error in both U-Pb ratios (± 0.4%) and the uncertainty associated with the $^{207}Pb/^{206}Pb$ ratio (± 0.1%).

Figure 20. Interpretation of provenance evolution of the Goulburn Supergroup on the basis of paleocurrent and detrital zircon U-Pb data. Paleocurrent data from Figure 5.

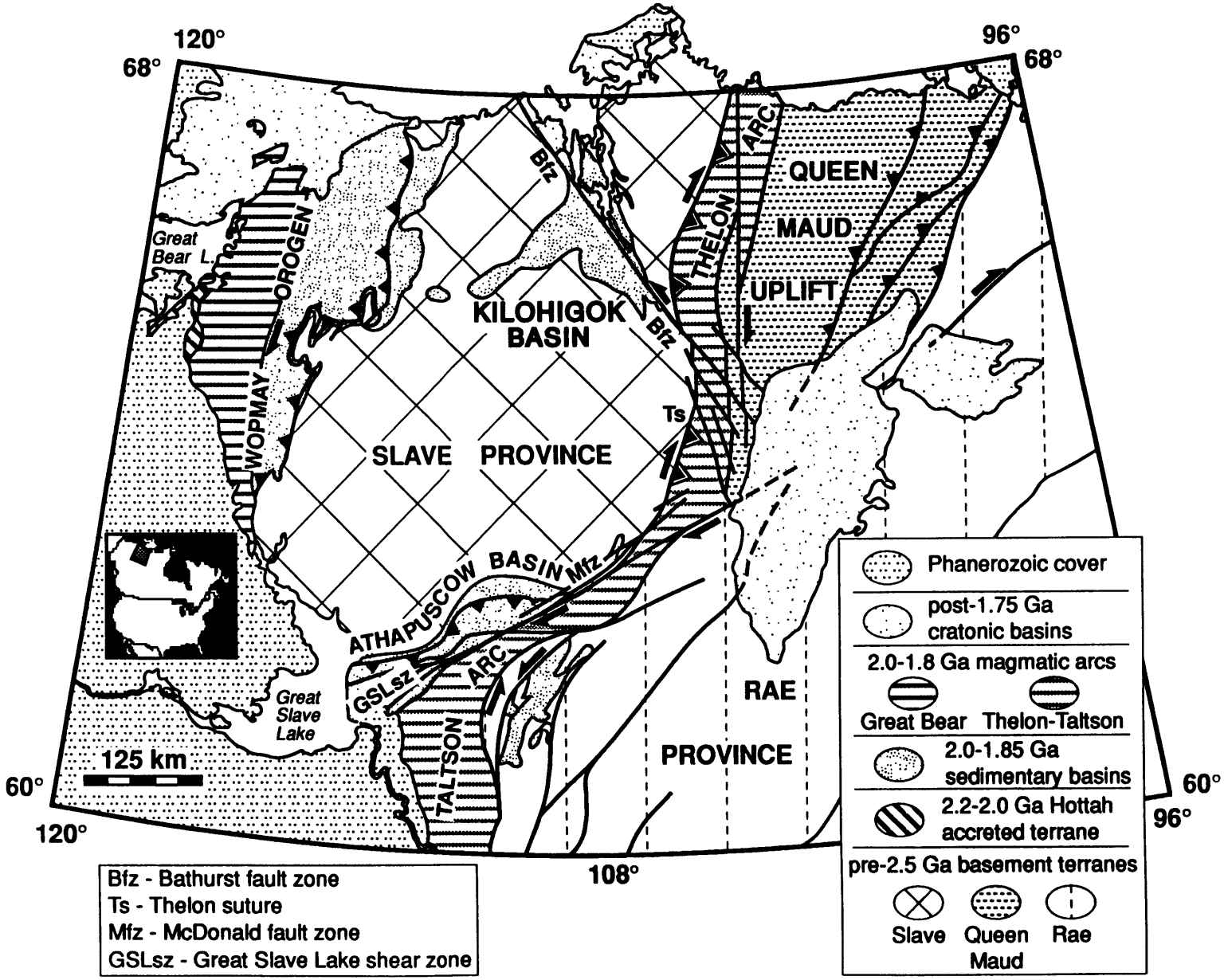
120°
68°
96°
68°
Great Bear L.
WOPMAY OROGEN
Bfz
THELON ARC
QUEEN MAUD UPLIFT
KILOHIGOK BASIN
Bfz
Ts
SLAVE PROVINCE
ATHAPUSCOW BASIN
Mfz
GSLsz
ARC
Great Slave Lake
TALTSON
RAE PROVINCE
125 km
60°
120°
108°
60°
96°
Bfz - Bathurst fault zone
Ts - Thelon suture
Mfz - McDonald fault zone
GSLsz - Great Slave Lake shear zone
Phanerozoic cover
post-1.75 Ga cratonic basins
2.0-1.8 Ga magmatic arcs
Great Bear
Thelon-Taltson
2.0-1.85 Ga sedimentary basins
2.2-2.0 Ga Hottah accreted terrane
pre-2.5 Ga basement terranes
Slave
Queen Maud
Rae

Figure 1.

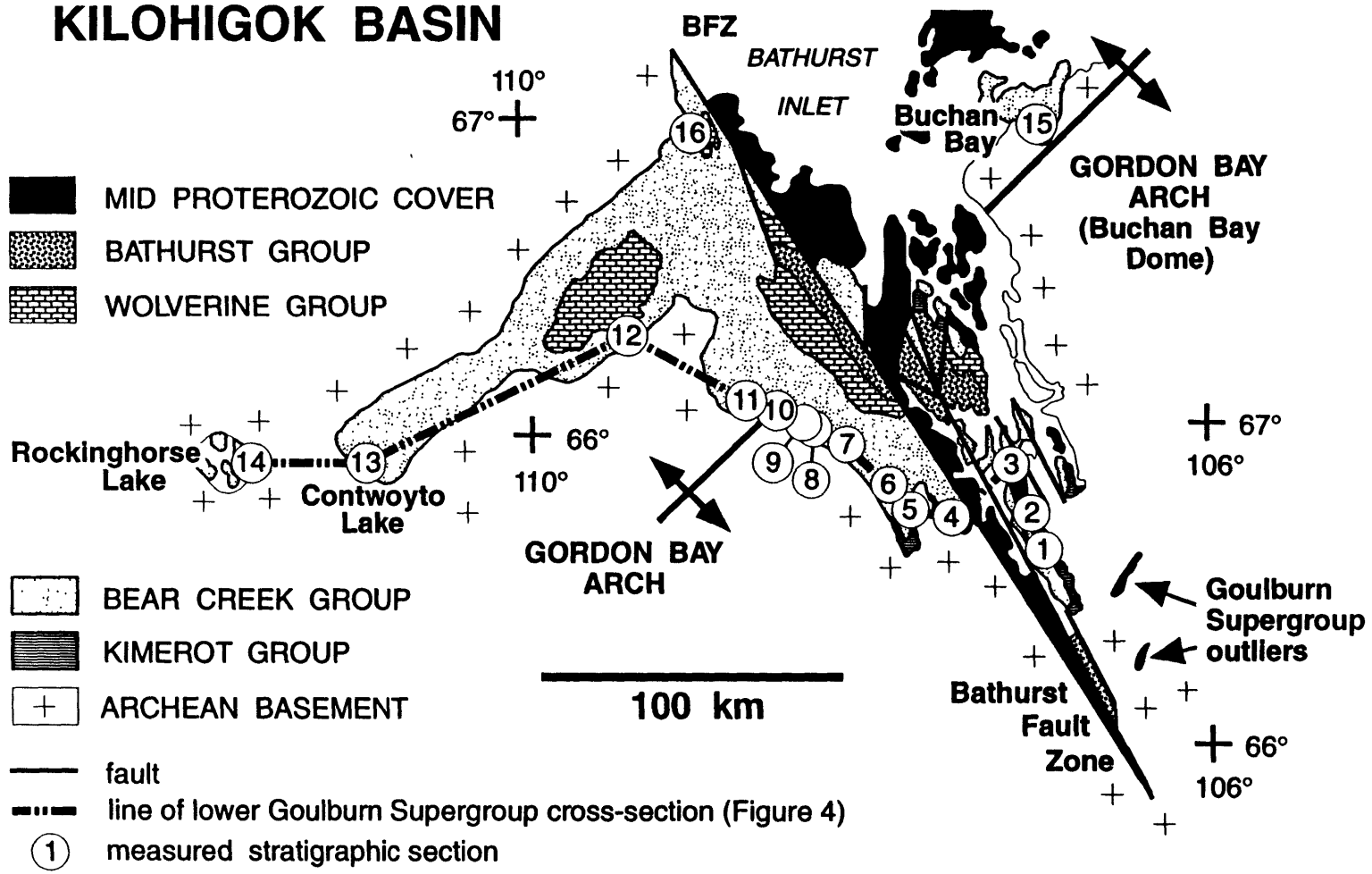
KILOHIGOK BASIN
BFZ
BATHURST
INLET
110°
67°
16
Buchan
Bay
15
GORDON BAY
ARCH
(Buchan Bay
Dome)
MID PROTEROZOIC COVER
BATHURST GROUP
WOLVERINE GROUP
12
11
10
9
8
7
6
5
4
3
2
1
66°
110°
67°
106°
Rockinghorse
Lake
14
13
Contwoyto
Lake
GORDON BAY
ARCH
BEAR CREEK GROUP
KIMEROT GROUP
ARCHEAN BASEMENT
100 km
Goulburn
Supergroup
outliers
Bathurst
Fault
Zone
66°
106°
fault
line of lower Goulburn Supergroup cross-section (Figure 4)
1 measured stratigraphic section

Figure 2.

a

lower Goulburn Supergroup				
lithostratigraphy groups	lithostratigraphy formations	sedimentary environment	tectonic interpretation	volcanic ash age (Ma)
Upper Bear Creek Group	Quadyuk Mara Burnside	carbonate platform marine shelf braid delta / braided alluvial	hinterland unroofing & alluvial progradation over craton	1882 ± 2
Lower Bear Creek Group	Link Beechey Rifle Hackett	siliciclastic marine shelf / minor shelf carbonates / basinal turbidites	Bear Creek foredeep flexural subsidence and infilling of marine foredeep	1963 ± 6 1969 ± 1
Kimerot Group	Peg Kenyon	siliciclastic to carbonate platform	Kimerot passive margin	

b

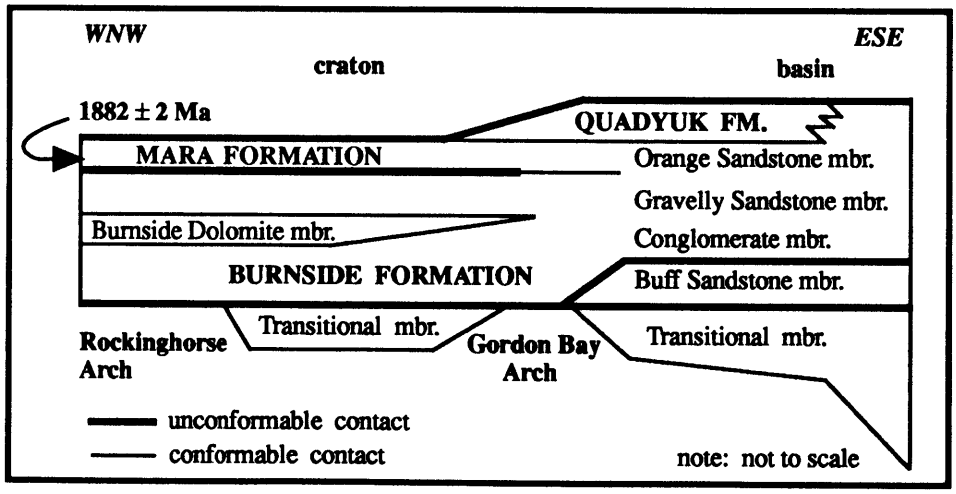

Figure 3.

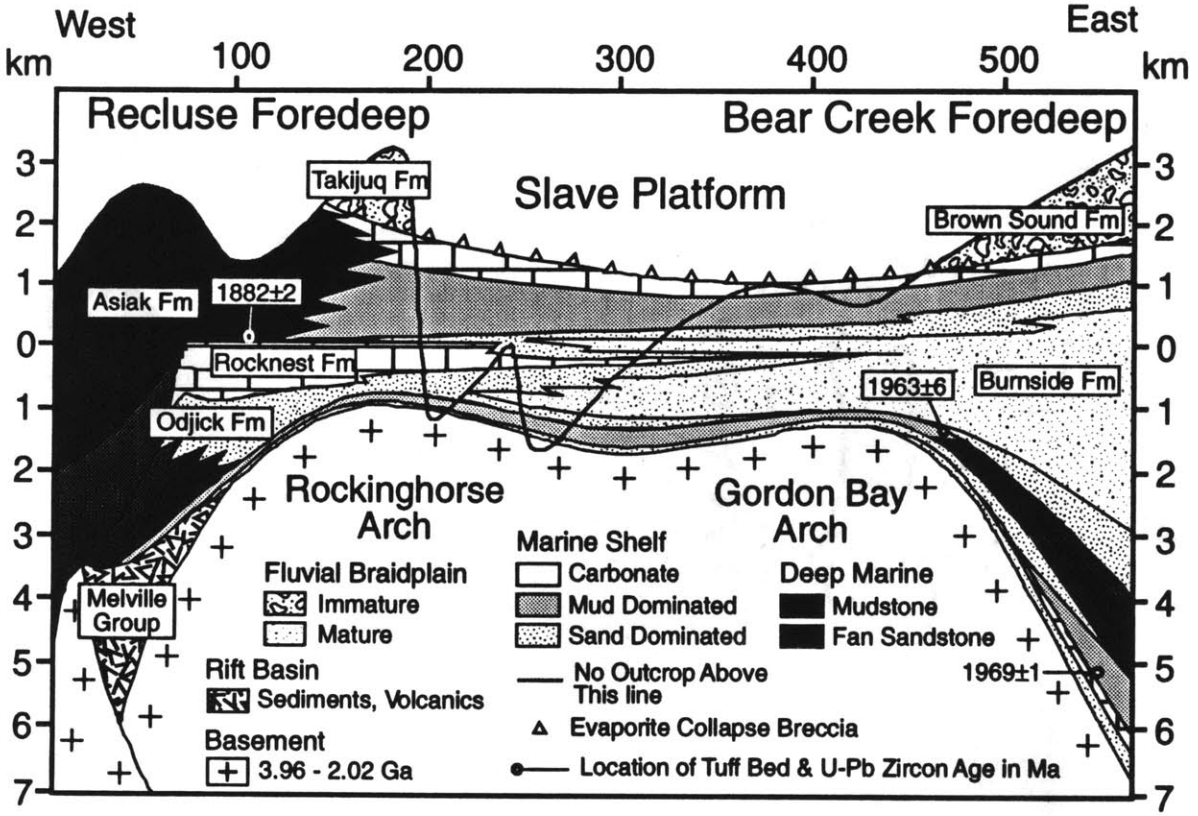
West
East
km
100
200
300
400
500
km
Recluse Foredeep
Bear Creek Foredeep
Slave Platform
Takijuq Fm
Brown Sound Fm
Asiak Fm
1882±2
Rocknest Fm
Odjick Fm
1963±6
Burnside Fm
Rockinghorse Arch
Gordon Bay Arch
Melville Group
Fluvial Braidplain
Immature
Mature
Rift Basin
Sediments, Volcanics
Basement
3.96 - 2.02 Ga
Marine Shelf
Carbonate
Mud Dominated
Sand Dominated
Deep Marine
Mudstone
Fan Sandstone
No Outcrop Above This line
1969±1
Evaporite Collapse Breccia
Location of Tuff Bed & U-Pb Zircon Age in Ma

Figure 4.

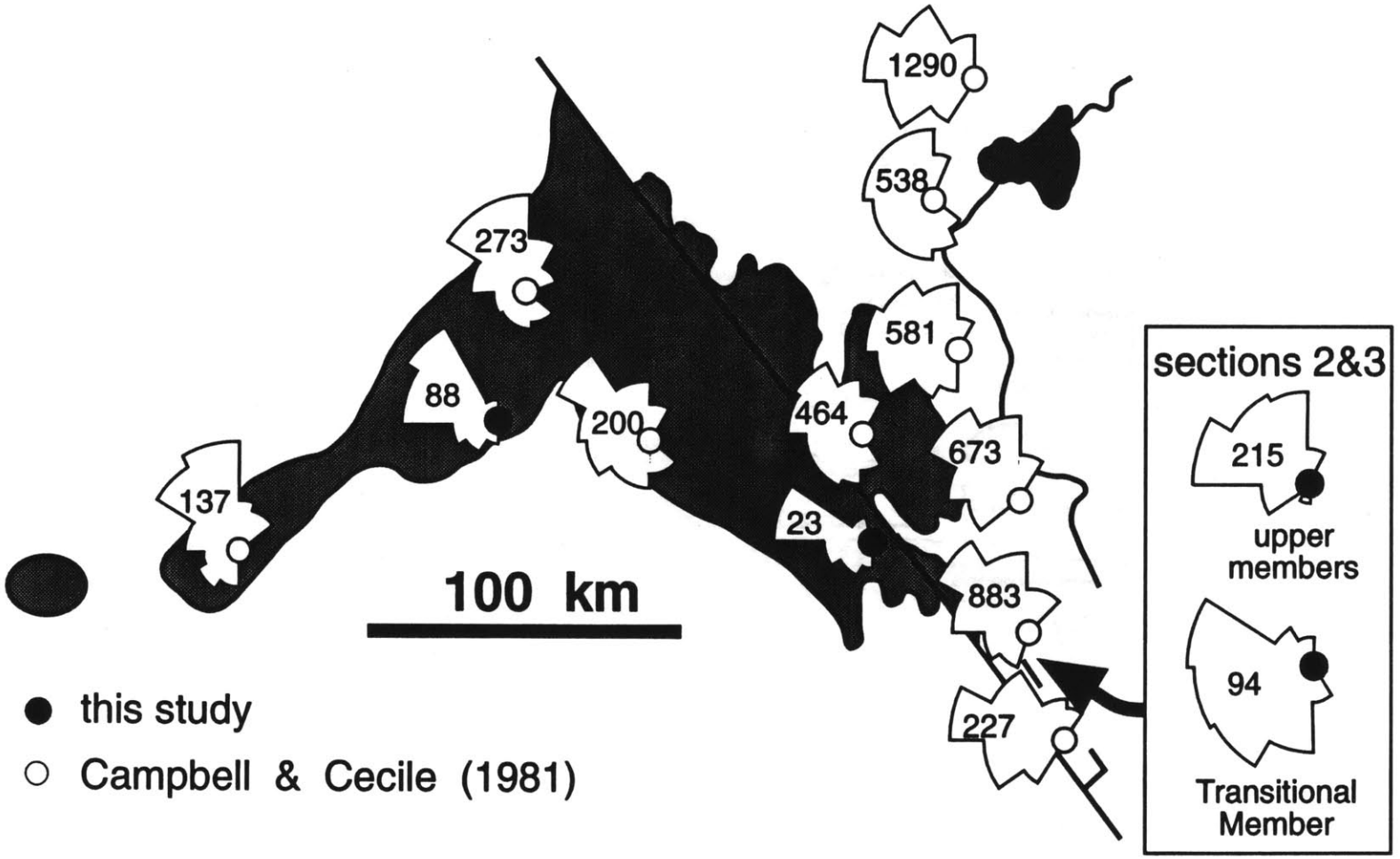
1290
538
273
581
88
200
464
673
137
23
883
227
100 km
this study
Campbell & Cecile (1981)
sections 2&3
215
upper members
94
Transitional Member

Figure 5.

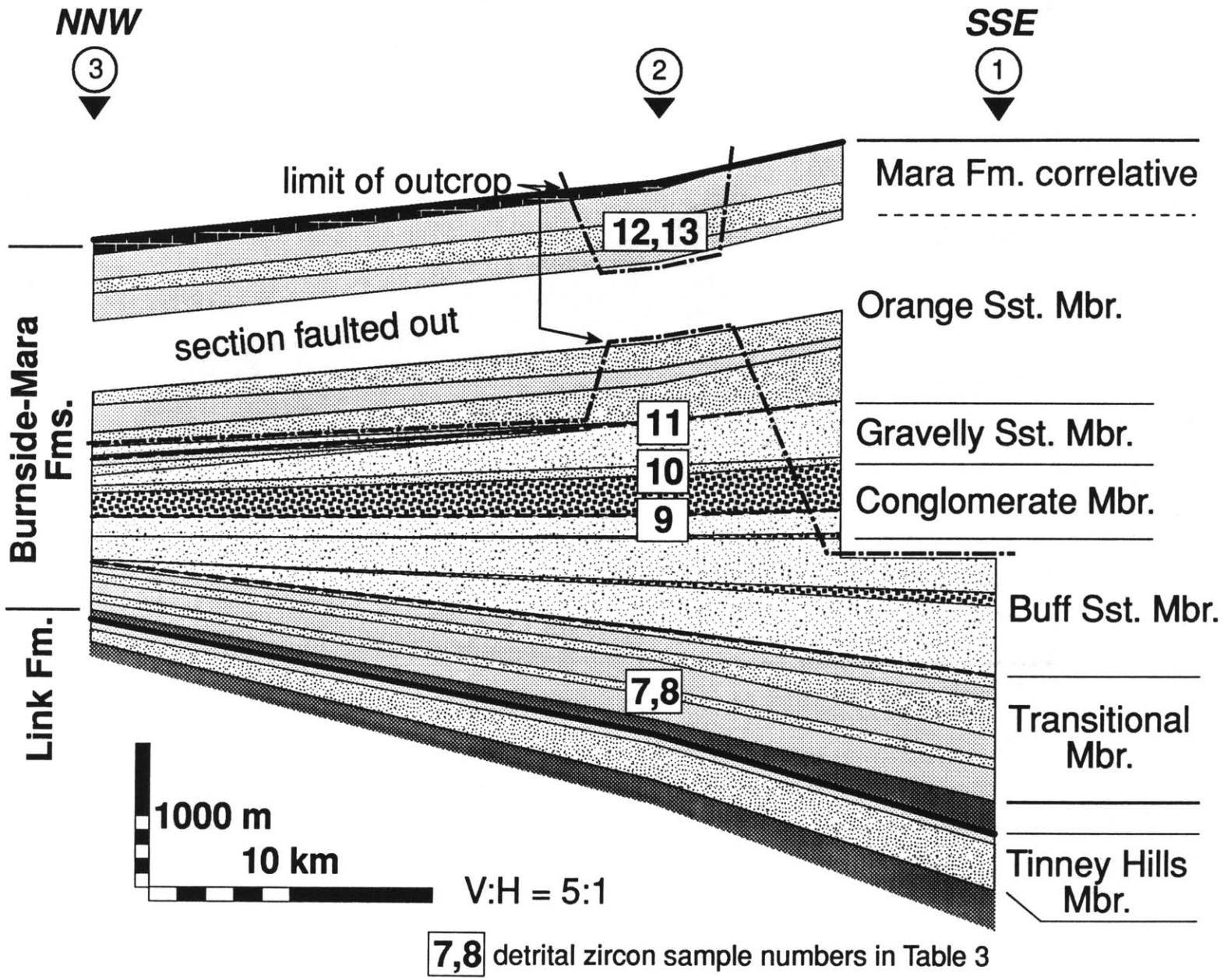
NNW
SSE
3
2
1
limit of outcrop
12,13
Mara Fm. correlative
Orange Sst. Mbr.
section faulted out
Burnside-Mara Fms.
11
Gravelly Sst. Mbr.
10
Conglomerate Mbr.
9
Buff Sst. Mbr.
Link Fm.
7,8
Transitional Mbr.
Tinney Hills Mbr.
1000 m
10 km
V:H = 5:1
7,8 detrital zircon sample numbers in Table 3

Figure 6.

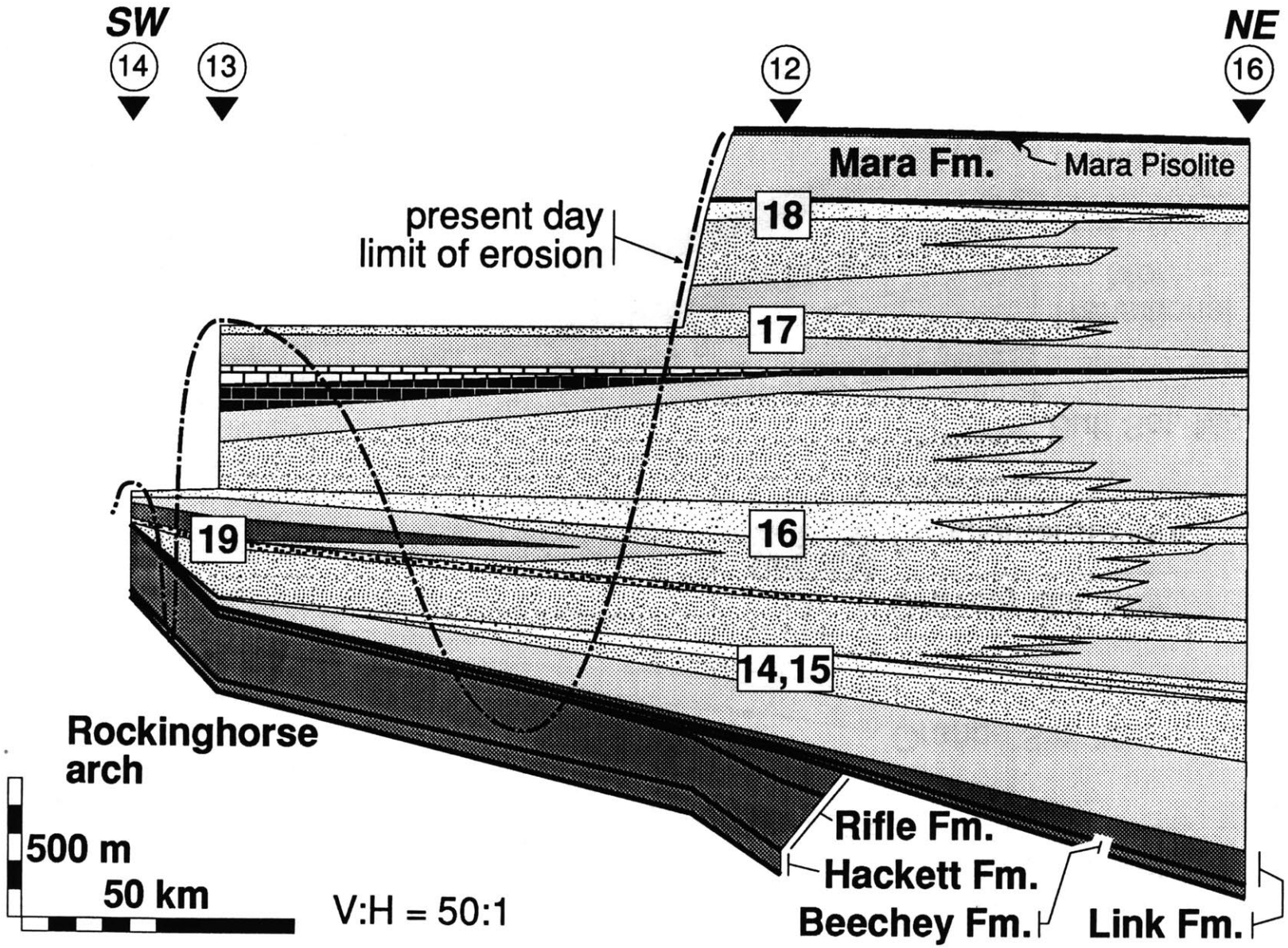

Figure 7. 17 detrital zircon sample number in Table 3

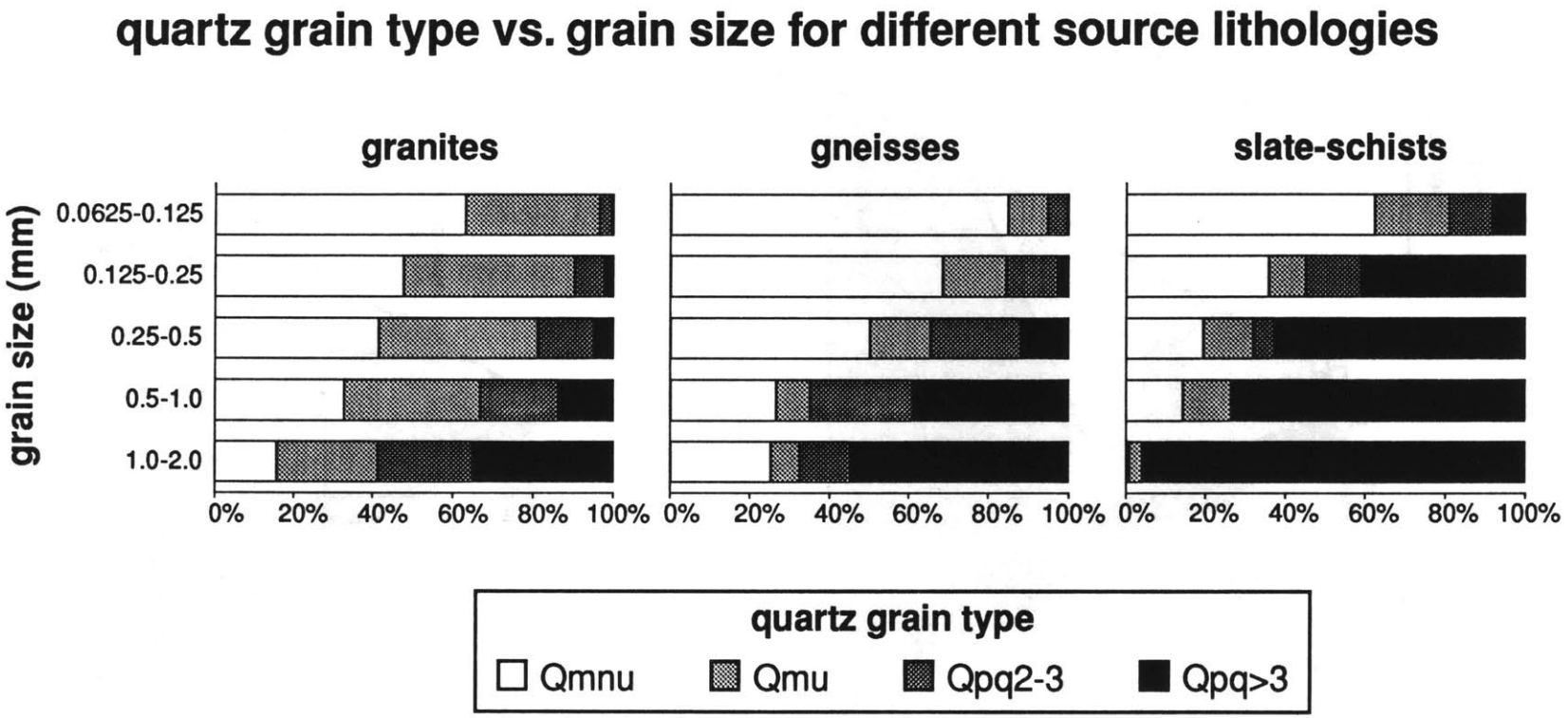

Figure 8.

data from Tortosa et al. (1991)

Figure 9.

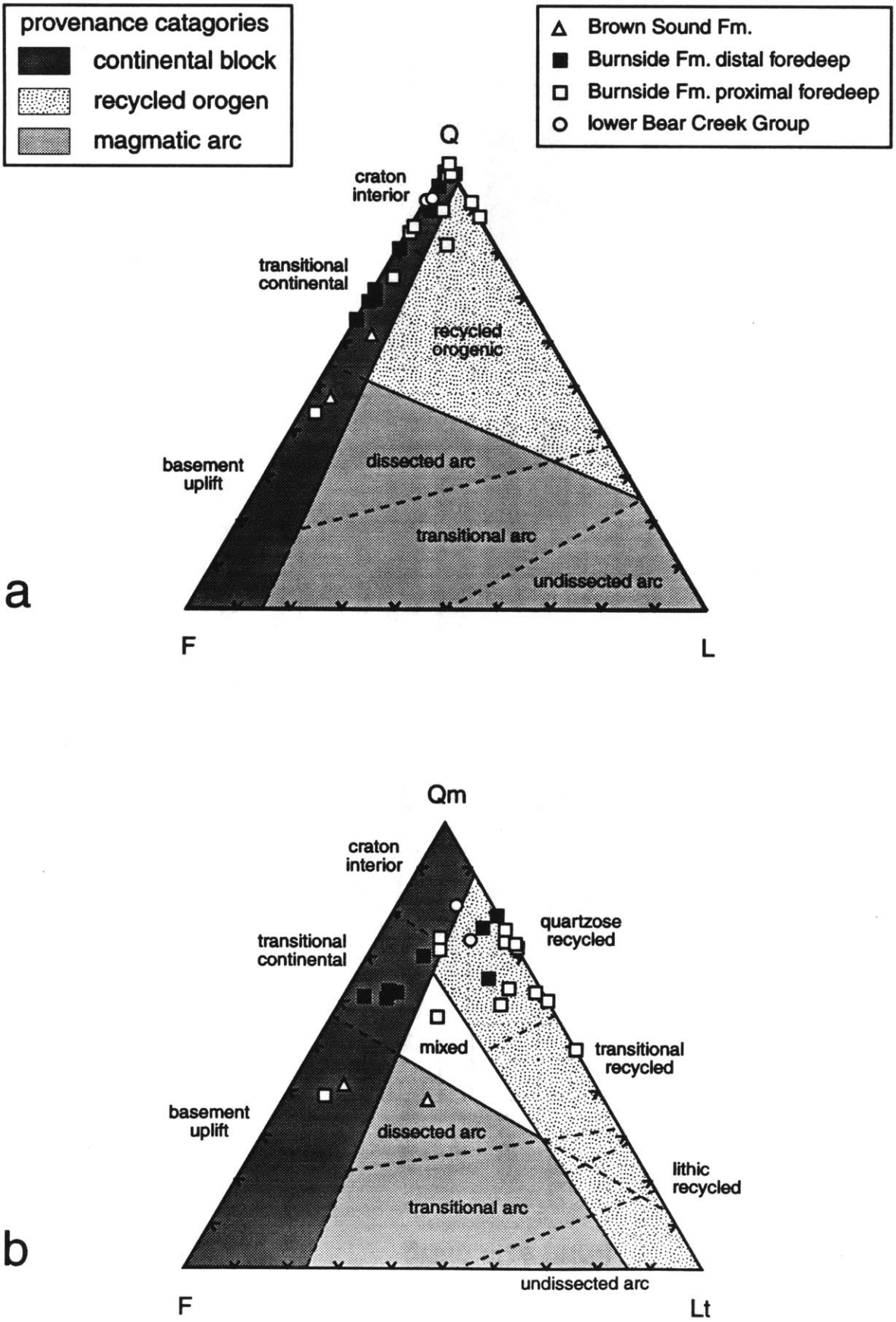
provenance catagories
continental block
recycled orogen
magmatic arc
Brown Sound Fm.
Burnside Fm. distal foredeep
Burnside Fm. proximal foredeep
lower Bear Creek Group
Q
craton interior
transitional continental
recycled orogenic
basement uplift
dissected arc
transitional arc
undissected arc
a
F
L
Qm
craton interior
transitional continental
quartzose recycled
mixed
transitional recycled
basement uplift
dissected arc
lithic recycled
transitional arc
undissected arc
b
F
Lt

Figure 10.

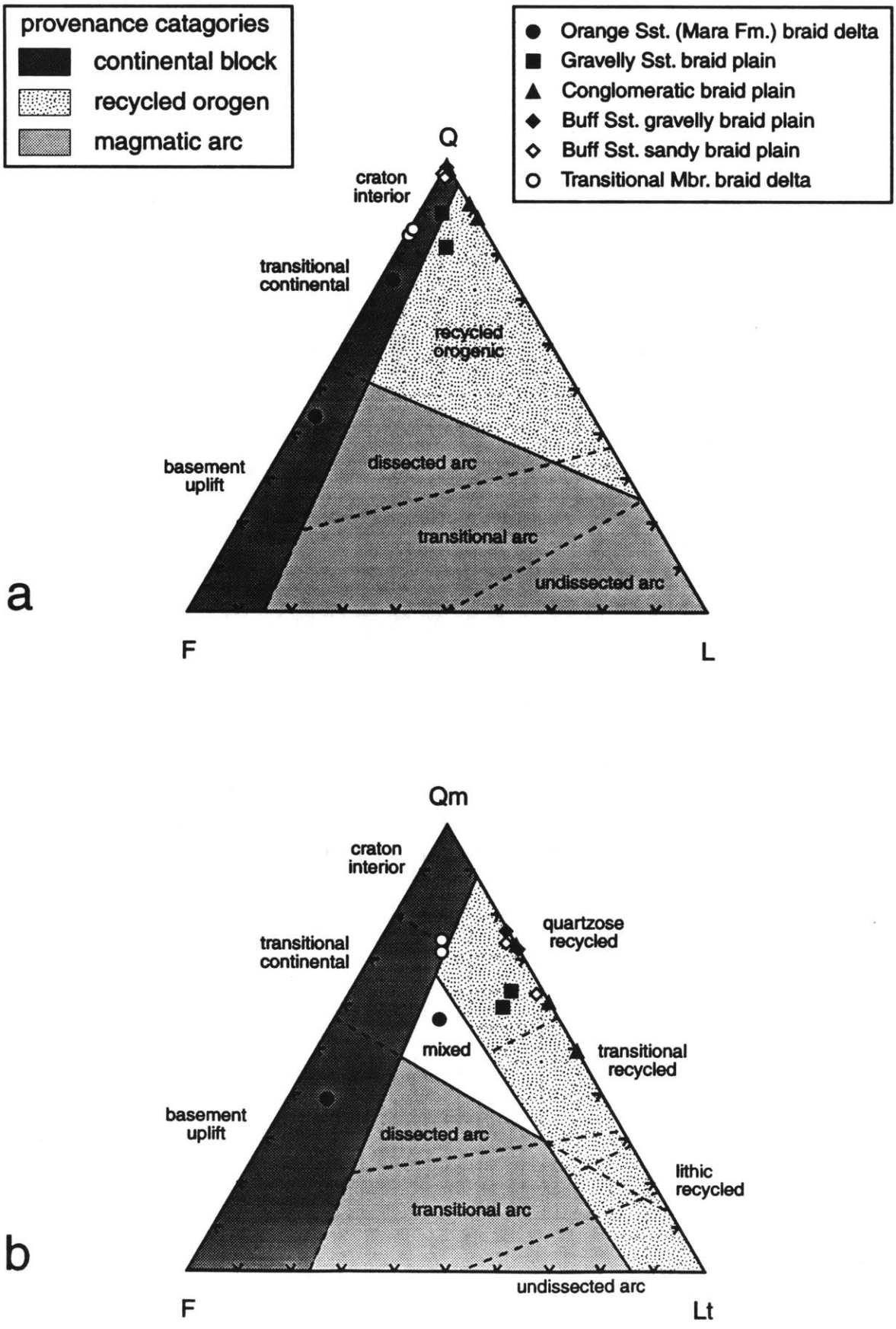
provenance catagories
continental block
recycled orogen
magmatic arc
Orange Sst. (Mara Fm.) braid delta
Gravelly Sst. braid plain
Conglomeratic braid plain
Buff Sst. gravelly braid plain
Buff Sst. sandy braid plain
Transitional Mbr. braid delta
Q
craton interior
transitional continental
recycled orogenic
basement uplift
dissected arc
transitional arc
undissected arc
F
L
a
Qm
craton interior
transitional continental
quartzose recycled
mixed
transitional recycled
basement uplift
dissected arc
lithic recycled
transitional arc
undissected arc
F
Lt
b

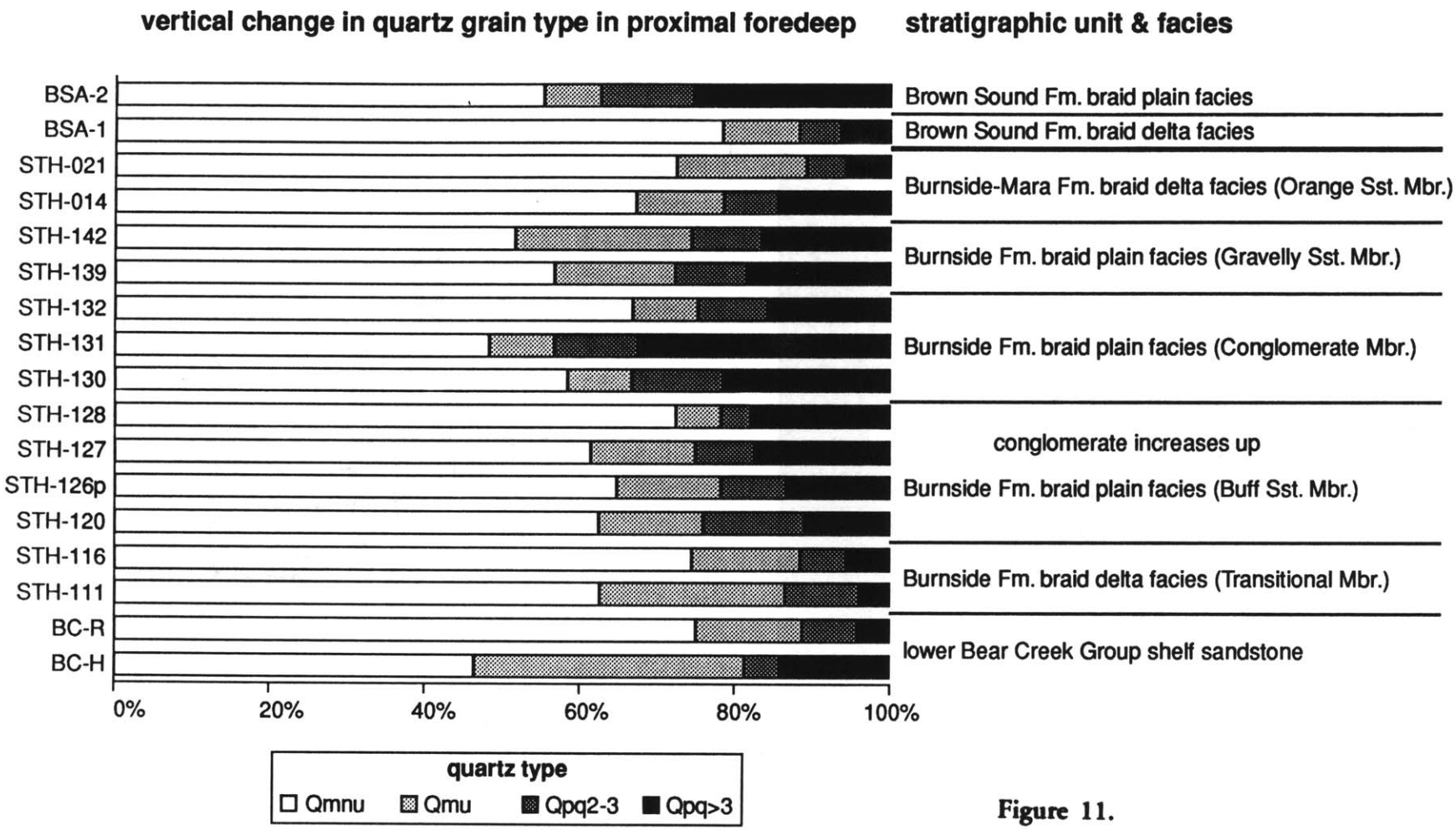
vertical change in quartz grain type in proximal foredeep
stratigraphic unit & facies
BSA-2
BSA-1
STH-021
STH-014
STH-142
STH-139
STH-132
STH-131
STH-130
STH-128
STH-127
STH-126p
STH-120
STH-116
STH-111
BC-R
BC-H
Brown Sound Fm. braid plain facies
Brown Sound Fm. braid delta facies
Burnside-Mara Fm. braid delta facies (Orange Sst. Mbr.)
Burnside Fm. braid plain facies (Gravelly Sst. Mbr.)
Burnside Fm. braid plain facies (Conglomerate Mbr.)
conglomerate increases up
Burnside Fm. braid plain facies (Buff Sst. Mbr.)
Burnside Fm. braid delta facies (Transitional Mbr.)
lower Bear Creek Group shelf sandstone
0%
20%
40%
60%
80%
100%
quartz type
Qmnu
Qmu
Qpq2-3
Qpq>3

Figure 11.

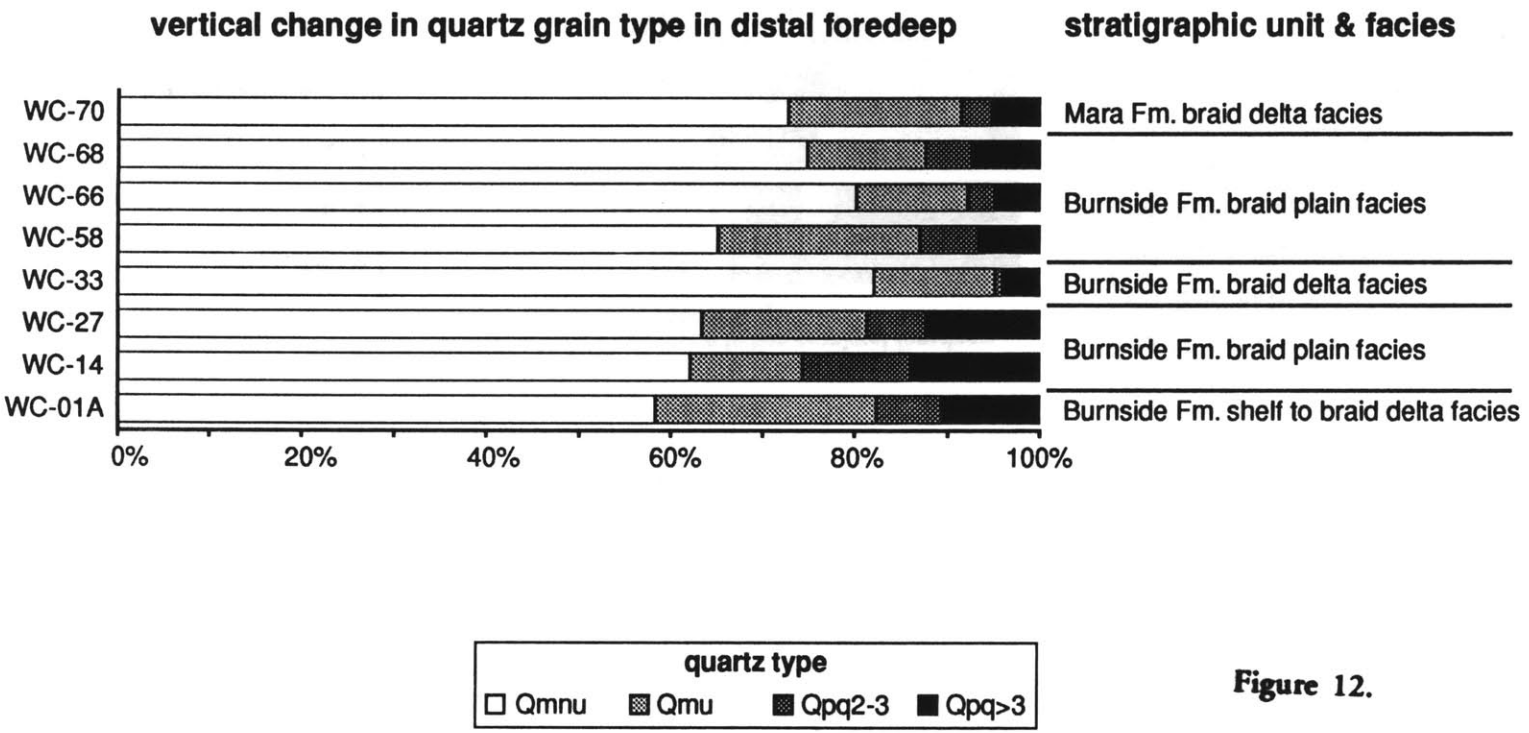
vertical change in quartz grain type in distal foredeep
stratigraphic unit & facies
WC-70
WC-68
WC-66
WC-58
WC-33
WC-27
WC-14
WC-01A
0%
20%
40%
60%
80%
100%
Mara Fm. braid delta facies
Burnside Fm. braid plain facies
Burnside Fm. braid delta facies
Burnside Fm. braid plain facies
Burnside Fm. shelf to braid delta facies
quartz type
Qmnu
Qmu
Qpq2-3
Qpq>3

Figure 12.

a

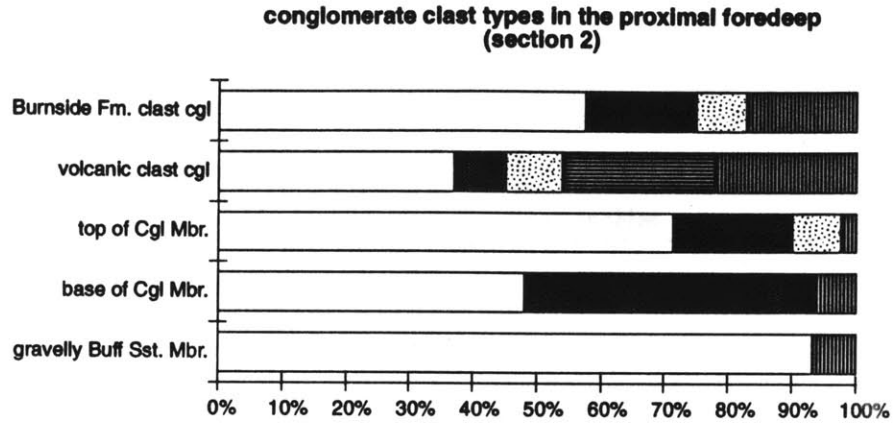
conglomerate clast types in the proximal foredeep
(section 2)
Burnside Fm. clast cgl
volcanic clast cgl
top of Cgl Mbr.
base of Cgl Mbr.
gravelly Buff Sst. Mbr.
0%
10%
20%
30%
40%
50%
60%
70%
80%
90%
100%

b

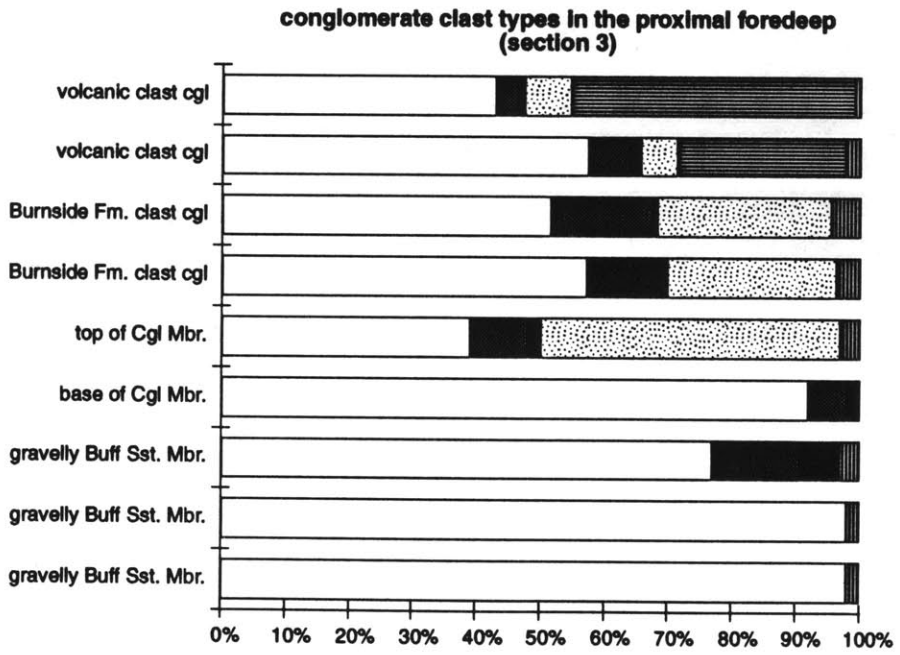
conglomerate clast types in the proximal foredeep
(section 3)
volcanic clast cgl
volcanic clast cgl
Burnside Fm. clast cgl
Burnside Fm. clast cgl
top of Cgl Mbr.
base of Cgl Mbr.
gravelly Buff Sst. Mbr.
gravelly Buff Sst. Mbr.
gravelly Buff Sst. Mbr.
0%
10%
20%
30%
40%
50%
60%
70%
80%
90%
100%

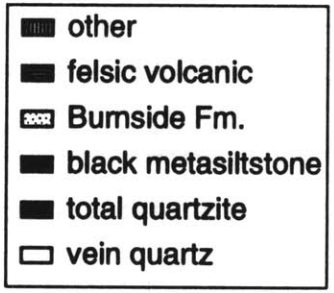
other
felsic volcanic
Burnside Fm.
black metasiltstone
total quartzite
vein quartz

Figure 13.

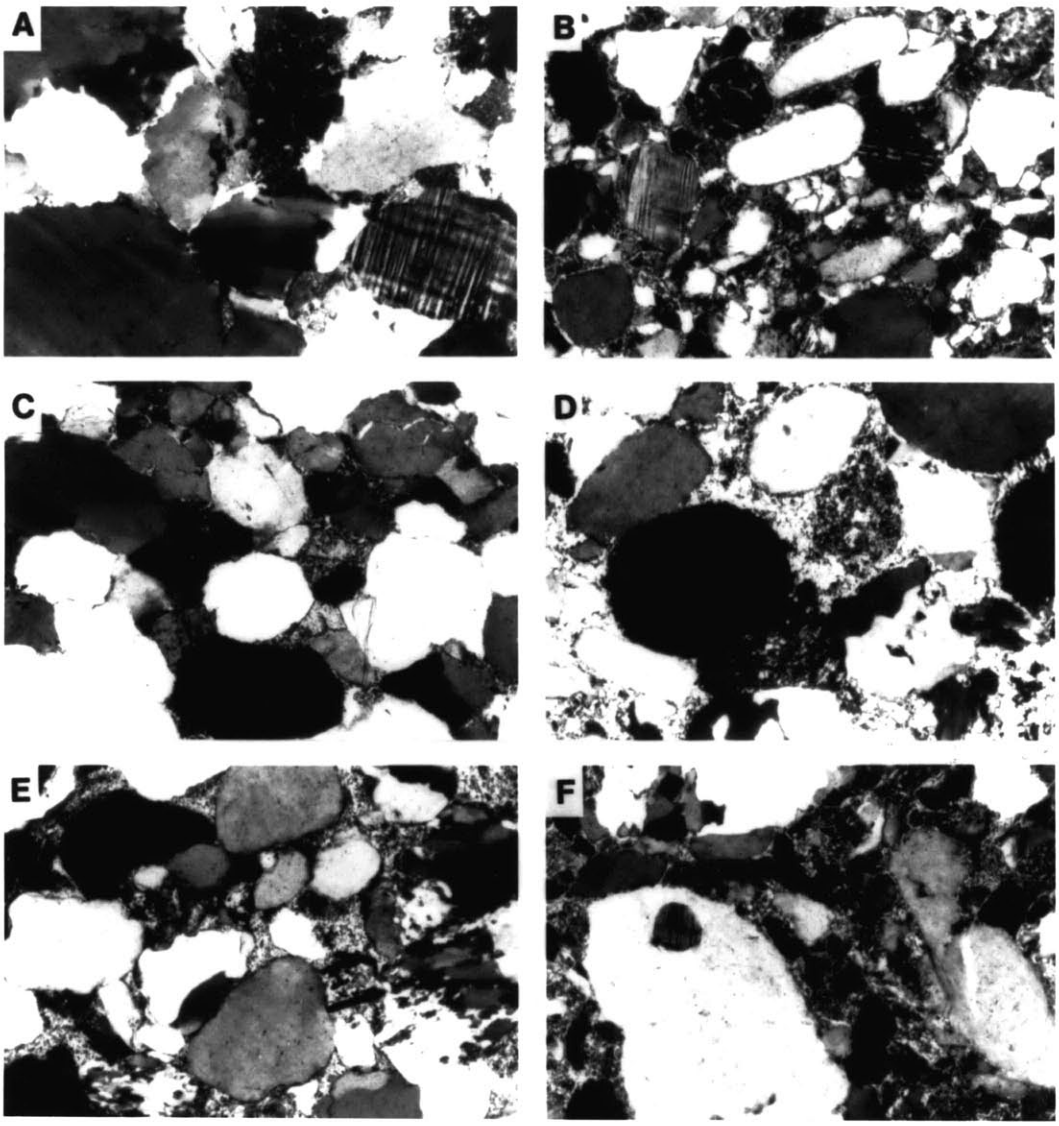

Figure 14.

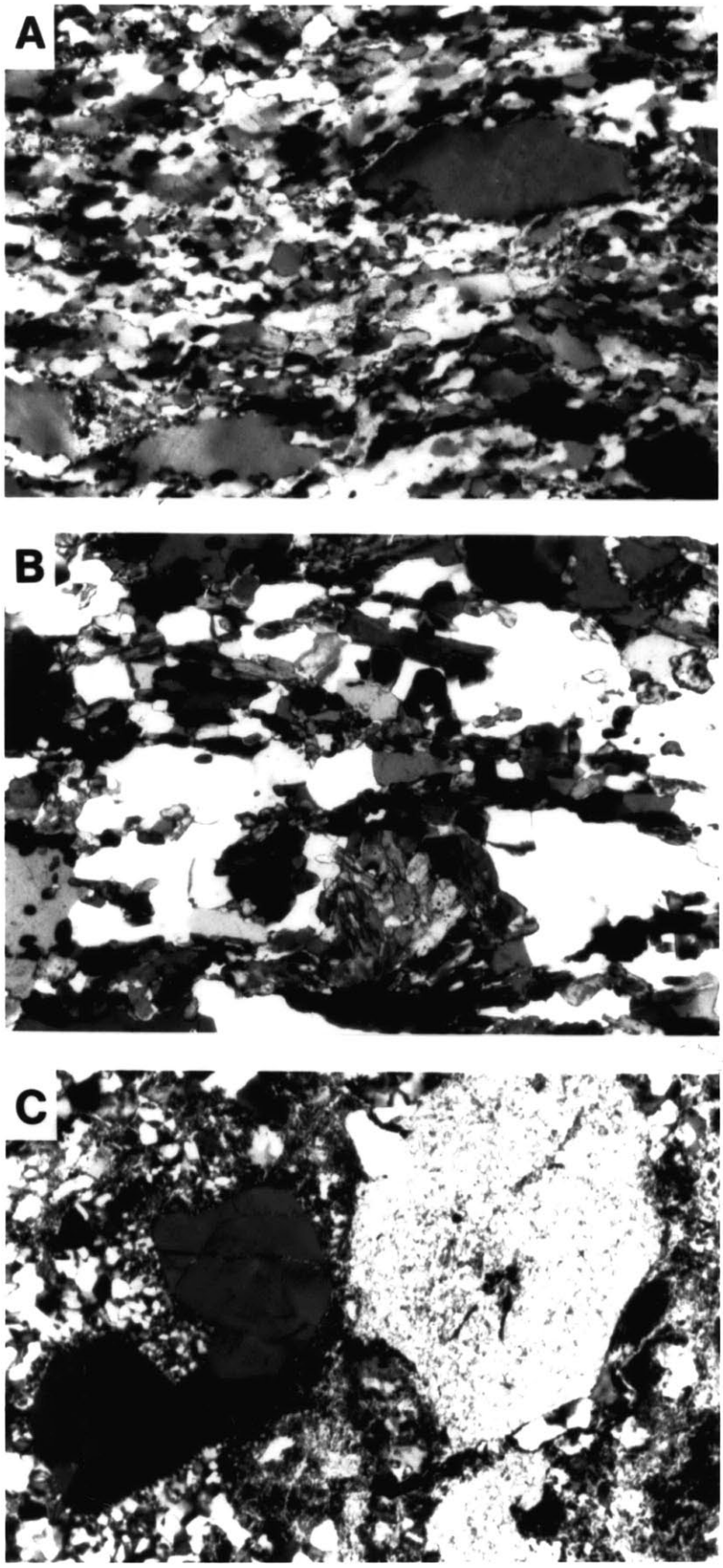

Figure 15.

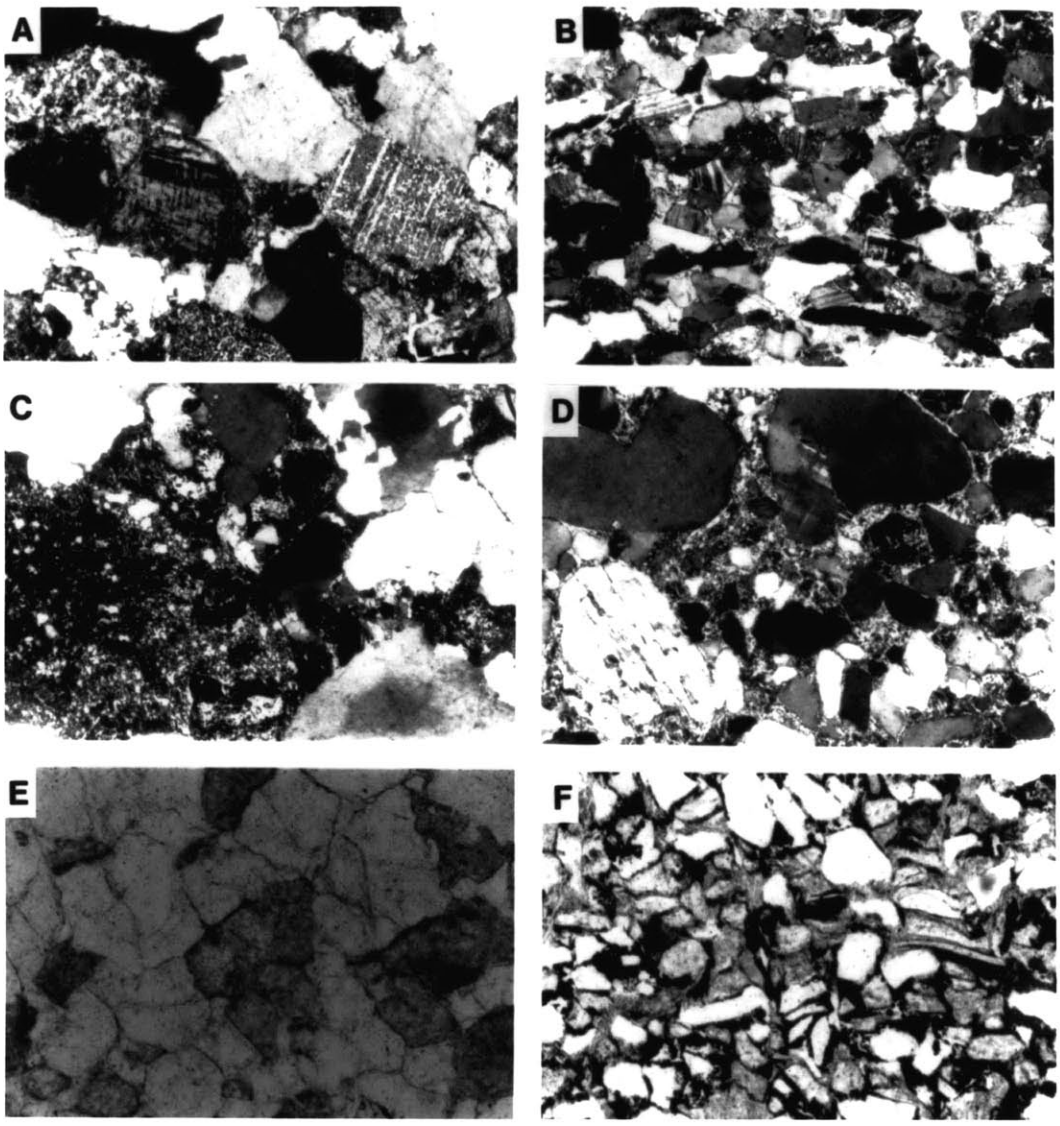

Figure 16.

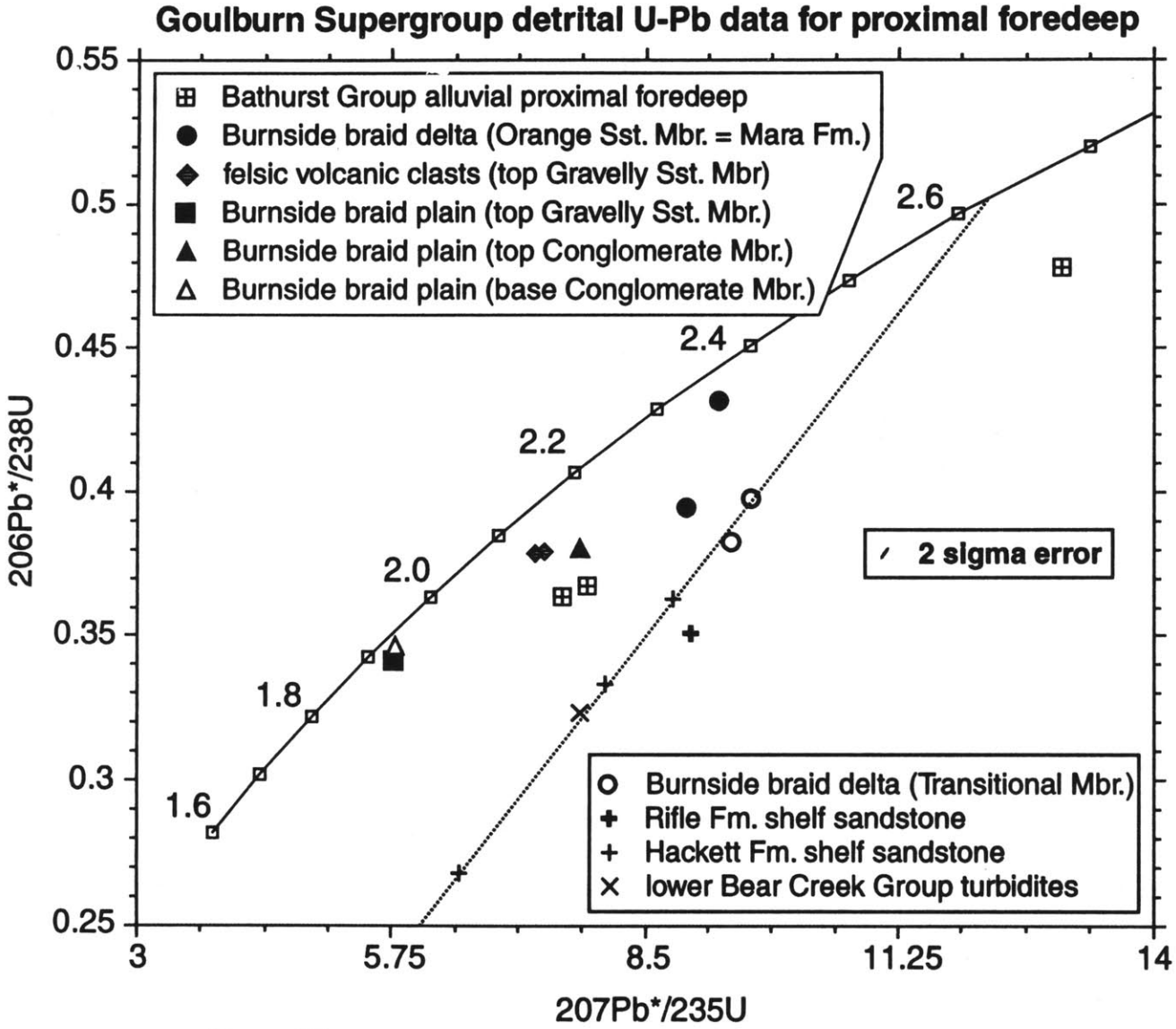
Goulburn Supergroup detrital U-Pb data for proximal foredeep
Bathurst Group alluvial proximal foredeep
Burnside braid delta (Orange Sst. Mbr. = Mara Fm.)
felsic volcanic clasts (top Gravelly Sst. Mbr)
Burnside braid plain (top Gravelly Sst. Mbr.)
Burnside braid plain (top Conglomerate Mbr.)
Burnside braid plain (base Conglomerate Mbr.)
2 sigma error
Burnside braid delta (Transitional Mbr.)
Rifle Fm. shelf sandstone
Hackett Fm. shelf sandstone
lower Bear Creek Group turbidites
1.6
1.8
2.0
2.2
2.4
2.6
0.55
0.5
0.45
0.4
0.35
0.3
0.25
206Pb*/238U
3
5.75
8.5
11.25
14
207Pb*/235U

Figure 17.

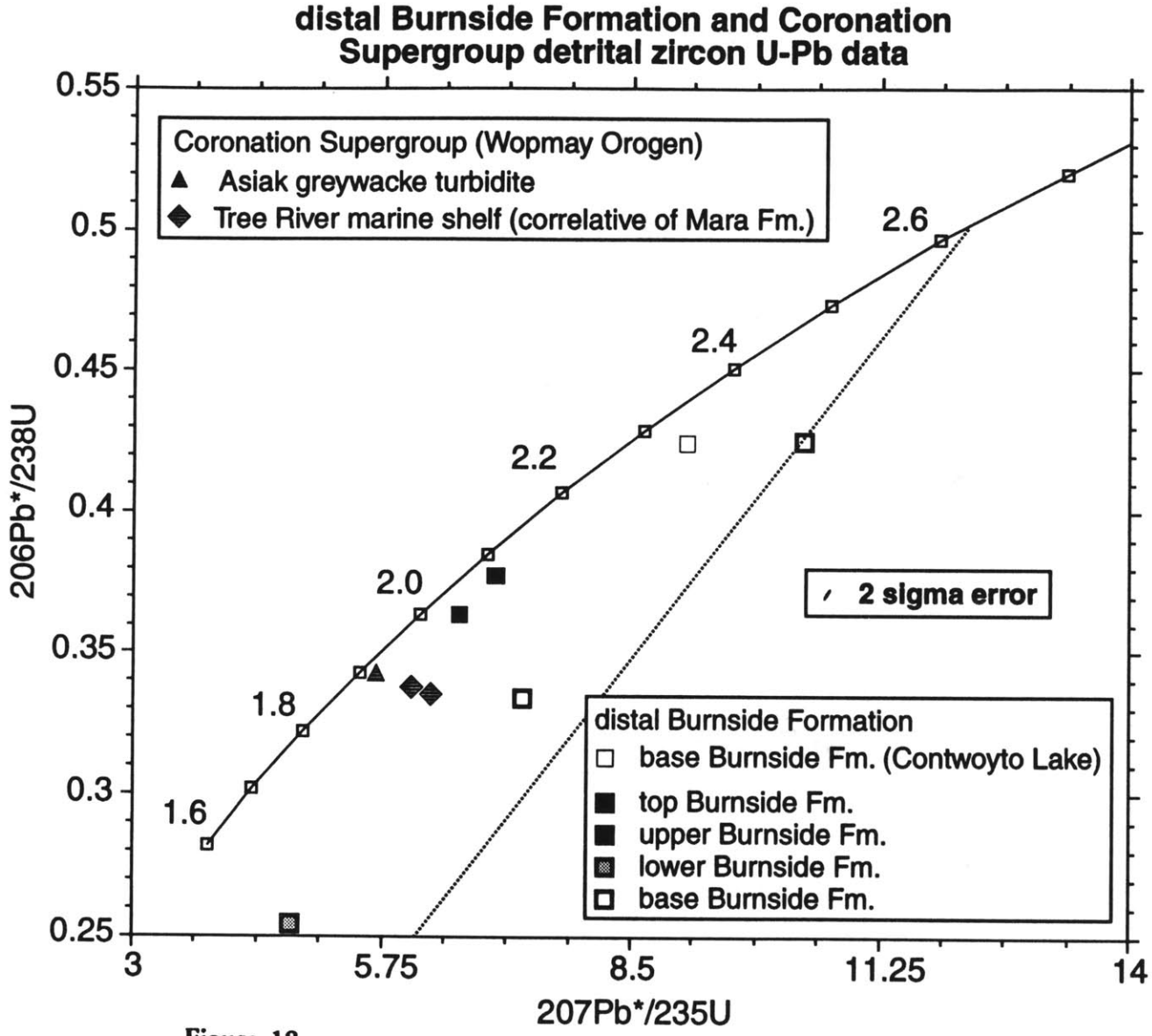
distal Burnside Formation and Coronation Supergroup detrital zircon U-Pb data
Coronation Supergroup (Wopmay Orogen)
Asiak greywacke turbidite
Tree River marine shelf (correlative of Mara Fm.)
2 sigma error
distal Burnside Formation
base Burnside Fm. (Contwoyto Lake)
top Burnside Fm.
upper Burnside Fm.
lower Burnside Fm.
base Burnside Fm.
1.6
1.8
2.0
2.2
2.4
2.6
206Pb*/238U
207Pb*/235U
0.55
0.5
0.45
0.4
0.35
0.3
0.25
3
5.75
8.5
11.25
14

Figure 18.

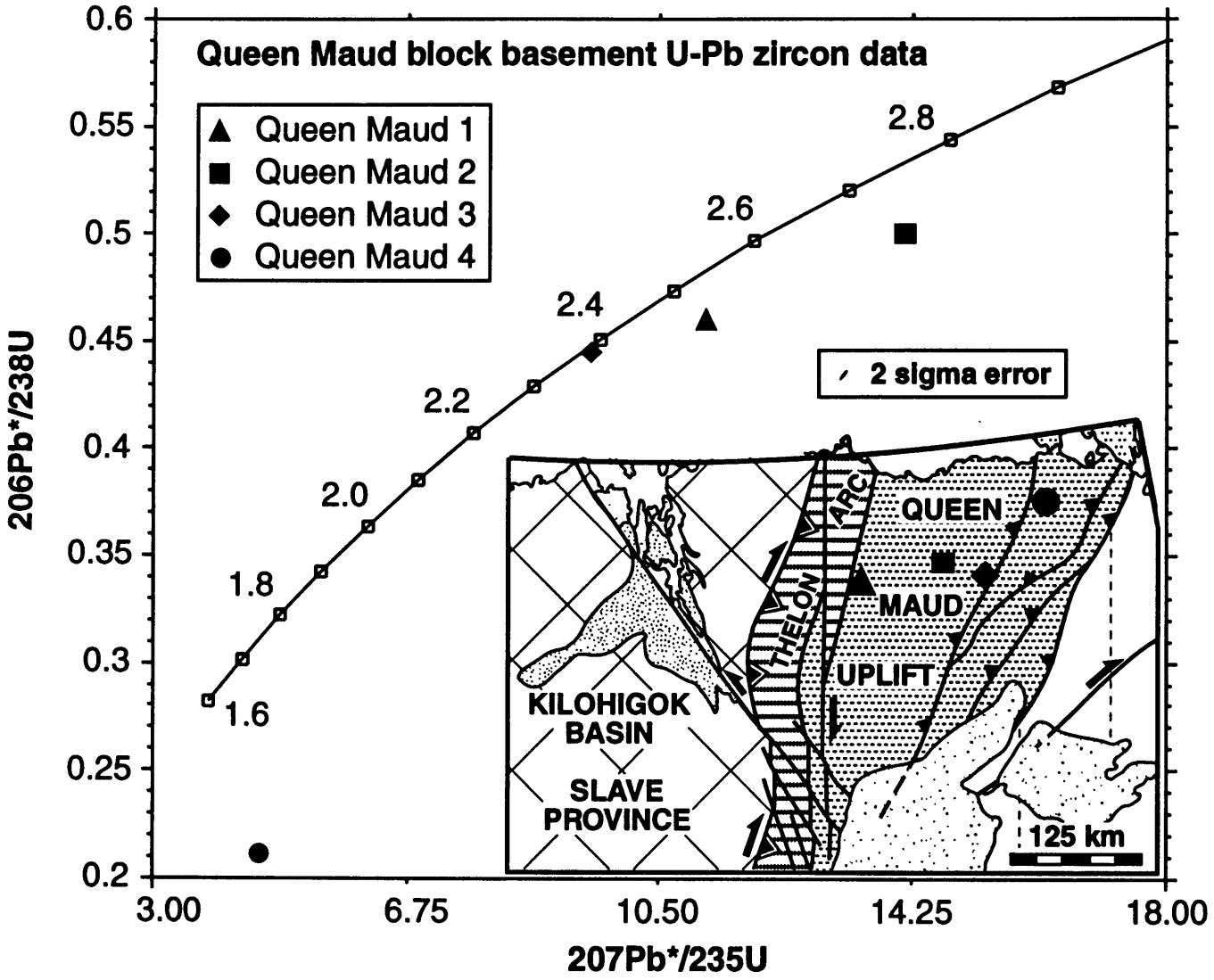
Queen Maud block basement U-Pb zircon data
Queen Maud 1
Queen Maud 2
Queen Maud 3
Queen Maud 4
2 sigma error
206Pb*/238U
207Pb*/235U
0.6
0.55
0.5
0.45
0.4
0.35
0.3
0.25
0.2
3.00
6.75
10.50
14.25
18.00
1.6
1.8
2.0
2.2
2.4
2.6
2.8
ARC
THELON
QUEEN
MAUD
UPLIFT
KILOHIGOK
BASIN
SLAVE
PROVINCE
125 km

Figure 19.

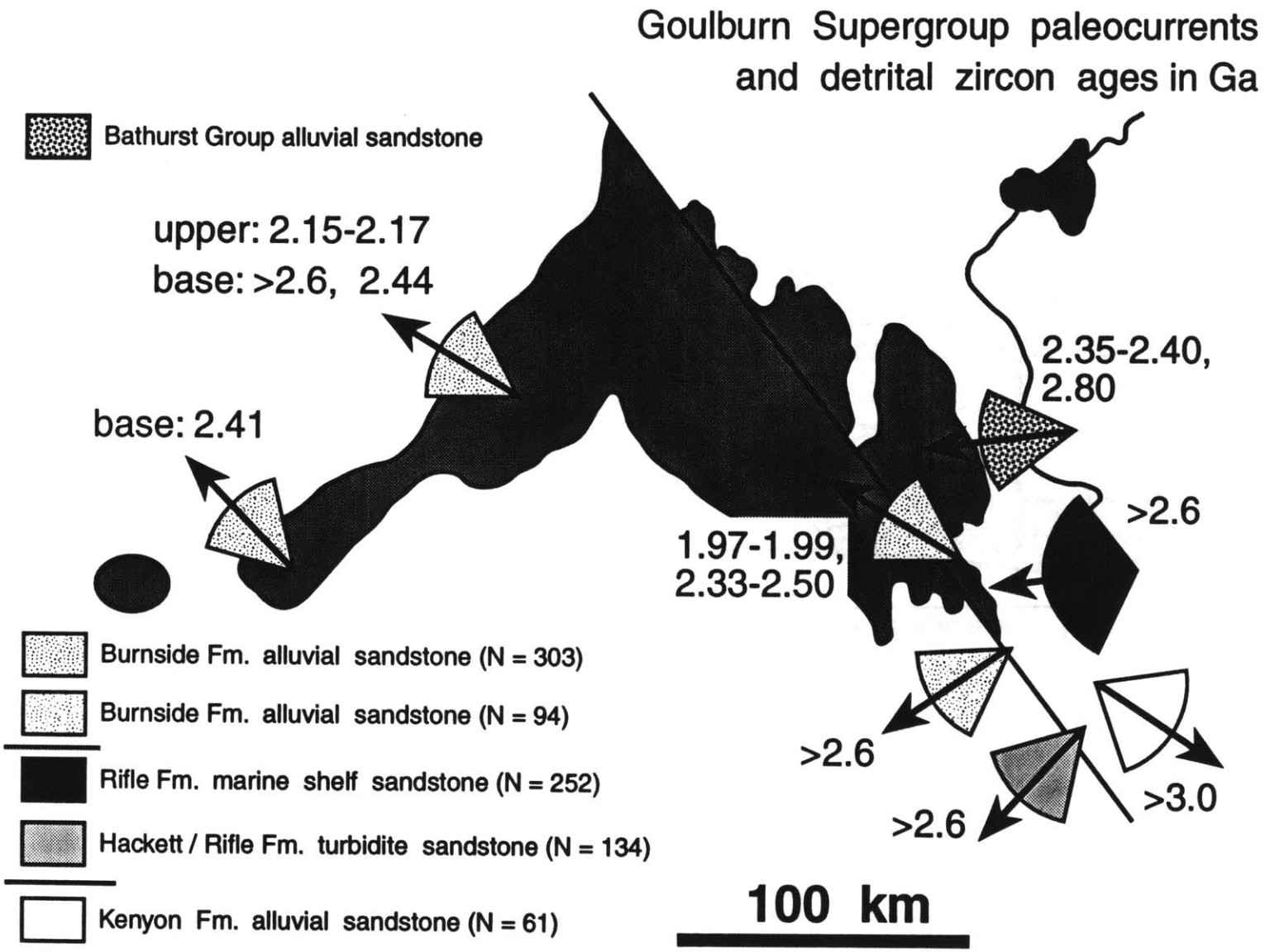
Goulburn Supergroup paleocurrents
and detrital zircon ages in Ga
Bathurst Group alluvial sandstone
upper: 2.15-2.17
base: >2.6, 2.44
base: 2.41
2.35-2.40,
2.80
>2.6
1.97-1.99,
2.33-2.50
>2.6
>2.6
>3.0
Burnside Fm. alluvial sandstone (N = 303)
Burnside Fm. alluvial sandstone (N = 94)
Rifle Fm. marine shelf sandstone (N = 252)
Hackett / Rifle Fm. turbidite sandstone (N = 134)
Kenyon Fm. alluvial sandstone (N = 61)
100 km

Figure 20.

Appendices

Appendix A:
Measured stratigraphic sections in the Burnside Formation

Appendix B:
Petrographic data from the Goulburn Supergroup

Appendix C:
Zircon sample locations

Appendix A:
Measured stratigraphic sections in the Burnside Formation

Burnside Formation measured section locations				
section number	map sheet (1:250 000 scale)	latitude N	longitude W	notes
1	Tinney Hills (76-J)	66° 36.75'	107° 27.5'	Bear Creek Hills
2	Tinney Hills (76-J)	66° 45.0' 66° 43.8'	107° 35.5' 107° 39.5'	south Tinney Hills; lower section moves obliquely with respect to bedding to northwest and ends at T-shaped penninsula; upper section heads across southern end of Tinney Cove at southern limit of the Tinney Hills
3	Tinney Hills (76-J)	66° 56.6' 66° 57.0'	107° 40.5' 107° 44.0'	north Tinney Hills
	Tinney Hills (76-J)	66° 58.8'	107° 41.5'	Manning Penninsula detailed section illustrated in chapter 1
4	Beechey Lake (76-G)	65° 50.5'	106° 35.5'	southeast folds near Bathurst Fault
5	Beechey Lake (76-G)	65° 51.7'	106° 45.5'	northwest folds near Bathurst Fault
6	Beechey Lake (76-G)	65° 51.1'	107° 12.5'	Rifle Lake
7	Beechey Lake (76-G)	65° 58.6'	107° 31.5'	south Link Lake
8	Tinney Hills (76-J)	66° 00.8'	107° 46.25'	mid Link Lake
9	Tinney Hills (76-J)	66° 02.8'	107° 52.0'	northwest Link Lake
10	Mara River (76-K)	66° 05.6'	108° 04.5'	southeast Hackett River
11	Mara River (76-K)	66° 07.5'	108° 12.5'	northwest Hackett River
12	Mara River (76-K)	66° 19.25' 66° 20.25'	109° 06.8' 109° 12.0'	Wolverine Canyon; Burnside Fm. section base of Mara Fm. section
13	Contwoyto Lake (76-E)	65° 52.5'	111° 03.0'	Contwoyto Lake
14	Point Lake (84-H)	65° 49.5'	112° 10.0'	Rockinghorse Lake
15	Rideout Island (76-O)	67° 56.2'	107° 26.5'	Buchan Bay
16	Mara River (76-K)	66° 59.9'	108° 38.25'	Wilberforce Hills; section stradles the lowermost part of Arctic Sound (76-N) sheet

legend for measured sections

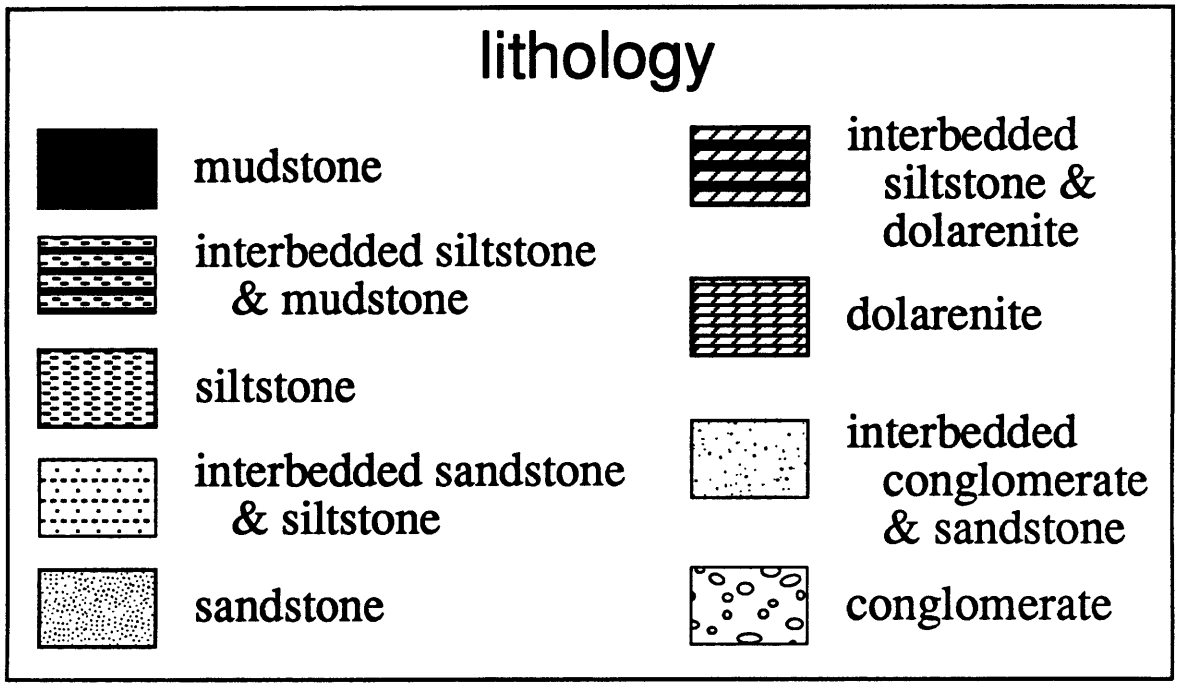

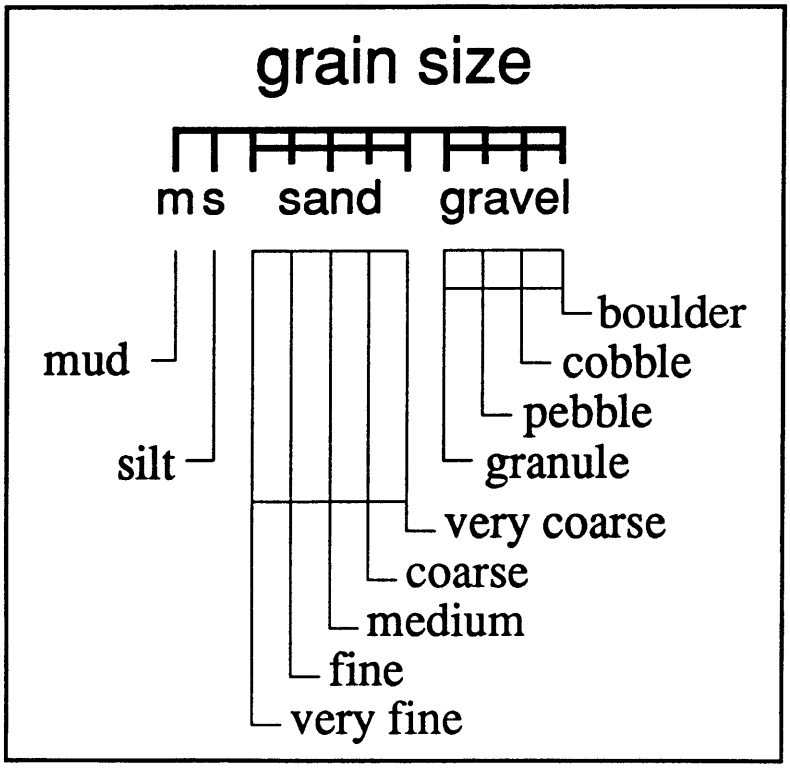

sedimentary structures

planar cross-bedding

trough cross-bedding

hummocky/swaley cross-stratification

wavy laminae

interference ripples

current, wave ripples

starved current, wave ripples

parallel laminae

low-angle cross laminae

graded beds

slump, soft-sediment deformation

gutter

paleocurrent indicators

unidirectional (e.g., current ripples, trough cross-beds)

bidirectional (e.g., wave ripple crests, gutter casts)

miscellaneous

mudstone clasts

lithologic sample

bulk sample for detrital zircon geochronology

Abbreviations used in measured section notes

grain size modifiers

mdst	mudstone
sltst	siltstone
	sand
sst	sandstone
(vf)	very fine sand
(f)	fine sand
(m)	medium sand
(c)	coarse sand
(vc)	very coarse
	gravel
cgl	conglomerate
(gran)	granule
(peb)	pebble
(cbl)	cobble
(bld)	boulder

bedding and cross-bedding

lam, lam'd	laminae, laminated
bds, bdg	beds, bedding
xlam	cross laminae
xbds, xbdg	cross beds, cross bedding

section 1: Bear Creek Hills

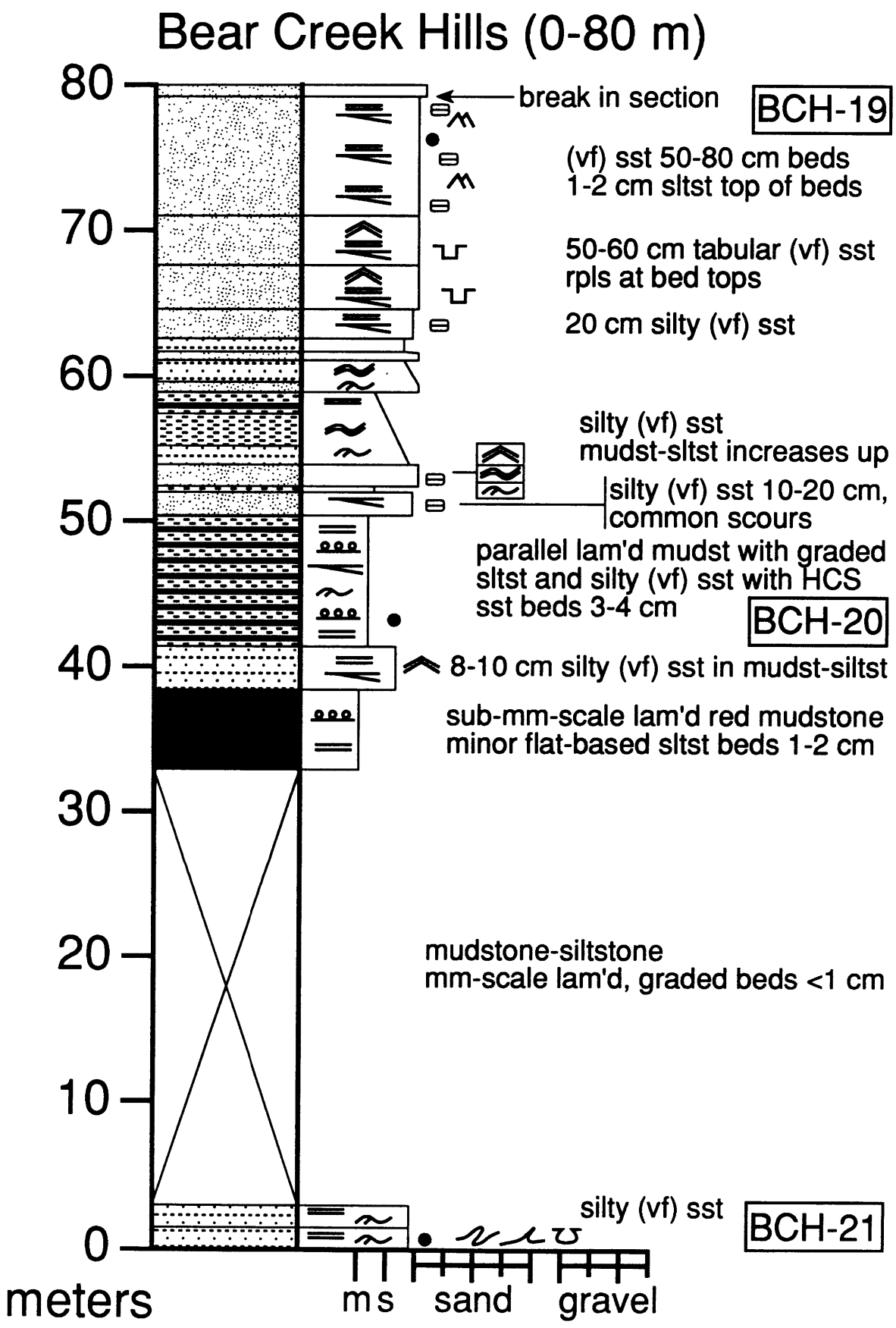
Bear Creek Hills (0-80 m)
80
70
60
50
40
30
20
10
0
meters
break in section
BCH-19
(vf) sst 50-80 cm beds
1-2 cm sltst top of beds
50-60 cm tabular (vf) sst
rpls at bed tops
20 cm silty (vf) sst
silty (vf) sst
mudst-sltst increases up
silty (vf) sst 10-20 cm,
common scours
parallel lam'd mudst with graded
sltst and silty (vf) sst with HCS
sst beds 3-4 cm
BCH-20
8-10 cm silty (vf) sst in mudst-siltst
sub-mm-scale lam'd red mudstone
minor flat-based sltst beds 1-2 cm
mudstone-siltstone
mm-scale lam'd, graded beds <1 cm
silty (vf) sst
BCH-21
ms
sand
gravel

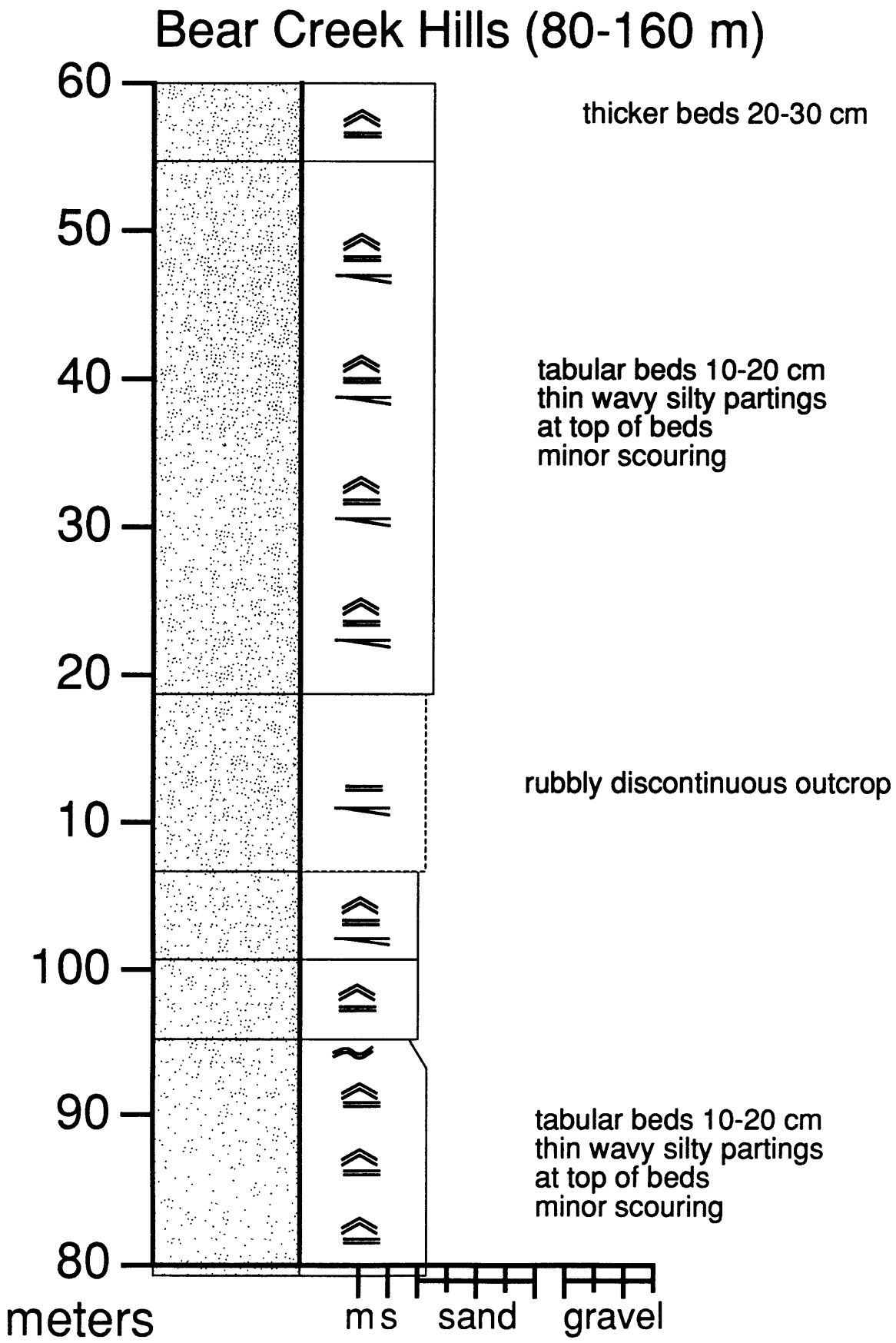
Bear Creek Hills (80-160 m)
60
50
40
30
20
10
100
90
80
meters
thicker beds 20-30 cm
tabular beds 10-20 cm
thin wavy silty partings
at top of beds
minor scouring
rubbly discontinuous outcrop
tabular beds 10-20 cm
thin wavy silty partings
at top of beds
minor scouring
ms
sand
gravel

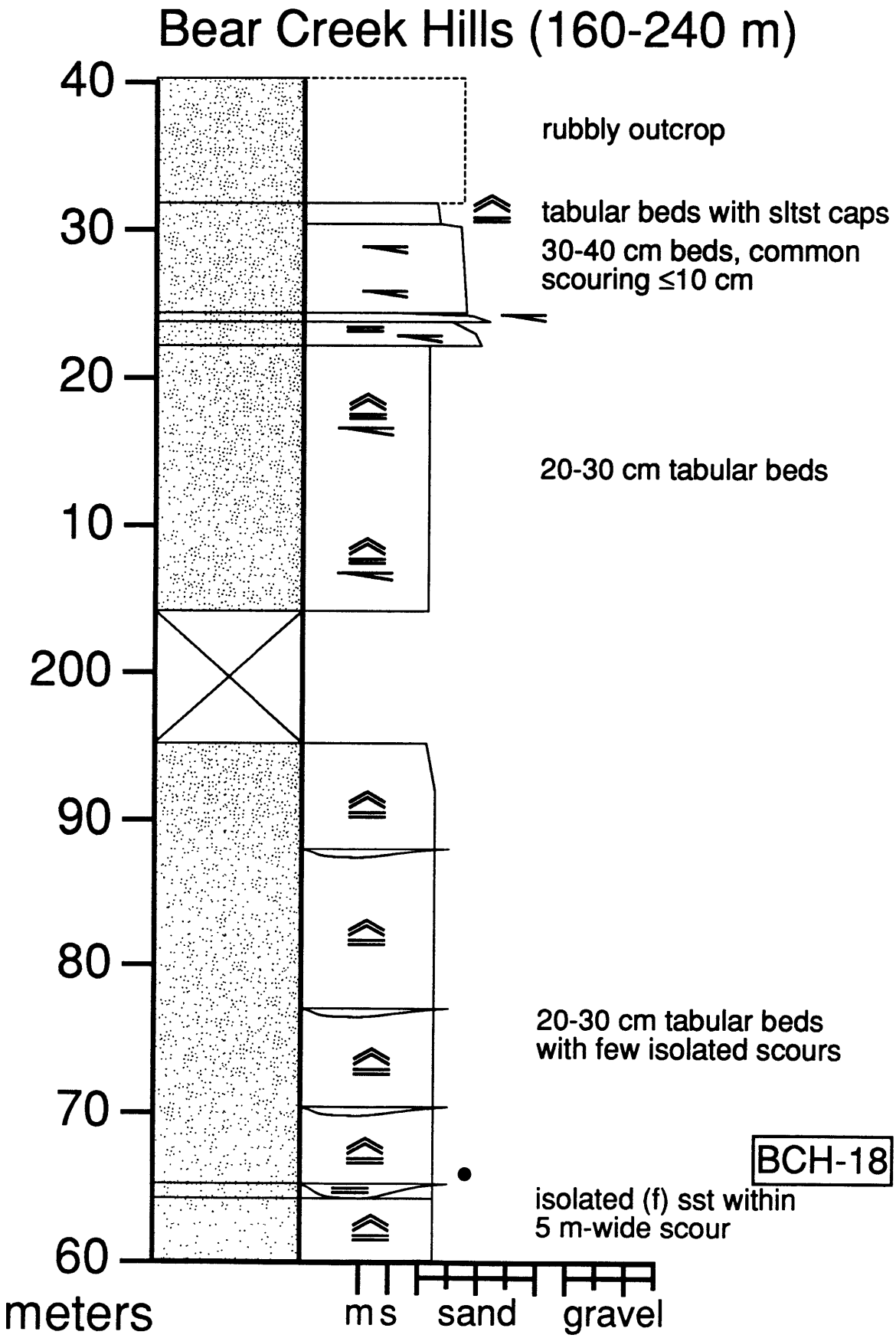
Bear Creek Hills (160-240 m)
40
30
20
10
200
90
80
70
60
meters
rubbly outcrop
tabular beds with sltst caps
30-40 cm beds, common
scouring ≤10 cm
20-30 cm tabular beds
20-30 cm tabular beds
with few isolated scours
BCH-18
isolated (f) sst within
5 m-wide scour
ms
sand
gravel

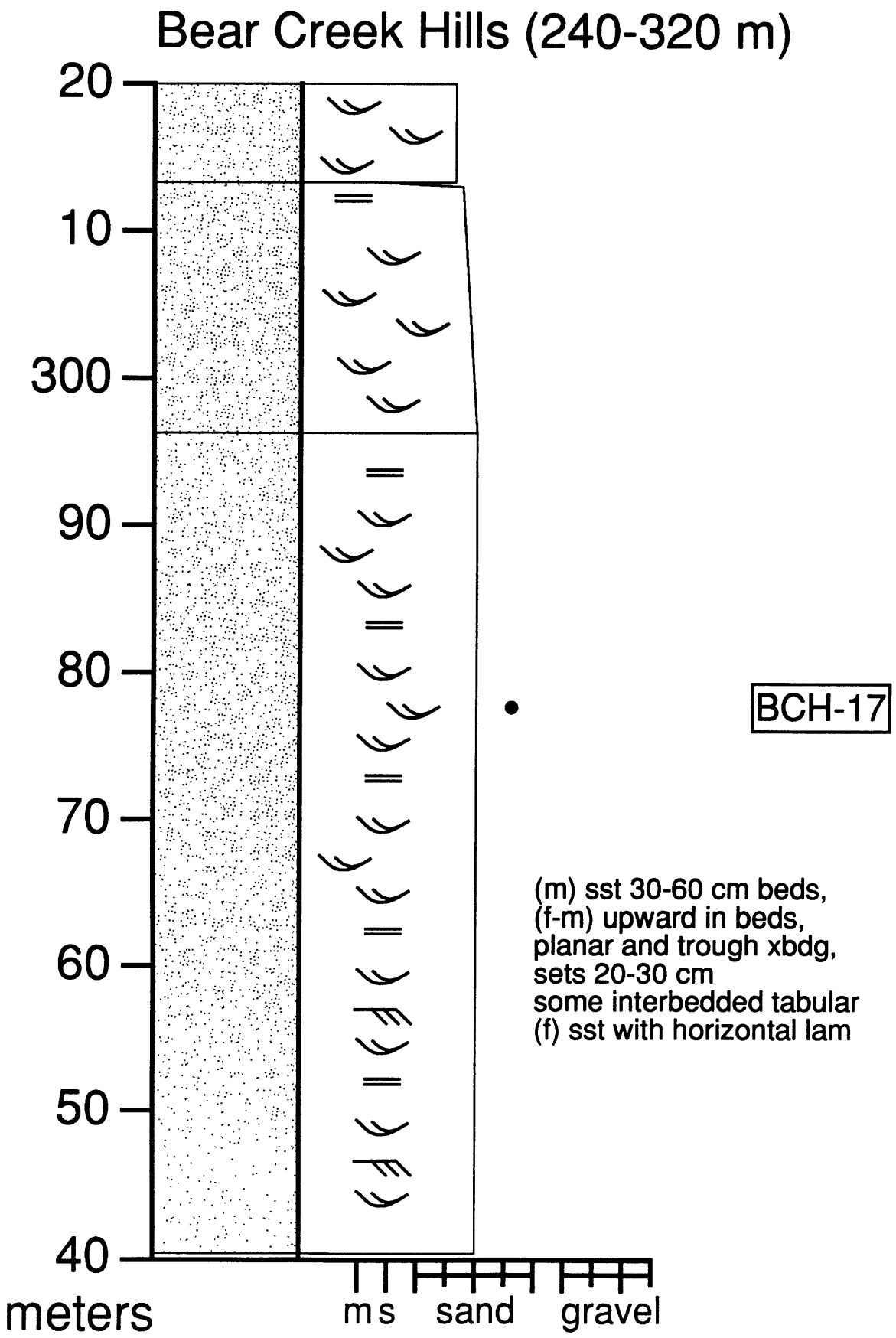
Bear Creek Hills (240-320 m)
20
10
300
90
80
70
60
50
40
meters
m s
sand
gravel
BCH-17
(m) sst 30-60 cm beds,
(f-m) upward in beds,
planar and trough xbdg,
sets 20-30 cm
some interbedded tabular
(f) sst with horizontal lam

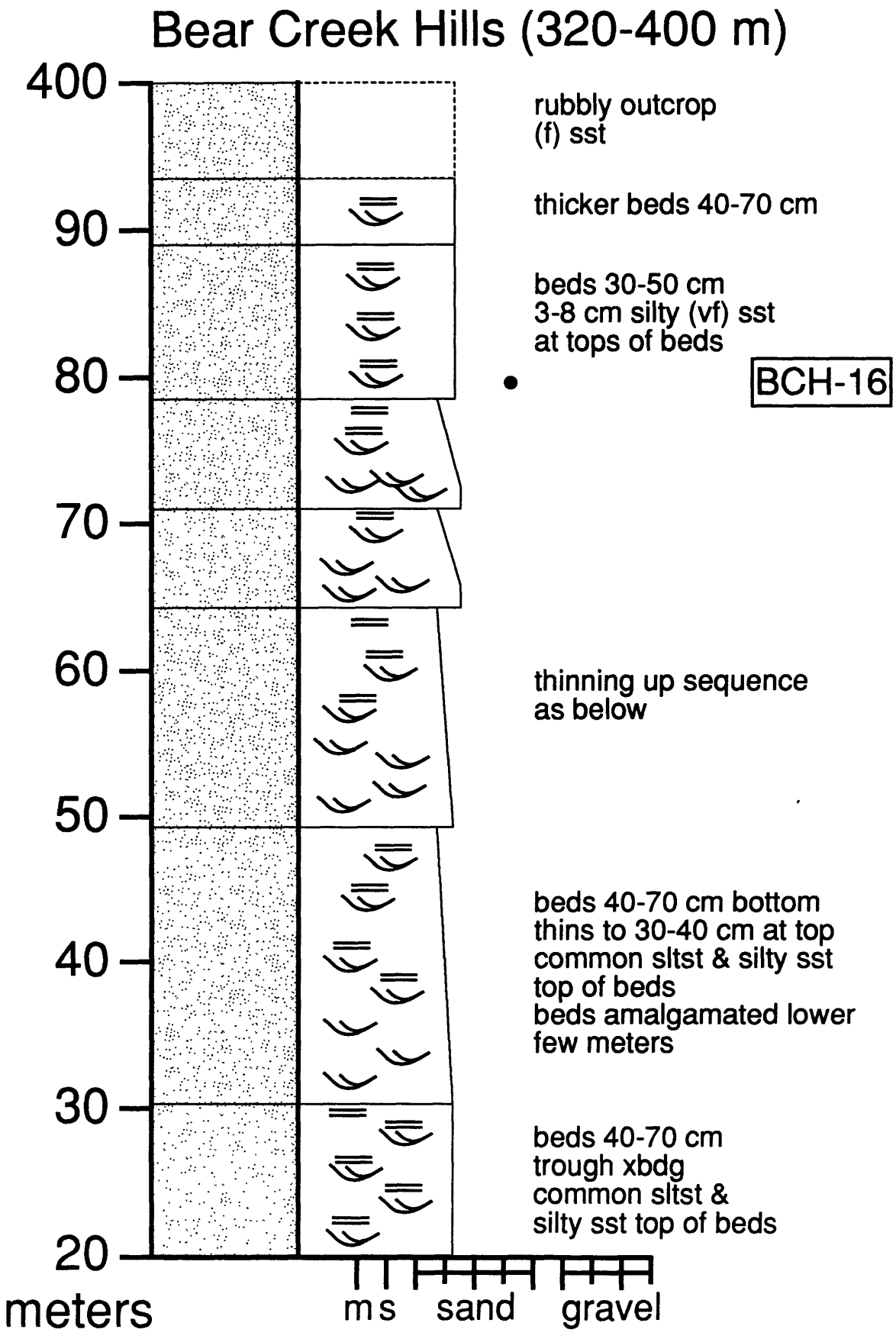
Bear Creek Hills (320-400 m)
400
90
80
70
60
50
40
30
20
meters
rubbly outcrop
(f) sst
thicker beds 40-70 cm
beds 30-50 cm
3-8 cm silty (vf) sst
at tops of beds
BCH-16
thinning up sequence
as below
beds 40-70 cm bottom
thins to 30-40 cm at top
common sltst & silty sst
top of beds
beds amalgamated lower
few meters
beds 40-70 cm
trough xbdg
common sltst &
silty sst top of beds
m s
sand
gravel

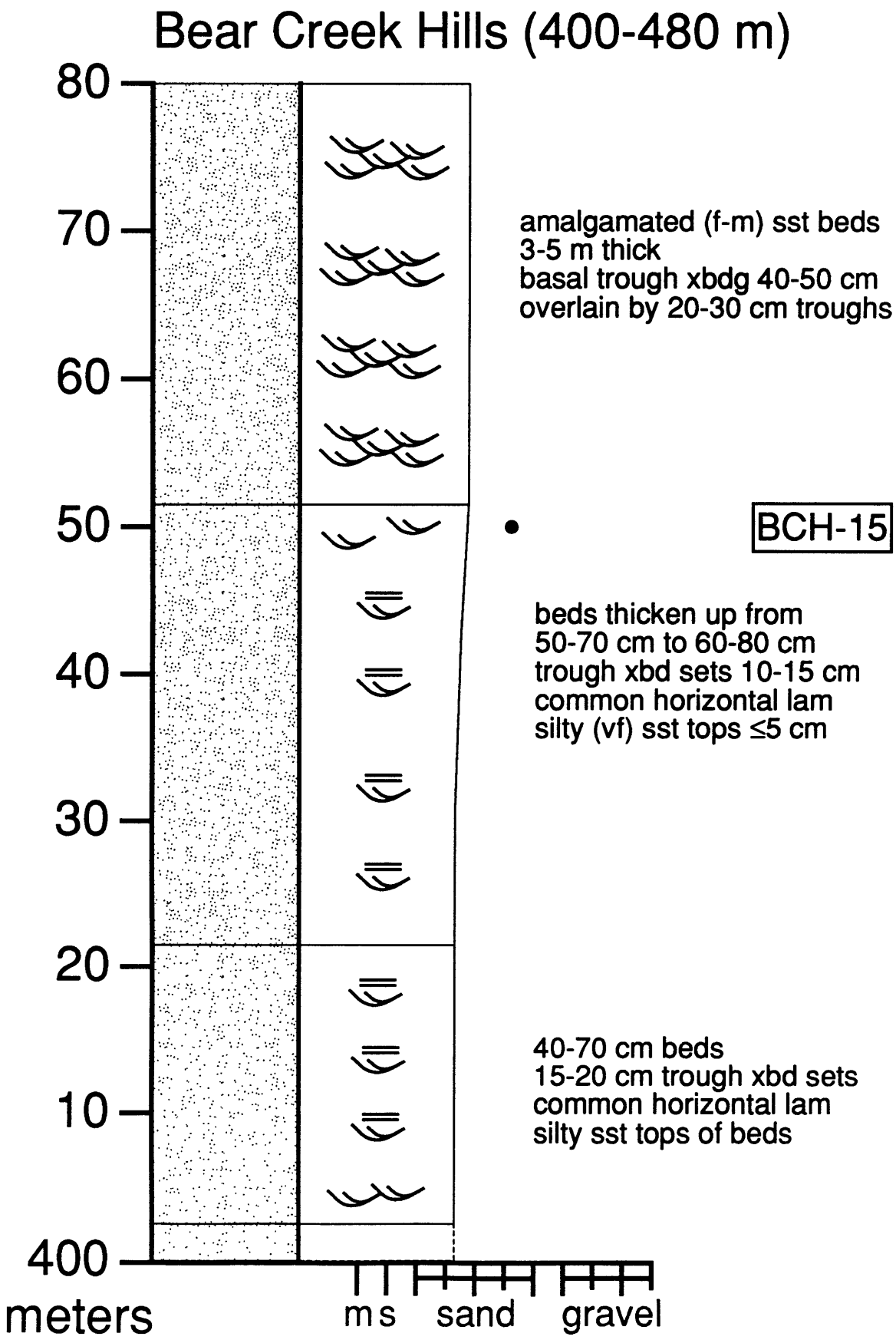
Bear Creek Hills (400-480 m)
80
70
60
50
40
30
20
10
400
meters
amalgamated (f-m) sst beds
3-5 m thick
basal trough xbdg 40-50 cm
overlain by 20-30 cm troughs
BCH-15
beds thicken up from
50-70 cm to 60-80 cm
trough xbd sets 10-15 cm
common horizontal lam
silty (vf) sst tops ≤5 cm
40-70 cm beds
15-20 cm trough xbd sets
common horizontal lam
silty sst tops of beds
ms
sand
gravel

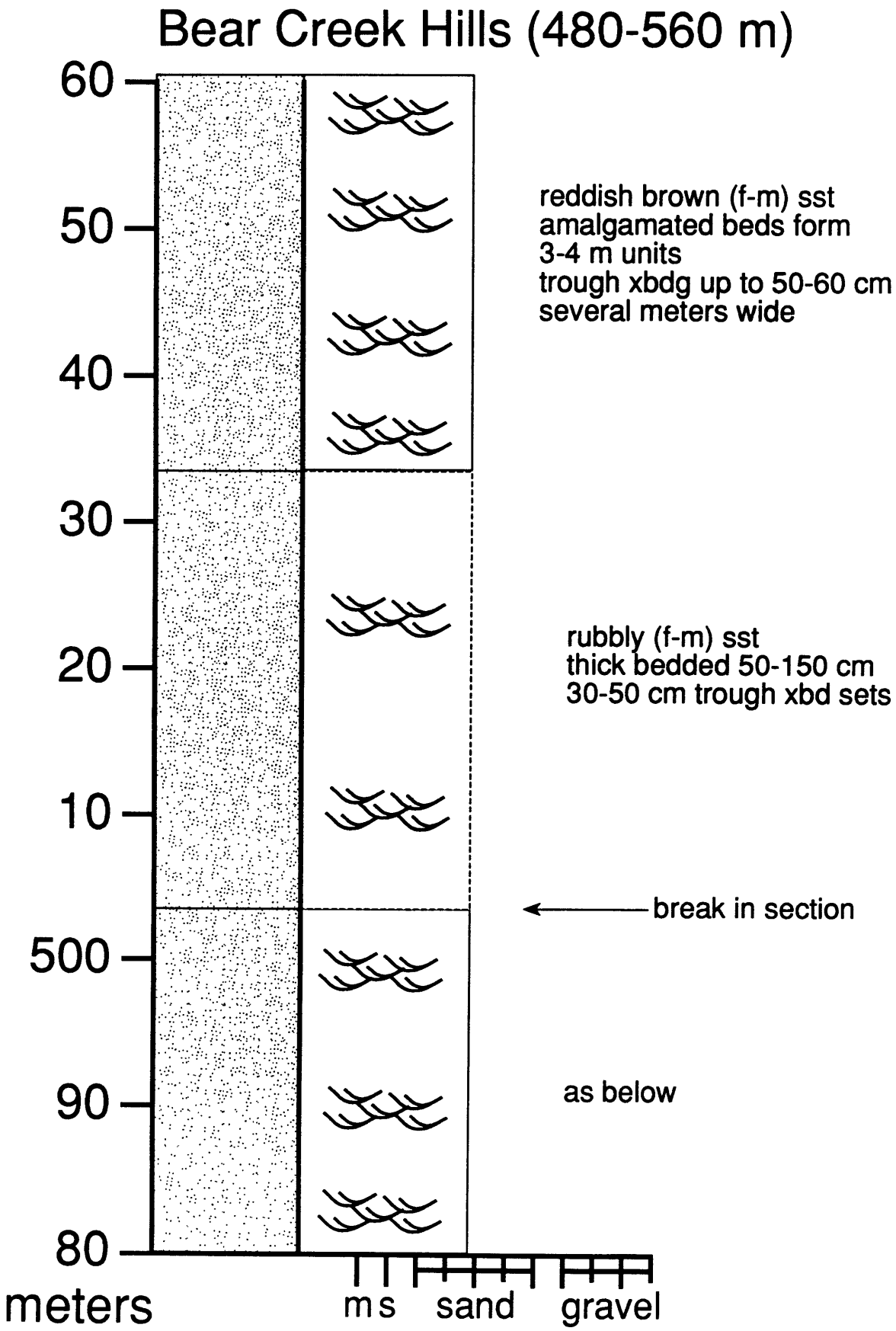
Bear Creek Hills (480-560 m)
60
50
40
30
20
10
500
90
80
meters
m s
sand
gravel
reddish brown (f-m) sst
amalgamated beds form
3-4 m units
trough xbdg up to 50-60 cm
several meters wide
rubbly (f-m) sst
thick bedded 50-150 cm
30-50 cm trough xbd sets
break in section
as below

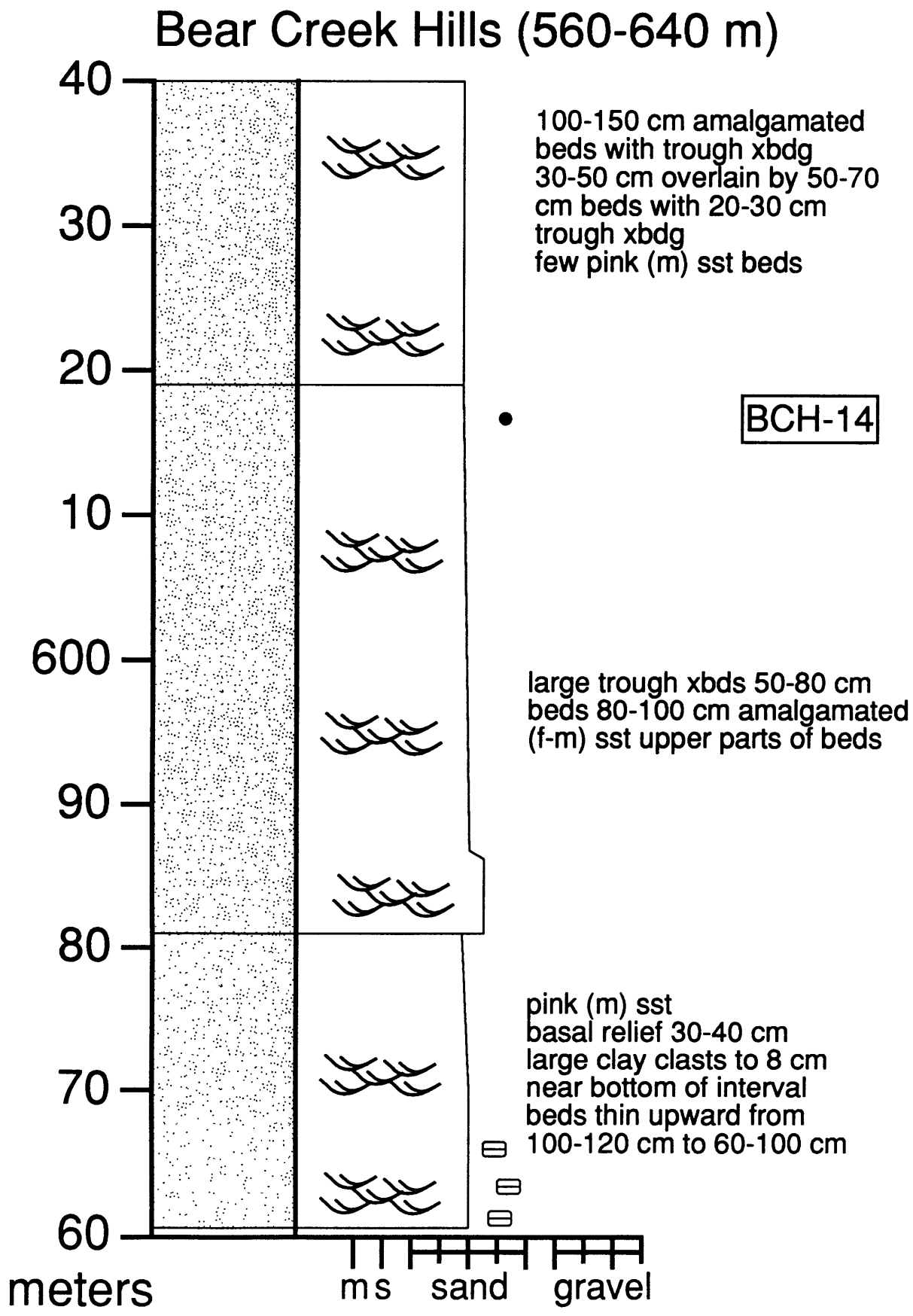
Bear Creek Hills (560-640 m)
40
30
20
10
600
90
80
70
60
meters
100-150 cm amalgamated
beds with trough xbdg
30-50 cm overlain by 50-70
cm beds with 20-30 cm
trough xbdg
few pink (m) sst beds
BCH-14
large trough xbds 50-80 cm
beds 80-100 cm amalgamated
(f-m) sst upper parts of beds
pink (m) sst
basal relief 30-40 cm
large clay clasts to 8 cm
near bottom of interval
beds thin upward from
100-120 cm to 60-100 cm
m s
sand
gravel

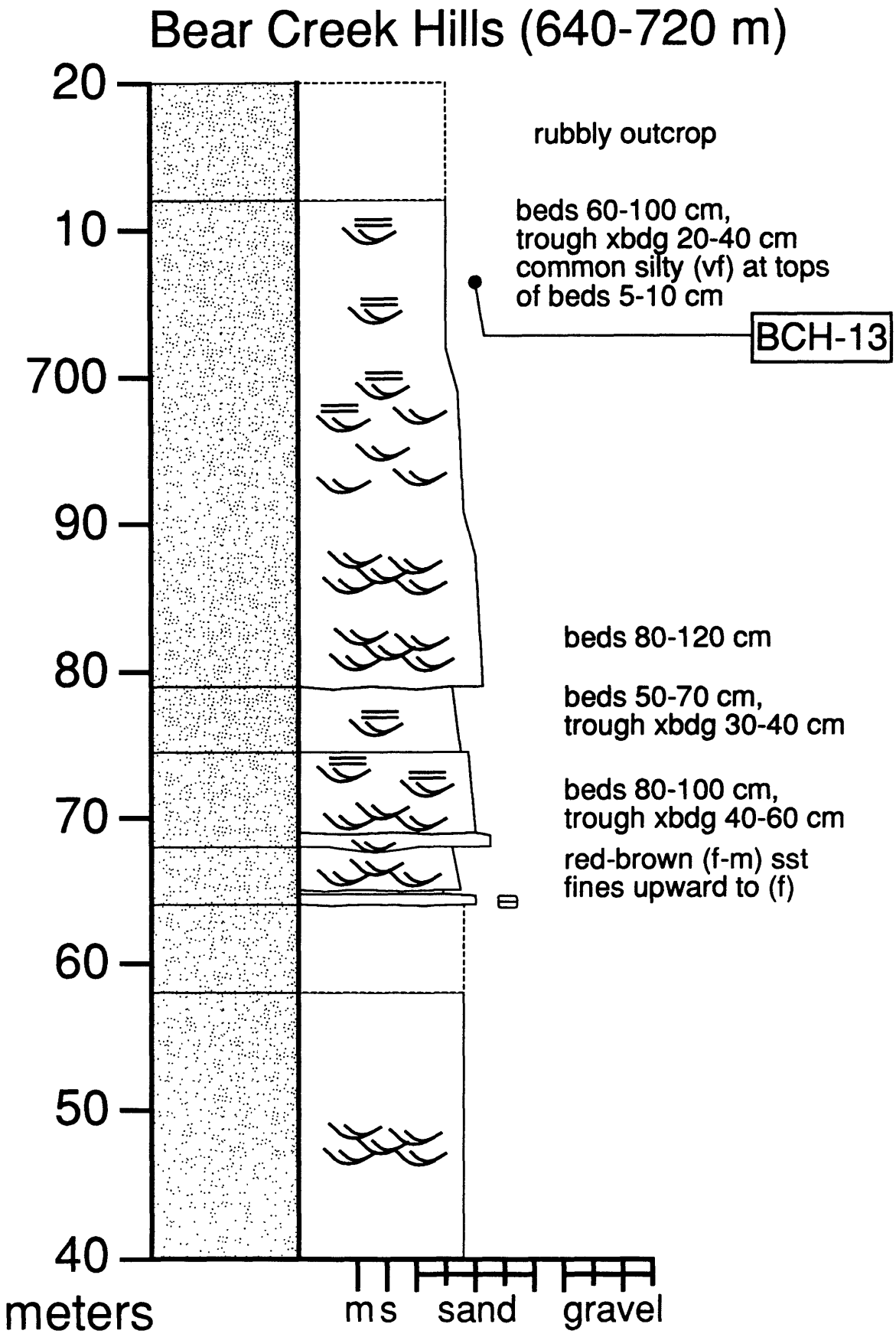
Bear Creek Hills (640-720 m)
20
10
700
90
80
70
60
50
40
meters
rubbly outcrop
beds 60-100 cm,
trough xbdg 20-40 cm
common silty (vf) at tops
of beds 5-10 cm
BCH-13
beds 80-120 cm
beds 50-70 cm,
trough xbdg 30-40 cm
beds 80-100 cm,
trough xbdg 40-60 cm
red-brown (f-m) sst
fines upward to (f)
m s
sand
gravel

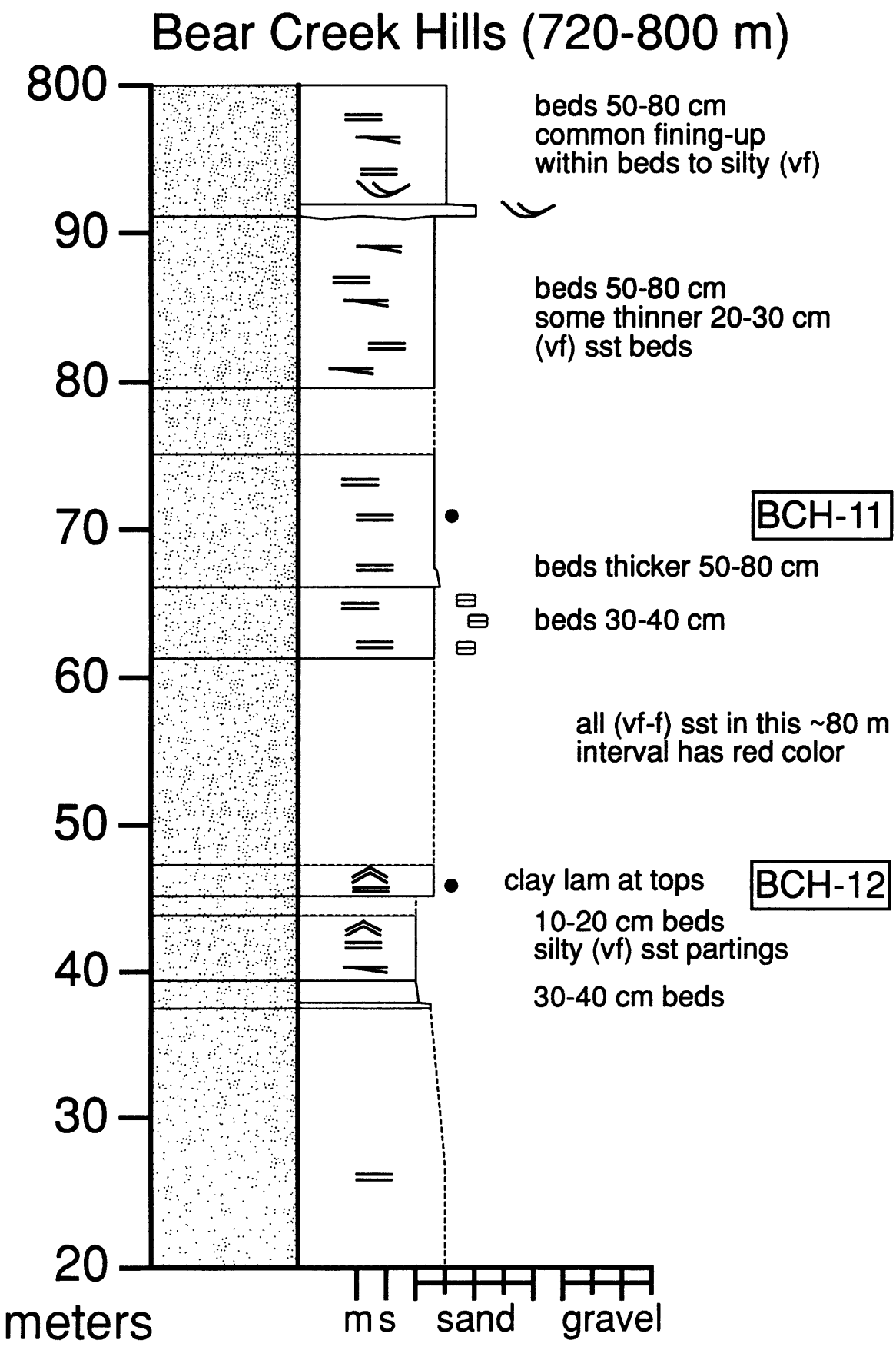
Bear Creek Hills (720-800 m)
800
90
80
70
60
50
40
30
20
meters
beds 50-80 cm
common fining-up
within beds to silty (vf)
beds 50-80 cm
some thinner 20-30 cm
(vf) sst beds
BCH-11
beds thicker 50-80 cm
beds 30-40 cm
all (vf-f) sst in this ~80 m
interval has red color
clay lam at tops
BCH-12
10-20 cm beds
silty (vf) sst partings
30-40 cm beds
ms
sand
gravel

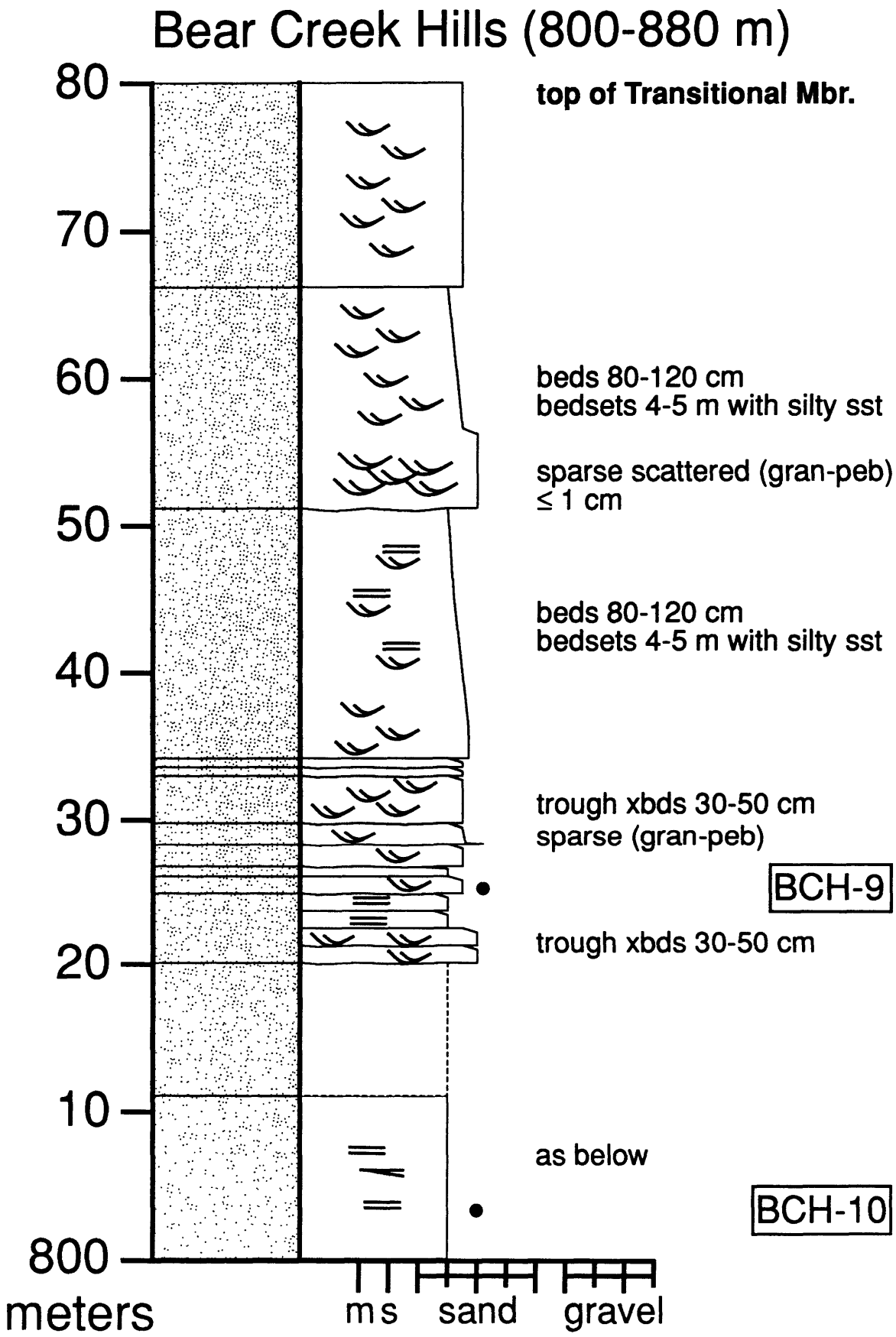
Bear Creek Hills (800-880 m)
80
70
60
50
40
30
20
10
800
meters
top of Transitional Mbr.
beds 80-120 cm
bedsets 4-5 m with silty sst
sparse scattered (gran-peb)
≤ 1 cm
beds 80-120 cm
bedsets 4-5 m with silty sst
trough xbds 30-50 cm
sparse (gran-peb)
BCH-9
trough xbds 30-50 cm
as below
BCH-10
ms
sand
gravel

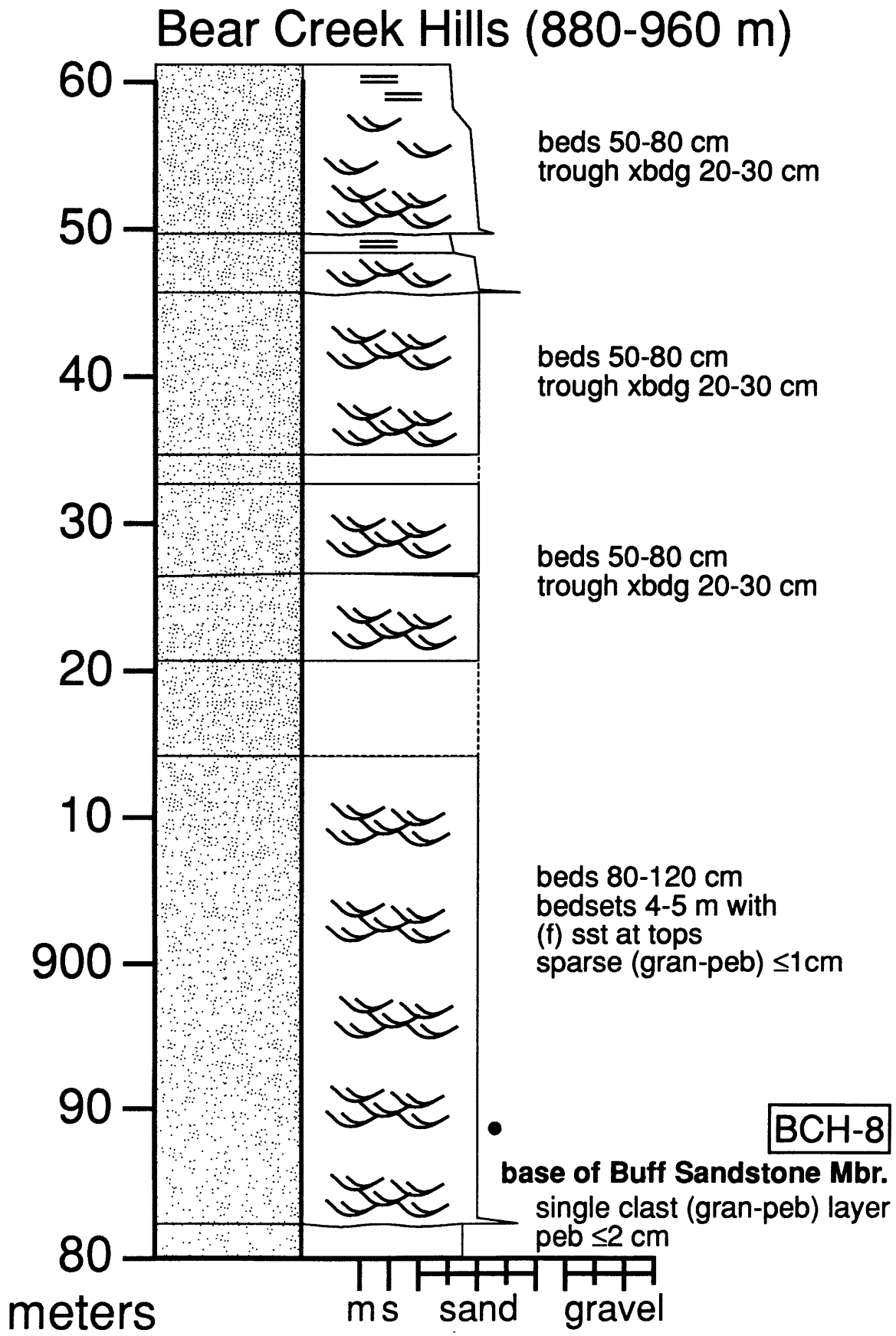
Bear Creek Hills (880-960 m)
60
50
40
30
20
10
900
90
80
meters
beds 50-80 cm
trough xbdg 20-30 cm
beds 50-80 cm
trough xbdg 20-30 cm
beds 50-80 cm
trough xbdg 20-30 cm
beds 80-120 cm
bedsets 4-5 m with
(f) sst at tops
sparse (gran-peb) ≤1cm
BCH-8
base of Buff Sandstone Mbr.
single clast (gran-peb) layer
peb ≤2 cm
m s
sand
gravel

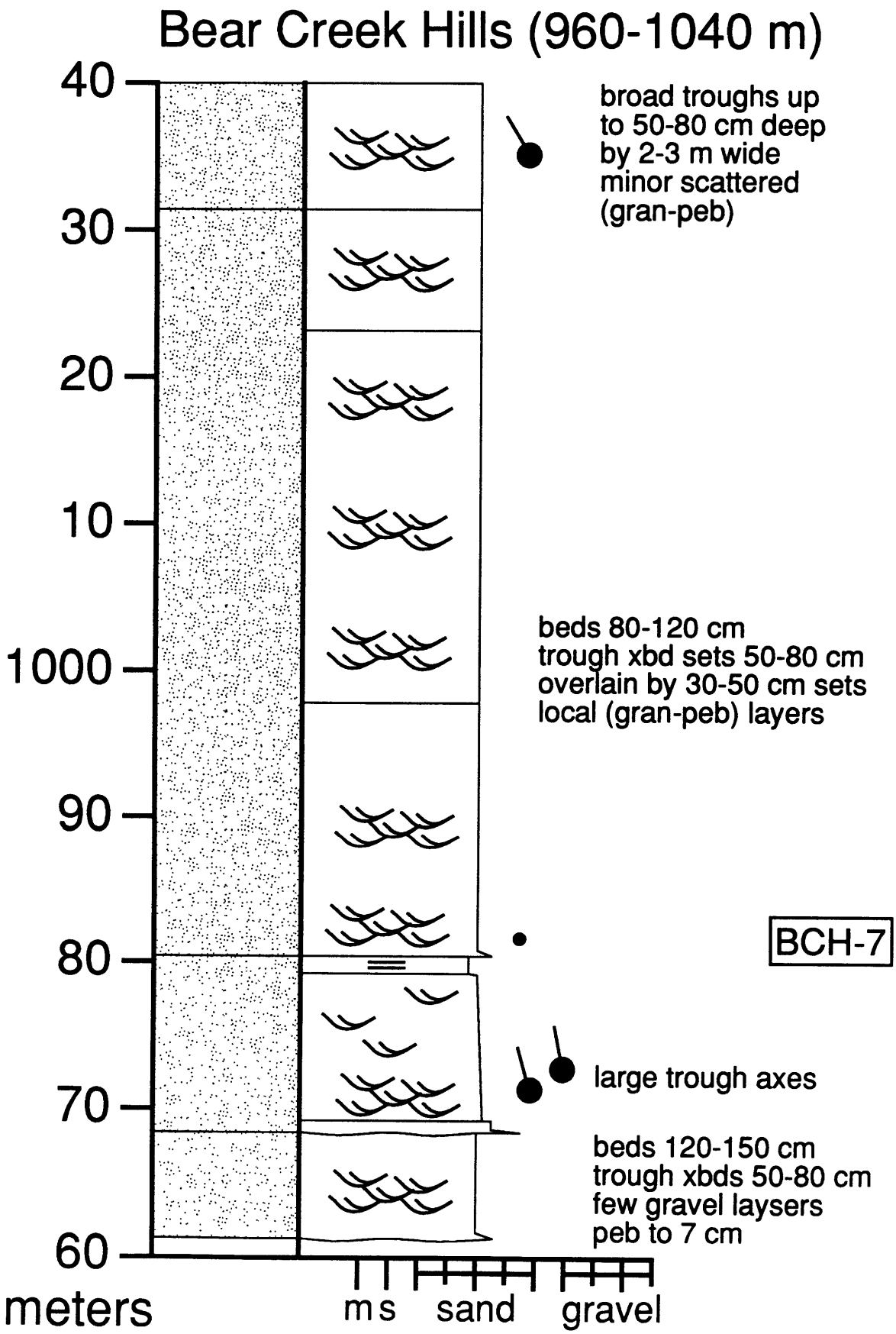
Bear Creek Hills (960-1040 m)
40
30
20
10
1000
90
80
70
60
meters
broad troughs up
to 50-80 cm deep
by 2-3 m wide
minor scattered
(gran-peb)
beds 80-120 cm
trough xbd sets 50-80 cm
overlain by 30-50 cm sets
local (gran-peb) layers
BCH-7
large trough axes
beds 120-150 cm
trough xbds 50-80 cm
few gravel laysers
peb to 7 cm
ms
sand
gravel

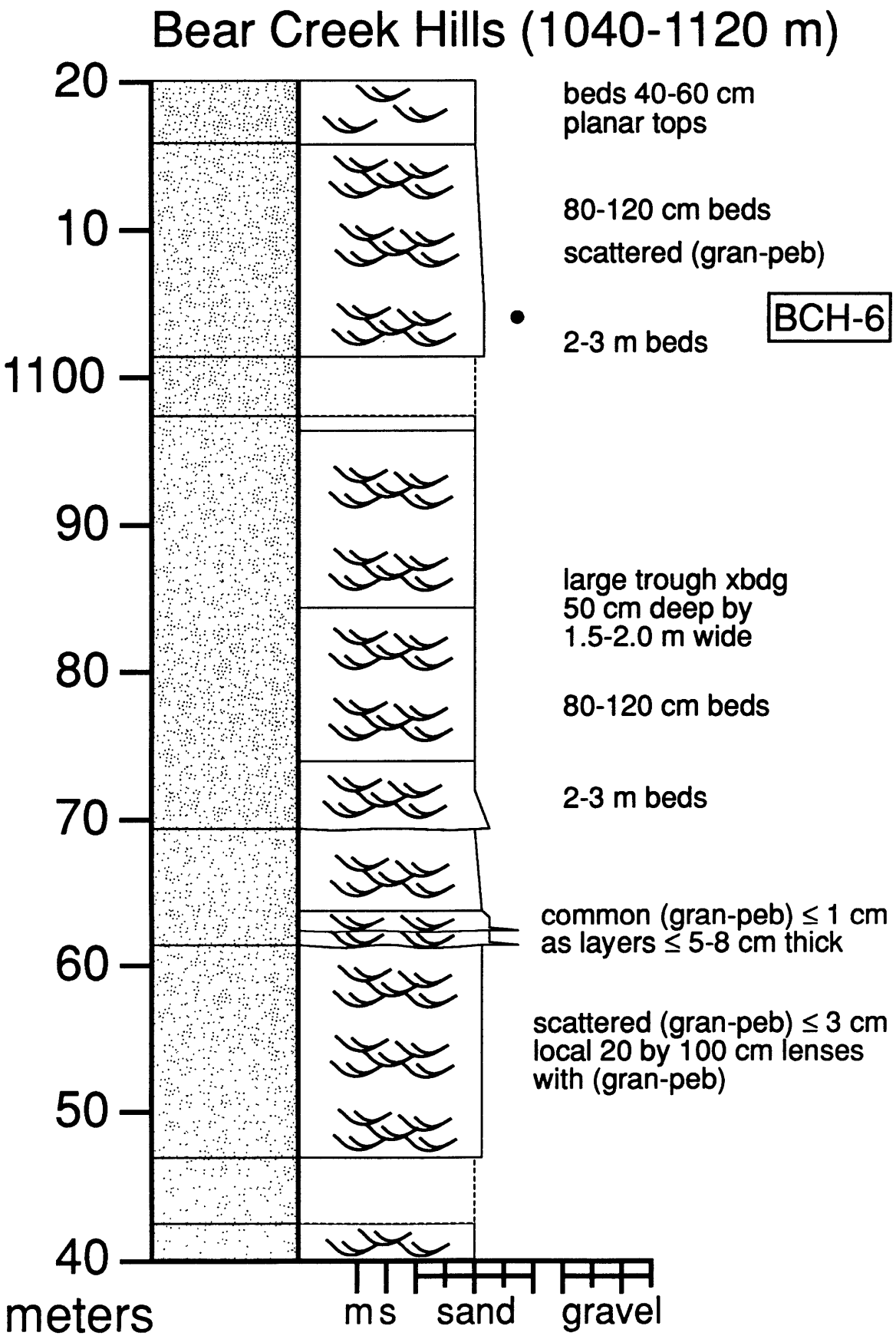
Bear Creek Hills (1040-1120 m)
20
10
1100
90
80
70
60
50
40
meters
beds 40-60 cm
planar tops
80-120 cm beds
scattered (gran-peb)
BCH-6
2-3 m beds
large trough xbdg
50 cm deep by
1.5-2.0 m wide
80-120 cm beds
2-3 m beds
common (gran-peb) ≤ 1 cm
as layers ≤ 5-8 cm thick
scattered (gran-peb) ≤ 3 cm
local 20 by 100 cm lenses
with (gran-peb)
m s
sand
gravel

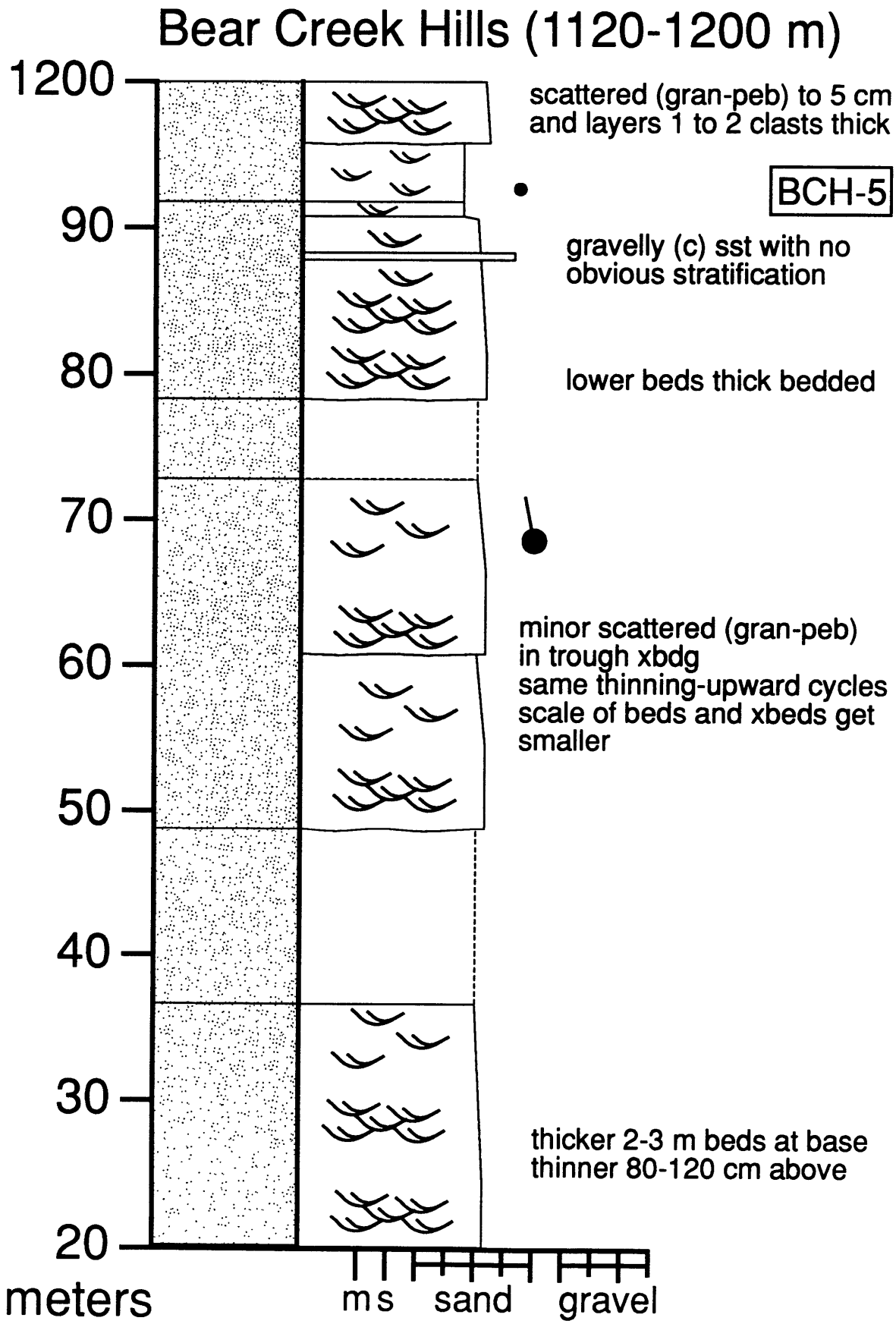
Bear Creek Hills (1120-1200 m)
1200
90
80
70
60
50
40
30
20
meters
scattered (gran-peb) to 5 cm
and layers 1 to 2 clasts thick
BCH-5
gravelly (c) sst with no
obvious stratification
lower beds thick bedded
minor scattered (gran-peb)
in trough xbdg
same thinning-upward cycles
scale of beds and xbeds get
smaller
thicker 2-3 m beds at base
thinner 80-120 cm above
ms
sand
gravel

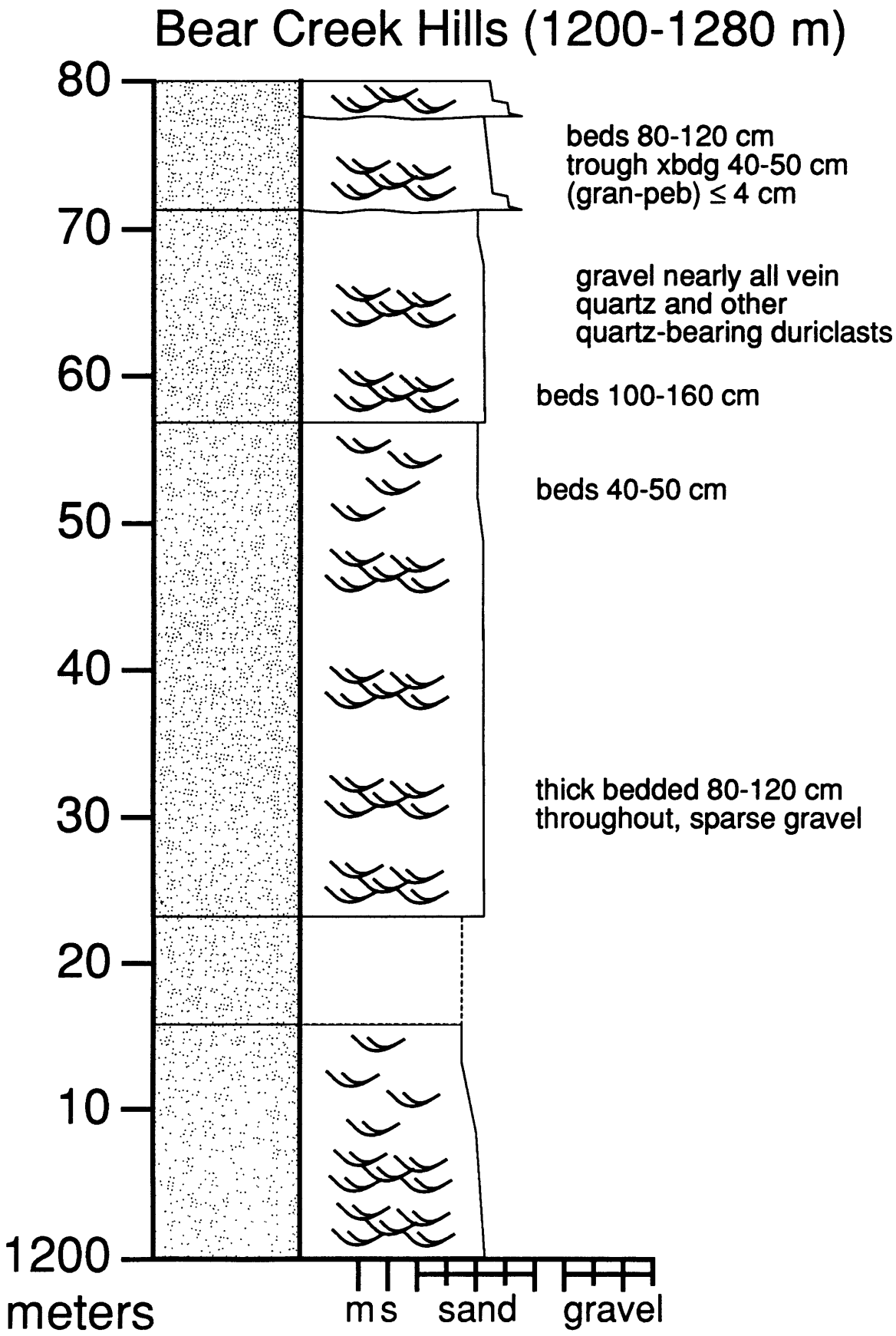
Bear Creek Hills (1200-1280 m)
80
70
60
50
40
30
20
10
1200
meters
beds 80-120 cm
trough xbdg 40-50 cm
(gran-peb) ≤ 4 cm
gravel nearly all vein
quartz and other
quartz-bearing duriclasts
beds 100-160 cm
beds 40-50 cm
thick bedded 80-120 cm
throughout, sparse gravel
m s
sand
gravel

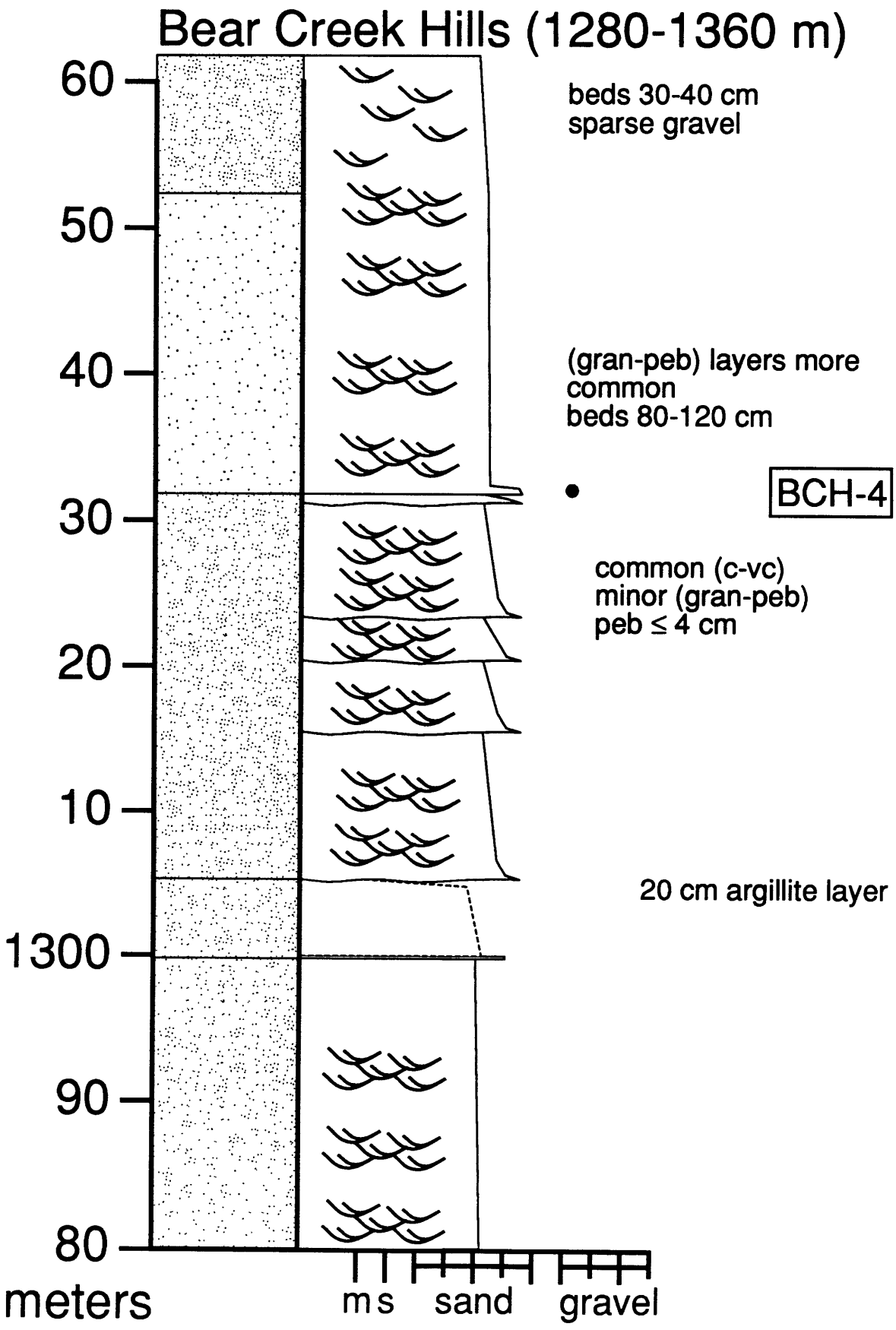
Bear Creek Hills (1280-1360 m)
60
50
40
30
20
10
1300
90
80
meters
ms
sand
gravel
beds 30-40 cm
sparse gravel
(gran-peb) layers more common
beds 80-120 cm
BCH-4
common (c-vc)
minor (gran-peb)
peb ≤ 4 cm
20 cm argillite layer

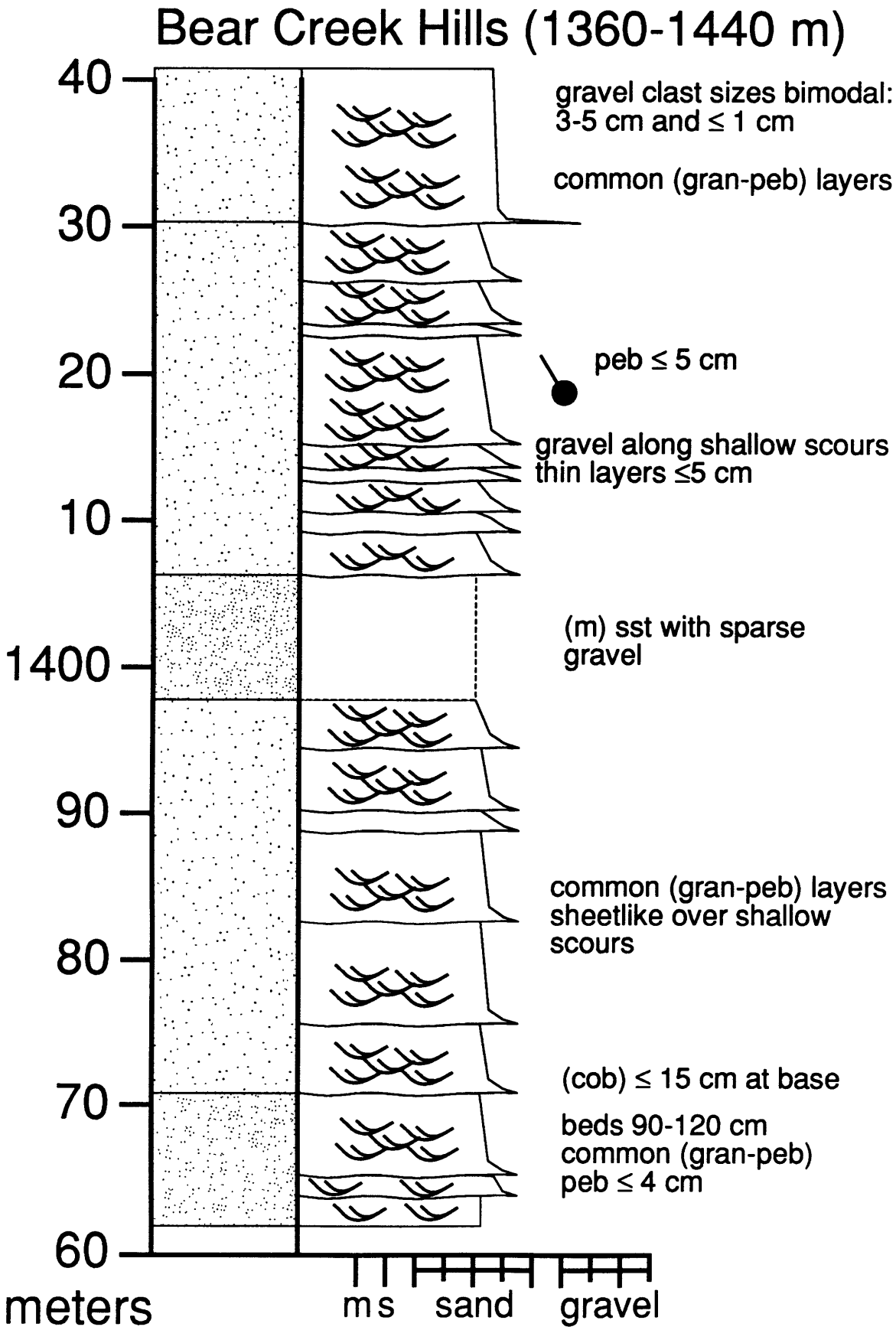
Bear Creek Hills (1360-1440 m)
40
30
20
10
1400
90
80
70
60
meters
gravel clast sizes bimodal:
3-5 cm and ≤ 1 cm
common (gran-peb) layers
peb ≤ 5 cm
gravel along shallow scours
thin layers ≤5 cm
(m) sst with sparse
gravel
common (gran-peb) layers
sheetlike over shallow
scours
(cob) ≤ 15 cm at base
beds 90-120 cm
common (gran-peb)
peb ≤ 4 cm
ms
sand
gravel

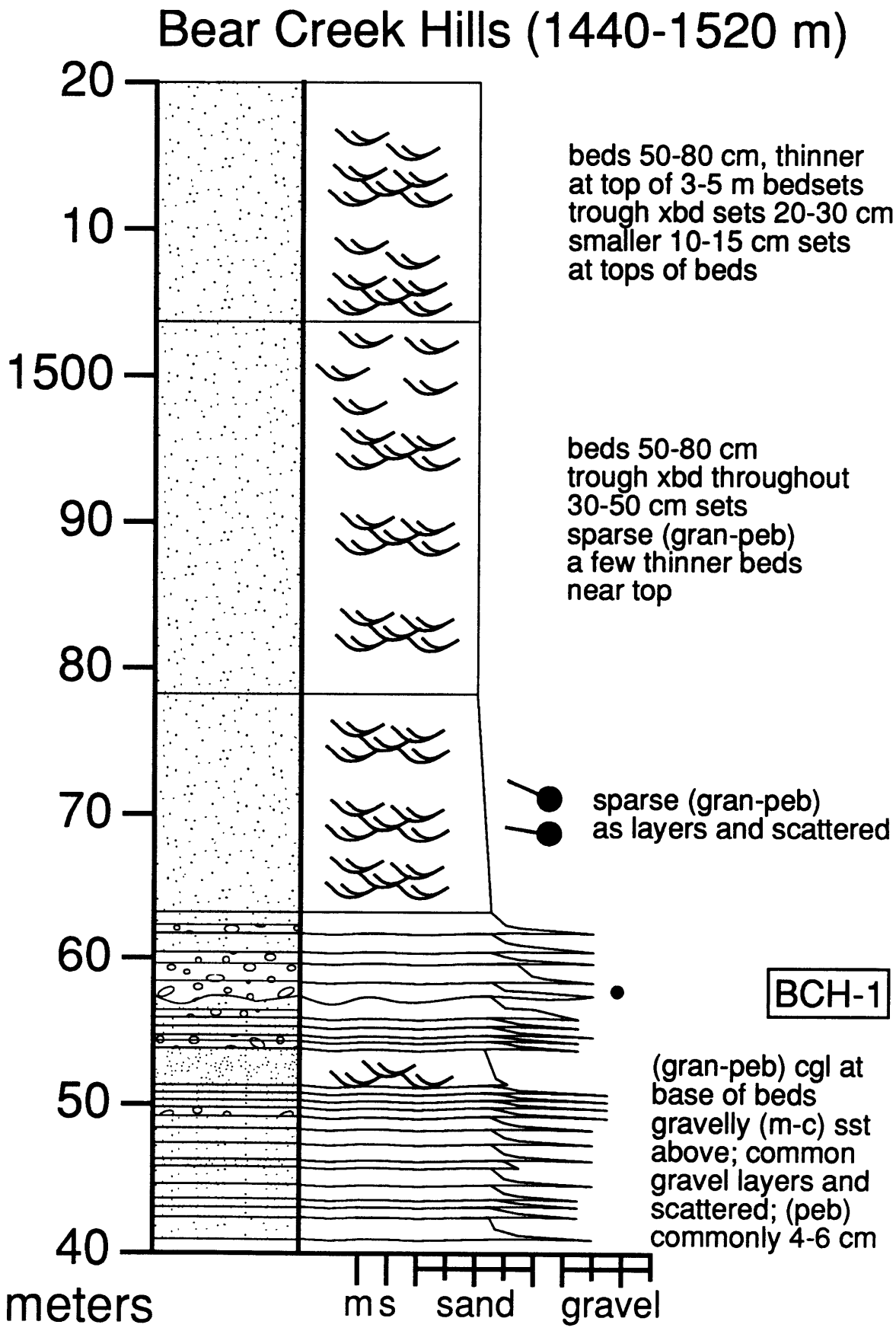
Bear Creek Hills (1440-1520 m)
20
10
1500
90
80
70
60
50
40
meters
beds 50-80 cm, thinner
at top of 3-5 m bedsets
trough xbd sets 20-30 cm
smaller 10-15 cm sets
at tops of beds
beds 50-80 cm
trough xbd throughout
30-50 cm sets
sparse (gran-peb)
a few thinner beds
near top
sparse (gran-peb)
as layers and scattered
BCH-1
(gran-peb) cgl at
base of beds
gravelly (m-c) sst
above; common
gravel layers and
scattered; (peb)
commonly 4-6 cm
ms
sand
gravel

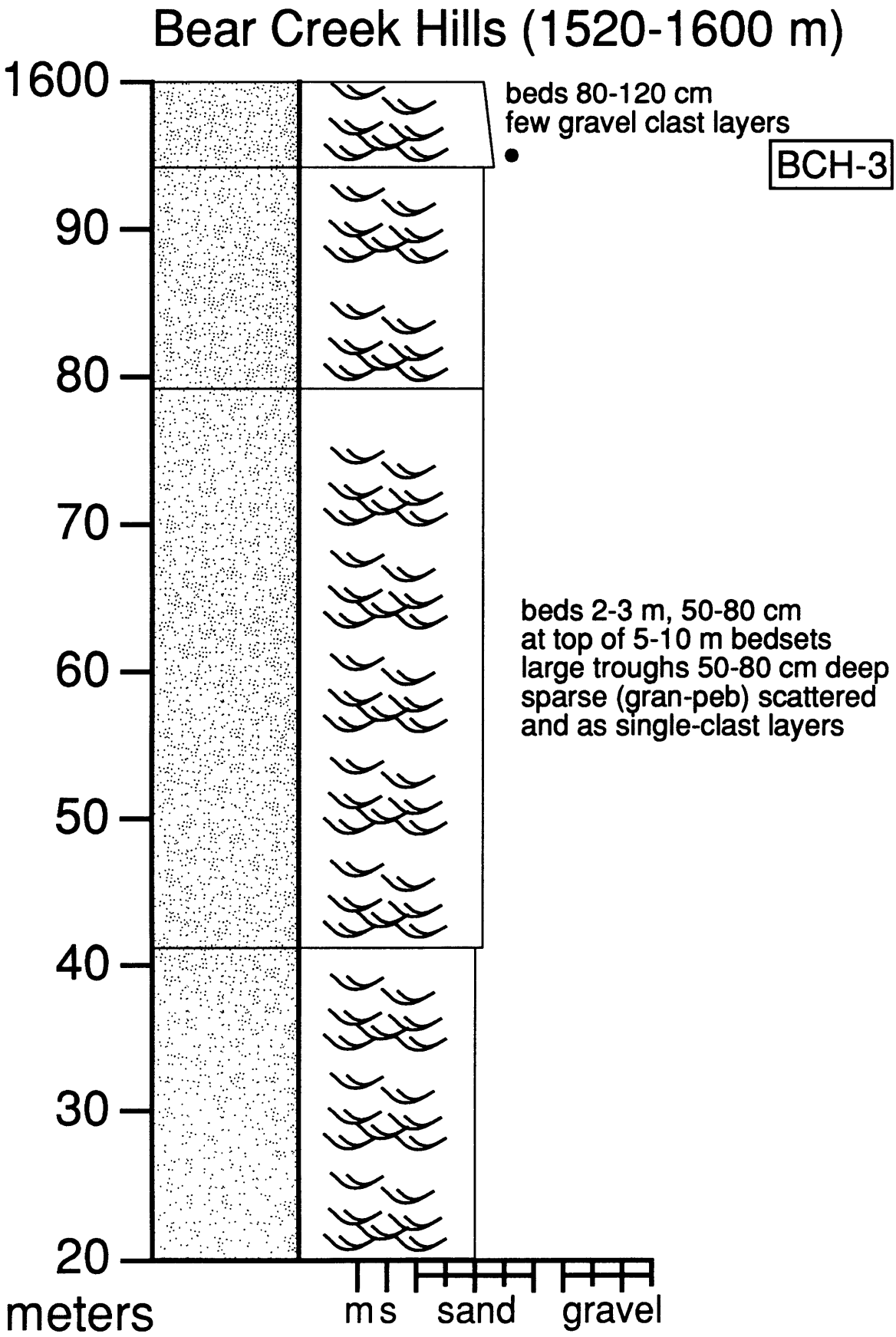
Bear Creek Hills (1520-1600 m)
1600
90
80
70
60
50
40
30
20
meters
beds 80-120 cm
few gravel clast layers
BCH-3
beds 2-3 m, 50-80 cm
at top of 5-10 m bedsets
large troughs 50-80 cm deep
sparse (gran-peb) scattered
and as single-clast layers
m s
sand
gravel

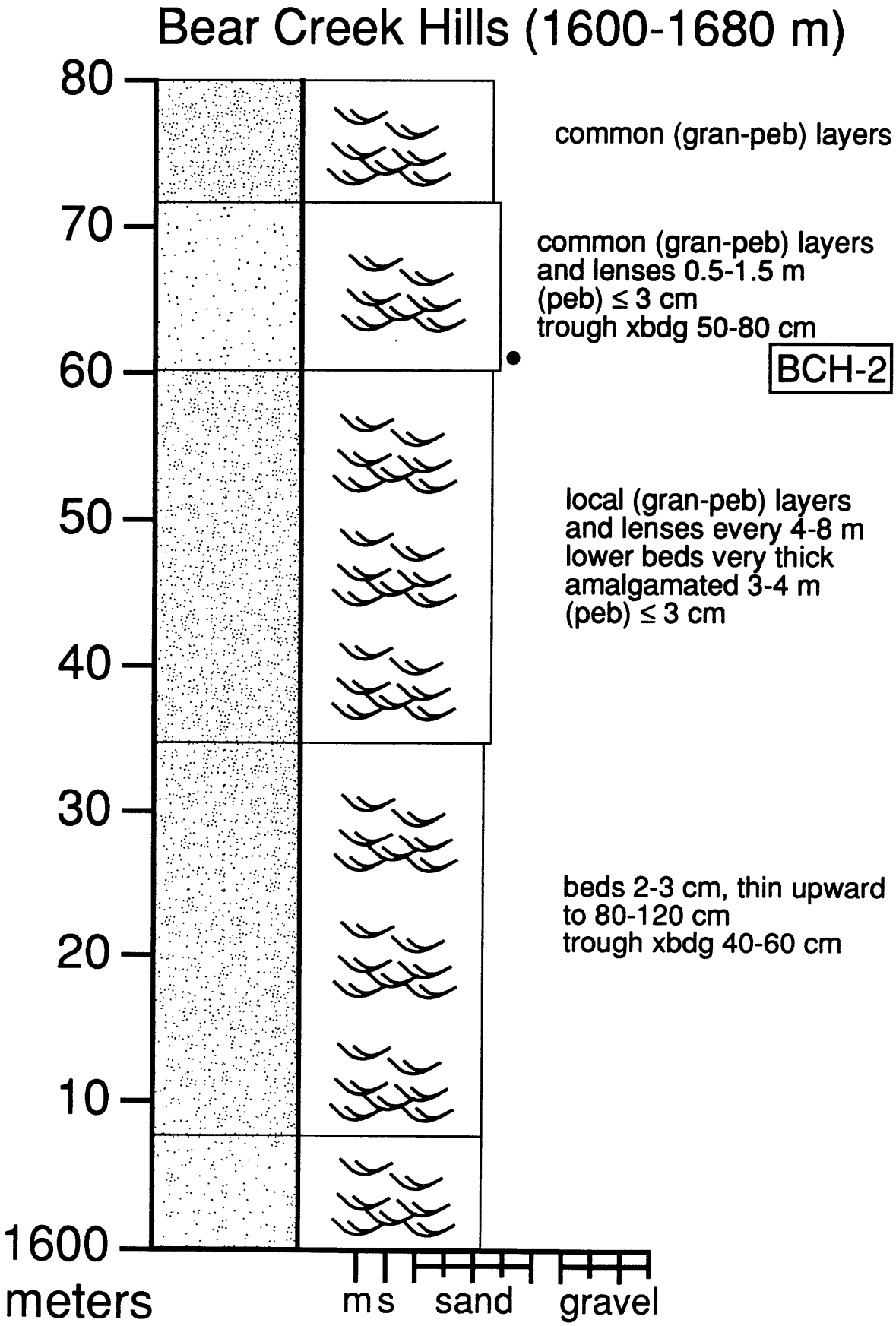
Bear Creek Hills (1600-1680 m)
80
70
60
50
40
30
20
10
1600
meters
common (gran-peb) layers
common (gran-peb) layers
and lenses 0.5-1.5 m
(peb) ≤ 3 cm
trough xbdg 50-80 cm
BCH-2
local (gran-peb) layers
and lenses every 4-8 m
lower beds very thick
amalgamated 3-4 m
(peb) ≤ 3 cm
beds 2-3 cm, thin upward
to 80-120 cm
trough xbdg 40-60 cm
m s
sand
gravel

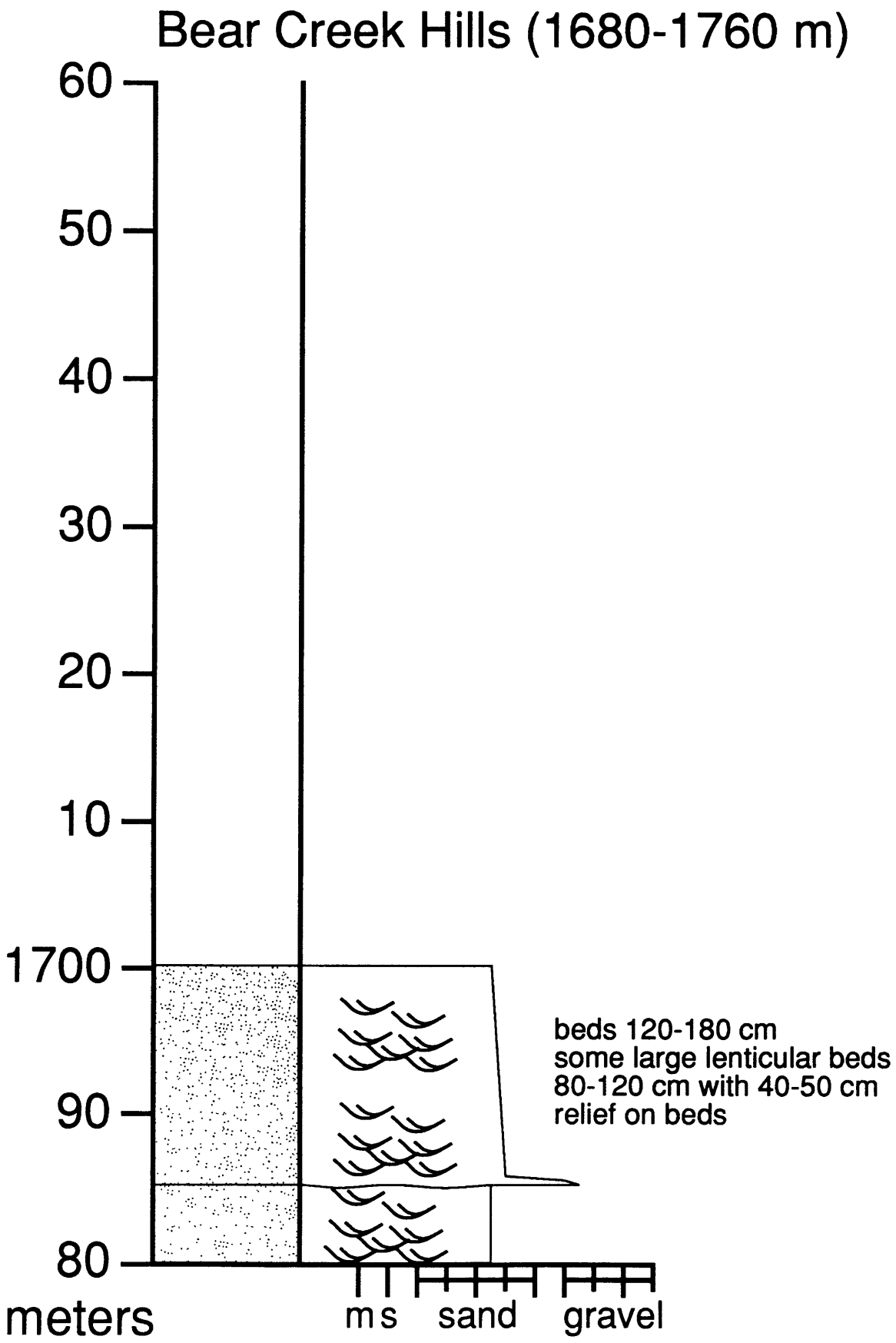
Bear Creek Hills (1680-1760 m)
60
50
40
30
20
10
1700
90
80
meters
beds 120-180 cm
some large lenticular beds
80-120 cm with 40-50 cm
relief on beds
m s
sand
gravel

section 2: South TInney Hills & south Tinney Hills-upper section

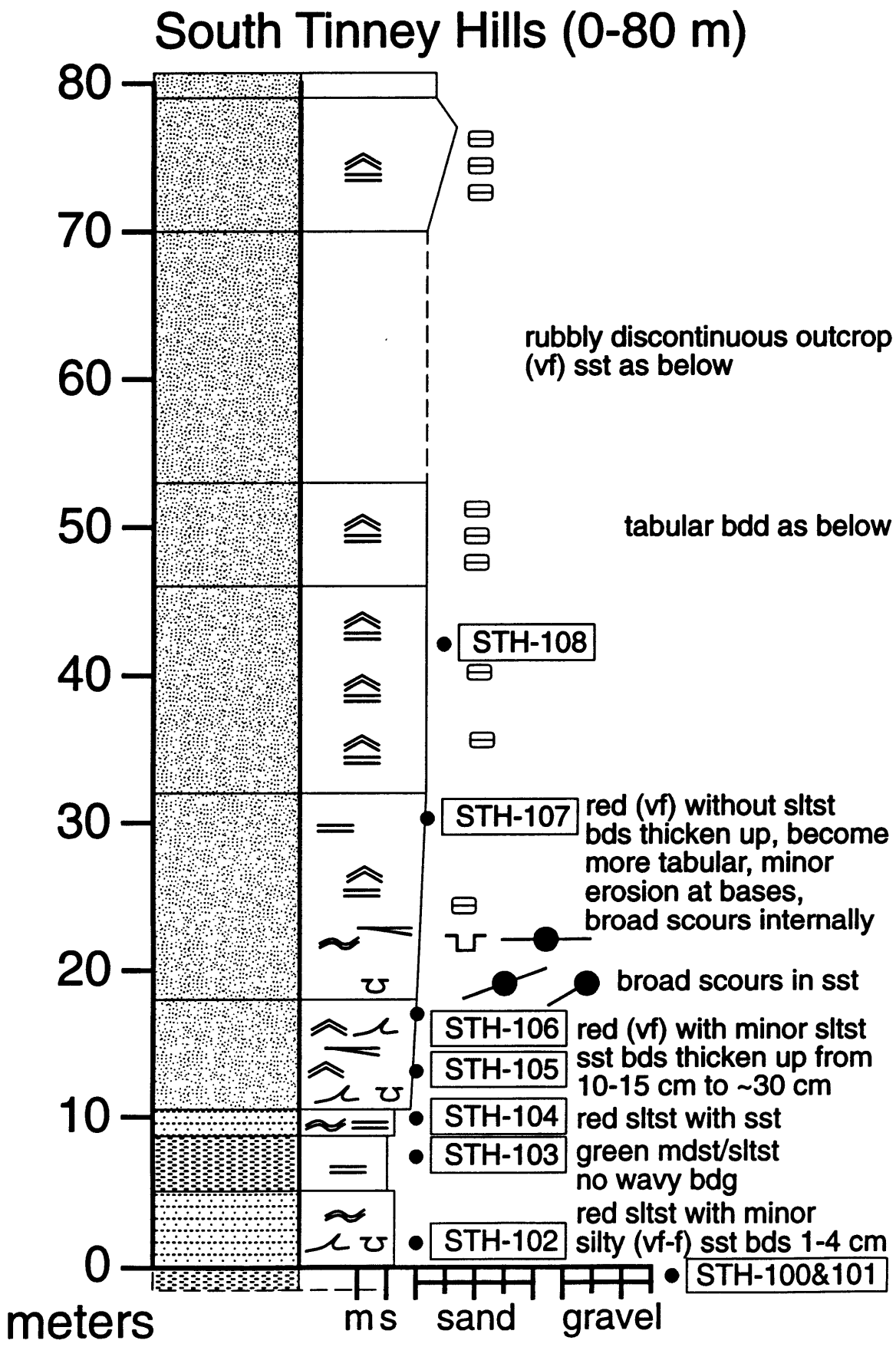
South Tinney Hills (0-80 m)
80
70
60
50
40
30
20
10
0
meters
m s
sand
gravel
rubbly discontinuous outcrop
(vf) sst as below
tabular bdd as below
STH-108
STH-107
red (vf) without sltst
bds thicken up, become
more tabular, minor
erosion at bases,
broad scours internally
broad scours in sst
STH-106
red (vf) with minor sltst
STH-105
sst bds thicken up from
10-15 cm to ~30 cm
STH-104
red sltst with sst
STH-103
green mdst/sltst
no wavy bdg
red sltst with minor
STH-102
silty (vf-f) sst bds 1-4 cm
STH-100&101

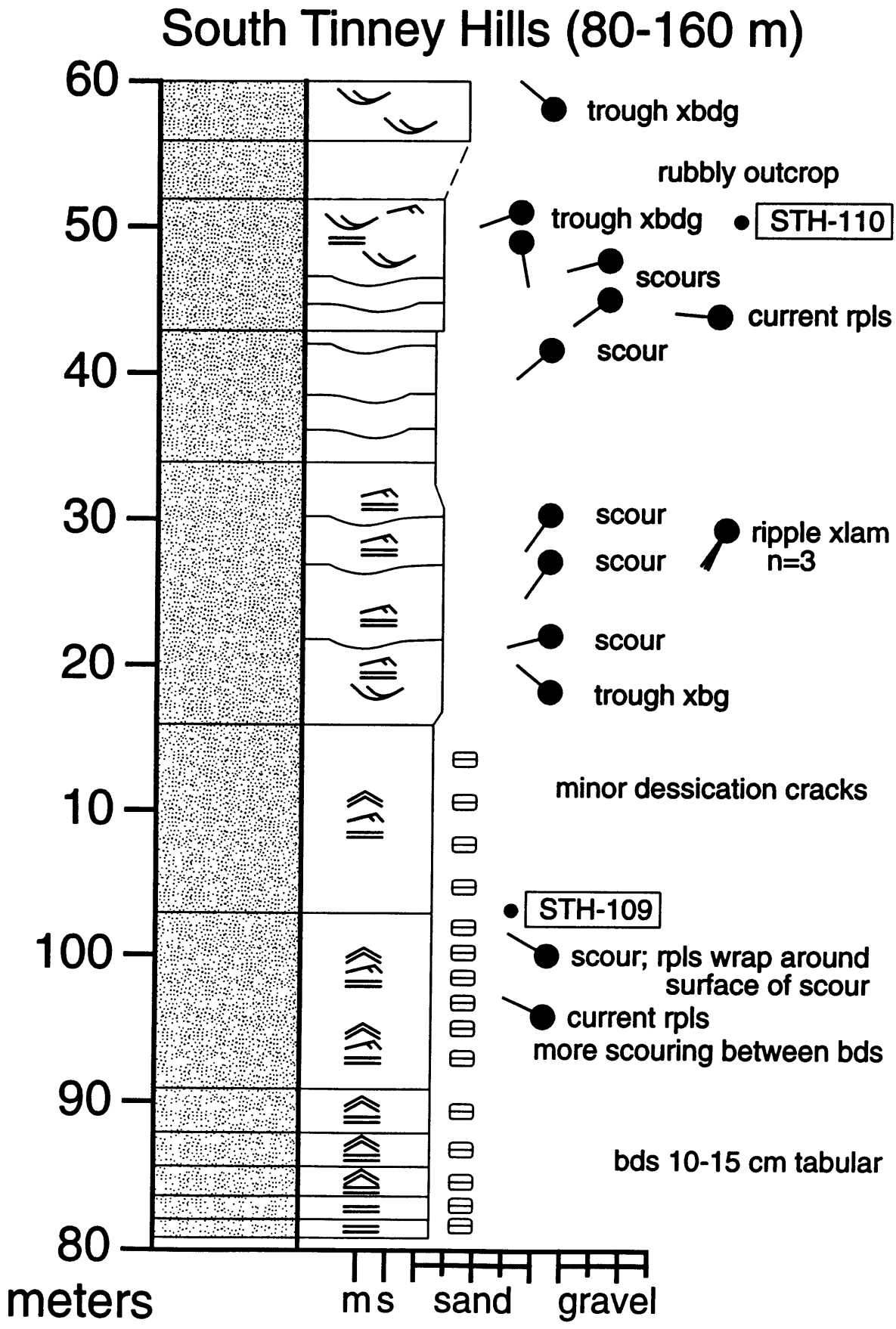
South Tinney Hills (80-160 m)
60
50
40
30
20
10
100
90
80
meters
trough xbdg
rubbly outcrop
trough xbdg
STH-110
scours
current rpls
scour
scour
scour
ripple xlam
n=3
scour
trough xbg
minor dessication cracks
STH-109
scour; rpls wrap around
surface of scour
current rpls
more scouring between bds
bds 10-15 cm tabular
m s
sand
gravel

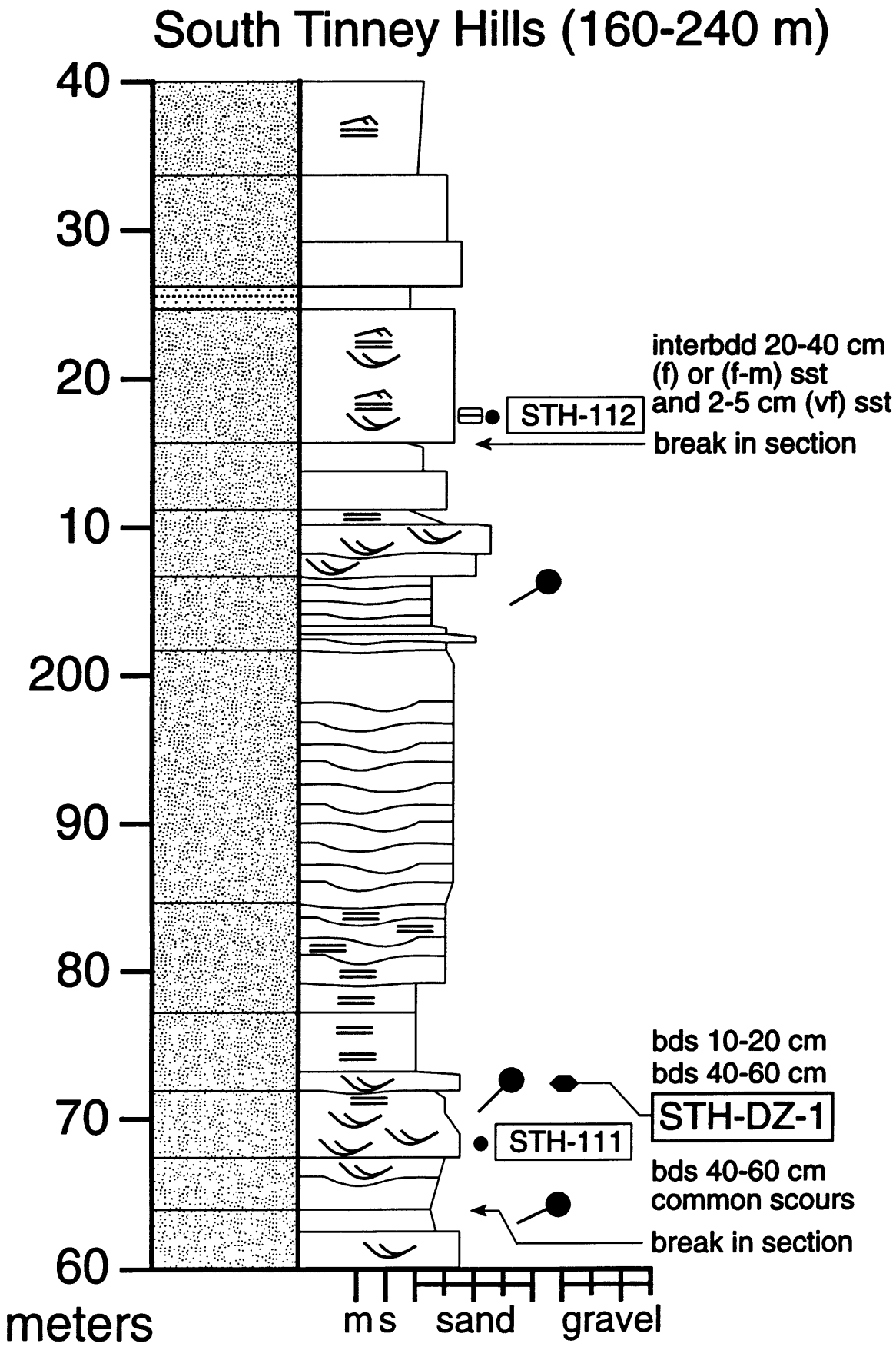
South Tinney Hills (160-240 m)
40
30
20
10
200
90
80
70
60
meters
m s
sand
gravel
interbdd 20-40 cm
(f) or (f-m) sst
and 2-5 cm (vf) sst
STH-112
break in section
bds 10-20 cm
bds 40-60 cm
STH-DZ-1
STH-111
bds 40-60 cm
common scours
break in section

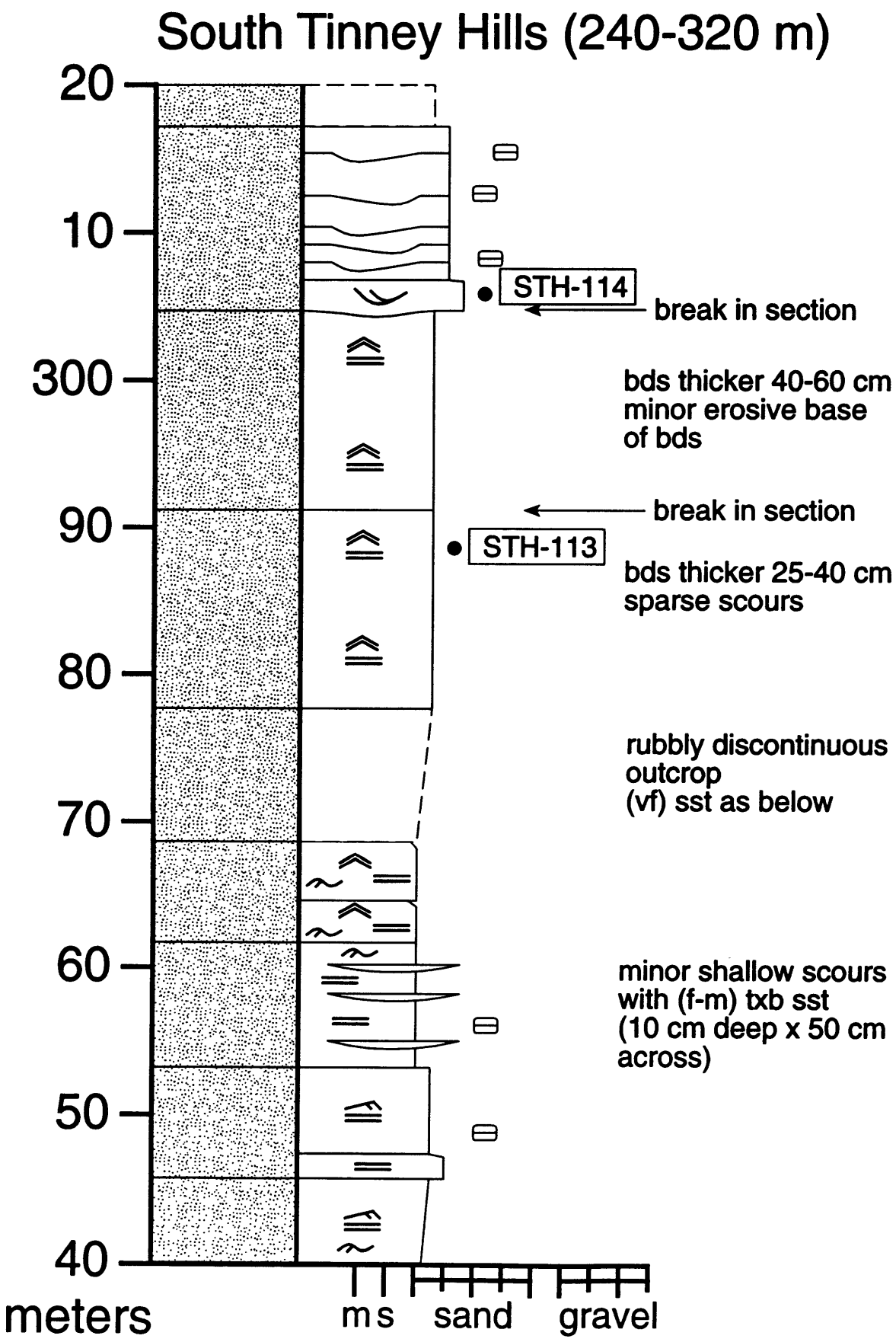
South Tinney Hills (240-320 m)
20
10
300
90
80
70
60
50
40
meters
STH-114
break in section
bds thicker 40-60 cm
minor erosive base
of bds
break in section
STH-113
bds thicker 25-40 cm
sparse scours
rubbly discontinuous
outcrop
(vf) sst as below
minor shallow scours
with (f-m) txb sst
(10 cm deep x 50 cm
across)
m s
sand
gravel

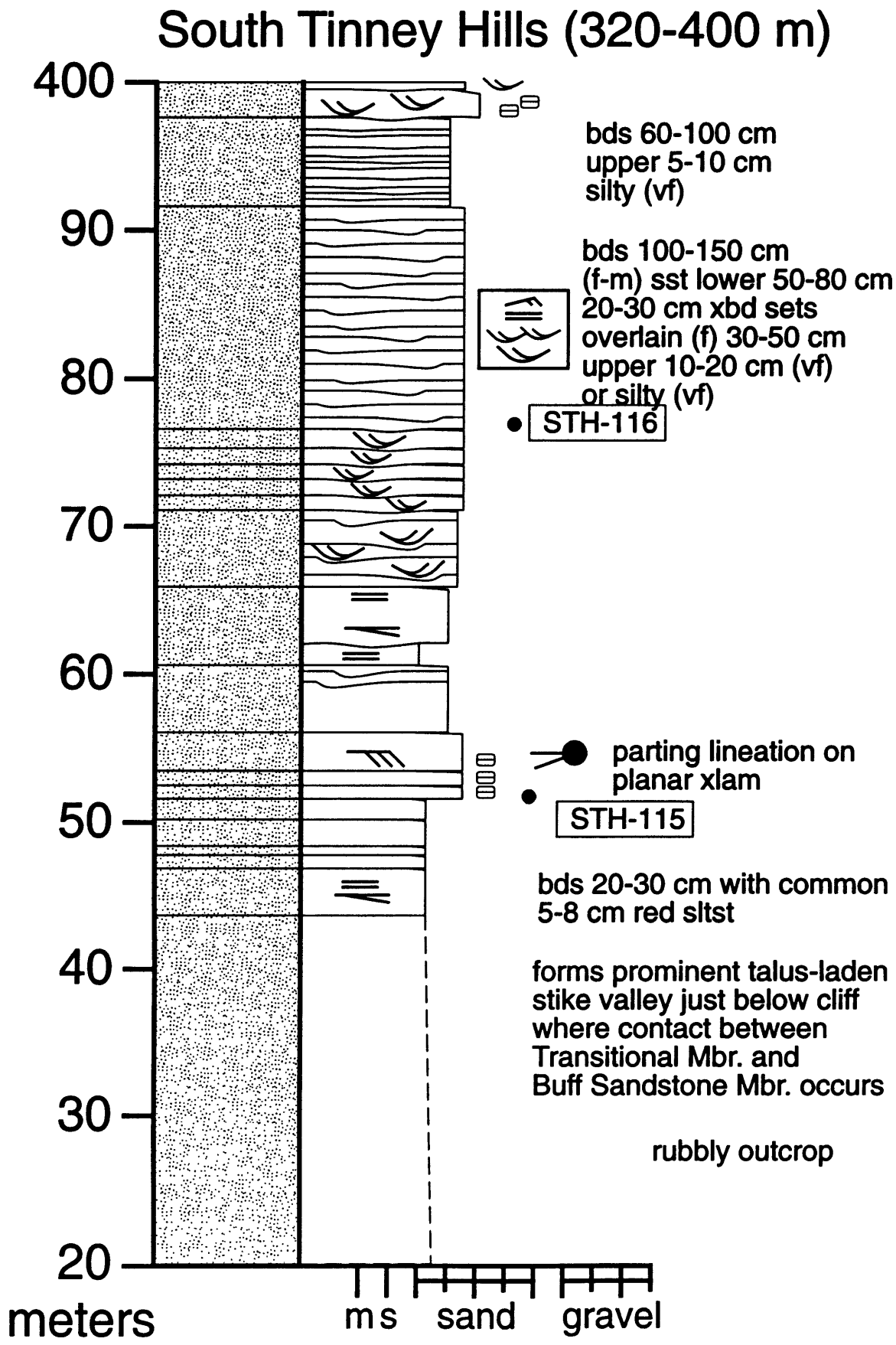
South Tinney Hills (320-400 m)
400
90
80
70
60
50
40
30
20
meters
m s
sand
gravel
bds 60-100 cm
upper 5-10 cm
silty (vf)
bds 100-150 cm
(f-m) sst lower 50-80 cm
20-30 cm xbd sets
overlain (f) 30-50 cm
upper 10-20 cm (vf)
or silty (vf)
STH-116
parting lineation on
planar xlam
STH-115
bds 20-30 cm with common
5-8 cm red sltst
forms prominent talus-laden
stike valley just below cliff
where contact between
Transitional Mbr. and
Buff Sandstone Mbr. occurs
rubbly outcrop

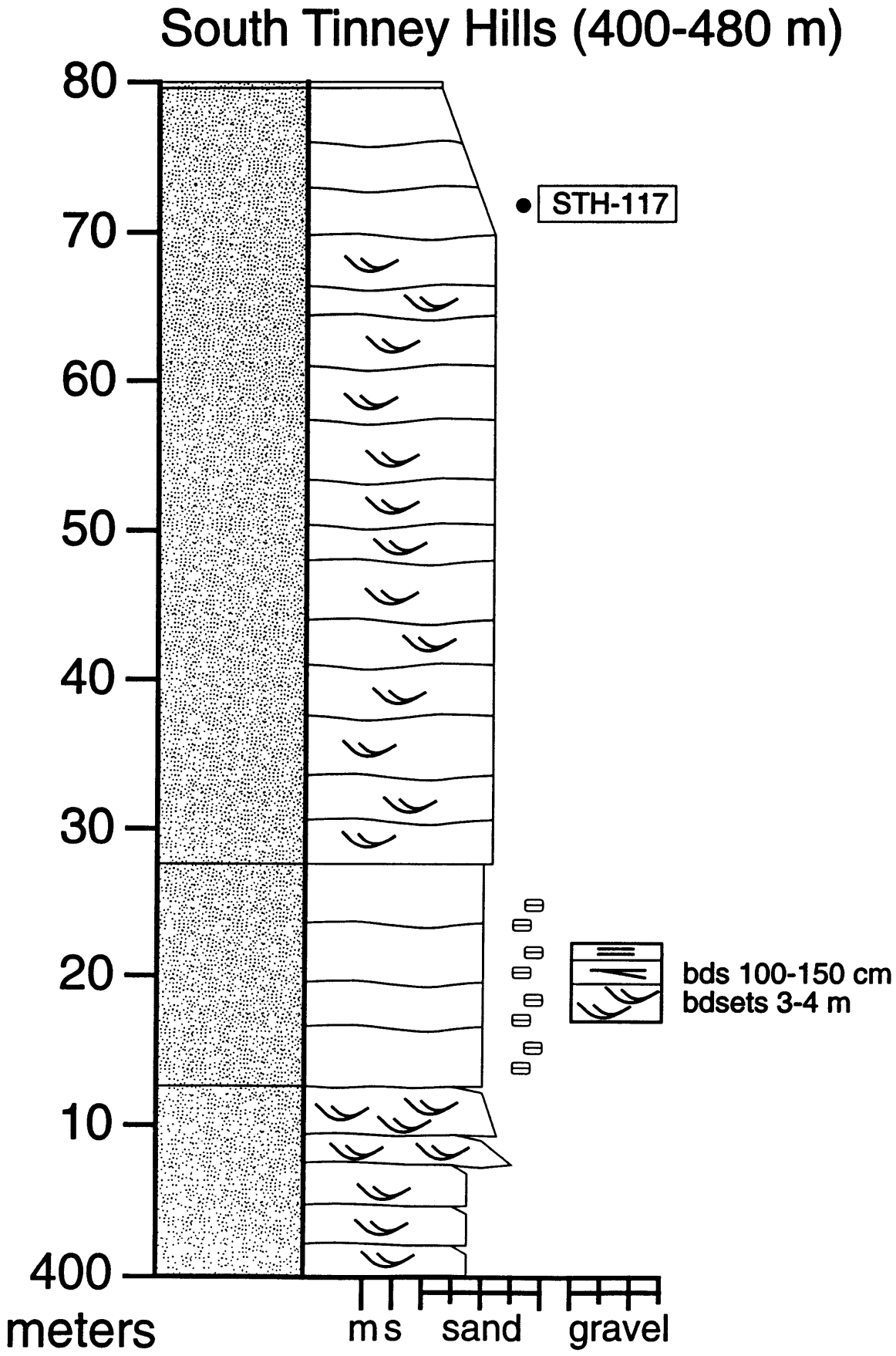
South Tinney Hills (400-480 m)
80
70
60
50
40
30
20
10
400
meters
STH-117
bds 100-150 cm
bdsets 3-4 m
m s
sand
gravel

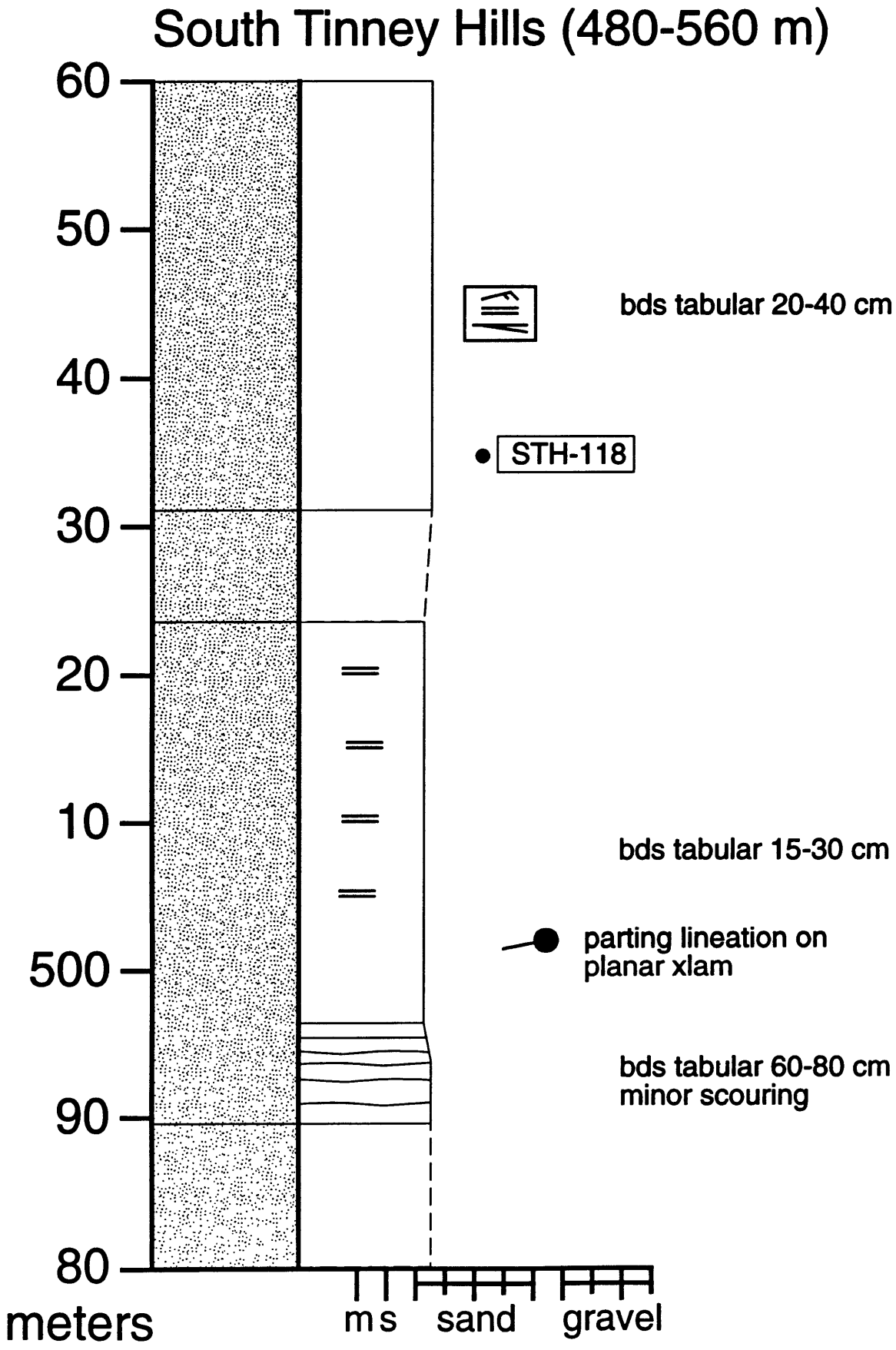
South Tinney Hills (480-560 m)
60
50
40
30
20
10
500
90
80
meters
bds tabular 20-40 cm
STH-118
bds tabular 15-30 cm
parting lineation on planar xlam
bds tabular 60-80 cm minor scouring
ms
sand
gravel

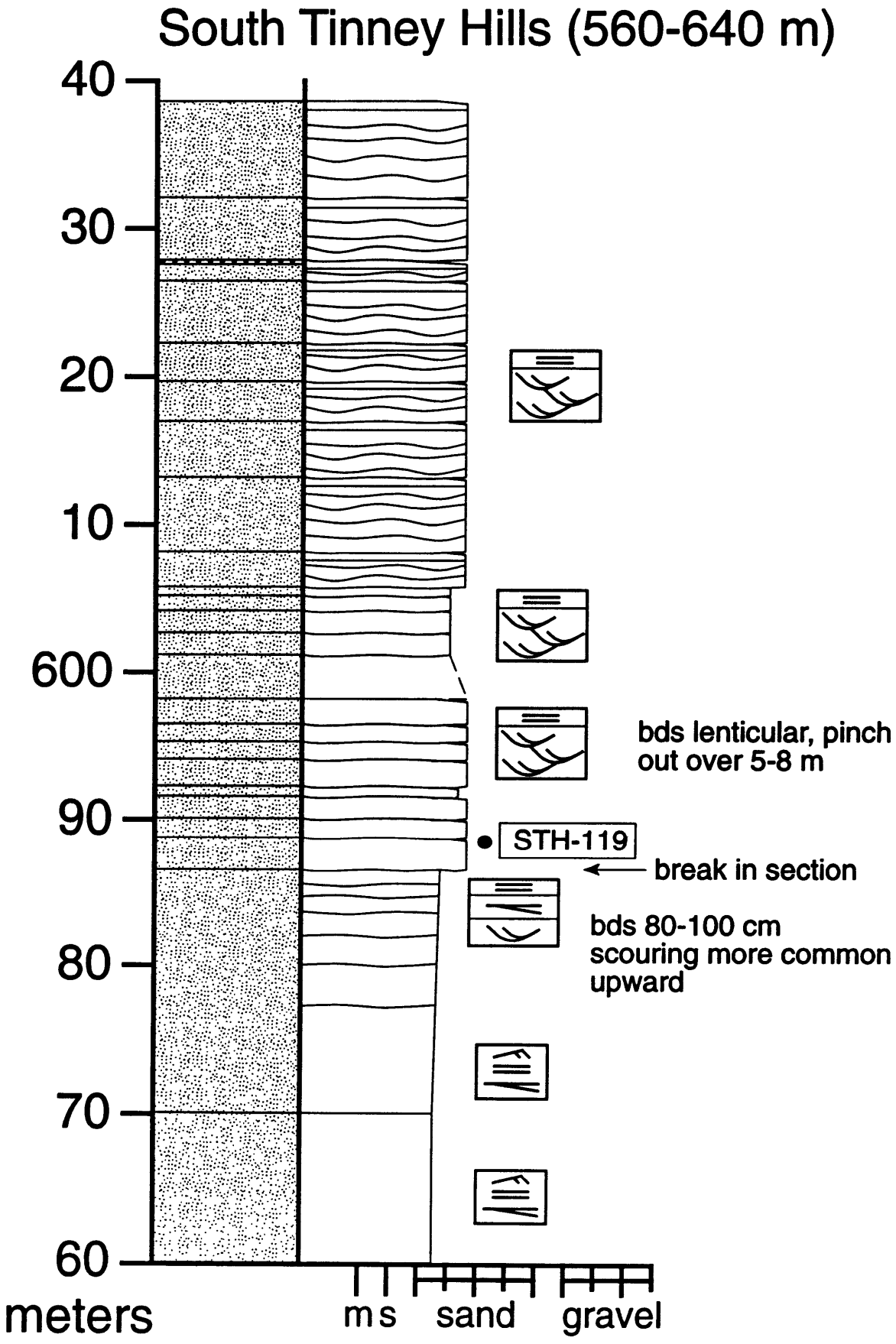
South Tinney Hills (560-640 m)
40
30
20
10
600
90
80
70
60
meters
m s
sand
gravel
bds lenticular, pinch out over 5-8 m
STH-119
break in section
bds 80-100 cm
scouring more common upward

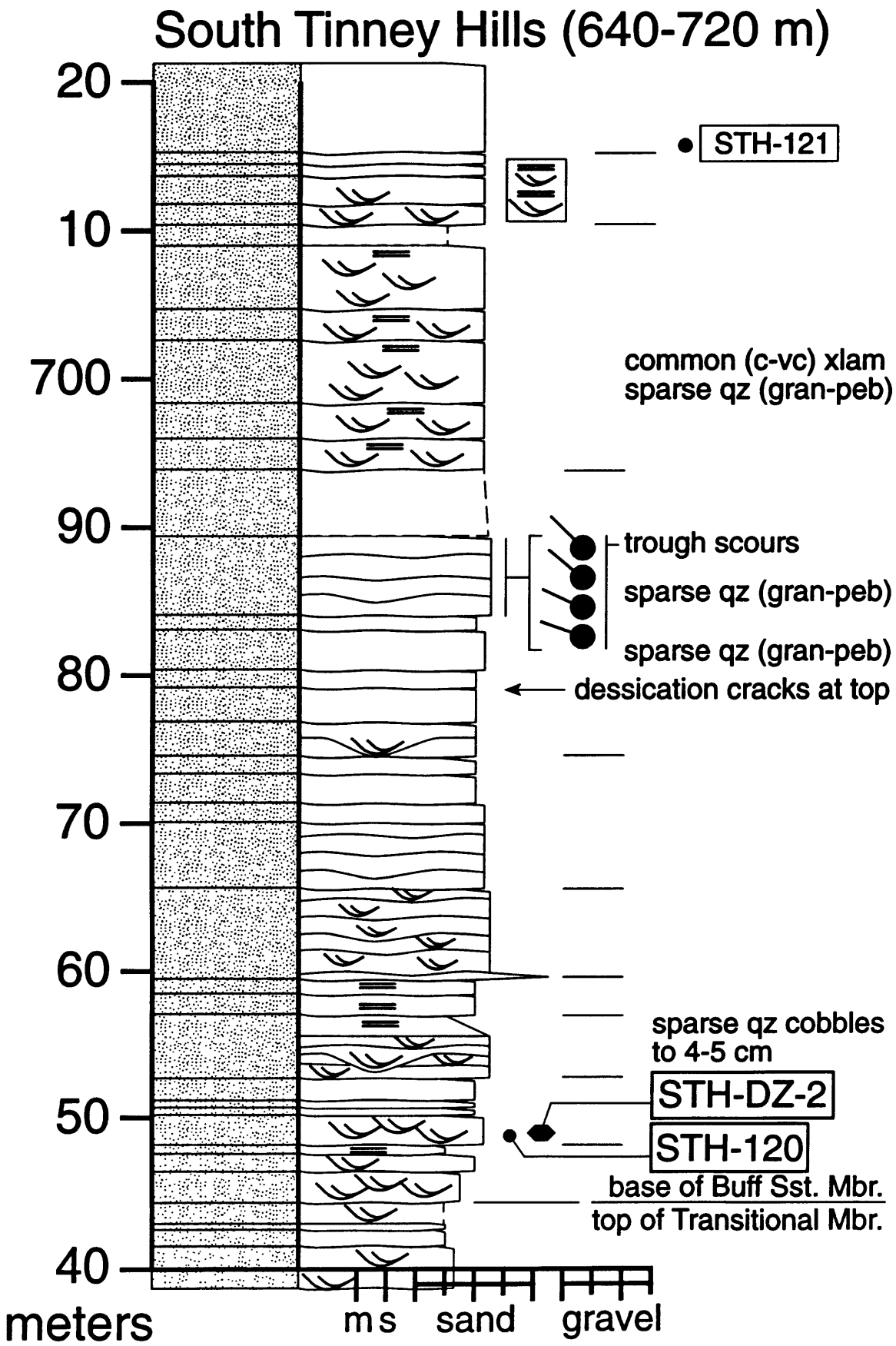
South Tinney Hills (640-720 m)
20
10
700
90
80
70
60
50
40
meters
STH-121
common (c-vc) xlam
sparse qz (gran-peb)
trough scours
sparse qz (gran-peb)
sparse qz (gran-peb)
dessication cracks at top
sparse qz cobbles
to 4-5 cm
STH-DZ-2
STH-120
base of Buff Sst. Mbr.
top of Transitional Mbr.
m s
sand
gravel

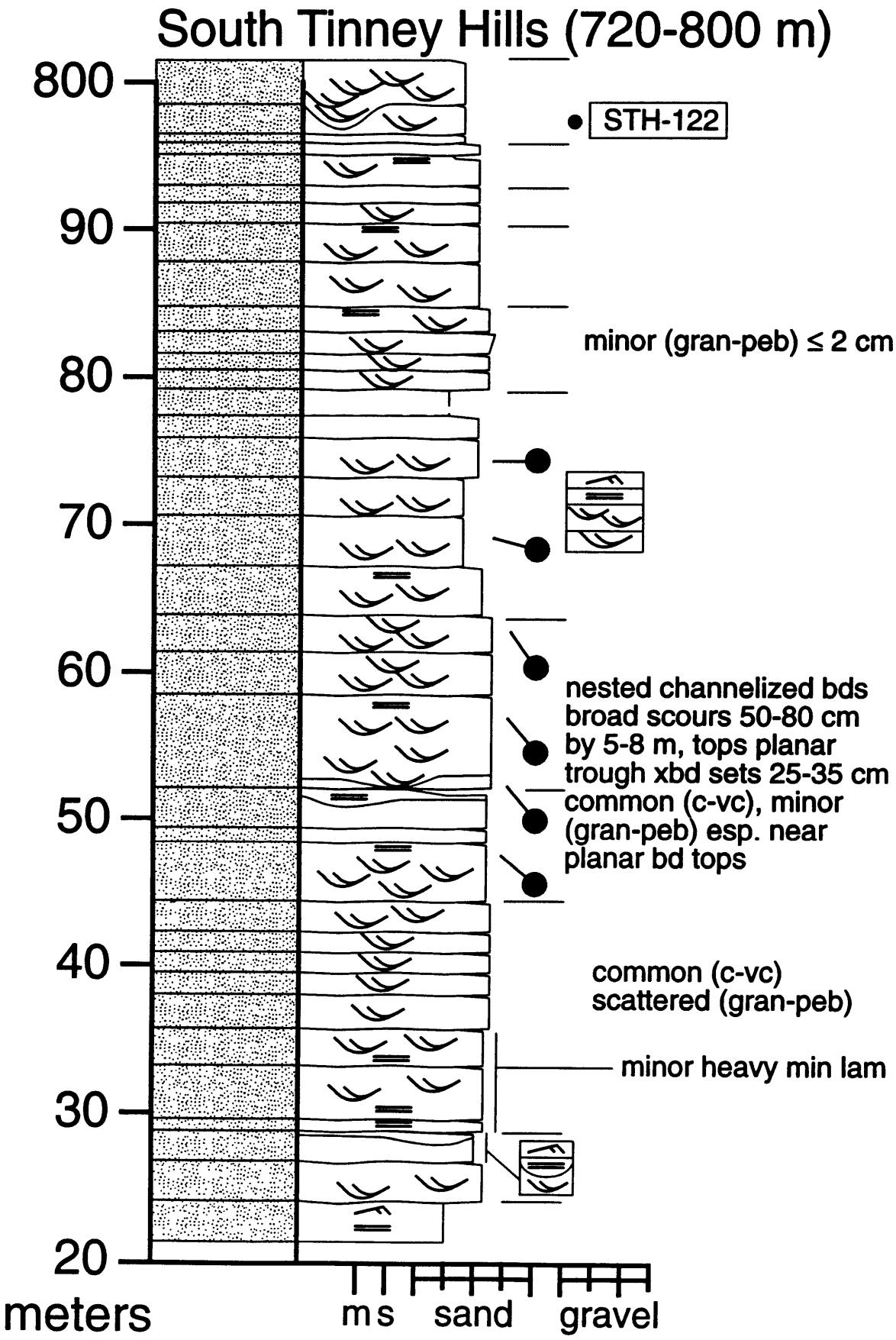
South Tinney Hills (720-800 m)
800
90
80
70
60
50
40
30
20
meters
STH-122
minor (gran-peb) ≤ 2 cm
nested channelized bds
broad scours 50-80 cm
by 5-8 m, tops planar
trough xbd sets 25-35 cm
common (c-vc), minor
(gran-peb) esp. near
planar bd tops
common (c-vc)
scattered (gran-peb)
minor heavy min lam
m s
sand
gravel

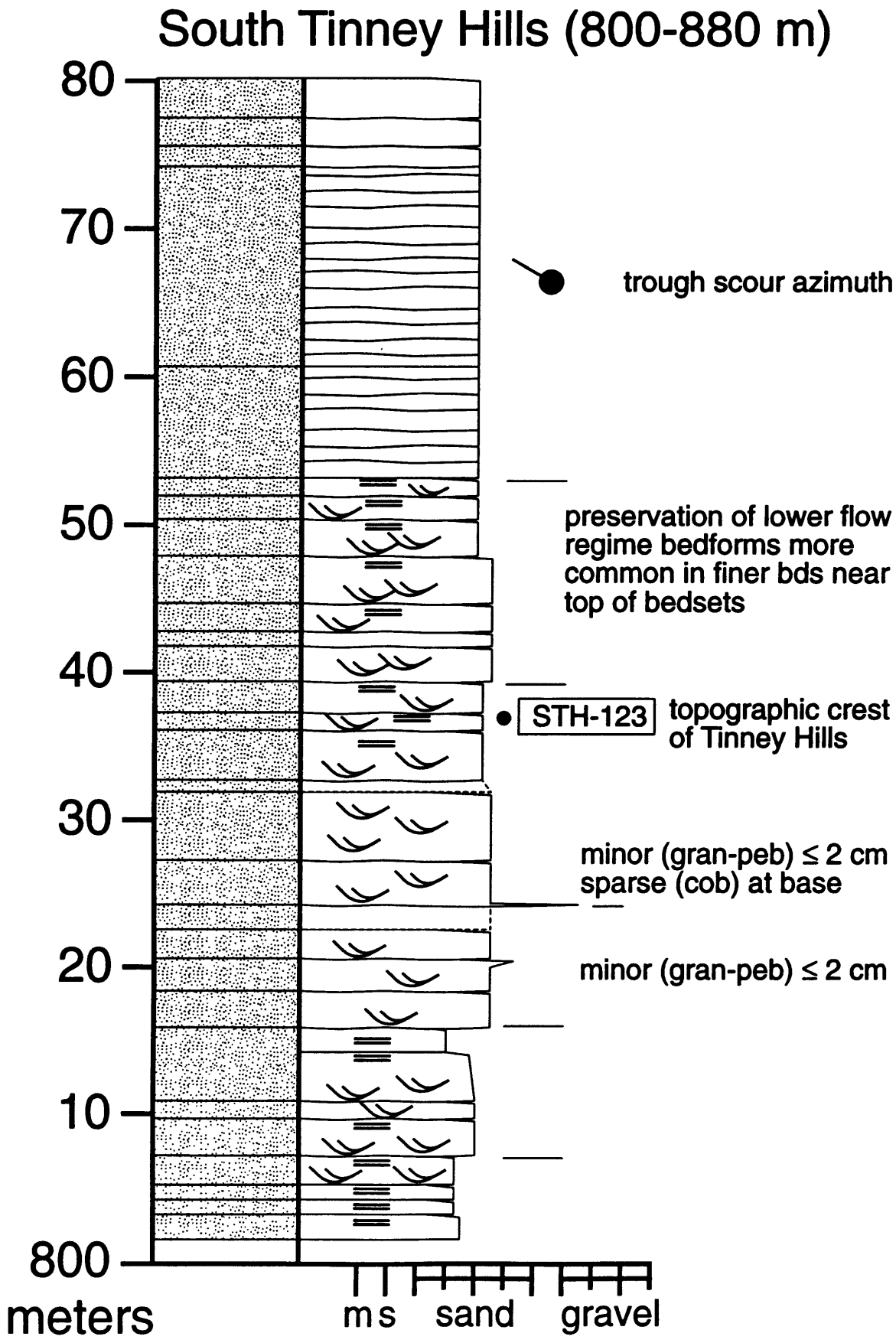
South Tinney Hills (800-880 m)
80
70
60
50
40
30
20
10
800
meters
trough scour azimuth
preservation of lower flow regime bedforms more common in finer bds near top of bedsets
STH-123
topographic crest of Tinney Hills
minor (gran-peb) ≤ 2 cm sparse (cob) at base
minor (gran-peb) ≤ 2 cm
m s
sand
gravel

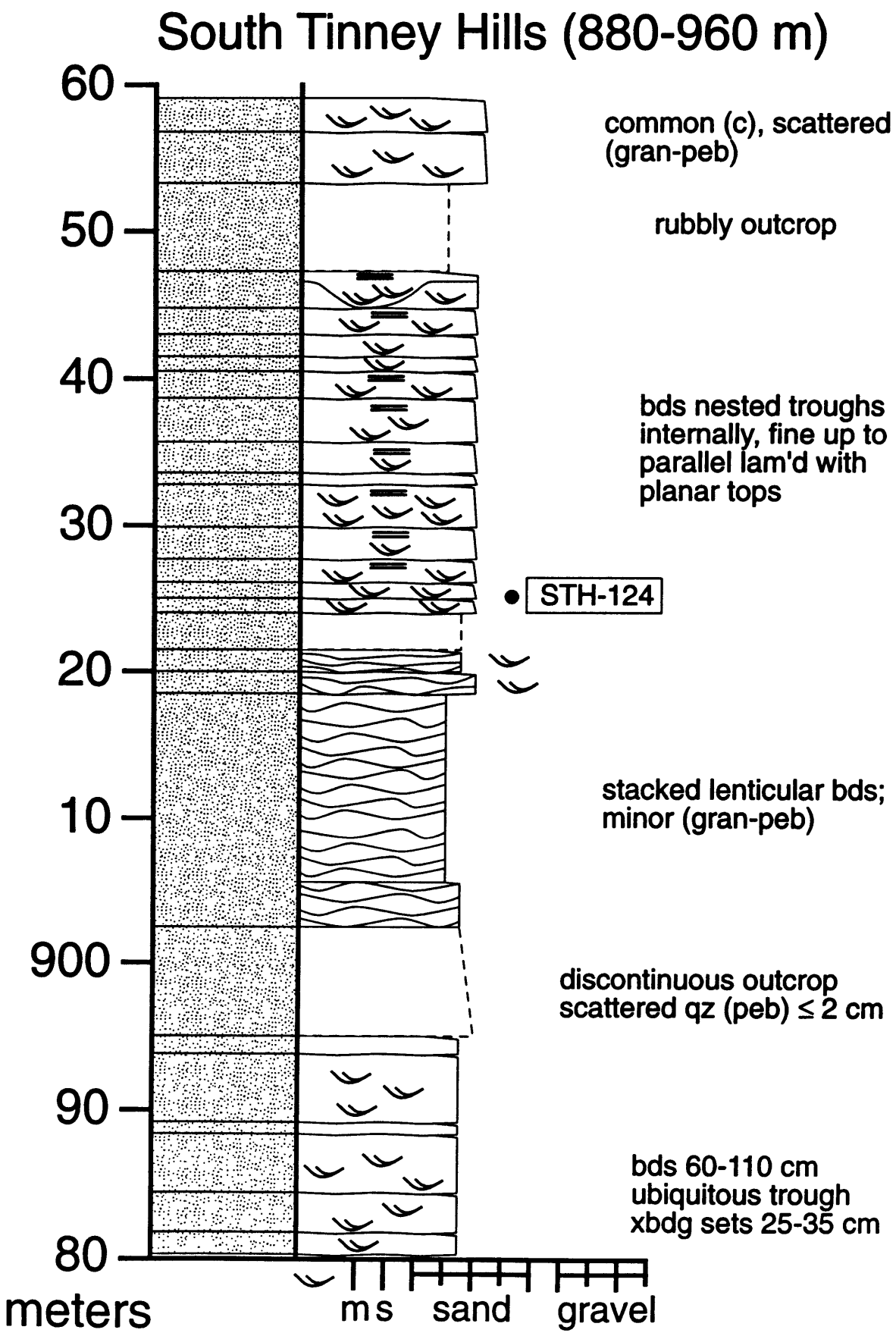
South Tinney Hills (880-960 m)
60
50
40
30
20
10
900
90
80
meters
m s
sand
gravel
common (c), scattered (gran-peb)
rubbly outcrop
bds nested troughs internally, fine up to parallel lam'd with planar tops
STH-124
stacked lenticular bds; minor (gran-peb)
discontinuous outcrop
scattered qz (peb) ≤ 2 cm
bds 60-110 cm
ubiquitous trough xbdg sets 25-35 cm

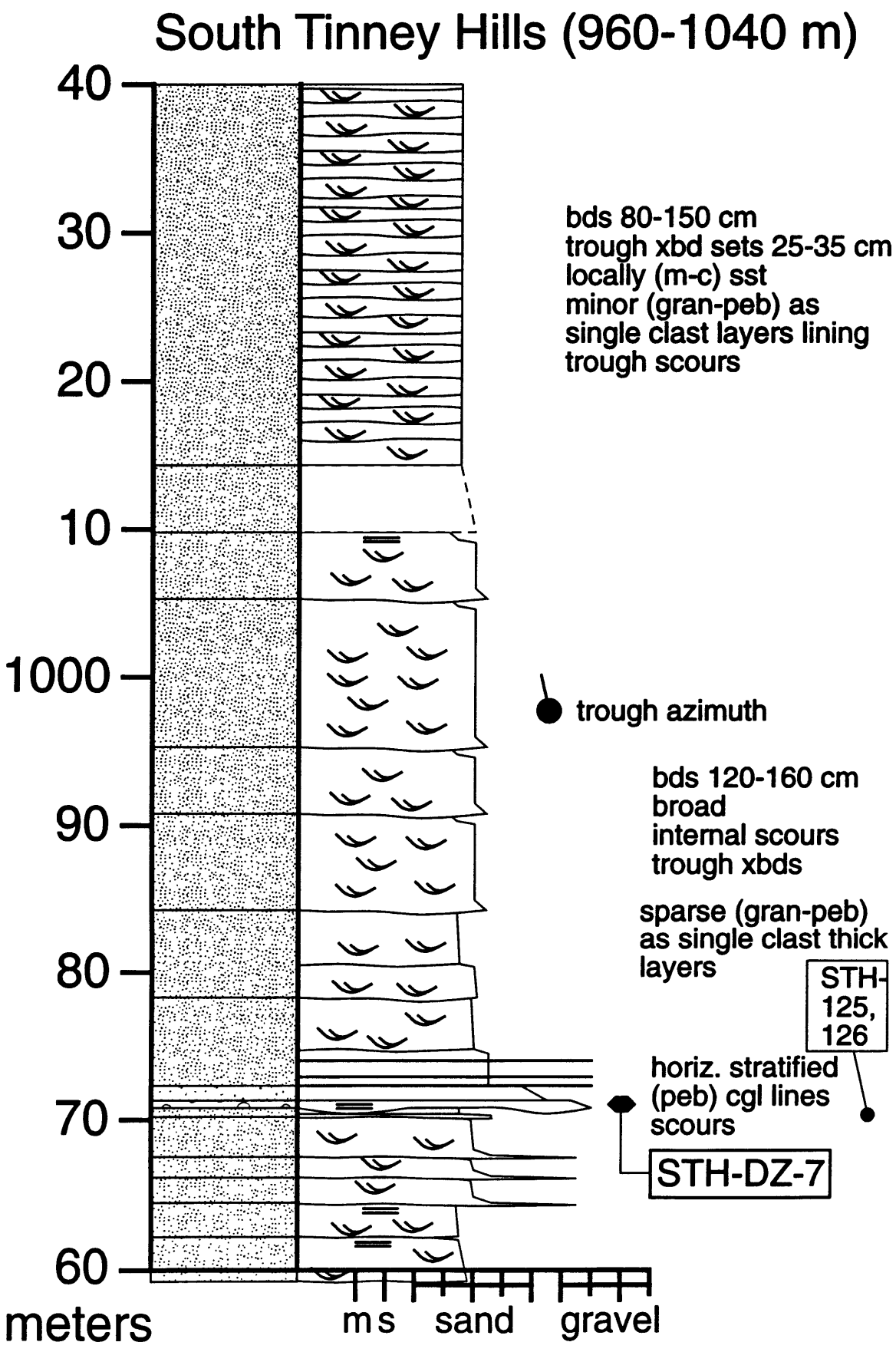
South Tinney Hills (960-1040 m)
40
30
20
10
1000
90
80
70
60
meters
m s
sand
gravel
bds 80-150 cm
trough xbd sets 25-35 cm
locally (m-c) sst
minor (gran-peb) as
single clast layers lining
trough scours
trough azimuth
bds 120-160 cm
broad
internal scours
trough xbds
sparse (gran-peb)
as single clast thick
layers
STH-
125,
126
horiz. stratified
(peb) cgl lines
scours
STH-DZ-7

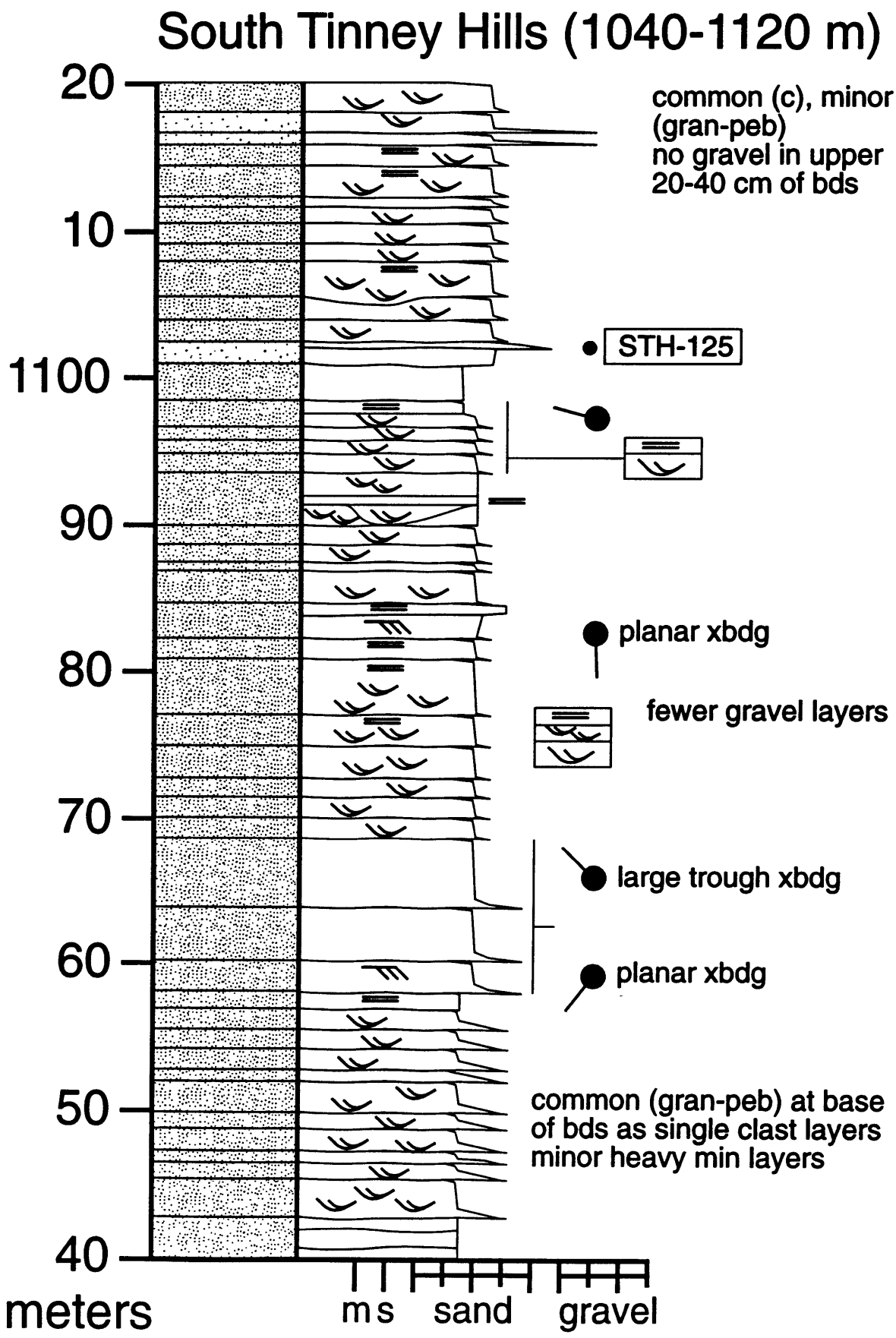
South Tinney Hills (1040-1120 m)
20
10
1100
90
80
70
60
50
40
meters
m s
sand
gravel
common (c), minor (gran-peb)
no gravel in upper 20-40 cm of bds
STH-125
planar xbdg
fewer gravel layers
large trough xbdg
planar xbdg
common (gran-peb) at base of bds as single clast layers
minor heavy min layers

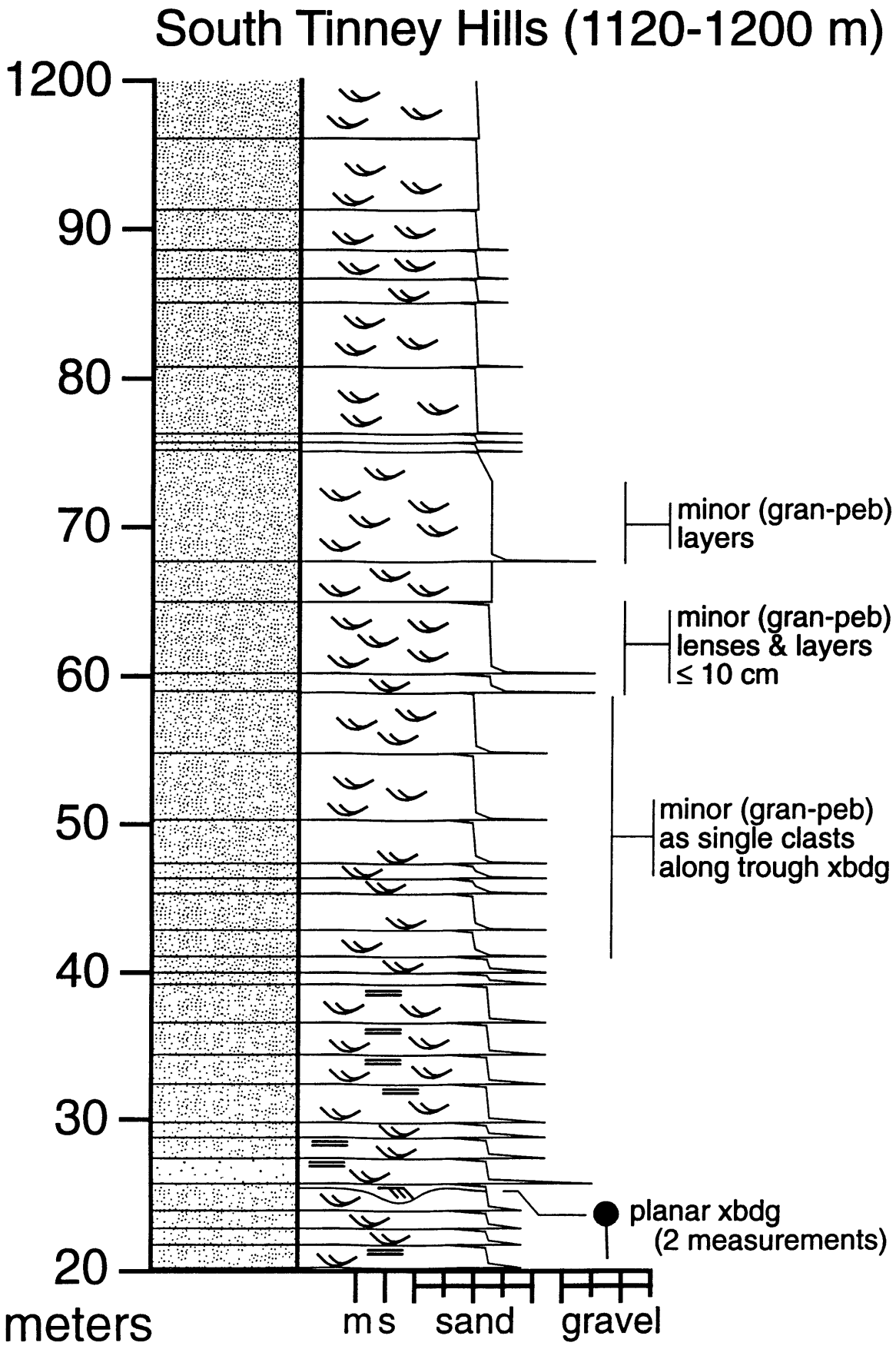
South Tinney Hills (1120-1200 m)
1200
90
80
70
60
50
40
30
20
meters
minor (gran-peb)
layers
minor (gran-peb)
lenses & layers
≤ 10 cm
minor (gran-peb)
as single clasts
along trough xbdg
planar xbdg
(2 measurements)
m s
sand
gravel

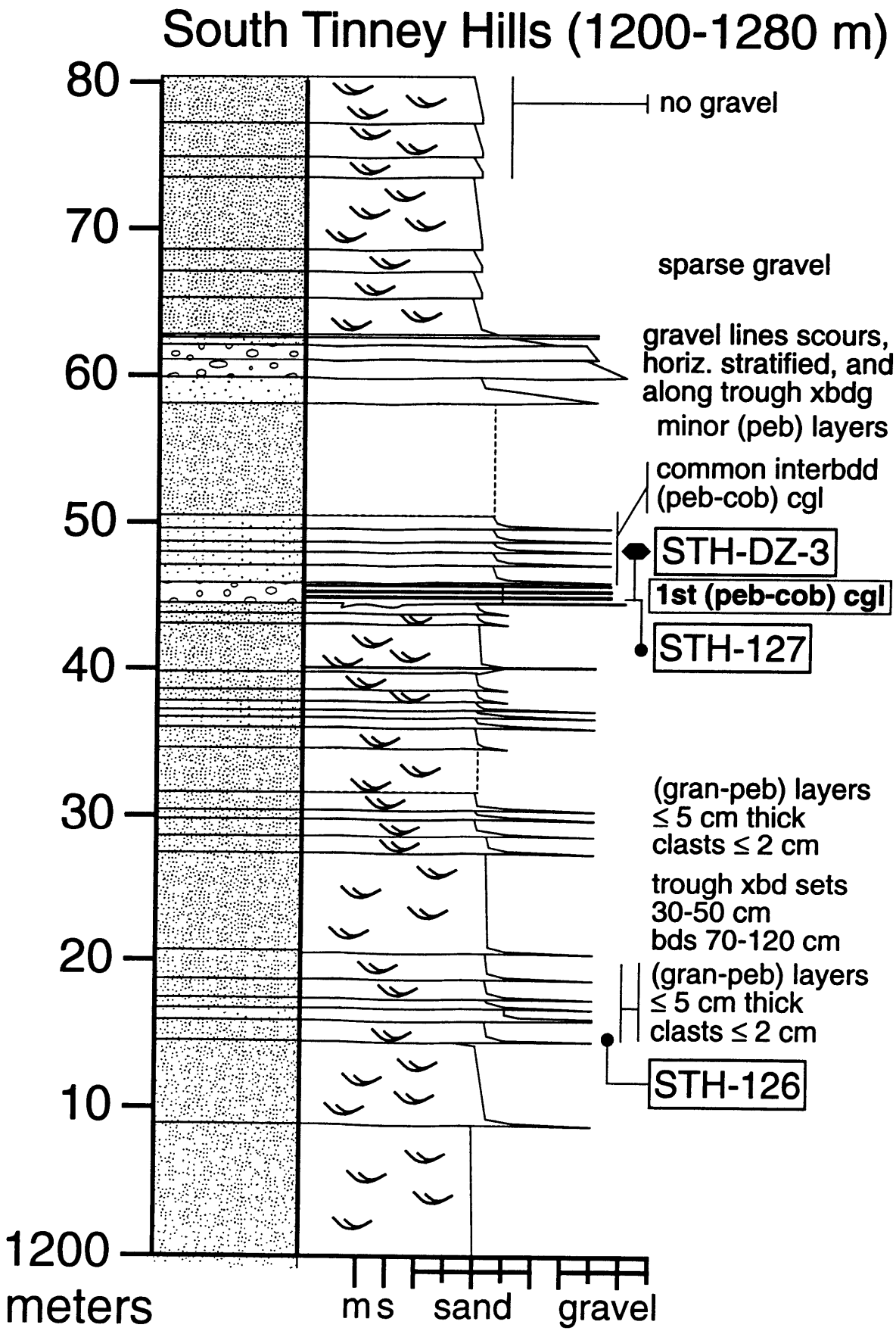
South Tinney Hills (1200-1280 m)
80
70
60
50
40
30
20
10
1200
meters
m s
sand
gravel
no gravel
sparse gravel
gravel lines scours,
horiz. stratified, and
along trough xbdg
minor (peb) layers
common interbdd
(peb-cob) cgl
STH-DZ-3
1st (peb-cob) cgl
STH-127
(gran-peb) layers
≤ 5 cm thick
clasts ≤ 2 cm
trough xbd sets
30-50 cm
bds 70-120 cm
(gran-peb) layers
≤ 5 cm thick
clasts ≤ 2 cm
STH-126

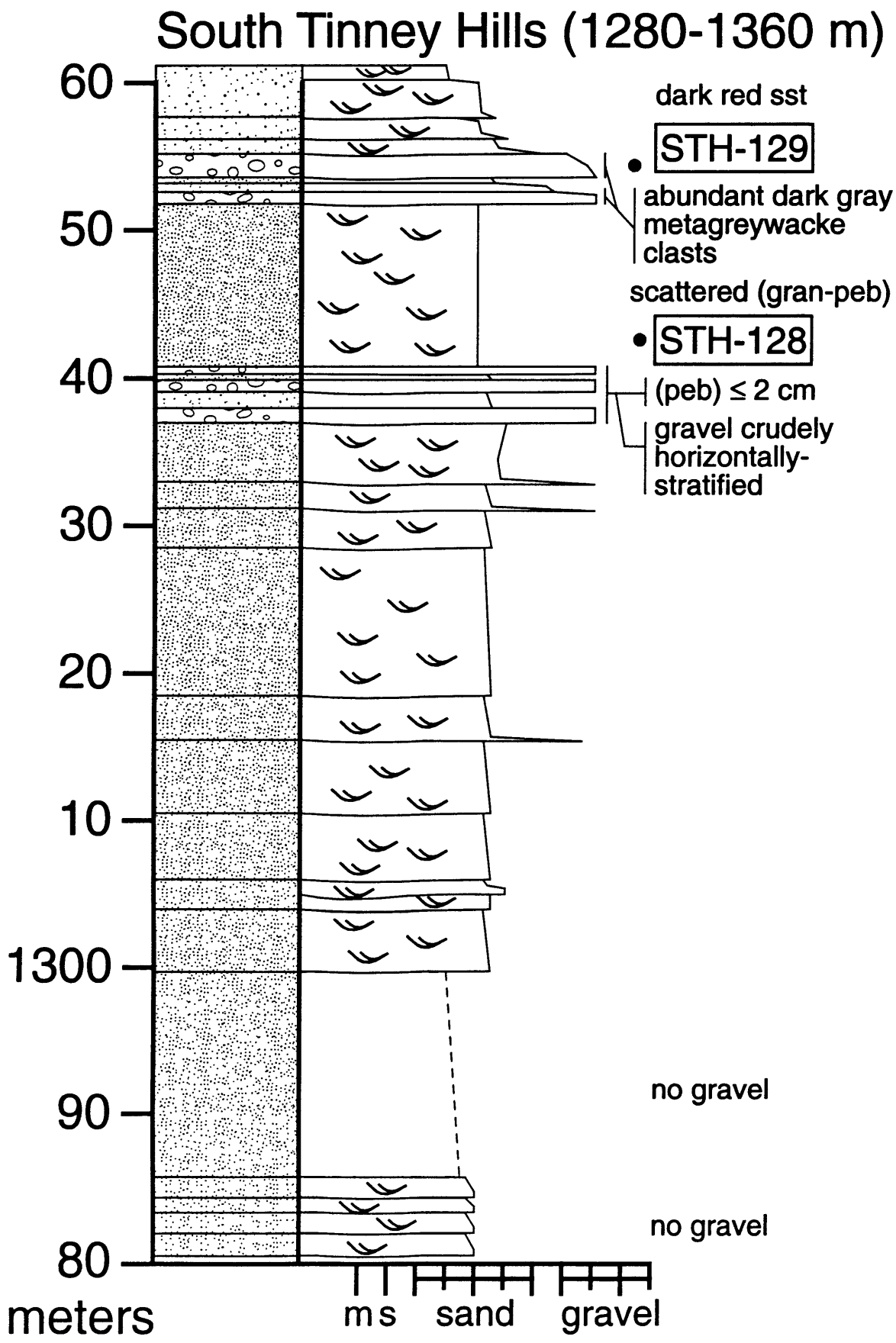
South Tinney Hills (1280-1360 m)
60
50
40
30
20
10
1300
90
80
meters
dark red sst
STH-129
abundant dark gray metagreywacke clasts
scattered (gran-peb)
STH-128
(peb) ≤ 2 cm
gravel crudely horizontally-stratified
no gravel
no gravel
m s
sand
gravel

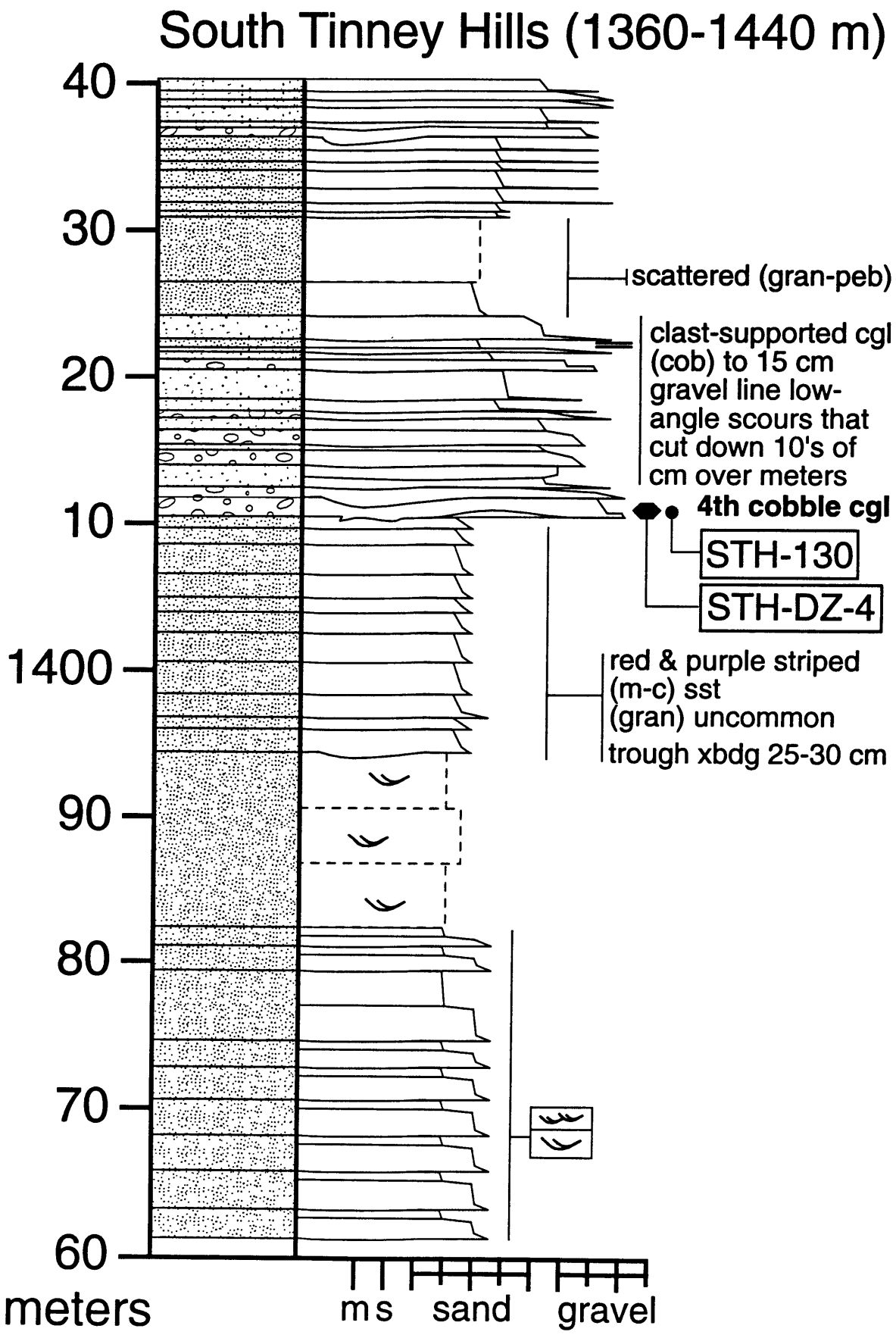
South Tinney Hills (1360-1440 m)
40
30
20
10
1400
90
80
70
60
meters
m s
sand
gravel
scattered (gran-peb)
clast-supported cgl (cob) to 15 cm gravel line low-angle scours that cut down 10's of cm over meters
4th cobble cgl
STH-130
STH-DZ-4
red & purple striped (m-c) sst (gran) uncommon trough xbdg 25-30 cm

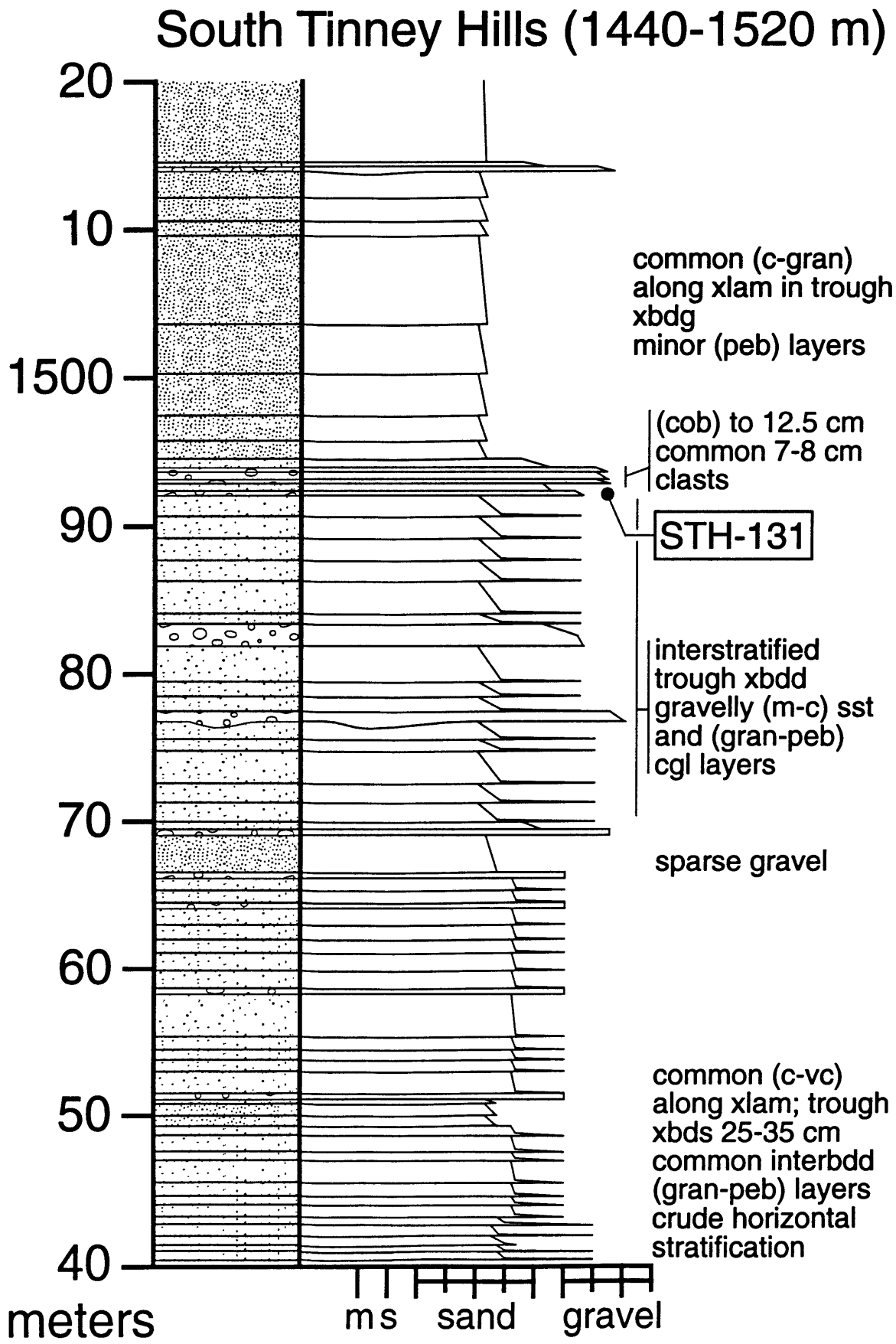
South Tinney Hills (1440-1520 m)
20
10
1500
90
80
70
60
50
40
meters
common (c-gran)
along xlam in trough
xbdg
minor (peb) layers
(cob) to 12.5 cm
common 7-8 cm
clasts
STH-131
interstratified
trough xbdd
gravelly (m-c) sst
and (gran-peb)
cgl layers
sparse gravel
common (c-vc)
along xlam; trough
xbds 25-35 cm
common interbdd
(gran-peb) layers
crude horizontal
stratification
m s
sand
gravel

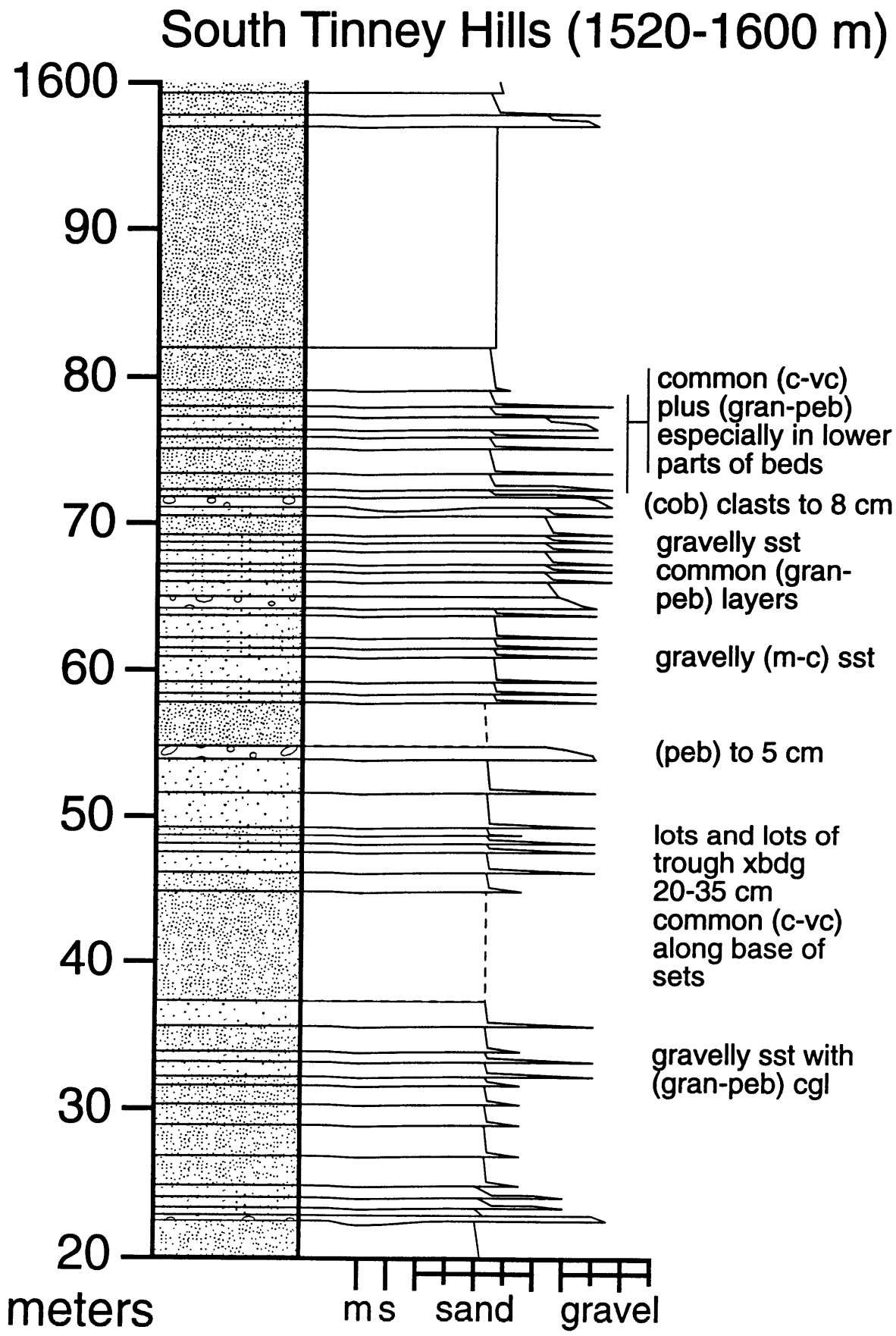
South Tinney Hills (1520-1600 m)
1600
90
80
70
60
50
40
30
20
meters
m s
sand
gravel
common (c-vc) plus (gran-peb) especially in lower parts of beds
(cob) clasts to 8 cm
gravelly sst common (gran-peb) layers
gravelly (m-c) sst
(peb) to 5 cm
lots and lots of trough xbdg 20-35 cm common (c-vc) along base of sets
gravelly sst with (gran-peb) cgl

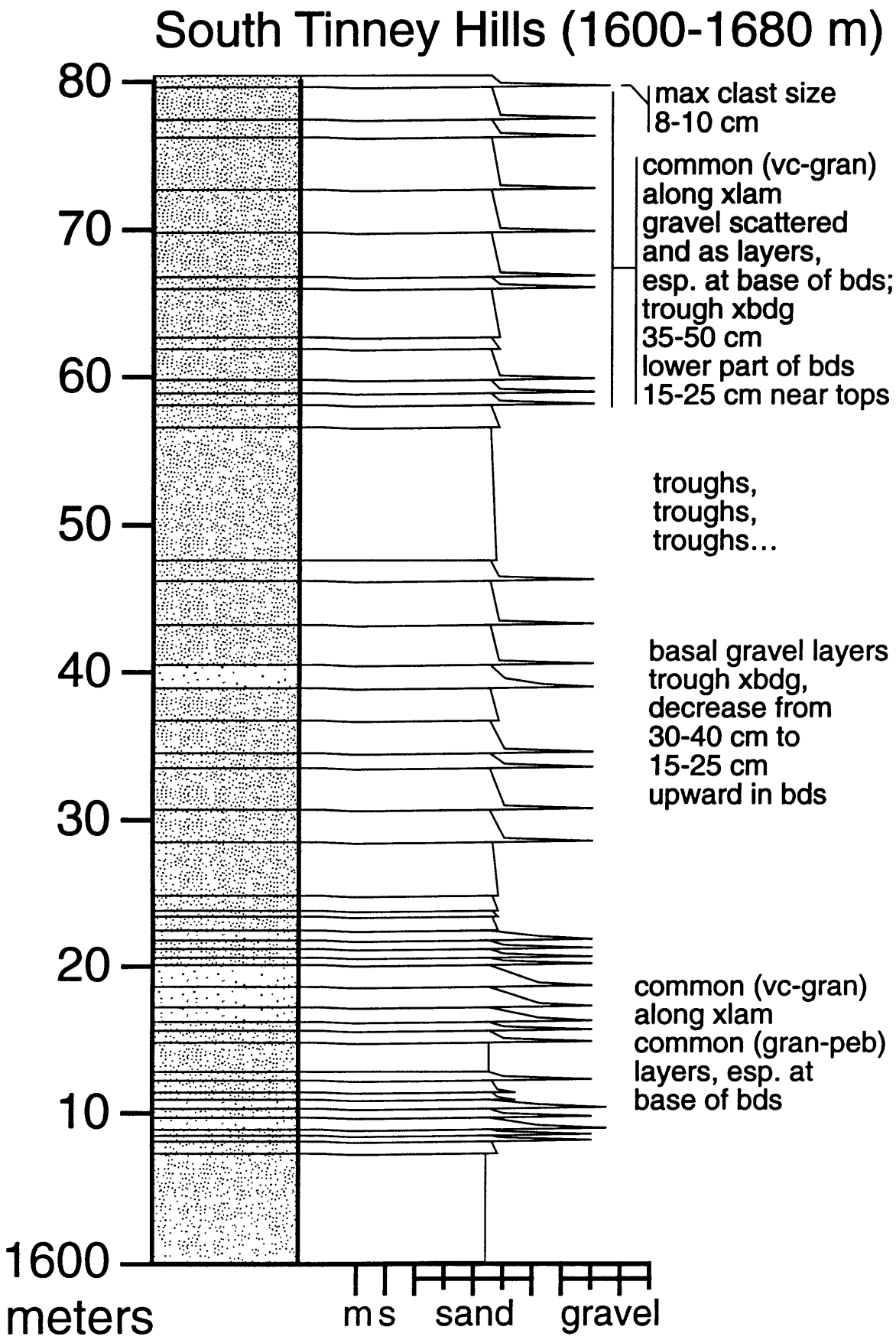
South Tinney Hills (1600-1680 m)
80
70
60
50
40
30
20
10
1600
meters
max clast size
8-10 cm
common (vc-gran)
along xlam
gravel scattered
and as layers,
esp. at base of bds;
trough xbdg
35-50 cm
lower part of bds
15-25 cm near tops
troughs,
troughs,
troughs...
basal gravel layers
trough xbdg,
decrease from
30-40 cm to
15-25 cm
upward in bds
common (vc-gran)
along xlam
common (gran-peb)
layers, esp. at
base of bds
m s
sand
gravel

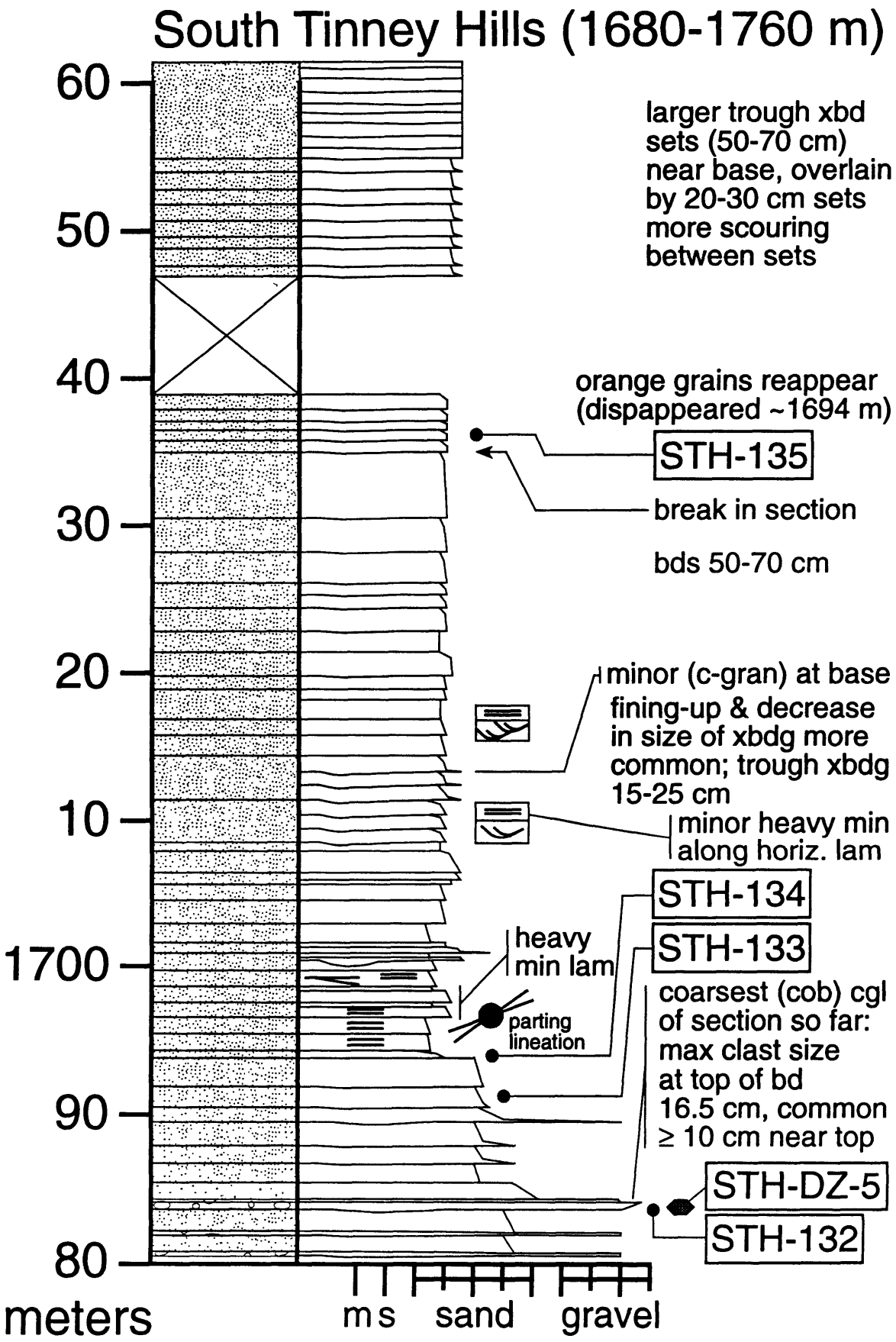
South Tinney Hills (1680-1760 m)
60
50
40
30
20
10
1700
90
80
meters
m s
sand
gravel
larger trough xbd sets (50-70 cm) near base, overlain by 20-30 cm sets more scouring between sets
orange grains reappear (dispappeared ~1694 m)
STH-135
break in section
bds 50-70 cm
minor (c-gran) at base fining-up & decrease in size of xbdg more common; trough xbdg 15-25 cm
minor heavy min along horiz. lam
STH-134
STH-133
heavy min lam
parting lineation
coarsest (cob) cgl of section so far: max clast size at top of bd 16.5 cm, common ≥ 10 cm near top
STH-DZ-5
STH-132

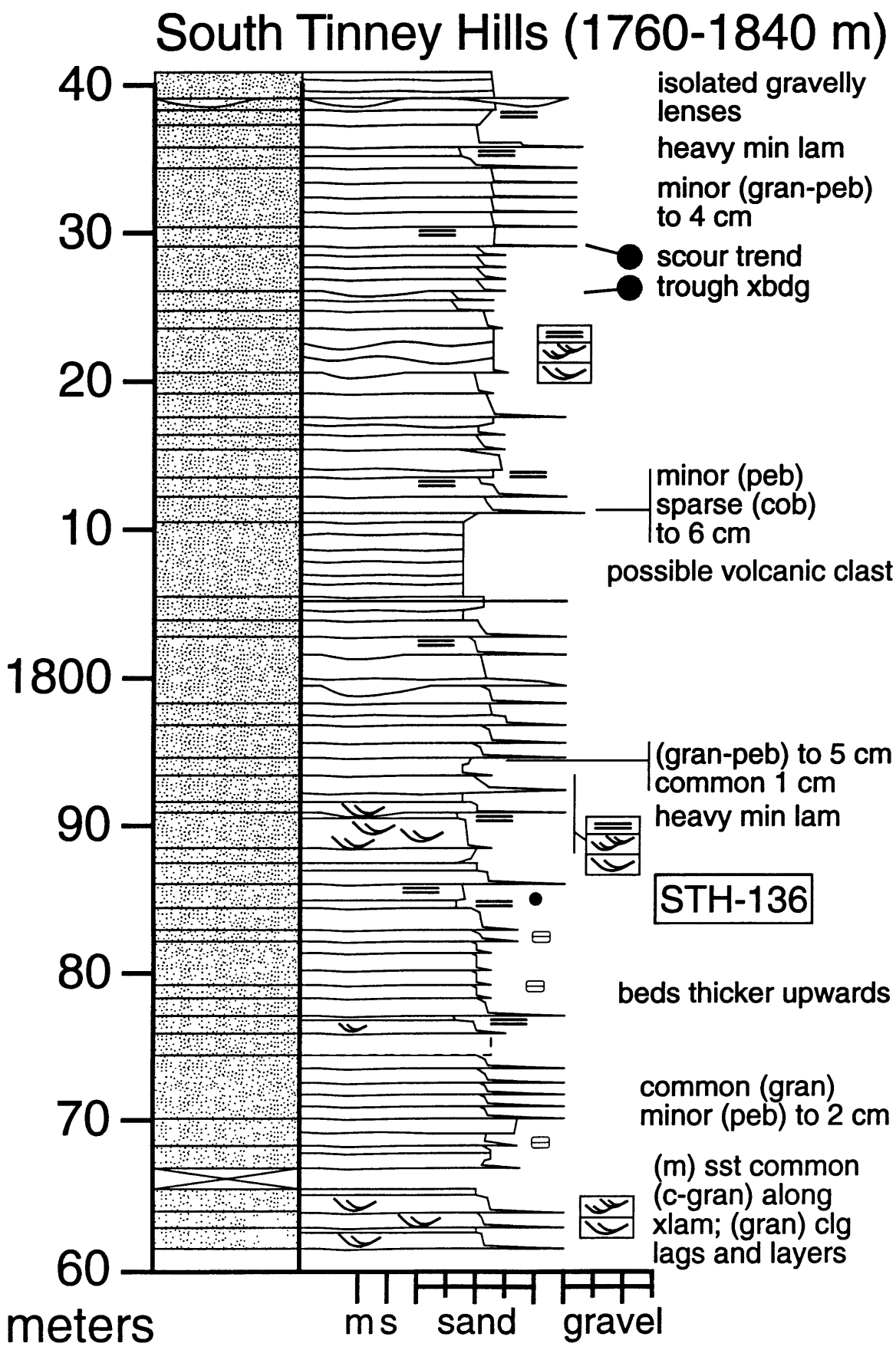
South Tinney Hills (1760-1840 m)
40
30
20
10
1800
90
80
70
60
meters
isolated gravelly lenses
heavy min lam
minor (gran-peb) to 4 cm
scour trend
trough xbdg
minor (peb) sparse (cob) to 6 cm
possible volcanic clast
(gran-peb) to 5 cm common 1 cm
heavy min lam
STH-136
beds thicker upwards
common (gran) minor (peb) to 2 cm
(m) sst common (c-gran) along xlam; (gran) clg lags and layers
m s
sand
gravel

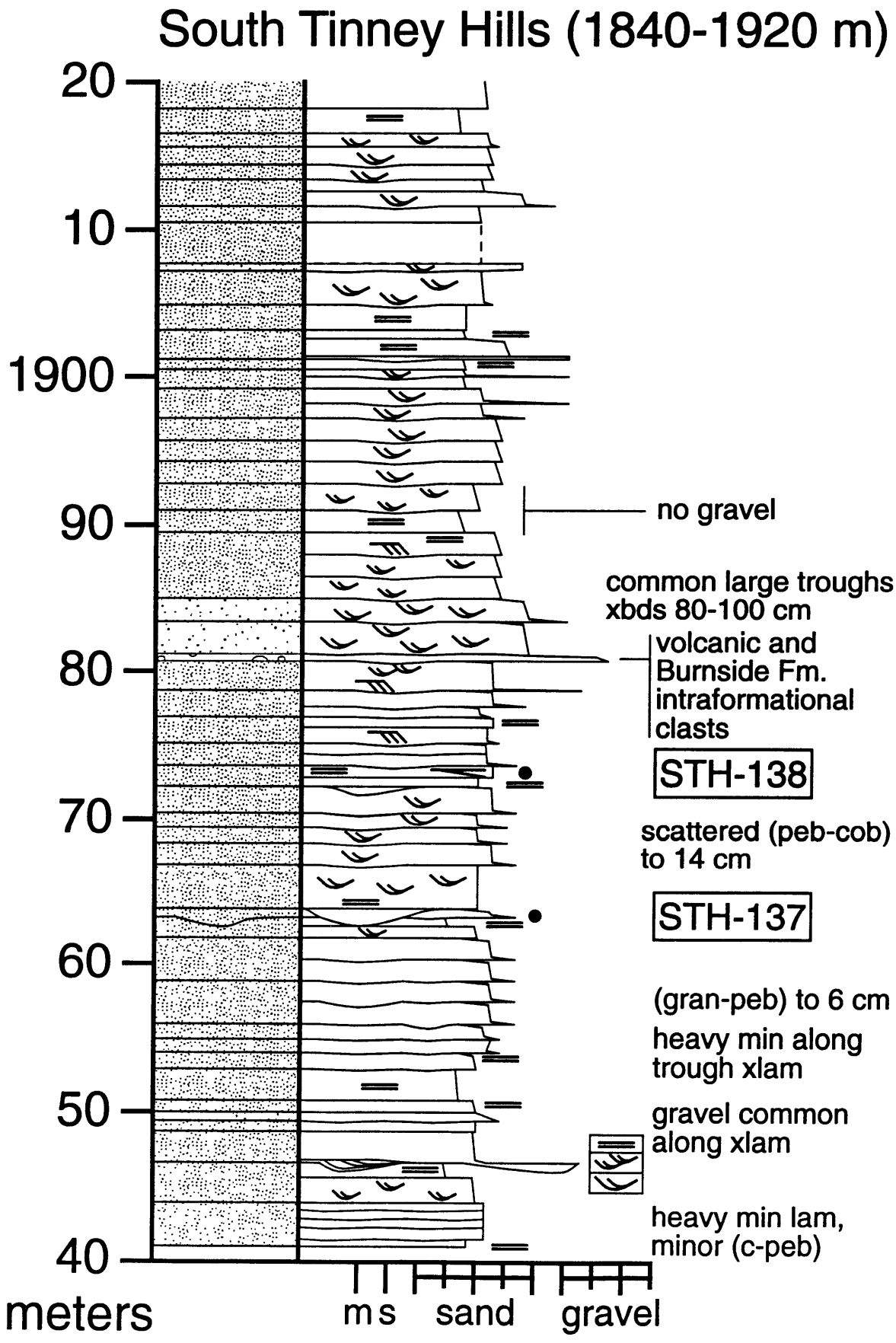
South Tinney Hills (1840-1920 m)
20
10
1900
90
80
70
60
50
40
meters
ms
sand
gravel
no gravel
common large troughs
xbds 80-100 cm
volcanic and
Burnside Fm.
intraformational
clasts
STH-138
scattered (peb-cob)
to 14 cm
STH-137
(gran-peb) to 6 cm
heavy min along
trough xlam
gravel common
along xlam
heavy min lam,
minor (c-peb)

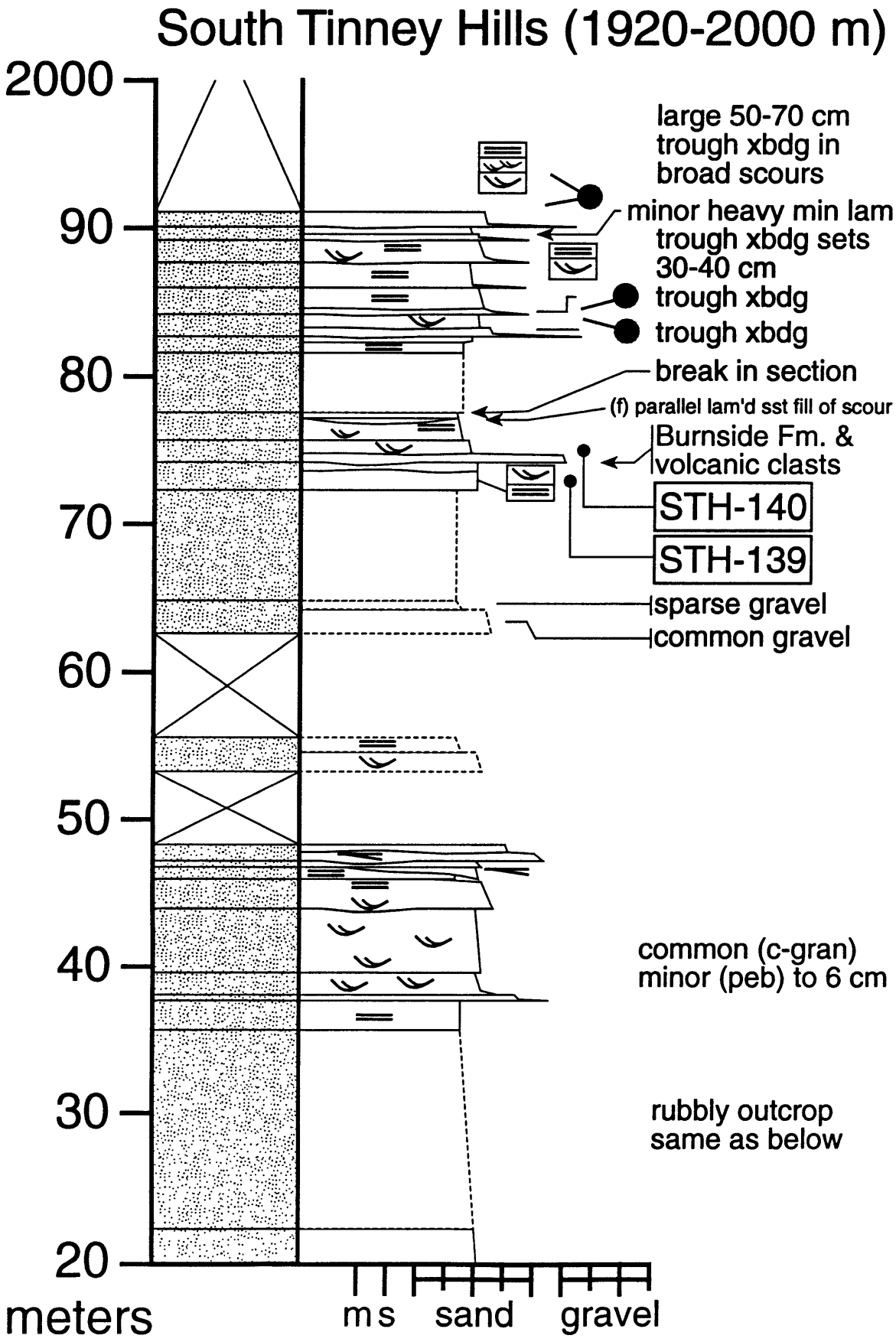
South Tinney Hills (1920-2000 m)
2000
90
80
70
60
50
40
30
20
meters
m s
sand
gravel
large 50-70 cm trough xbdg in broad scours
minor heavy min lam trough xbdg sets 30-40 cm
trough xbdg
trough xbdg
break in section
(f) parallel lam'd sst fill of scour
Burnside Fm. & volcanic clasts
STH-140
STH-139
sparse gravel
common gravel
common (c-gran) minor (peb) to 6 cm
rubbly outcrop same as below

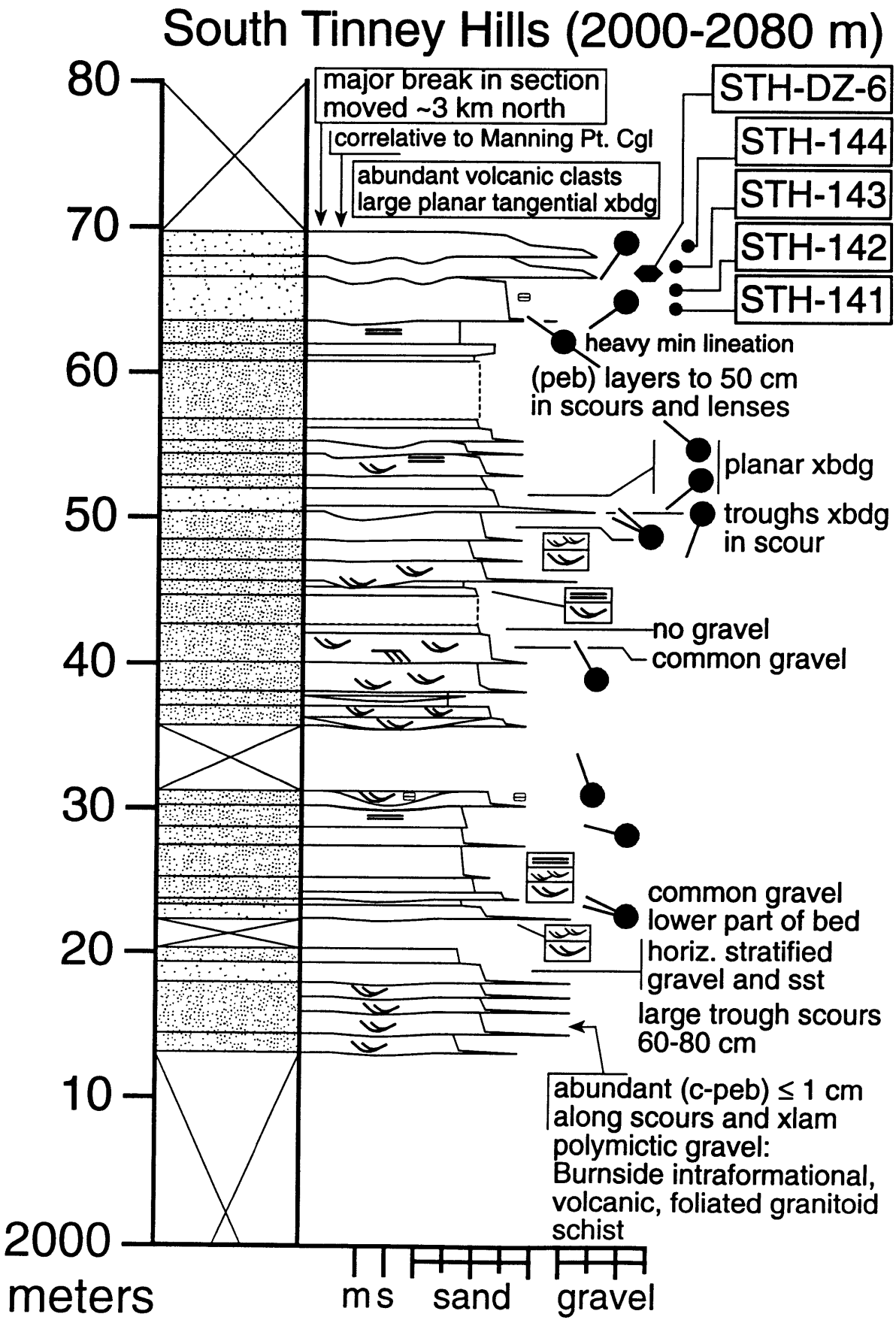
South Tinney Hills (2000-2080 m)
80
70
60
50
40
30
20
10
2000
meters
major break in section
moved ~3 km north
correlative to Manning Pt. Cgl
abundant volcanic clasts
large planar tangential xbdg
STH-DZ-6
STH-144
STH-143
STH-142
STH-141
heavy min lineation
(peb) layers to 50 cm
in scours and lenses
planar xbdg
troughs xbdg
in scour
no gravel
common gravel
common gravel
lower part of bed
horiz. stratified
gravel and sst
large trough scours
60-80 cm
abundant (c-peb) ≤ 1 cm
along scours and xlam
polymictic gravel:
Burnside intraformational,
volcanic, foliated granitoid
schist
m s
sand
gravel

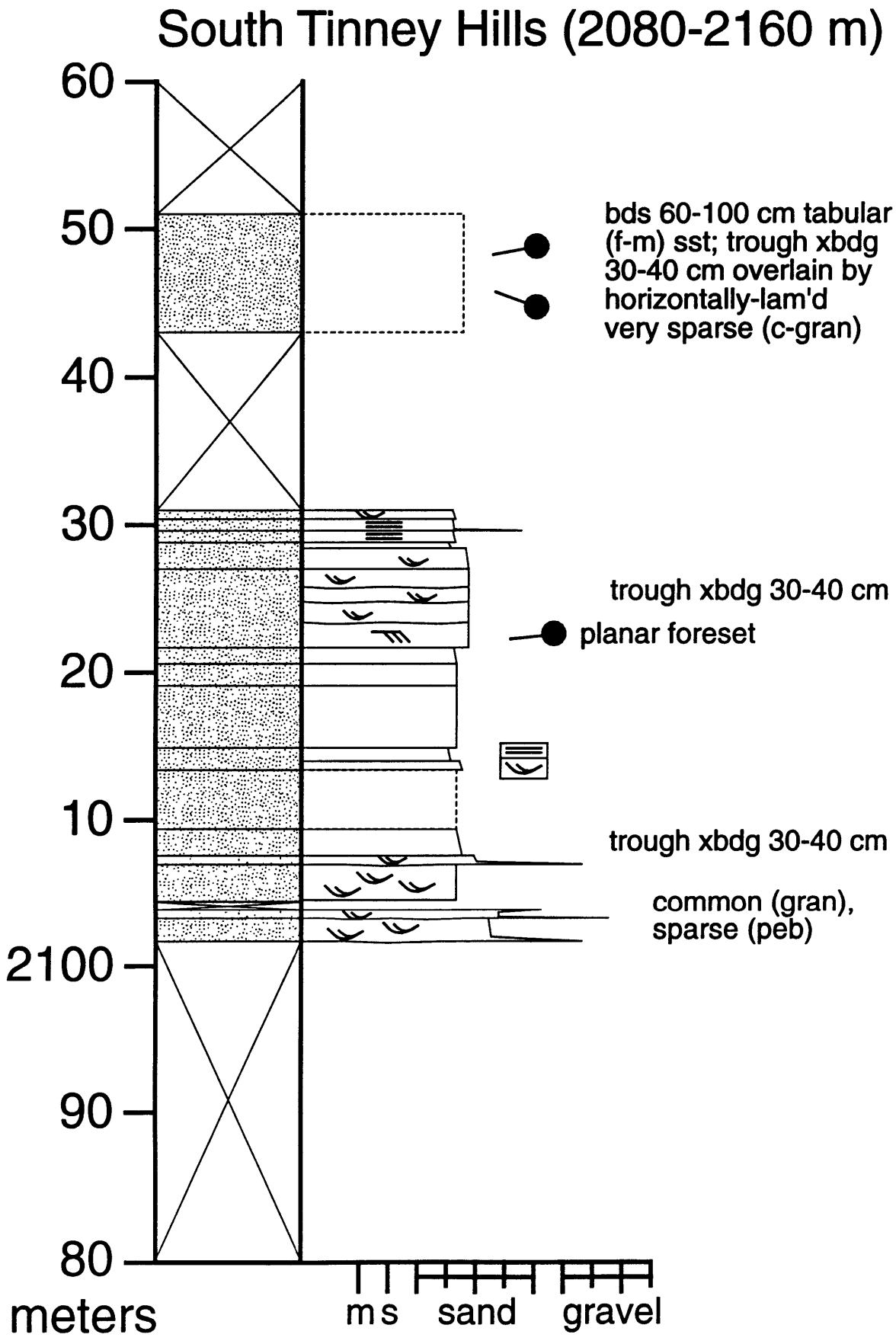
South Tinney Hills (2080-2160 m)
60
50
40
30
20
10
2100
90
80
meters
bds 60-100 cm tabular (f-m) sst; trough xbdg 30-40 cm overlain by horizontally-lam'd very sparse (c-gran)
trough xbdg 30-40 cm
planar foreset
trough xbdg 30-40 cm
common (gran), sparse (peb)
m s
sand
gravel

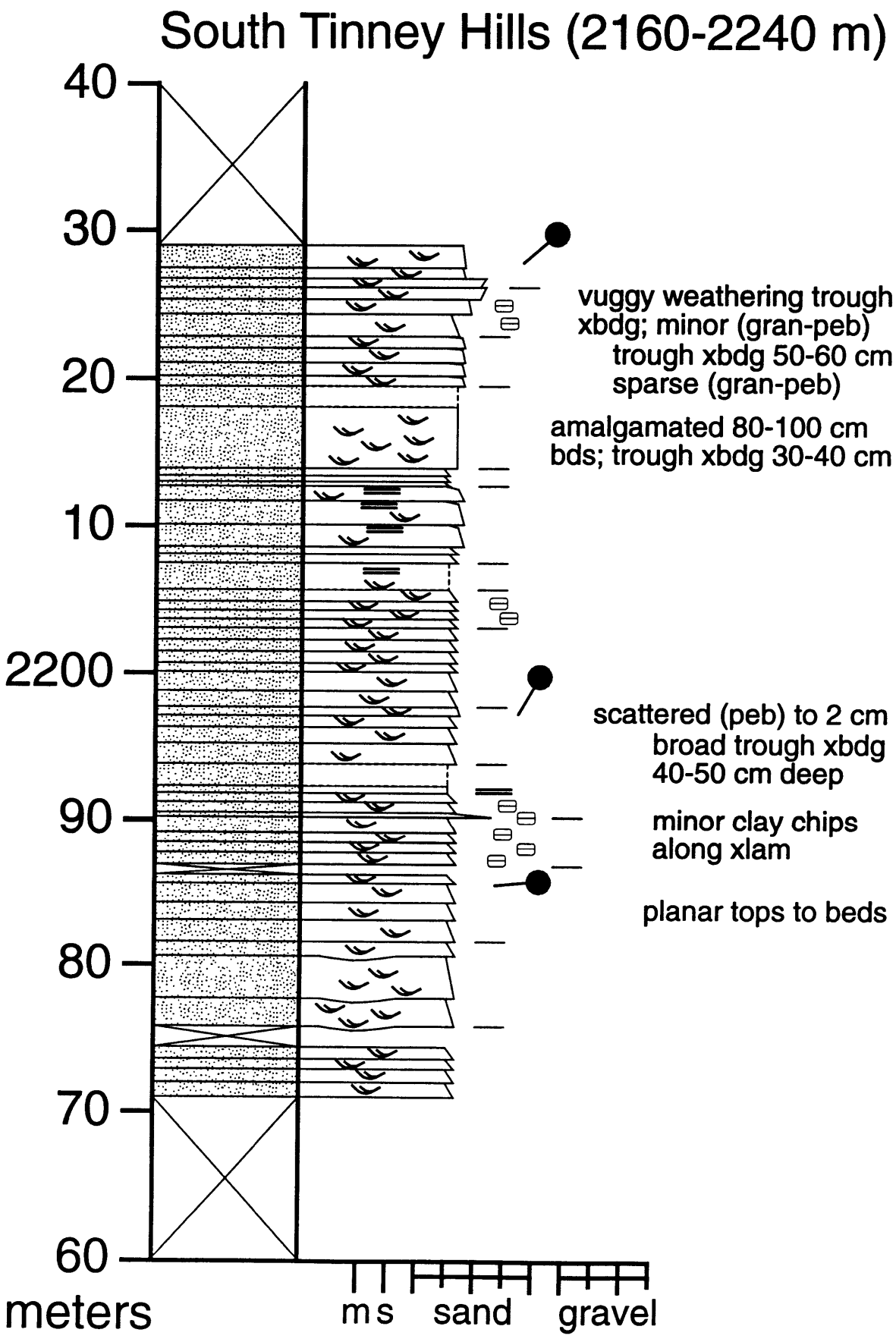
South Tinney Hills (2160-2240 m)
40
30
20
10
2200
90
80
70
60
meters
m s
sand
gravel
vuggy weathering trough xbdg; minor (gran-peb) trough xbdg 50-60 cm sparse (gran-peb)
amalgamated 80-100 cm bds; trough xbdg 30-40 cm
scattered (peb) to 2 cm broad trough xbdg 40-50 cm deep
minor clay chips along xlam
planar tops to beds

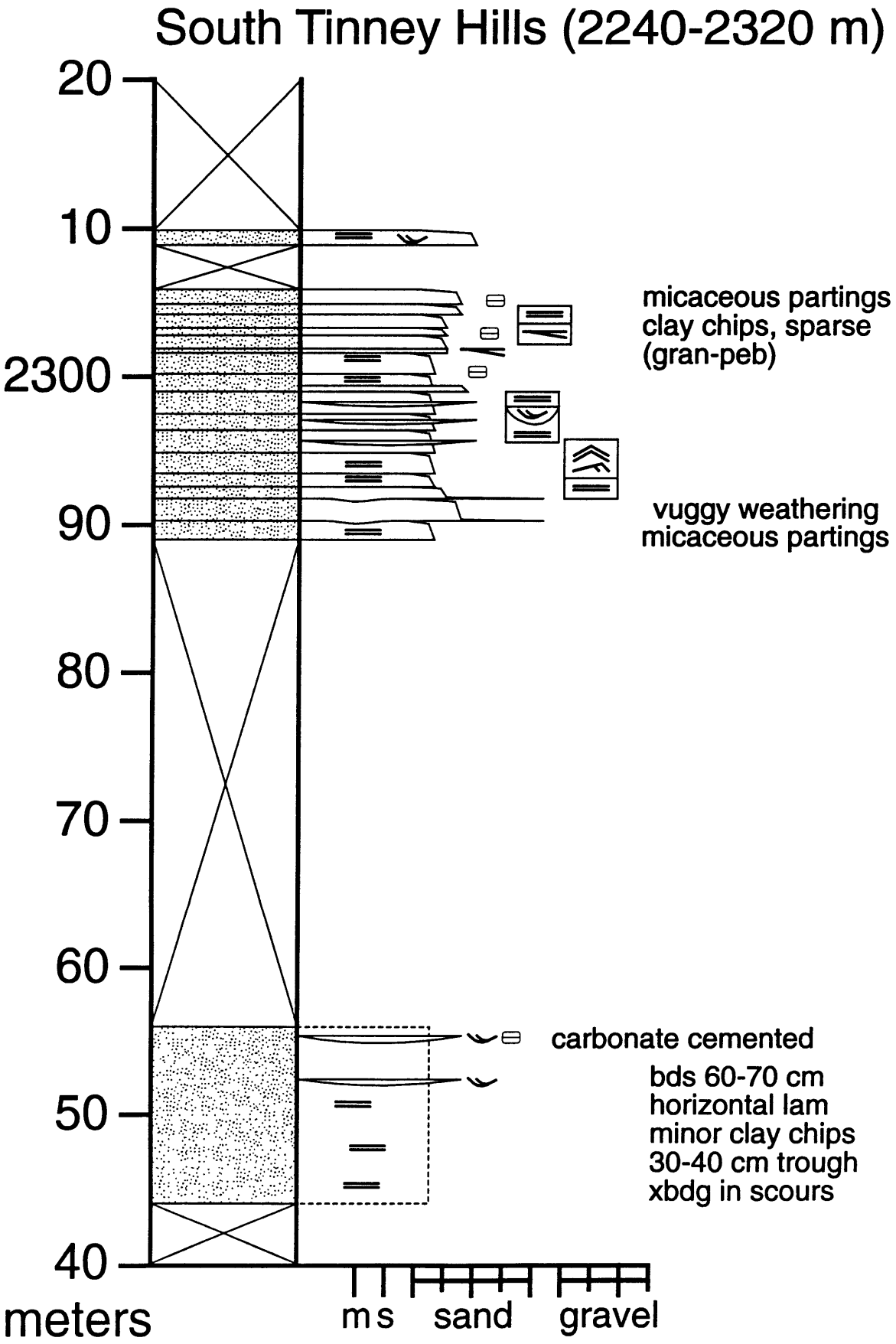
South Tinney Hills (2240-2320 m)
20
10
2300
90
80
70
60
50
40
meters
micaceous partings
clay chips, sparse
(gran-peb)
vuggy weathering
micaceous partings
carbonate cemented
bds 60-70 cm
horizontal lam
minor clay chips
30-40 cm trough
xbdg in scours
m s
sand
gravel

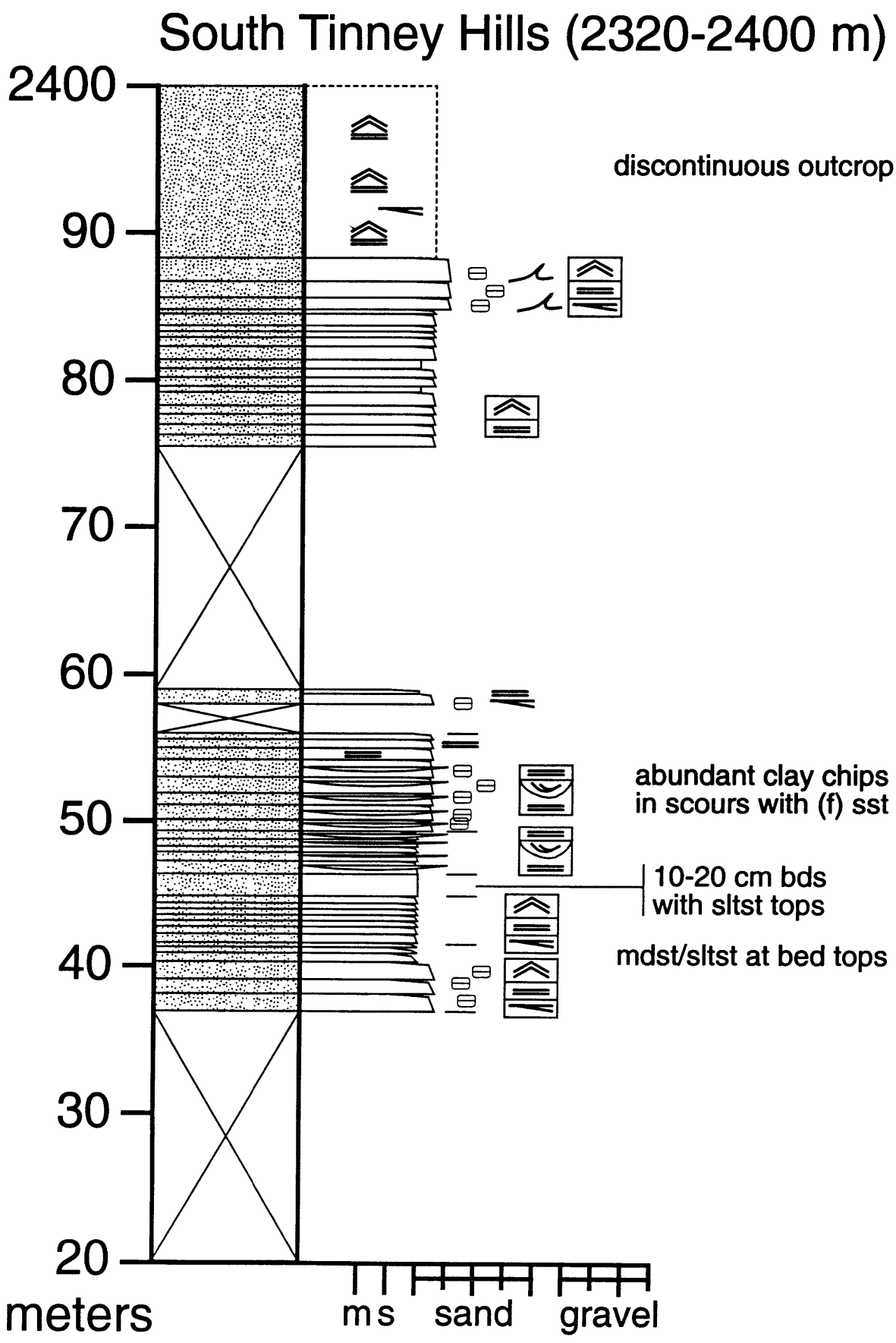
South Tinney Hills (2320-2400 m)
2400
90
80
70
60
50
40
30
20
meters
discontinuous outcrop
abundant clay chips
in scours with (f) sst
10-20 cm bds
with sltst tops
mdst/sltst at bed tops
m s
sand
gravel

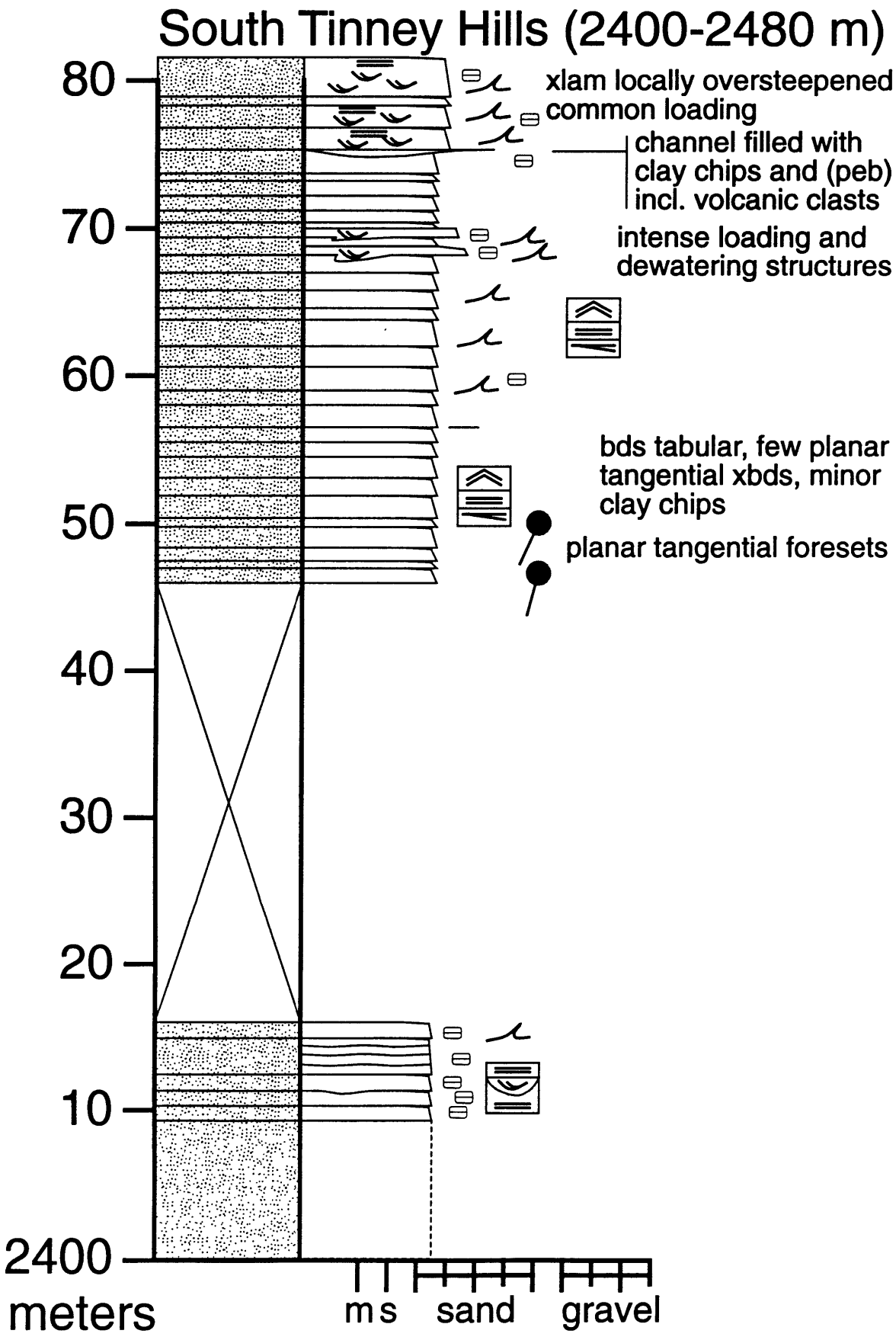
South Tinney Hills (2400-2480 m)
80
70
60
50
40
30
20
10
2400
meters
xlam locally oversteepened
common loading
channel filled with
clay chips and (peb)
incl. volcanic clasts
intense loading and
dewatering structures
bds tabular, few planar
tangential xbds, minor
clay chips
planar tangential foresets
m s
sand
gravel

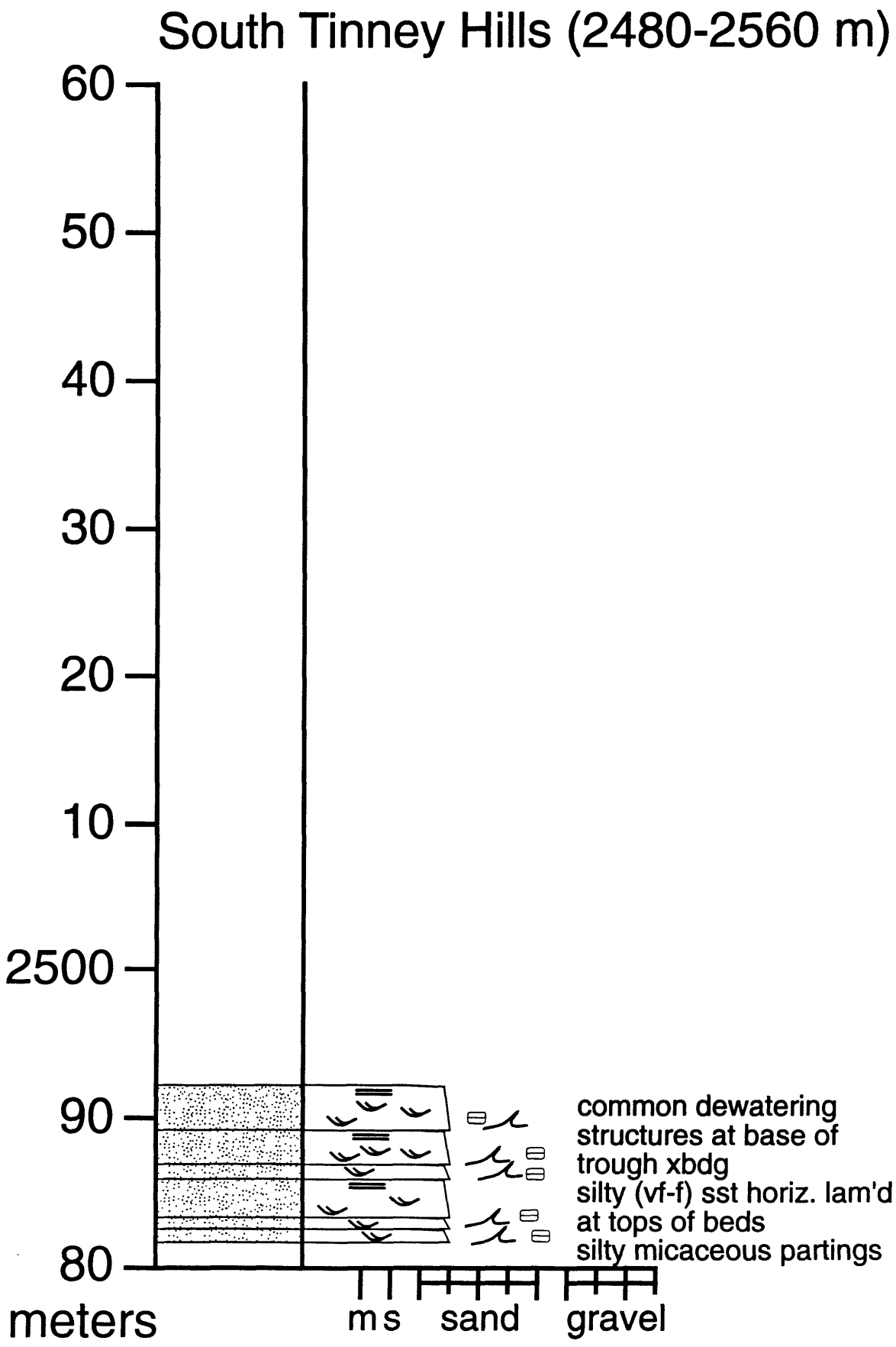
South Tinney Hills (2480-2560 m)
60
50
40
30
20
10
2500
90
80
meters
m s
sand
gravel
common dewatering
structures at base of
trough xbdg
silty (vf-f) sst horiz. lam'd
at tops of beds
silty micaceous partings

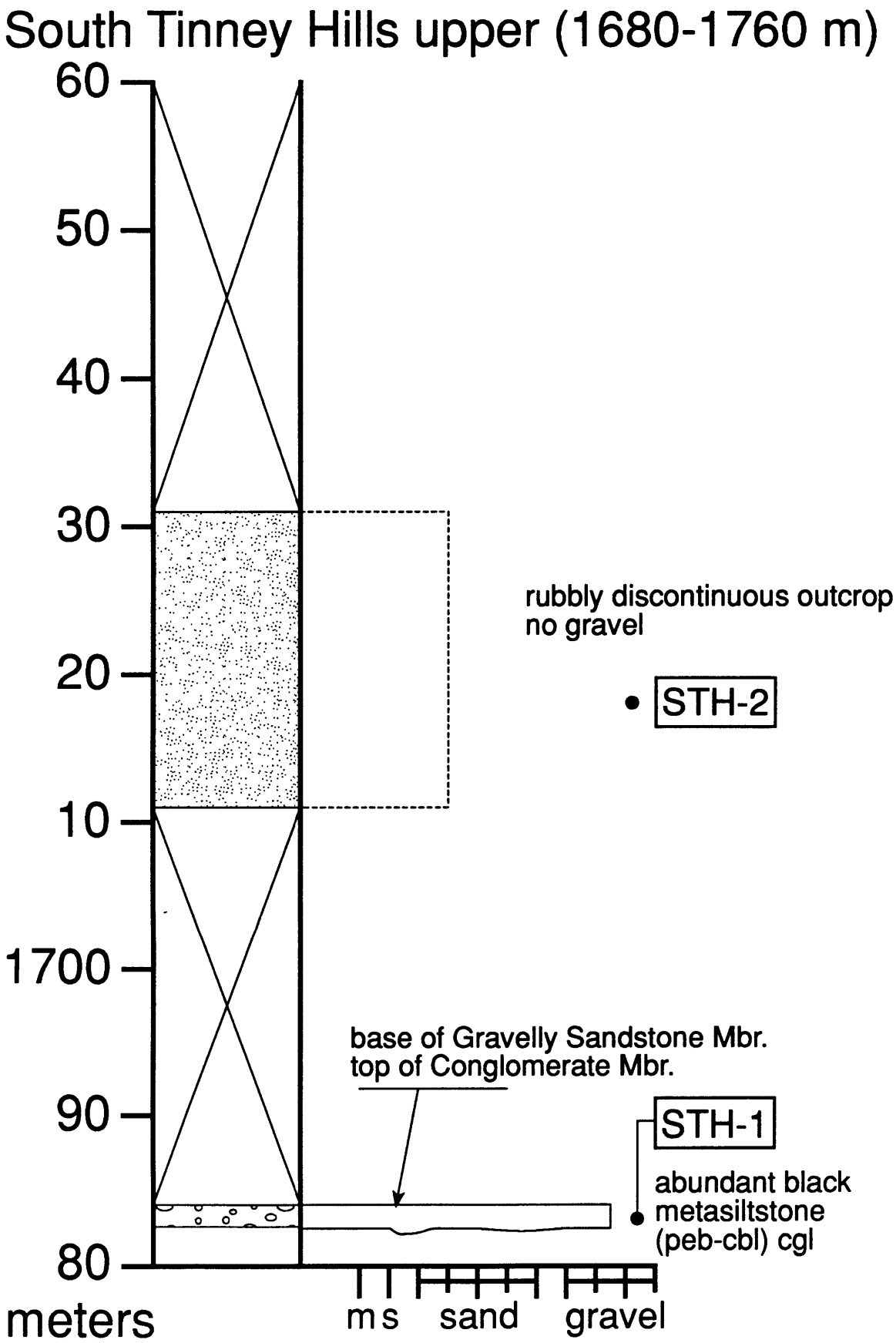
South Tinney Hills upper (1680-1760 m)
60
50
40
30
20
10
1700
90
80
meters
rubbly discontinuous outcrop
no gravel
STH-2
base of Gravelly Sandstone Mbr.
top of Conglomerate Mbr.
STH-1
abundant black
metasiltstone
(peb-cbl) cgl
ms
sand
gravel

South Tinney Hills upper (1760-1840 m)

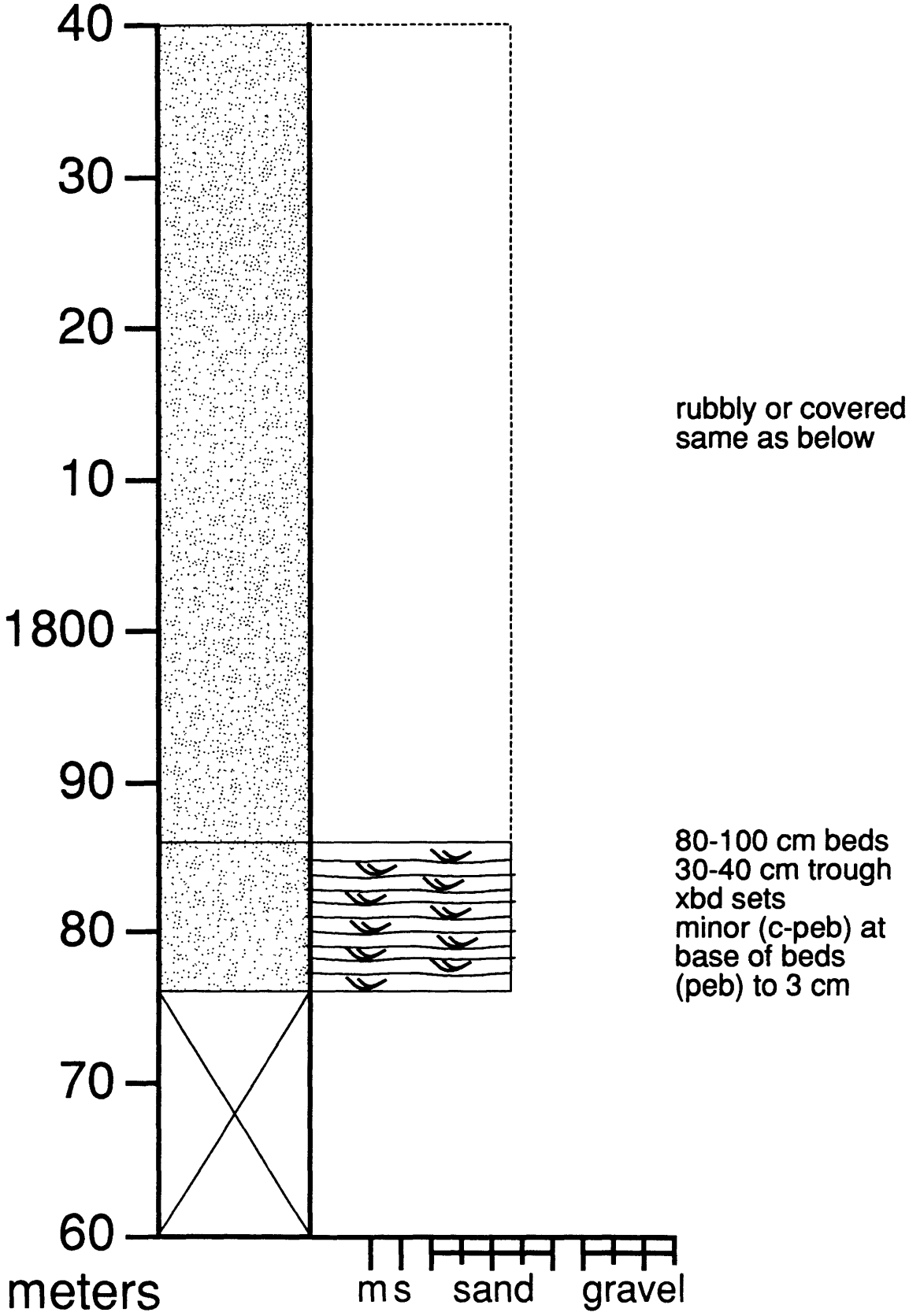

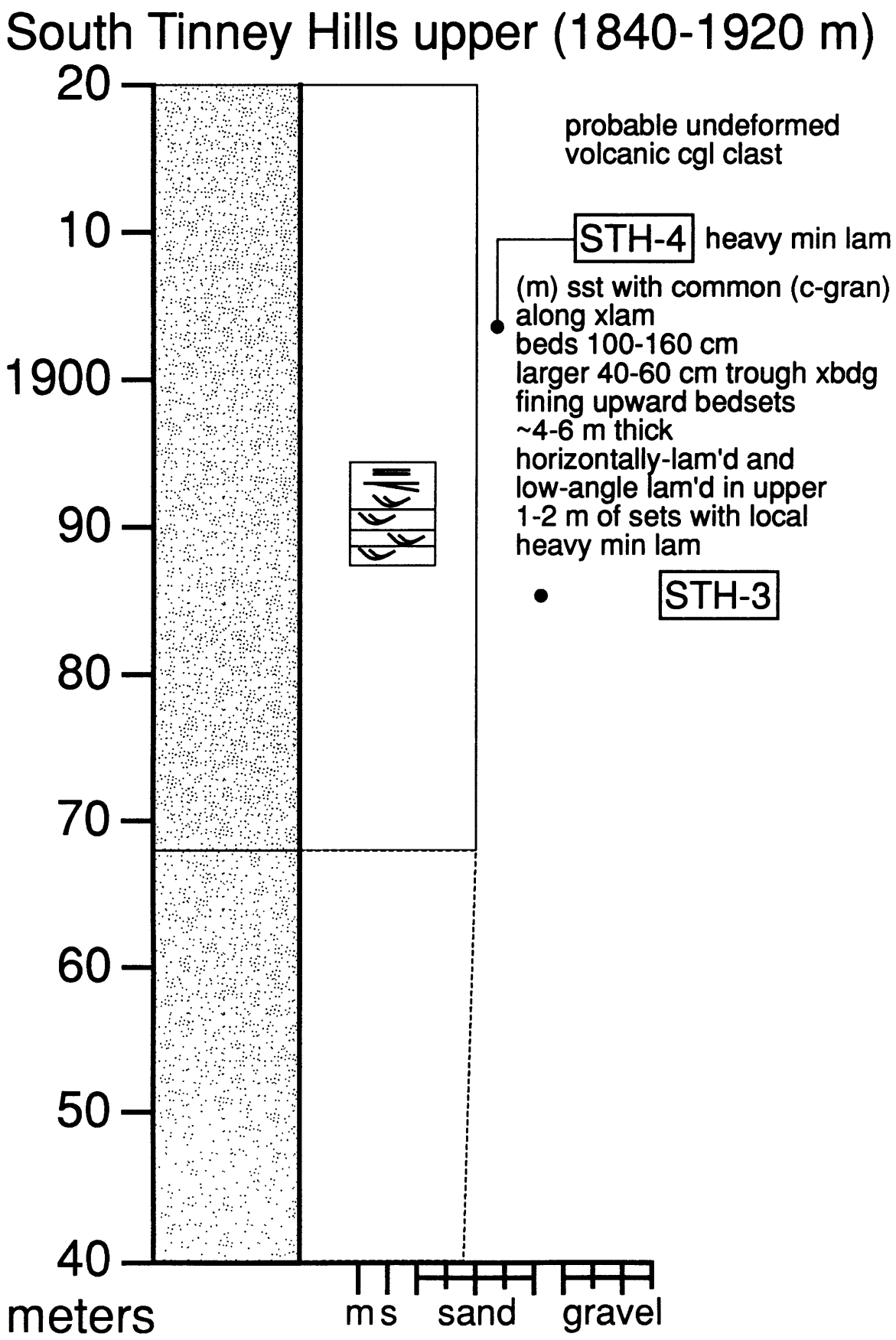
South Tinney Hills upper (1840-1920 m)
20
10
1900
90
80
70
60
50
40
meters
probable undeformed volcanic cgl clast
STH-4
heavy min lam
(m) sst with common (c-gran) along xlam
beds 100-160 cm
larger 40-60 cm trough xbdg
fining upward bedsets
~4-6 m thick
horizontally-lam'd and low-angle lam'd in upper 1-2 m of sets with local heavy min lam
STH-3
ms
sand
gravel

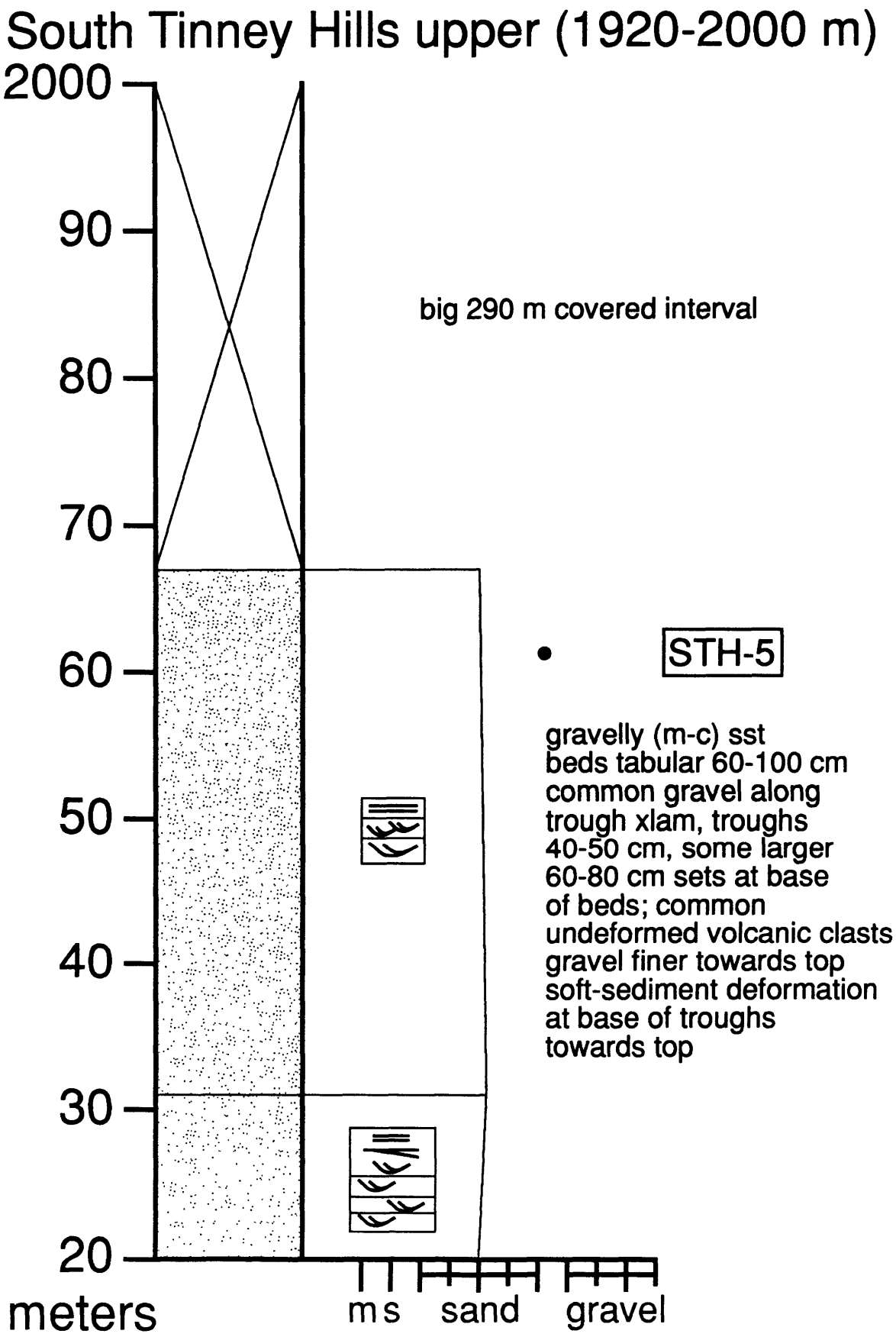
South Tinney Hills upper (1920-2000 m)
2000
90
80
70
60
50
40
30
20
meters
big 290 m covered interval
STH-5
gravelly (m-c) sst
beds tabular 60-100 cm
common gravel along
trough xlam, troughs
40-50 cm, some larger
60-80 cm sets at base
of beds; common
undeformed volcanic clasts
gravel finer towards top
soft-sediment deformation
at base of troughs
towards top
ms
sand
gravel

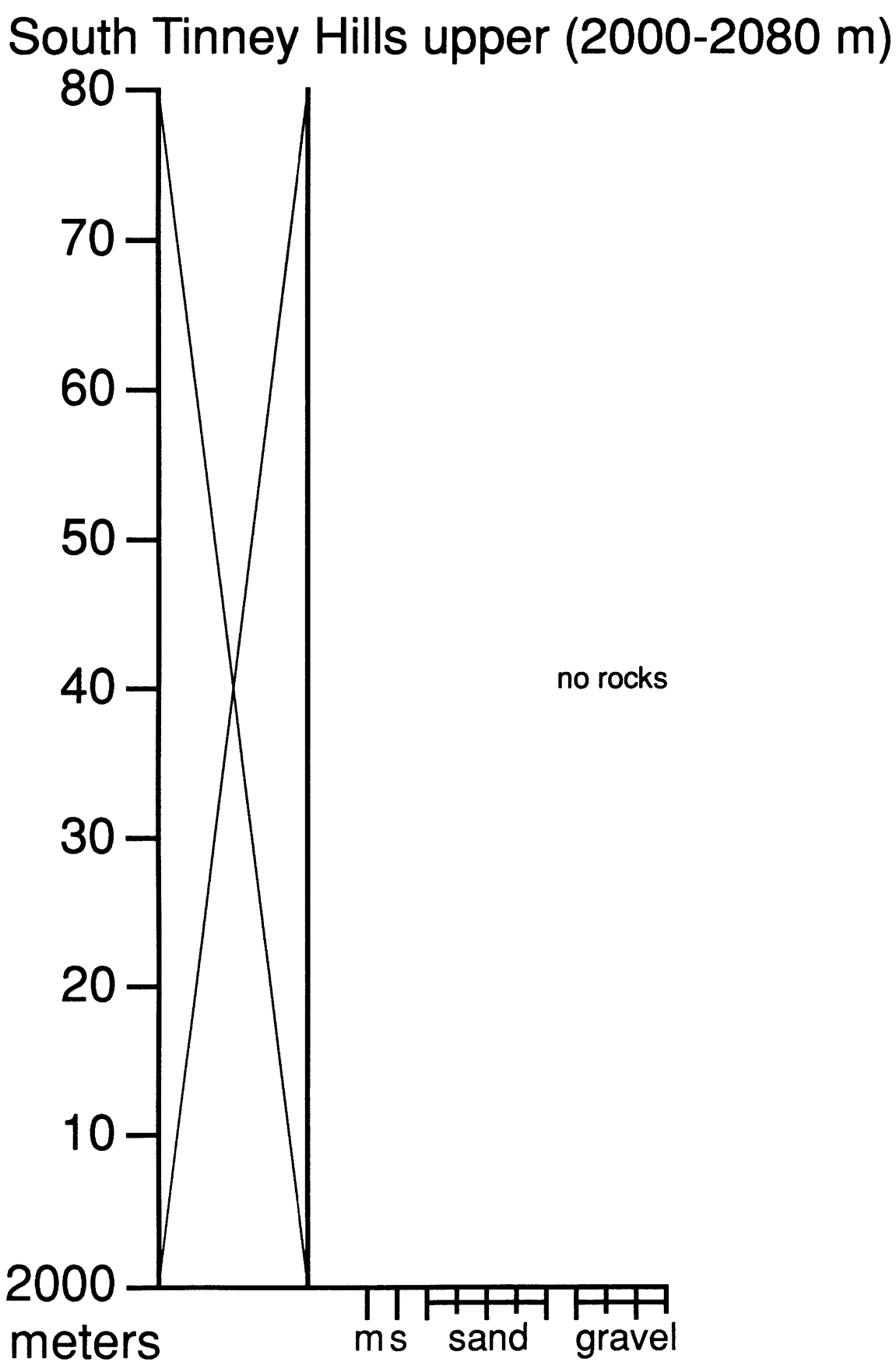
South Tinney Hills upper (2000-2080 m)
80
70
60
50
40
30
20
10
2000
meters
no rocks
m
s
sand
gravel

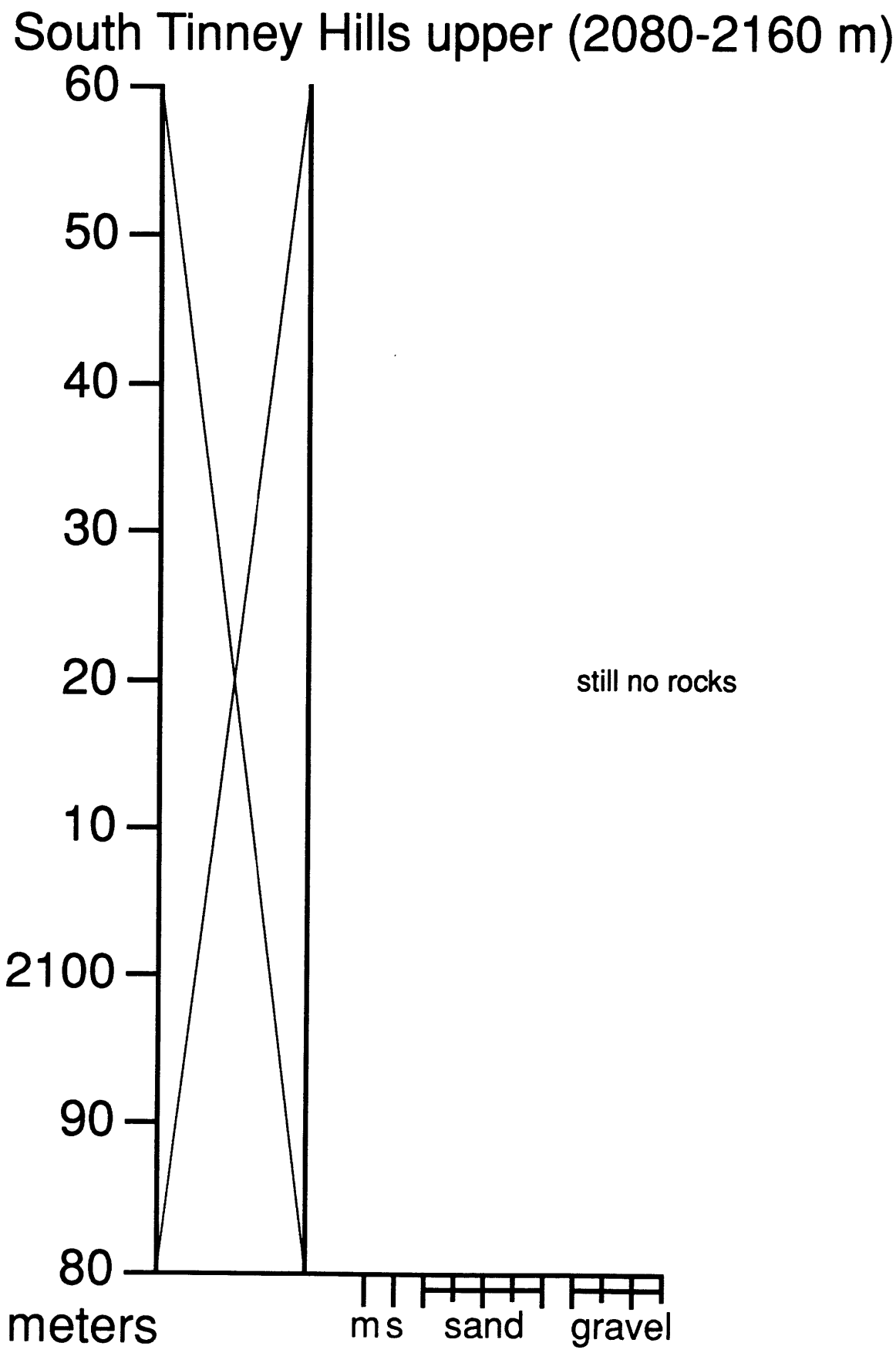
South Tinney Hills upper (2080-2160 m)
60
50
40
30
20
10
2100
90
80
meters
still no rocks
m s
sand
gravel

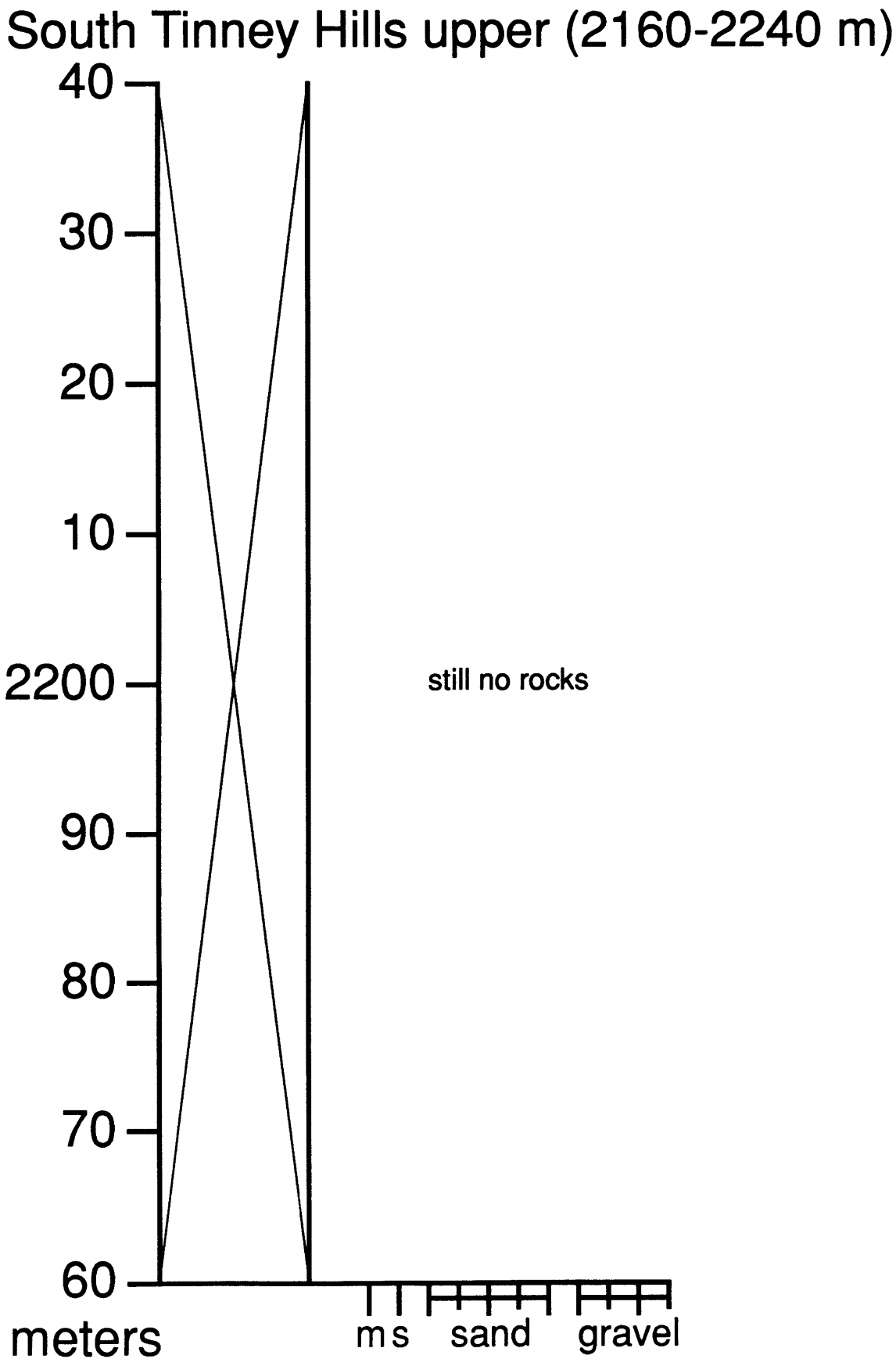
South Tinney Hills upper (2160-2240 m)
40
30
20
10
2200
90
80
70
60
meters
still no rocks
m s
sand
gravel

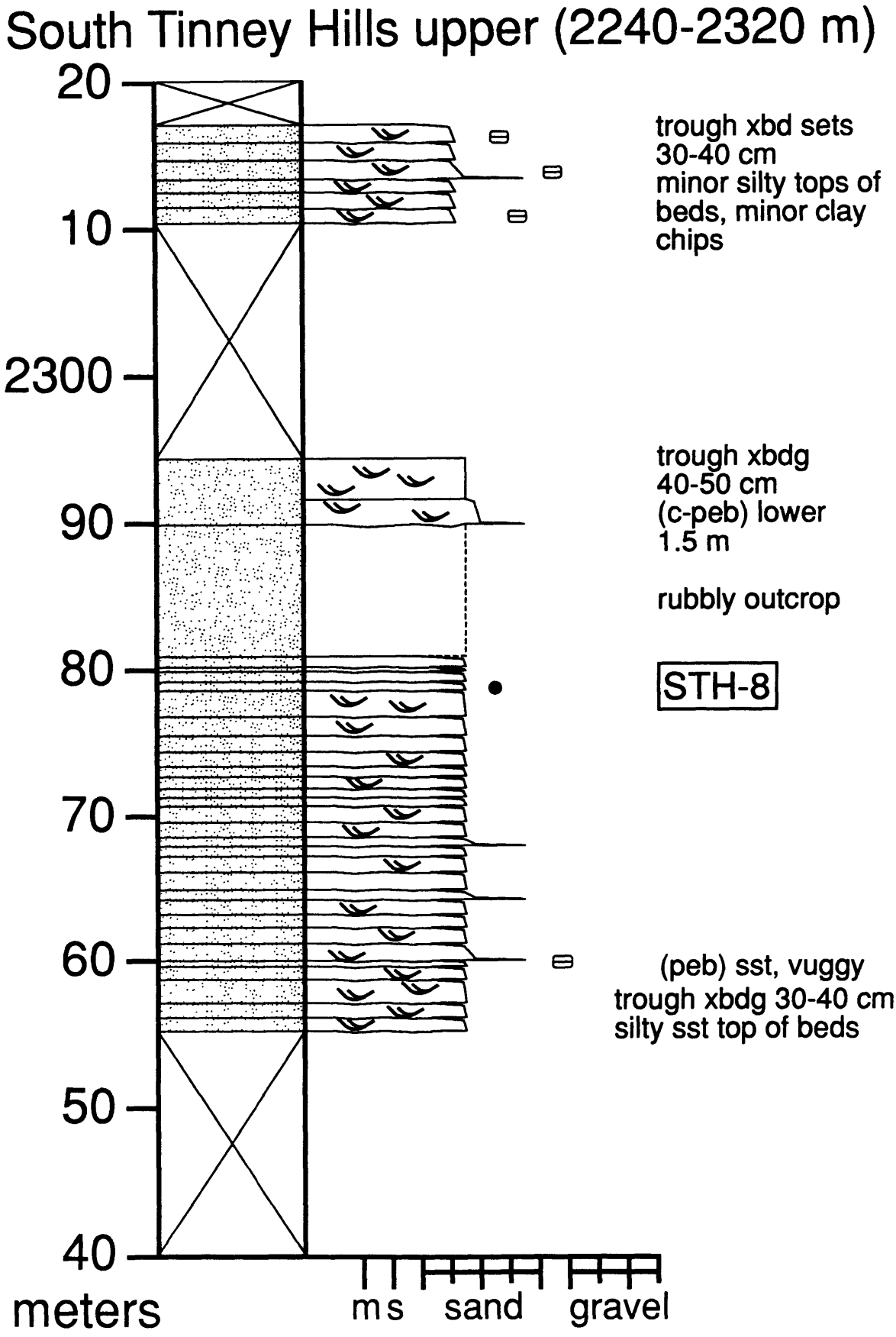
South Tinney Hills upper (2240-2320 m)
20
10
2300
90
80
70
60
50
40
meters
ms
sand
gravel
trough xbd sets
30-40 cm
minor silty tops of
beds, minor clay
chips
trough xbdg
40-50 cm
(c-peb) lower
1.5 m
rubbly outcrop
STH-8
(peb) sst, vuggy
trough xbdg 30-40 cm
silty sst top of beds

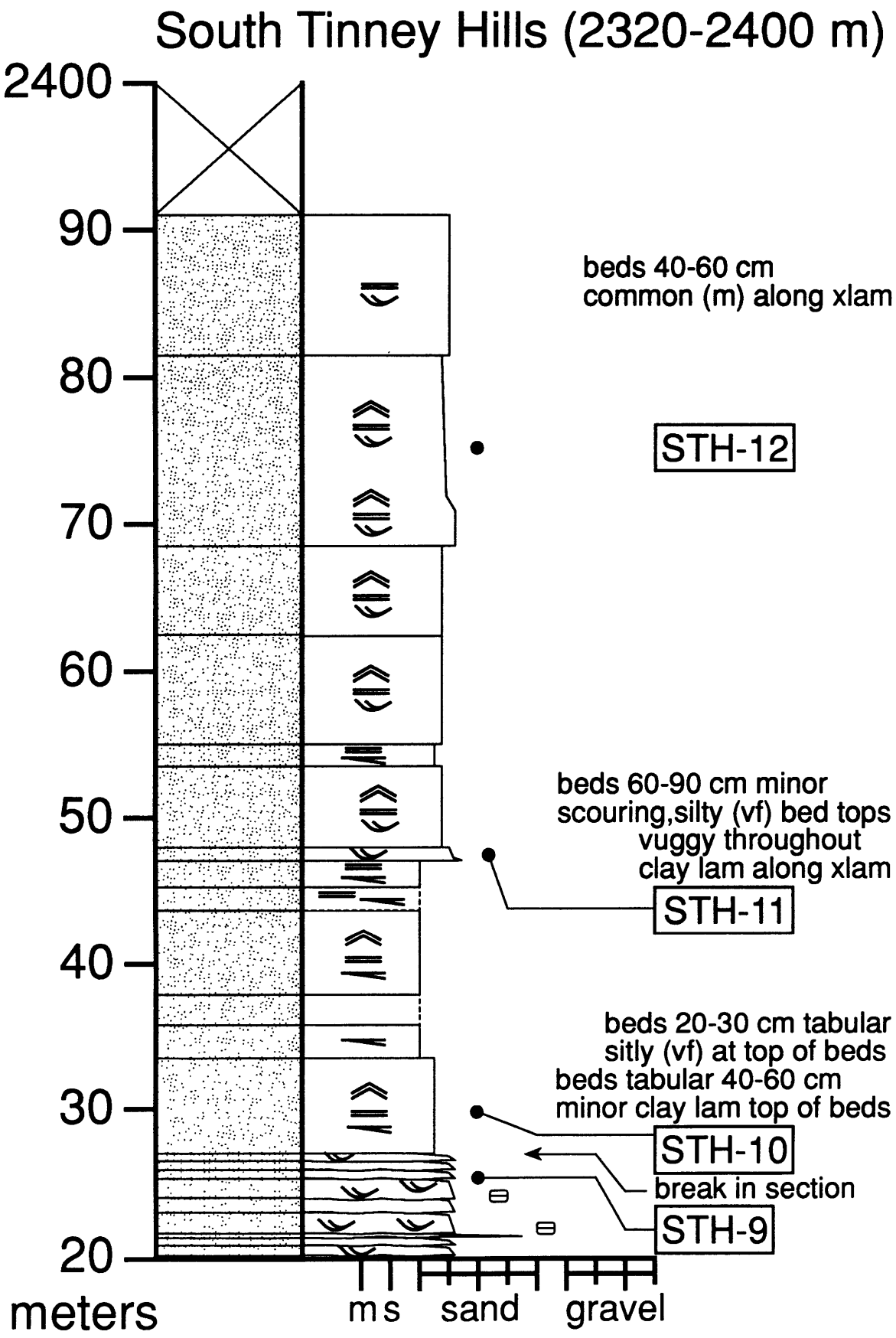
South Tinney Hills (2320-2400 m)
2400
90
80
70
60
50
40
30
20
meters
ms
sand
gravel
beds 40-60 cm
common (m) along xlam
STH-12
beds 60-90 cm minor
scouring,silty (vf) bed tops
vuggy throughout
clay lam along xlam
STH-11
beds 20-30 cm tabular
sitly (vf) at top of beds
beds tabular 40-60 cm
minor clay lam top of beds
STH-10
break in section
STH-9

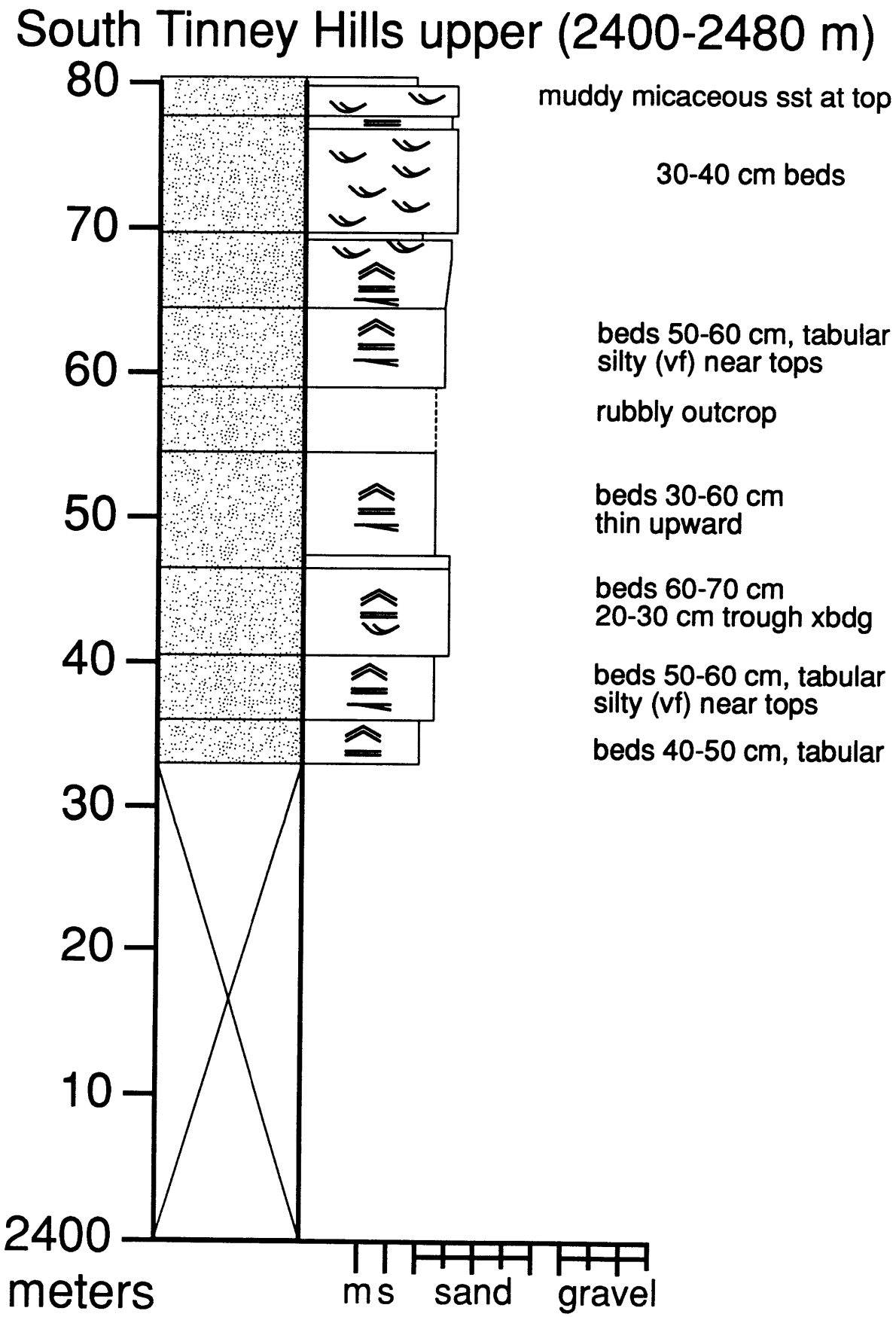
South Tinney Hills upper (2400-2480 m)
80
70
60
50
40
30
20
10
2400
meters
muddy micaceous sst at top
30-40 cm beds
beds 50-60 cm, tabular
silty (vf) near tops
rubbly outcrop
beds 30-60 cm
thin upward
beds 60-70 cm
20-30 cm trough xbdg
beds 50-60 cm, tabular
silty (vf) near tops
beds 40-50 cm, tabular
ms
sand
gravel

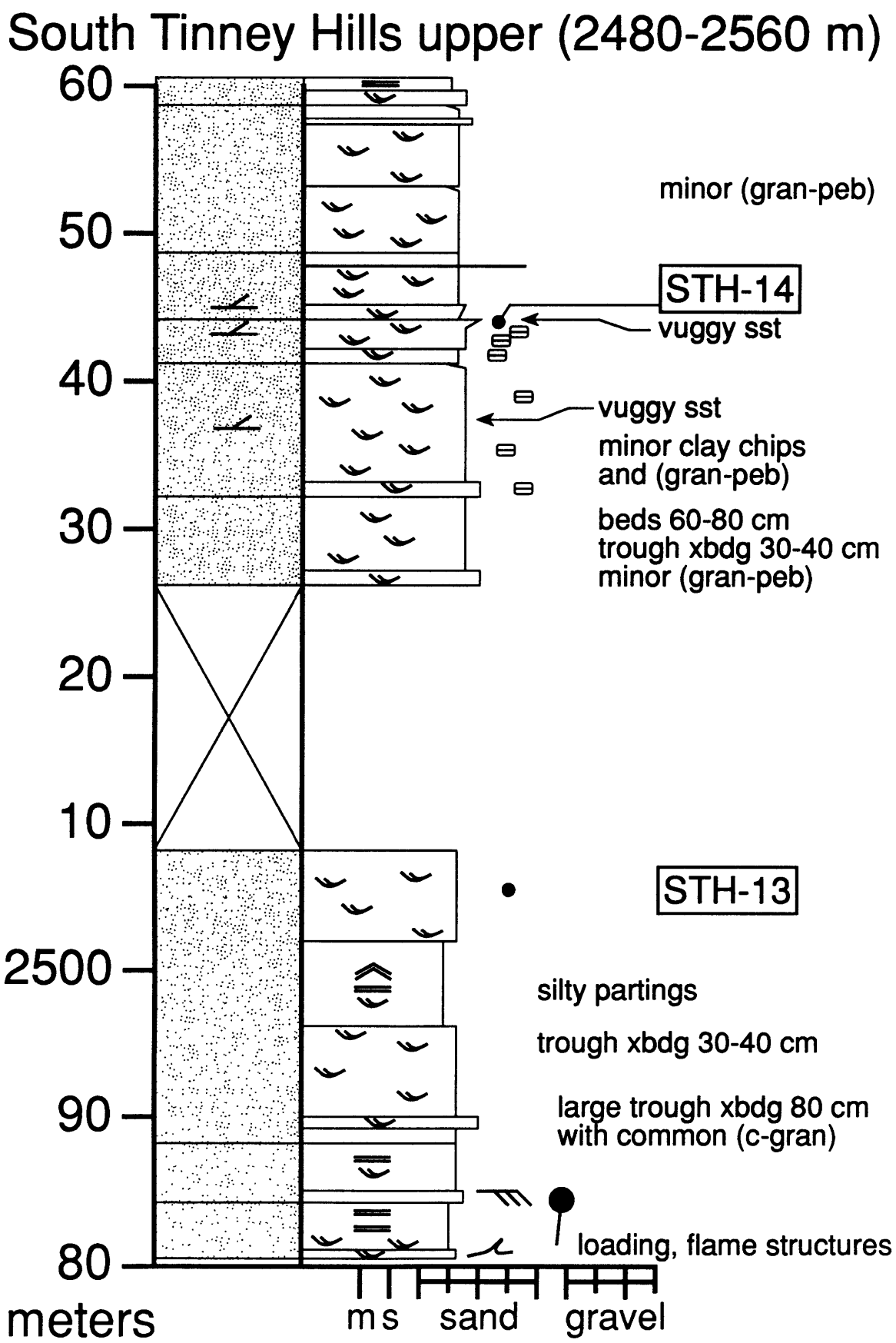
South Tinney Hills upper (2480-2560 m)
60
50
40
30
20
10
2500
90
80
meters
minor (gran-peb)
STH-14
vuggy sst
vuggy sst
minor clay chips
and (gran-peb)
beds 60-80 cm
trough xbdg 30-40 cm
minor (gran-peb)
STH-13
silty partings
trough xbdg 30-40 cm
large trough xbdg 80 cm
with common (c-gran)
loading, flame structures
ms
sand
gravel

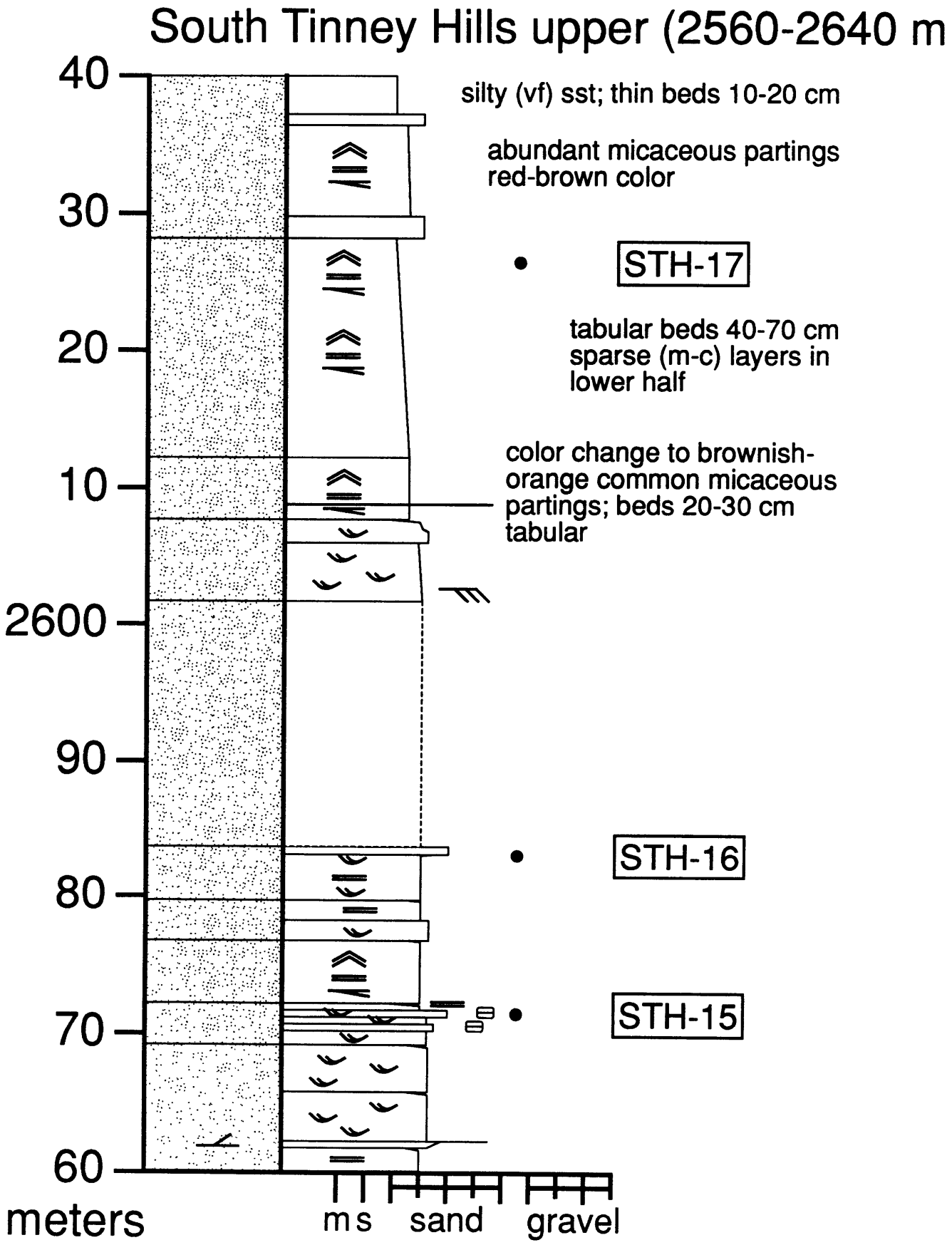
South Tinney Hills upper (2560-2640 m
40
30
20
10
2600
90
80
70
60
meters
silty (vf) sst; thin beds 10-20 cm
abundant micaceous partings
red-brown color
STH-17
tabular beds 40-70 cm
sparse (m-c) layers in
lower half
color change to brownish-
orange common micaceous
partings; beds 20-30 cm
tabular
STH-16
STH-15
m s
sand
gravel

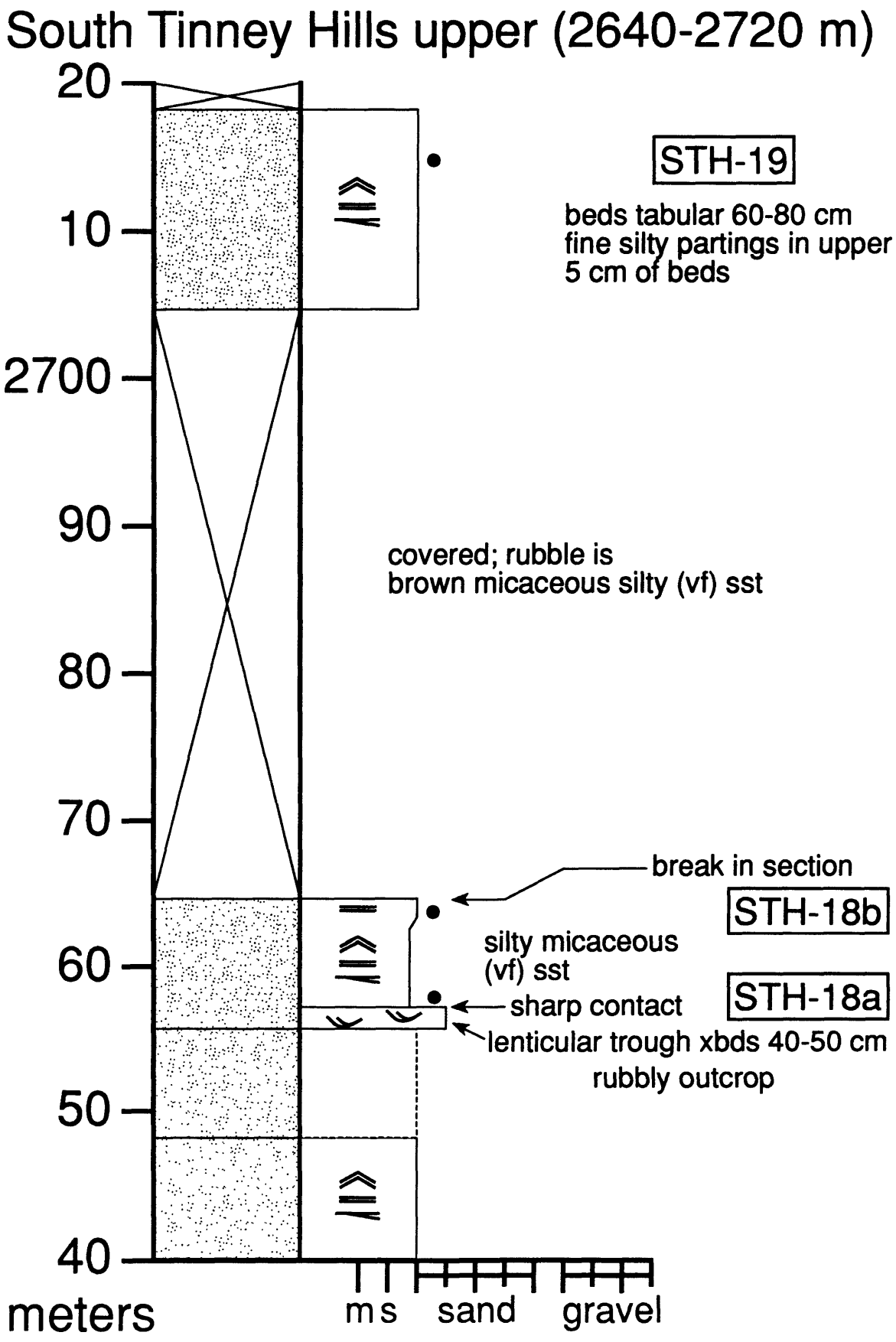
South Tinney Hills upper (2640-2720 m)
20
10
2700
90
80
70
60
50
40
meters
STH-19
beds tabular 60-80 cm
fine silty partings in upper
5 cm of beds
covered; rubble is
brown micaceous silty (vf) sst
break in section
STH-18b
silty micaceous
(vf) sst
sharp contact
STH-18a
lenticular trough xbds 40-50 cm
rubbly outcrop
m s
sand
gravel

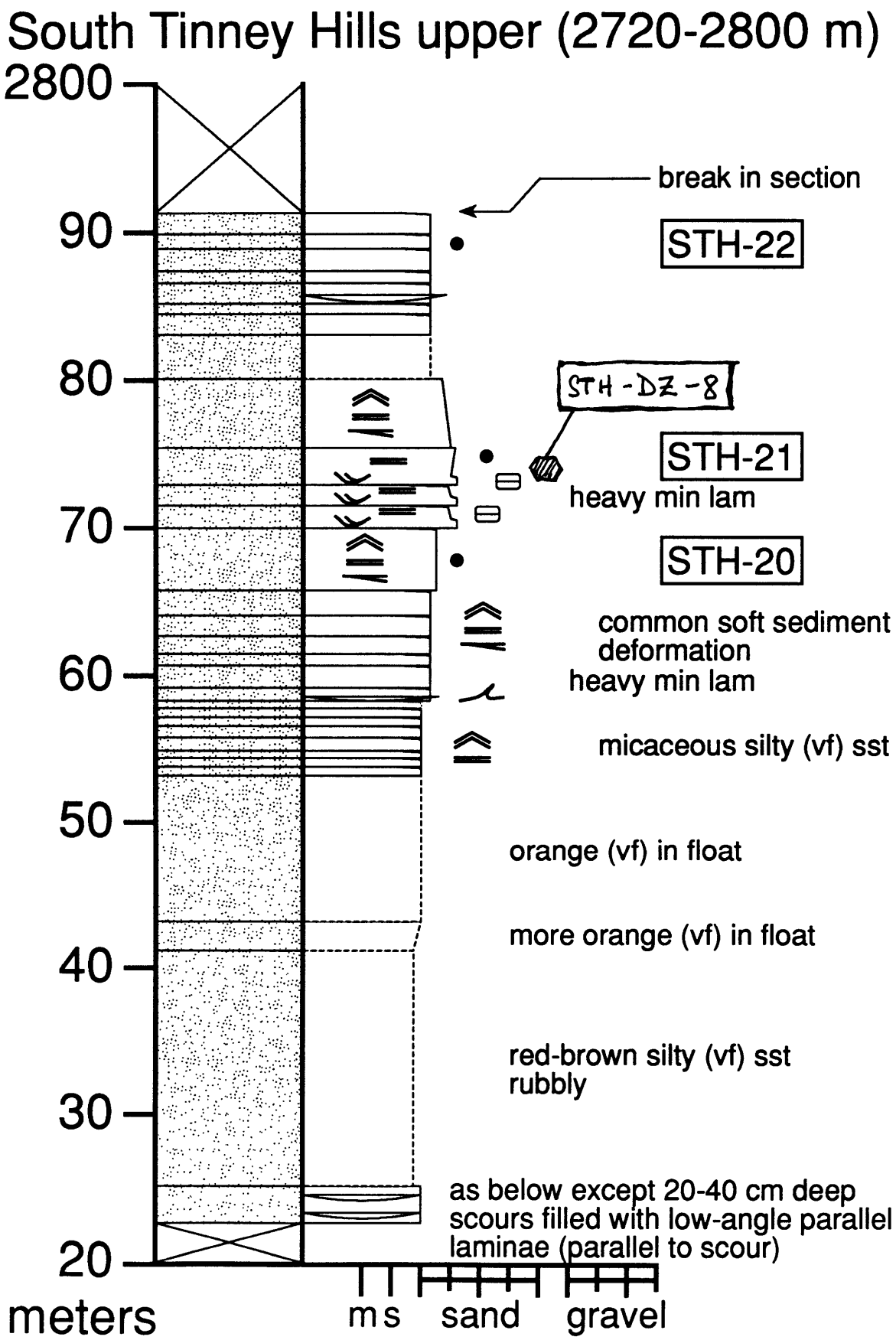
South Tinney Hills upper (2720-2800 m)
2800
90
80
70
60
50
40
30
20
meters
break in section
STH-22
STH-DZ-8
STH-21
heavy min lam
STH-20
common soft sediment deformation
heavy min lam
micaceous silty (vf) sst
orange (vf) in float
more orange (vf) in float
red-brown silty (vf) sst
rubbly
as below except 20-40 cm deep scours filled with low-angle parallel laminae (parallel to scour)
m s
sand
gravel

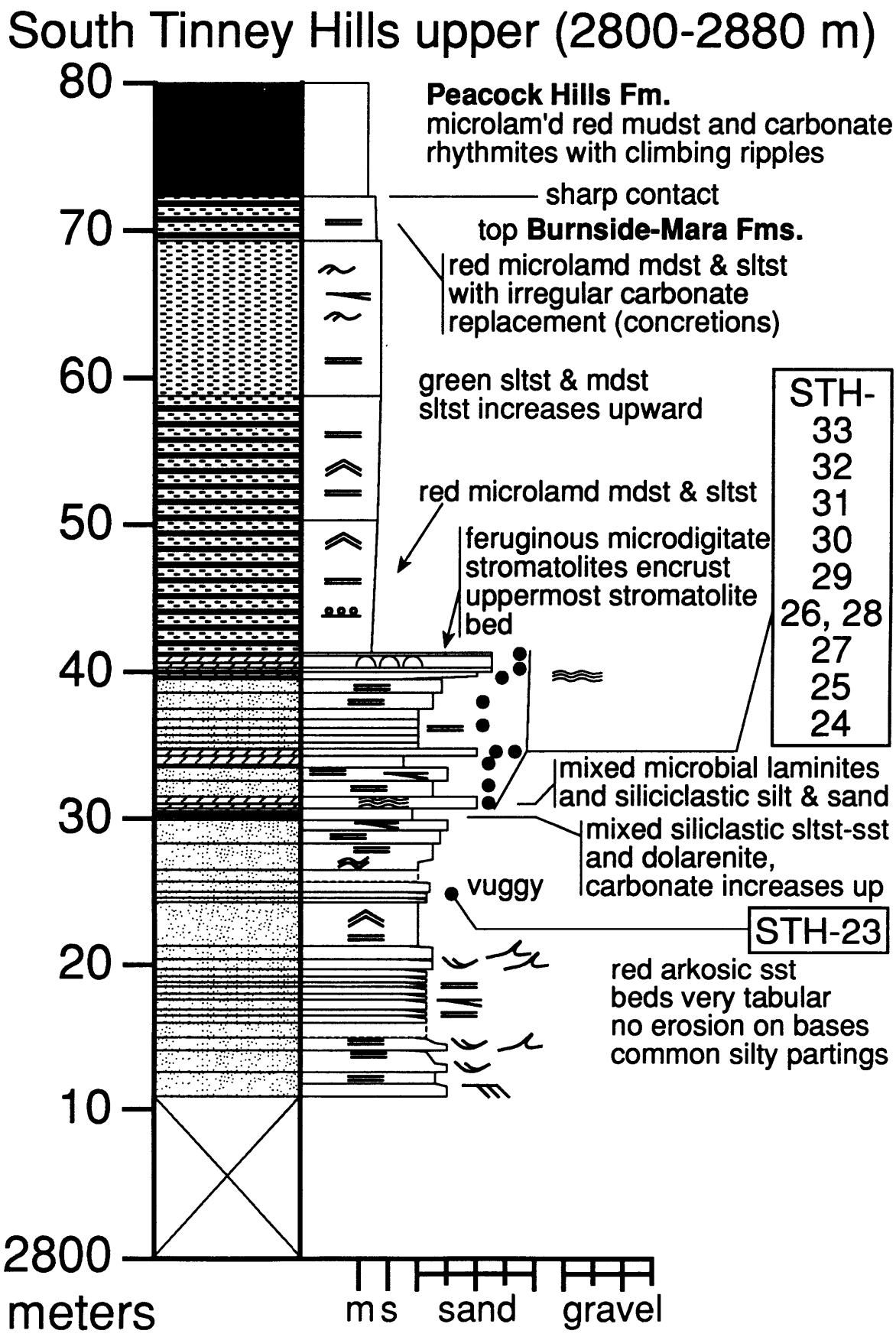
South Tinney Hills upper (2800-2880 m)
80
70
60
50
40
30
20
10
2800
meters
Peacock Hills Fm.
microlam'd red mudst and carbonate
rhythmites with climbing ripples
sharp contact
top Burnside-Mara Fms.
red microlamd mdst & sltst
with irregular carbonate
replacement (concretions)
green sltst & mdst
sltst increases upward
red microlamd mdst & sltst
feruginous microdigitate
stromatolites encrust
uppermost stromatolite
bed
STH-
33
32
31
30
29
26, 28
27
25
24
mixed microbial laminites
and siliciclastic silt & sand
mixed siliclastic sltst-sst
and dolarenite,
carbonate increases up
vuggy
STH-23
red arkosic sst
beds very tabular
no erosion on bases
common silty partings
m
s
sand
gravel

section 3: north Tinney Hills

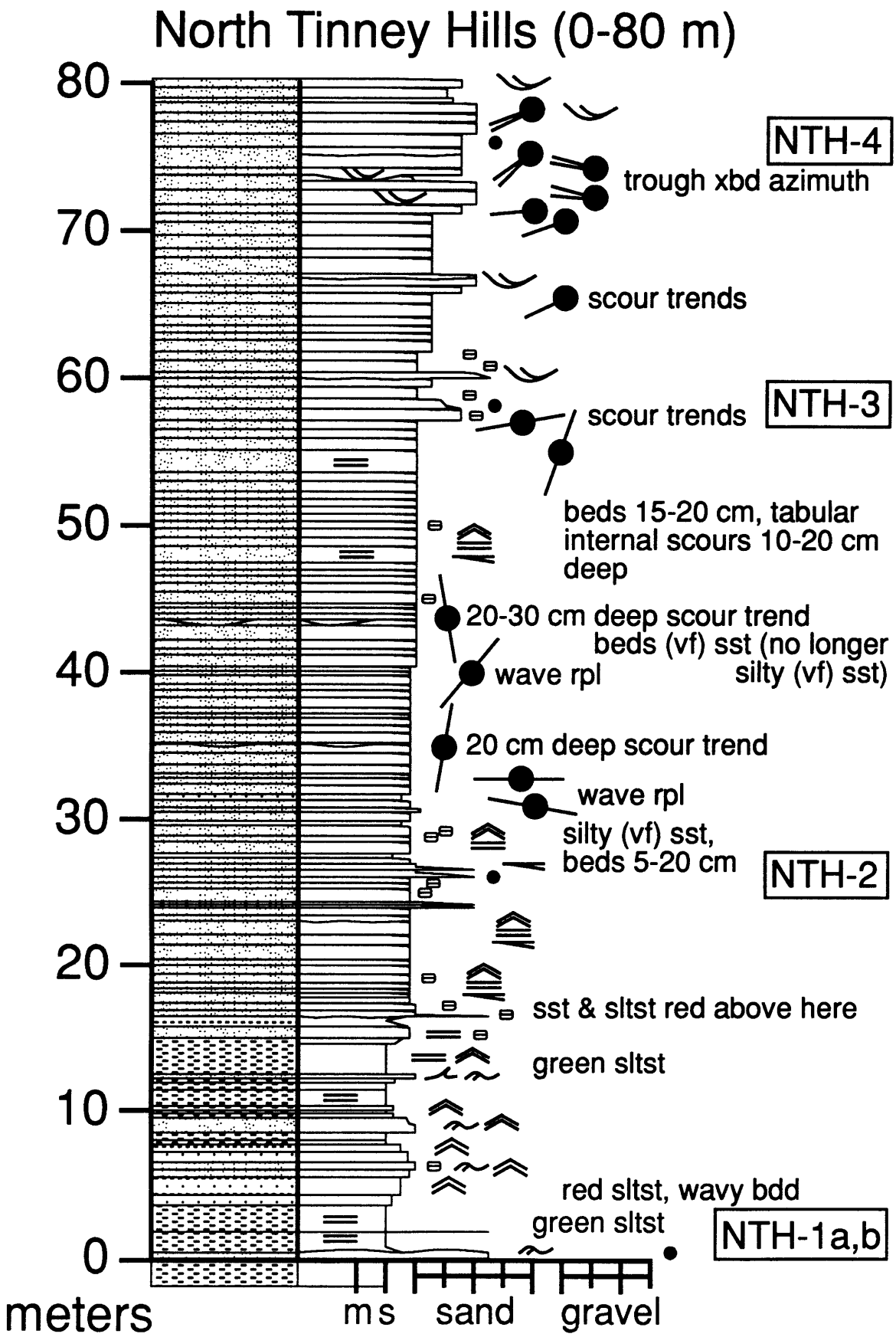
North Tinney Hills (0-80 m)
80
70
60
50
40
30
20
10
0
meters
ms
sand
gravel
NTH-4
trough xbd azimuth
scour trends
NTH-3
scour trends
beds 15-20 cm, tabular
internal scours 10-20 cm
deep
20-30 cm deep scour trend
beds (vf) sst (no longer
wave rpl
silty (vf) sst)
20 cm deep scour trend
wave rpl
silty (vf) sst,
beds 5-20 cm
NTH-2
sst & sltst red above here
green sltst
red sltst, wavy bdd
green sltst
NTH-1a,b

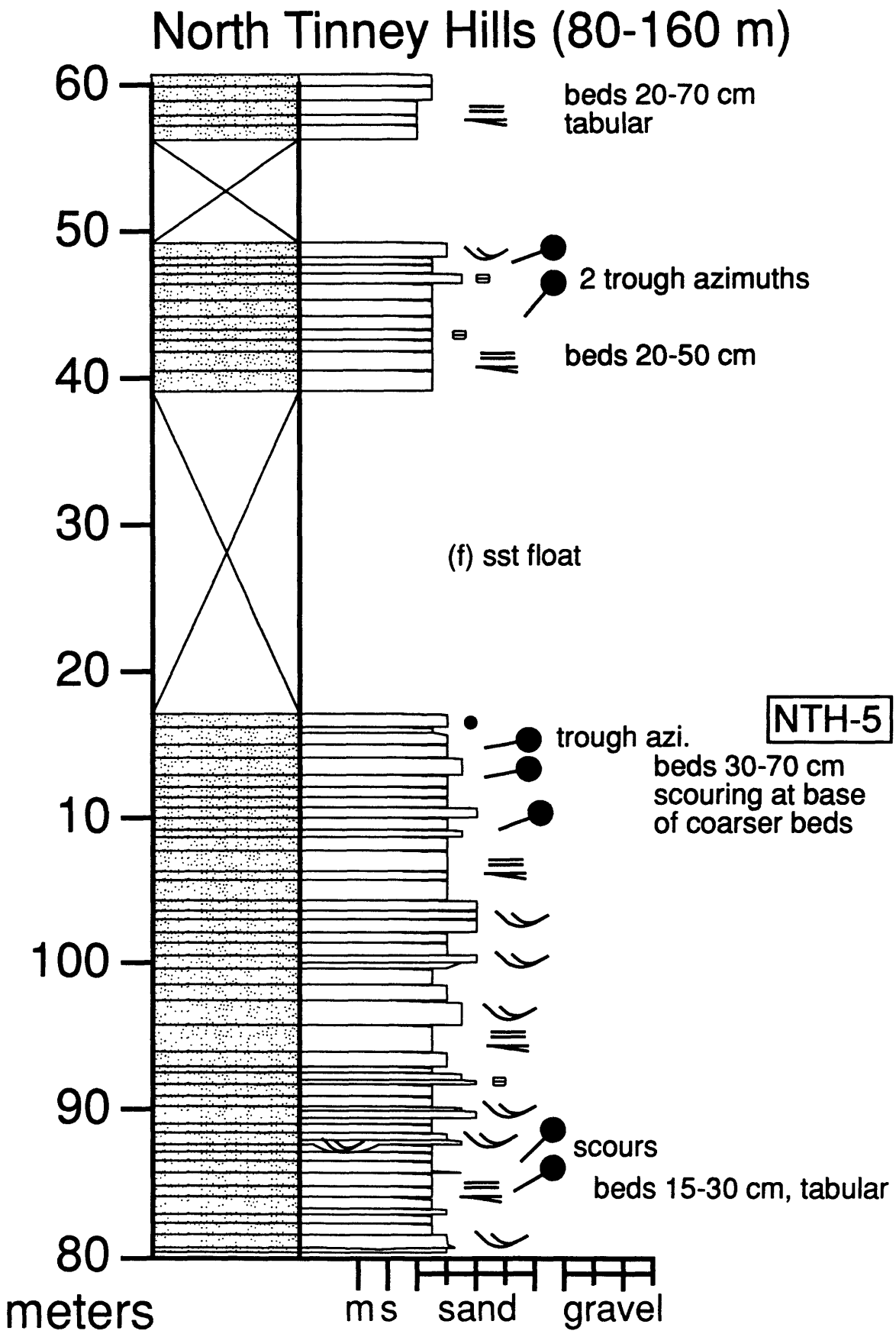
North Tinney Hills (80-160 m)
60
50
40
30
20
10
100
90
80
meters
beds 20-70 cm
tabular
2 trough azimuths
beds 20-50 cm
(f) sst float
NTH-5
trough azi.
beds 30-70 cm
scouring at base
of coarser beds
scours
beds 15-30 cm, tabular
ms
sand
gravel

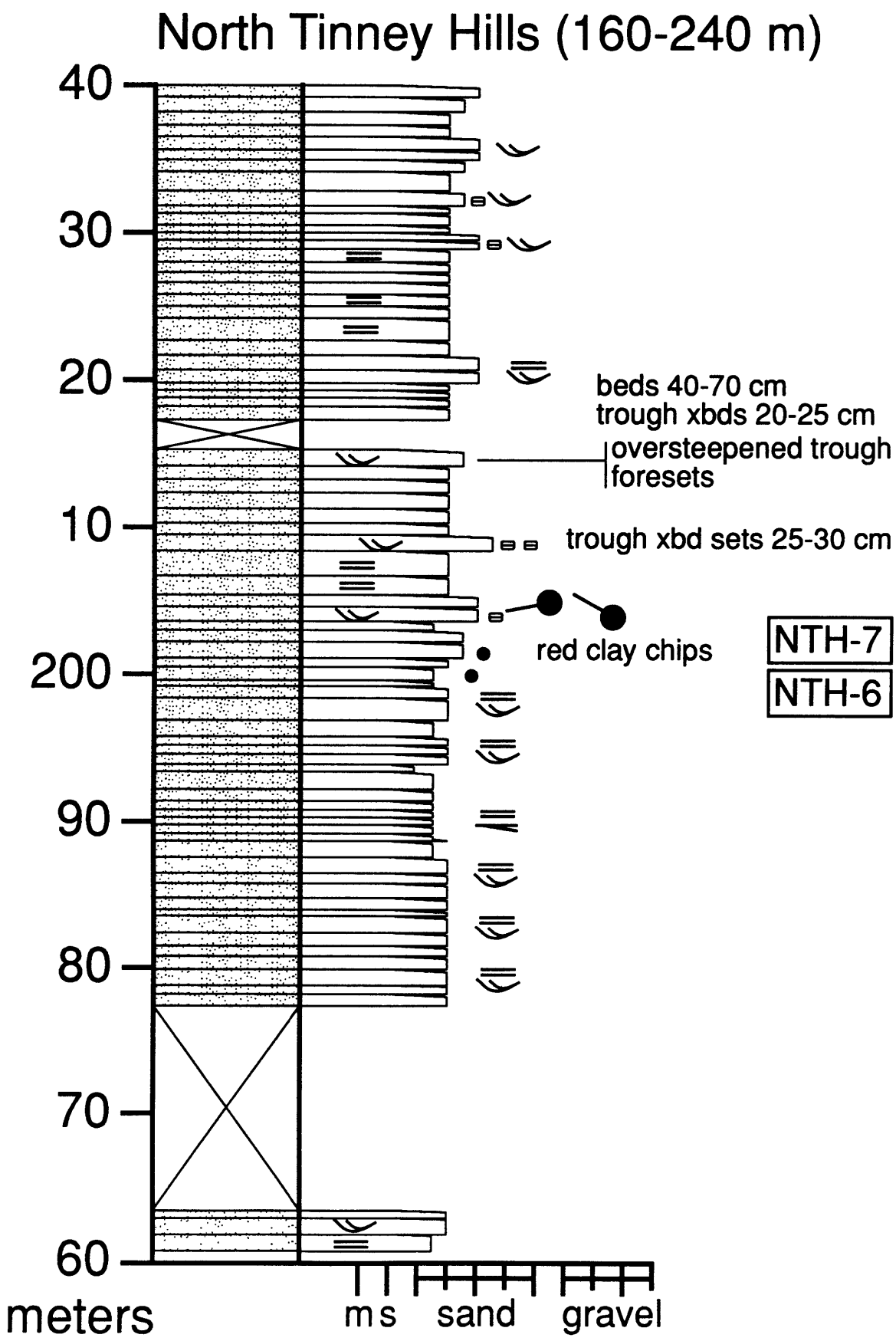
North Tinney Hills (160-240 m)
40
30
20
10
200
90
80
70
60
meters
beds 40-70 cm
trough xbds 20-25 cm
oversteepened trough foresets
trough xbd sets 25-30 cm
red clay chips
NTH-7
NTH-6
m s
sand
gravel

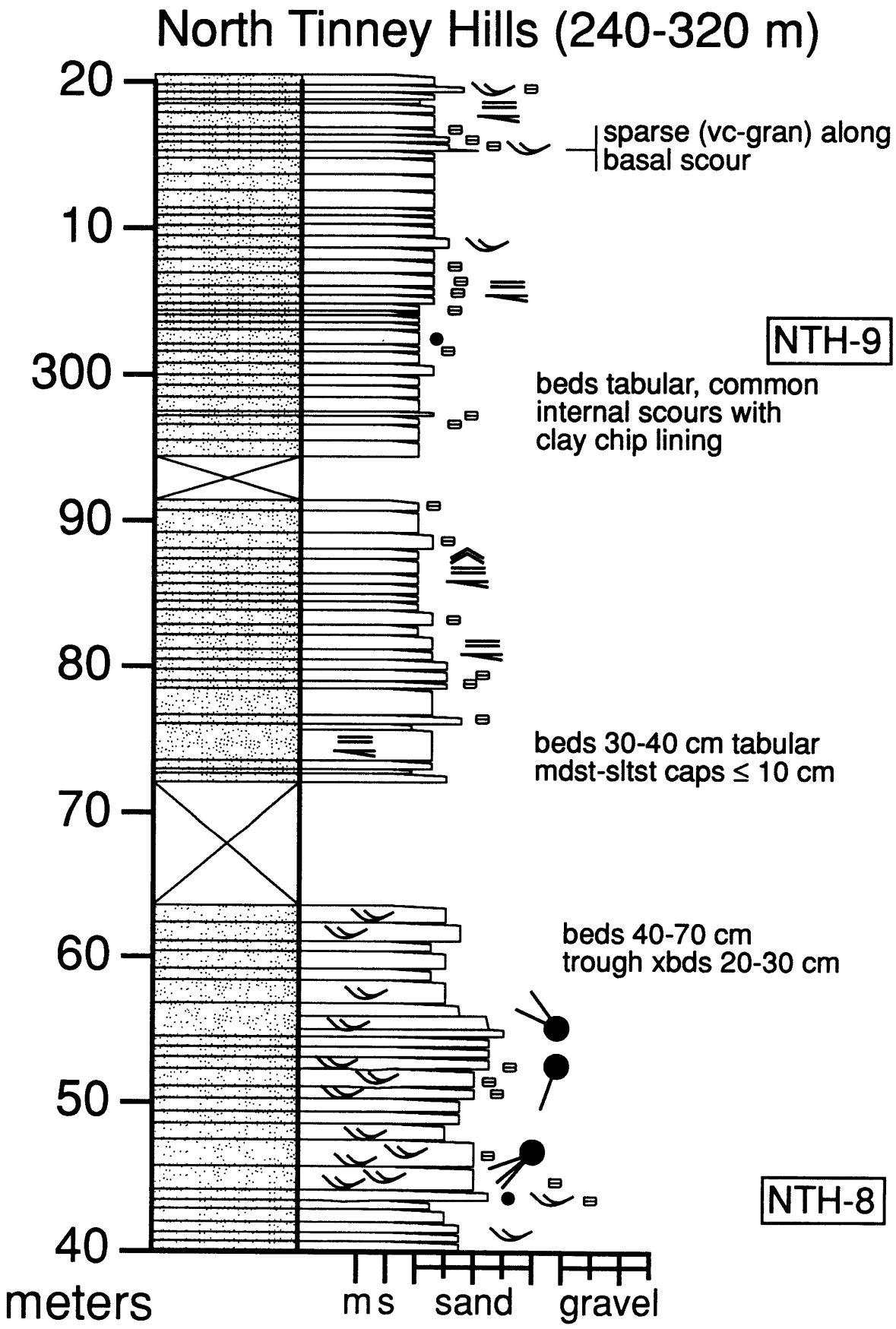
North Tinney Hills (240-320 m)
20
10
300
90
80
70
60
50
40
meters
m s
sand
gravel
sparse (vc-gran) along basal scour
NTH-9
beds tabular, common internal scours with clay chip lining
beds 30-40 cm tabular mdst-sltst caps ≤ 10 cm
beds 40-70 cm trough xbds 20-30 cm
NTH-8

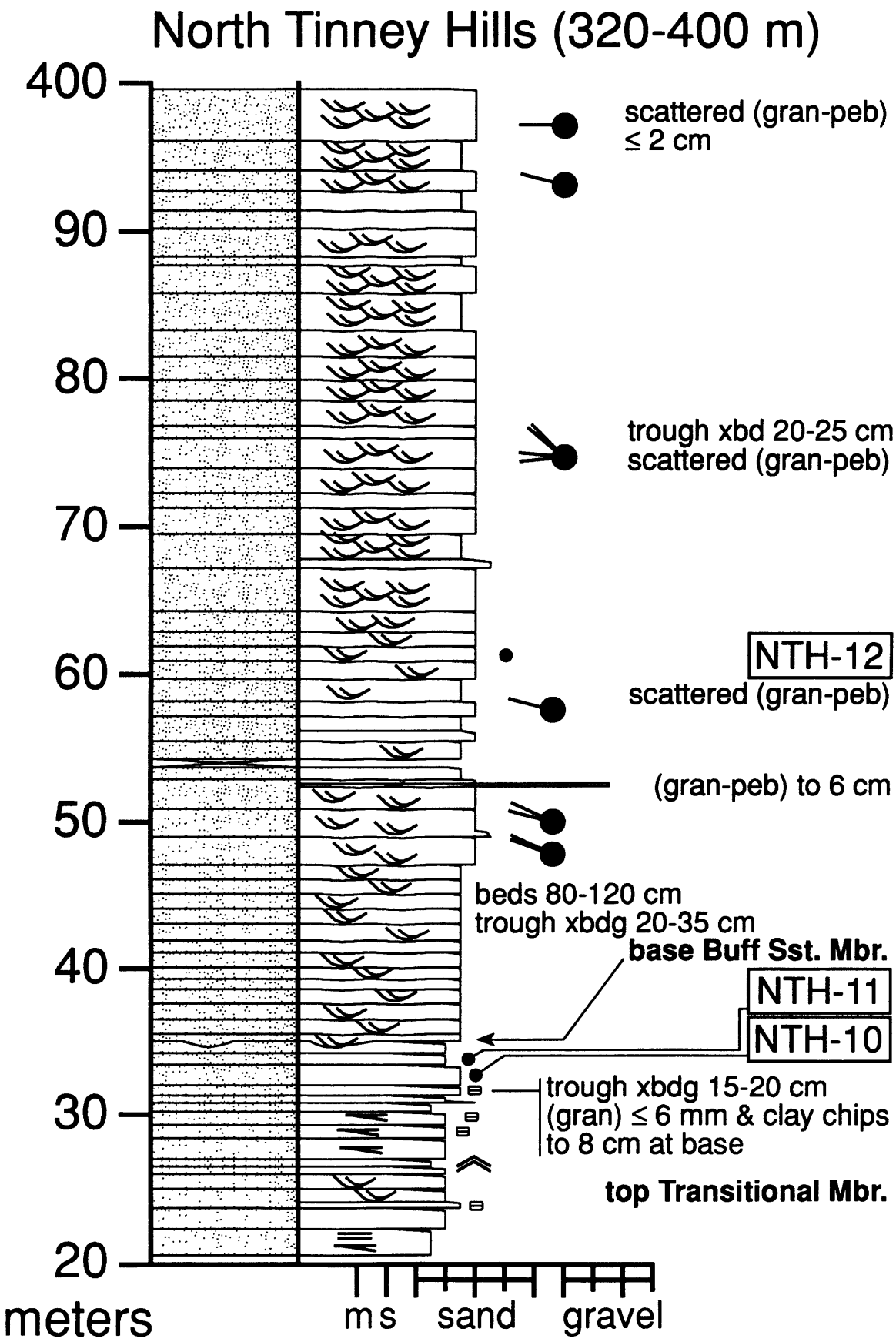
North Tinney Hills (320-400 m)
400
90
80
70
60
50
40
30
20
meters
m s
sand
gravel
scattered (gran-peb)
≤ 2 cm
trough xbd 20-25 cm
scattered (gran-peb)
NTH-12
scattered (gran-peb)
(gran-peb) to 6 cm
beds 80-120 cm
trough xbdg 20-35 cm
base Buff Sst. Mbr.
NTH-11
NTH-10
trough xbdg 15-20 cm
(gran) ≤ 6 mm & clay chips
to 8 cm at base
top Transitional Mbr.

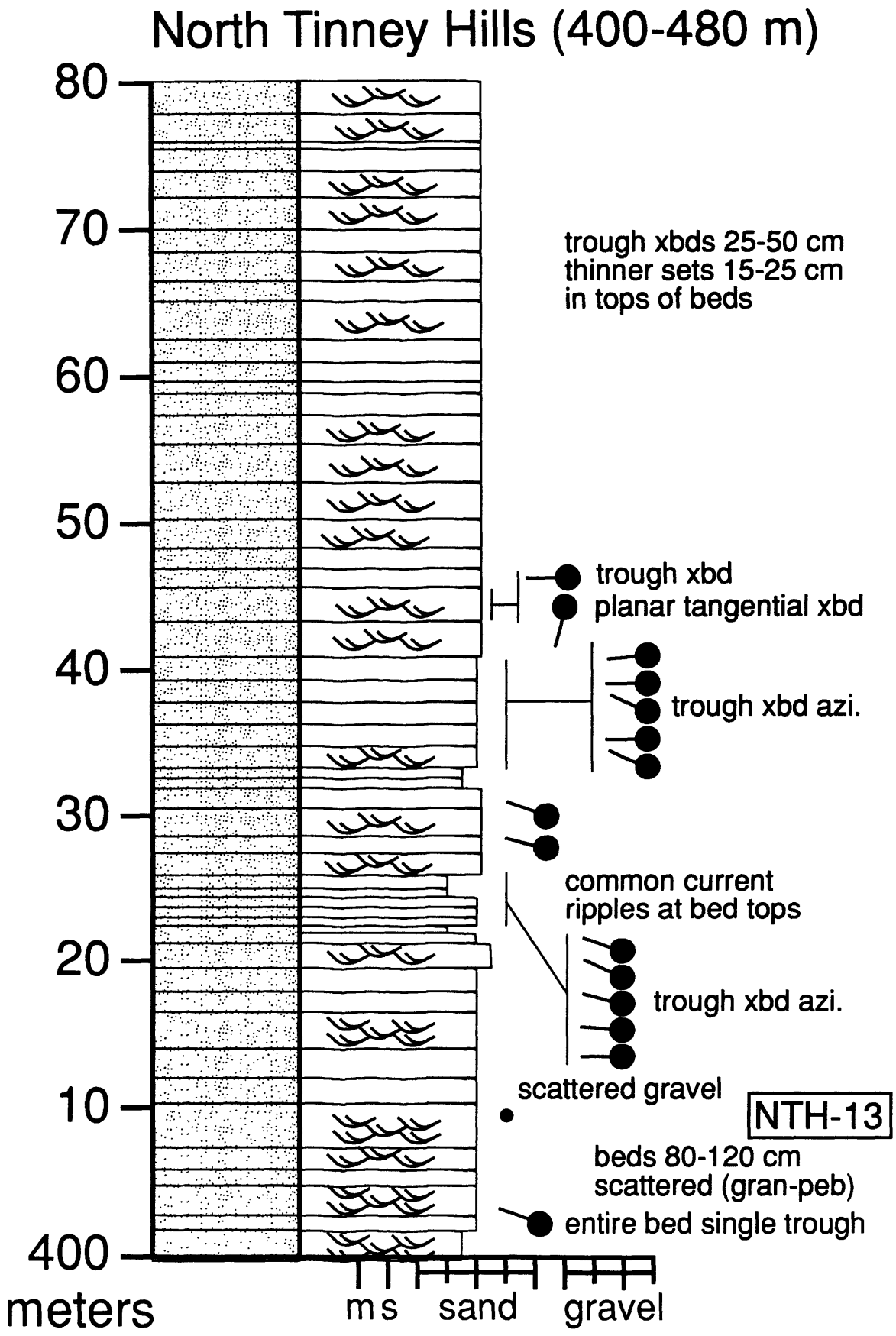
North Tinney Hills (400-480 m)
80
70
60
50
40
30
20
10
400
meters
trough xbds 25-50 cm
thinner sets 15-25 cm
in tops of beds
trough xbd
planar tangential xbd
trough xbd azi.
common current
ripples at bed tops
trough xbd azi.
scattered gravel
NTH-13
beds 80-120 cm
scattered (gran-peb)
entire bed single trough
ms
sand
gravel

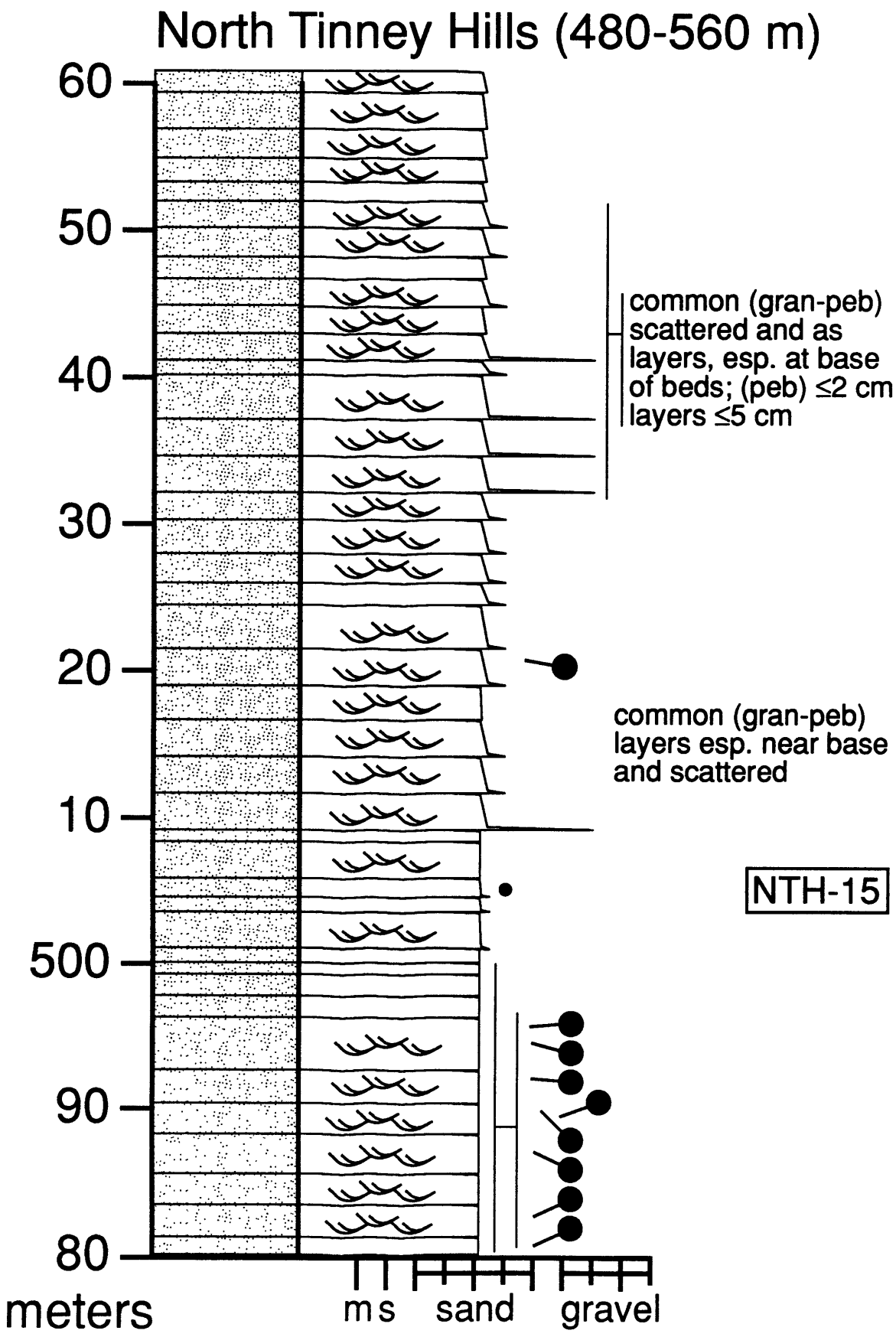
North Tinney Hills (480-560 m)
60
50
40
30
20
10
500
90
80
meters
m s
sand
gravel
common (gran-peb) scattered and as layers, esp. at base of beds; (peb) ≤2 cm layers ≤5 cm
common (gran-peb) layers esp. near base and scattered
NTH-15

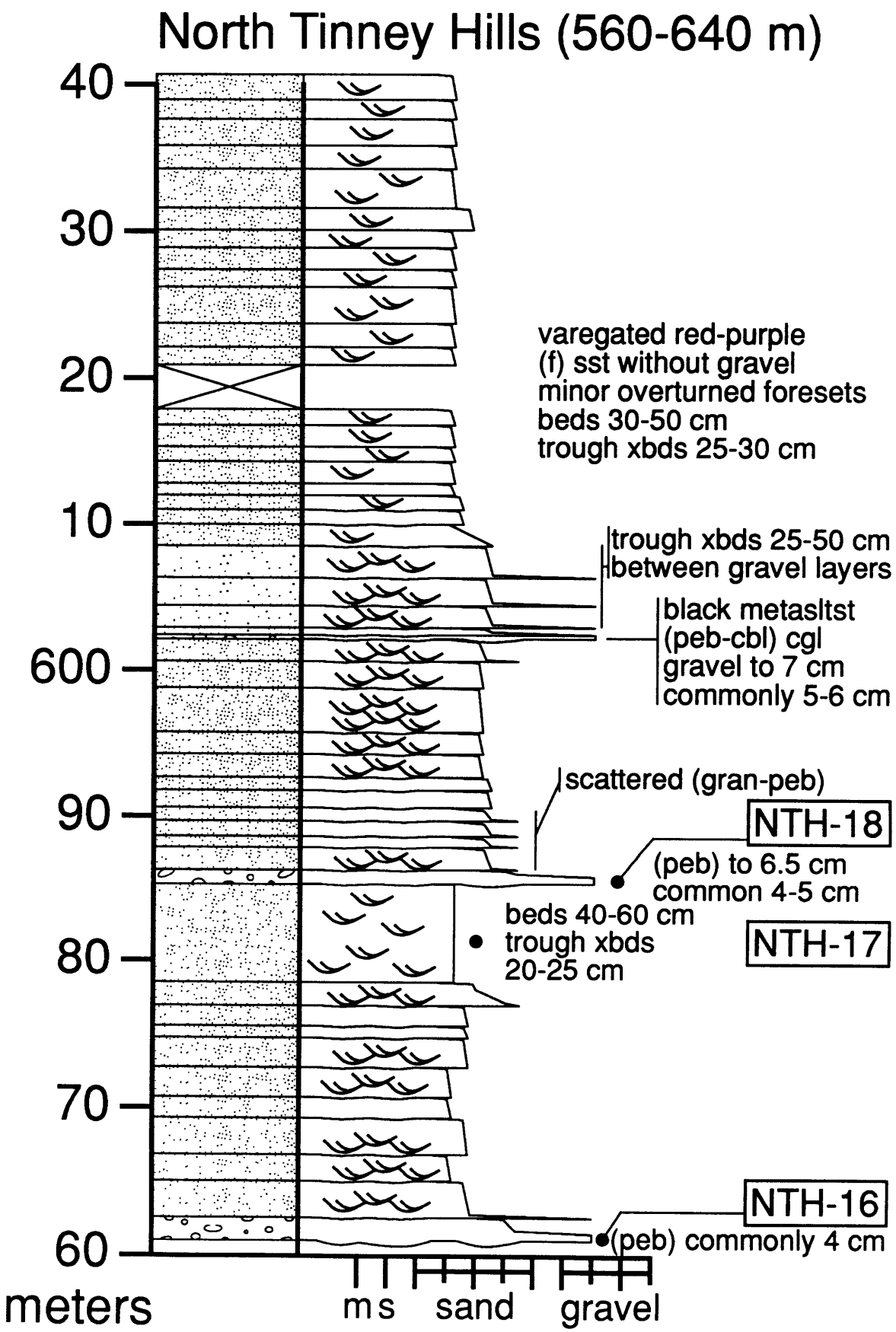
North Tinney Hills (560-640 m)
40
30
20
10
600
90
80
70
60
meters
varegated red-purple
(f) sst without gravel
minor overturned foresets
beds 30-50 cm
trough xbds 25-30 cm
trough xbds 25-50 cm
between gravel layers
black metasltst
(peb-cbl) cgl
gravel to 7 cm
commonly 5-6 cm
scattered (gran-peb)
NTH-18
(peb) to 6.5 cm
common 4-5 cm
beds 40-60 cm
trough xbds
20-25 cm
NTH-17
NTH-16
(peb) commonly 4 cm
ms
sand
gravel

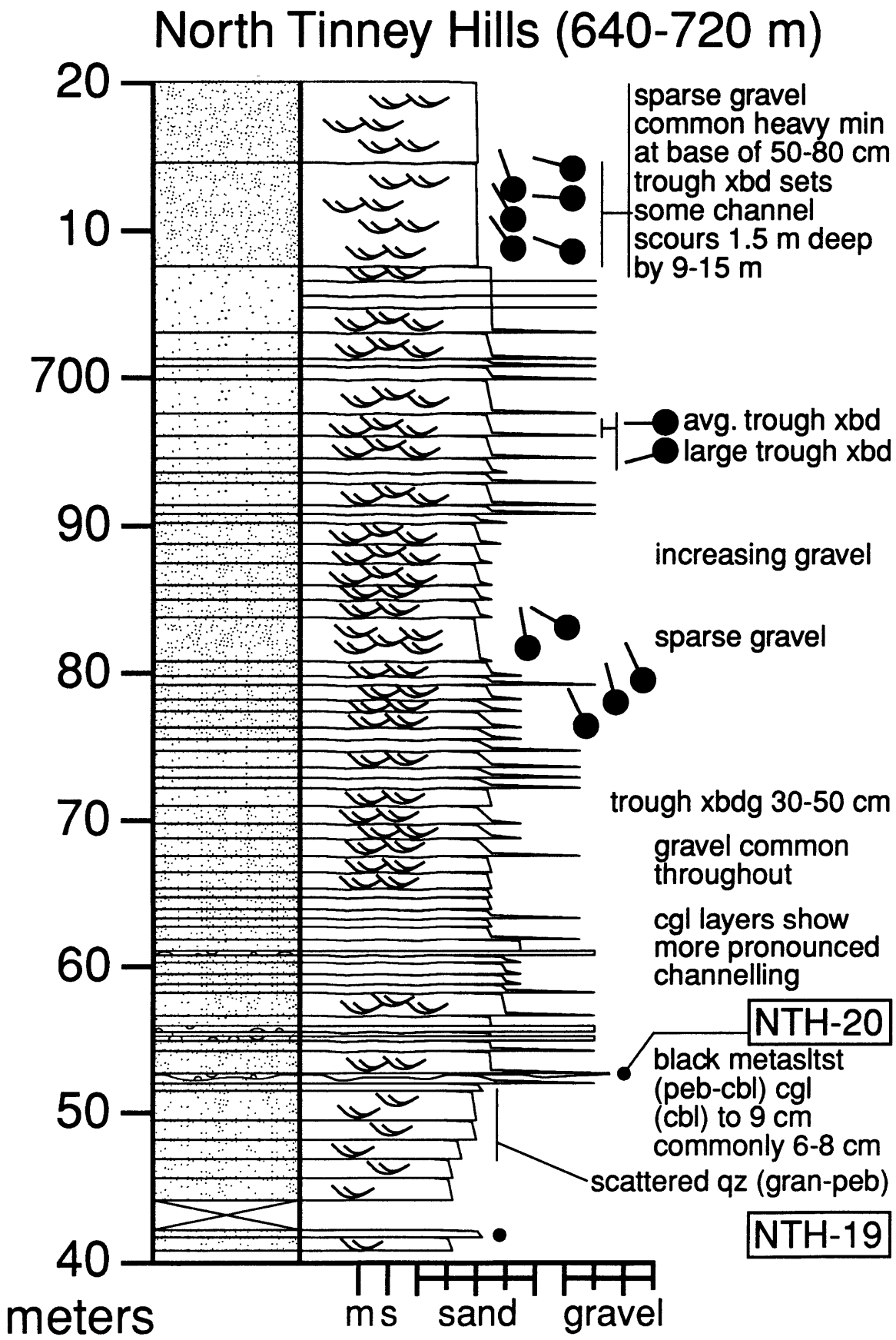
North Tinney Hills (640-720 m)
20
10
700
90
80
70
60
50
40
meters
m s
sand
gravel
sparse gravel
common heavy min
at base of 50-80 cm
trough xbd sets
some channel
scours 1.5 m deep
by 9-15 m
avg. trough xbd
large trough xbd
increasing gravel
sparse gravel
trough xbdg 30-50 cm
gravel common
throughout
cgl layers show
more pronounced
channelling
NTH-20
black metasltst
(peb-cbl) cgl
(cbl) to 9 cm
commonly 6-8 cm
scattered qz (gran-peb)
NTH-19

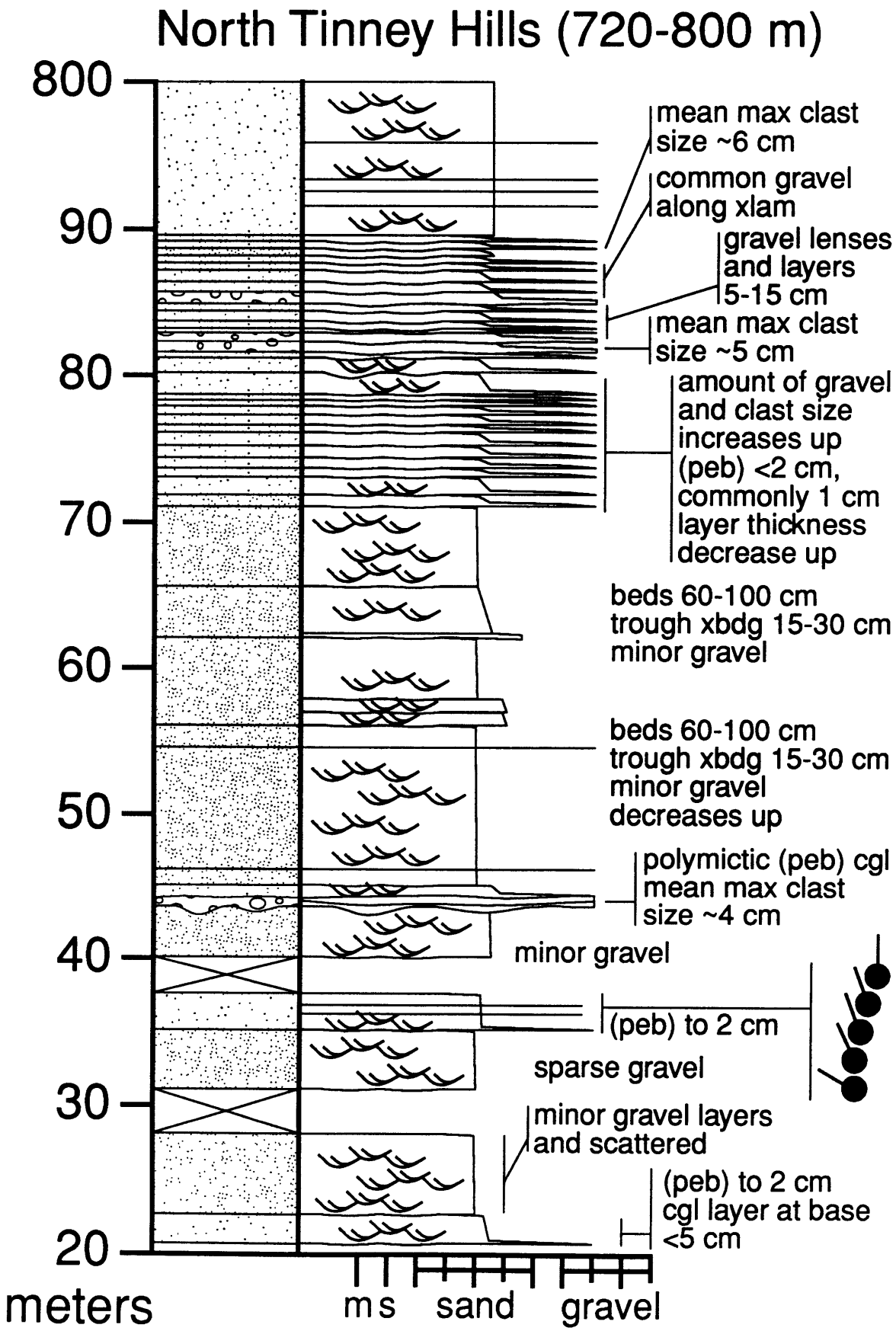
North Tinney Hills (720-800 m)
800
90
80
70
60
50
40
30
20
meters
mean max clast size ~6 cm
common gravel along xlam
gravel lenses and layers 5-15 cm
mean max clast size ~5 cm
amount of gravel and clast size increases up (peb) <2 cm, commonly 1 cm layer thickness decrease up
beds 60-100 cm trough xbdg 15-30 cm minor gravel
beds 60-100 cm trough xbdg 15-30 cm minor gravel decreases up
polymictic (peb) cgl mean max clast size ~4 cm
minor gravel
(peb) to 2 cm
sparse gravel
minor gravel layers and scattered
(peb) to 2 cm cgl layer at base <5 cm
ms
sand
gravel

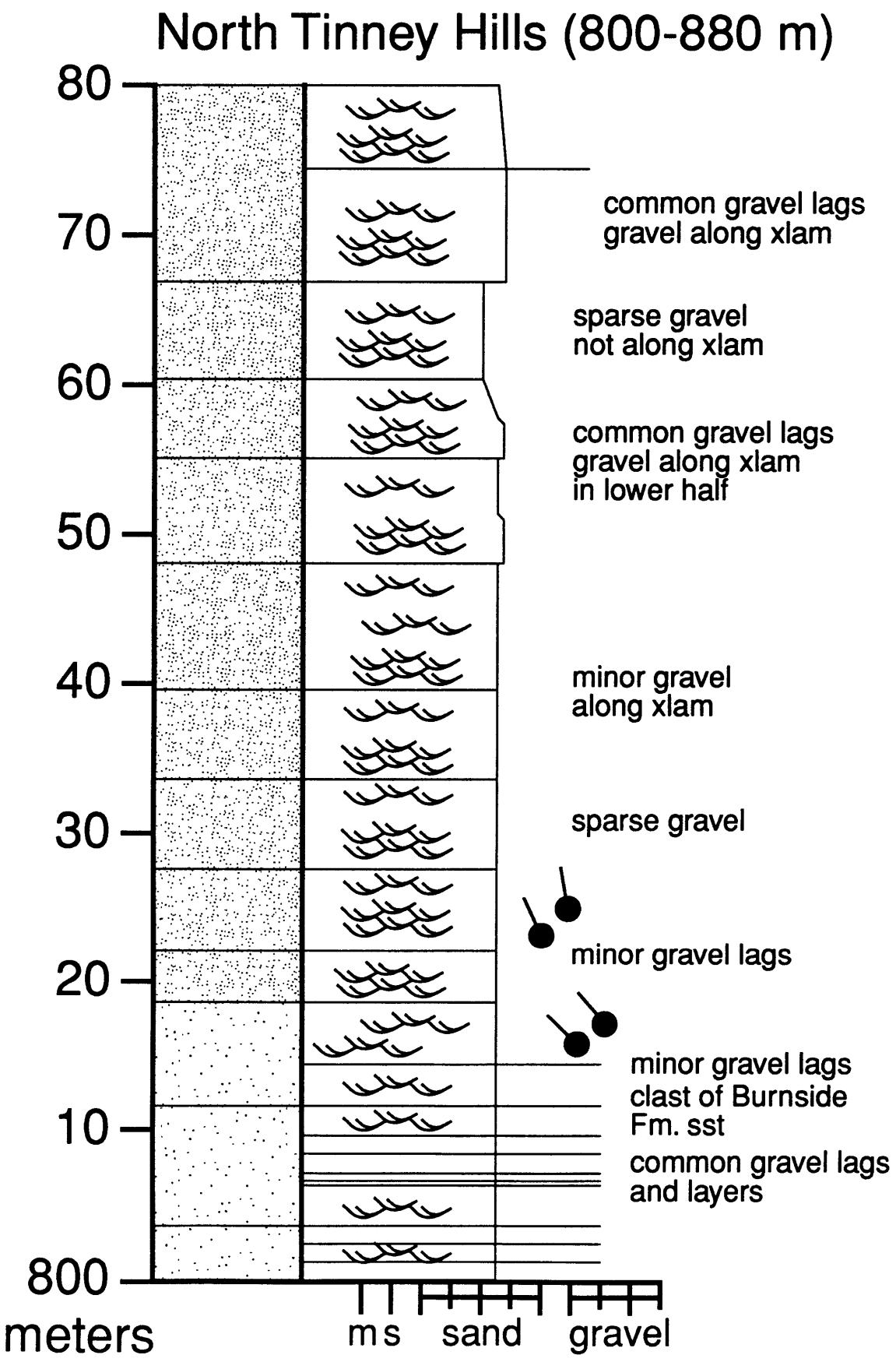
North Tinney Hills (800-880 m)
80
70
60
50
40
30
20
10
800
meters
common gravel lags
gravel along xlam
sparse gravel
not along xlam
common gravel lags
gravel along xlam
in lower half
minor gravel
along xlam
sparse gravel
minor gravel lags
minor gravel lags
clast of Burnside
Fm. sst
common gravel lags
and layers
ms
sand
gravel

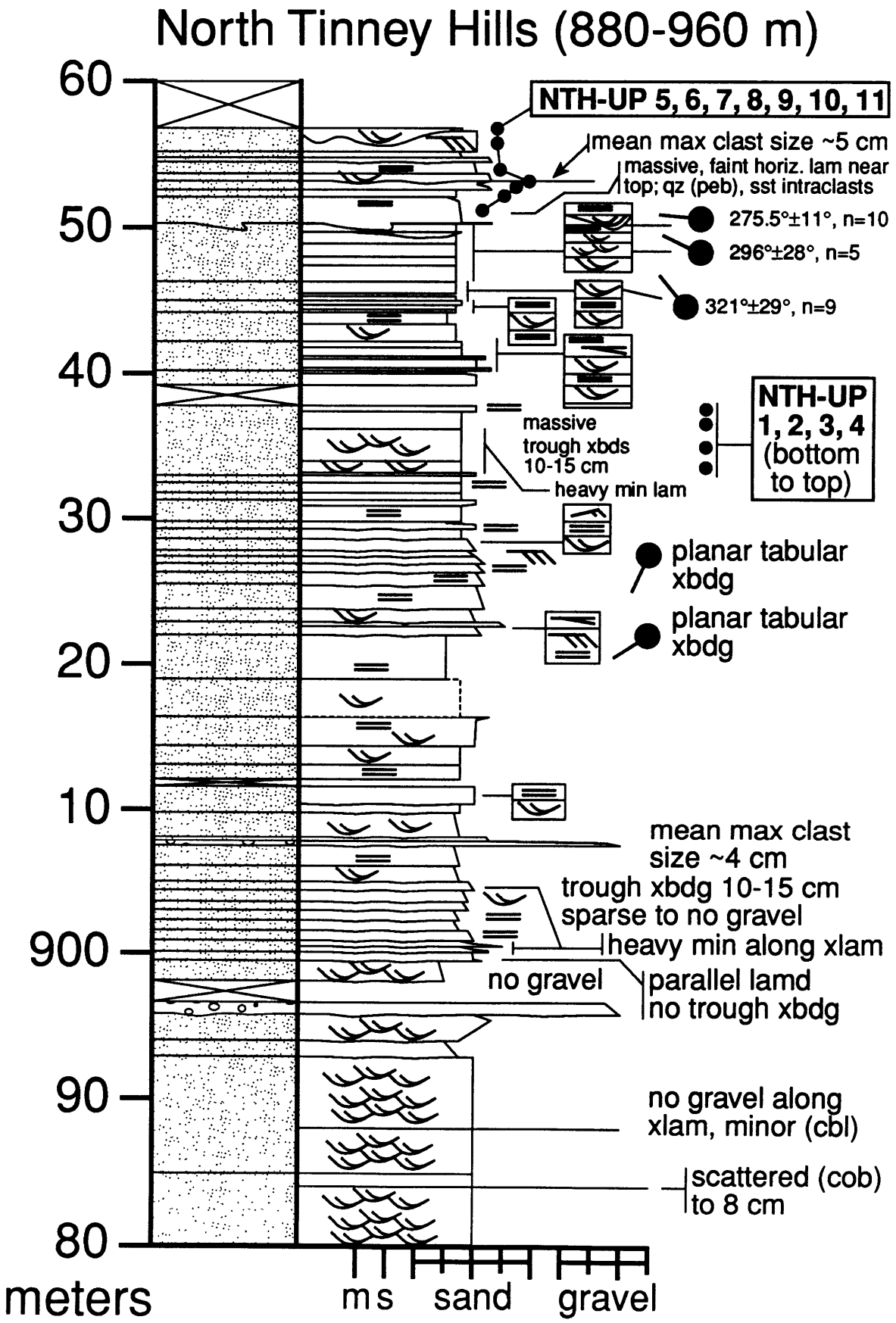
North Tinney Hills (880-960 m)
60
50
40
30
20
10
900
90
80
meters
NTH-UP 5, 6, 7, 8, 9, 10, 11
mean max clast size ~5 cm
massive, faint horiz. lam near top; qz (peb), sst intraclasts
275.5°±11°, n=10
296°±28°, n=5
321°±29°, n=9
massive
trough xbds 10-15 cm
heavy min lam
NTH-UP 1, 2, 3, 4 (bottom to top)
planar tabular xbdg
planar tabular xbdg
mean max clast size ~4 cm
trough xbdg 10-15 cm
sparse to no gravel
heavy min along xlam
no gravel
parallel lamd
no trough xbdg
no gravel along xlam, minor (cbl)
scattered (cob) to 8 cm
ms
sand
gravel

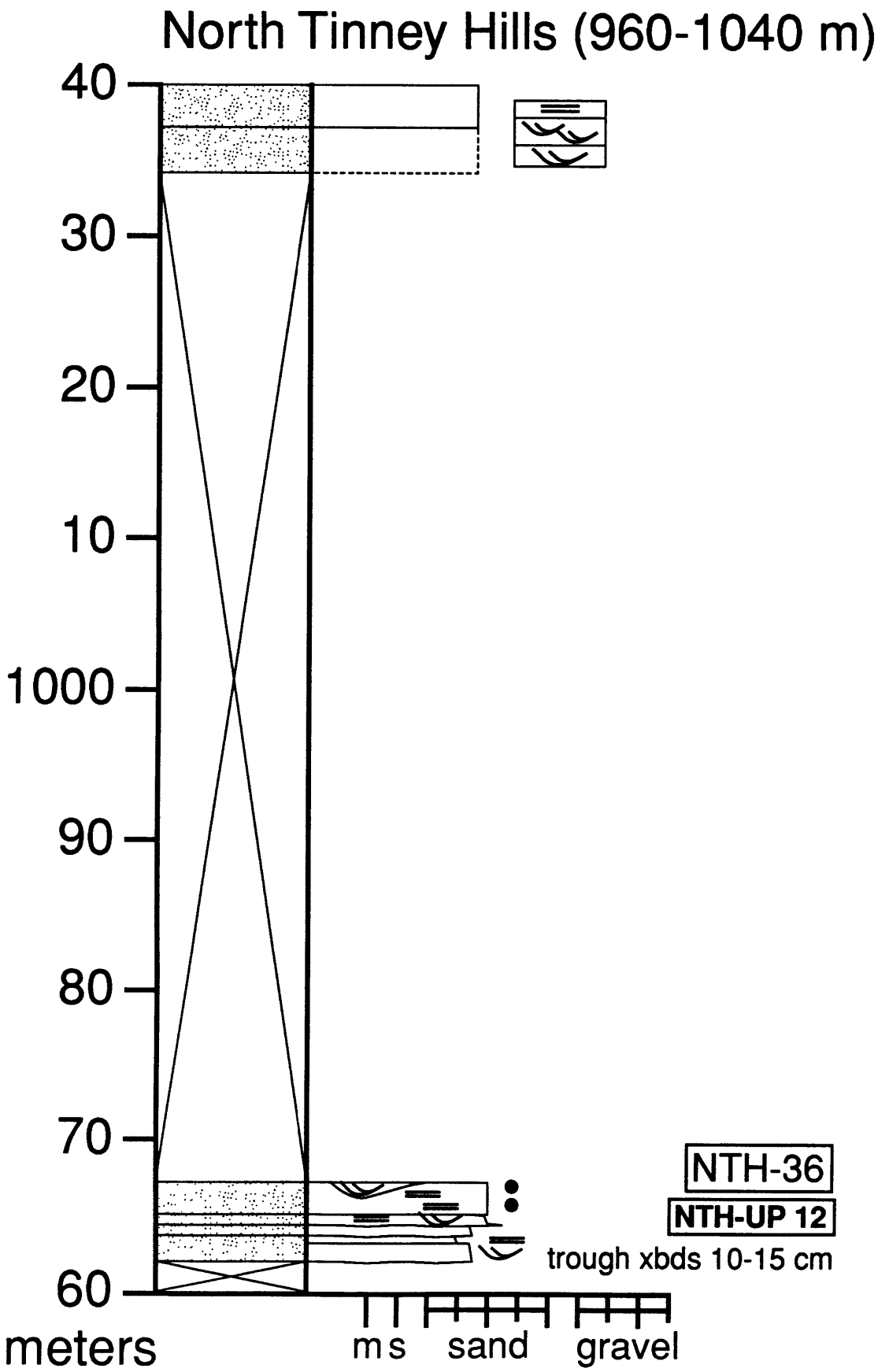
North Tinney Hills (960-1040 m)
40
30
20
10
1000
90
80
70
60
meters
NTH-36
NTH-UP 12
trough xbds 10-15 cm
m s
sand
gravel

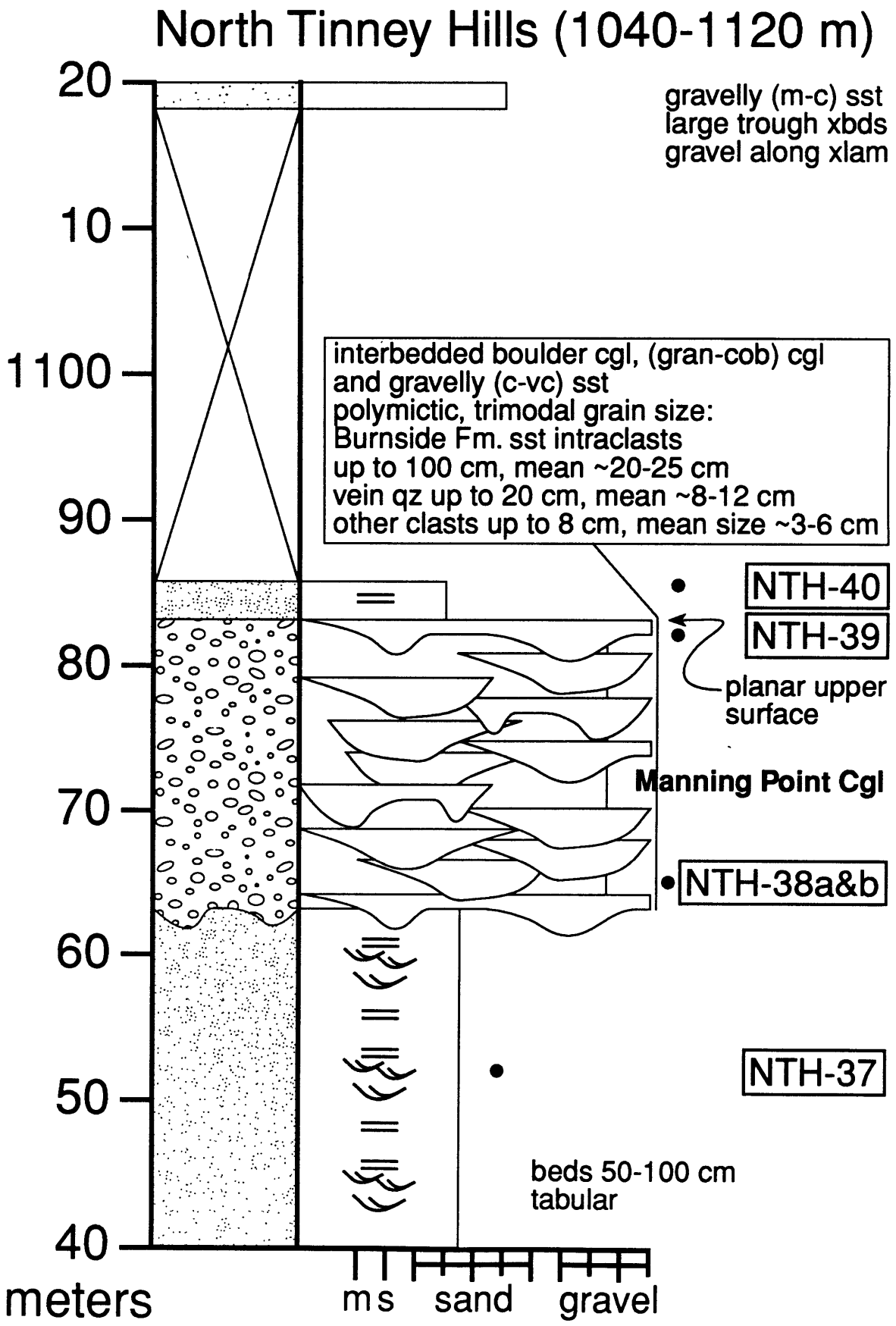
North Tinney Hills (1040-1120 m)
20
10
1100
90
80
70
60
50
40
meters
gravelly (m-c) sst
large trough xbds
gravel along xlam
interbedded boulder cgl, (gran-cob) cgl
and gravelly (c-vc) sst
polymictic, trimodal grain size:
Burnside Fm. sst intraclasts
up to 100 cm, mean ~20-25 cm
vein qz up to 20 cm, mean ~8-12 cm
other clasts up to 8 cm, mean size ~3-6 cm
NTH-40
NTH-39
planar upper
surface
Manning Point Cgl
NTH-38a&b
NTH-37
beds 50-100 cm
tabular
ms
sand
gravel

North Tinney Hills (1120-1200 m)

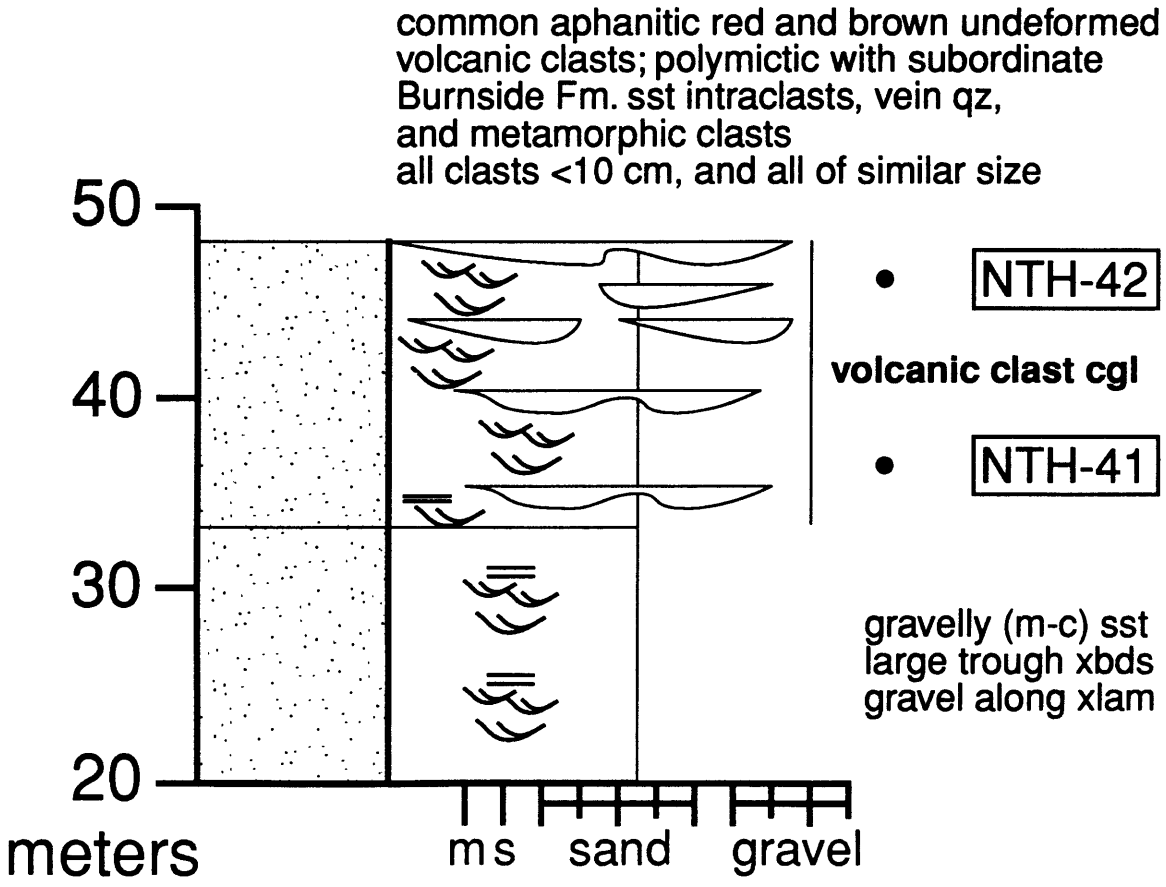

section 4: SE Folds

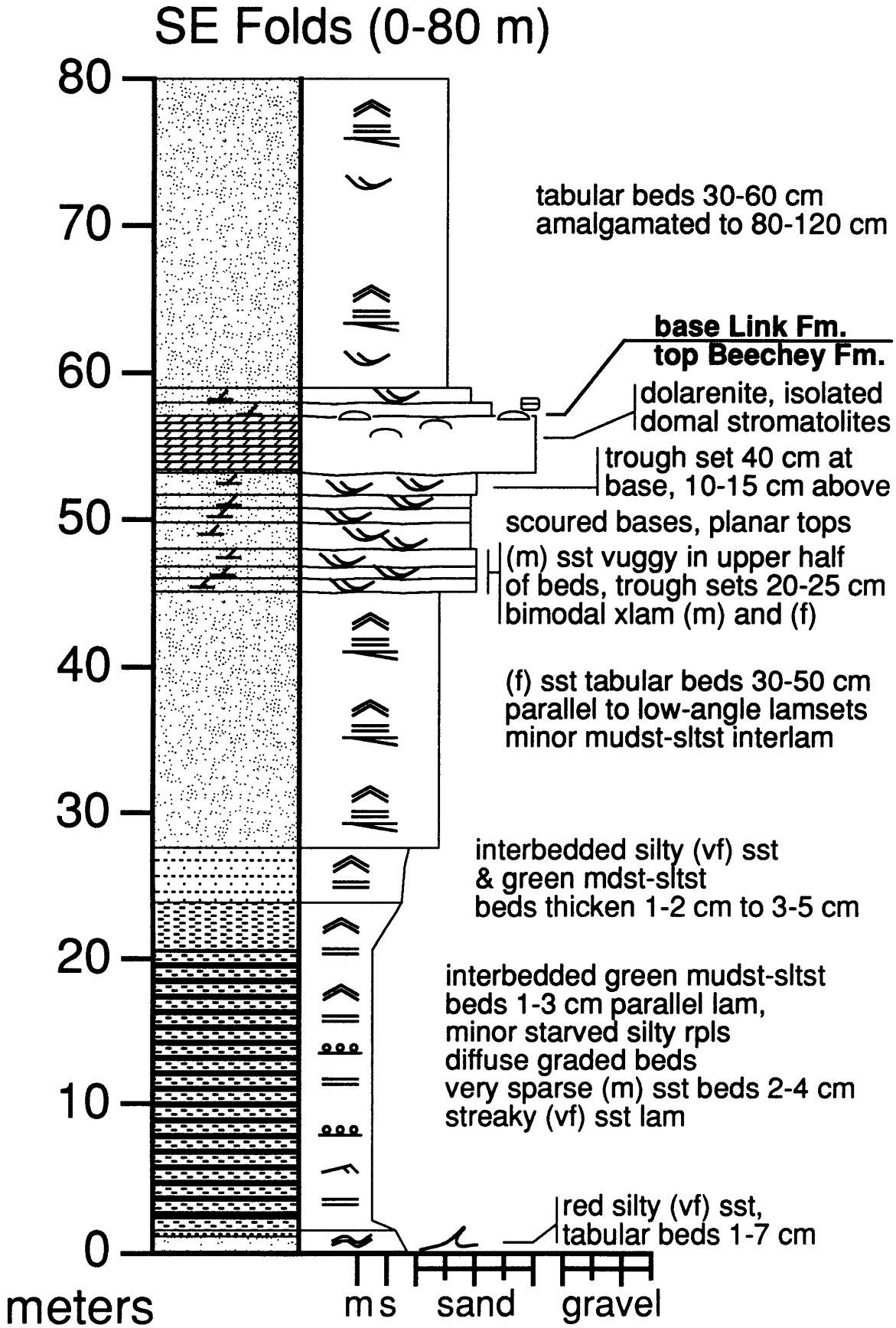
SE Folds (0-80 m)
80
70
60
50
40
30
20
10
0
meters
tabular beds 30-60 cm
amalgamated to 80-120 cm
base Link Fm.
top Beechey Fm.
dolarenite, isolated
domal stromatolites
trough set 40 cm at
base, 10-15 cm above
scoured bases, planar tops
(m) sst vuggy in upper half
of beds, trough sets 20-25 cm
bimodal xlam (m) and (f)
(f) sst tabular beds 30-50 cm
parallel to low-angle lamsets
minor mudst-sltst interlam
interbedded silty (vf) sst
& green mdst-sltst
beds thicken 1-2 cm to 3-5 cm
interbedded green mudst-sltst
beds 1-3 cm parallel lam,
minor starved silty rpls
diffuse graded beds
very sparse (m) sst beds 2-4 cm
streaky (vf) sst lam
red silty (vf) sst,
tabular beds 1-7 cm
m s
sand
gravel

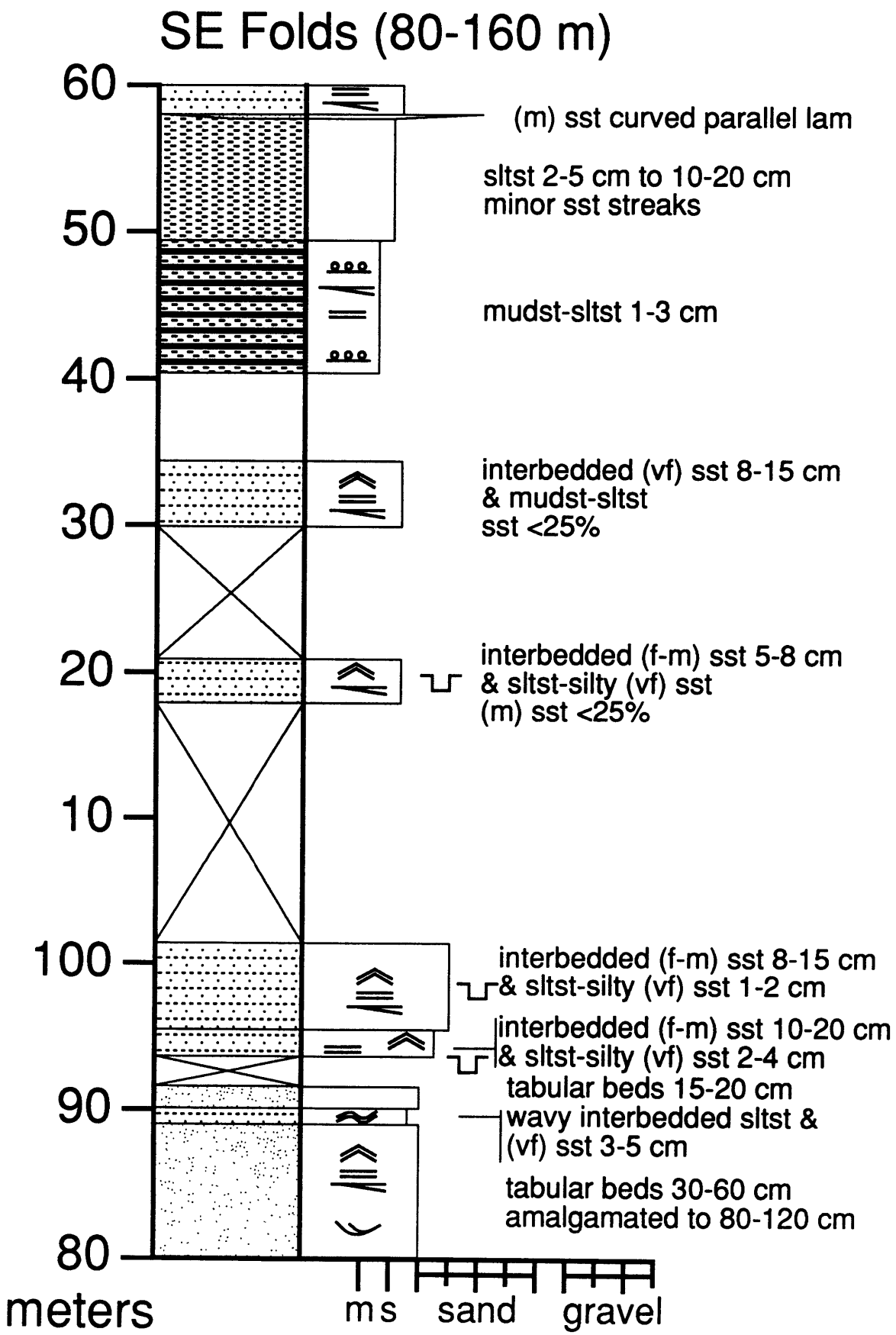
SE Folds (80-160 m)
60
50
40
30
20
10
100
90
80
meters
(m) sst curved parallel lam
sltst 2-5 cm to 10-20 cm
minor sst streaks
mudst-sltst 1-3 cm
interbedded (vf) sst 8-15 cm
& mudst-sltst
sst <25%
interbedded (f-m) sst 5-8 cm
& sltst-silty (vf) sst
(m) sst <25%
interbedded (f-m) sst 8-15 cm
& sltst-silty (vf) sst 1-2 cm
interbedded (f-m) sst 10-20 cm
& sltst-silty (vf) sst 2-4 cm
tabular beds 15-20 cm
wavy interbedded sltst &
(vf) sst 3-5 cm
tabular beds 30-60 cm
amalgamated to 80-120 cm
ms
sand
gravel

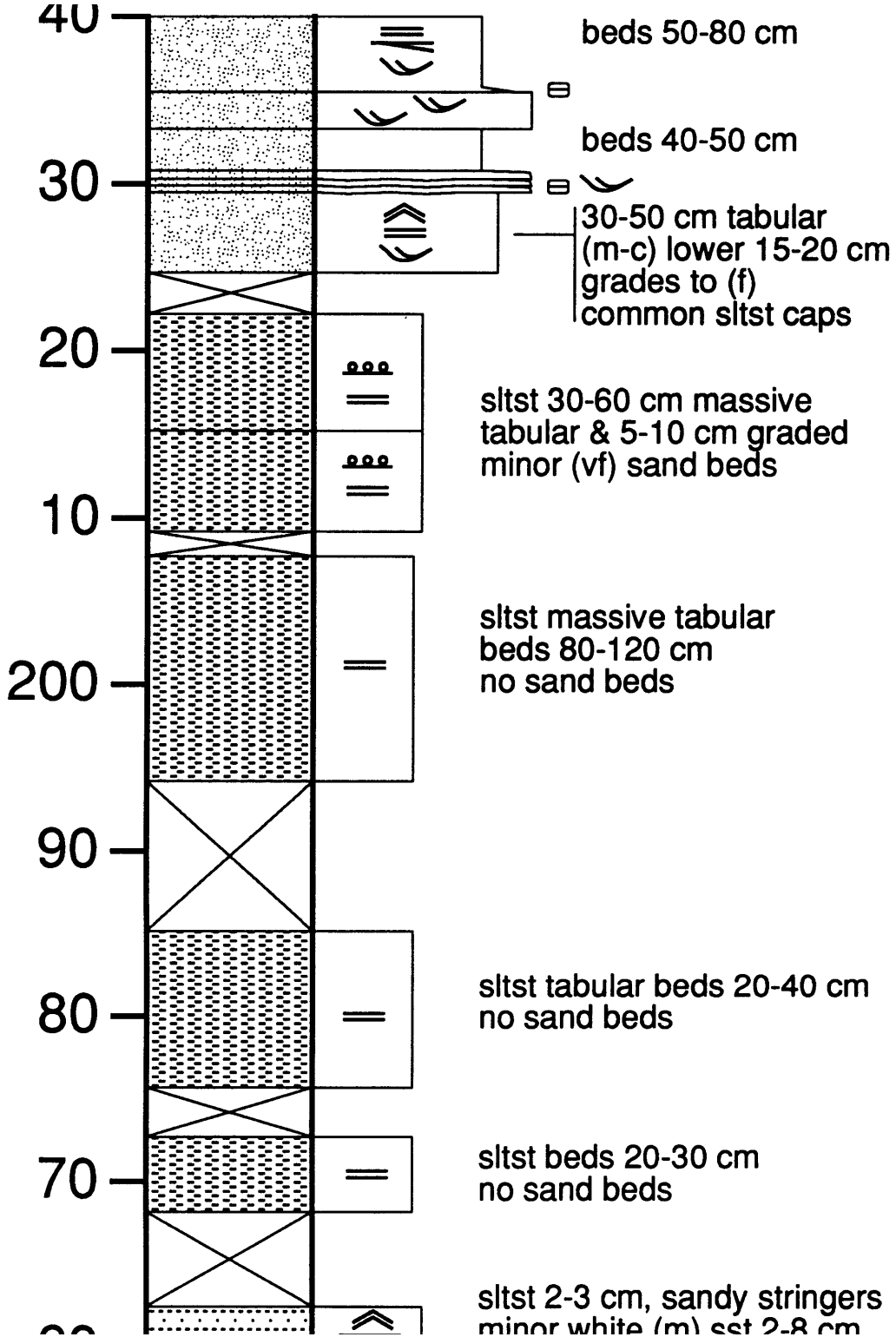
40
30
20
10
200
90
80
70
beds 50-80 cm
beds 40-50 cm
30-50 cm tabular
(m-c) lower 15-20 cm
grades to (f)
common sltst caps
sltst 30-60 cm massive
tabular & 5-10 cm graded
minor (vf) sand beds
sltst massive tabular
beds 80-120 cm
no sand beds
sltst tabular beds 20-40 cm
no sand beds
sltst beds 20-30 cm
no sand beds
sltst 2-3 cm, sandy stringers
minor white (m) sst 2-8 cm

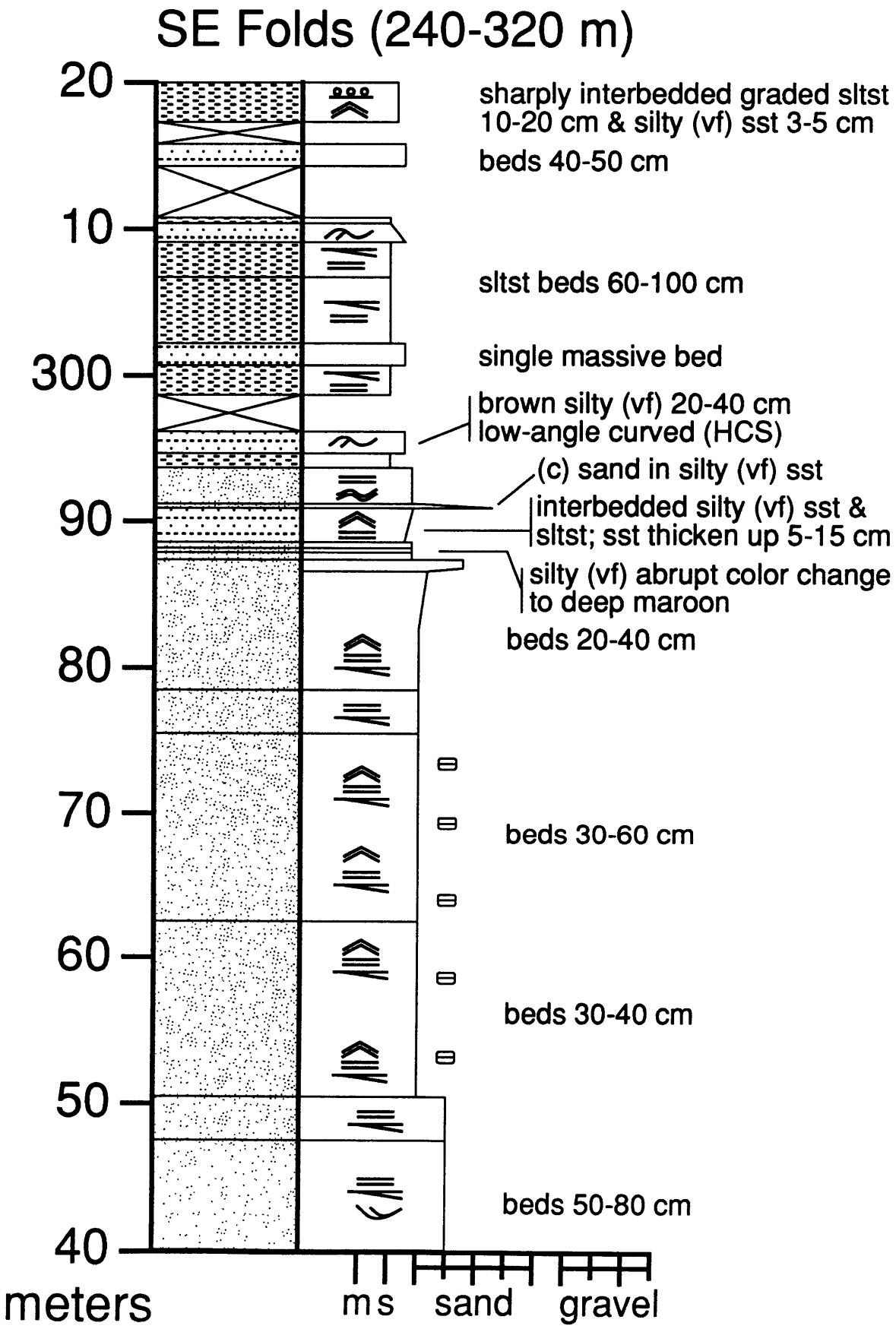
SE Folds (240-320 m)
20
10
300
90
80
70
60
50
40
meters
sharply interbedded graded sltst
10-20 cm & silty (vf) sst 3-5 cm
beds 40-50 cm
sltst beds 60-100 cm
single massive bed
brown silty (vf) 20-40 cm
low-angle curved (HCS)
(c) sand in silty (vf) sst
interbedded silty (vf) sst &
sltst; sst thicken up 5-15 cm
silty (vf) abrupt color change
to deep maroon
beds 20-40 cm
beds 30-60 cm
beds 30-40 cm
beds 50-80 cm
ms
sand
gravel

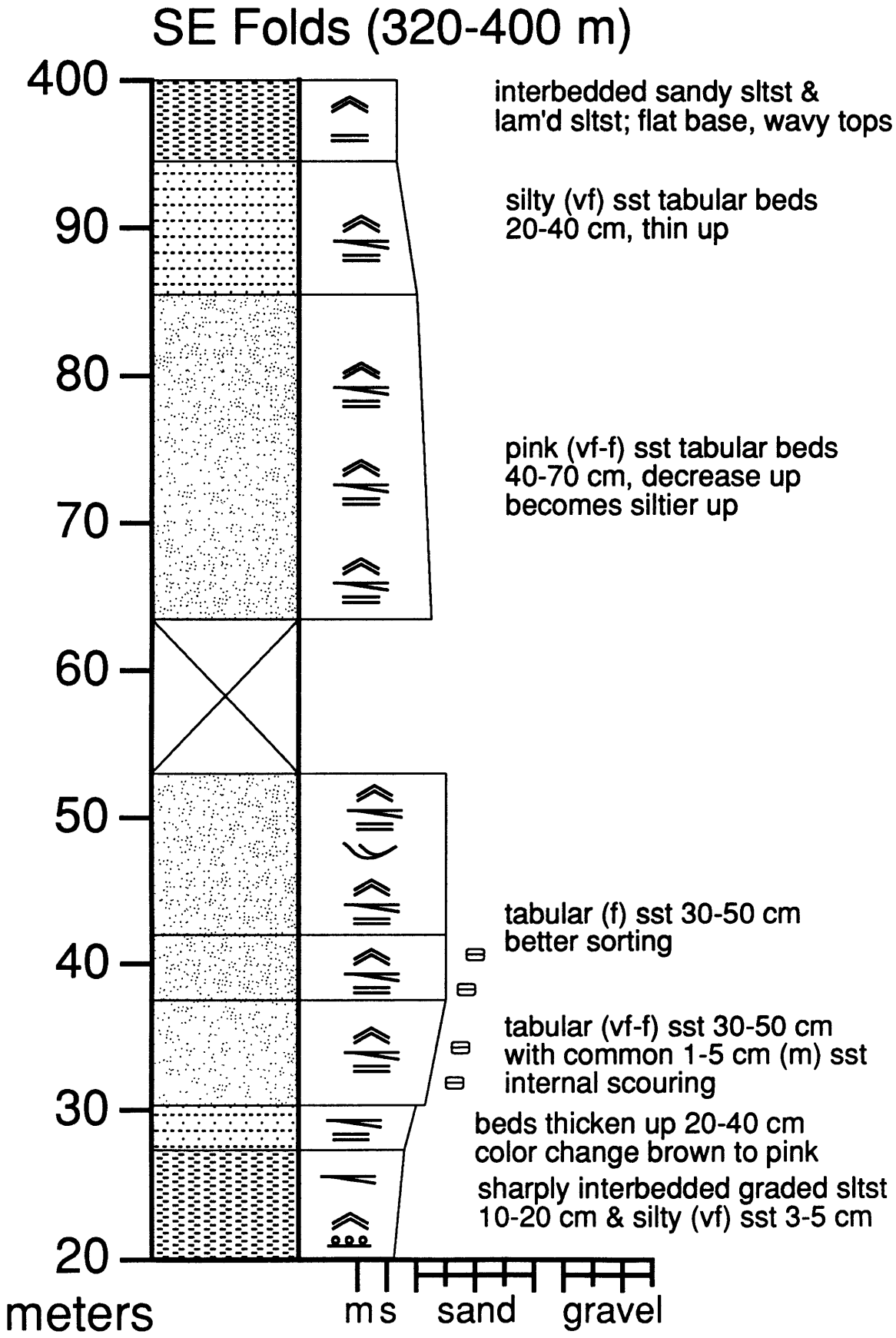
SE Folds (320-400 m)
400
90
80
70
60
50
40
30
20
meters
interbedded sandy sltst &
lam'd sltst; flat base, wavy tops
silty (vf) sst tabular beds
20-40 cm, thin up
pink (vf-f) sst tabular beds
40-70 cm, decrease up
becomes siltier up
tabular (f) sst 30-50 cm
better sorting
tabular (vf-f) sst 30-50 cm
with common 1-5 cm (m) sst
internal scouring
beds thicken up 20-40 cm
color change brown to pink
sharply interbedded graded sltst
10-20 cm & silty (vf) sst 3-5 cm
m s
sand
gravel

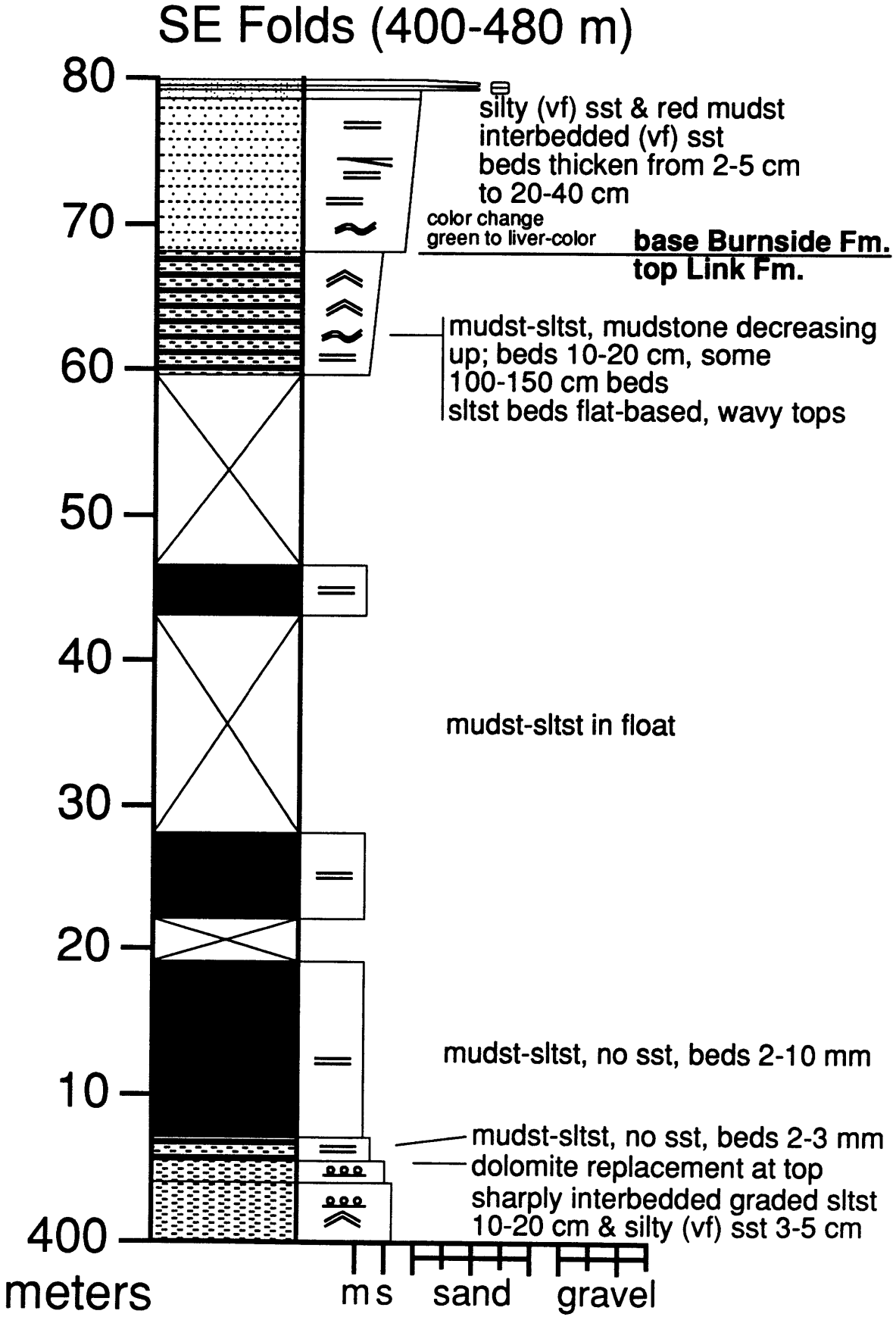
SE Folds (400-480 m)
80
70
60
50
40
30
20
10
400
meters
silty (vf) sst & red mudst
interbedded (vf) sst
beds thicken from 2-5 cm
to 20-40 cm
color change
green to liver-color
base Burnside Fm.
top Link Fm.
mudst-sltst, mudstone decreasing
up; beds 10-20 cm, some
100-150 cm beds
sltst beds flat-based, wavy tops
mudst-sltst in float
mudst-sltst, no sst, beds 2-10 mm
mudst-sltst, no sst, beds 2-3 mm
dolomite replacement at top
sharply interbedded graded sltst
10-20 cm & silty (vf) sst 3-5 cm
m s
sand
gravel

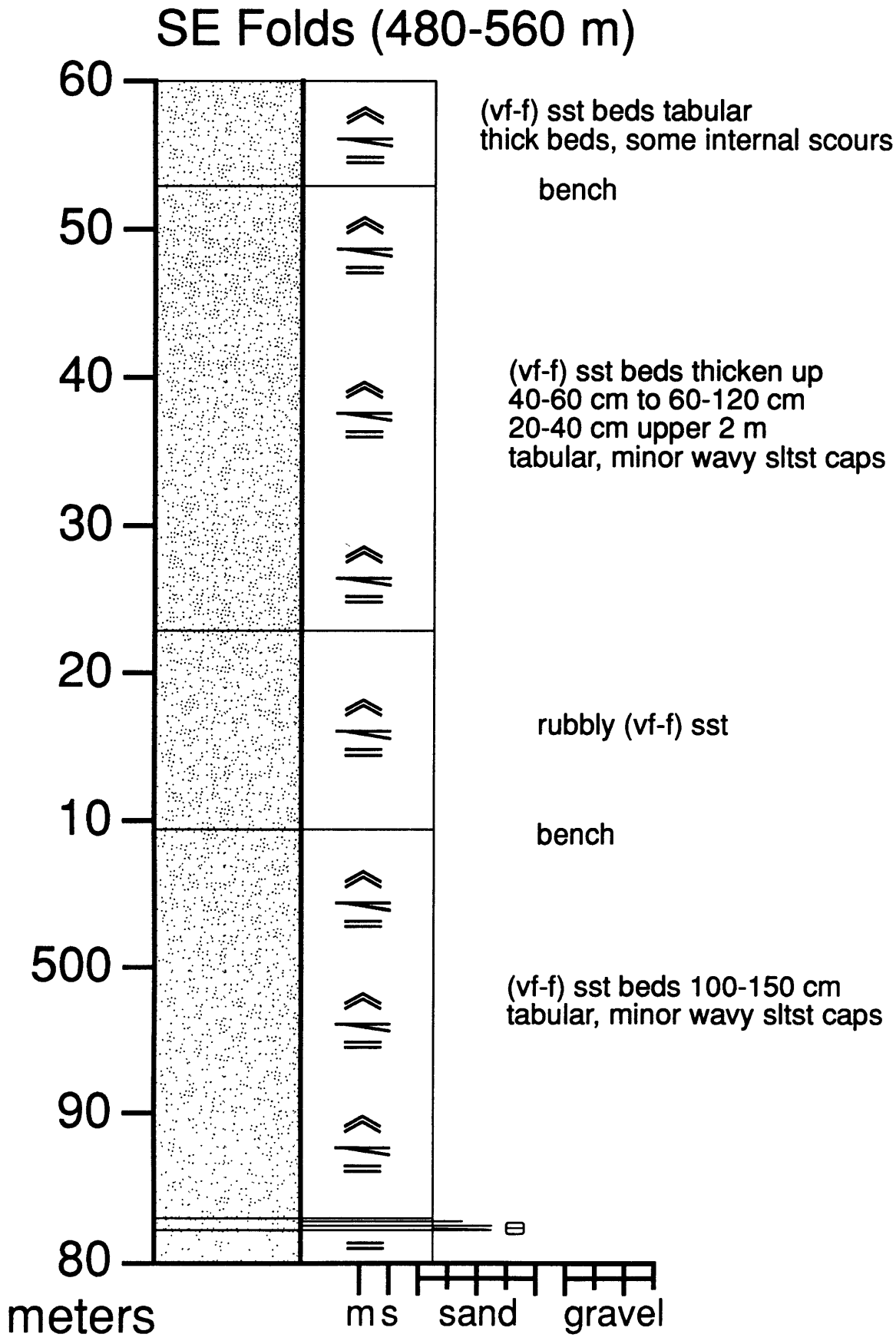
SE Folds (480-560 m)
60
50
40
30
20
10
500
90
80
meters
(vf-f) sst beds tabular
thick beds, some internal scours
bench
(vf-f) sst beds thicken up
40-60 cm to 60-120 cm
20-40 cm upper 2 m
tabular, minor wavy sltst caps
rubbly (vf-f) sst
bench
(vf-f) sst beds 100-150 cm
tabular, minor wavy sltst caps
m s
sand
gravel

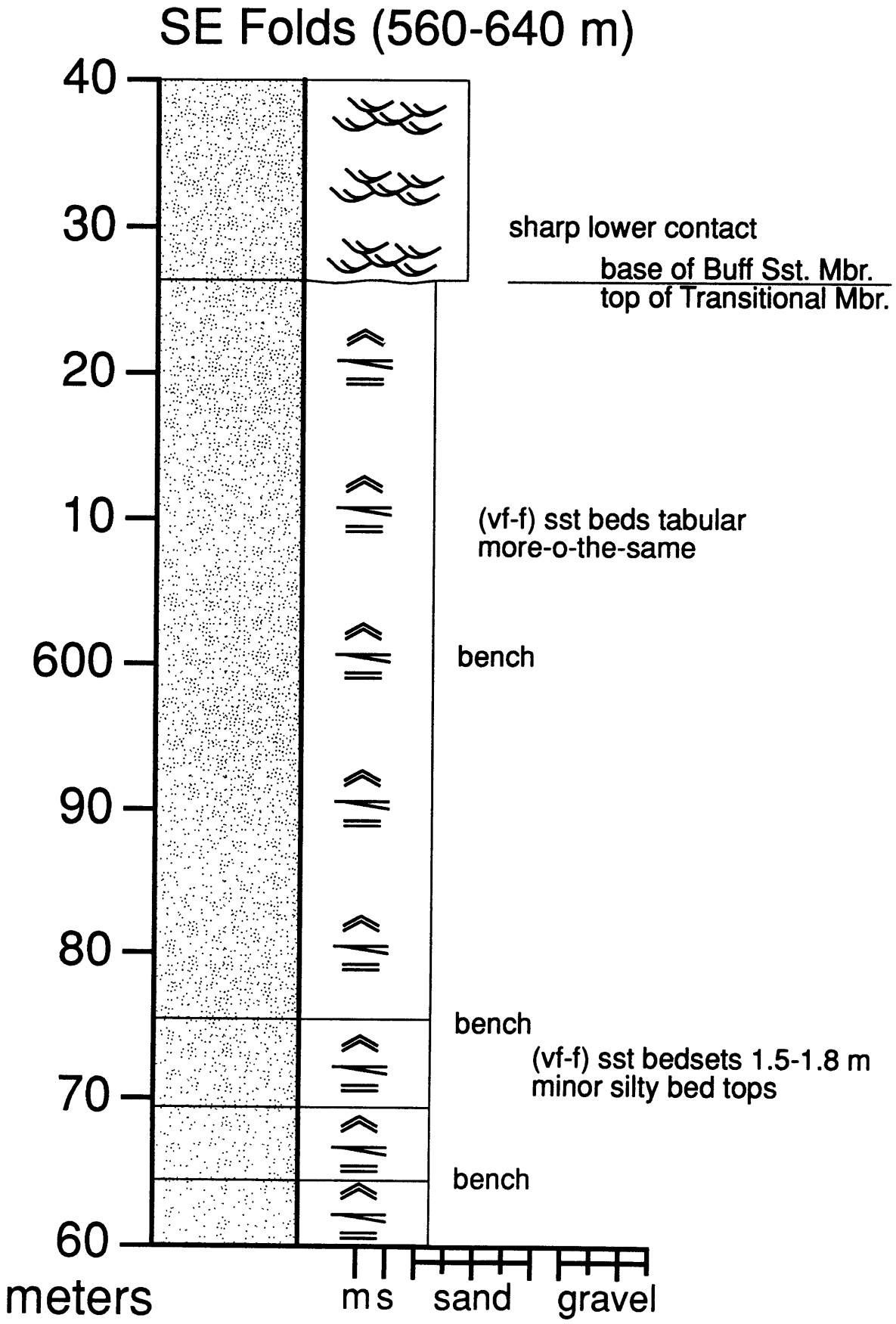
SE Folds (560-640 m)
40
30
20
10
600
90
80
70
60
meters
sharp lower contact
base of Buff Sst. Mbr.
top of Transitional Mbr.
(vf-f) sst beds tabular
more-o-the-same
bench
bench
(vf-f) sst bedsets 1.5-1.8 m
minor silty bed tops
bench
m s
sand
gravel

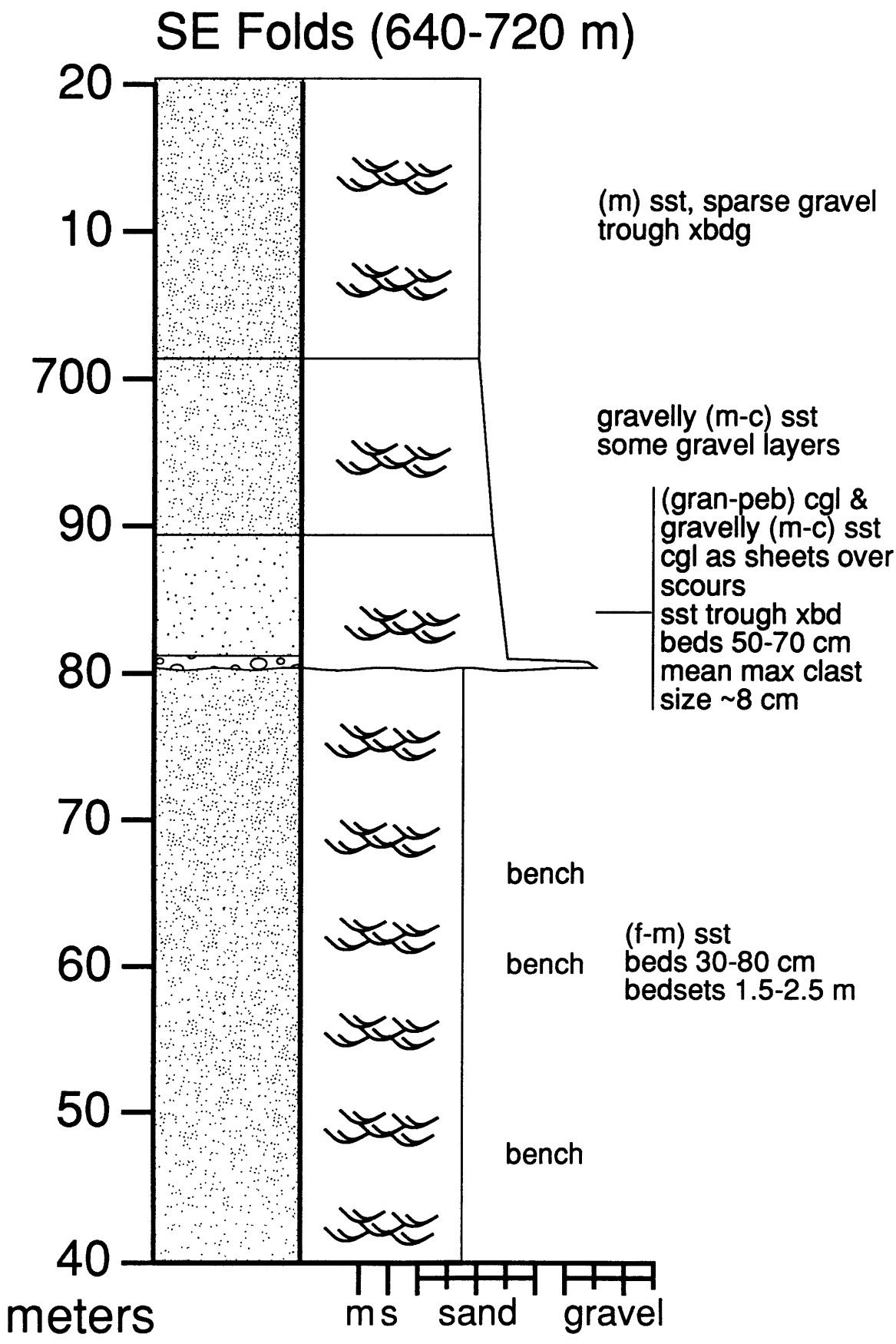
SE Folds (640-720 m)
20
10
700
90
80
70
60
50
40
meters
(m) sst, sparse gravel
trough xbdg
gravelly (m-c) sst
some gravel layers
(gran-peb) cgl &
gravelly (m-c) sst
cgl as sheets over
scours
sst trough xbd
beds 50-70 cm
mean max clast
size ~8 cm
bench
bench
(f-m) sst
beds 30-80 cm
bedsets 1.5-2.5 m
bench
m s
sand
gravel

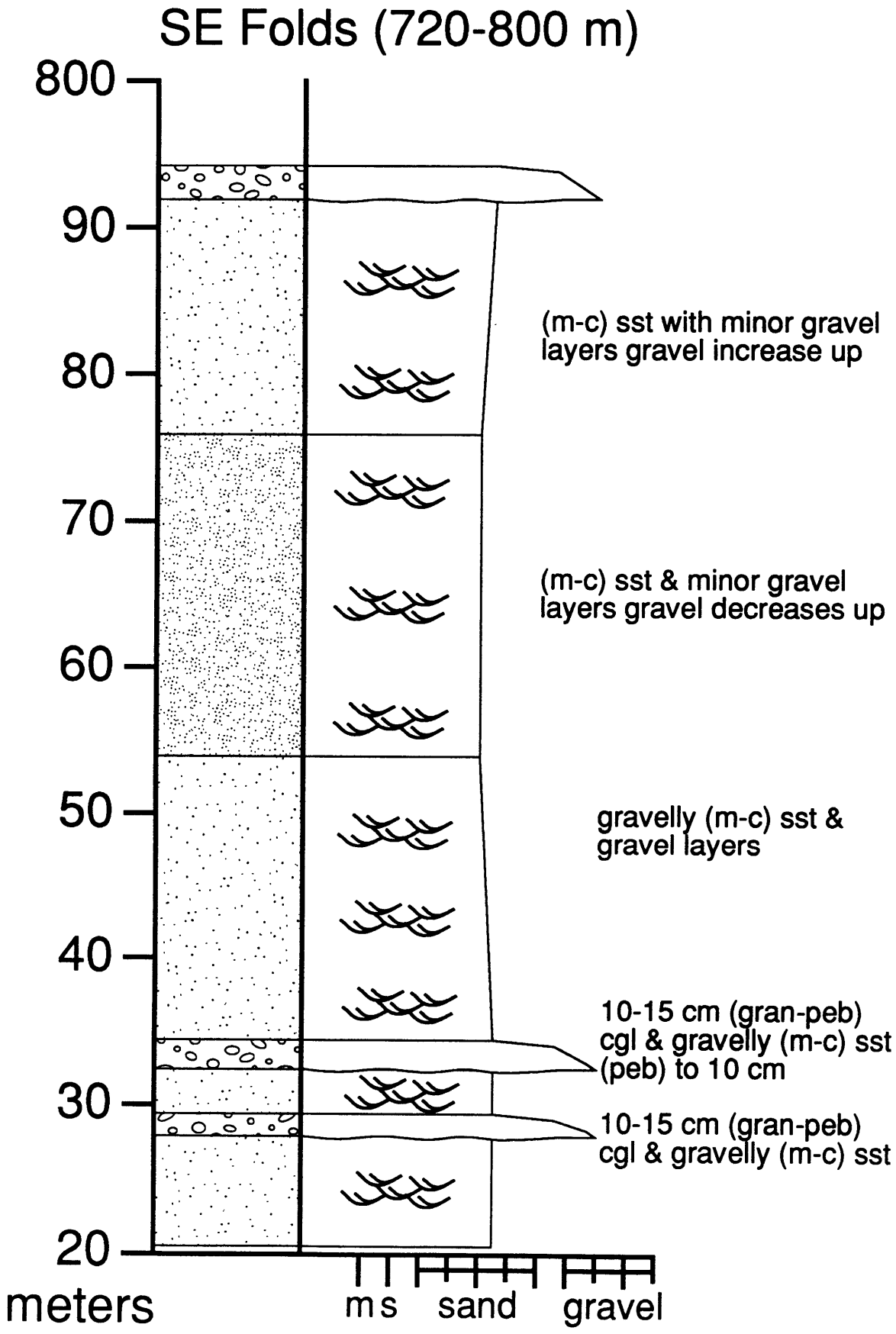
SE Folds (720-800 m)
800
90
80
70
60
50
40
30
20
meters
(m-c) sst with minor gravel layers gravel increase up
(m-c) sst & minor gravel layers gravel decreases up
gravelly (m-c) sst & gravel layers
10-15 cm (gran-peb) cgl & gravelly (m-c) sst (peb) to 10 cm
10-15 cm (gran-peb) cgl & gravelly (m-c) sst
m s
sand
gravel

section 5: NW Folds

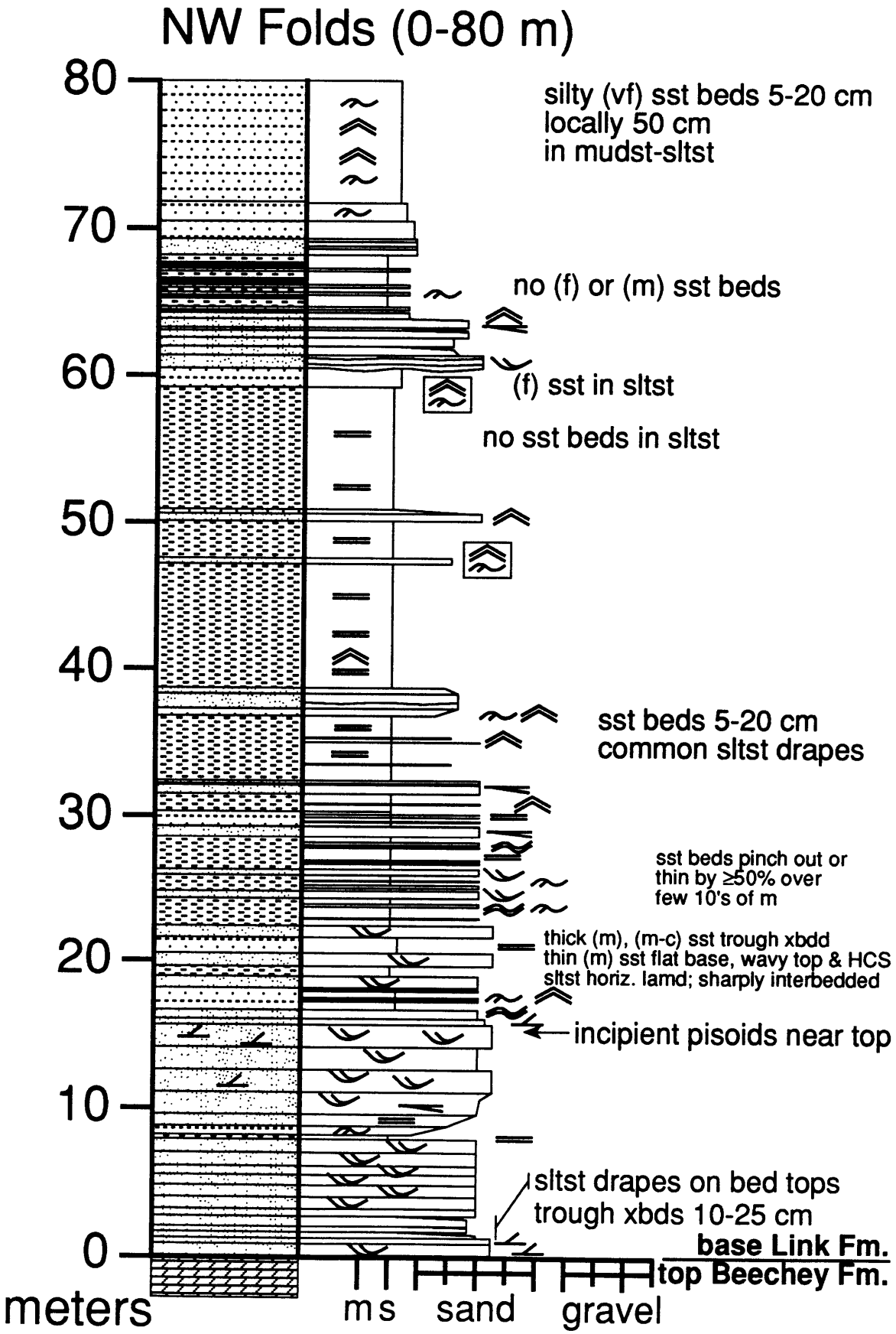
NW Folds (0-80 m)
80
70
60
50
40
30
20
10
0
meters
m s
sand
gravel
silty (vf) sst beds 5-20 cm
locally 50 cm
in mudst-sltst
no (f) or (m) sst beds
(f) sst in sltst
no sst beds in sltst
sst beds 5-20 cm
common sltst drapes
sst beds pinch out or
thin by ≥50% over
few 10's of m
thick (m), (m-c) sst trough xbdd
thin (m) sst flat base, wavy top & HCS
sltst horiz. lamd; sharply interbedded
incipient pisoids near top
sltst drapes on bed tops
trough xbds 10-25 cm
base Link Fm.
top Beechey Fm.

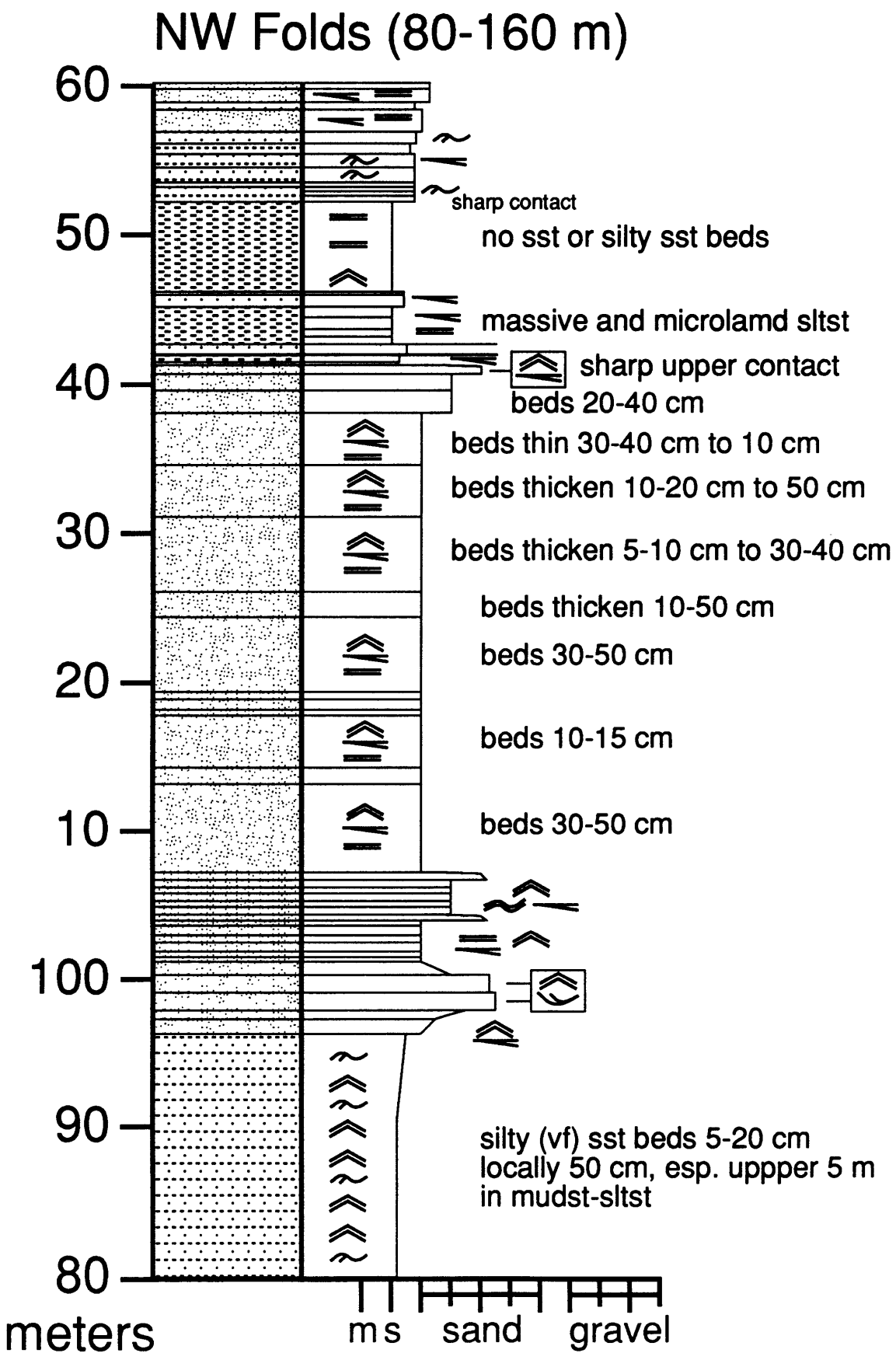
NW Folds (80-160 m)
60
50
40
30
20
10
100
90
80
meters
sharp contact
no sst or silty sst beds
massive and microlamd sltst
sharp upper contact
beds 20-40 cm
beds thin 30-40 cm to 10 cm
beds thicken 10-20 cm to 50 cm
beds thicken 5-10 cm to 30-40 cm
beds thicken 10-50 cm
beds 30-50 cm
beds 10-15 cm
beds 30-50 cm
silty (vf) sst beds 5-20 cm
locally 50 cm, esp. uppper 5 m
in mudst-sltst
m s
sand
gravel

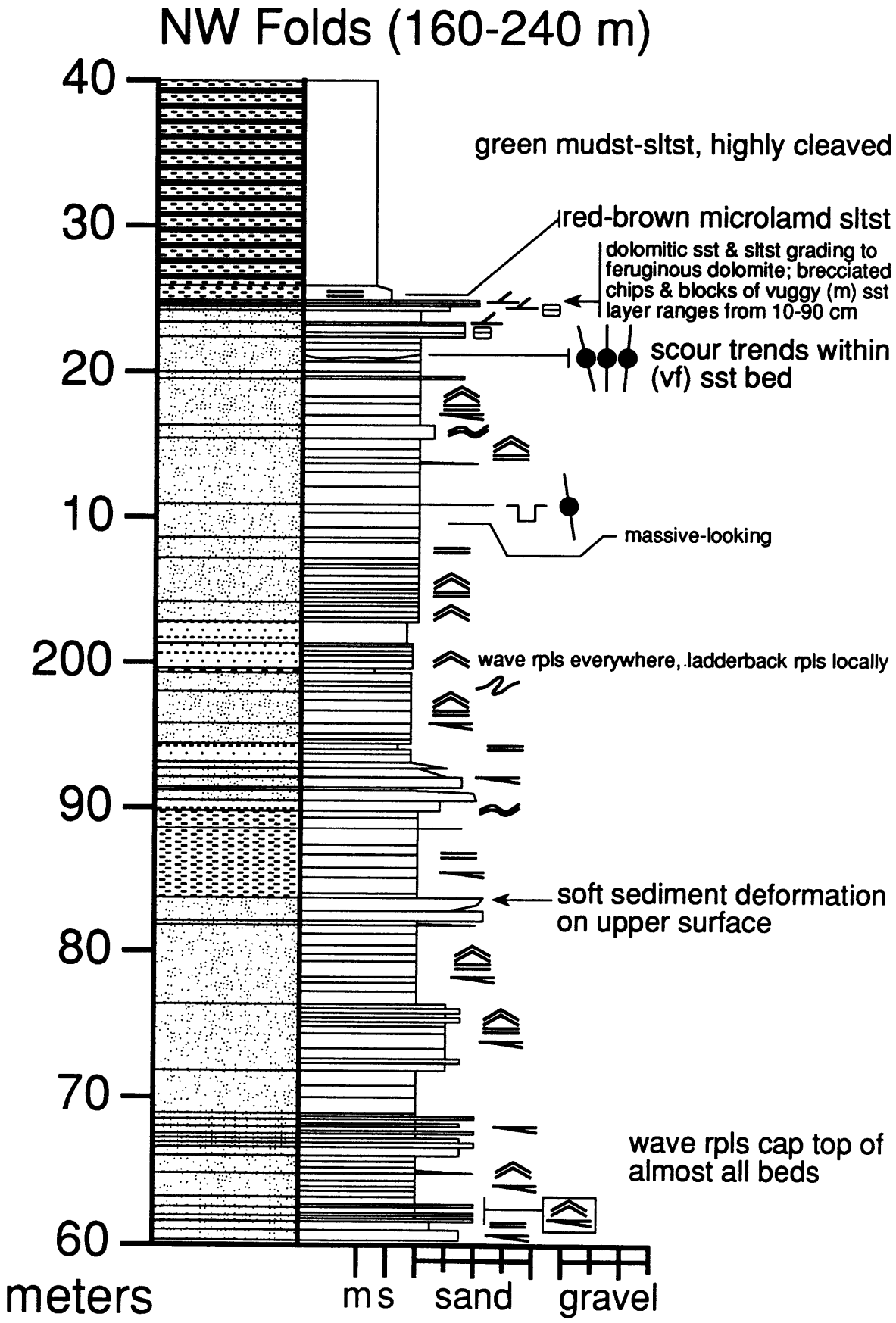
NW Folds (160-240 m)
40
30
20
10
200
90
80
70
60
meters
green mudst-sltst, highly cleaved
red-brown microlamd sltst
dolomitic sst & sltst grading to feruginous dolomite; brecciated chips & blocks of vuggy (m) sst layer ranges from 10-90 cm
scour trends within (vf) sst bed
massive-looking
wave rpls everywhere, ladderback rpls locally
soft sediment deformation on upper surface
wave rpls cap top of almost all beds
m s
sand
gravel

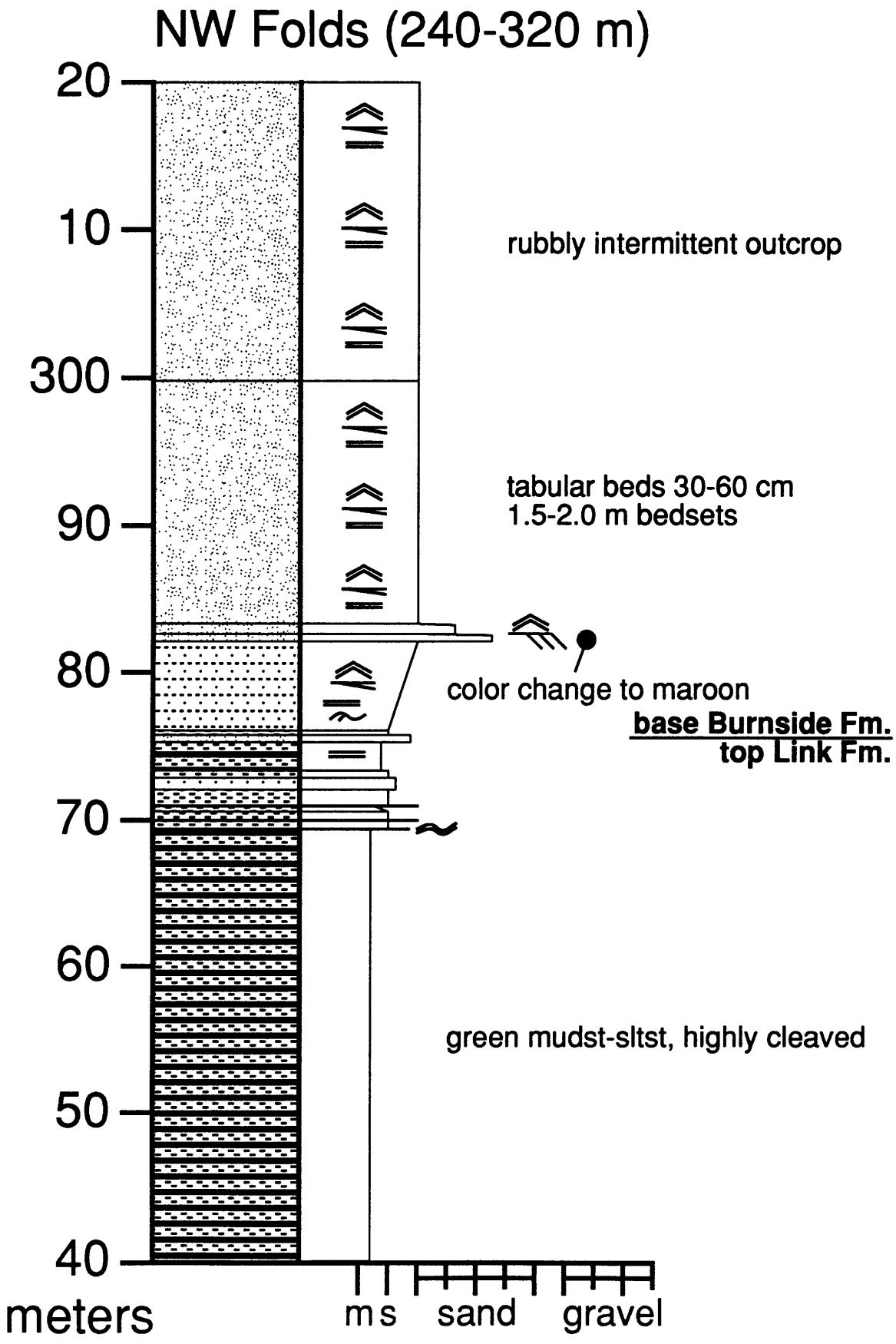
NW Folds (240-320 m)
20
10
300
90
80
70
60
50
40
meters
rubbly intermittent outcrop
tabular beds 30-60 cm
1.5-2.0 m bedsets
color change to maroon
base Burnside Fm.
top Link Fm.
green mudst-sltst, highly cleaved
m s
sand
gravel

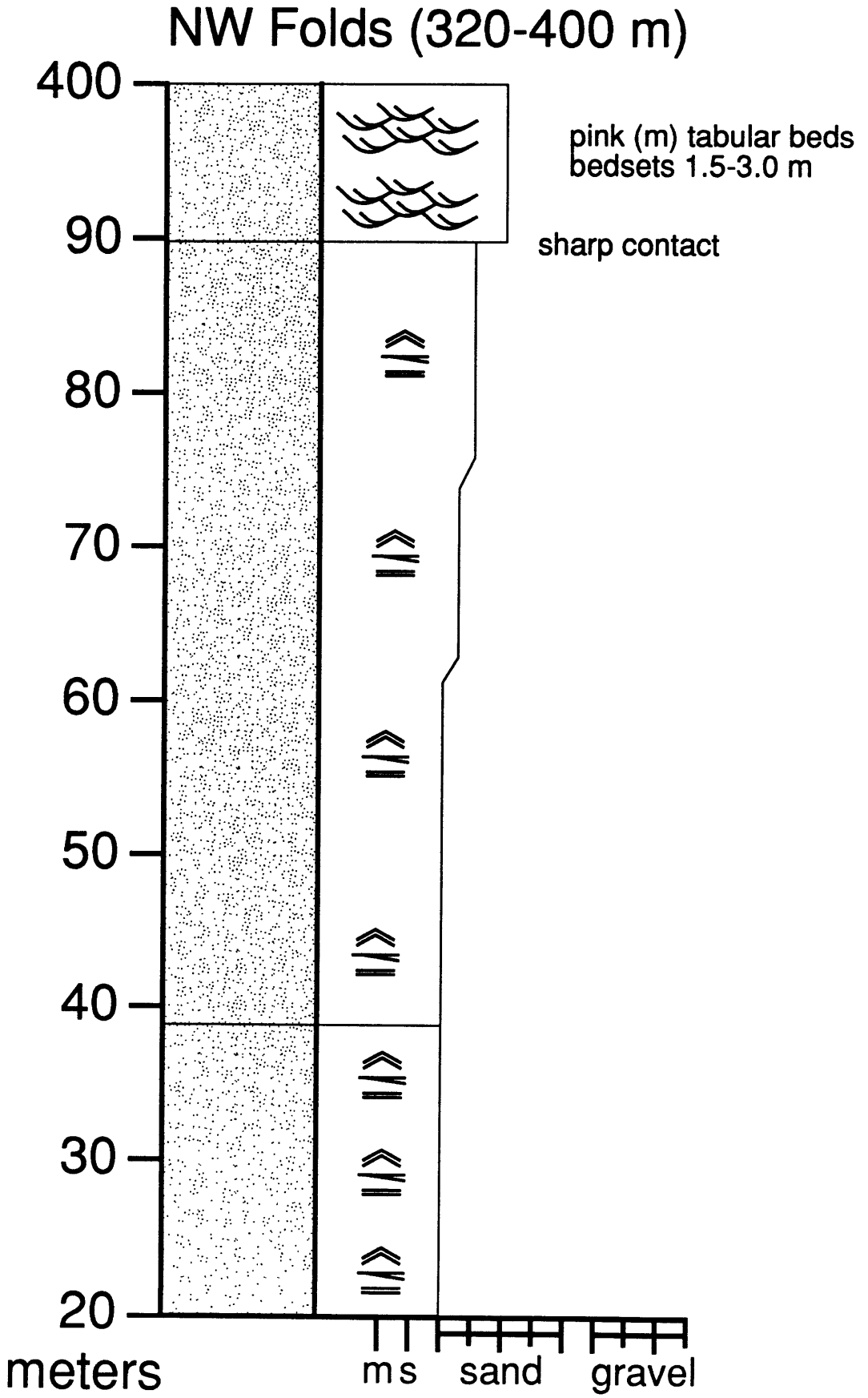
NW Folds (320-400 m)
400
90
80
70
60
50
40
30
20
meters
pink (m) tabular beds
bedsets 1.5-3.0 m
sharp contact
m s
sand
gravel

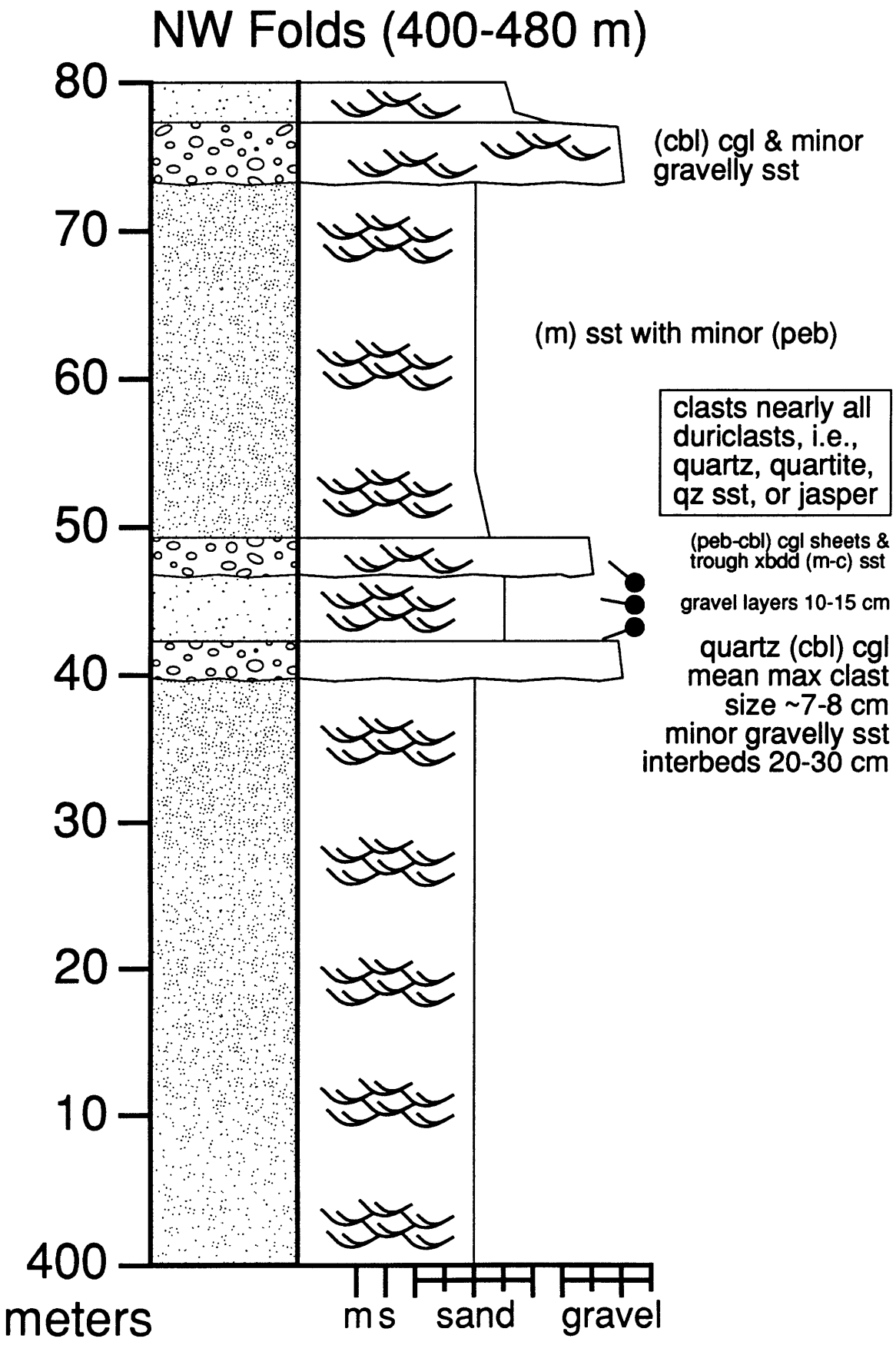
NW Folds (400-480 m)
80
70
60
50
40
30
20
10
400
meters
(cbl) cgl & minor gravelly sst
(m) sst with minor (peb)
clasts nearly all duriclasts, i.e., quartz, quartite, qz sst, or jasper
(peb-cbl) cgl sheets & trough xbdd (m-c) sst
gravel layers 10-15 cm
quartz (cbl) cgl mean max clast size ~7-8 cm
minor gravelly sst interbeds 20-30 cm
m s
sand
gravel

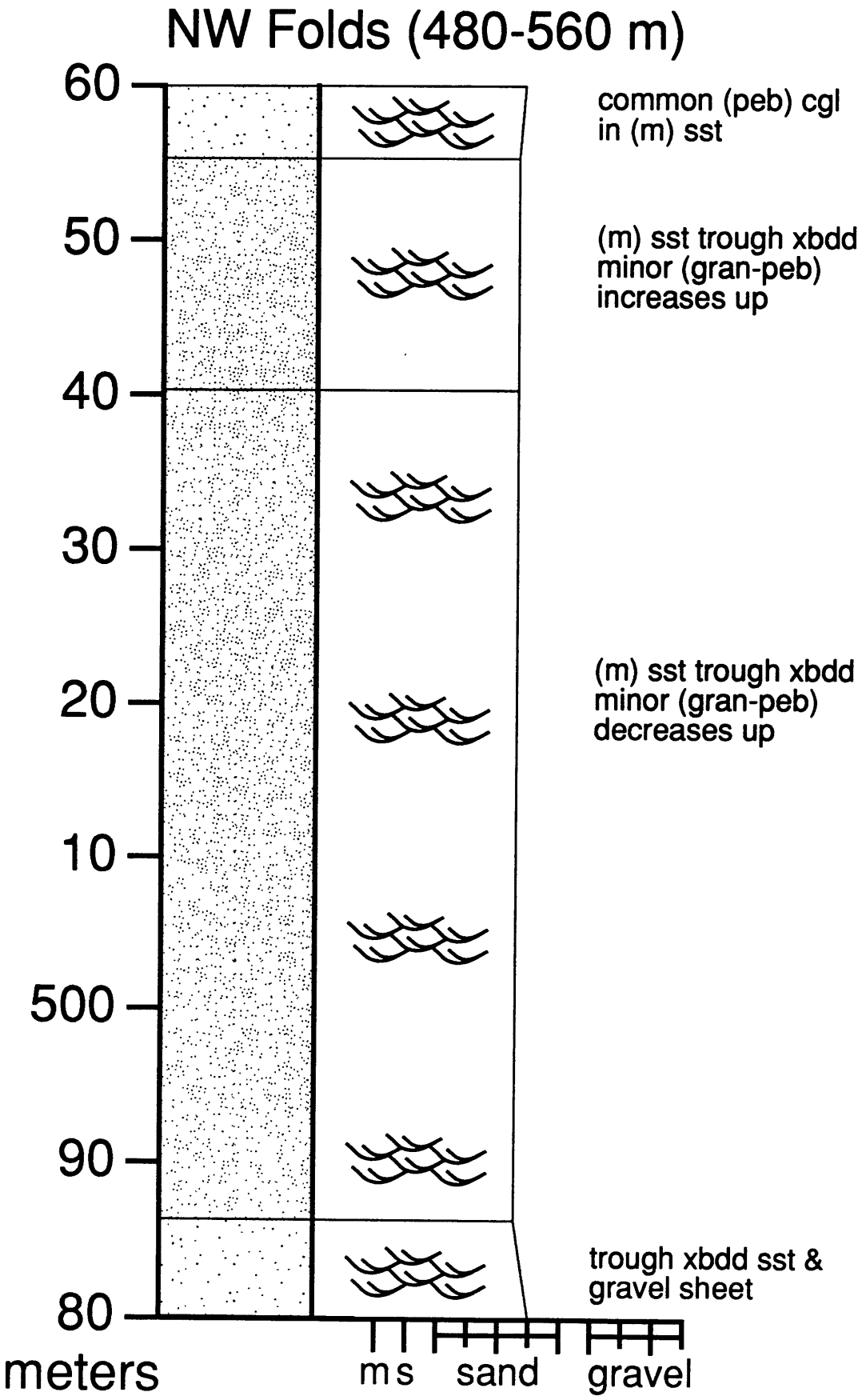
NW Folds (480-560 m)
60
50
40
30
20
10
500
90
80
meters
common (peb) cgl
in (m) sst
(m) sst trough xbdd
minor (gran-peb)
increases up
(m) sst trough xbdd
minor (gran-peb)
decreases up
trough xbdd sst &
gravel sheet
m s
sand
gravel

NW Folds (560-575 m)

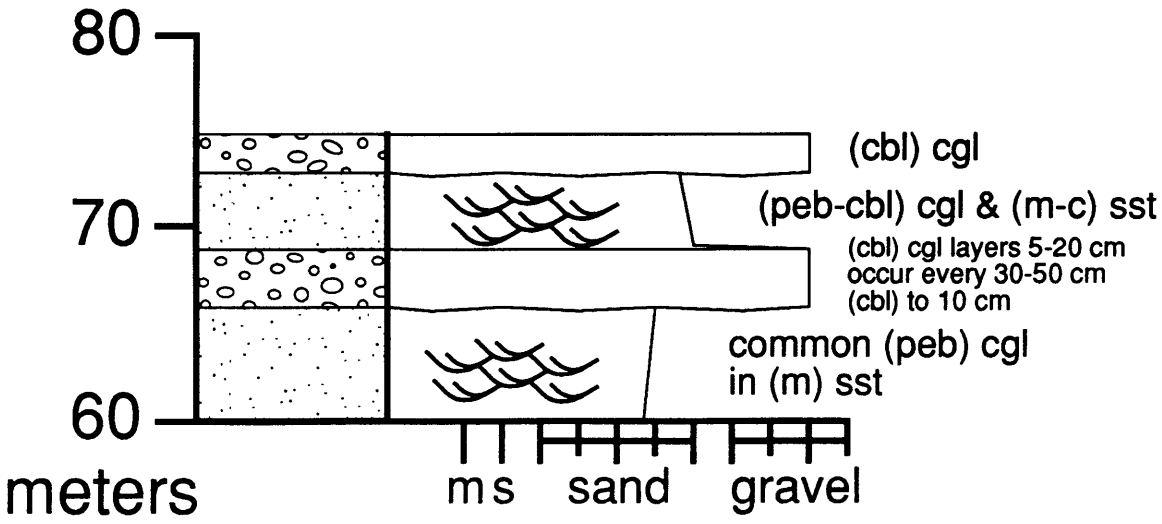

section 6: Rifle Lake

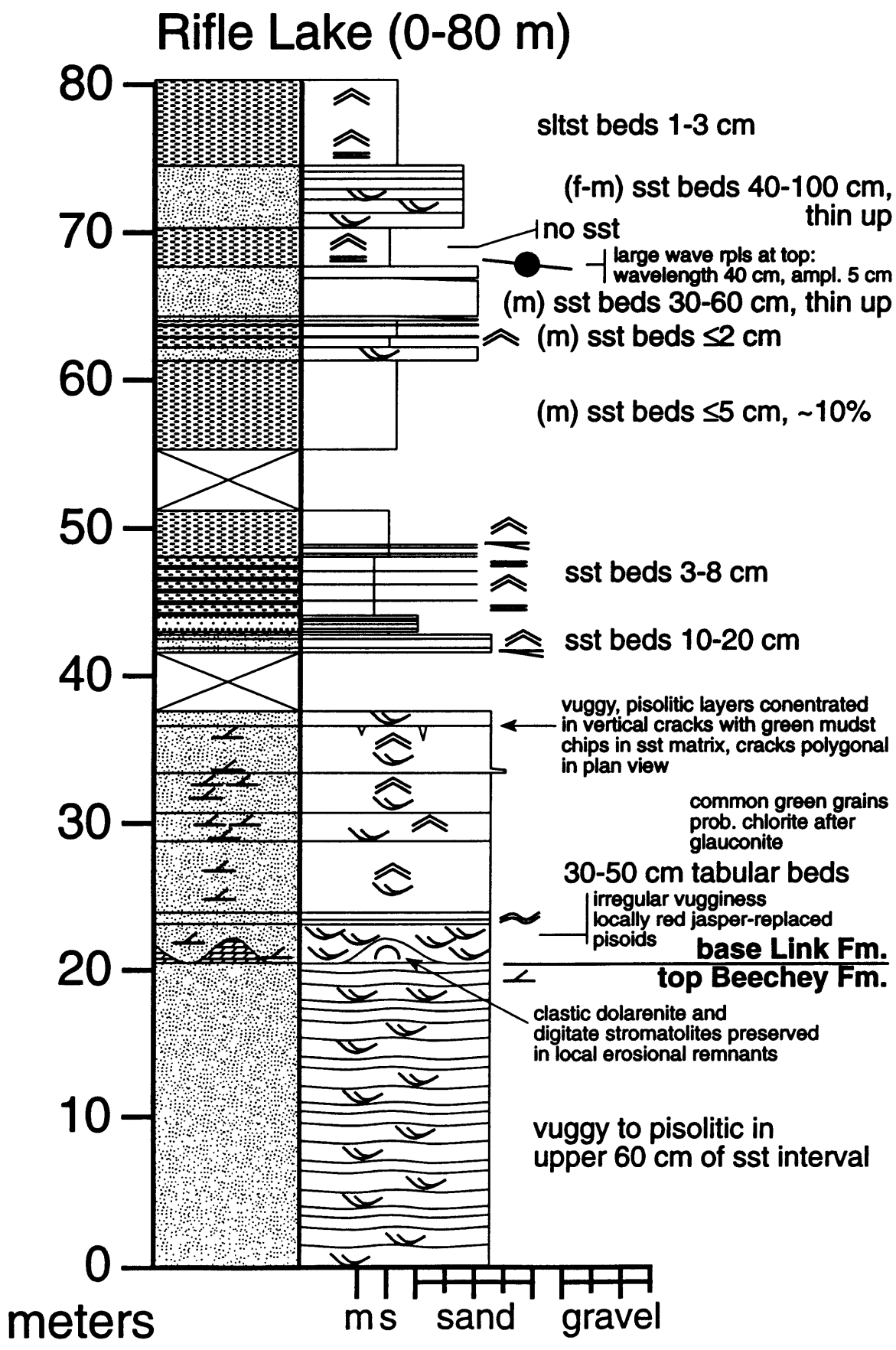
Rifle Lake (0-80 m)
80
70
60
50
40
30
20
10
0
meters
m s
sand
gravel
sltst beds 1-3 cm
(f-m) sst beds 40-100 cm, thin up
no sst
large wave rpls at top: wavelength 40 cm, ampl. 5 cm
(m) sst beds 30-60 cm, thin up
(m) sst beds ≤2 cm
(m) sst beds ≤5 cm, ~10%
sst beds 3-8 cm
sst beds 10-20 cm
vuggy, pisolitic layers conentrated in vertical cracks with green mudst chips in sst matrix, cracks polygonal in plan view
common green grains prob. chlorite after glauconite
30-50 cm tabular beds
irregular vugginess locally red jasper-replaced pisoids
base Link Fm.
top Beechey Fm.
clastic dolarenite and digitate stromatolites preserved in local erosional remnants
vuggy to pisolitic in upper 60 cm of sst interval

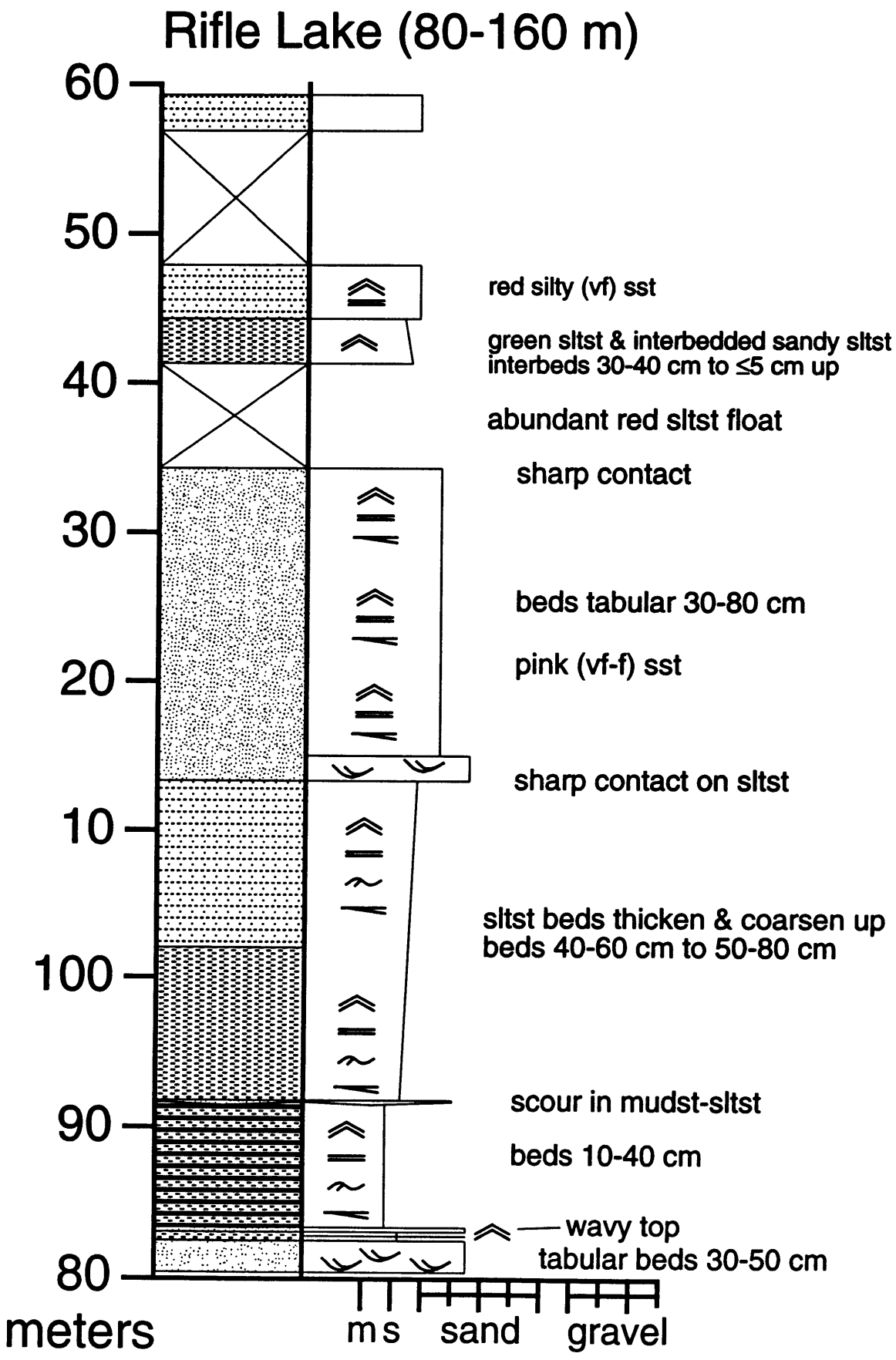
Rifle Lake (80-160 m)
60
50
40
30
20
10
100
90
80
meters
red silty (vf) sst
green sltst & interbedded sandy sltst
interbeds 30-40 cm to ≤5 cm up
abundant red sltst float
sharp contact
beds tabular 30-80 cm
pink (vf-f) sst
sharp contact on sltst
sltst beds thicken & coarsen up
beds 40-60 cm to 50-80 cm
scour in mudst-sltst
beds 10-40 cm
wavy top
tabular beds 30-50 cm
ms
sand
gravel

Rifle Lake (160-177 m)

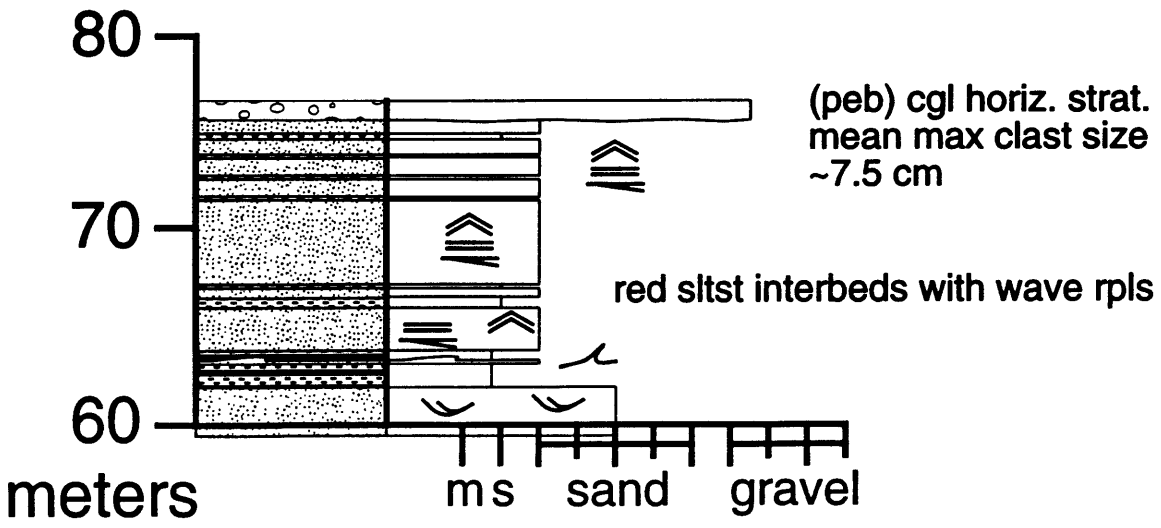

section 7: south Link Lake

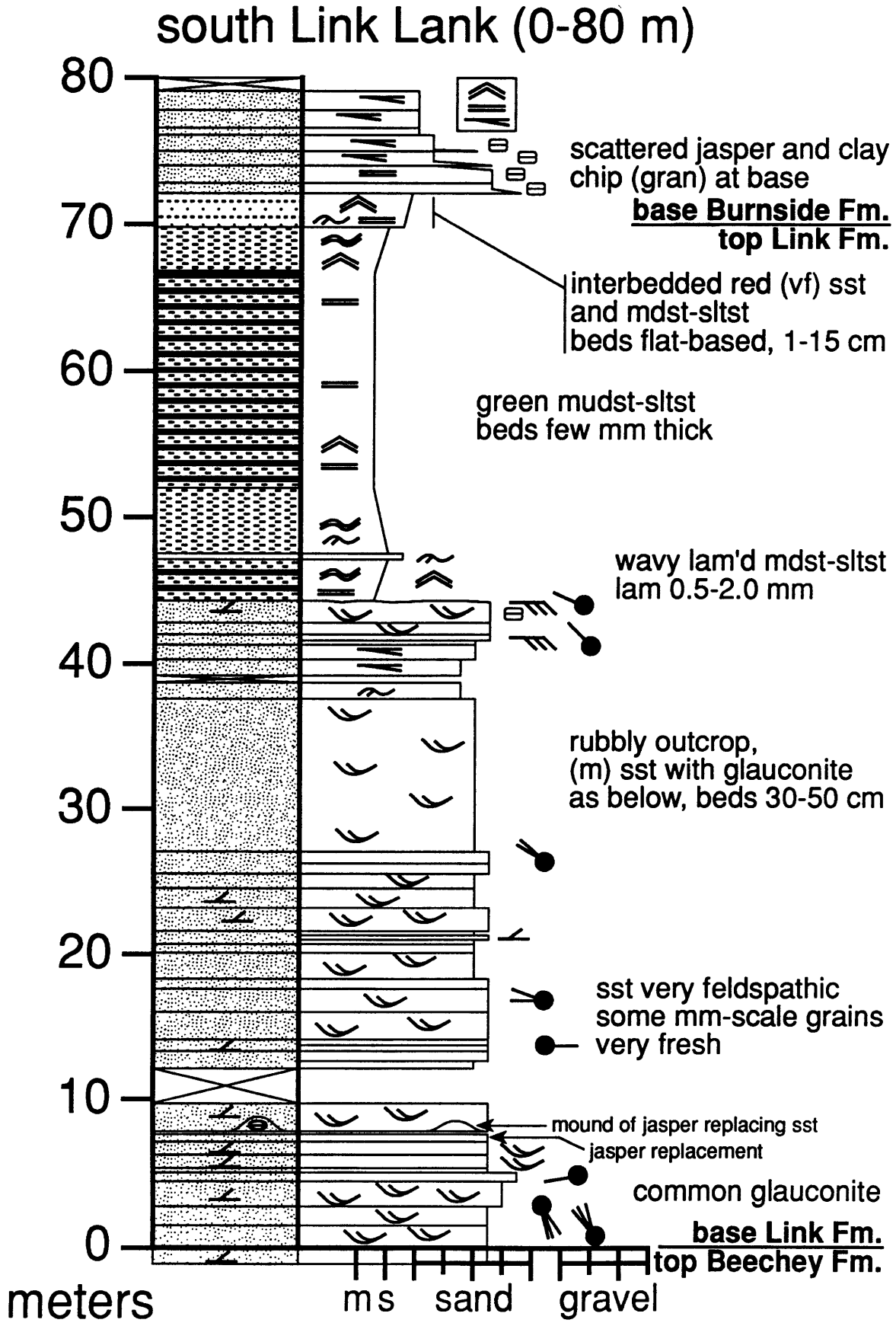
south Link Lank (0-80 m)
80
70
60
50
40
30
20
10
0
meters
ms
sand
gravel
scattered jasper and clay chip (gran) at base
base Burnside Fm.
top Link Fm.
interbedded red (vf) sst and mdst-sltst beds flat-based, 1-15 cm
green mudst-sltst beds few mm thick
wavy lam'd mdst-sltst lam 0.5-2.0 mm
rubbly outcrop, (m) sst with glauconite as below, beds 30-50 cm
sst very feldspathic some mm-scale grains very fresh
mound of jasper replacing sst
jasper replacement
common glauconite
base Link Fm.
top Beechey Fm.

south Link Lake (80-110 m)

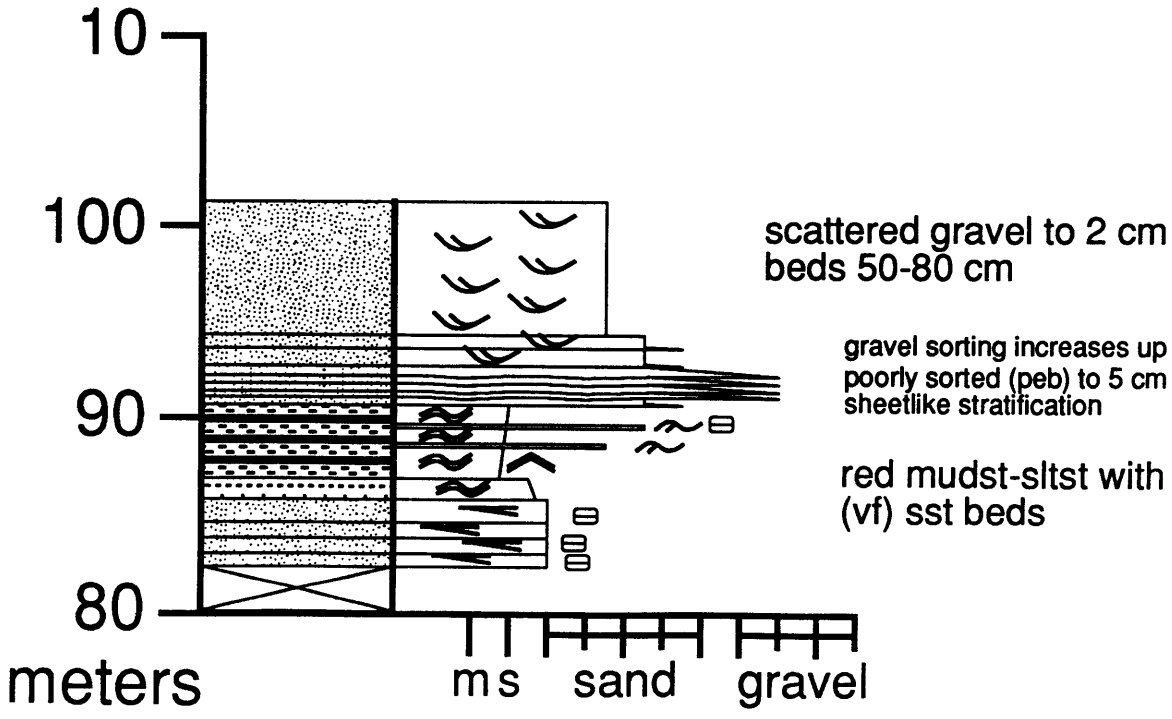

section 8: middle Link Lake

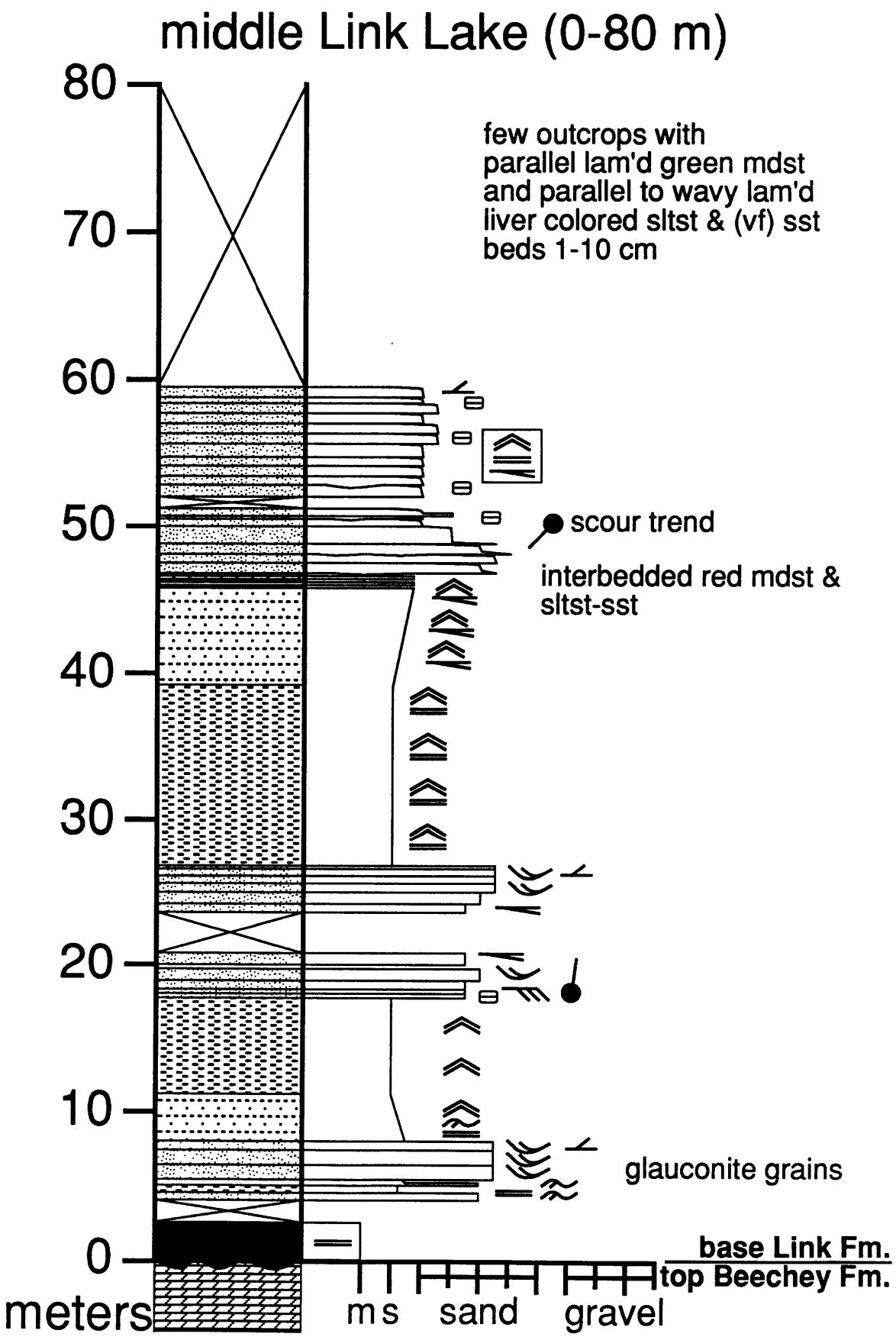
middle Link Lake (0-80 m)
80
70
60
50
40
30
20
10
0
meters
few outcrops with
parallel lam'd green mdst
and parallel to wavy lam'd
liver colored sltst & (vf) sst
beds 1-10 cm
scour trend
interbedded red mdst &
sltst-sst
glauconite grains
base Link Fm.
top Beechey Fm.
m s
sand
gravel

middle Link Lake (80-100 m)

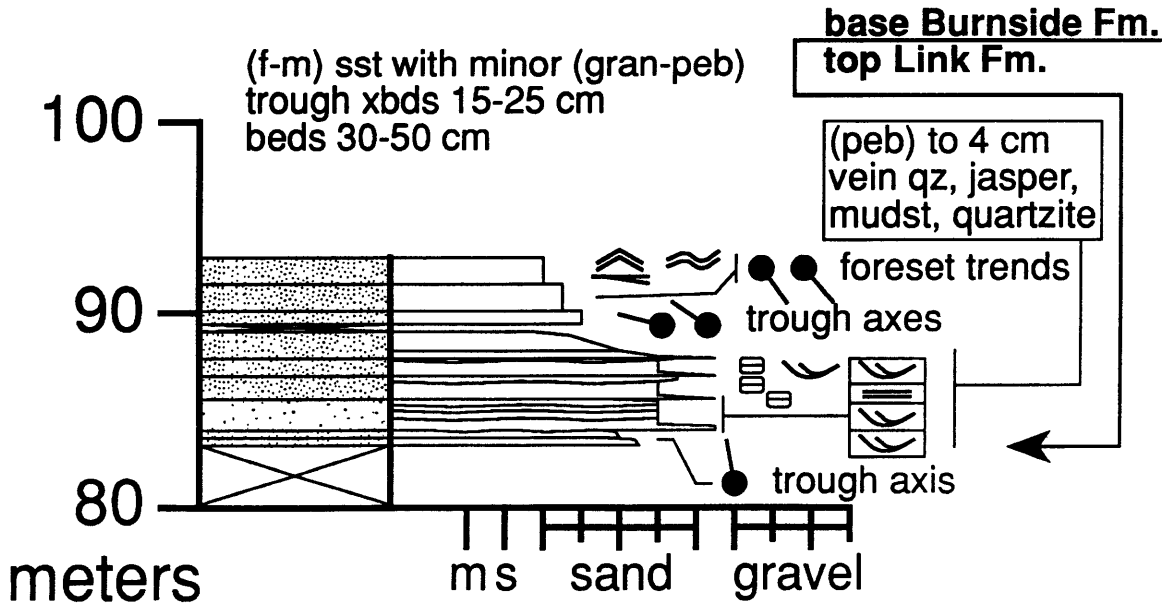

section 9: north Link Lake

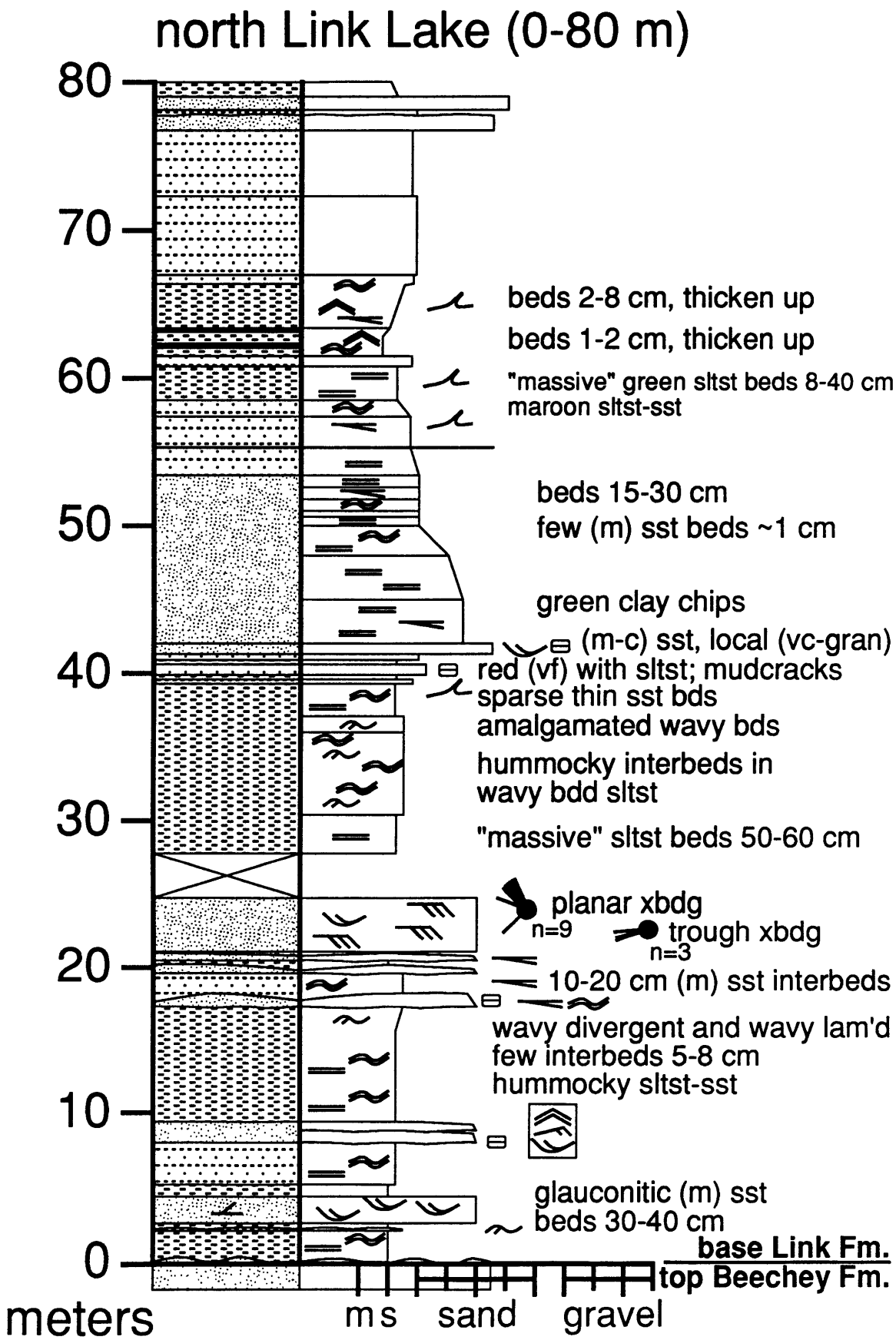
north Link Lake (0-80 m)
80
70
60
50
40
30
20
10
0
meters
m
s
sand
gravel
beds 2-8 cm, thicken up
beds 1-2 cm, thicken up
"massive" green sltst beds 8-40 cm
maroon sltst-sst
beds 15-30 cm
few (m) sst beds ~1 cm
green clay chips
(m-c) sst, local (vc-gran)
red (vf) with sltst; mudcracks
sparse thin sst bds
amalgamated wavy bds
hummocky interbeds in
wavy bdd sltst
"massive" sltst beds 50-60 cm
planar xbdg
n=9
trough xbdg
n=3
10-20 cm (m) sst interbeds
wavy divergent and wavy lam'd
few interbeds 5-8 cm
hummocky sltst-sst
glauconitic (m) sst
beds 30-40 cm
base Link Fm.
top Beechey Fm.

north Link Lake (80-90 m)

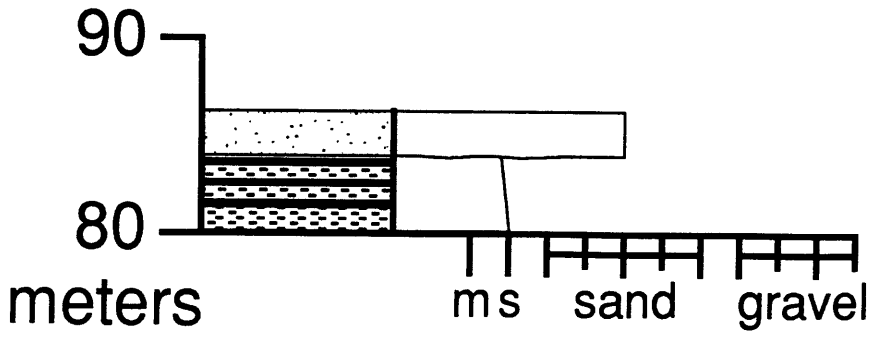

section 10: Hackett River

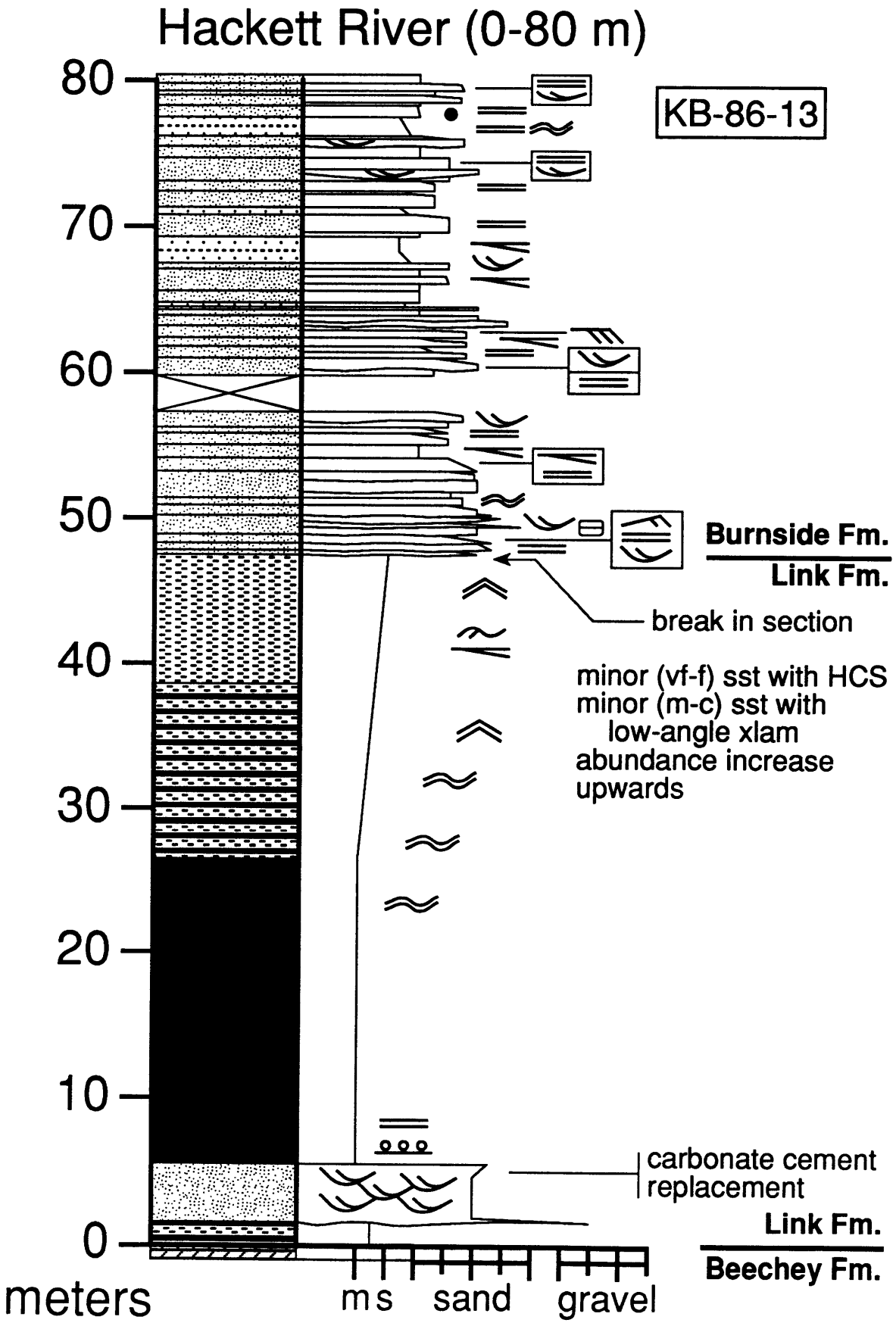
Hackett River (0-80 m)
KB-86-13
80
70
60
50
40
30
20
10
0
meters
Burnside Fm.
Link Fm.
break in section
minor (vf-f) sst with HCS
minor (m-c) sst with
low-angle xlam
abundance increase
upwards
carbonate cement
replacement
Link Fm.
Beechey Fm.
m s
sand
gravel

Hackett River (80-97 m)

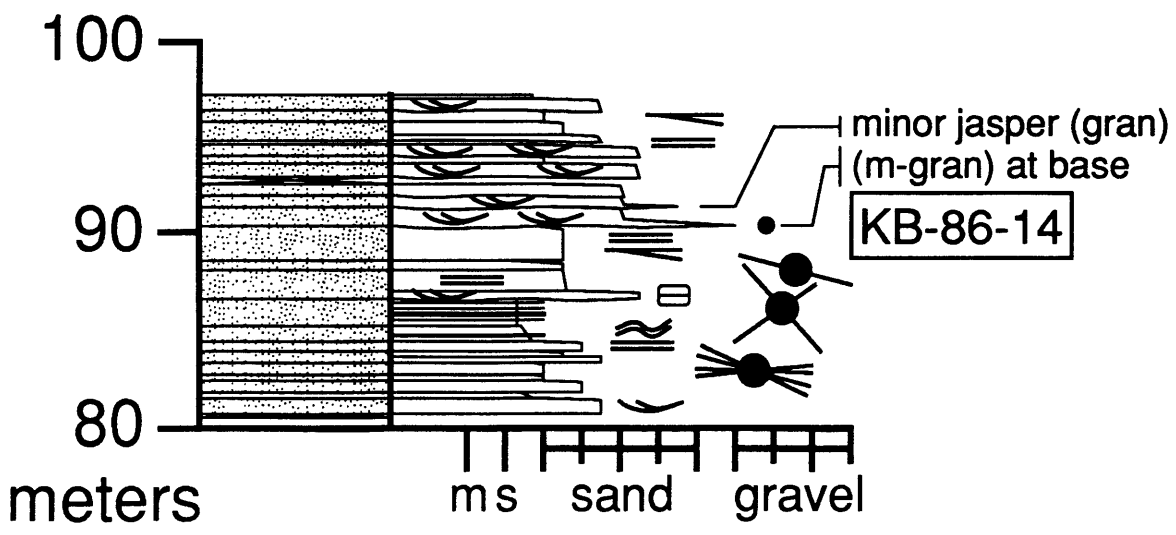

section 11: northwest Hackett River

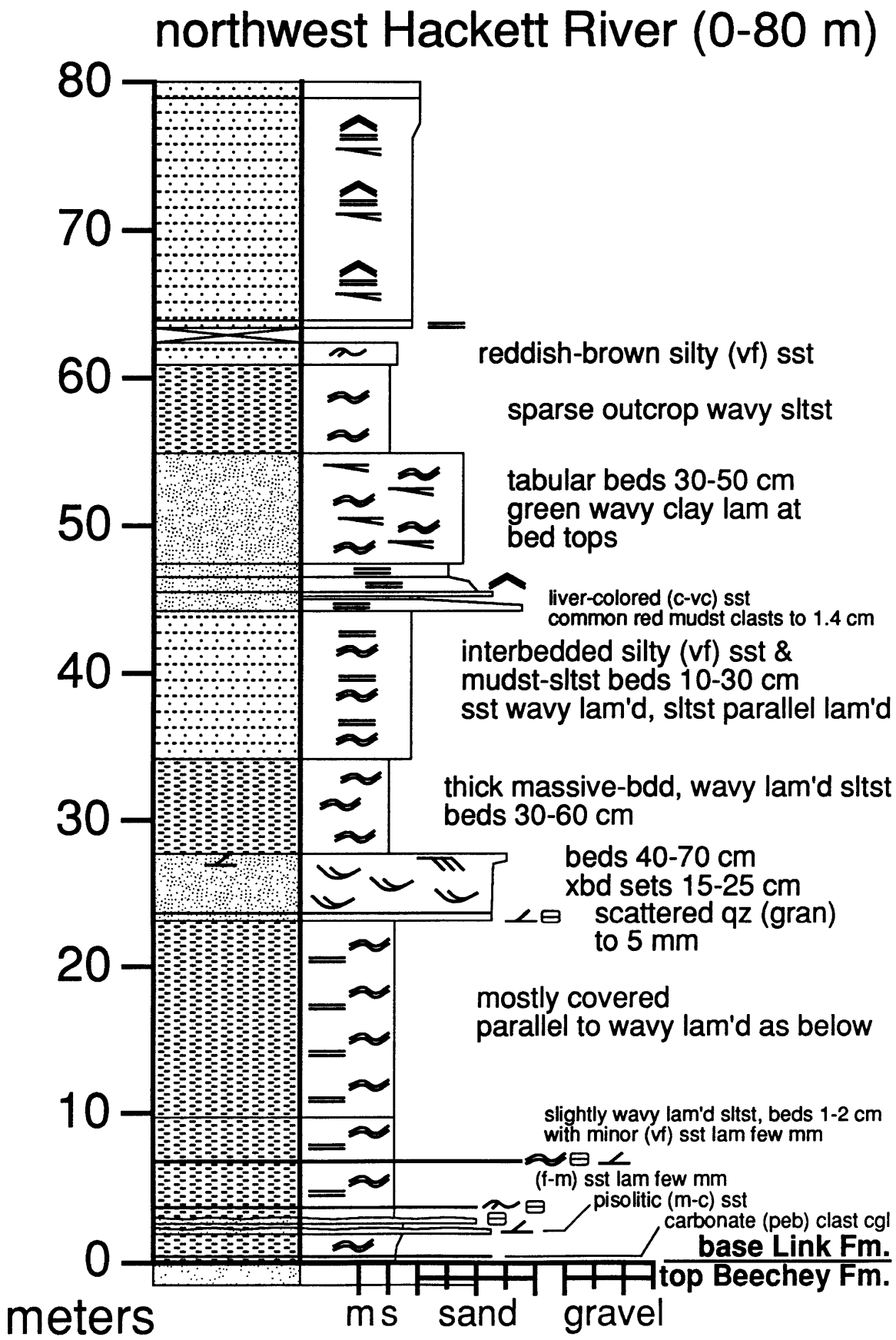
northwest Hackett River (0-80 m)
80
70
60
50
40
30
20
10
0
meters
reddish-brown silty (vf) sst
sparse outcrop wavy sltst
tabular beds 30-50 cm
green wavy clay lam at
bed tops
liver-colored (c-vc) sst
common red mudst clasts to 1.4 cm
interbedded silty (vf) sst &
mudst-sltst beds 10-30 cm
sst wavy lam'd, sltst parallel lam'd
thick massive-bdd, wavy lam'd sltst
beds 30-60 cm
beds 40-70 cm
xbd sets 15-25 cm
scattered qz (gran)
to 5 mm
mostly covered
parallel to wavy lam'd as below
slightly wavy lam'd sltst, beds 1-2 cm
with minor (vf) sst lam few mm
(f-m) sst lam few mm
pisolitic (m-c) sst
carbonate (peb) clast cgl
base Link Fm.
top Beechey Fm.
m s
sand
gravel

northwest Hackett River (80-120 m)

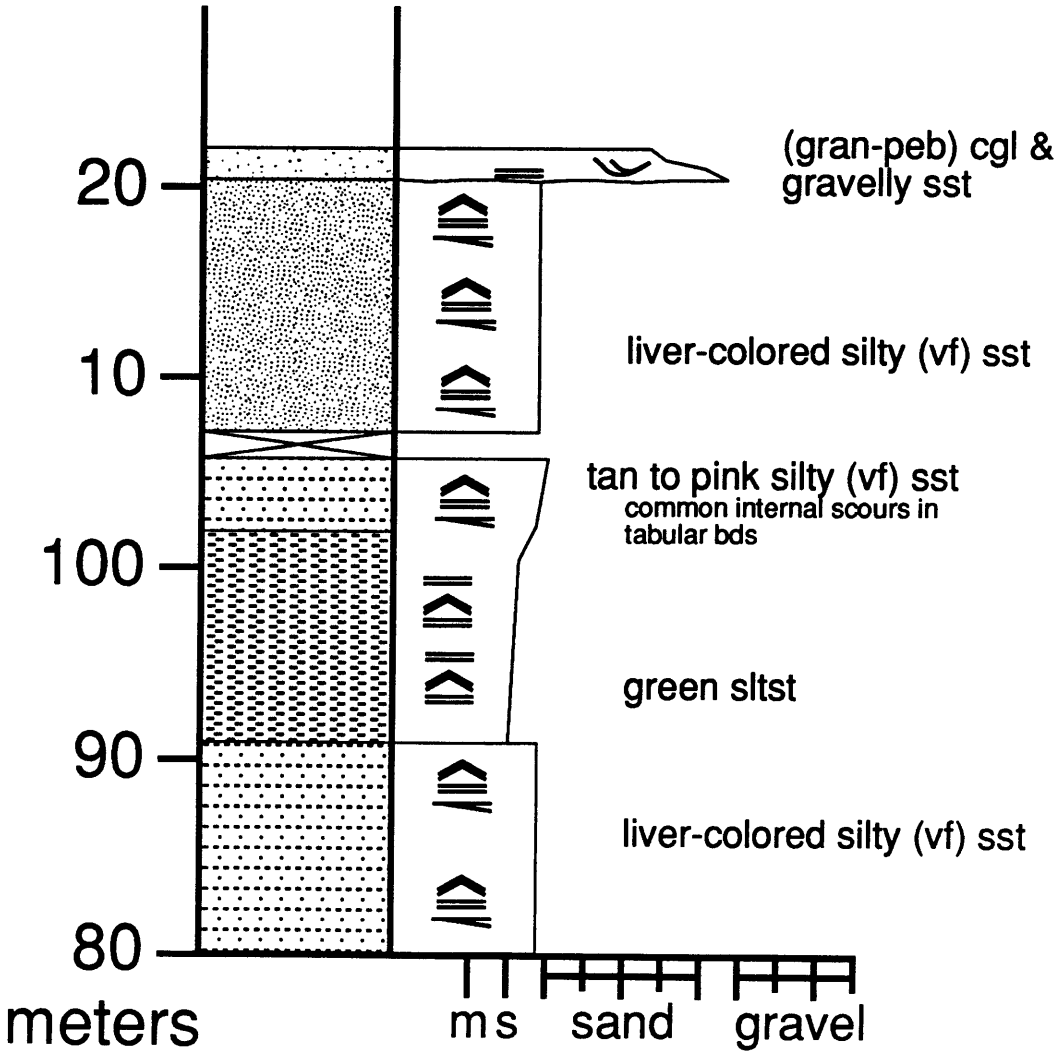

section 12: Wolverine Canyon

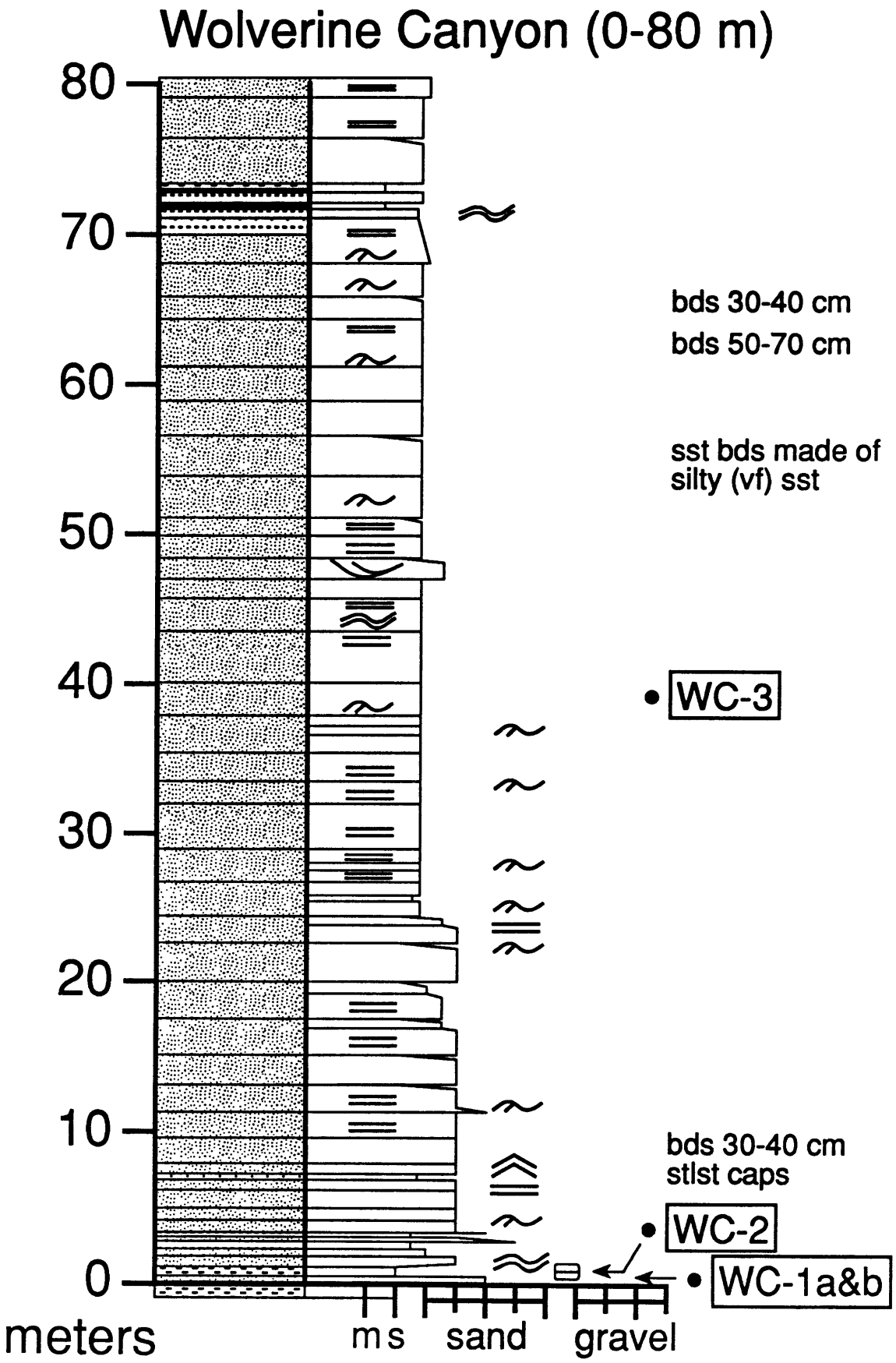
Wolverine Canyon (0-80 m)
80
70
60
50
40
30
20
10
0
meters
ms
sand
gravel
bds 30-40 cm
bds 50-70 cm
sst bds made of
silty (vf) sst
WC-3
bds 30-40 cm
stlst caps
WC-2
WC-1a&b

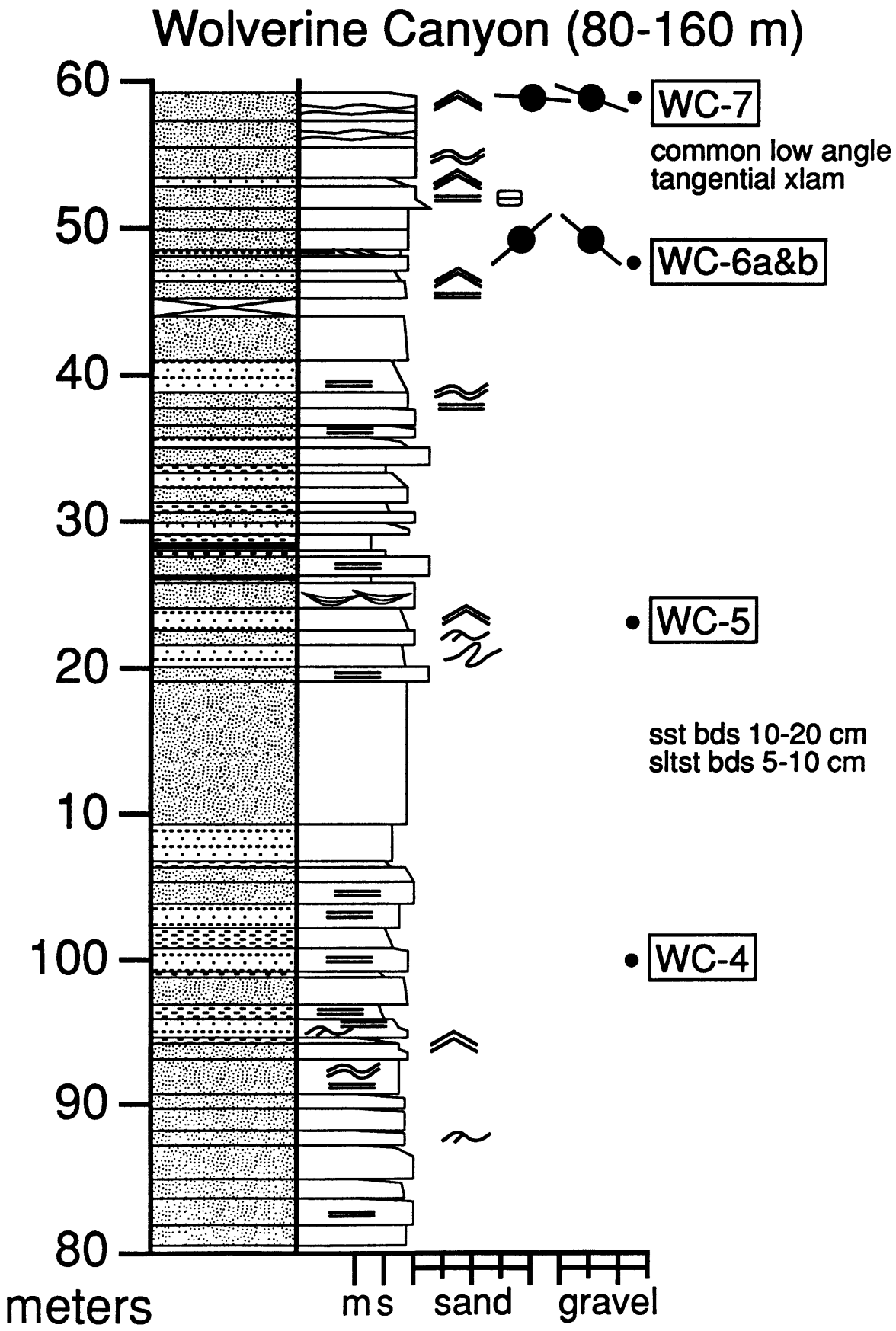
Wolverine Canyon (80-160 m)
60
50
40
30
20
10
100
90
80
meters
WC-7
common low angle
tangential xlam
WC-6a&b
WC-5
sst bds 10-20 cm
sltst bds 5-10 cm
WC-4
m s
sand
gravel

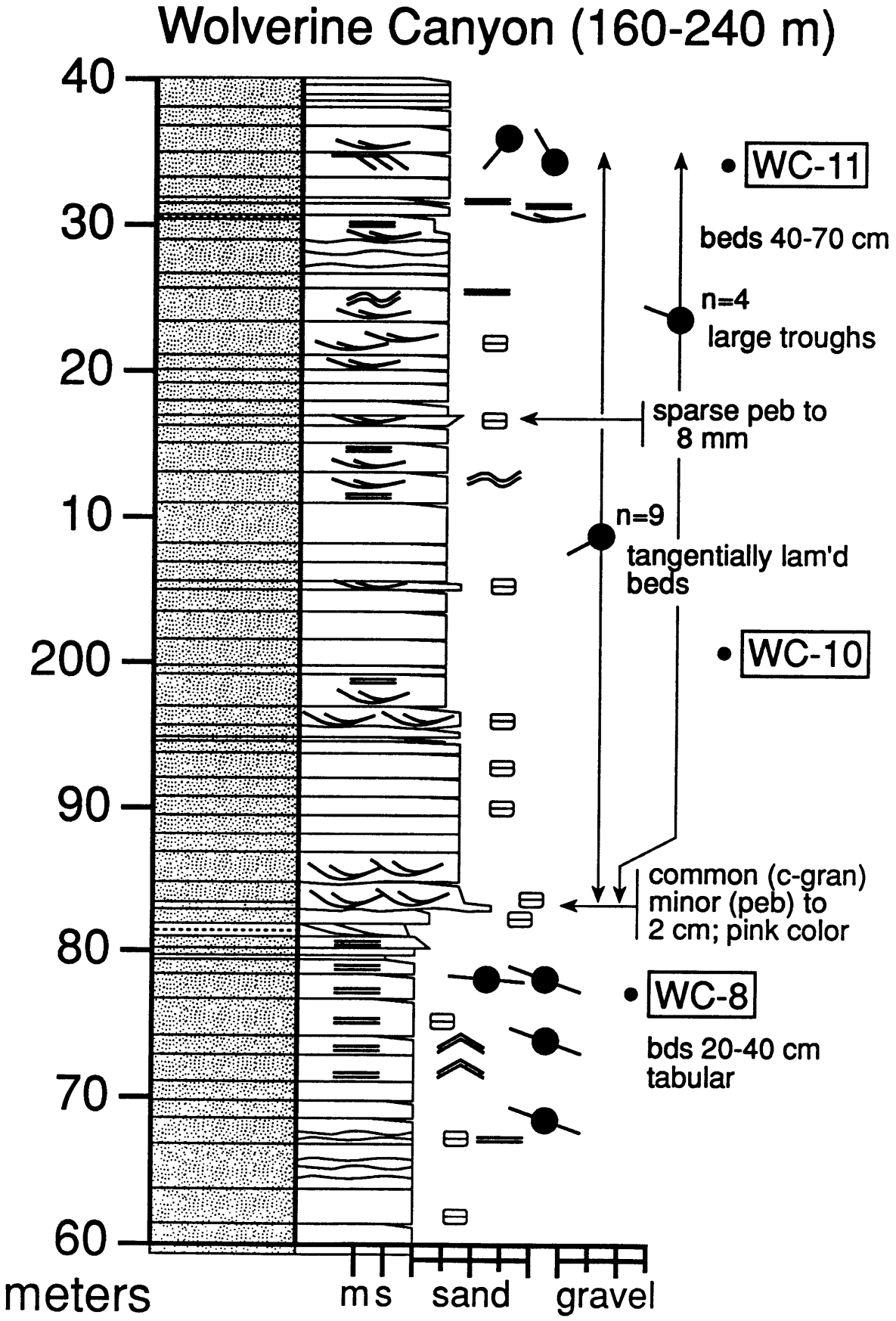
Wolverine Canyon (160-240 m)
40
30
20
10
200
90
80
70
60
meters
m s
sand
gravel
WC-11
beds 40-70 cm
n=4
large troughs
sparse peb to
8 mm
n=9
tangentially lam'd
beds
WC-10
common (c-gran)
minor (peb) to
2 cm; pink color
WC-8
bds 20-40 cm
tabular

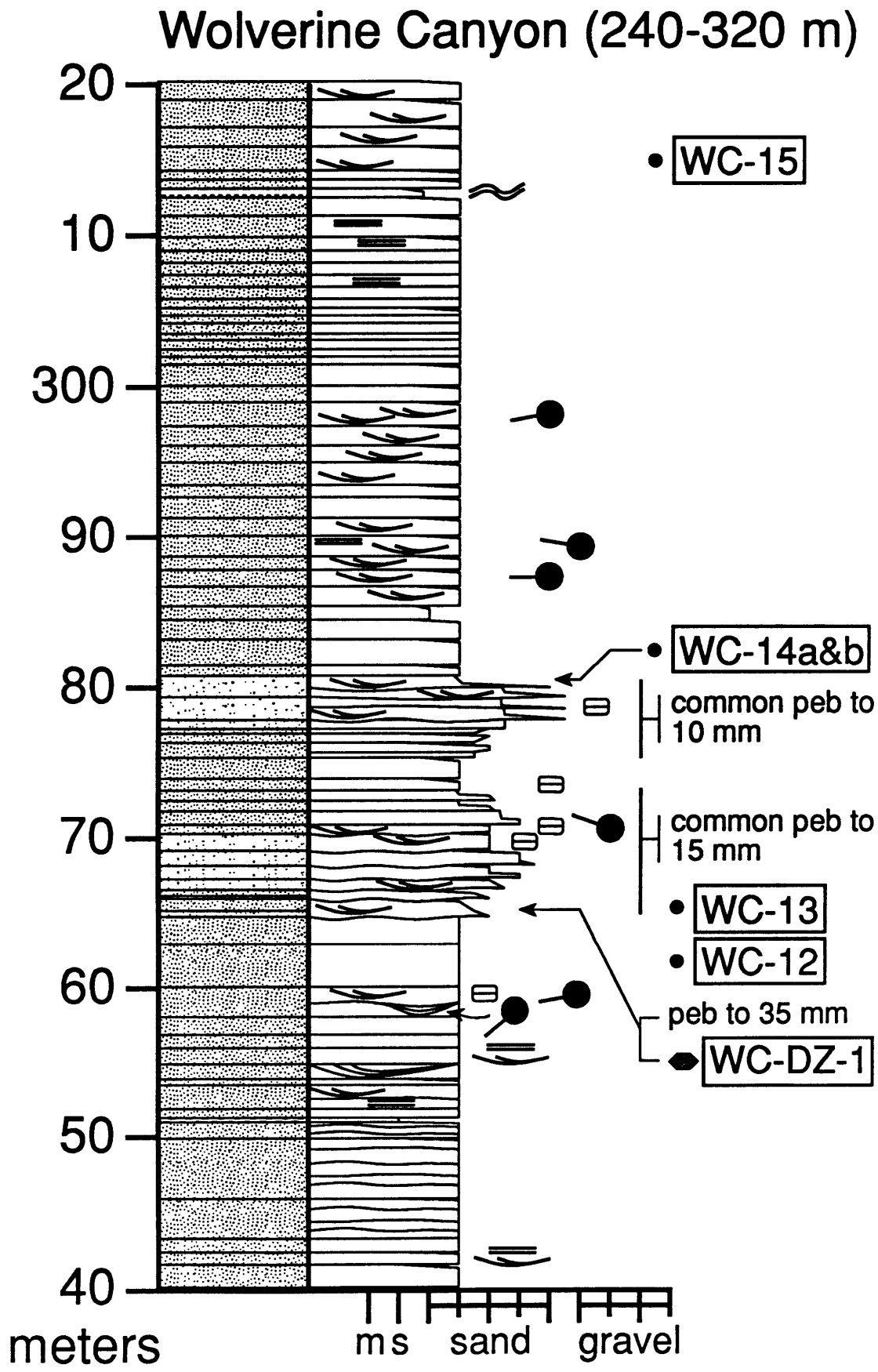
Wolverine Canyon (240-320 m)
20
10
300
90
80
70
60
50
40
meters
WC-15
WC-14a&b
common peb to 10 mm
common peb to 15 mm
WC-13
WC-12
peb to 35 mm
WC-DZ-1
ms
sand
gravel

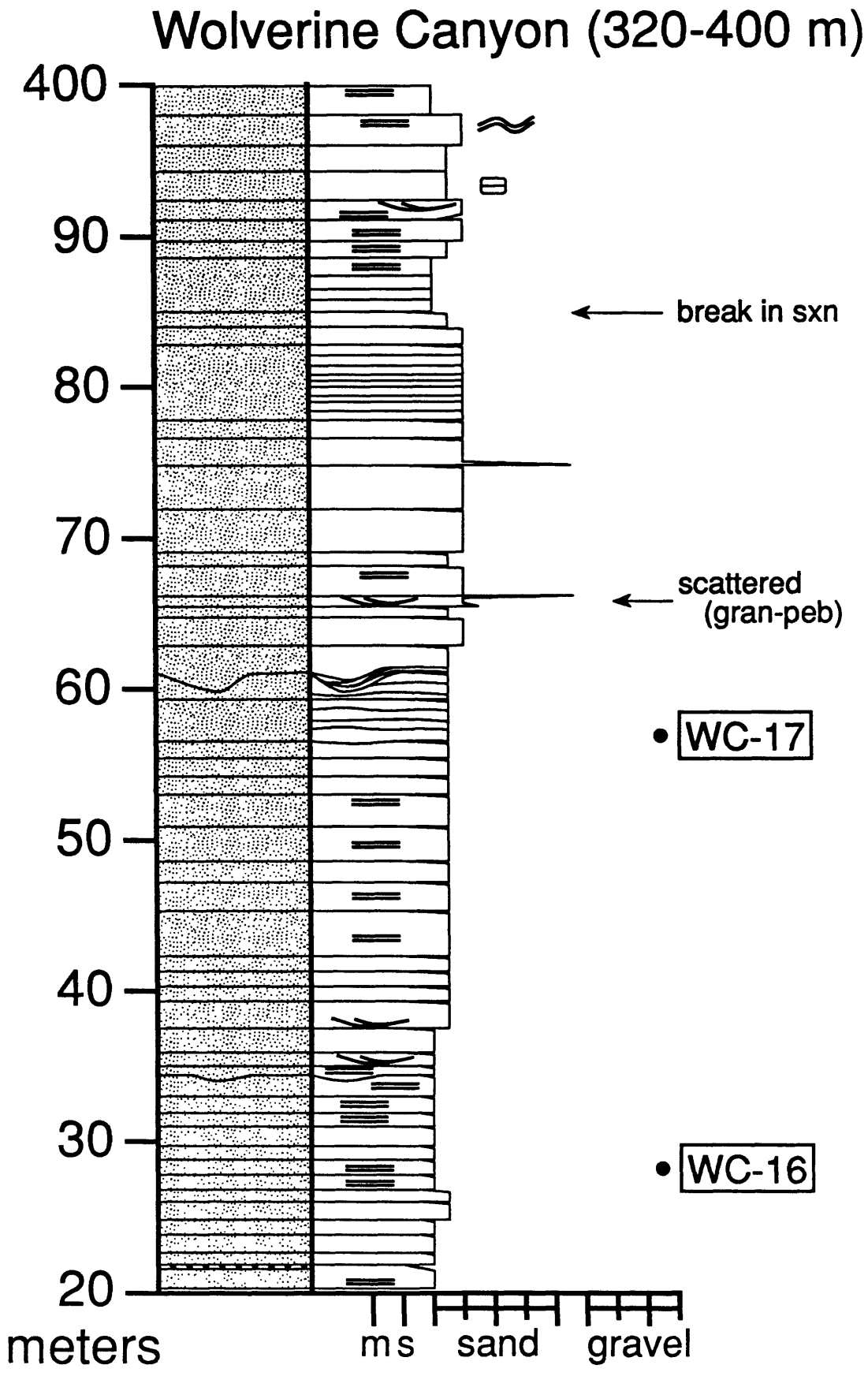
Wolverine Canyon (320-400 m)
400
90
80
70
60
50
40
30
20
meters
break in sxn
scattered
(gran-peb)
WC-17
WC-16
m s
sand
gravel

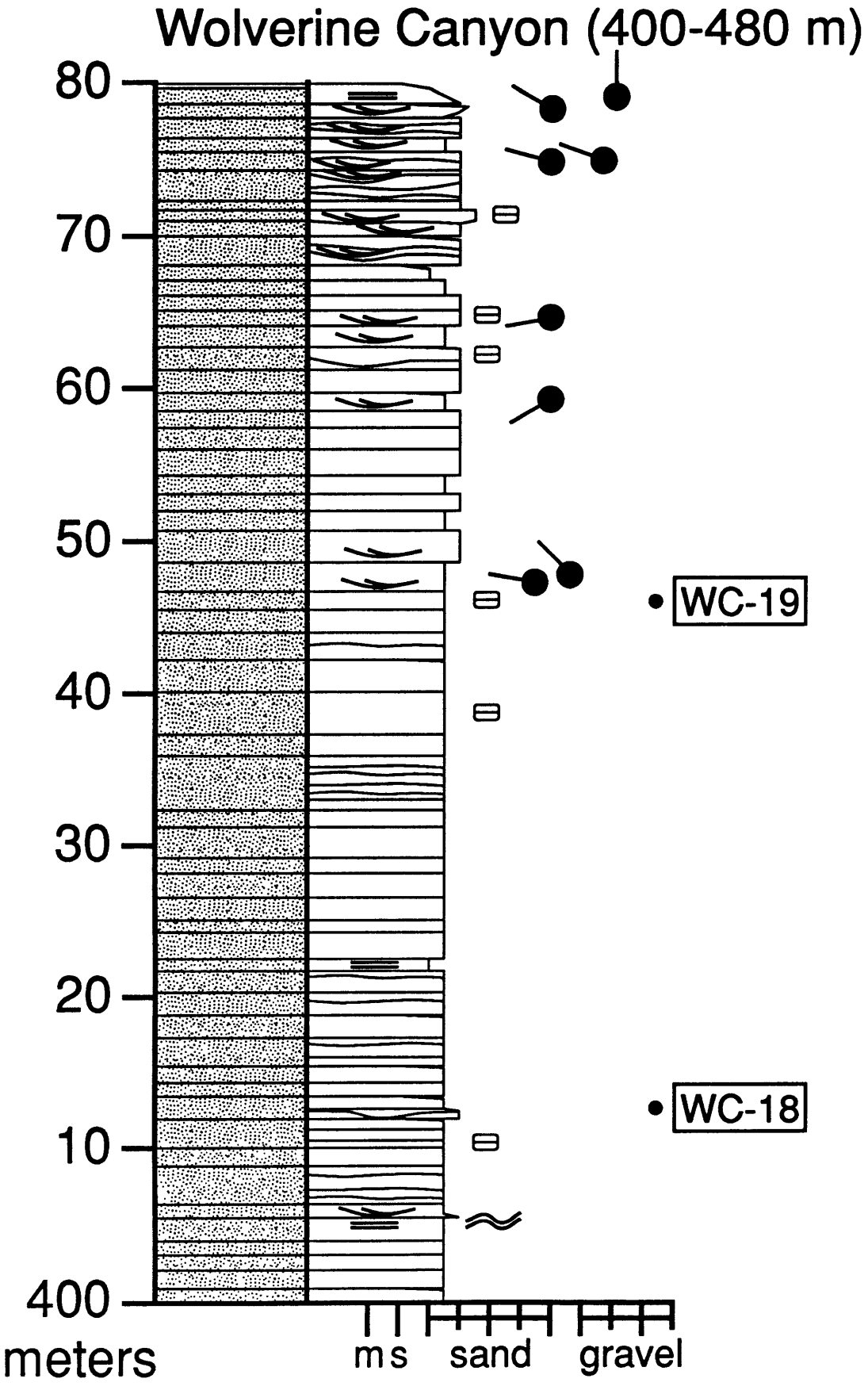
Wolverine Canyon (400-480 m)
80
70
60
50
40
30
20
10
400
meters
WC-19
WC-18
ms
sand
gravel

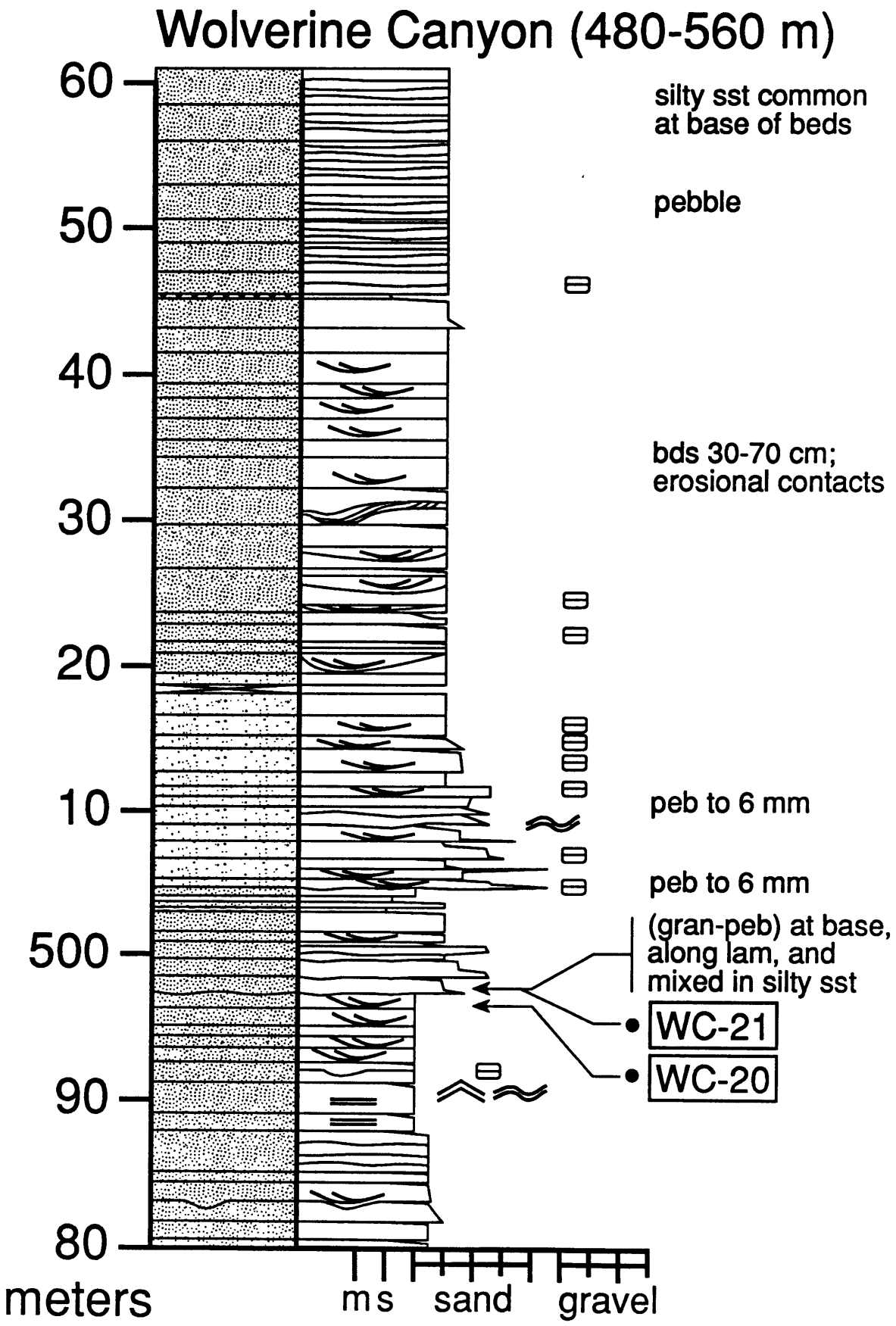
Wolverine Canyon (480-560 m)
60
50
40
30
20
10
500
90
80
meters
m s
sand
gravel
silty sst common at base of beds
pebble
bds 30-70 cm; erosional contacts
peb to 6 mm
peb to 6 mm
(gran-peb) at base, along lam, and mixed in silty sst
WC-21
WC-20

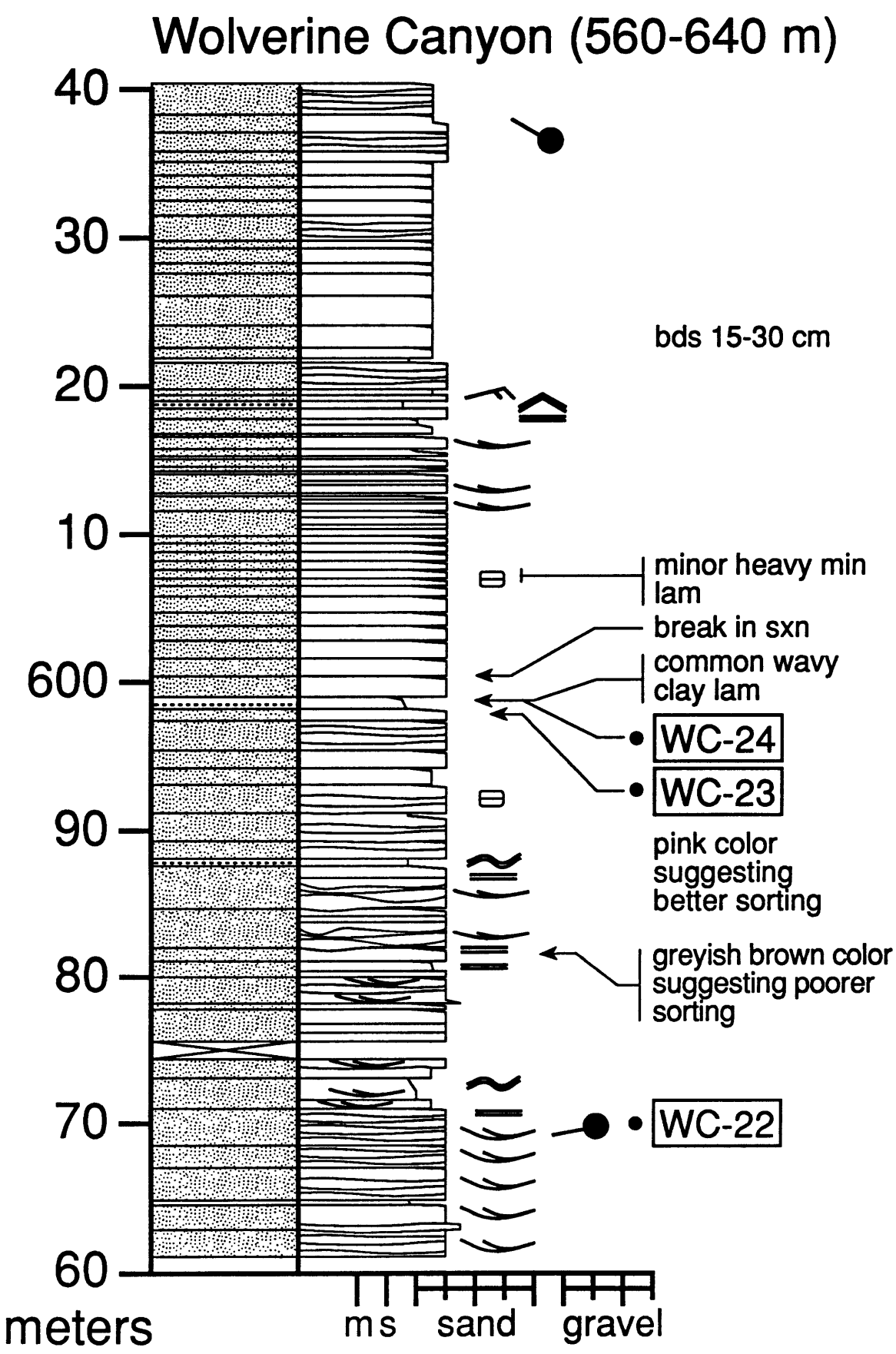
Wolverine Canyon (560-640 m)
40
30
20
10
600
90
80
70
60
meters
ms
sand
gravel
bds 15-30 cm
minor heavy min lam
break in sxn
common wavy clay lam
WC-24
WC-23
pink color suggesting better sorting
greyish brown color suggesting poorer sorting
WC-22

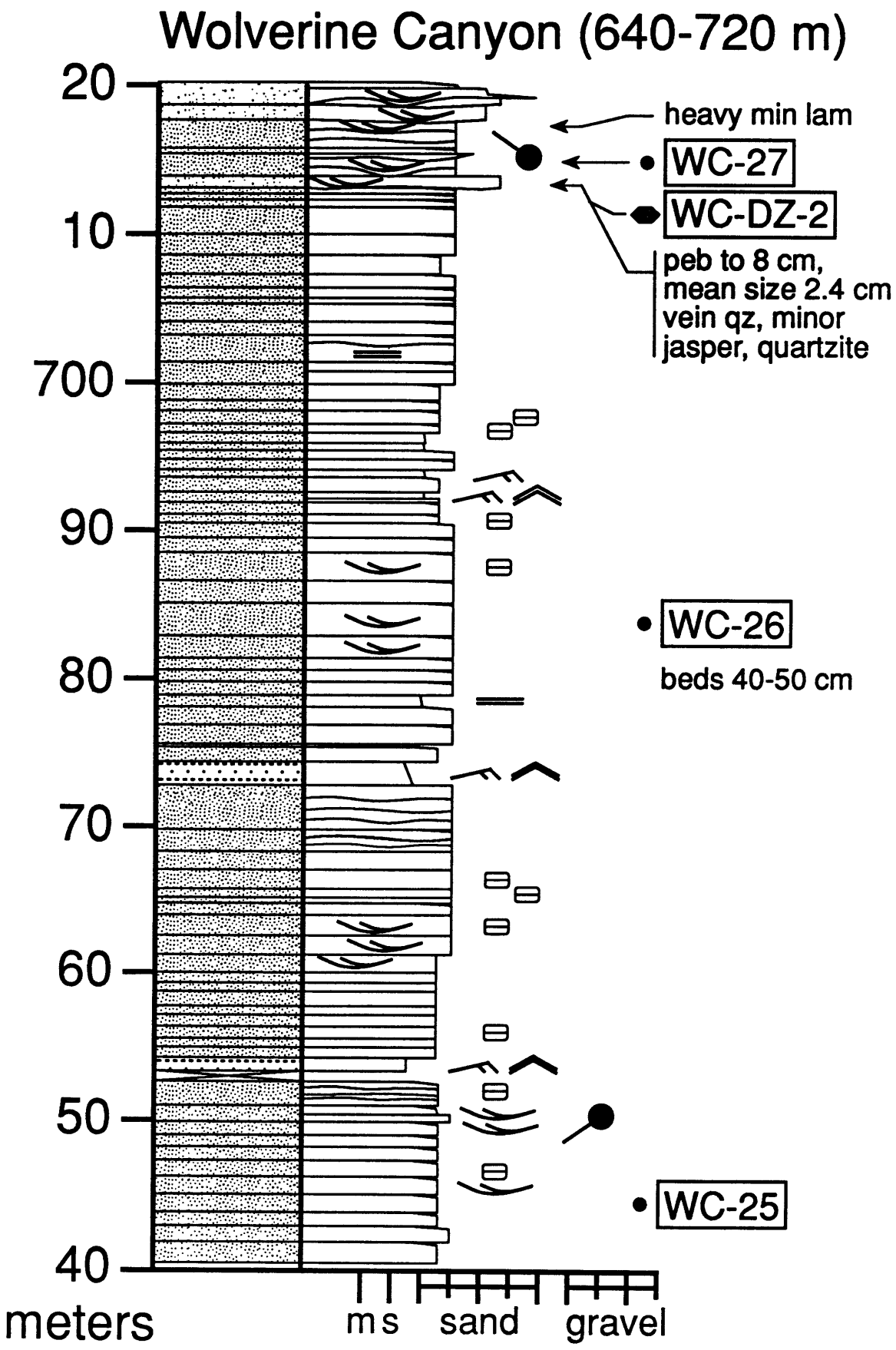
Wolverine Canyon (640-720 m)
20
10
700
90
80
70
60
50
40
meters
m s
sand
gravel
heavy min lam
WC-27
WC-DZ-2
peb to 8 cm,
mean size 2.4 cm
vein qz, minor
jasper, quartzite
WC-26
beds 40-50 cm
WC-25

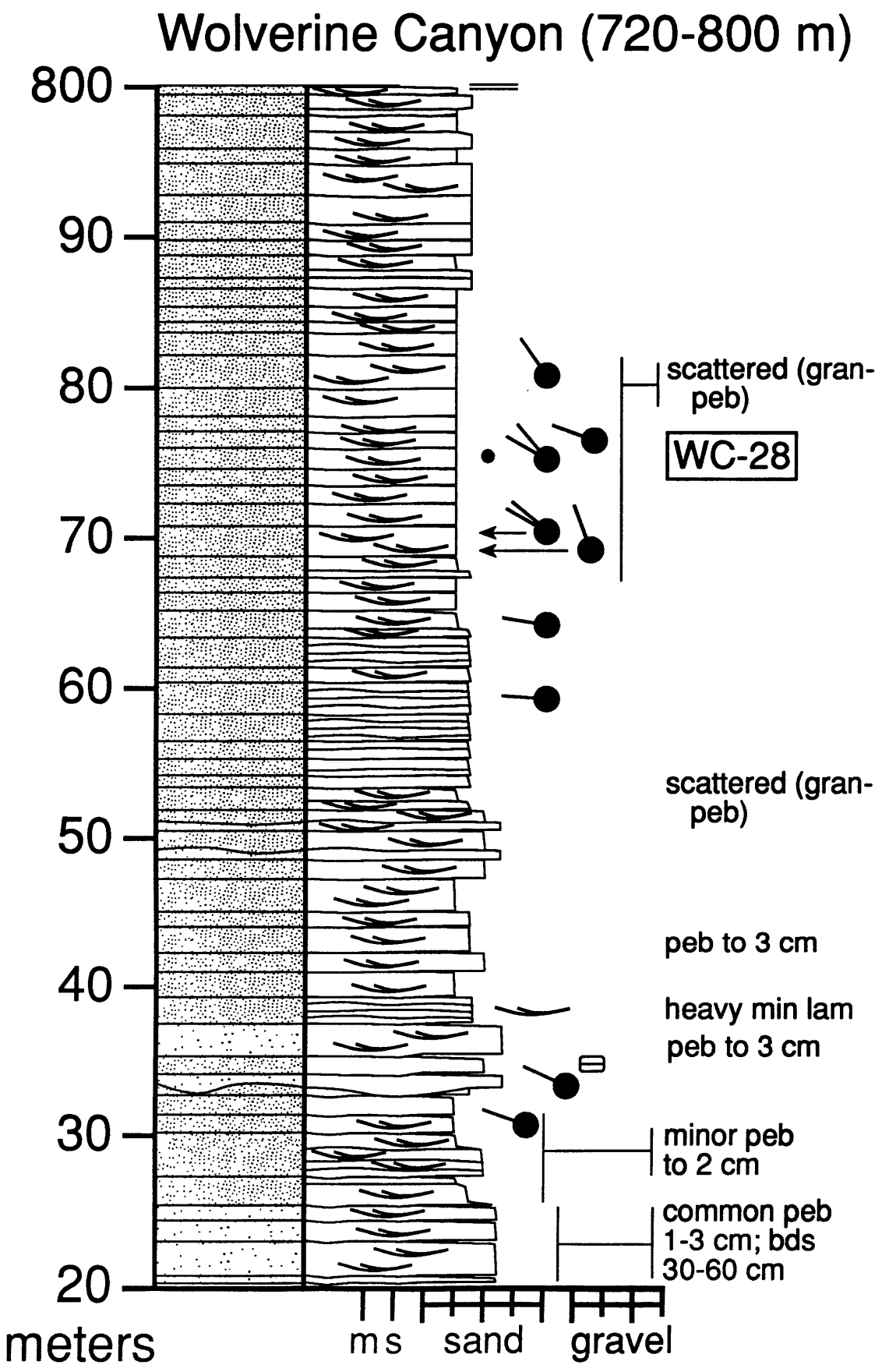
Wolverine Canyon (720-800 m)
800
90
80
70
60
50
40
30
20
meters
m s
sand
gravel
scattered (gran-peb)
WC-28
scattered (gran-peb)
peb to 3 cm
heavy min lam
peb to 3 cm
minor peb to 2 cm
common peb 1-3 cm; bds 30-60 cm

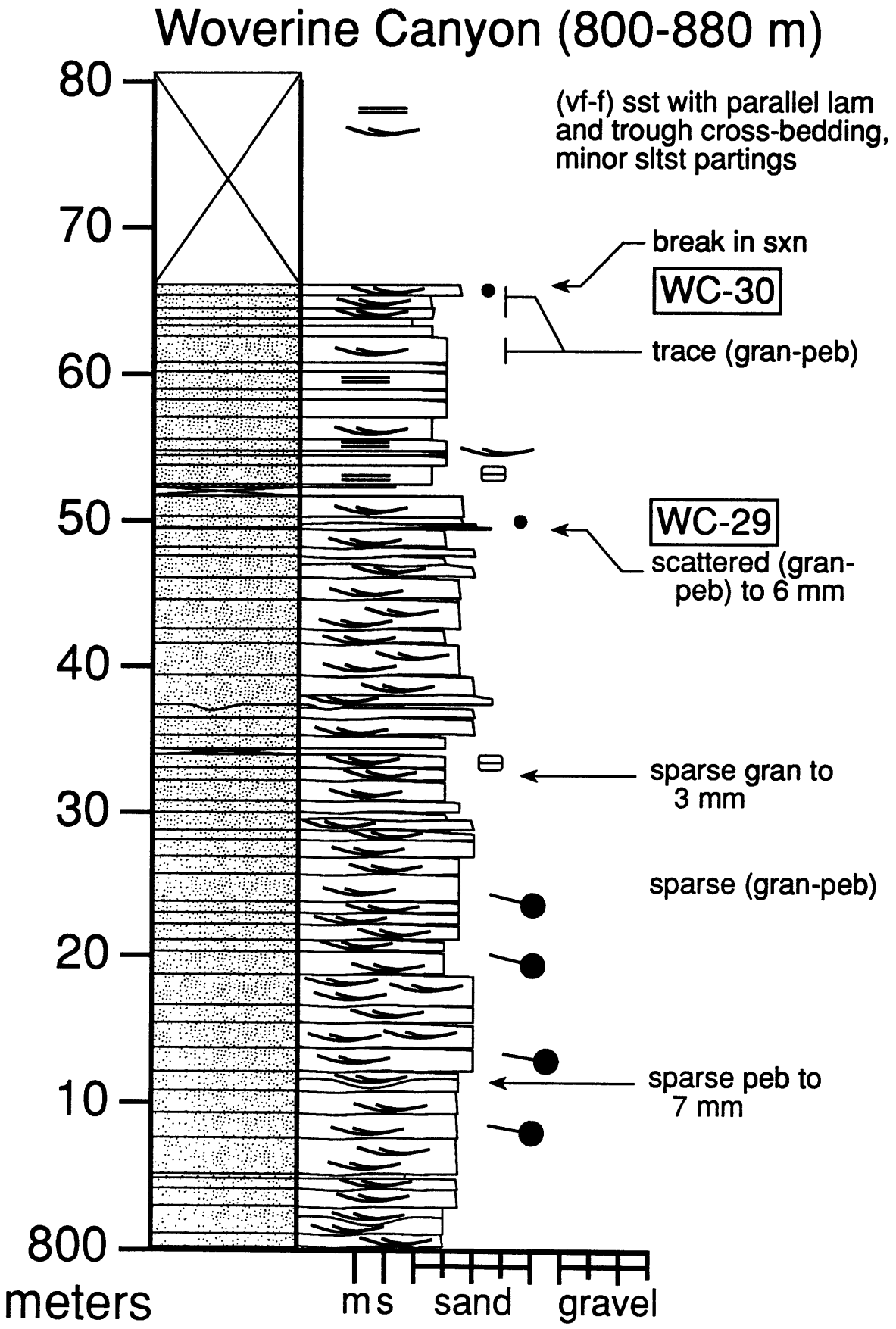
Woverine Canyon (800-880 m)
80
70
60
50
40
30
20
10
800
meters
(vf-f) sst with parallel lam and trough cross-bedding, minor sltst partings
break in sxn
WC-30
trace (gran-peb)
WC-29
scattered (gran-peb) to 6 mm
sparse gran to 3 mm
sparse (gran-peb)
sparse peb to 7 mm
ms
sand
gravel

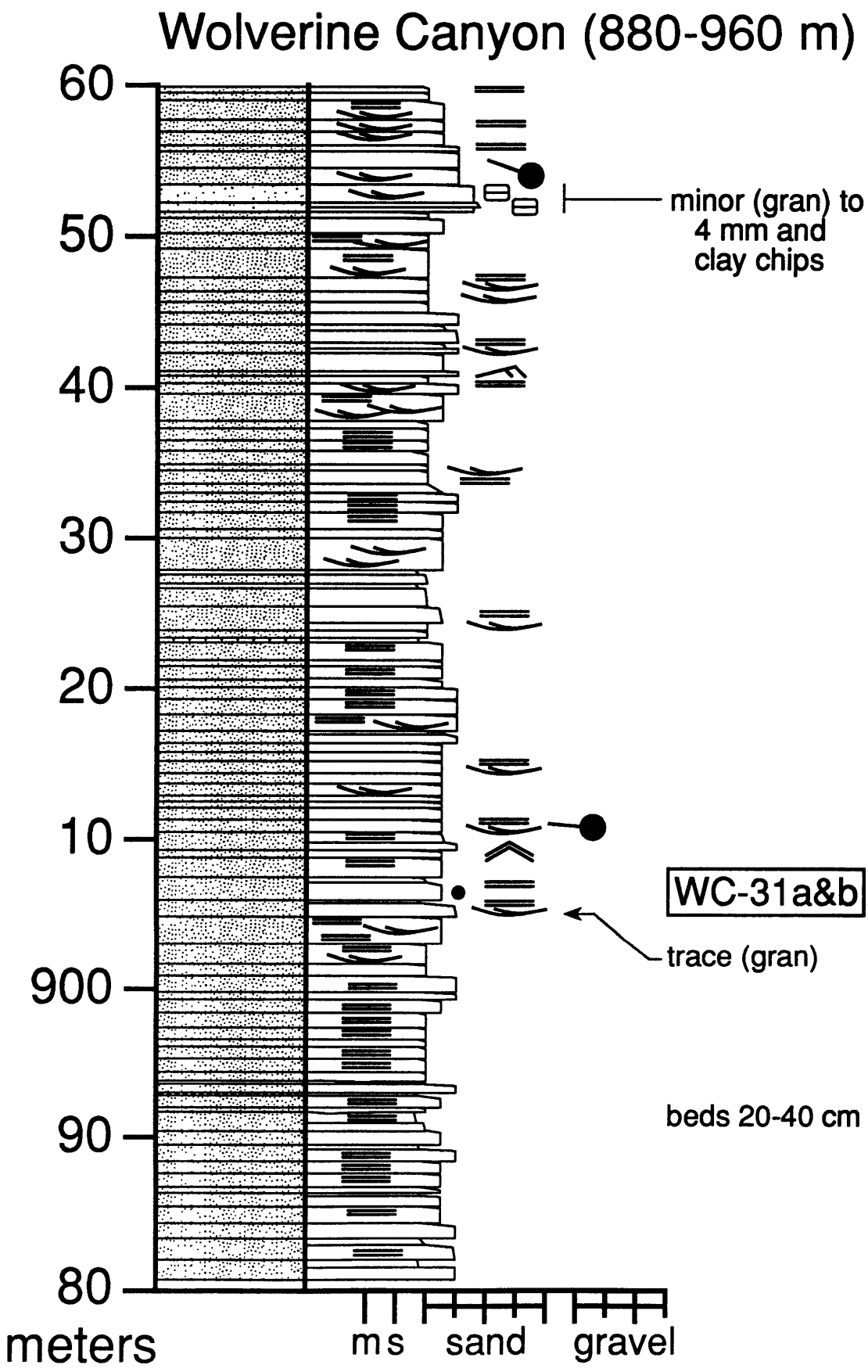
Wolverine Canyon (880-960 m)
60
50
40
30
20
10
900
90
80
meters
minor (gran) to 4 mm and clay chips
WC-31a&b
trace (gran)
beds 20-40 cm
ms
sand
gravel

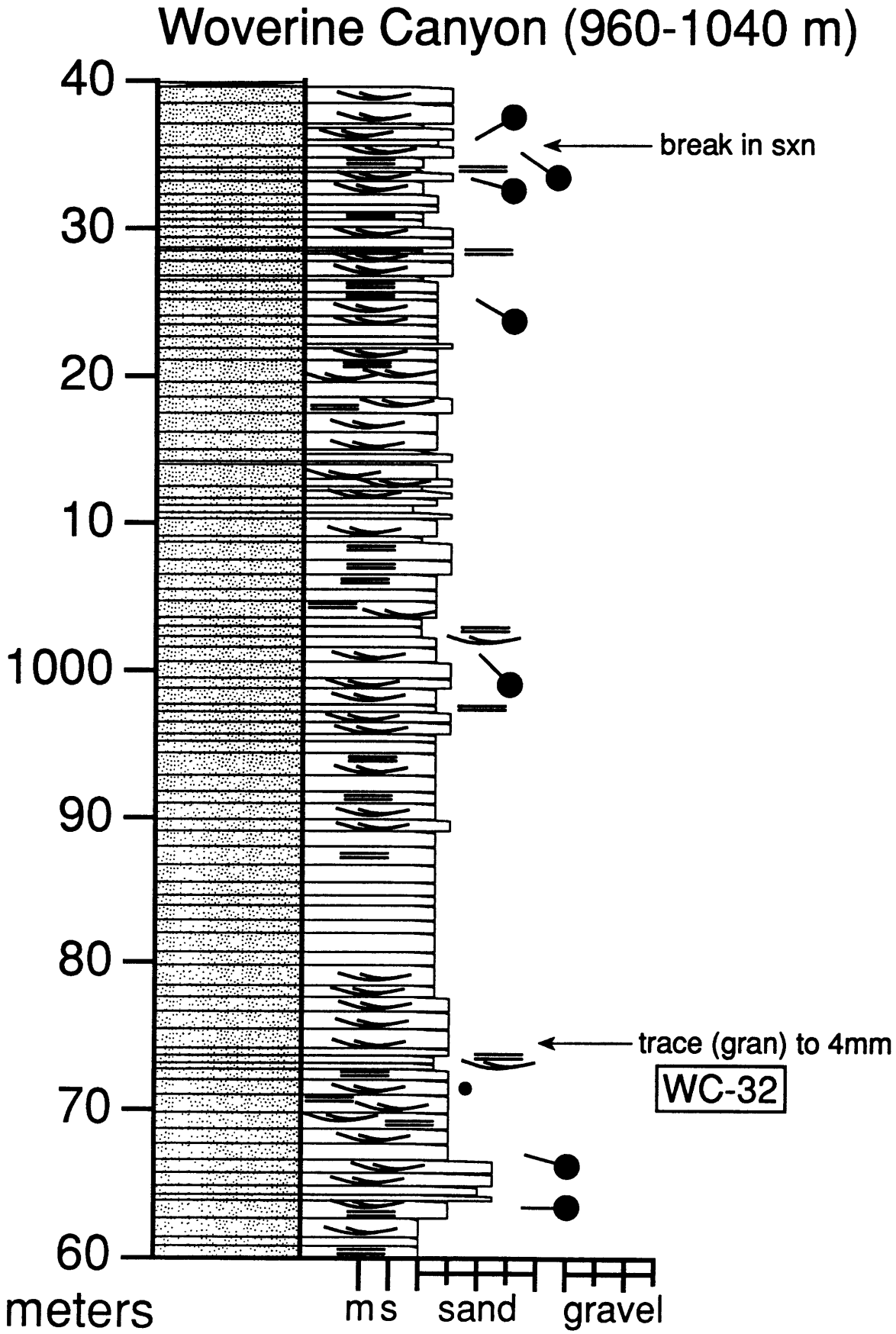
Woverine Canyon (960-1040 m)
40
30
20
10
1000
90
80
70
60
meters
break in sxn
trace (gran) to 4mm
WC-32
ms
sand
gravel

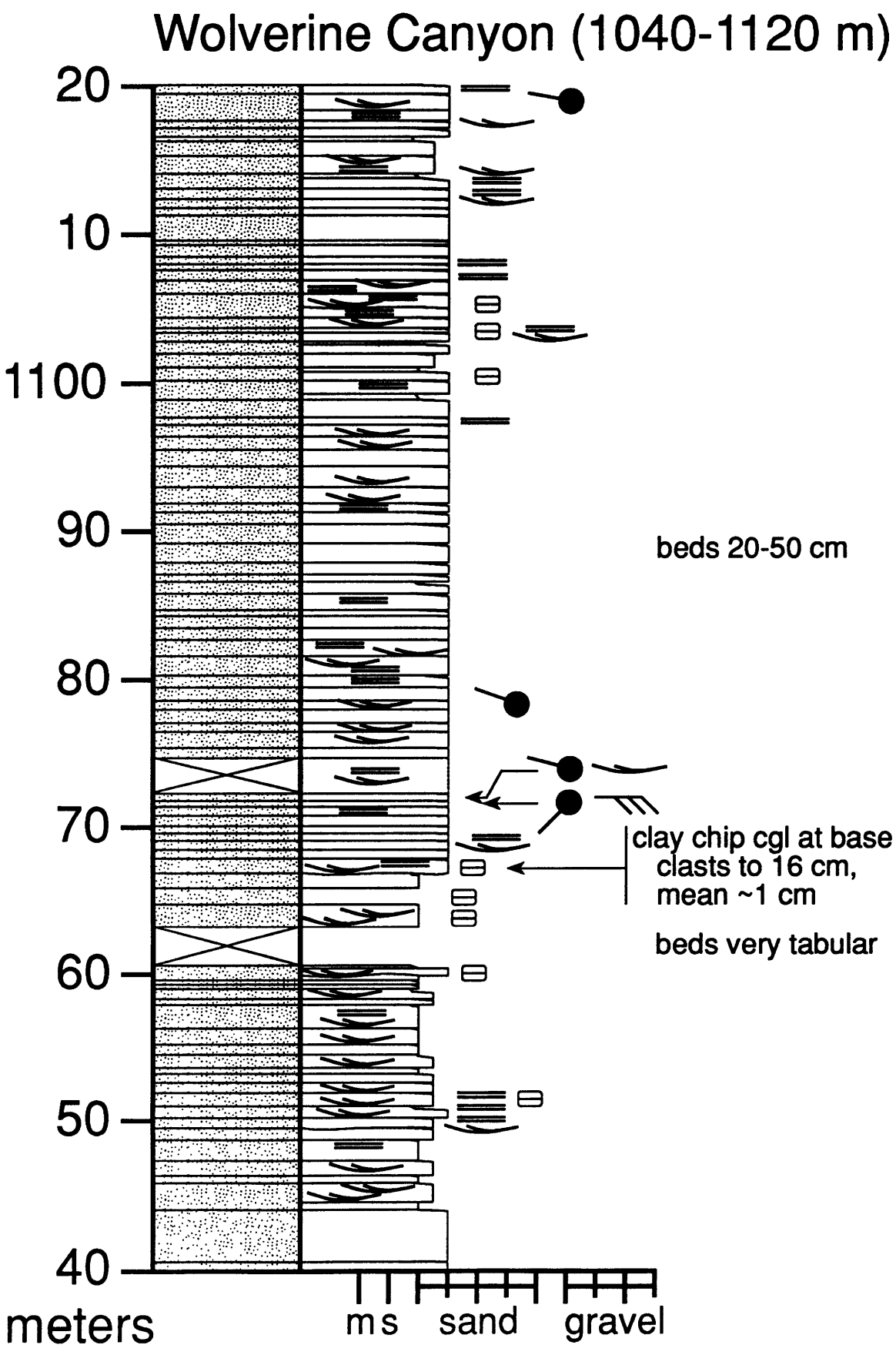
Wolverine Canyon (1040-1120 m)
20
10
1100
90
80
70
60
50
40
meters
ms
sand
gravel
beds 20-50 cm
clay chip cgl at base
clasts to 16 cm,
mean ~1 cm
beds very tabular

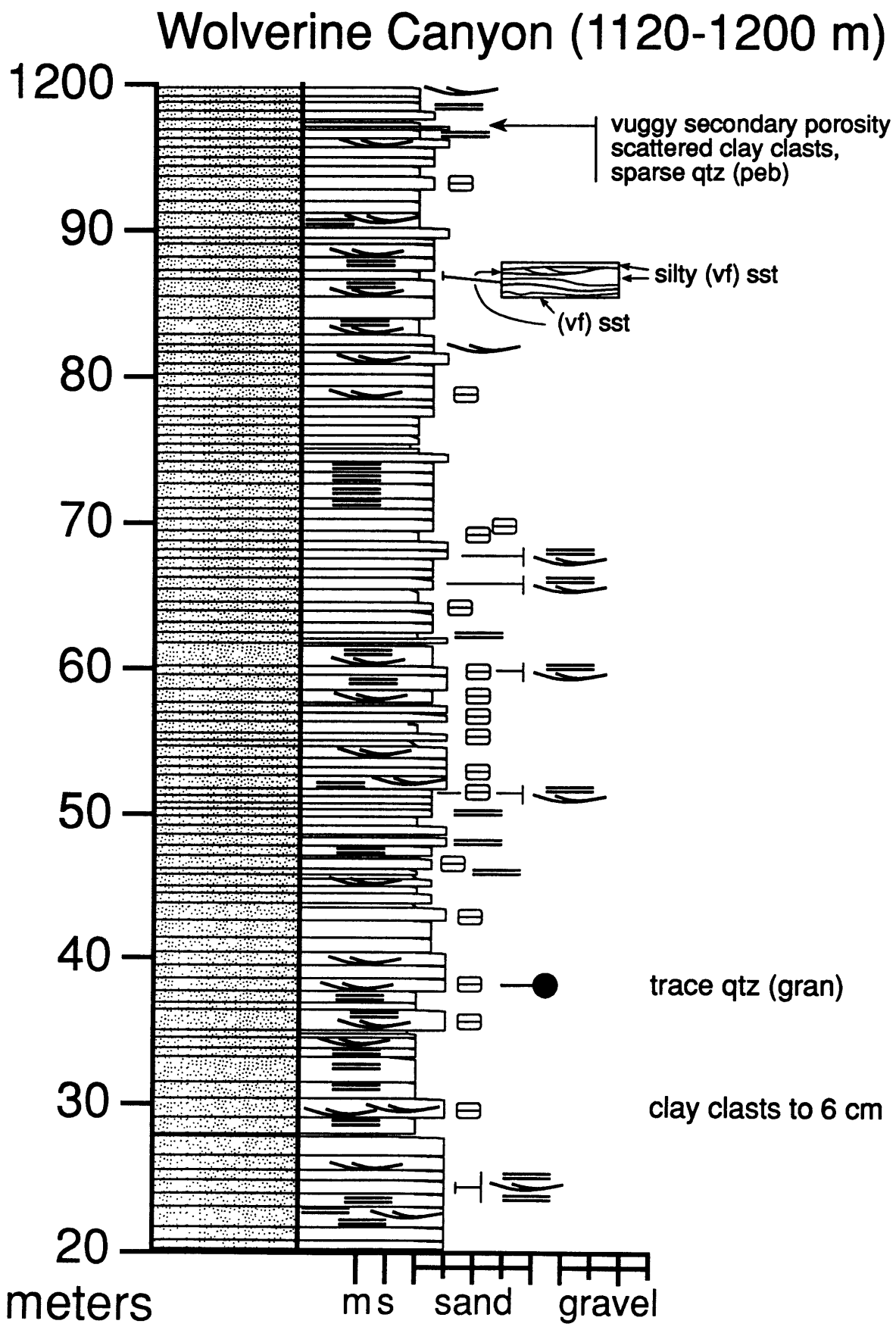
Wolverine Canyon (1120-1200 m)
1200
90
80
70
60
50
40
30
20
meters
m s
sand
gravel
vuggy secondary porosity
scattered clay clasts,
sparse qtz (peb)
silty (vf) sst
(vf) sst
trace qtz (gran)
clay clasts to 6 cm

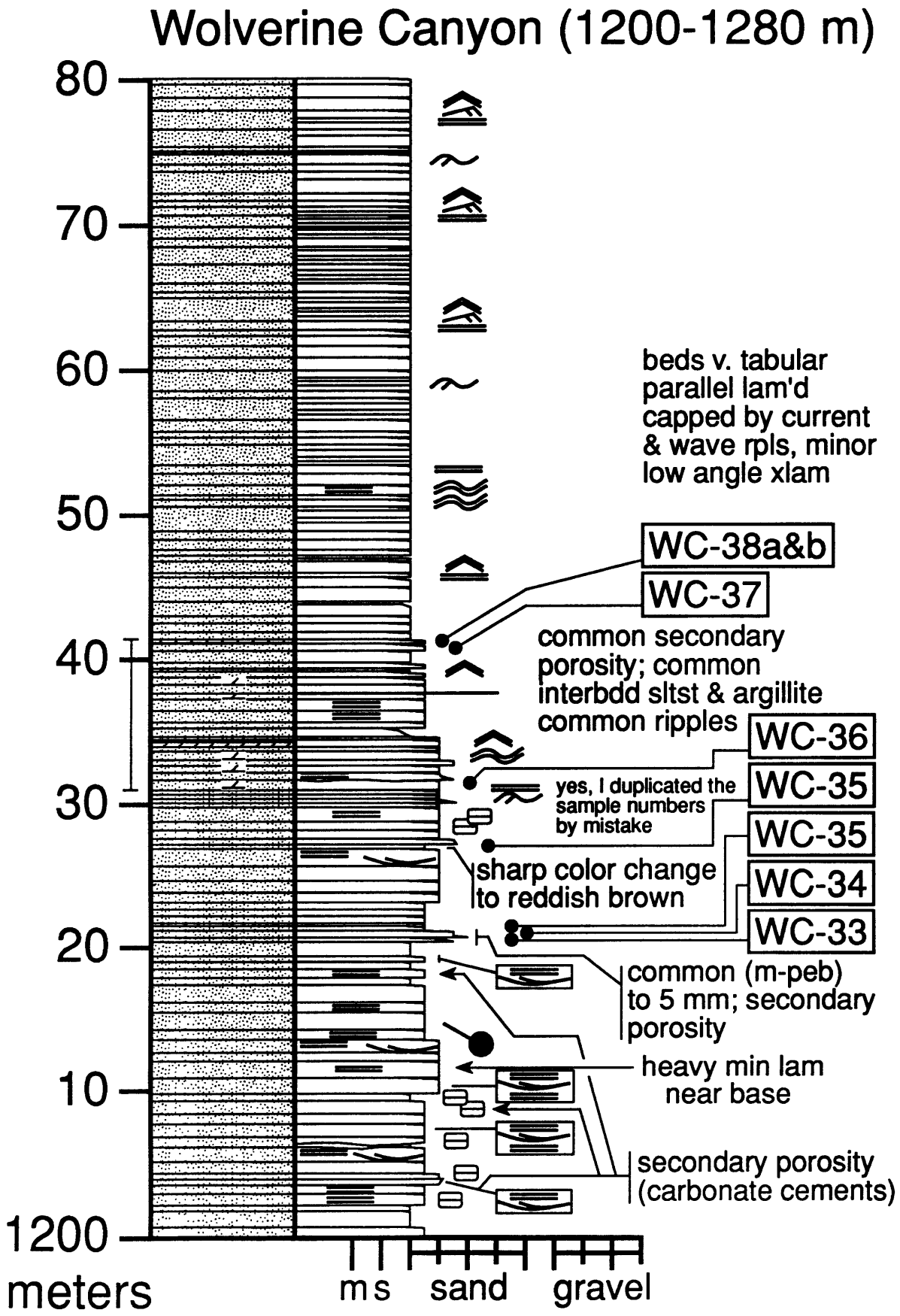
Wolverine Canyon (1200-1280 m)
80
70
60
50
40
30
20
10
1200
meters
ms
sand
gravel
beds v. tabular parallel lam'd capped by current & wave rpls, minor low angle xlam
WC-38a&b
WC-37
common secondary porosity; common interbdd sltst & argillite common ripples
WC-36
WC-35
yes, I duplicated the sample numbers by mistake
WC-35
sharp color change to reddish brown
WC-34
WC-33
common (m-peb) to 5 mm; secondary porosity
heavy min lam near base
secondary porosity (carbonate cements)

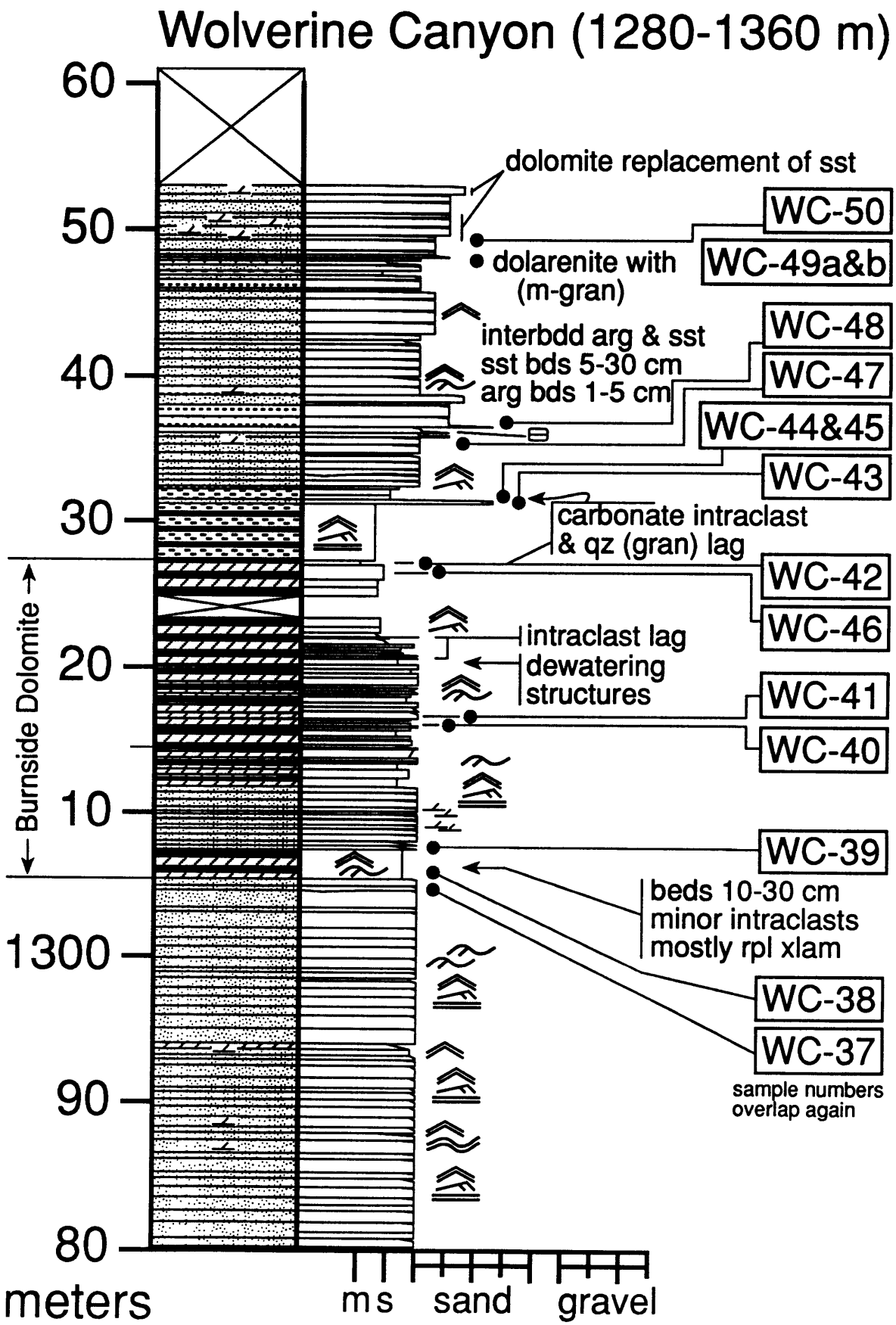
Wolverine Canyon (1280-1360 m)
60
50
40
30
20
10
1300
90
80
meters
Burnside Dolomite
dolomite replacement of sst
WC-50
dolarenite with (m-gran)
WC-49a&b
interbdd arg & sst
sst bds 5-30 cm
arg bds 1-5 cm
WC-48
WC-47
WC-44&45
WC-43
carbonate intraclast & qz (gran) lag
WC-42
WC-46
intraclast lag
dewatering structures
WC-41
WC-40
WC-39
beds 10-30 cm
minor intraclasts
mostly rpl xlam
WC-38
WC-37
sample numbers overlap again
ms
sand
gravel

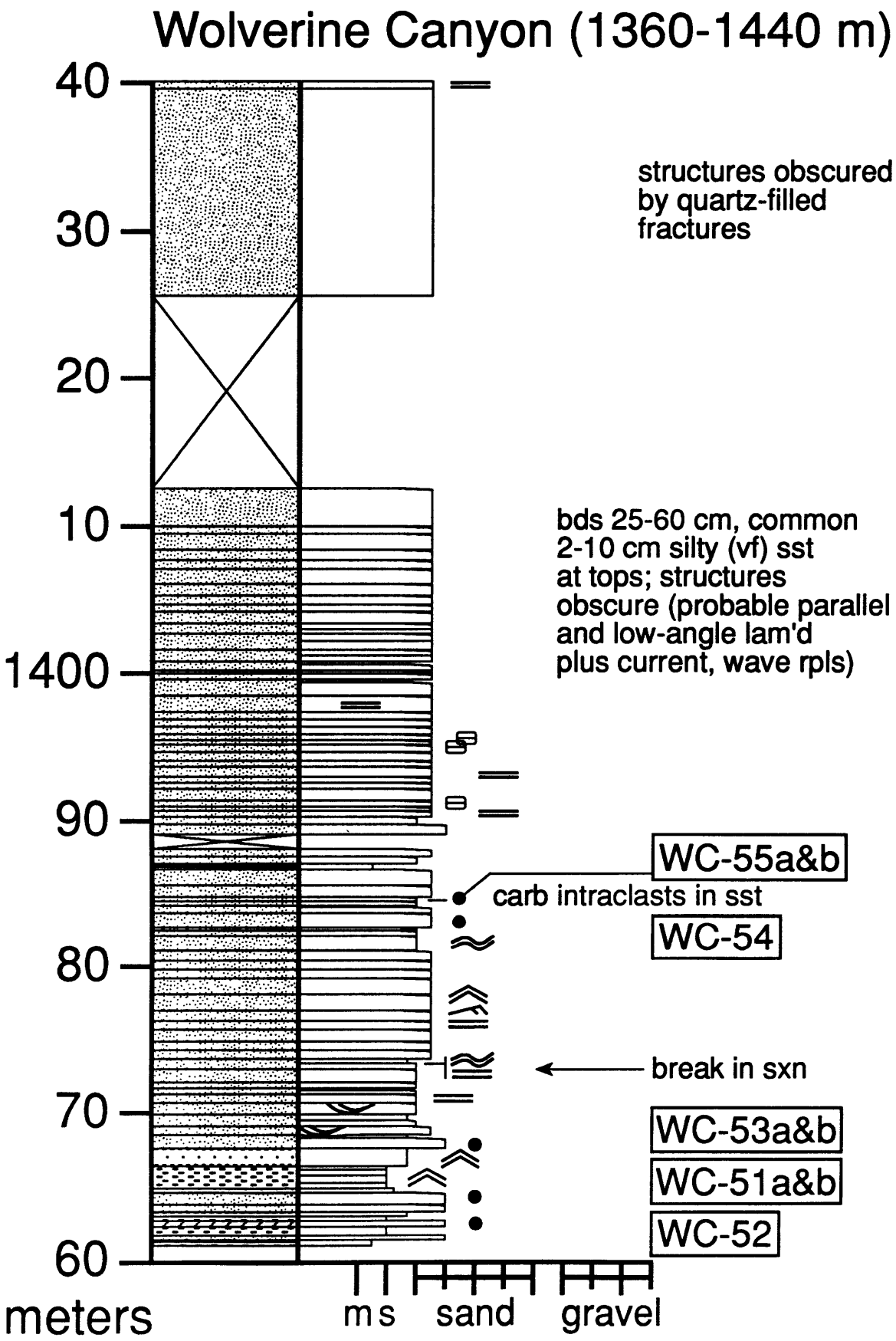
Wolverine Canyon (1360-1440 m)
40
30
20
10
1400
90
80
70
60
meters
structures obscured by quartz-filled fractures
bds 25-60 cm, common 2-10 cm silty (vf) sst at tops; structures obscure (probable parallel and low-angle lam'd plus current, wave rpls)
WC-55a&b
carb intraclasts in sst
WC-54
break in sxn
WC-53a&b
WC-51a&b
WC-52
ms
sand
gravel

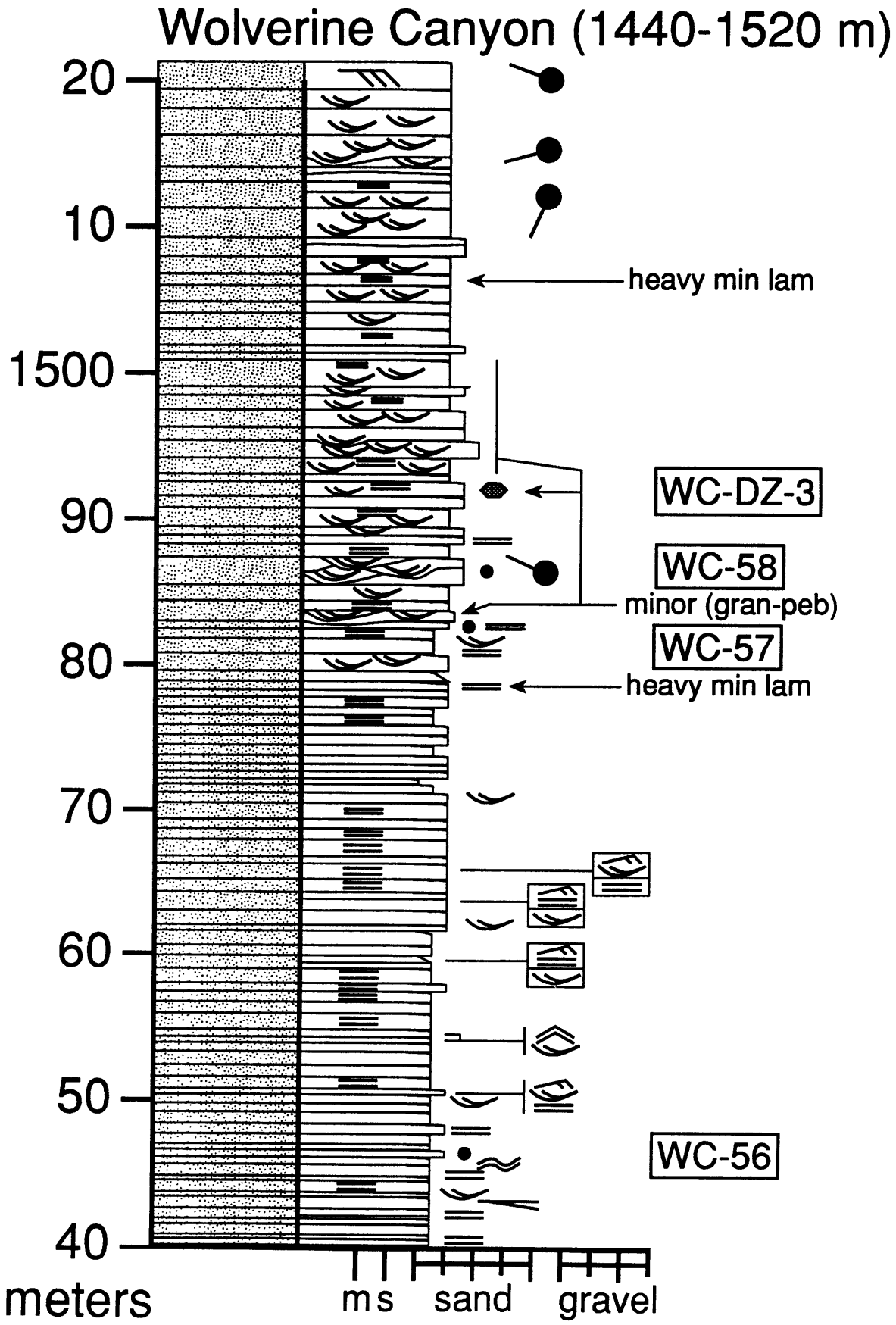
Wolverine Canyon (1440-1520 m)
20
10
1500
90
80
70
60
50
40
meters
heavy min lam
WC-DZ-3
WC-58
minor (gran-peb)
WC-57
heavy min lam
WC-56
ms
sand
gravel

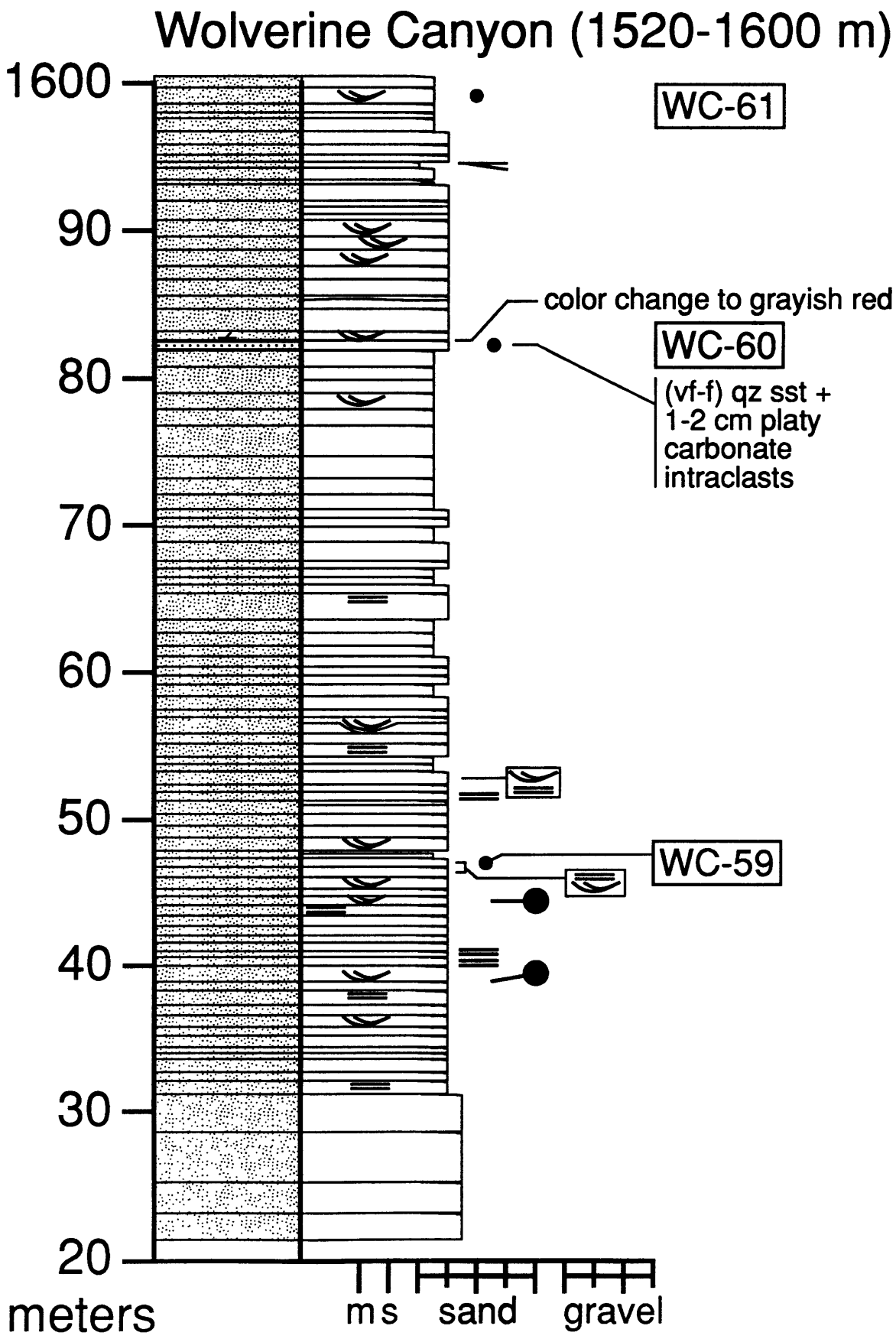
Wolverine Canyon (1520-1600 m)
1600
90
80
70
60
50
40
30
20
meters
WC-61
color change to grayish red
WC-60
(vf-f) qz sst +
1-2 cm platy
carbonate
intraclasts
WC-59
ms
sand
gravel

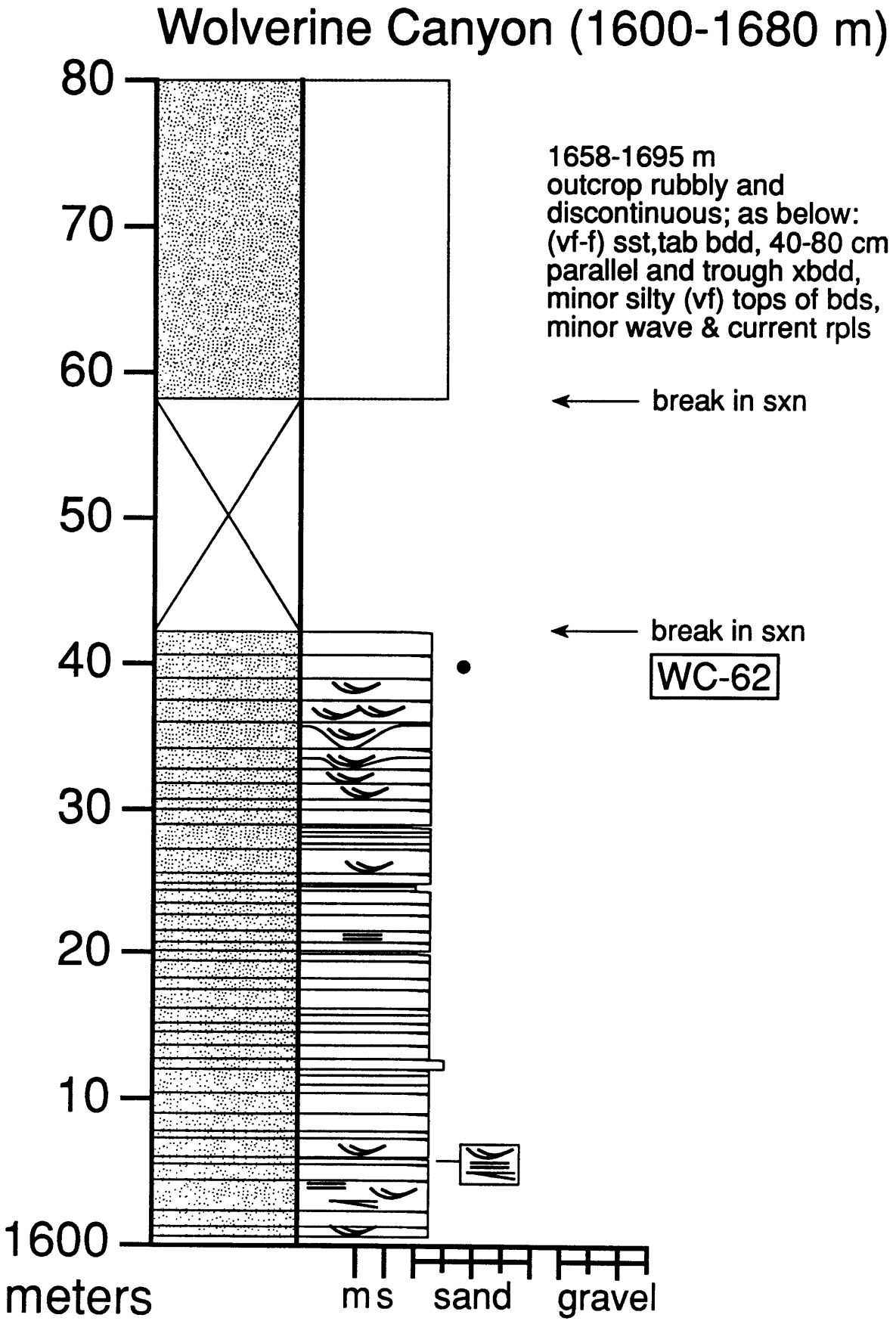
Wolverine Canyon (1600-1680 m)
80
70
60
50
40
30
20
10
1600
meters
1658-1695 m
outcrop rubbly and
discontinuous; as below:
(vf-f) sst,tab bdd, 40-80 cm
parallel and trough xbdd,
minor silty (vf) tops of bds,
minor wave & current rpls
break in sxn
break in sxn
WC-62
ms
sand
gravel

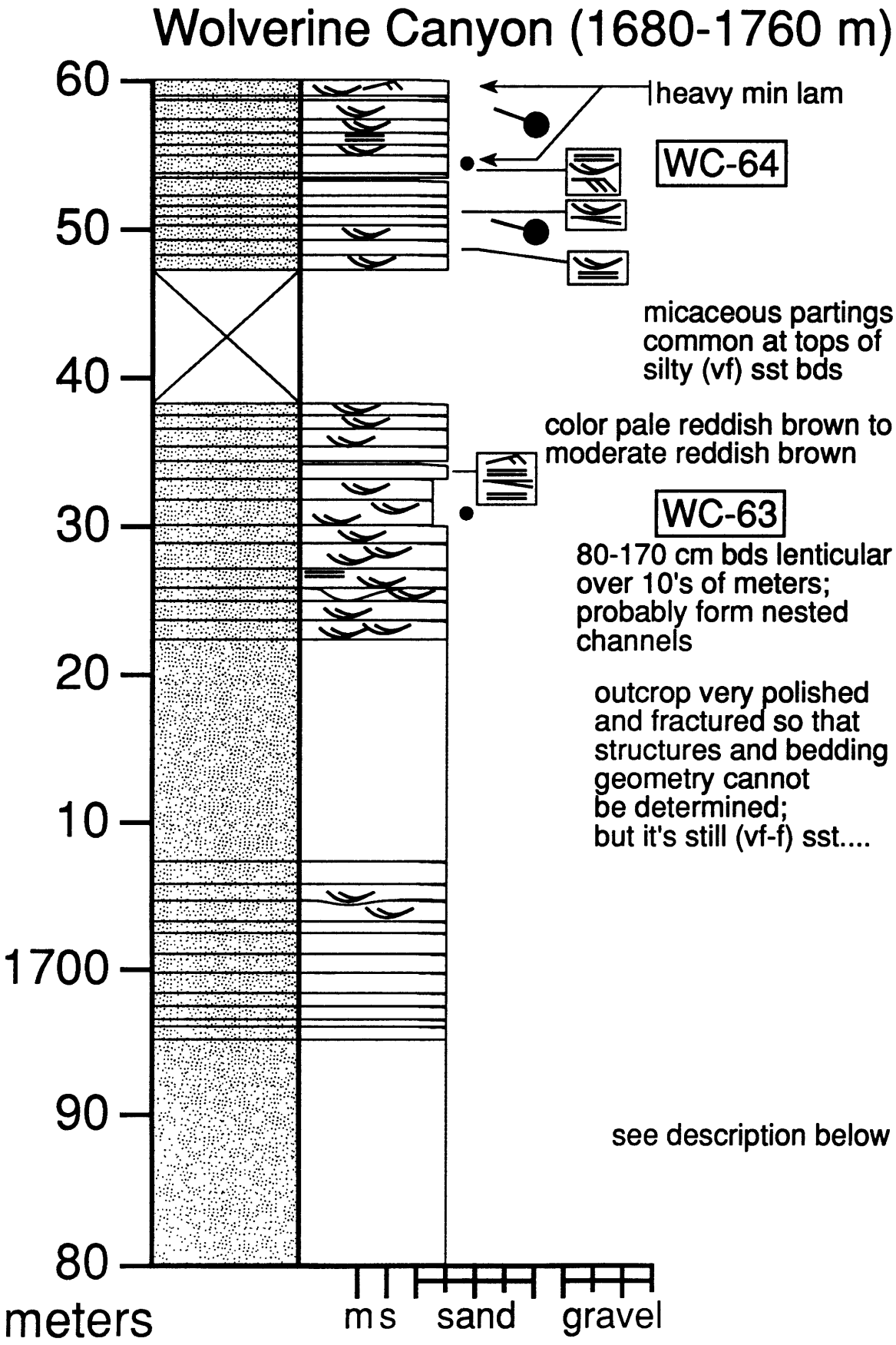
Wolverine Canyon (1680-1760 m)
60
50
40
30
20
10
1700
90
80
meters
heavy min lam
WC-64
micaceous partings common at tops of silty (vf) sst bds
color pale reddish brown to moderate reddish brown
WC-63
80-170 cm bds lenticular over 10's of meters; probably form nested channels
outcrop very polished and fractured so that structures and bedding geometry cannot be determined; but it's still (vf-f) sst....
see description below
ms
sand
gravel

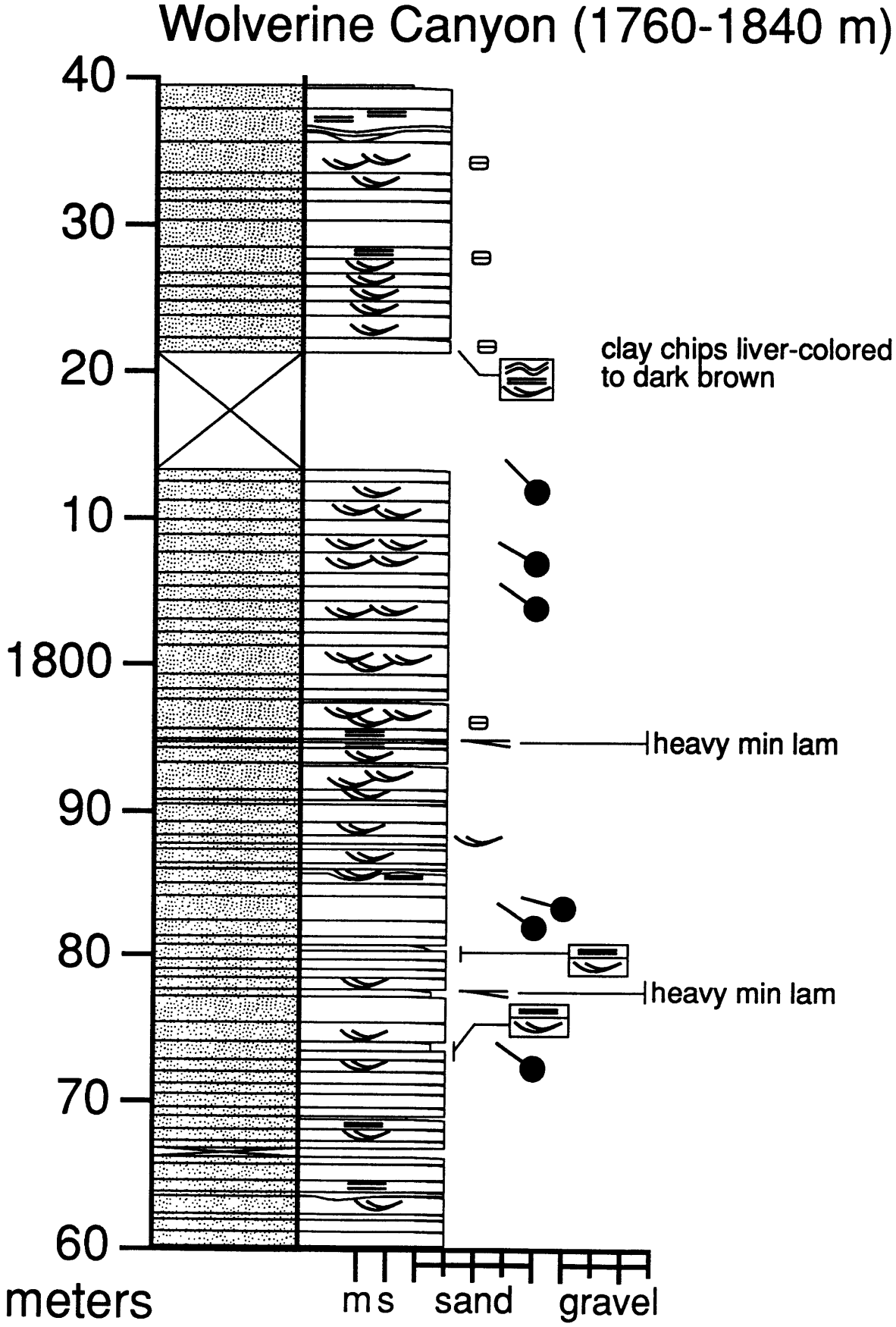
Wolverine Canyon (1760-1840 m)
40
30
20
10
1800
90
80
70
60
meters
clay chips liver-colored to dark brown
heavy min lam
heavy min lam
ms
sand
gravel

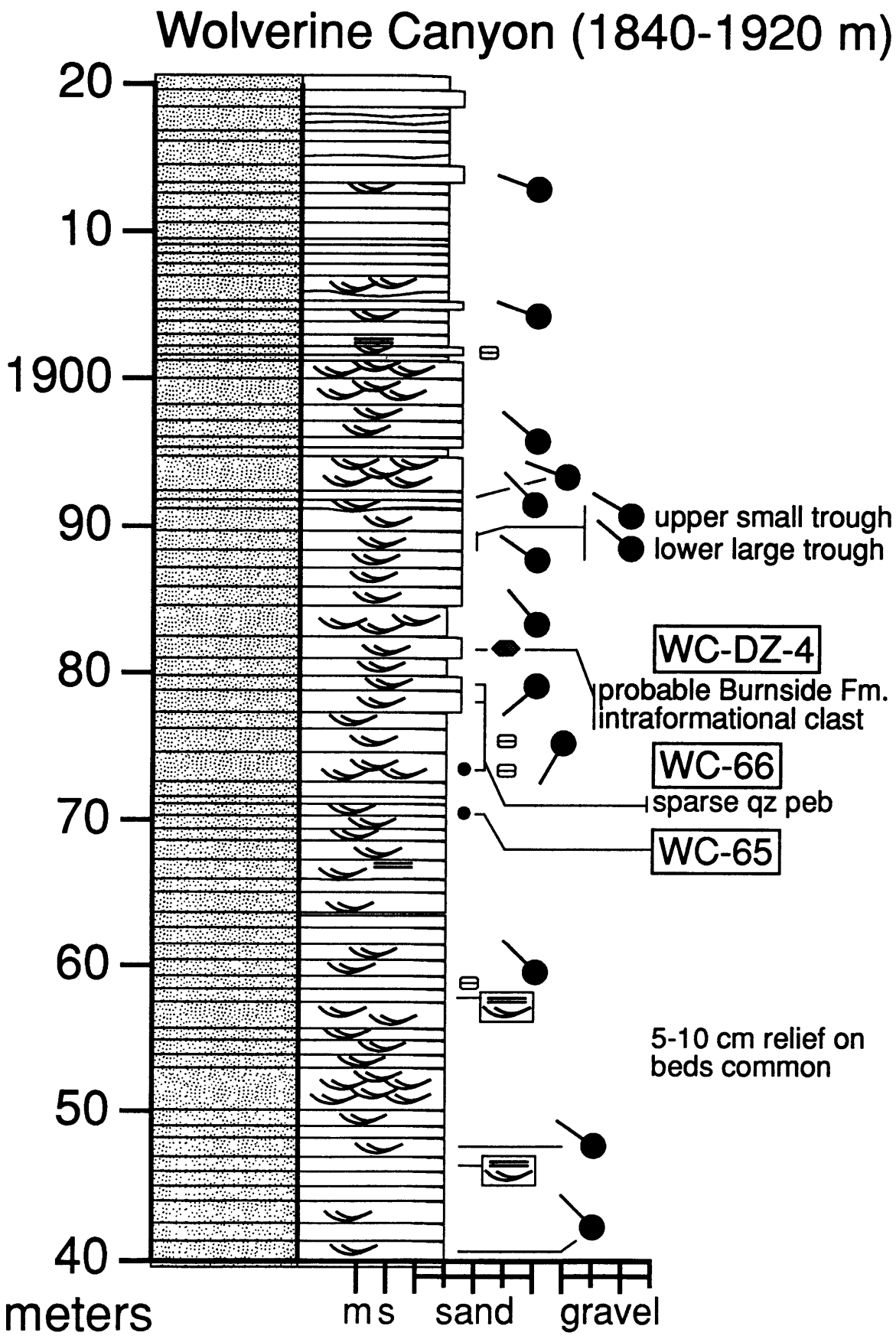
Wolverine Canyon (1840-1920 m)
20
10
1900
90
80
70
60
50
40
meters
m s
sand
gravel
upper small trough
lower large trough
WC-DZ-4
probable Burnside Fm.
intraformational clast
WC-66
sparse qz peb
WC-65
5-10 cm relief on
beds common

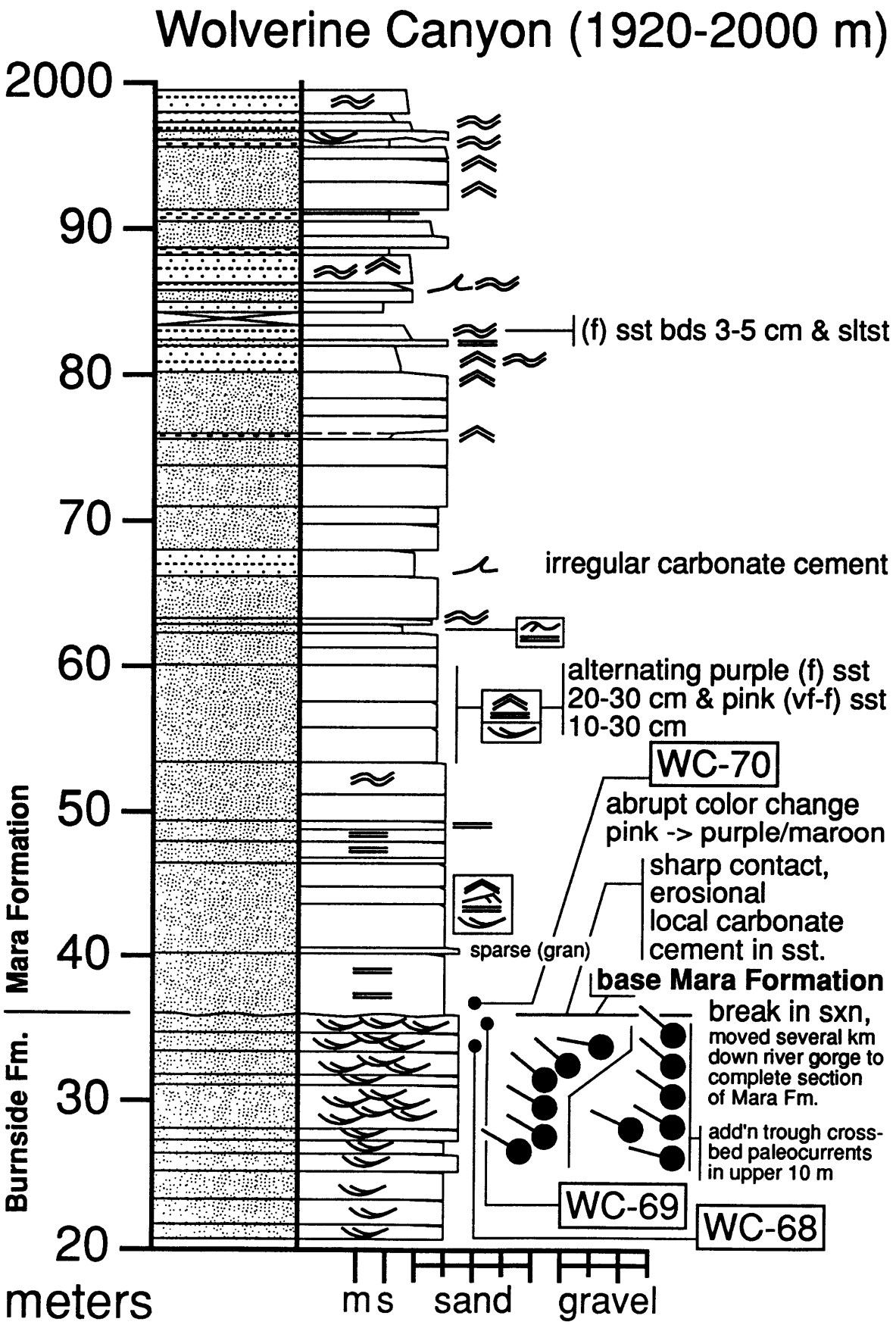
Wolverine Canyon (1920-2000 m)
2000
90
80
70
60
50
40
30
20
meters
Mara Formation
Burnside Fm.
(f) sst bds 3-5 cm & sltst
irregular carbonate cement
alternating purple (f) sst
20-30 cm & pink (vf-f) sst
10-30 cm
WC-70
abrupt color change
pink -> purple/maroon
sharp contact,
erosional
local carbonate
cement in sst.
sparse (gran)
base Mara Formation
break in sxn,
moved several km
down river gorge to
complete section
of Mara Fm.
add'n trough cross-
bed paleocurrents
in upper 10 m
WC-69
WC-68
m s
sand
gravel

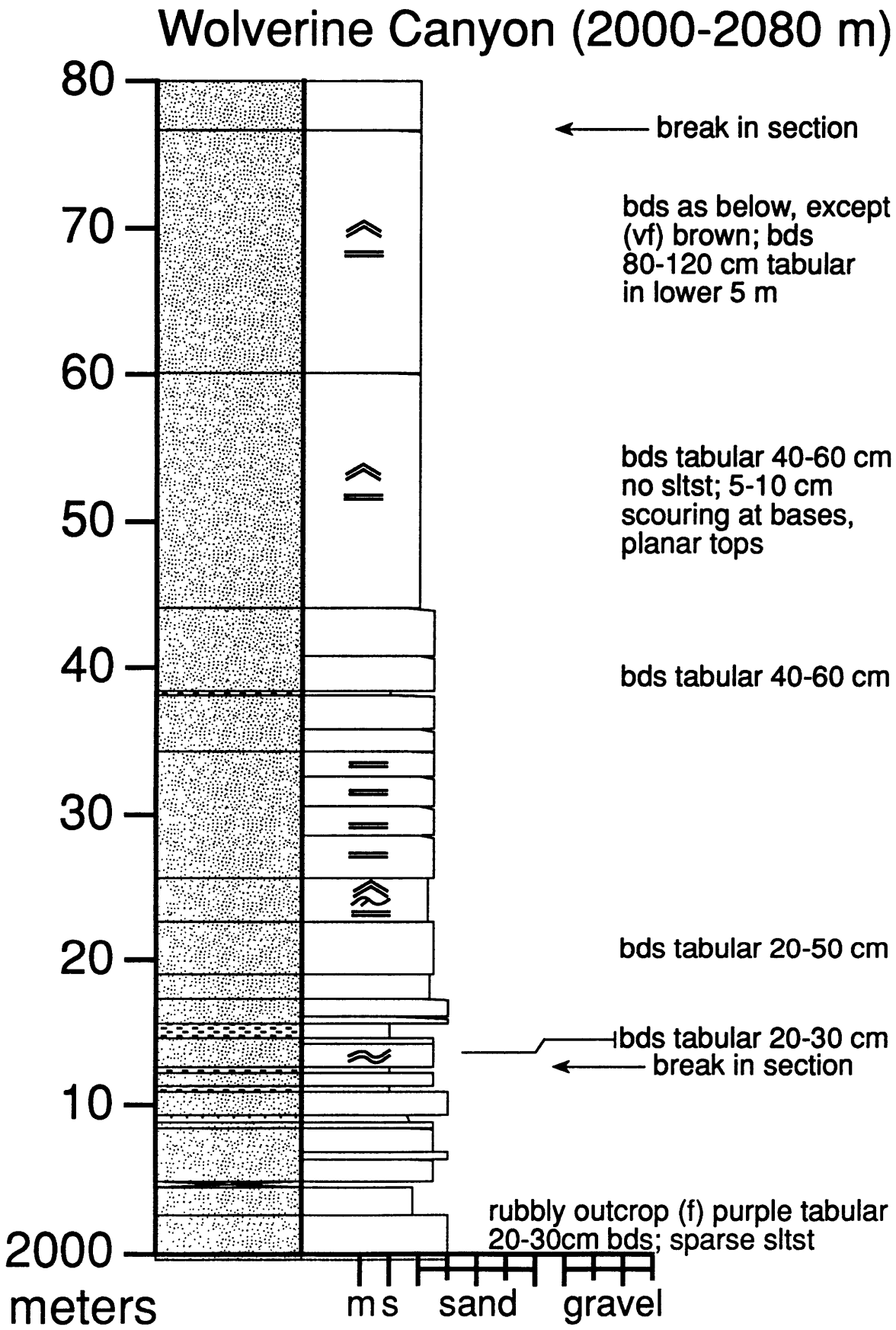
Wolverine Canyon (2000-2080 m)
80
70
60
50
40
30
20
10
2000
meters
break in section
bds as below, except (vf) brown; bds 80-120 cm tabular in lower 5 m
bds tabular 40-60 cm no sltst; 5-10 cm scouring at bases, planar tops
bds tabular 40-60 cm
bds tabular 20-50 cm
bds tabular 20-30 cm
break in section
rubbly outcrop (f) purple tabular 20-30cm bds; sparse sltst
m s
sand
gravel

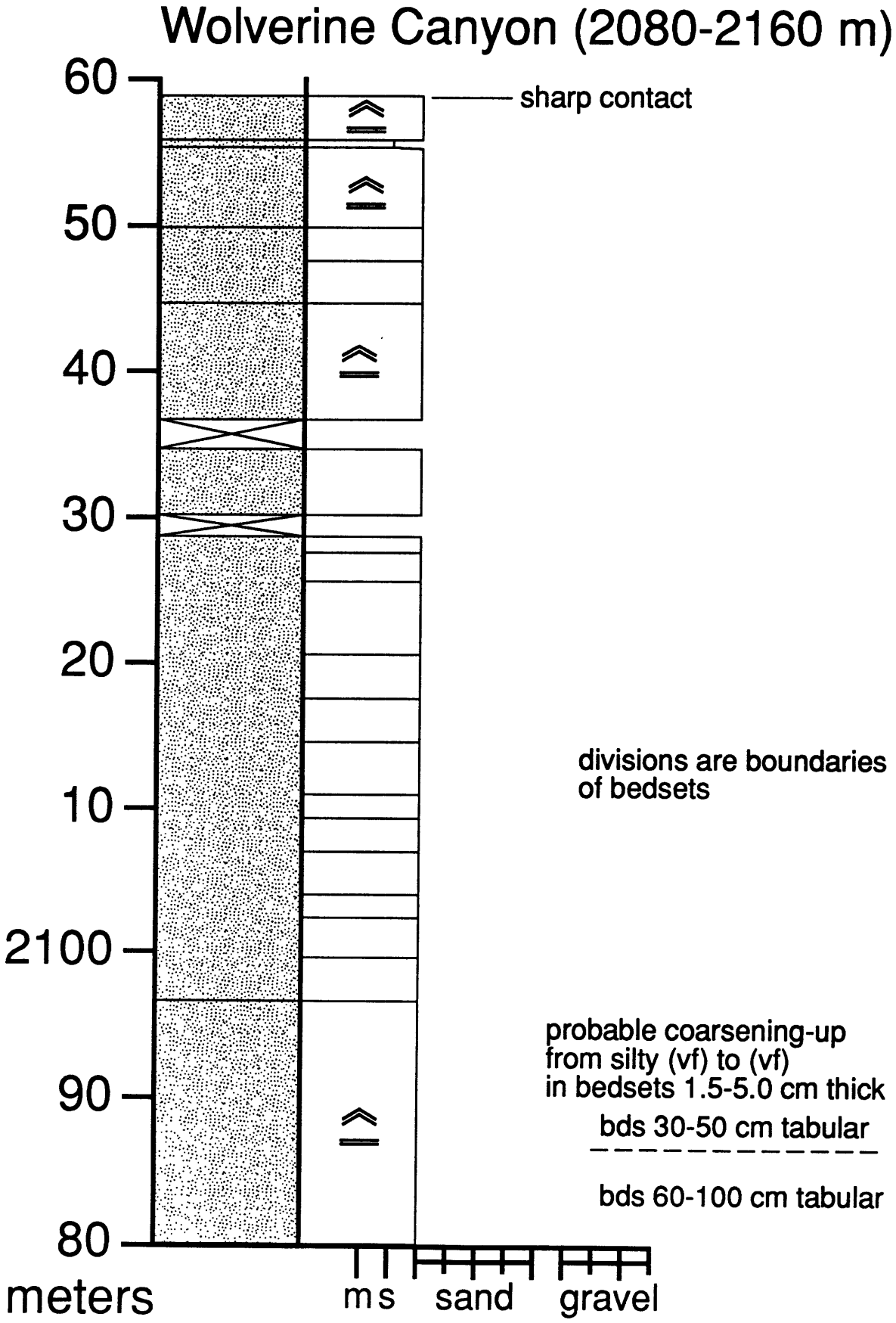
Wolverine Canyon (2080-2160 m)
60
50
40
30
20
10
2100
90
80
meters
sharp contact
divisions are boundaries
of bedsets
probable coarsening-up
from silty (vf) to (vf)
in bedsets 1.5-5.0 cm thick
bds 30-50 cm tabular
bds 60-100 cm tabular
ms
sand
gravel

Wolverine Canyon (2160-2178 m)

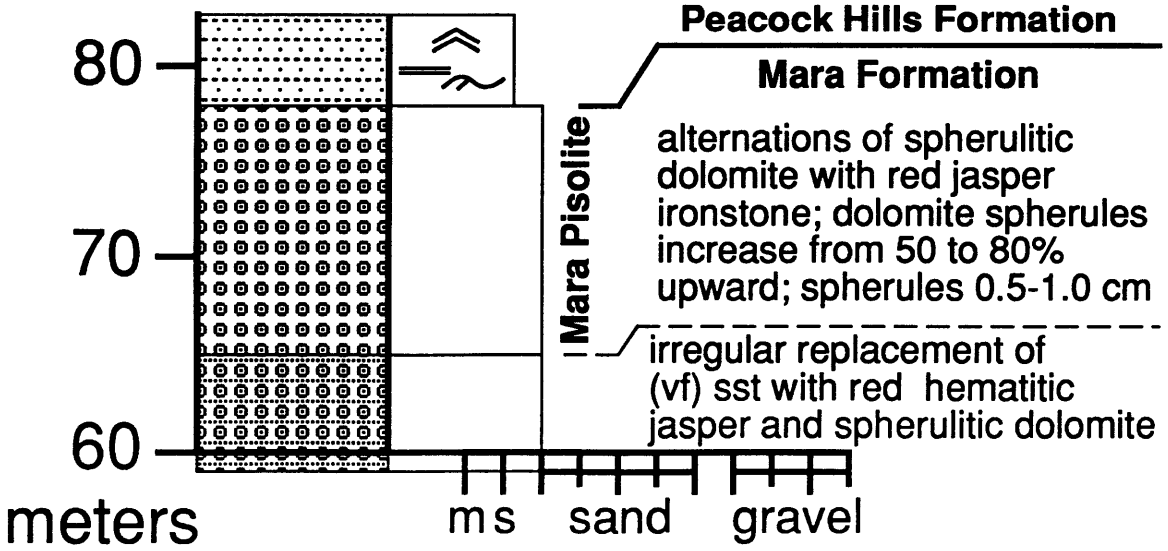

section 13: Contwoyto Lake

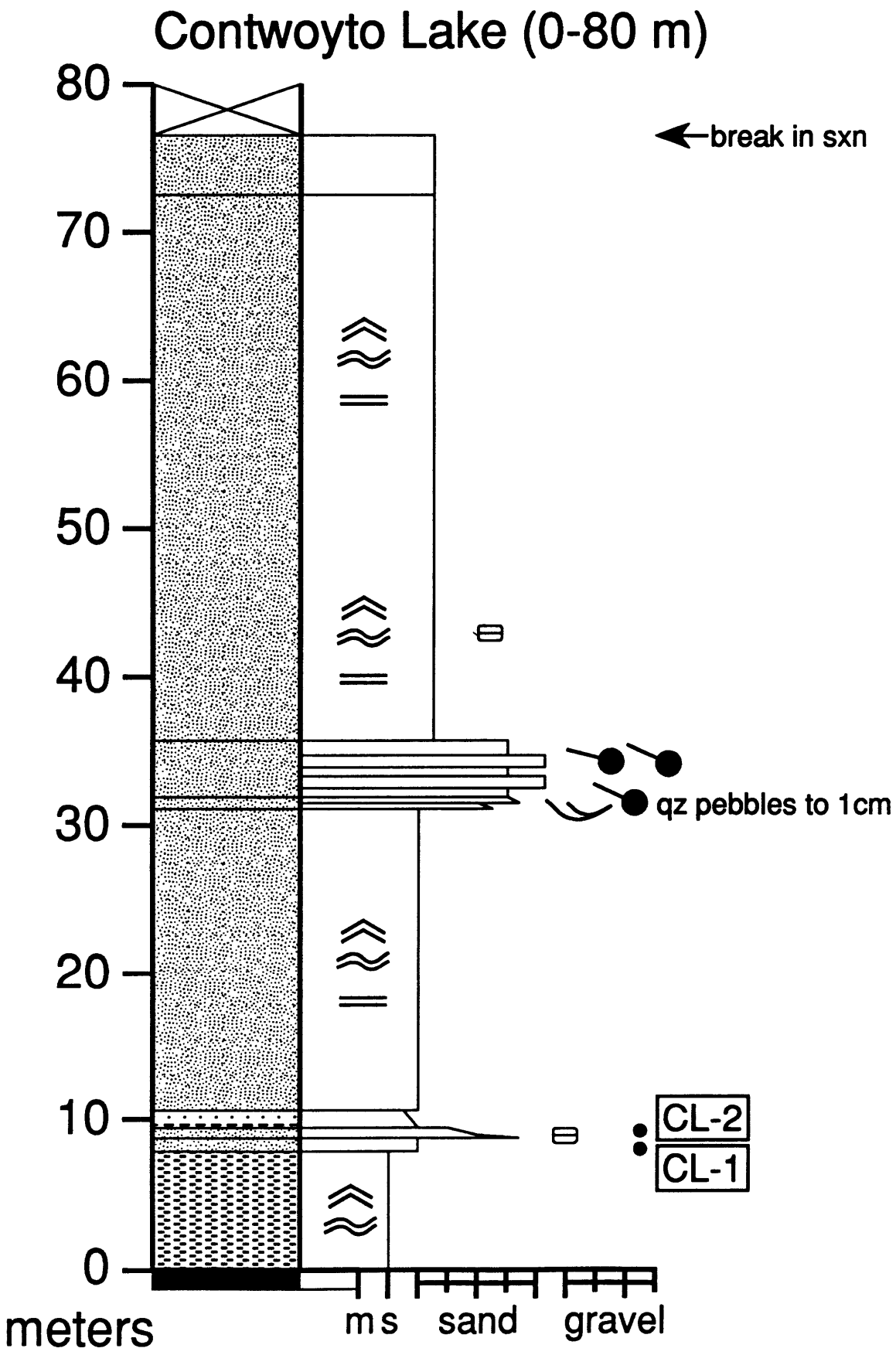
Contwoyto Lake (0-80 m)
80
70
60
50
40
30
20
10
0
meters
break in sxn
qz pebbles to 1cm
CL-2
CL-1
m s
sand
gravel

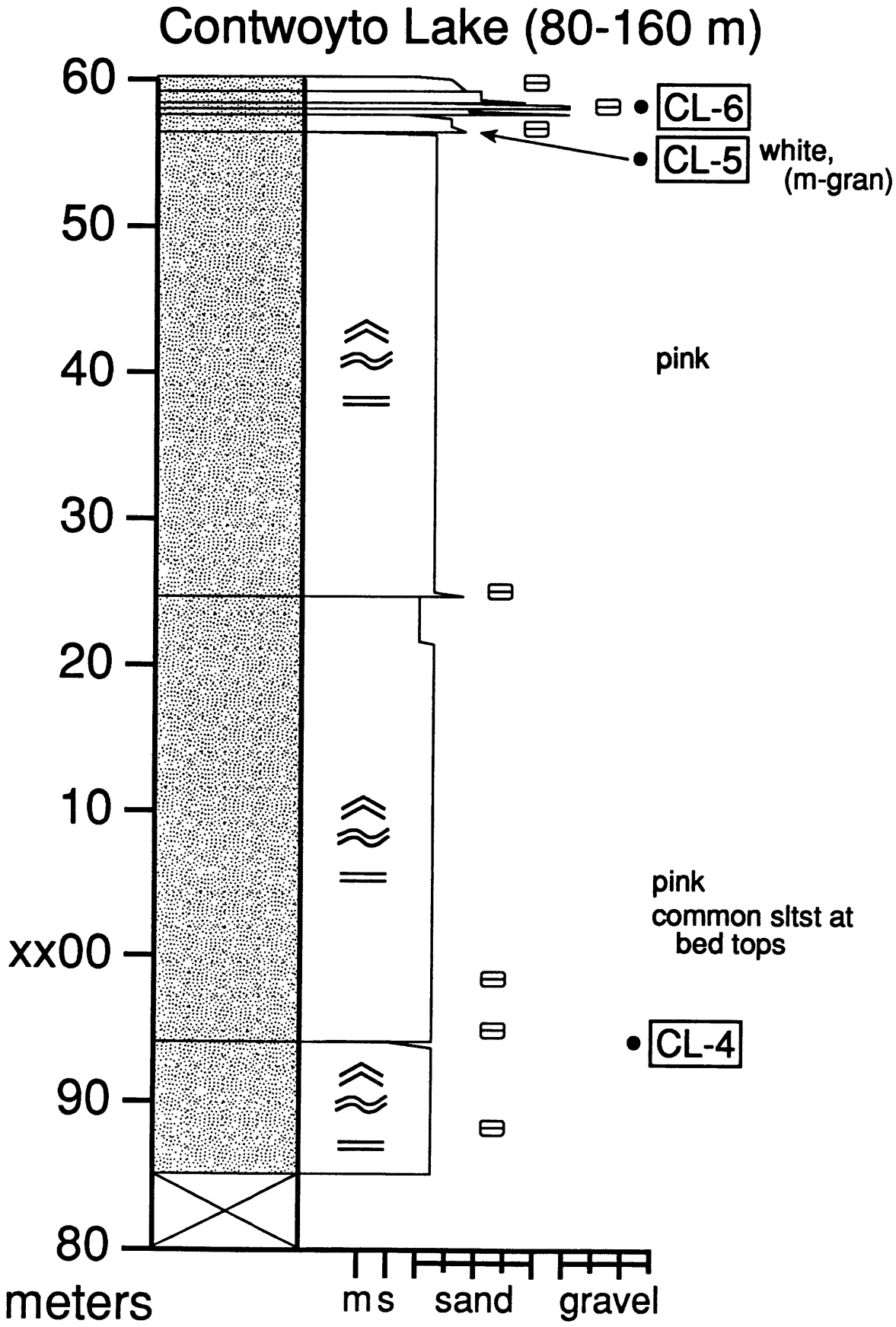
Contwoyto Lake (80-160 m)
60
50
40
30
20
10
xx00
90
80
meters
CL-6
CL-5
white,
(m-gran)
pink
pink
common sltst at
bed tops
CL-4
m s
sand
gravel

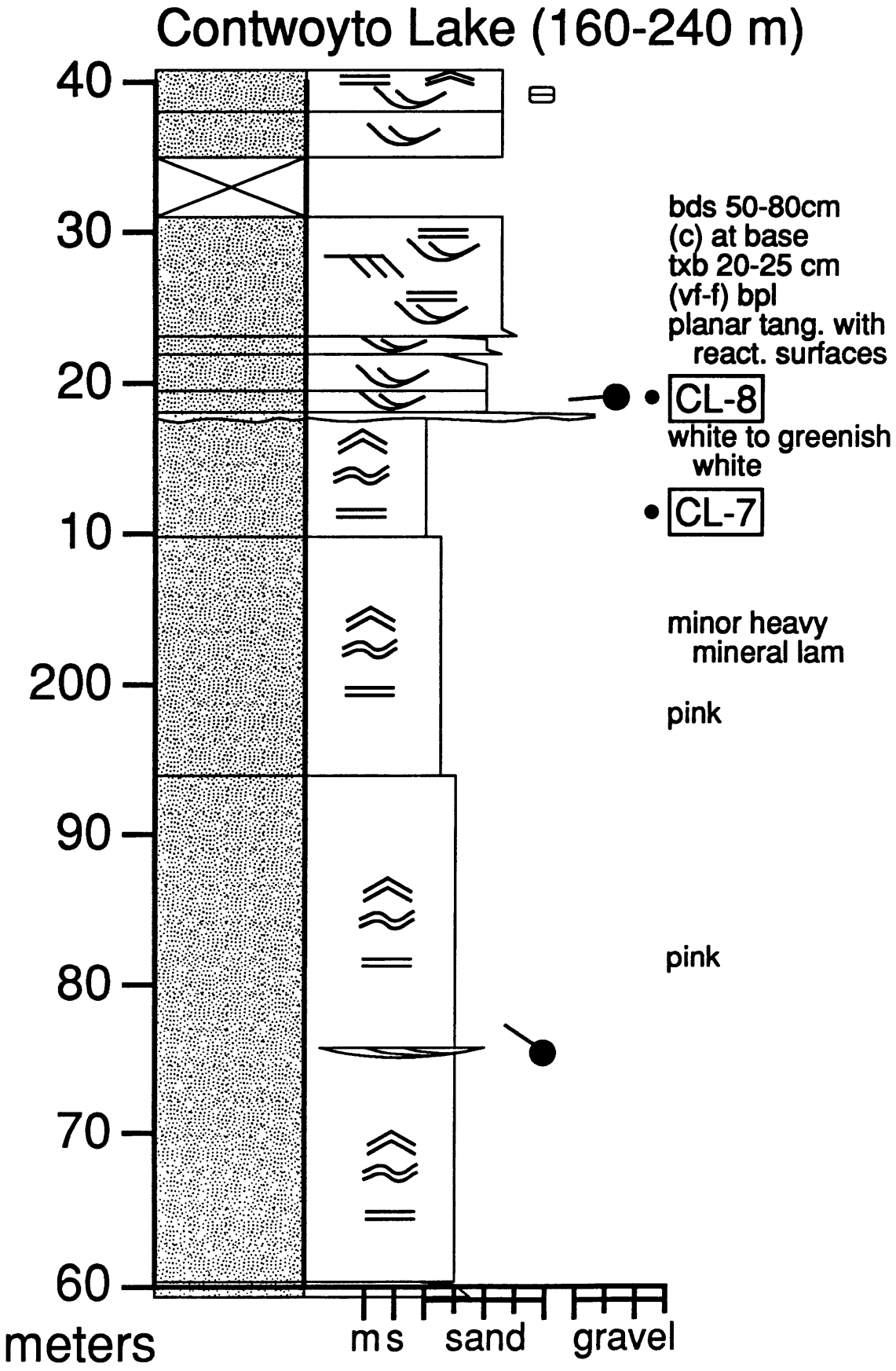
Contwoyto Lake (160-240 m)
40
30
20
10
200
90
80
70
60
meters
bds 50-80cm
(c) at base
txb 20-25 cm
(vf-f) bpl
planar tang. with
react. surfaces
CL-8
white to greenish
white
CL-7
minor heavy
mineral lam
pink
pink
ms
sand
gravel

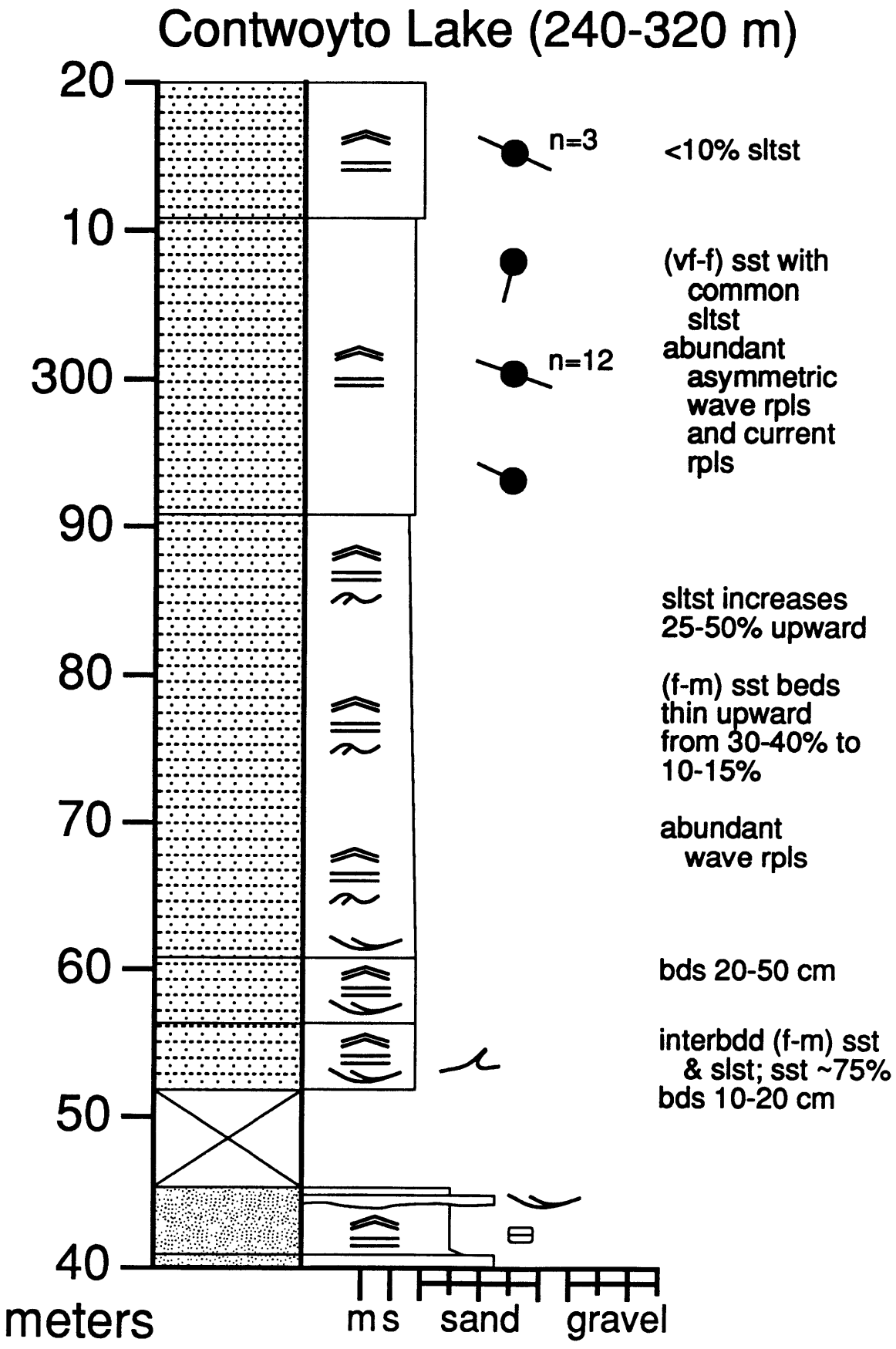
Contwoyto Lake (240-320 m)
20
10
300
90
80
70
60
50
40
meters
n=3
n=12
<10% sltst
(vf-f) sst with common sltst
abundant asymmetric wave rpls and current rpls
sltst increases 25-50% upward
(f-m) sst beds thin upward from 30-40% to 10-15%
abundant wave rpls
bds 20-50 cm
interbdd (f-m) sst & slst; sst ~75%
bds 10-20 cm
m s
sand
gravel

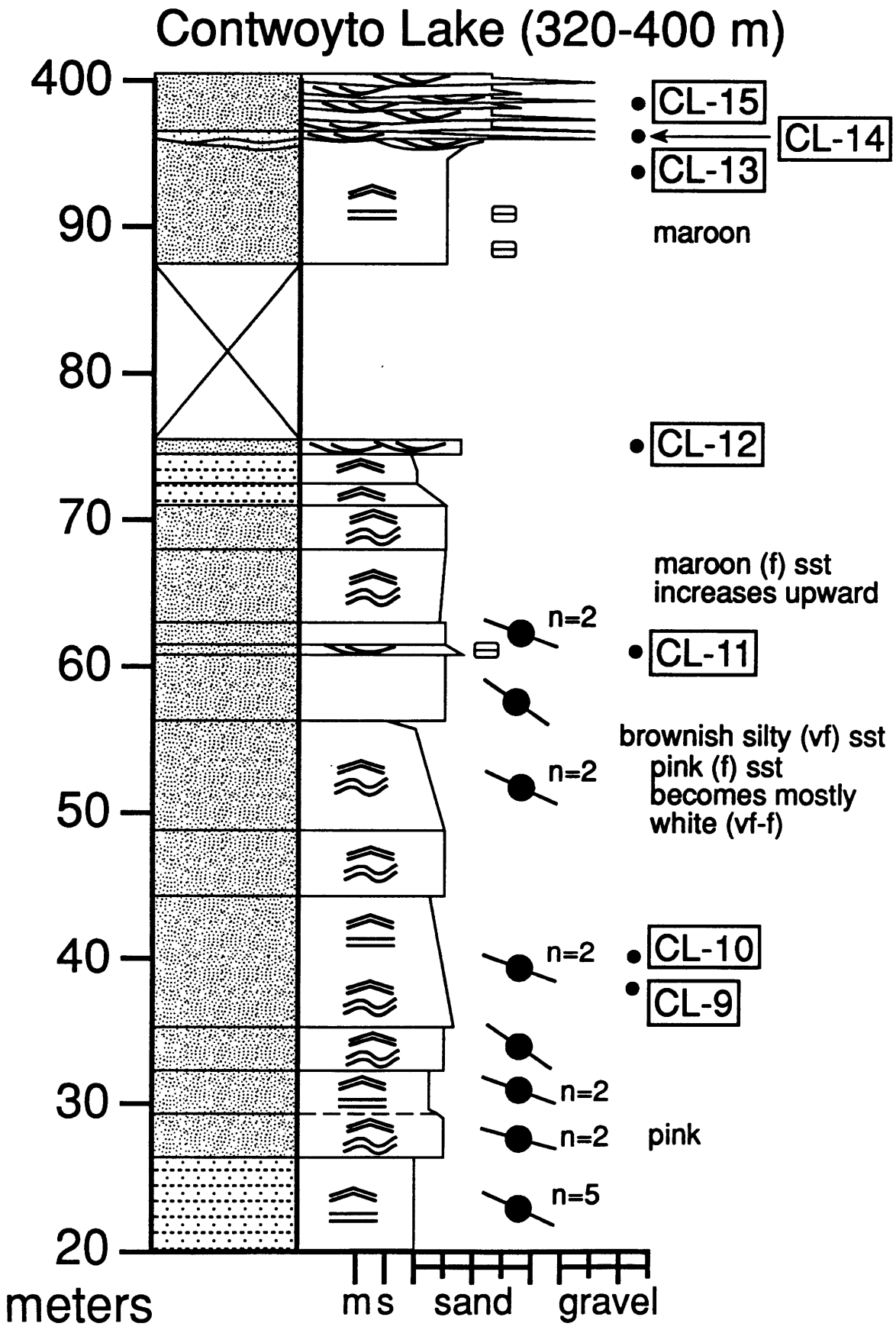
Contwoyto Lake (320-400 m)
400
90
80
70
60
50
40
30
20
meters
CL-15
CL-14
CL-13
maroon
CL-12
maroon (f) sst
increases upward
n=2
CL-11
brownish silty (vf) sst
pink (f) sst
becomes mostly
white (vf-f)
n=2
n=2
CL-10
CL-9
n=2
n=2
pink
n=5
ms
sand
gravel

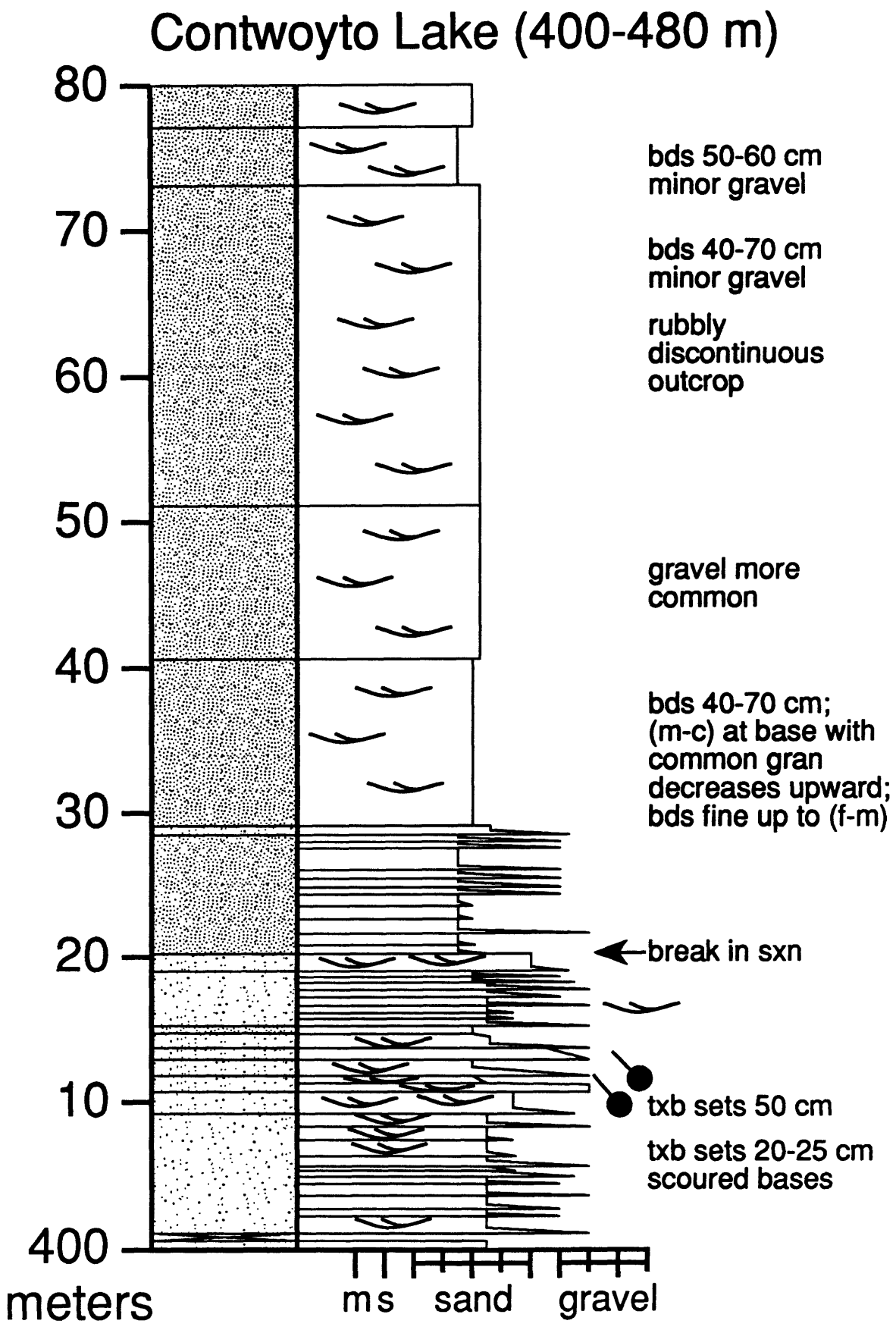
Contwoyto Lake (400-480 m)
80
70
60
50
40
30
20
10
400
meters
ms
sand
gravel
bds 50-60 cm
minor gravel
bds 40-70 cm
minor gravel
rubbly
discontinuous
outcrop
gravel more
common
bds 40-70 cm;
(m-c) at base with
common gran
decreases upward;
bds fine up to (f-m)
break in sxn
txb sets 50 cm
txb sets 20-25 cm
scoured bases

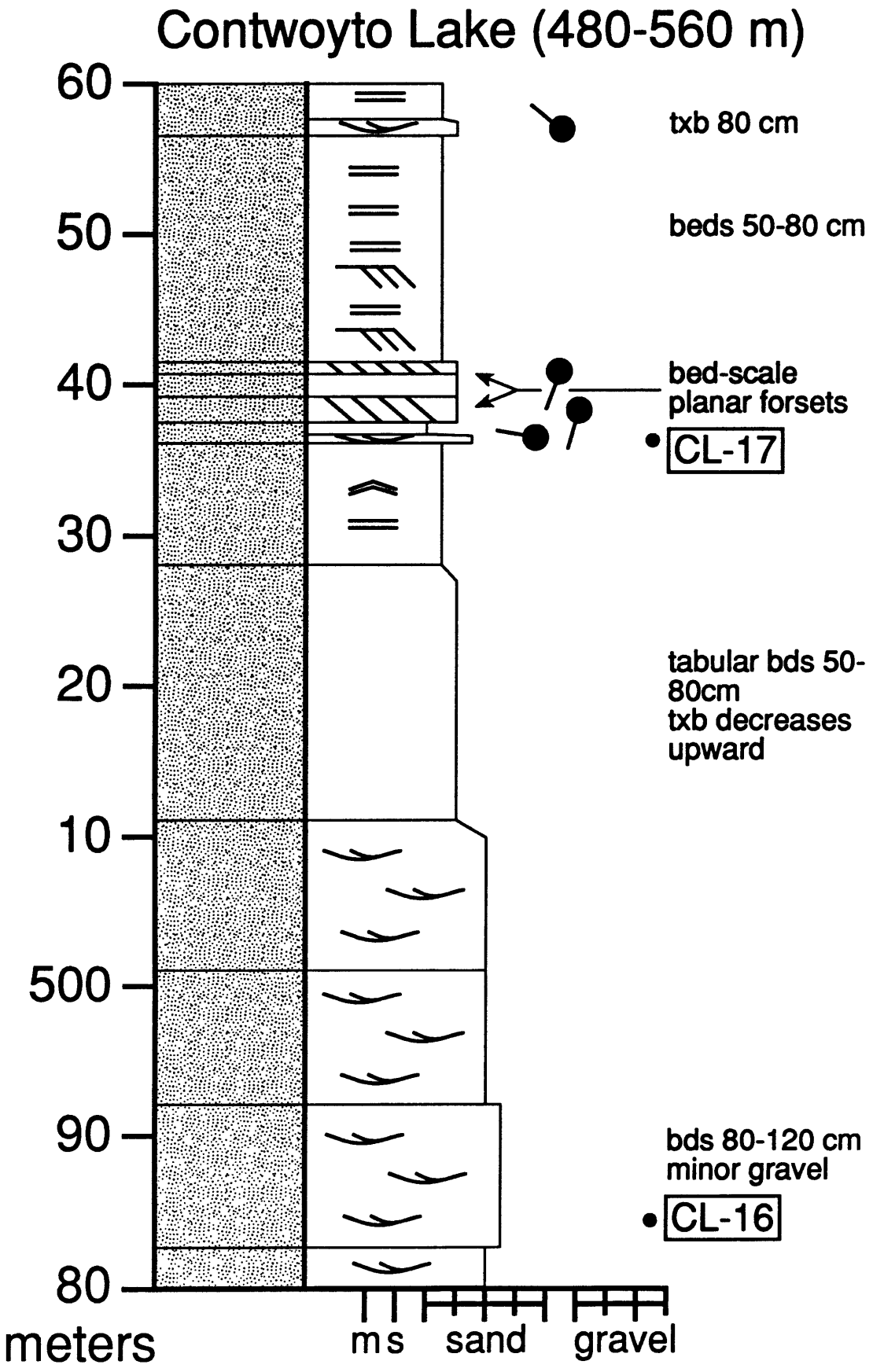
Contwoyto Lake (480-560 m)
60
50
40
30
20
10
500
90
80
meters
txb 80 cm
beds 50-80 cm
bed-scale
planar forsets
CL-17
tabular bds 50-
80cm
txb decreases
upward
bds 80-120 cm
minor gravel
CL-16
ms
sand
gravel

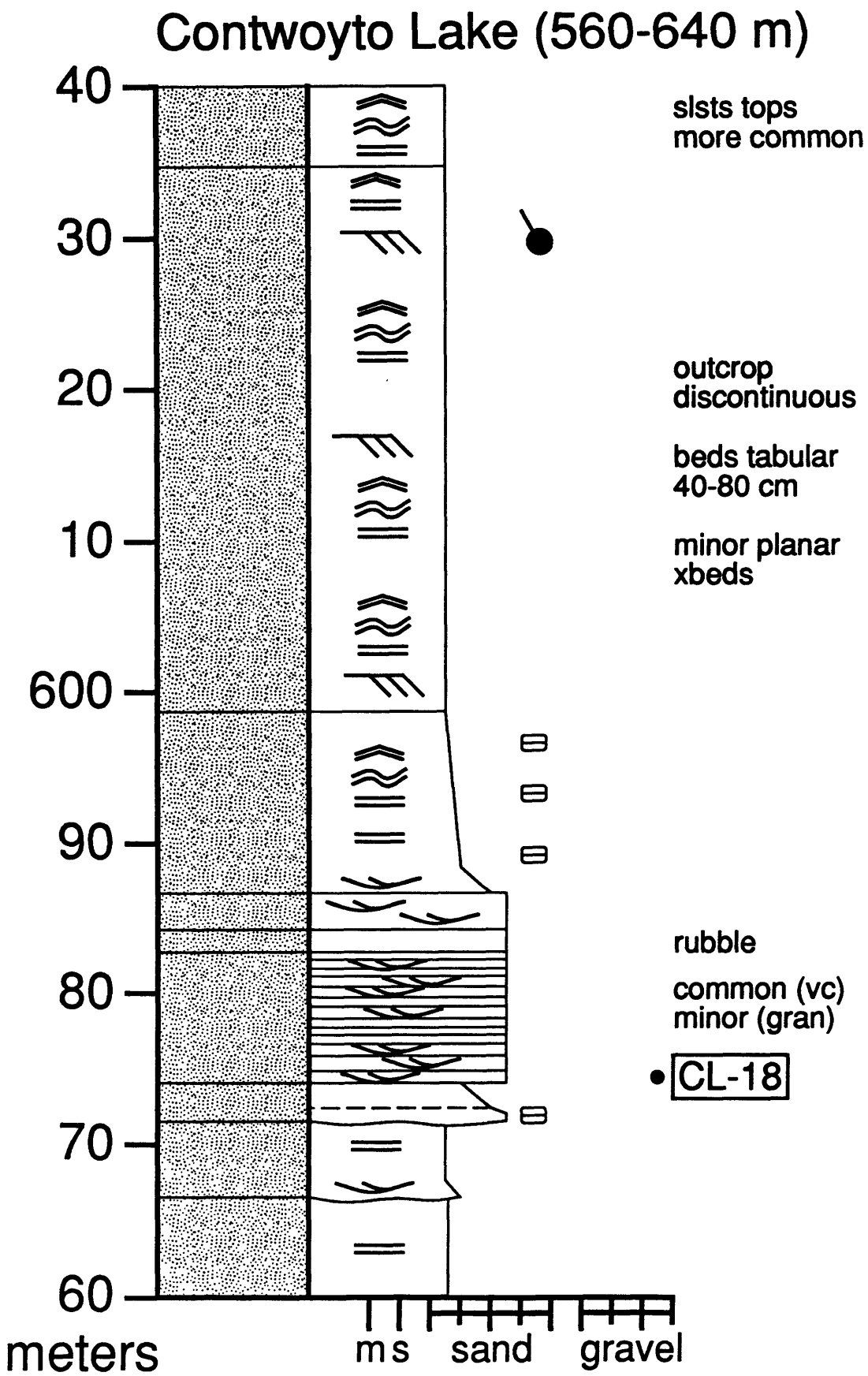
Contwoyto Lake (560-640 m)
40
30
20
10
600
90
80
70
60
meters
ms
sand
gravel
slsts tops
more common
outcrop
discontinuous
beds tabular
40-80 cm
minor planar
xbeds
rubble
common (vc)
minor (gran)
CL-18

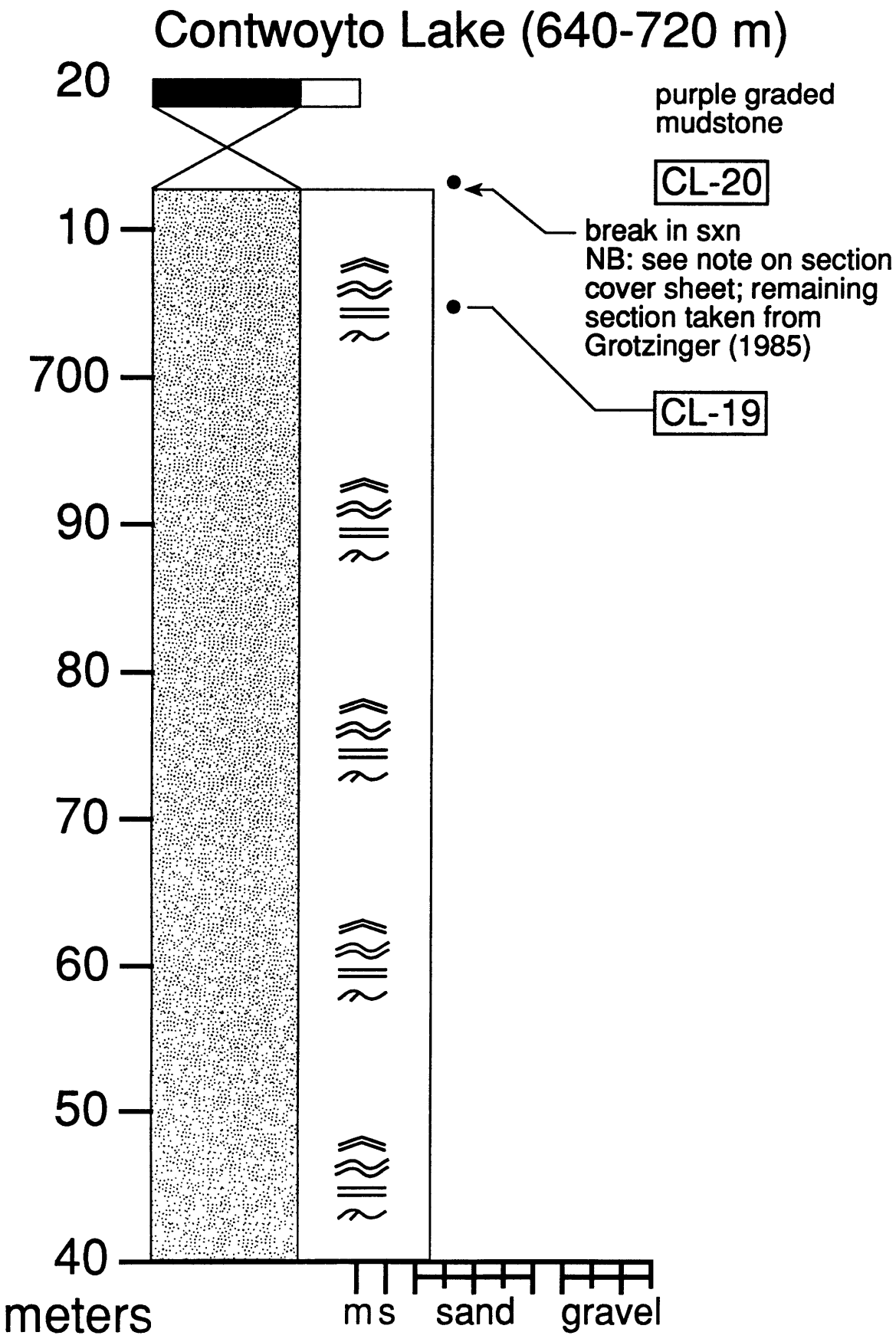
Contwoyto Lake (640-720 m)
20
10
700
90
80
70
60
50
40
meters
purple graded mudstone
CL-20
break in sxn
NB: see note on section cover sheet; remaining section taken from Grotzinger (1985)
CL-19
m s
sand
gravel

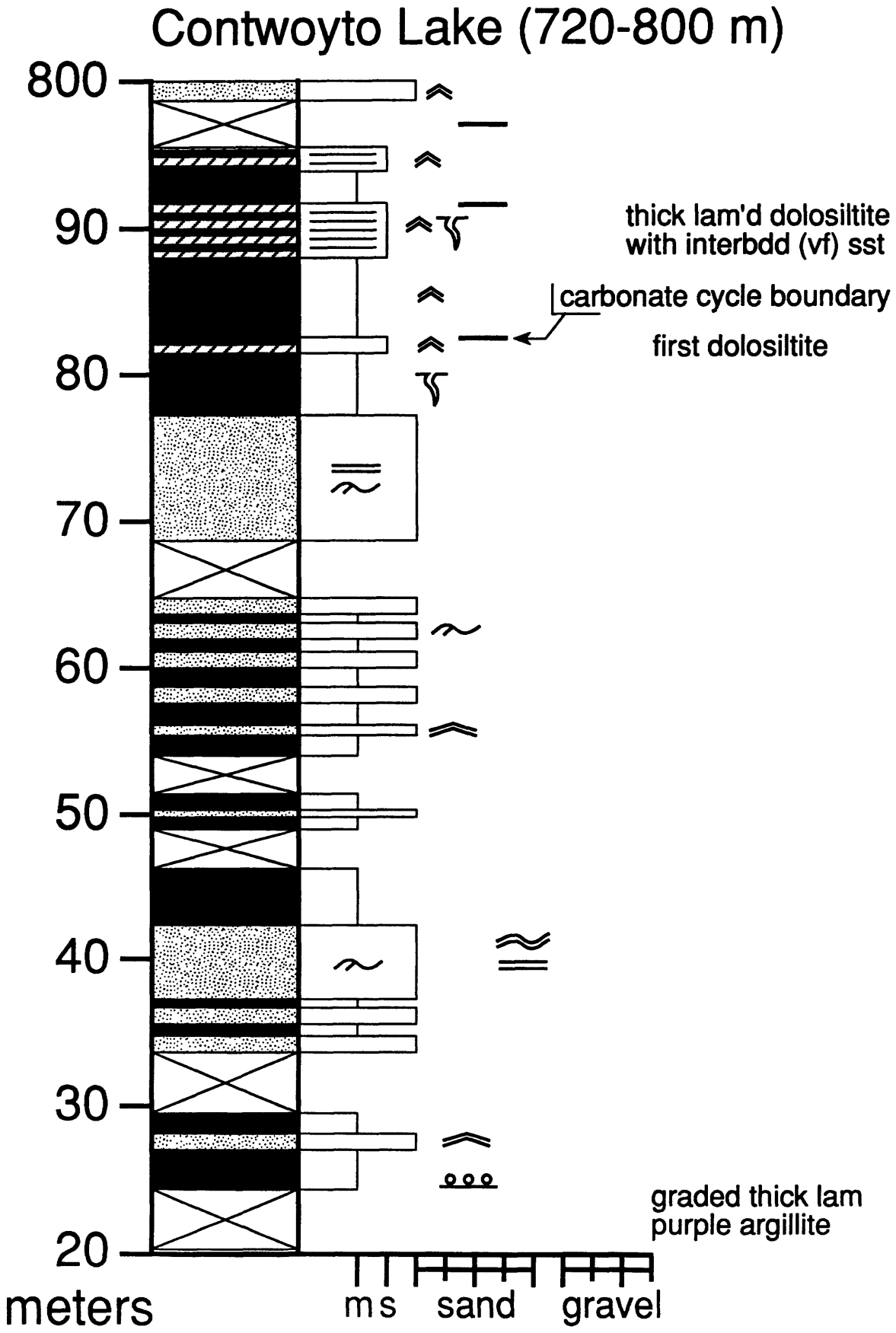
Contwoyto Lake (720-800 m)
800
90
80
70
60
50
40
30
20
meters
thick lam'd dolosiltite
with interbdd (vf) sst
carbonate cycle boundary
first dolosiltite
graded thick lam
purple argillite
ms
sand
gravel

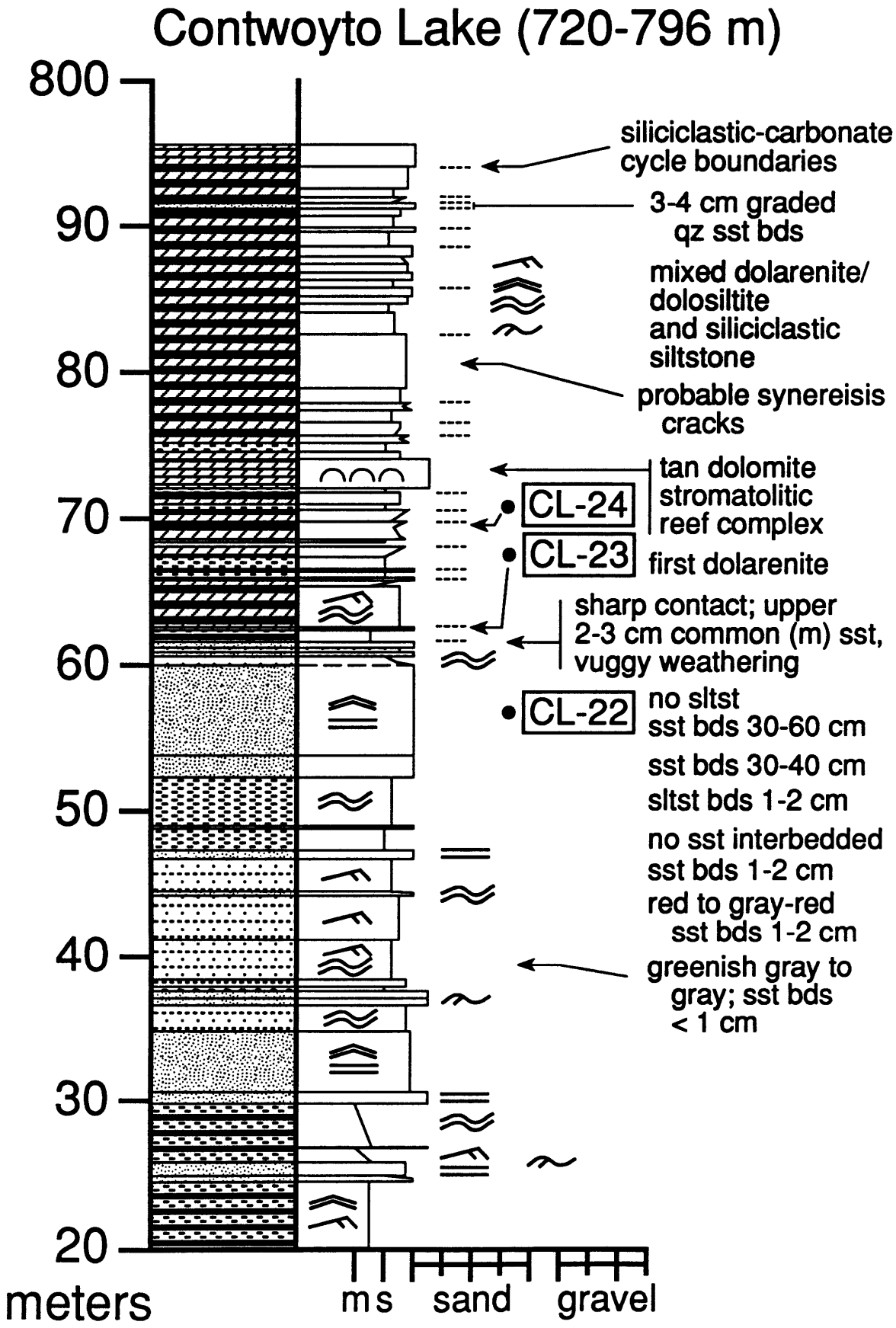
Contwoyto Lake (720-796 m)
800
90
80
70
60
50
40
30
20
meters
m s
sand
gravel
siliciclastic-carbonate cycle boundaries
3-4 cm graded qz sst bds
mixed dolarenite/ dolosiltite and siliciclastic siltstone
probable synereisis cracks
tan dolomite stromatolitic reef complex
CL-24
CL-23
first dolarenite
sharp contact; upper 2-3 cm common (m) sst, vuggy weathering
CL-22
no sltst
sst bds 30-60 cm
sst bds 30-40 cm
sltst bds 1-2 cm
no sst interbedded
sst bds 1-2 cm
red to gray-red sst bds 1-2 cm
greenish gray to gray; sst bds < 1 cm

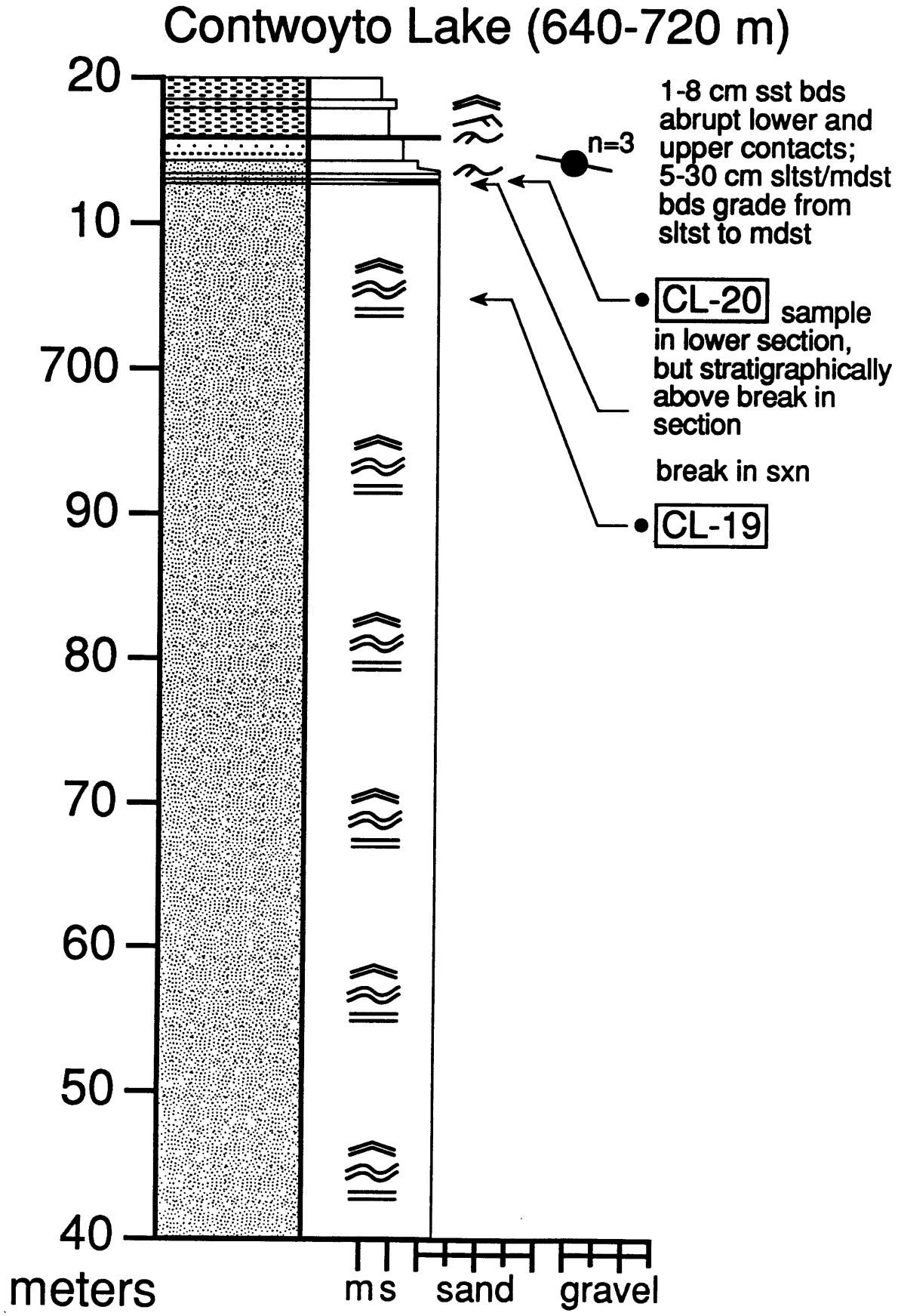
Contwoyto Lake (640-720 m)
20
10
700
90
80
70
60
50
40
meters
n=3
1-8 cm sst bds abrupt lower and upper contacts; 5-30 cm sltst/mdst bds grade from sltst to mdst
CL-20 sample in lower section, but stratigraphically above break in section
break in sxn
CL-19
ms
sand
gravel

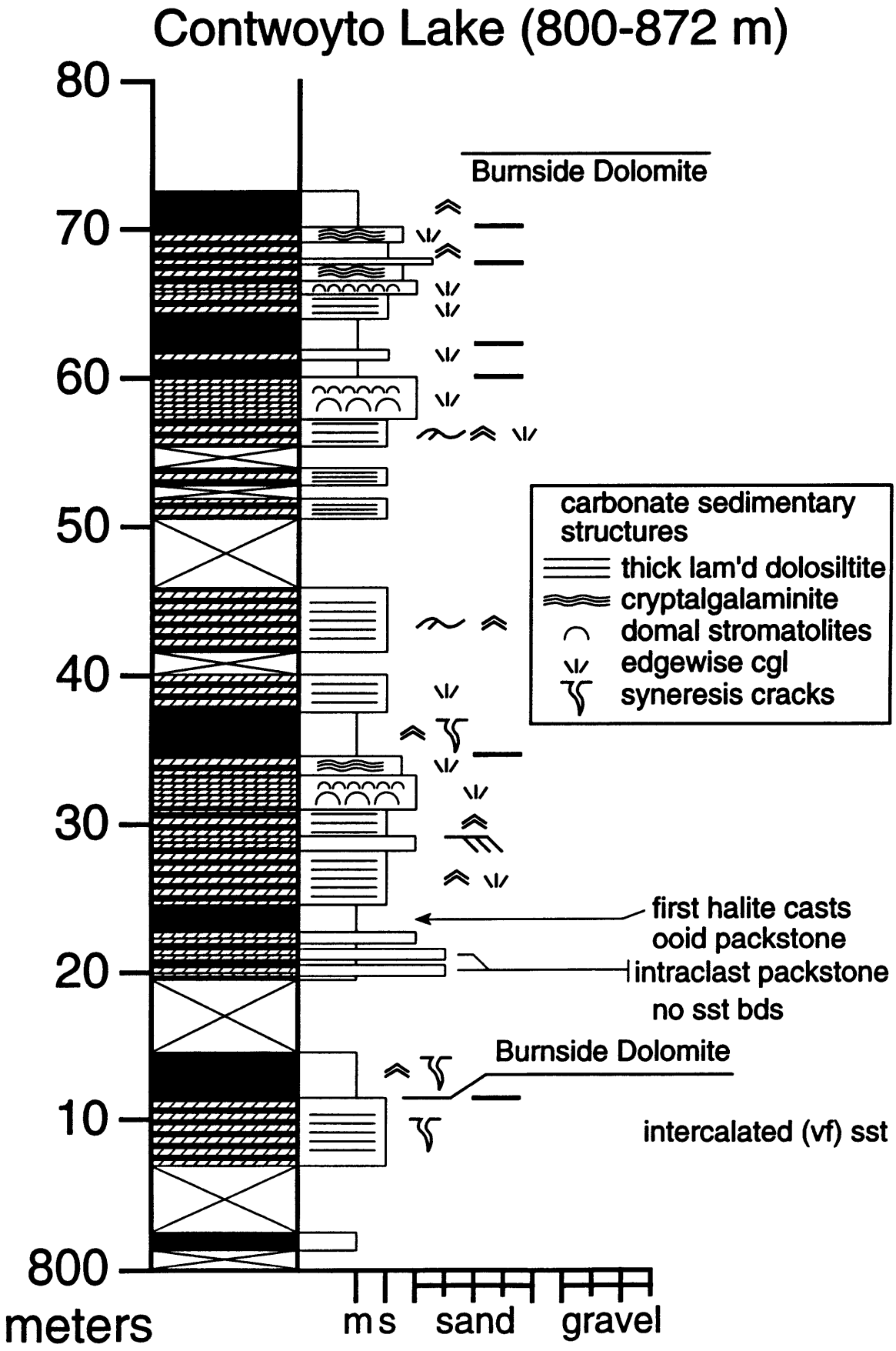
Contwoyto Lake (800-872 m)
80
70
60
50
40
30
20
10
800
meters
Burnside Dolomite
carbonate sedimentary structures
thick lam'd dolosiltite
cryptalgalaminite
domal stromatolites
edgewise cgl
syneresis cracks
first halite casts
ooid packstone
intraclast packstone
no sst bds
Burnside Dolomite
intercalated (vf) sst
ms
sand
gravel

section 14: Rockinghorse Lake

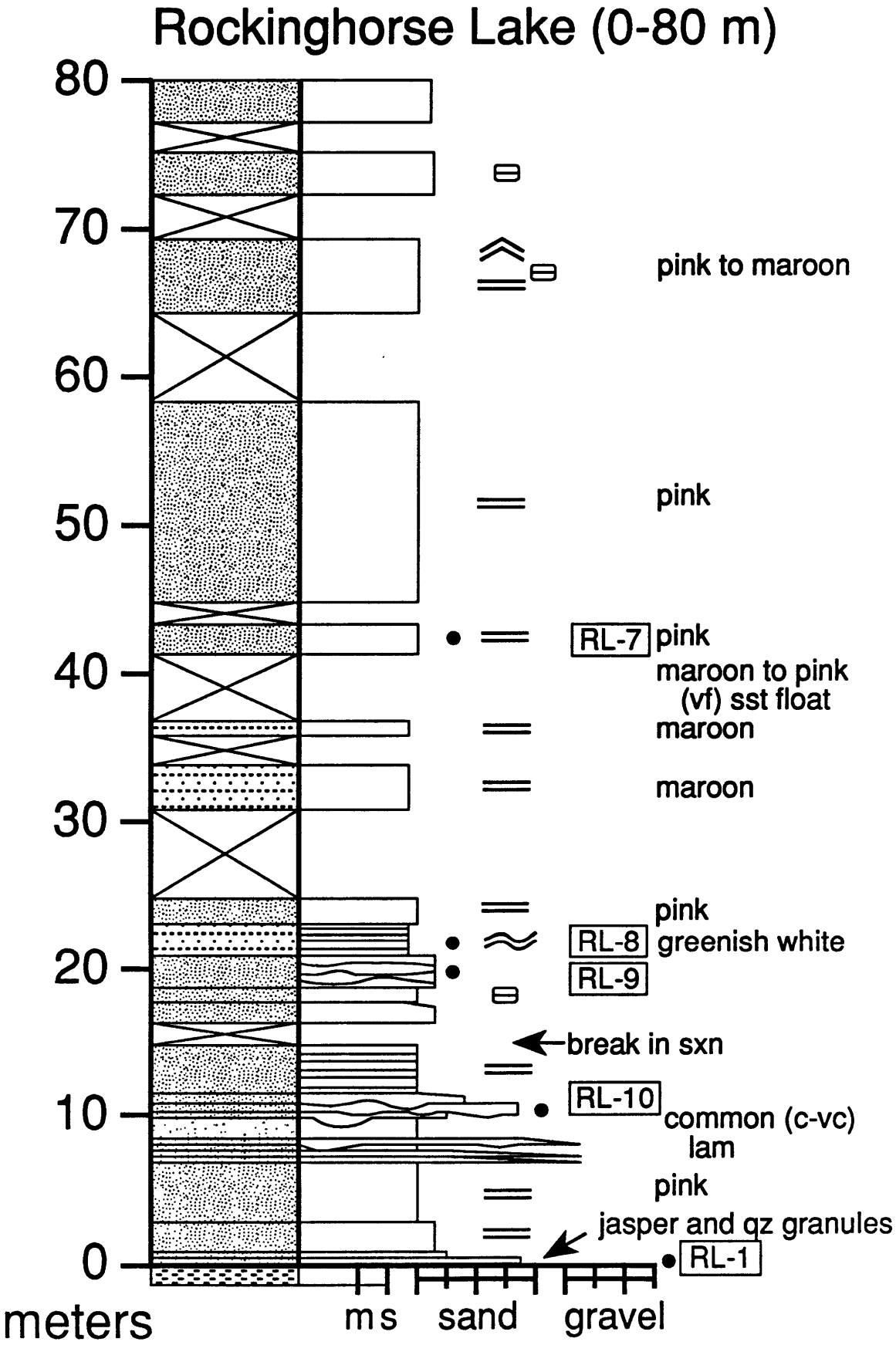
Rockinghorse Lake (0-80 m)
80
70
60
50
40
30
20
10
0
meters
ms
sand
gravel
pink to maroon
pink
RL-7
pink
maroon to pink
(vf) sst float
maroon
maroon
pink
RL-8
greenish white
RL-9
break in sxn
RL-10
common (c-vc)
lam
pink
jasper and qz granules
RL-1

Rockinghorse Lake (80-143.6 m)

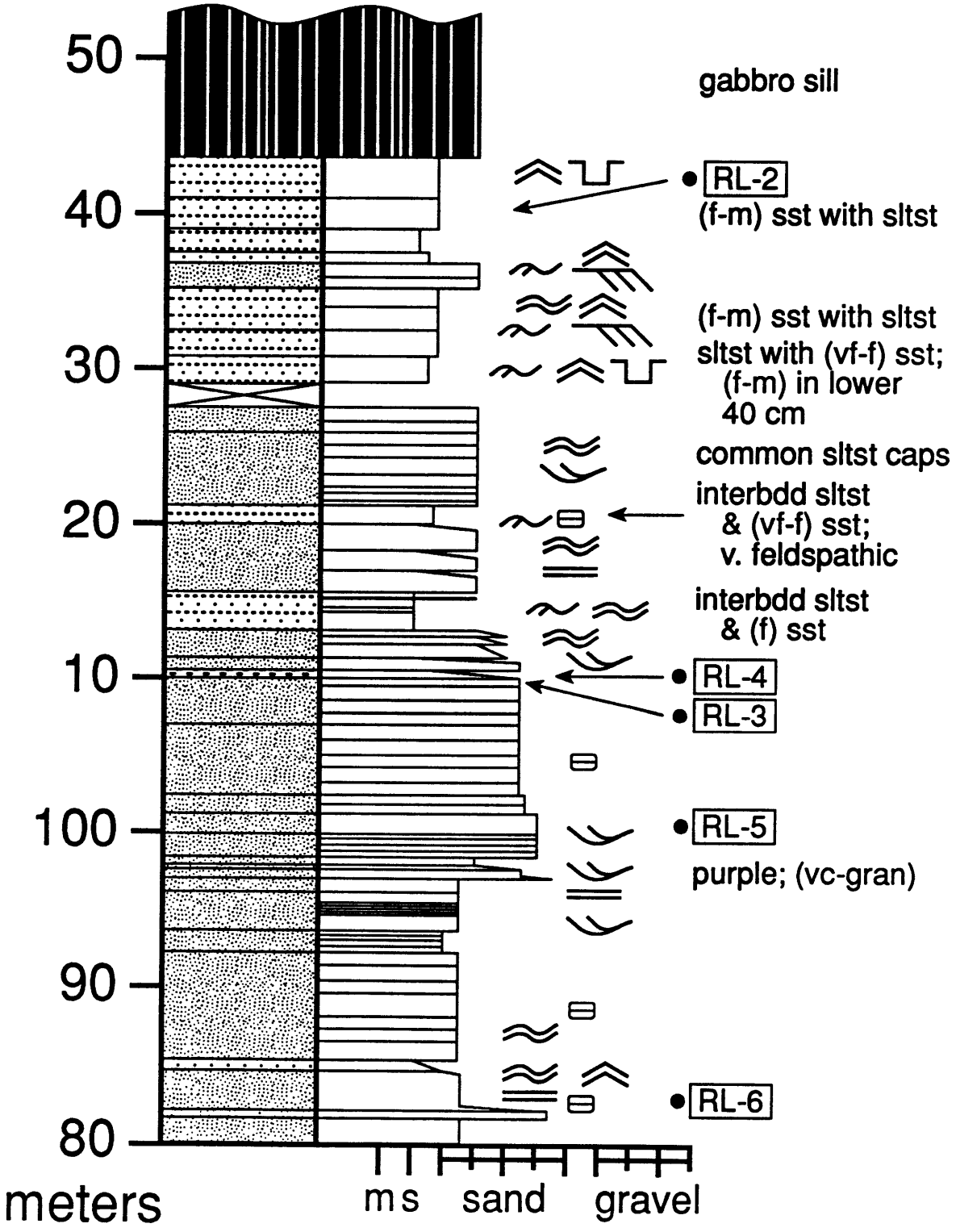

section 15: Buchan Bay

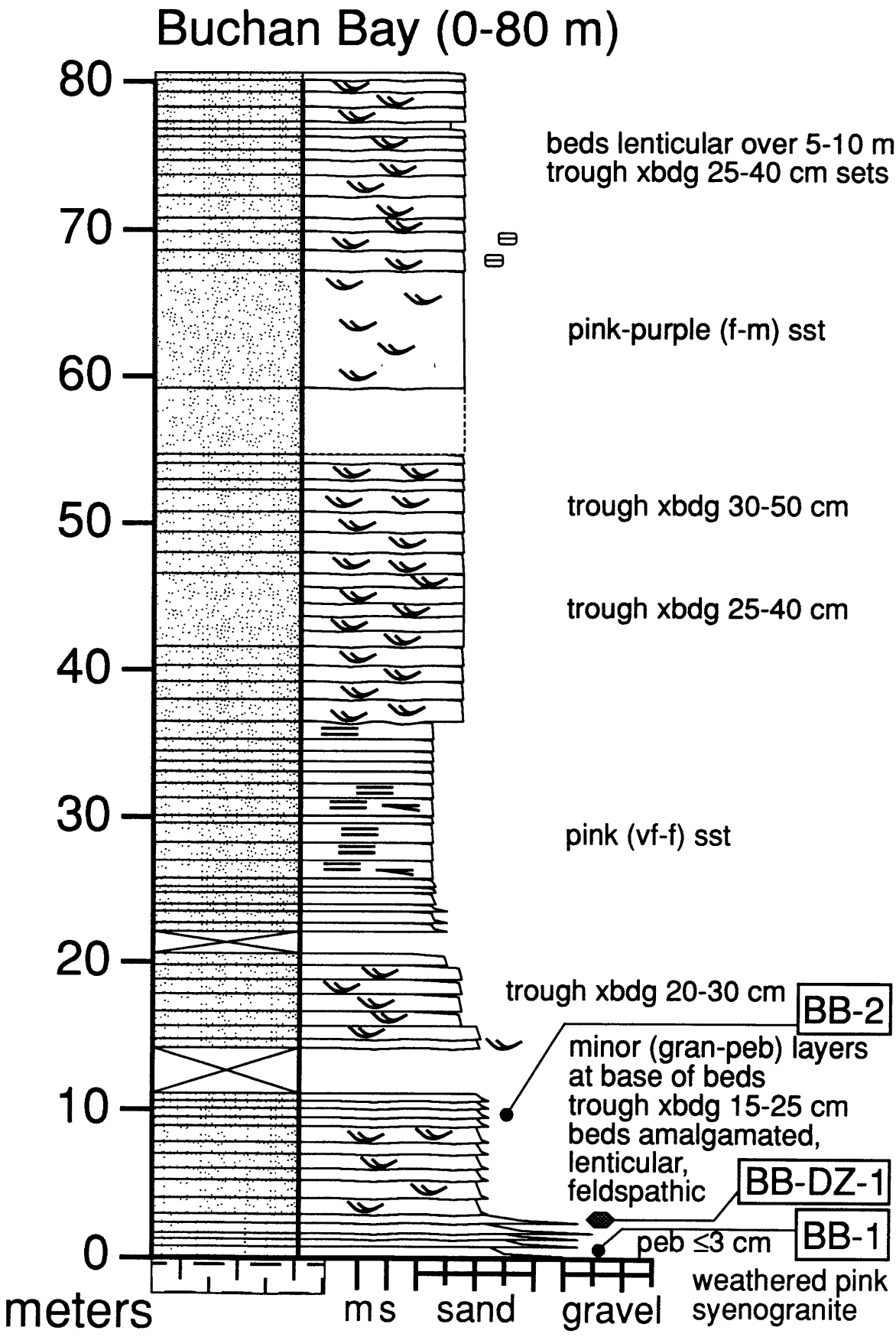
Buchan Bay (0-80 m)
80
70
60
50
40
30
20
10
0
meters
m s
sand
gravel
beds lenticular over 5-10 m
trough xbdg 25-40 cm sets
pink-purple (f-m) sst
trough xbdg 30-50 cm
trough xbdg 25-40 cm
pink (vf-f) sst
trough xbdg 20-30 cm
BB-2
minor (gran-peb) layers
at base of beds
trough xbdg 15-25 cm
beds amalgamated,
lenticular,
feldspathic
BB-DZ-1
peb ≤3 cm
BB-1
weathered pink
syenogranite

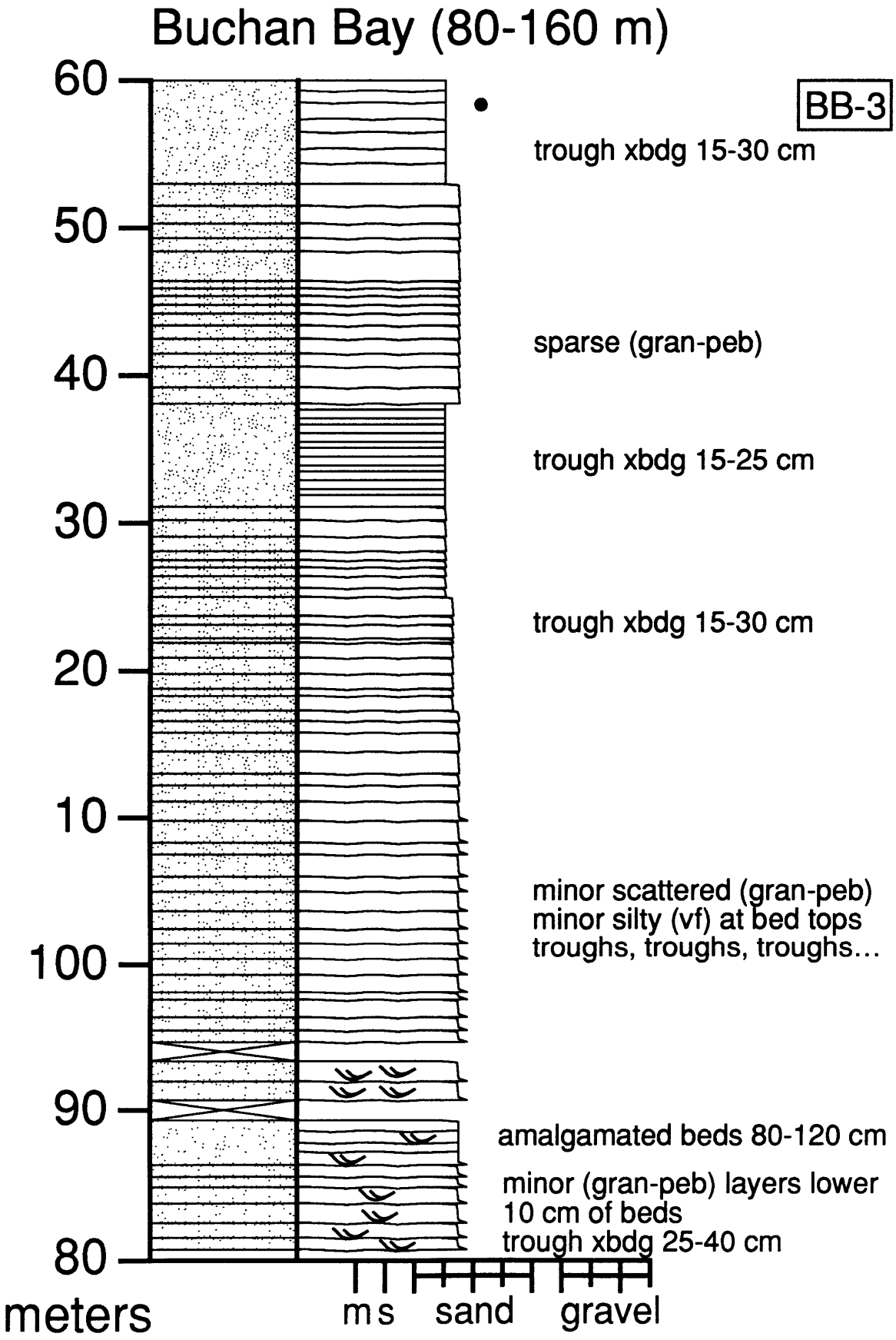
Buchan Bay (80-160 m)
60
50
40
30
20
10
100
90
80
meters
BB-3
trough xbdg 15-30 cm
sparse (gran-peb)
trough xbdg 15-25 cm
trough xbdg 15-30 cm
minor scattered (gran-peb)
minor silty (vf) at bed tops
troughs, troughs, troughs...
amalgamated beds 80-120 cm
minor (gran-peb) layers lower
10 cm of beds
trough xbdg 25-40 cm
m s
sand
gravel

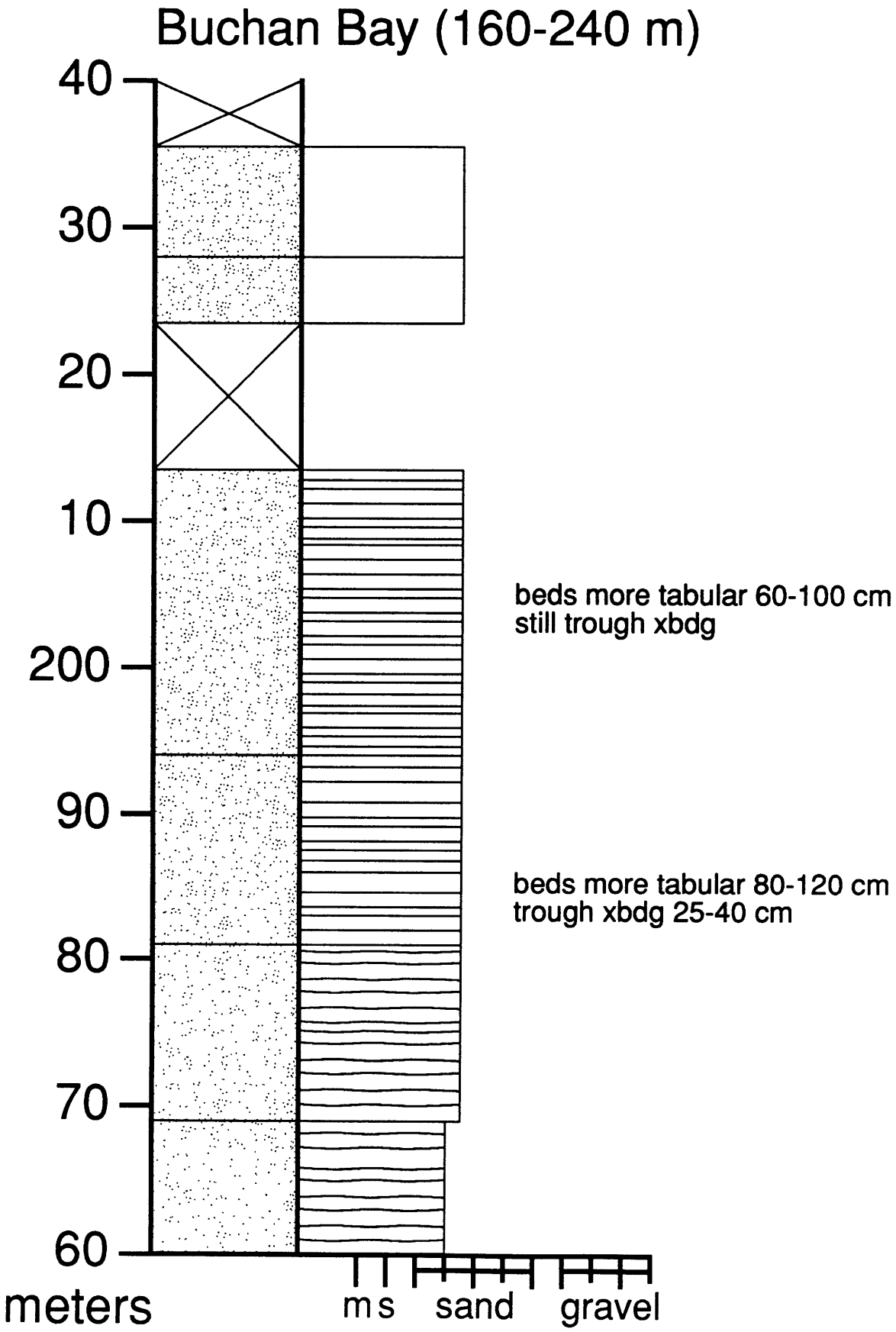
Buchan Bay (160-240 m)
40
30
20
10
200
90
80
70
60
meters
beds more tabular 60-100 cm
still trough xbdg
beds more tabular 80-120 cm
trough xbdg 25-40 cm
m s
sand
gravel

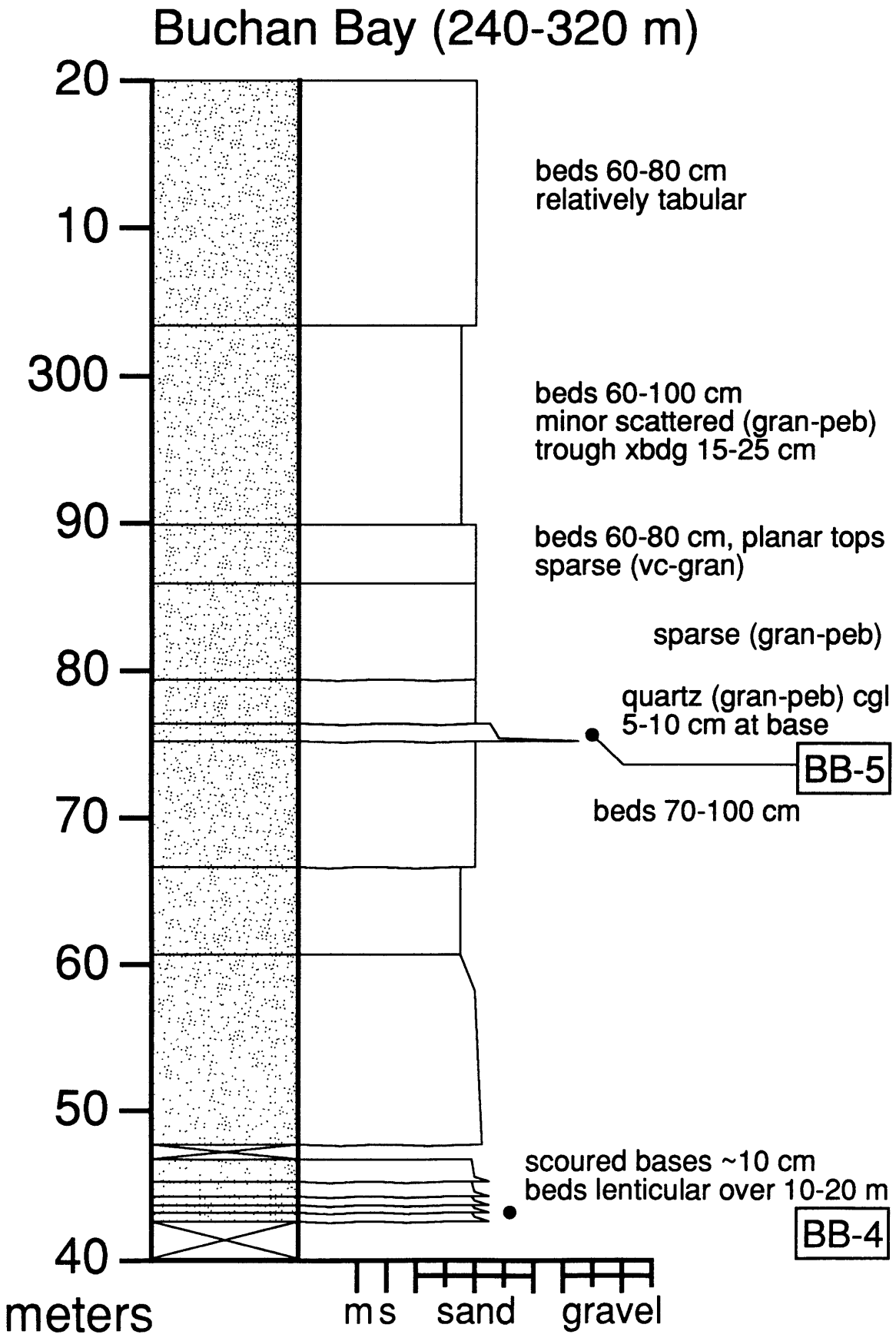
Buchan Bay (240-320 m)
20
10
300
90
80
70
60
50
40
meters
beds 60-80 cm
relatively tabular
beds 60-100 cm
minor scattered (gran-peb)
trough xbdg 15-25 cm
beds 60-80 cm, planar tops
sparse (vc-gran)
sparse (gran-peb)
quartz (gran-peb) cgl
5-10 cm at base
BB-5
beds 70-100 cm
scoured bases ~10 cm
beds lenticular over 10-20 m
BB-4
m s
sand
gravel

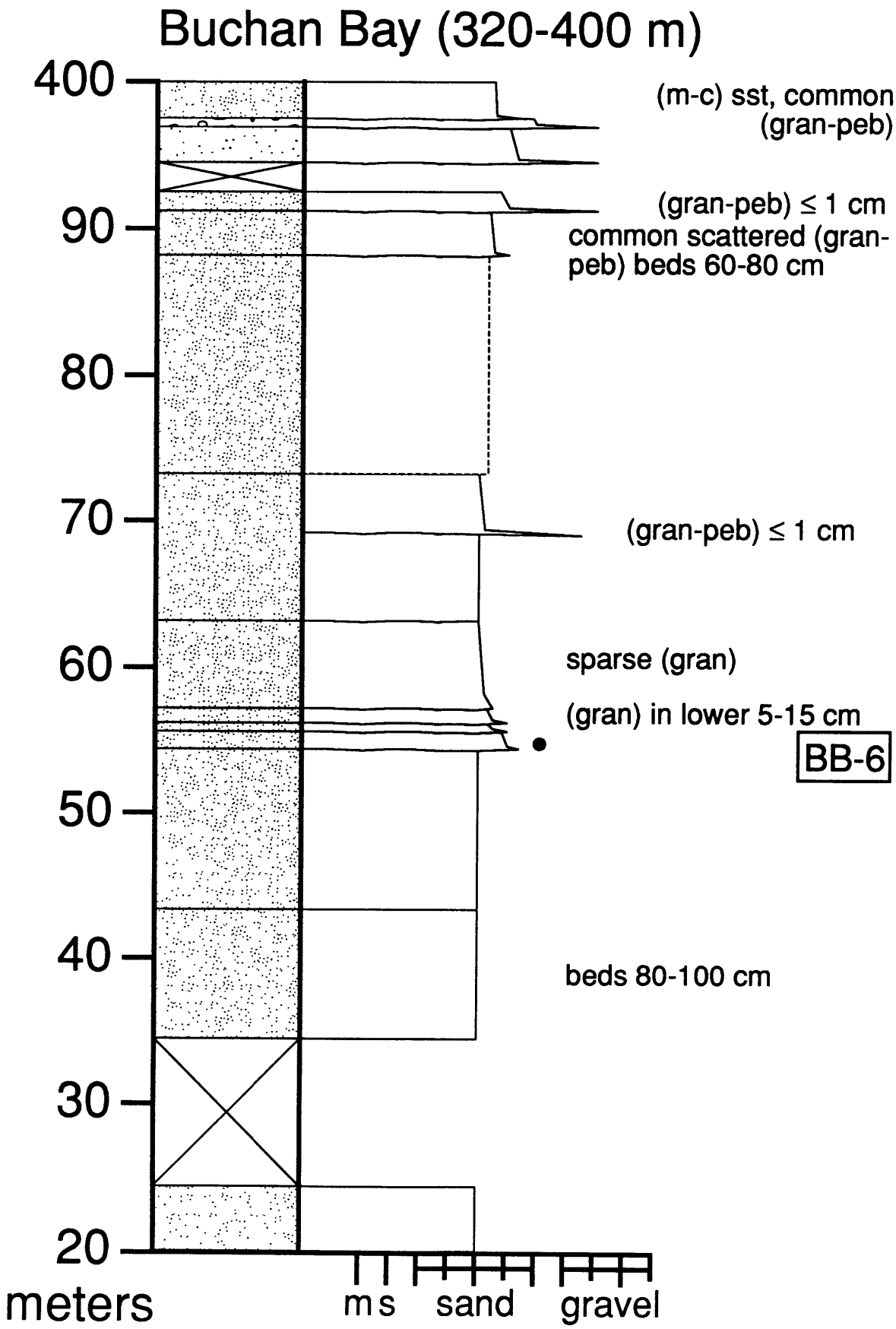
Buchan Bay (320-400 m)
400
90
80
70
60
50
40
30
20
meters
m s
sand
gravel
(m-c) sst, common (gran-peb)
(gran-peb) ≤ 1 cm
common scattered (gran-peb) beds 60-80 cm
(gran-peb) ≤ 1 cm
sparse (gran)
(gran) in lower 5-15 cm
BB-6
beds 80-100 cm

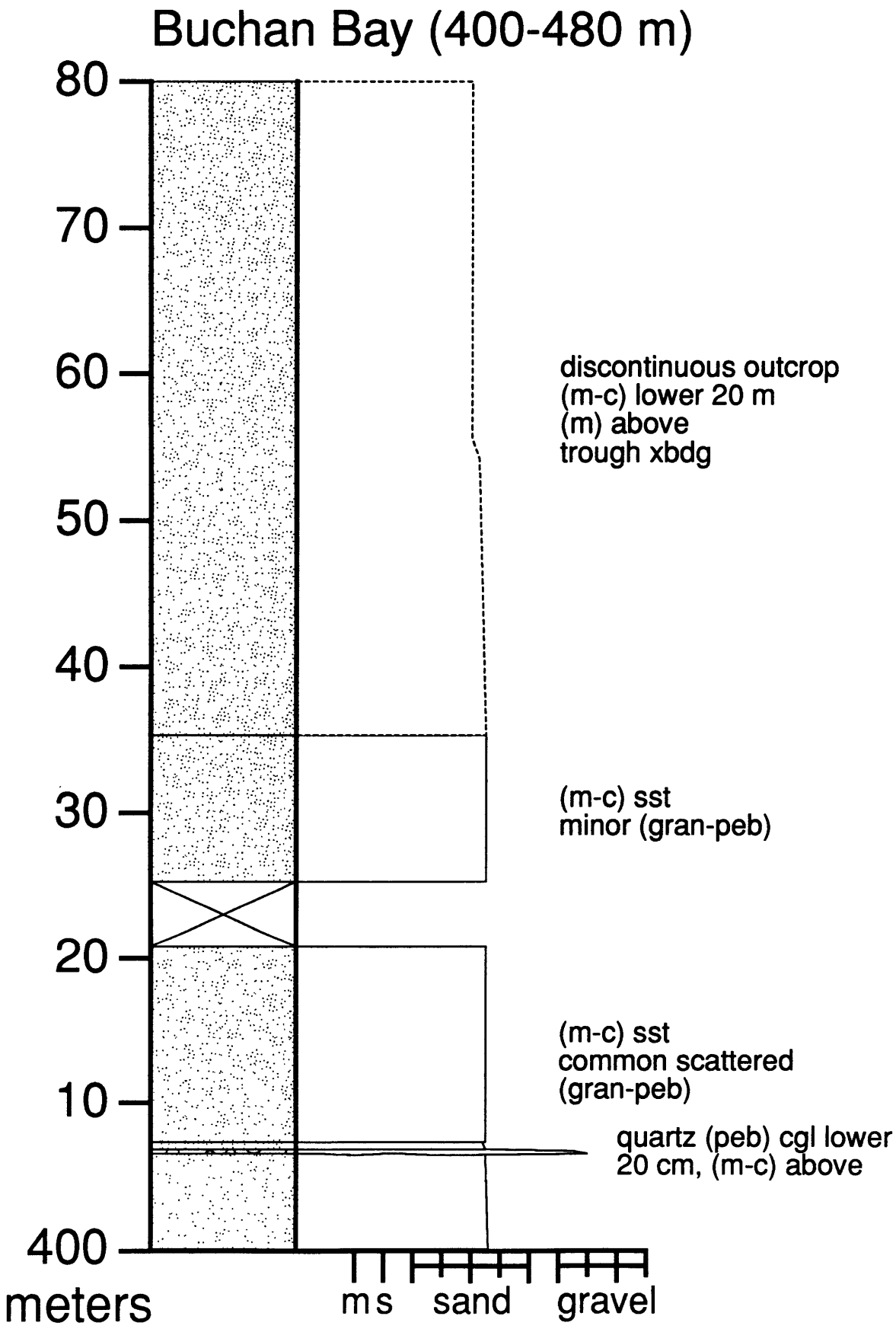
Buchan Bay (400-480 m)
80
70
60
50
40
30
20
10
400
meters
discontinuous outcrop
(m-c) lower 20 m
(m) above
trough xbdg
(m-c) sst
minor (gran-peb)
(m-c) sst
common scattered
(gran-peb)
quartz (peb) cgl lower
20 cm, (m-c) above
ms
sand
gravel

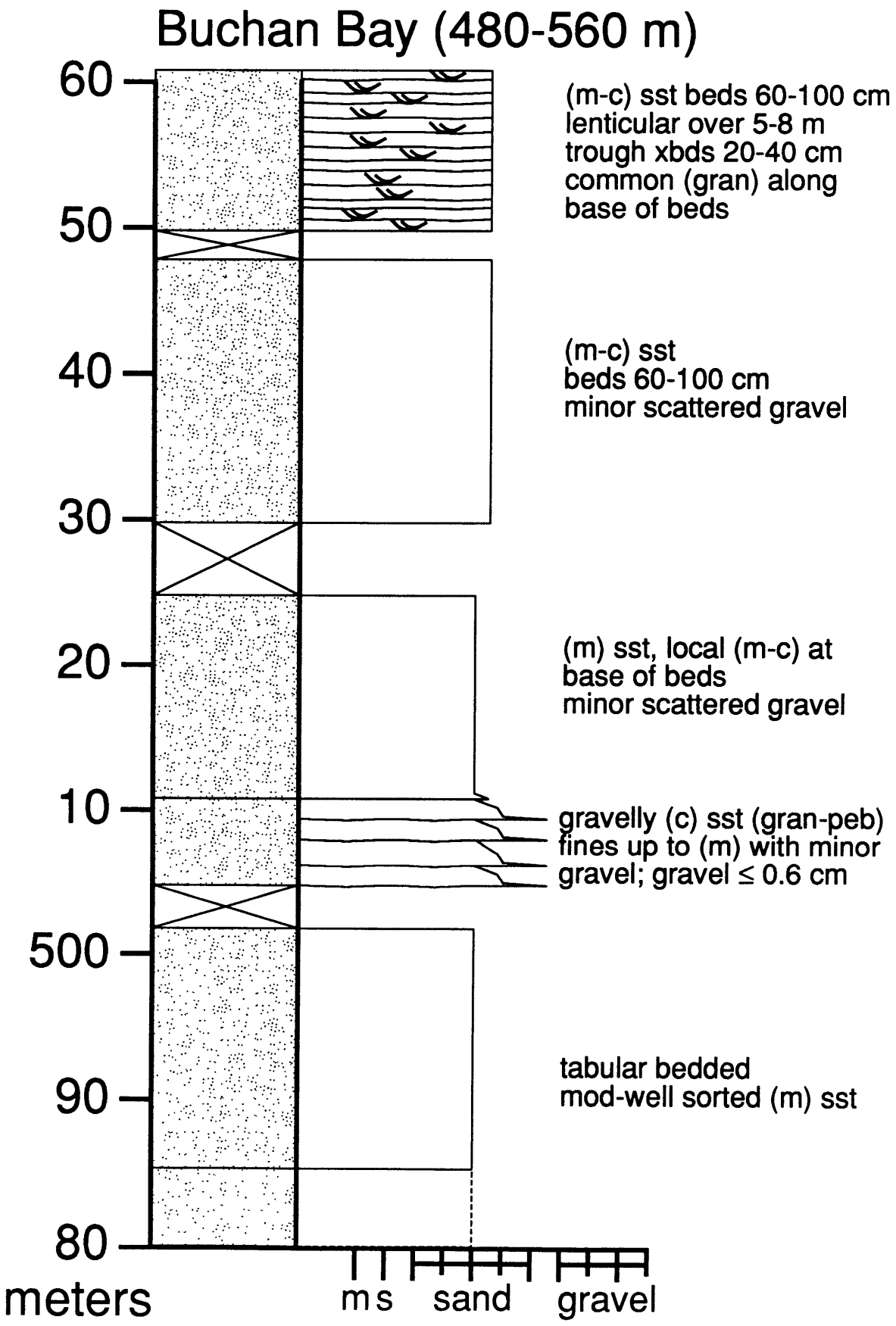
Buchan Bay (480-560 m)
60
50
40
30
20
10
500
90
80
meters
(m-c) sst beds 60-100 cm
lenticular over 5-8 m
trough xbds 20-40 cm
common (gran) along
base of beds
(m-c) sst
beds 60-100 cm
minor scattered gravel
(m) sst, local (m-c) at
base of beds
minor scattered gravel
gravelly (c) sst (gran-peb)
fines up to (m) with minor
gravel; gravel ≤ 0.6 cm
tabular bedded
mod-well sorted (m) sst
m s
sand
gravel

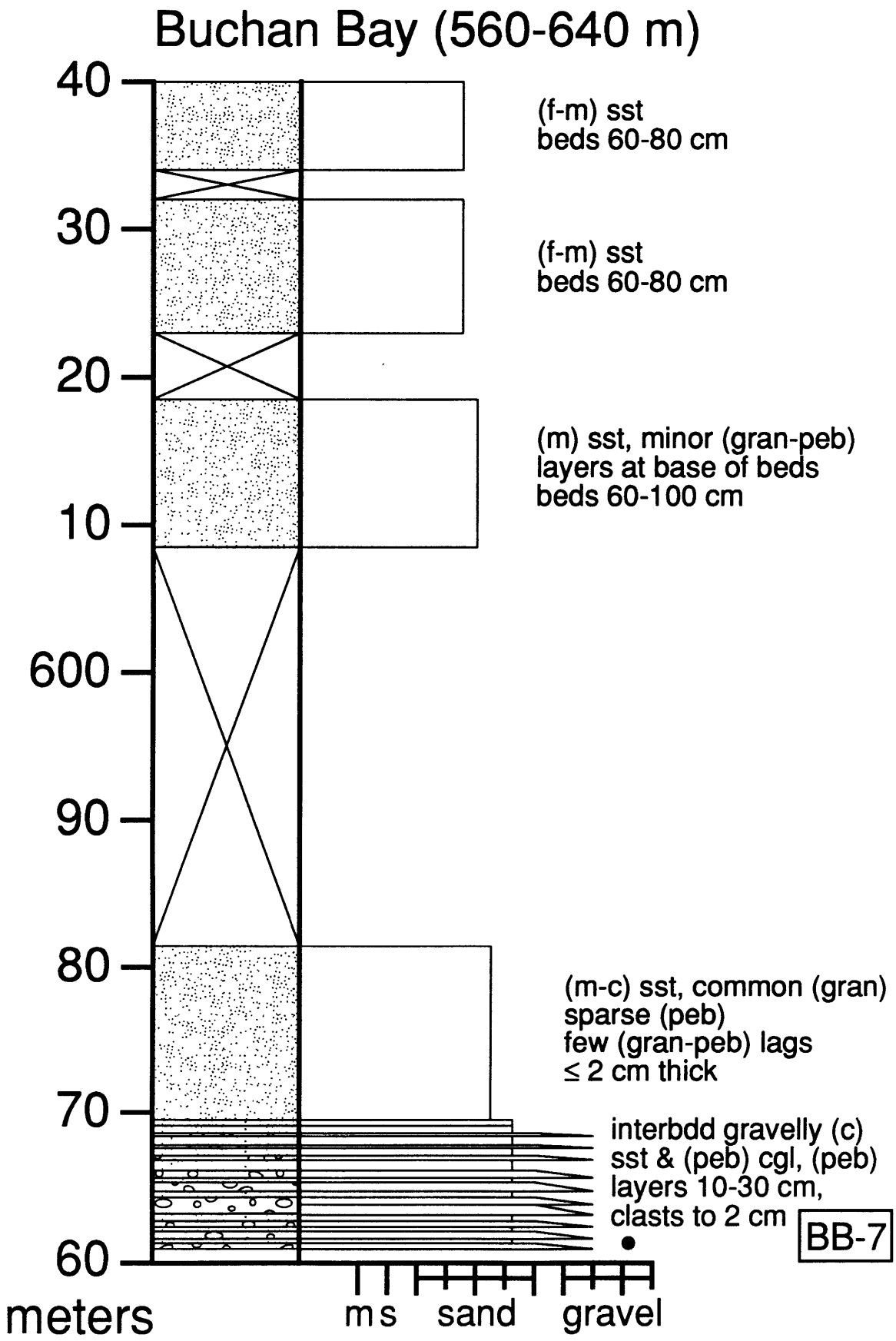
Buchan Bay (560-640 m)
40
30
20
10
600
90
80
70
60
meters
(f-m) sst
beds 60-80 cm
(f-m) sst
beds 60-80 cm
(m) sst, minor (gran-peb)
layers at base of beds
beds 60-100 cm
(m-c) sst, common (gran)
sparse (peb)
few (gran-peb) lags
≤ 2 cm thick
interbdd gravelly (c)
sst & (peb) cgl, (peb)
layers 10-30 cm,
clasts to 2 cm
BB-7
m s
sand
gravel

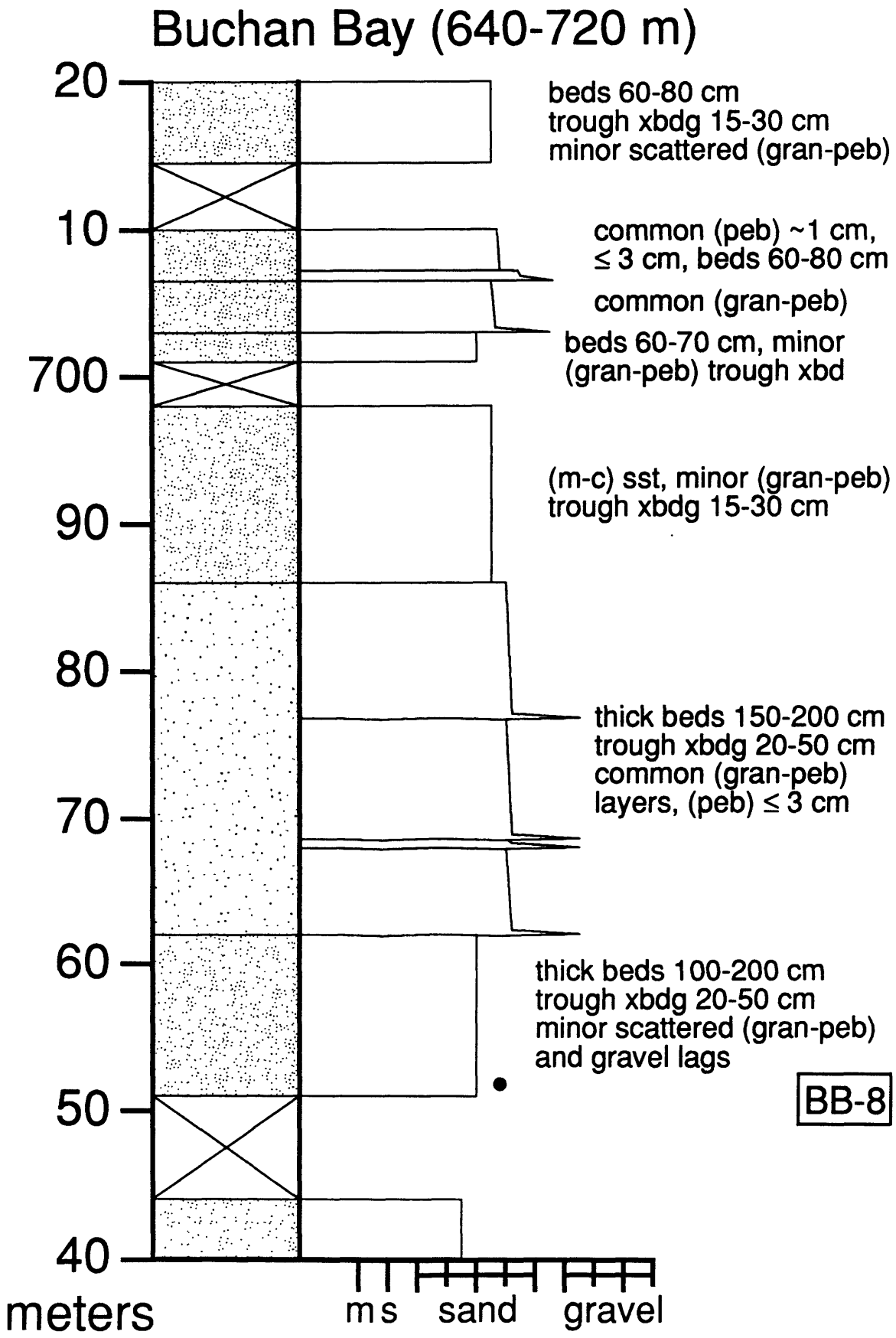
Buchan Bay (640-720 m)
20
10
700
90
80
70
60
50
40
meters
beds 60-80 cm
trough xbdg 15-30 cm
minor scattered (gran-peb)
common (peb) ~1 cm,
≤ 3 cm, beds 60-80 cm
common (gran-peb)
beds 60-70 cm, minor
(gran-peb) trough xbd
(m-c) sst, minor (gran-peb)
trough xbdg 15-30 cm
thick beds 150-200 cm
trough xbdg 20-50 cm
common (gran-peb)
layers, (peb) ≤ 3 cm
thick beds 100-200 cm
trough xbdg 20-50 cm
minor scattered (gran-peb)
and gravel lags
BB-8
ms
sand
gravel

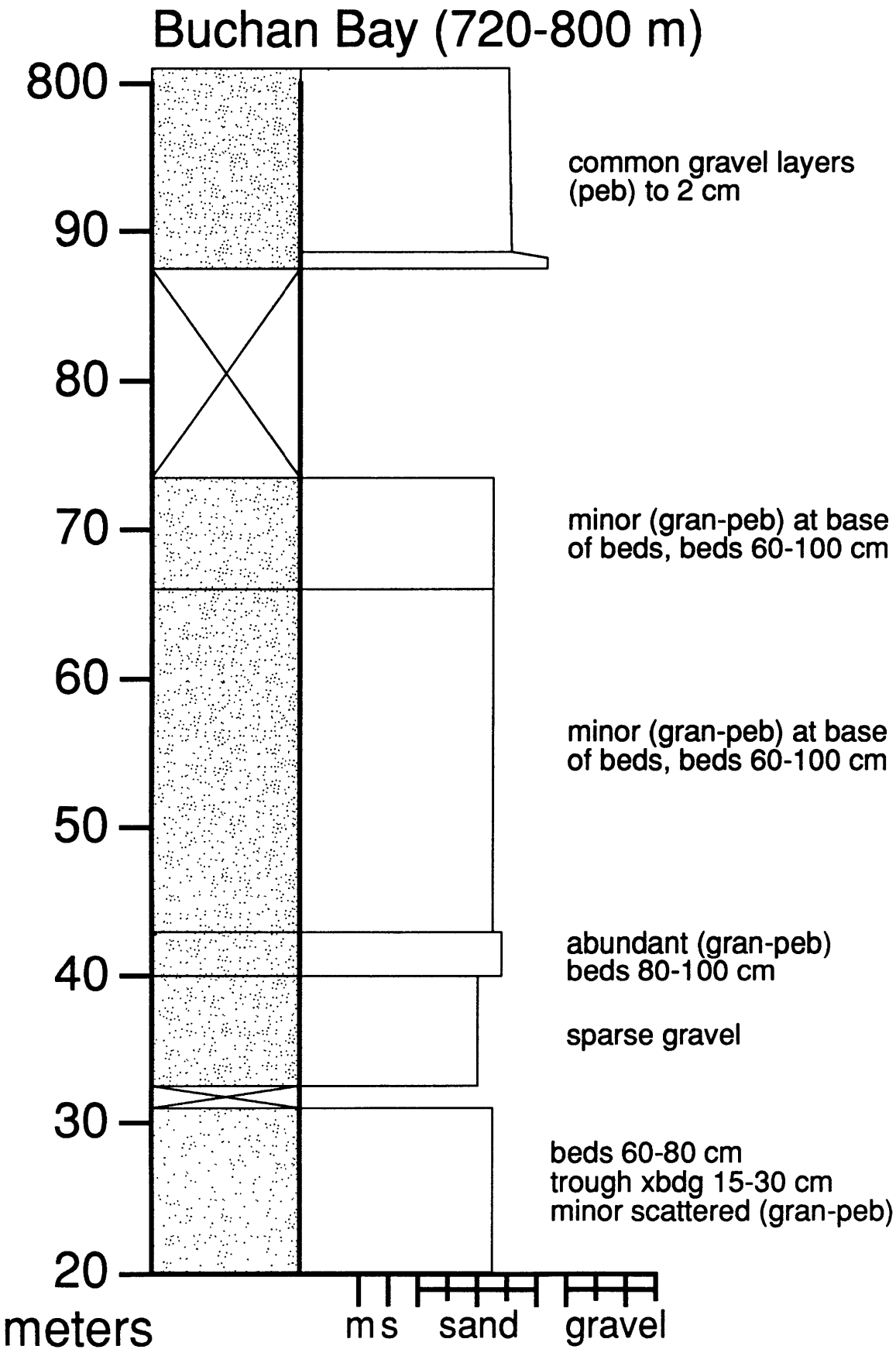
Buchan Bay (720-800 m)
800
90
80
70
60
50
40
30
20
meters
common gravel layers
(peb) to 2 cm
minor (gran-peb) at base
of beds, beds 60-100 cm
minor (gran-peb) at base
of beds, beds 60-100 cm
abundant (gran-peb)
beds 80-100 cm
sparse gravel
beds 60-80 cm
trough xbdg 15-30 cm
minor scattered (gran-peb)
ms
sand
gravel

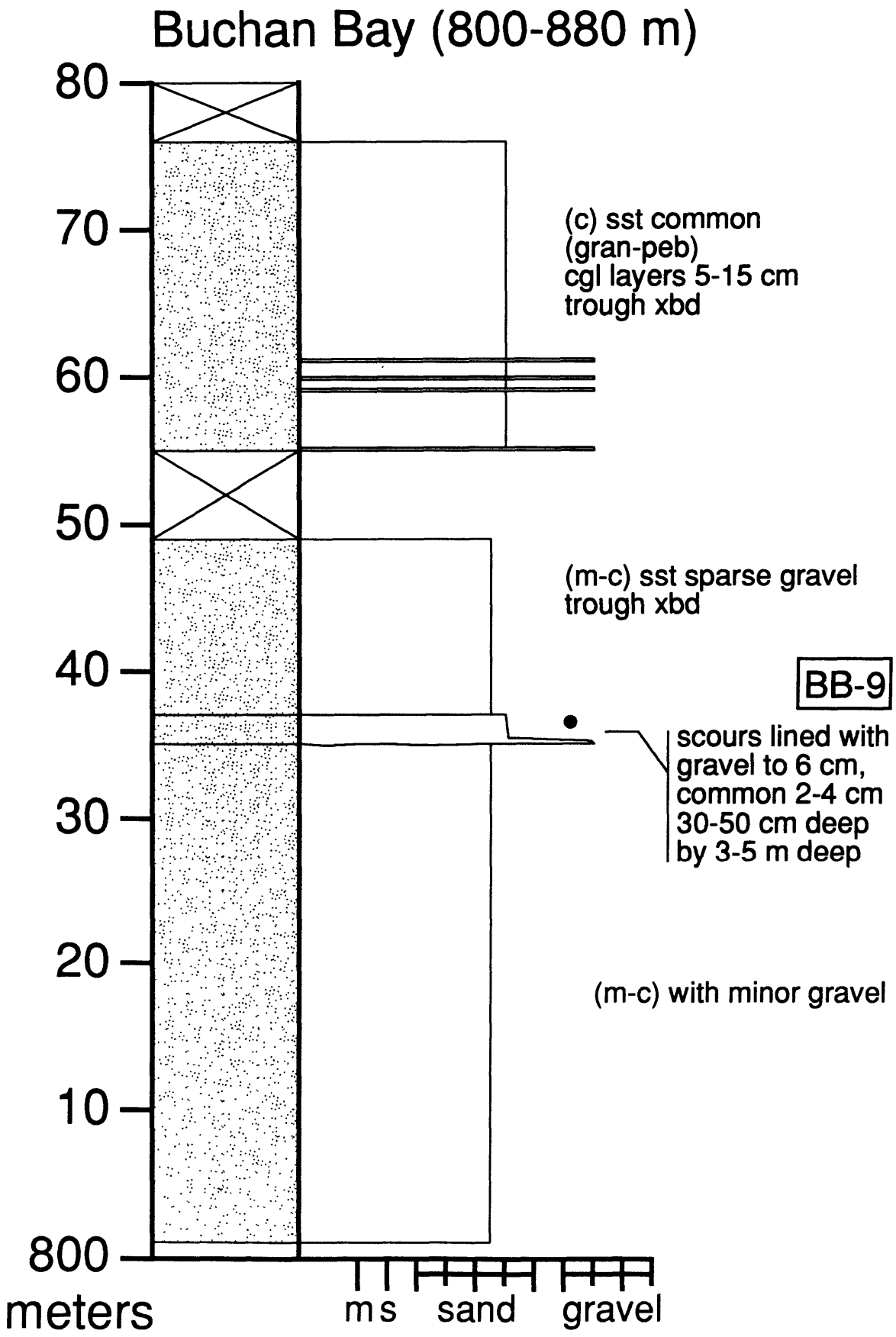
Buchan Bay (800-880 m)
80
70
60
50
40
30
20
10
800
meters
(c) sst common
(gran-peb)
cgl layers 5-15 cm
trough xbd
(m-c) sst sparse gravel
trough xbd
BB-9
scours lined with
gravel to 6 cm,
common 2-4 cm
30-50 cm deep
by 3-5 m deep
(m-c) with minor gravel
ms
sand
gravel

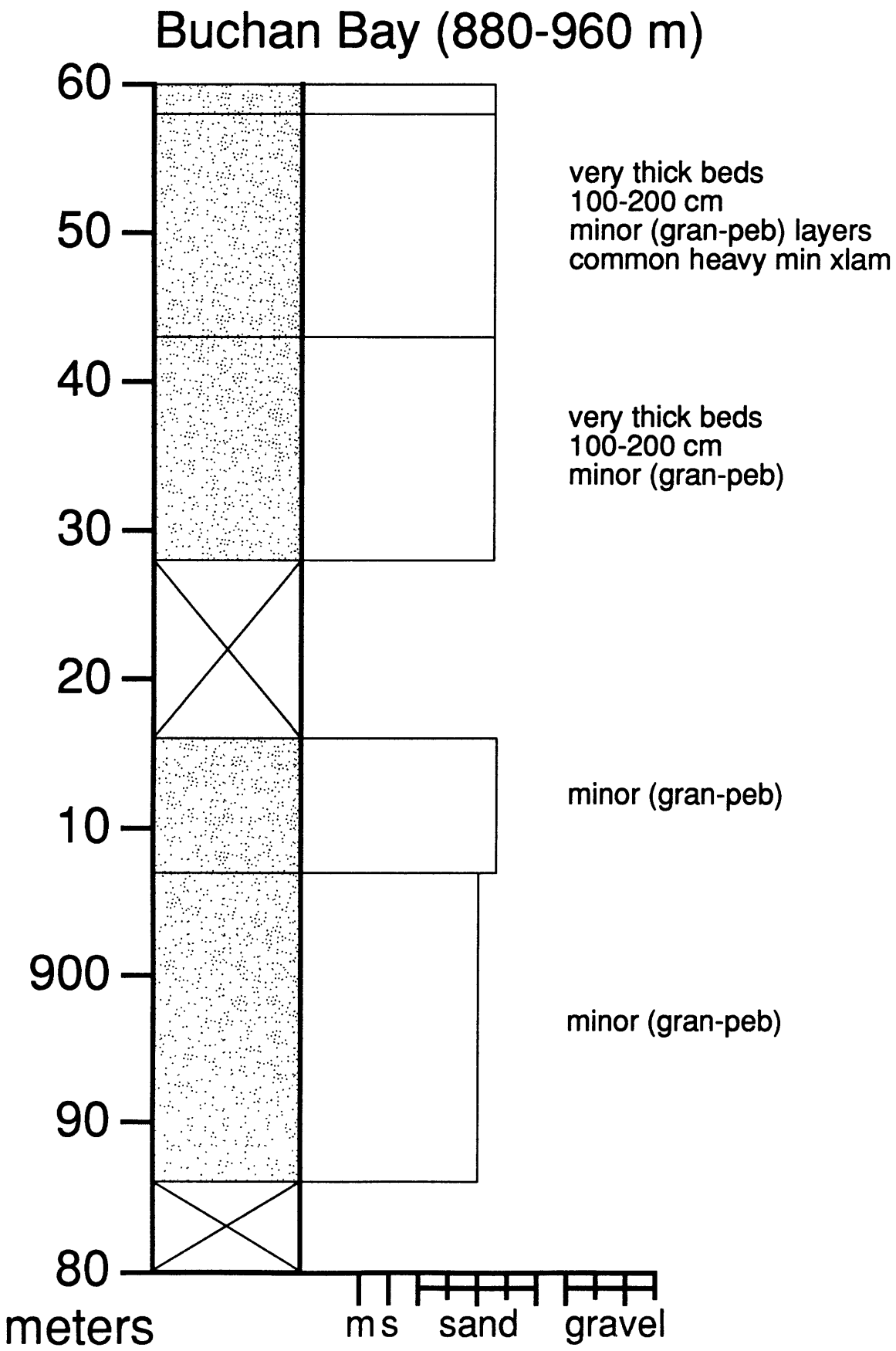
Buchan Bay (880-960 m)
60
50
40
30
20
10
900
90
80
meters
very thick beds
100-200 cm
minor (gran-peb) layers
common heavy min xlam
very thick beds
100-200 cm
minor (gran-peb)
minor (gran-peb)
minor (gran-peb)
m s
sand
gravel

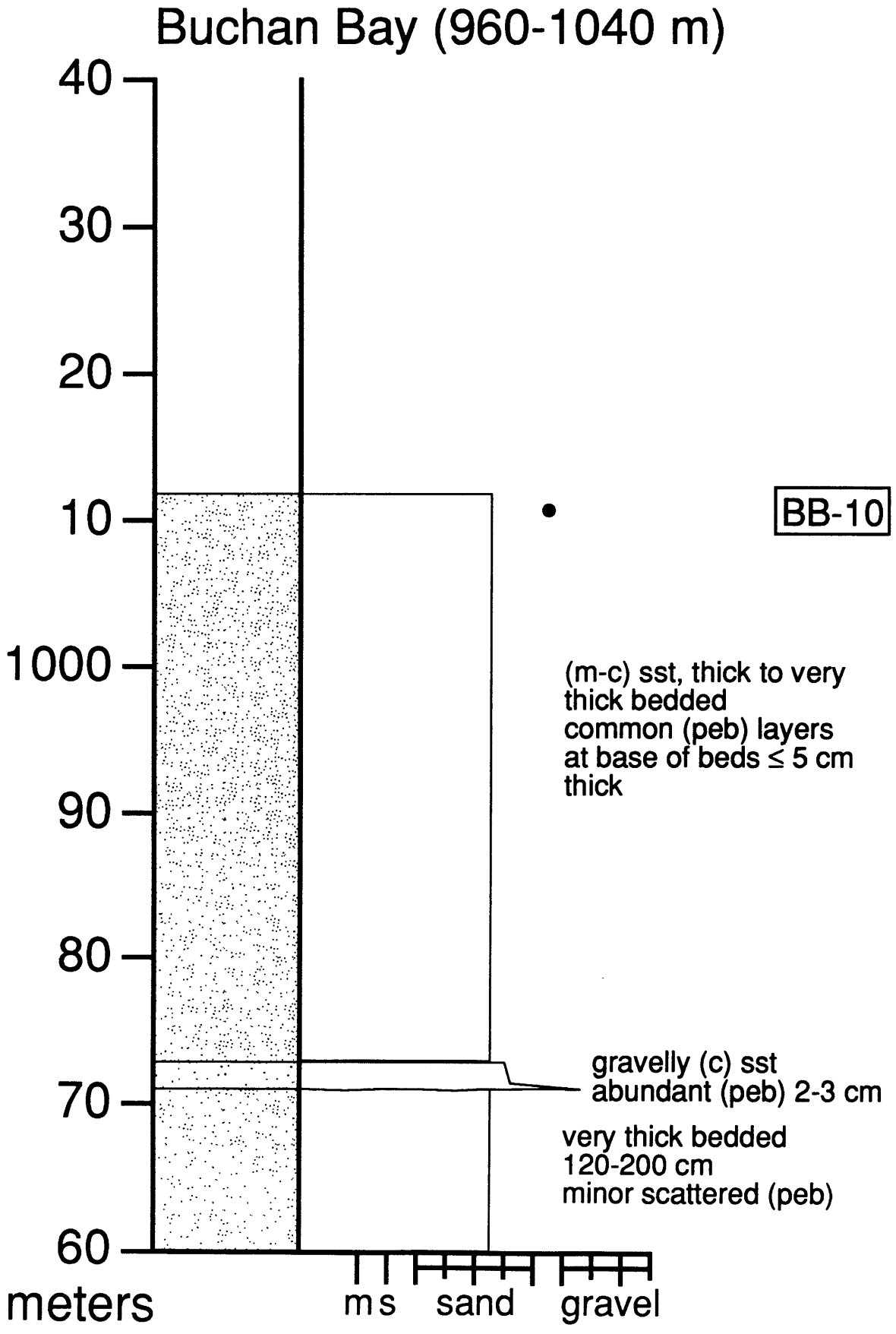
Buchan Bay (960-1040 m)
40
30
20
10
1000
90
80
70
60
meters
BB-10
(m-c) sst, thick to very thick bedded
common (peb) layers
at base of beds ≤ 5 cm thick
gravelly (c) sst
abundant (peb) 2-3 cm
very thick bedded
120-200 cm
minor scattered (peb)
m s
sand
gravel

section 16: Wilberforce Hills

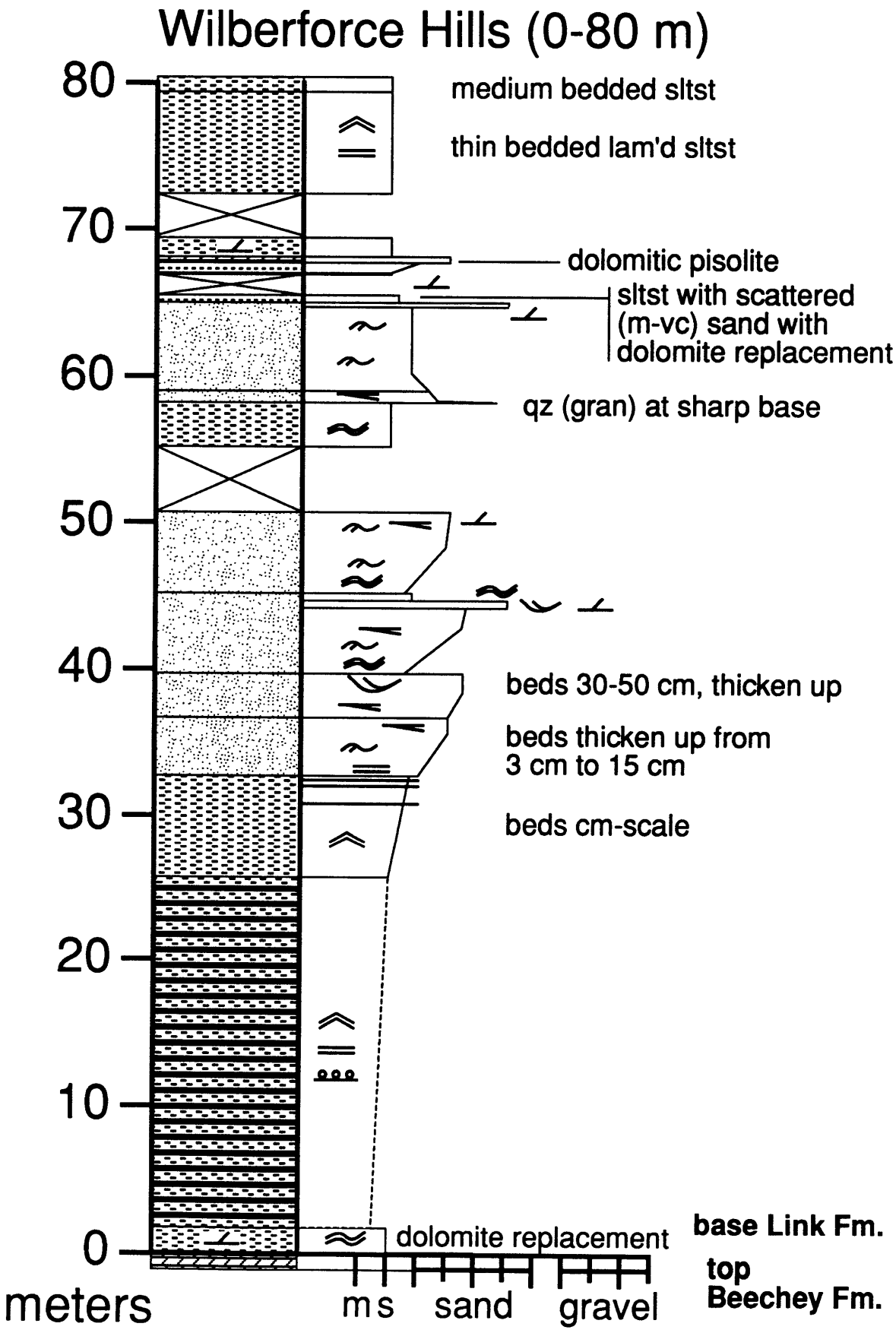
Wilberforce Hills (0-80 m)
80
70
60
50
40
30
20
10
0
meters
medium bedded sltst
thin bedded lam'd sltst
dolomitic pisolite
sltst with scattered
(m-vc) sand with
dolomite replacement
qz (gran) at sharp base
beds 30-50 cm, thicken up
beds thicken up from
3 cm to 15 cm
beds cm-scale
dolomite replacement
base Link Fm.
top
Beechey Fm.
m s
sand
gravel

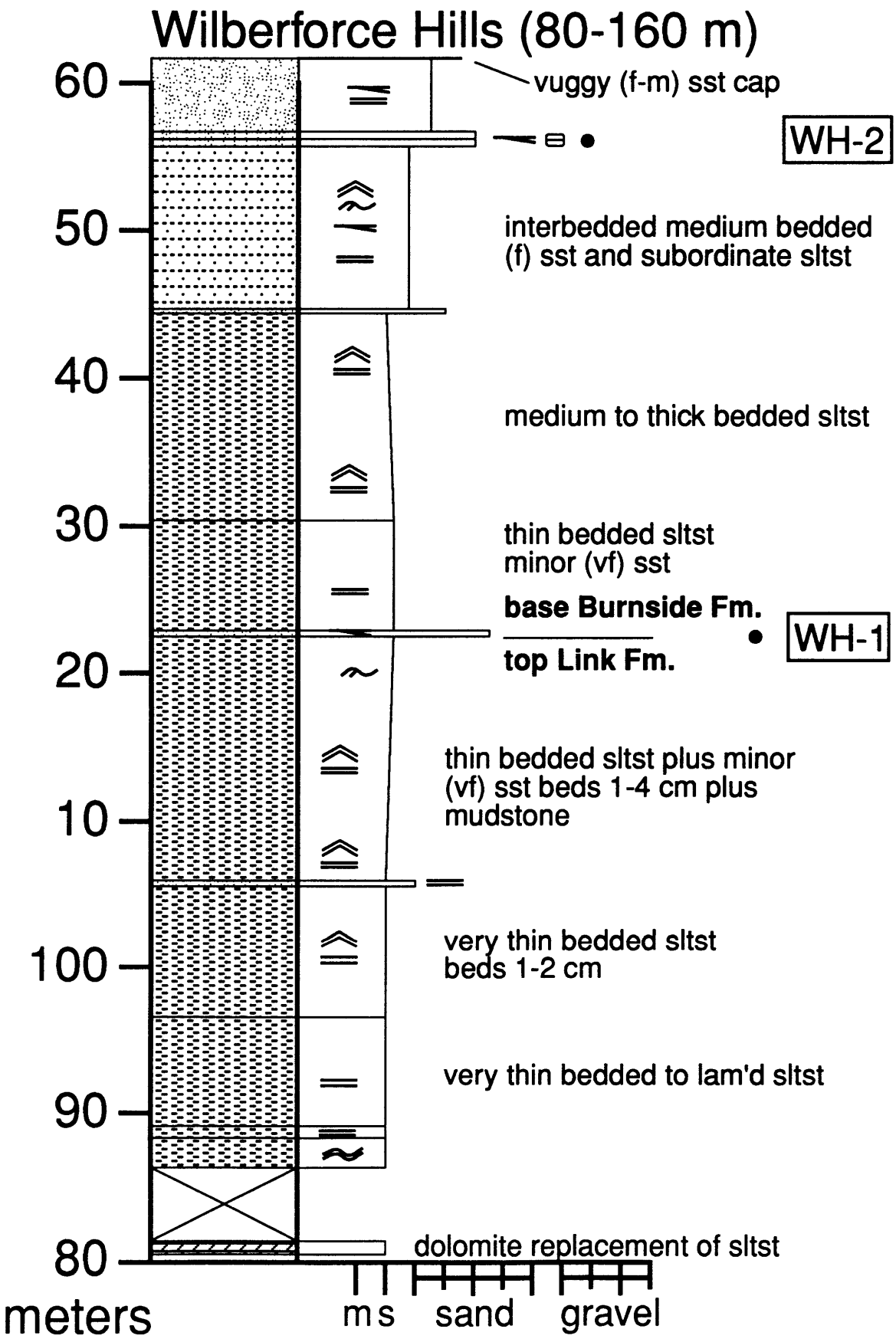
Wilberforce Hills (80-160 m)
60
50
40
30
20
10
100
90
80
meters
vuggy (f-m) sst cap
WH-2
interbedded medium bedded (f) sst and subordinate sltst
medium to thick bedded sltst
thin bedded sltst
minor (vf) sst
base Burnside Fm.
top Link Fm.
WH-1
thin bedded sltst plus minor (vf) sst beds 1-4 cm plus mudstone
very thin bedded sltst beds 1-2 cm
very thin bedded to lam'd sltst
dolomite replacement of sltst
m s
sand
gravel

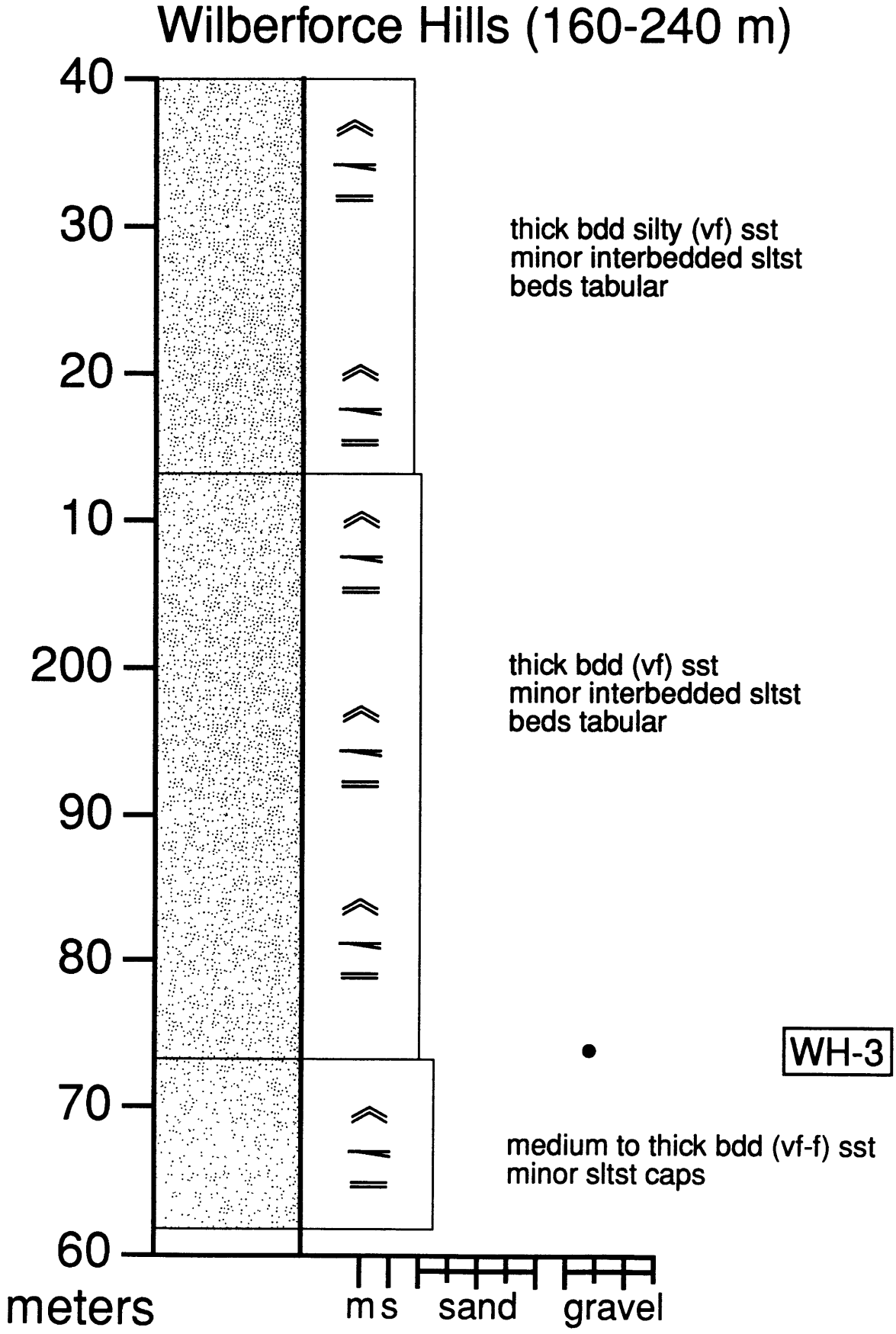
Wilberforce Hills (160-240 m)
40
30
20
10
200
90
80
70
60
meters
thick bdd silty (vf) sst
minor interbedded sltst
beds tabular
thick bdd (vf) sst
minor interbedded sltst
beds tabular
WH-3
medium to thick bdd (vf-f) sst
minor sltst caps
m s
sand
gravel

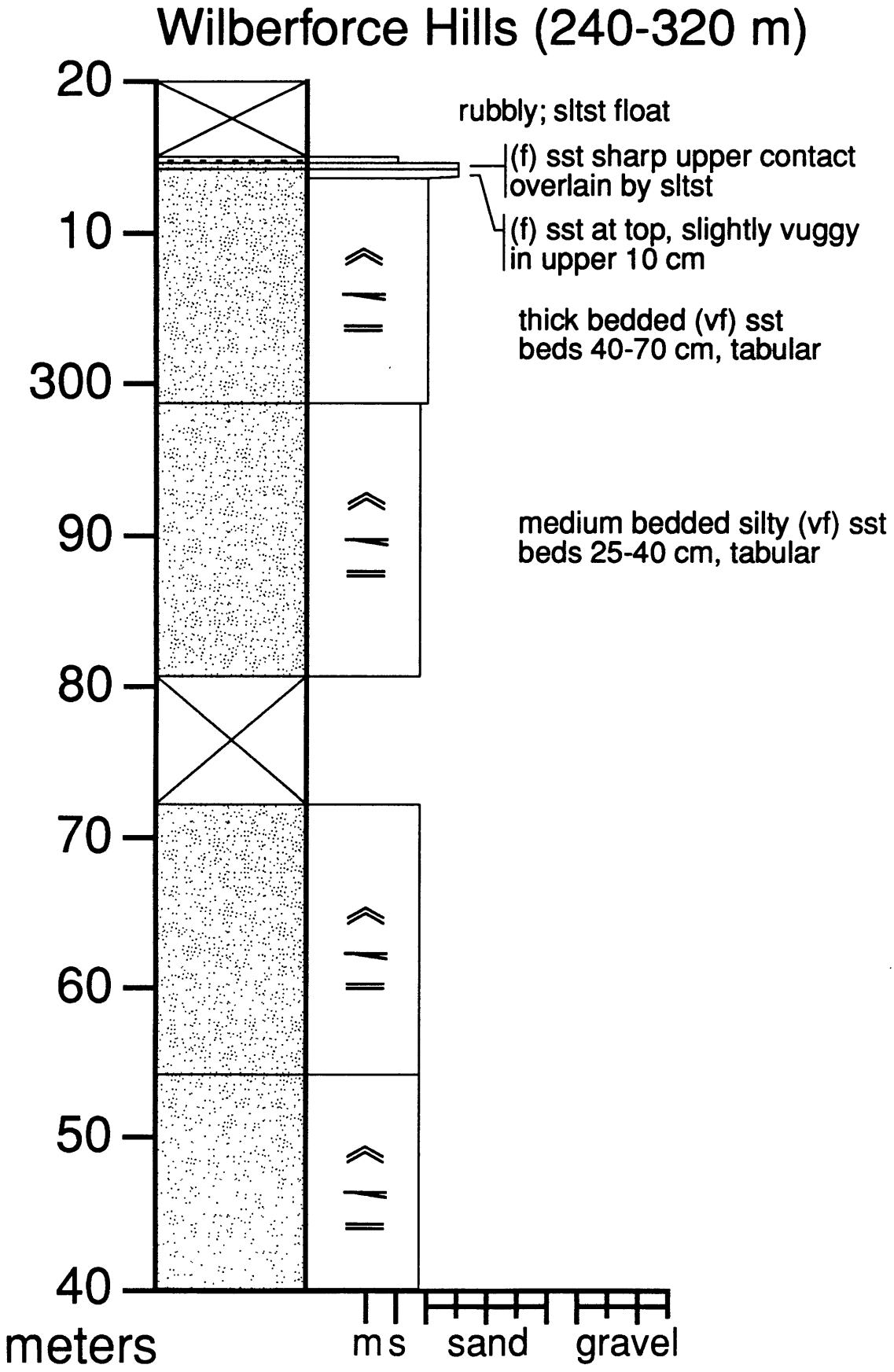
Wilberforce Hills (240-320 m)
20
10
300
90
80
70
60
50
40
meters
rubbly; sltst float
(f) sst sharp upper contact
overlain by sltst
(f) sst at top, slightly vuggy
in upper 10 cm
thick bedded (vf) sst
beds 40-70 cm, tabular
medium bedded silty (vf) sst
beds 25-40 cm, tabular
m s
sand
gravel

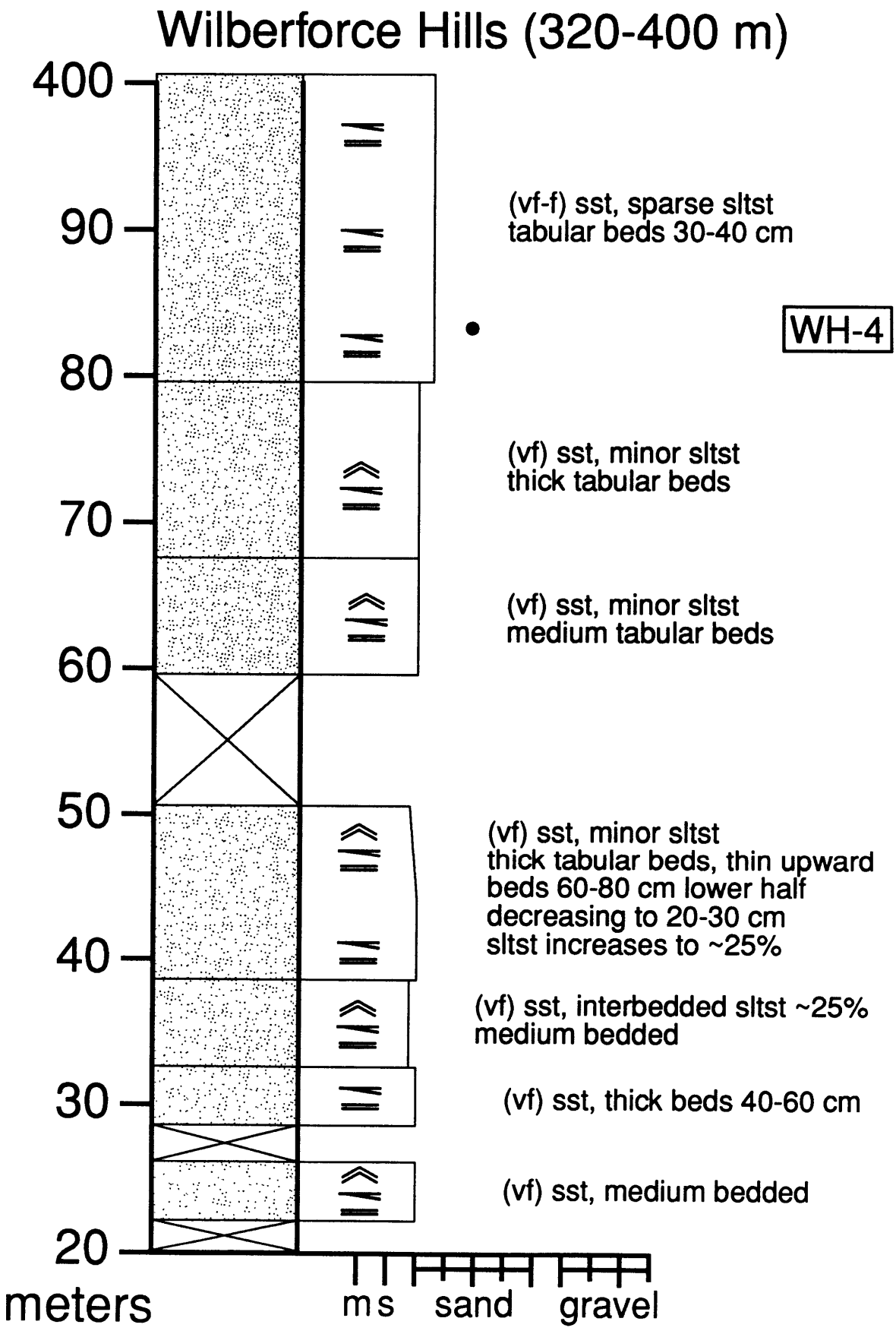
Wilberforce Hills (320-400 m)
400
90
80
70
60
50
40
30
20
meters
(vf-f) sst, sparse sltst
tabular beds 30-40 cm
WH-4
(vf) sst, minor sltst
thick tabular beds
(vf) sst, minor sltst
medium tabular beds
(vf) sst, minor sltst
thick tabular beds, thin upward
beds 60-80 cm lower half
decreasing to 20-30 cm
sltst increases to ~25%
(vf) sst, interbedded sltst ~25%
medium bedded
(vf) sst, thick beds 40-60 cm
(vf) sst, medium bedded
m s
sand
gravel

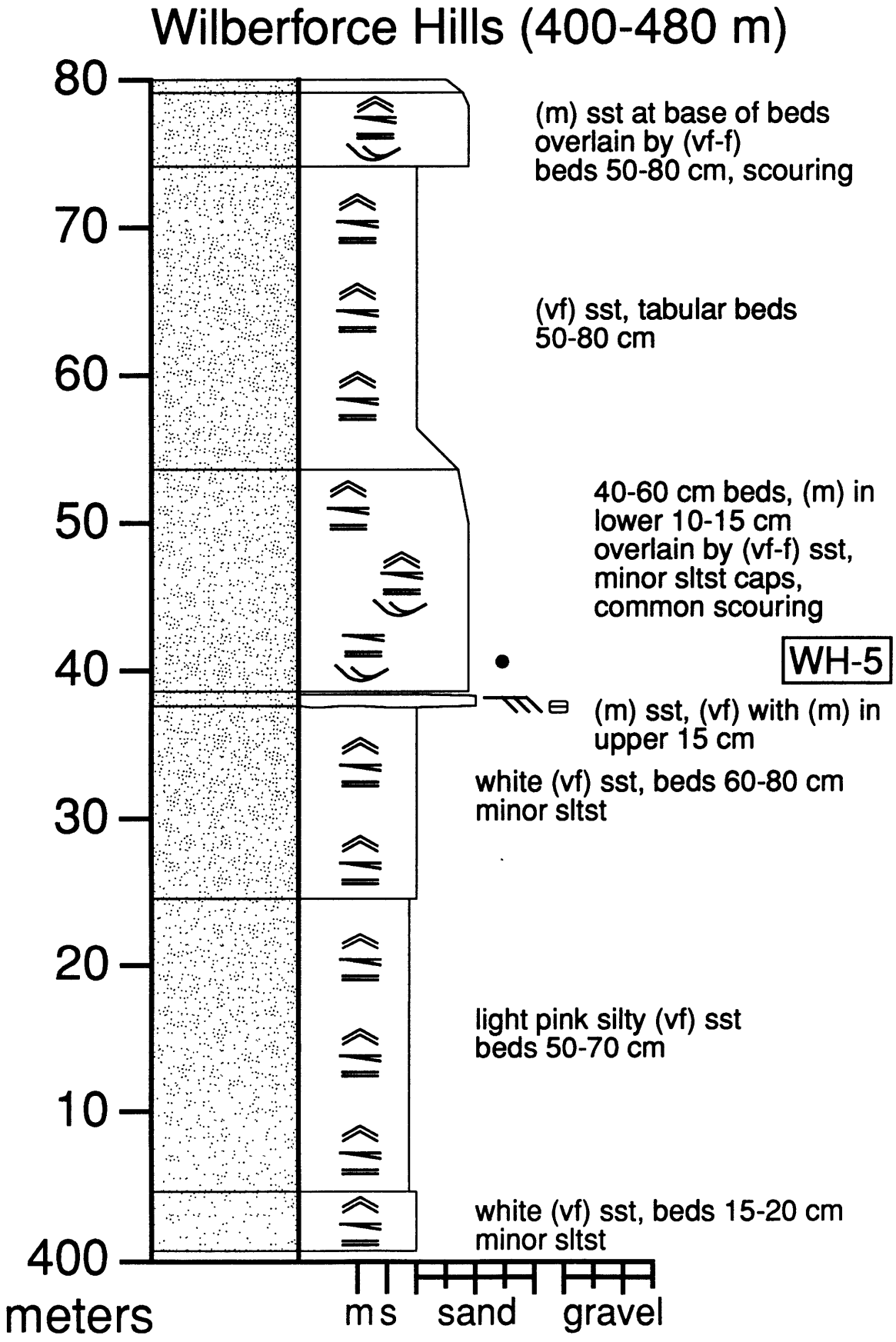
Wilberforce Hills (400-480 m)
80
70
60
50
40
30
20
10
400
meters
(m) sst at base of beds overlain by (vf-f) beds 50-80 cm, scouring
(vf) sst, tabular beds 50-80 cm
40-60 cm beds, (m) in lower 10-15 cm overlain by (vf-f) sst, minor sltst caps, common scouring
WH-5
(m) sst, (vf) with (m) in upper 15 cm
white (vf) sst, beds 60-80 cm minor sltst
light pink silty (vf) sst beds 50-70 cm
white (vf) sst, beds 15-20 cm minor sltst
m s
sand
gravel

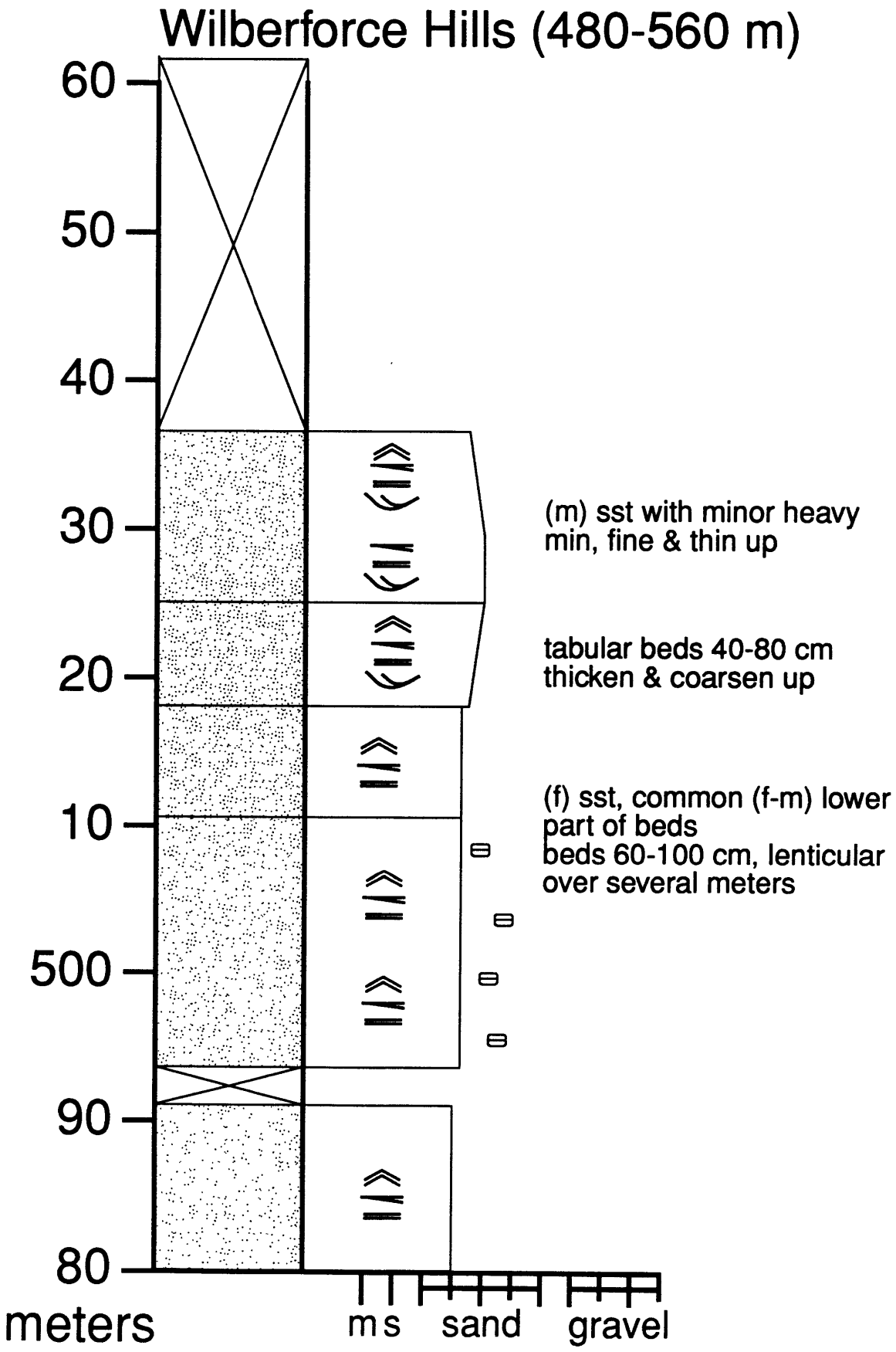
Wilberforce Hills (480-560 m)
60
50
40
30
20
10
500
90
80
meters
(m) sst with minor heavy min, fine & thin up
tabular beds 40-80 cm thicken & coarsen up
(f) sst, common (f-m) lower part of beds
beds 60-100 cm, lenticular over several meters
m s
sand
gravel

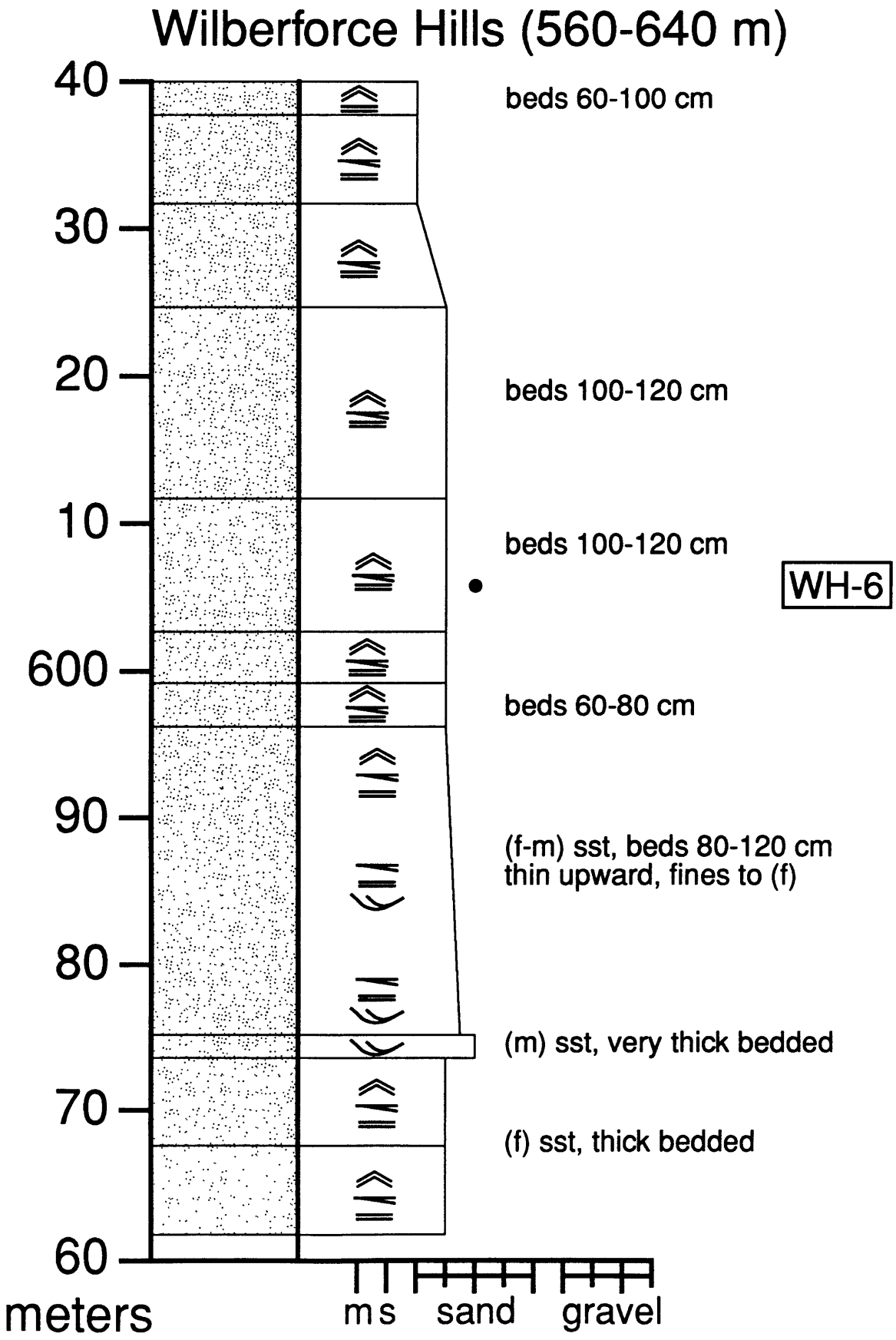
Wilberforce Hills (560-640 m)
40
30
20
10
600
90
80
70
60
meters
beds 60-100 cm
beds 100-120 cm
beds 100-120 cm
WH-6
beds 60-80 cm
(f-m) sst, beds 80-120 cm
thin upward, fines to (f)
(m) sst, very thick bedded
(f) sst, thick bedded
m s
sand
gravel

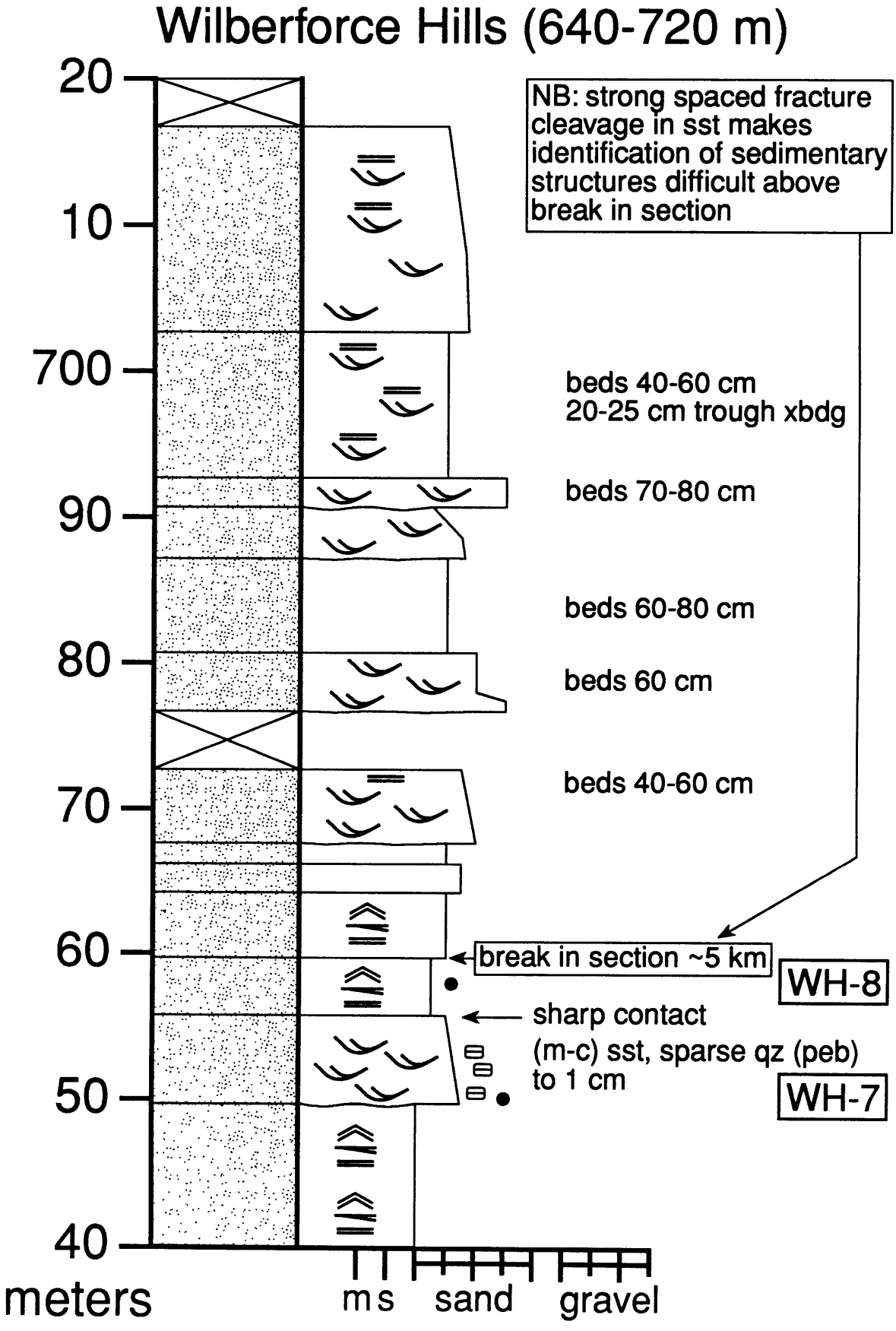
Wilberforce Hills (640-720 m)
20
10
700
90
80
70
60
50
40
meters
NB: strong spaced fracture cleavage in sst makes identification of sedimentary structures difficult above break in section
beds 40-60 cm
20-25 cm trough xbdg
beds 70-80 cm
beds 60-80 cm
beds 60 cm
beds 40-60 cm
break in section ~5 km
WH-8
sharp contact
(m-c) sst, sparse qz (peb) to 1 cm
WH-7
ms
sand
gravel

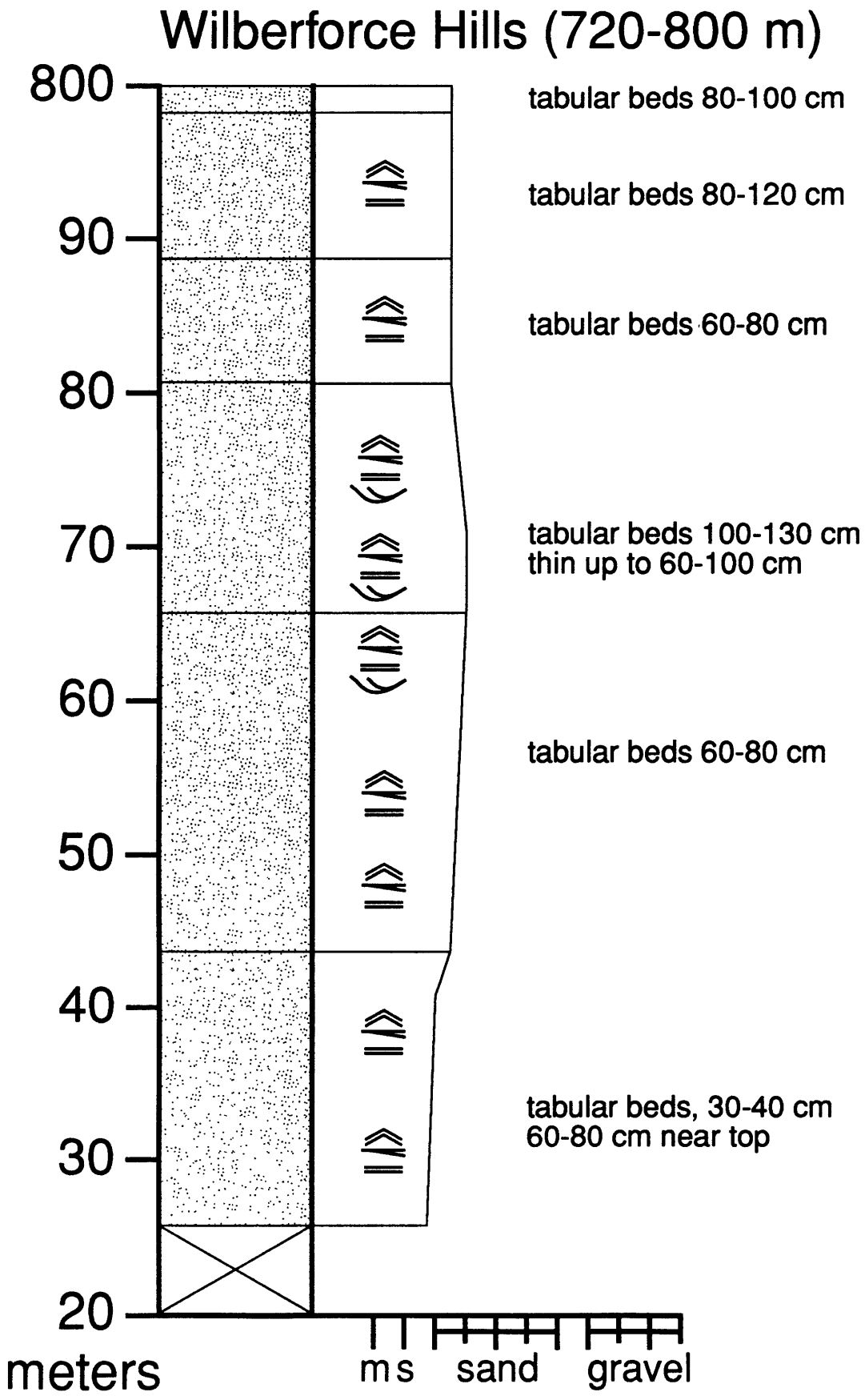
Wilberforce Hills (720-800 m)
800
90
80
70
60
50
40
30
20
meters
tabular beds 80-100 cm
tabular beds 80-120 cm
tabular beds 60-80 cm
tabular beds 100-130 cm
thin up to 60-100 cm
tabular beds 60-80 cm
tabular beds, 30-40 cm
60-80 cm near top
m s
sand
gravel

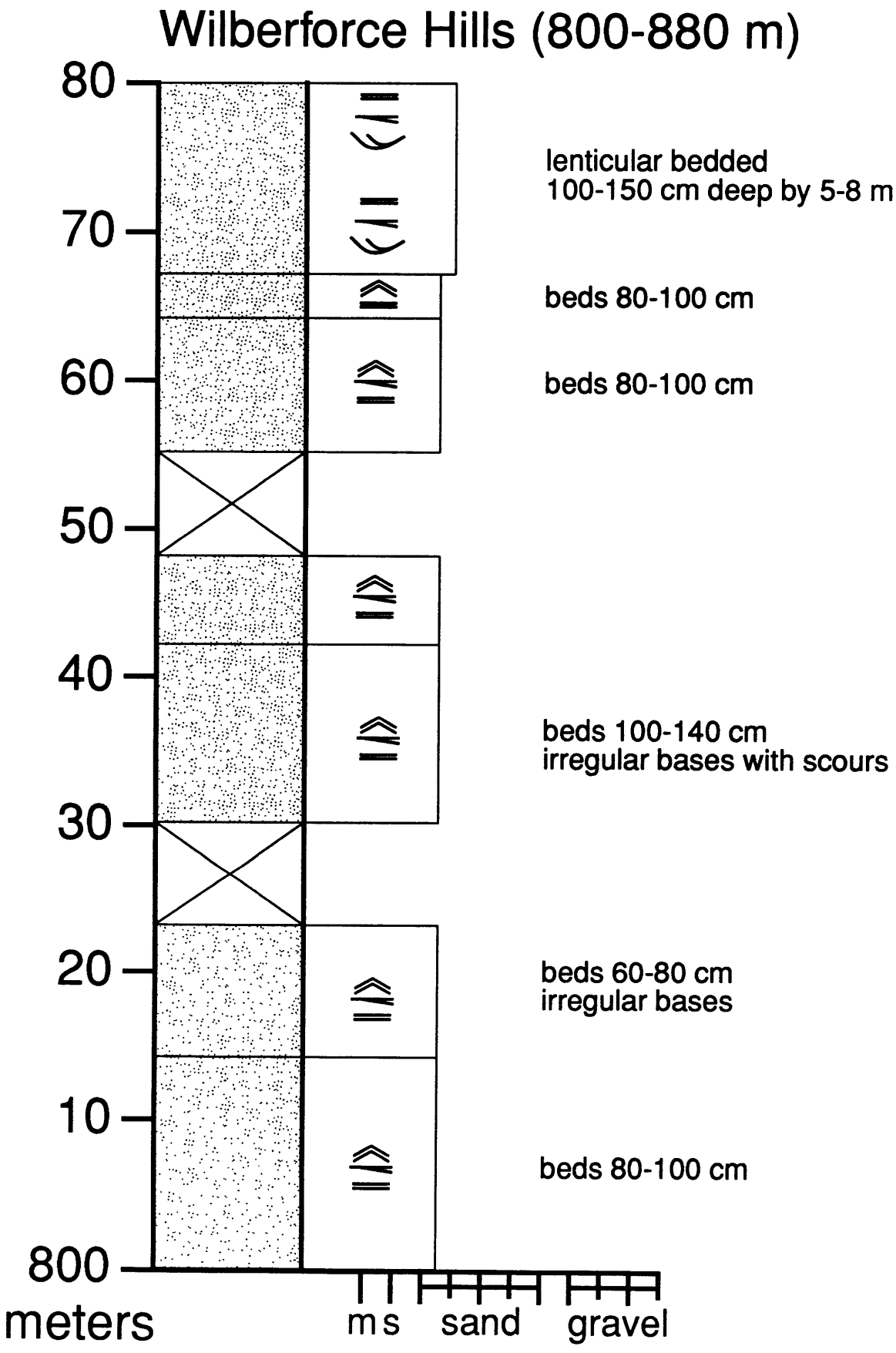
Wilberforce Hills (800-880 m)
80
70
60
50
40
30
20
10
800
meters
lenticular bedded
100-150 cm deep by 5-8 m
beds 80-100 cm
beds 80-100 cm
beds 100-140 cm
irregular bases with scours
beds 60-80 cm
irregular bases
beds 80-100 cm
m s
sand
gravel

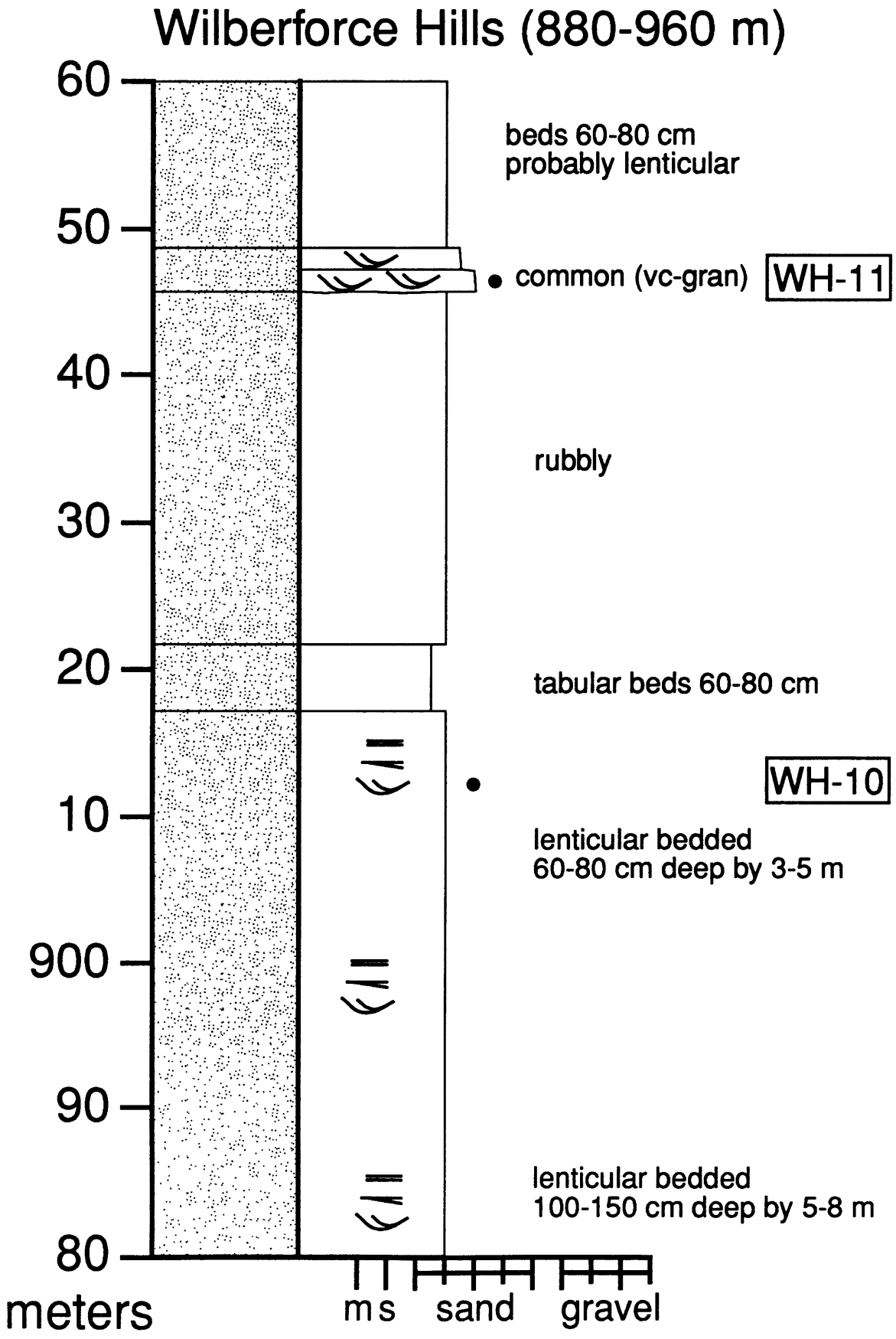
Wilberforce Hills (880-960 m)
60
50
40
30
20
10
900
90
80
meters
beds 60-80 cm
probably lenticular
common (vc-gran)
WH-11
rubbly
tabular beds 60-80 cm
WH-10
lenticular bedded
60-80 cm deep by 3-5 m
lenticular bedded
100-150 cm deep by 5-8 m
m s
sand
gravel

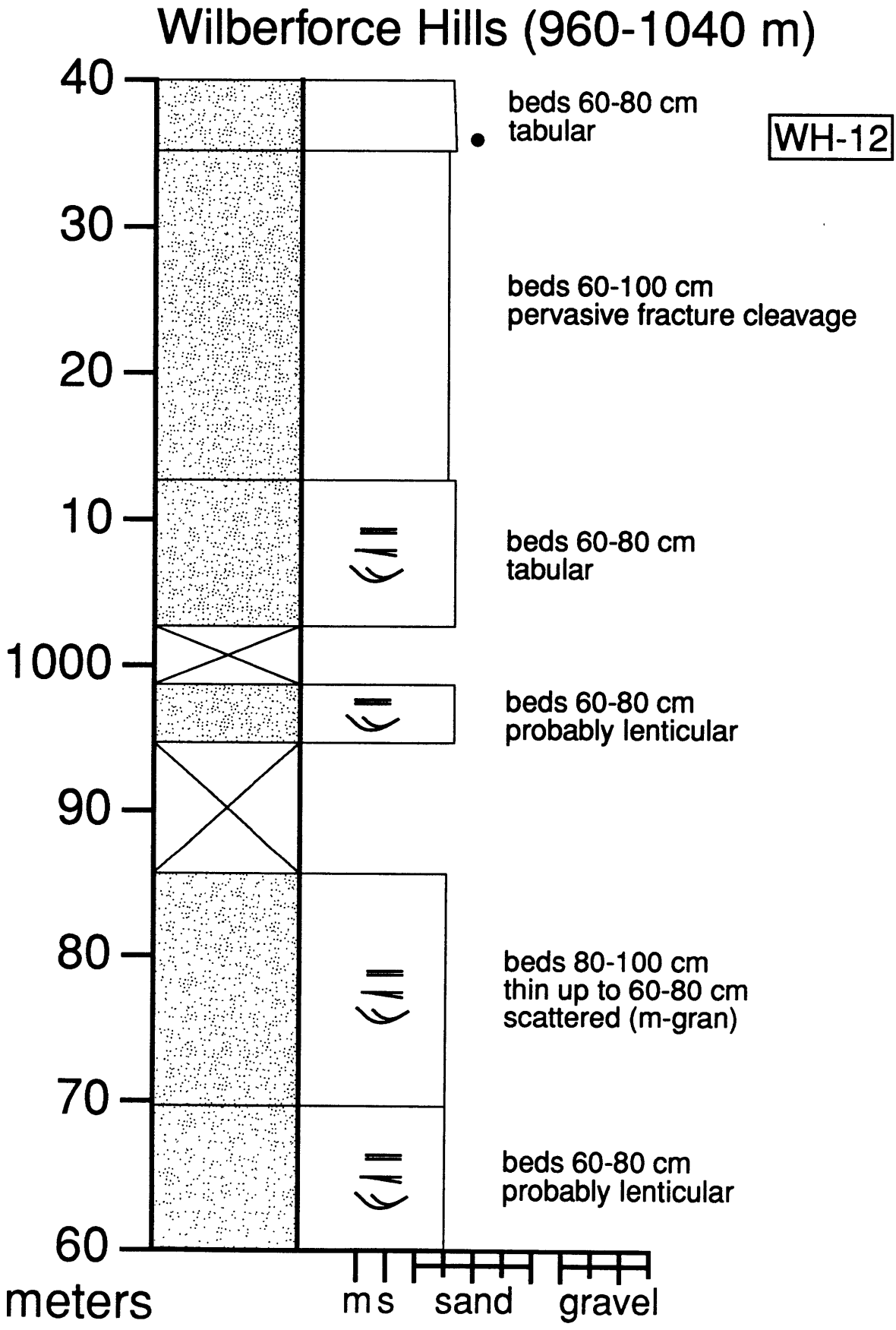
Wilberforce Hills (960-1040 m)
40
30
20
10
1000
90
80
70
60
meters
beds 60-80 cm
tabular
WH-12
beds 60-100 cm
pervasive fracture cleavage
beds 60-80 cm
tabular
beds 60-80 cm
probably lenticular
beds 80-100 cm
thin up to 60-80 cm
scattered (m-gran)
beds 60-80 cm
probably lenticular
m s
sand
gravel

Wilberforce Hills (1040-1120 m)

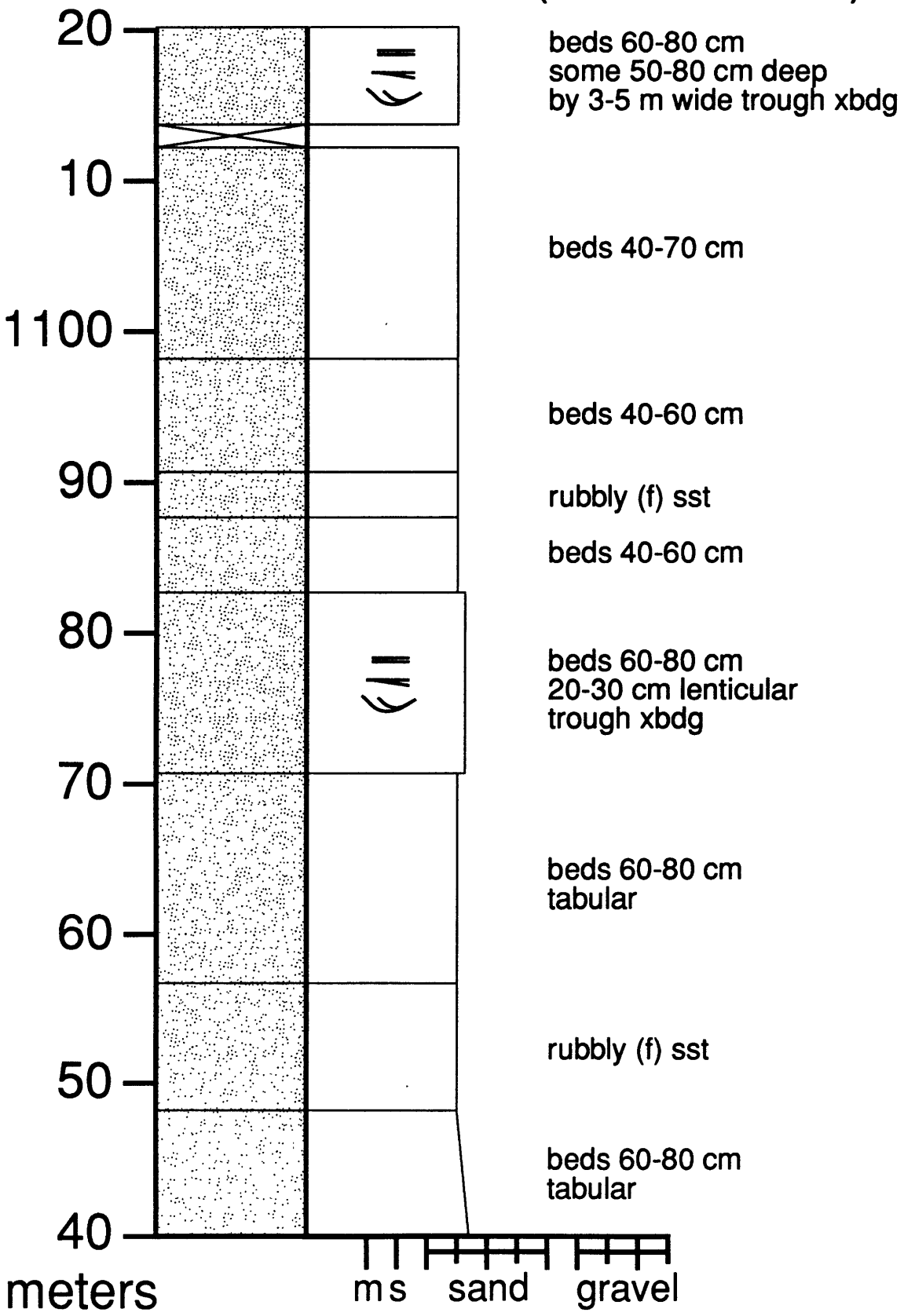

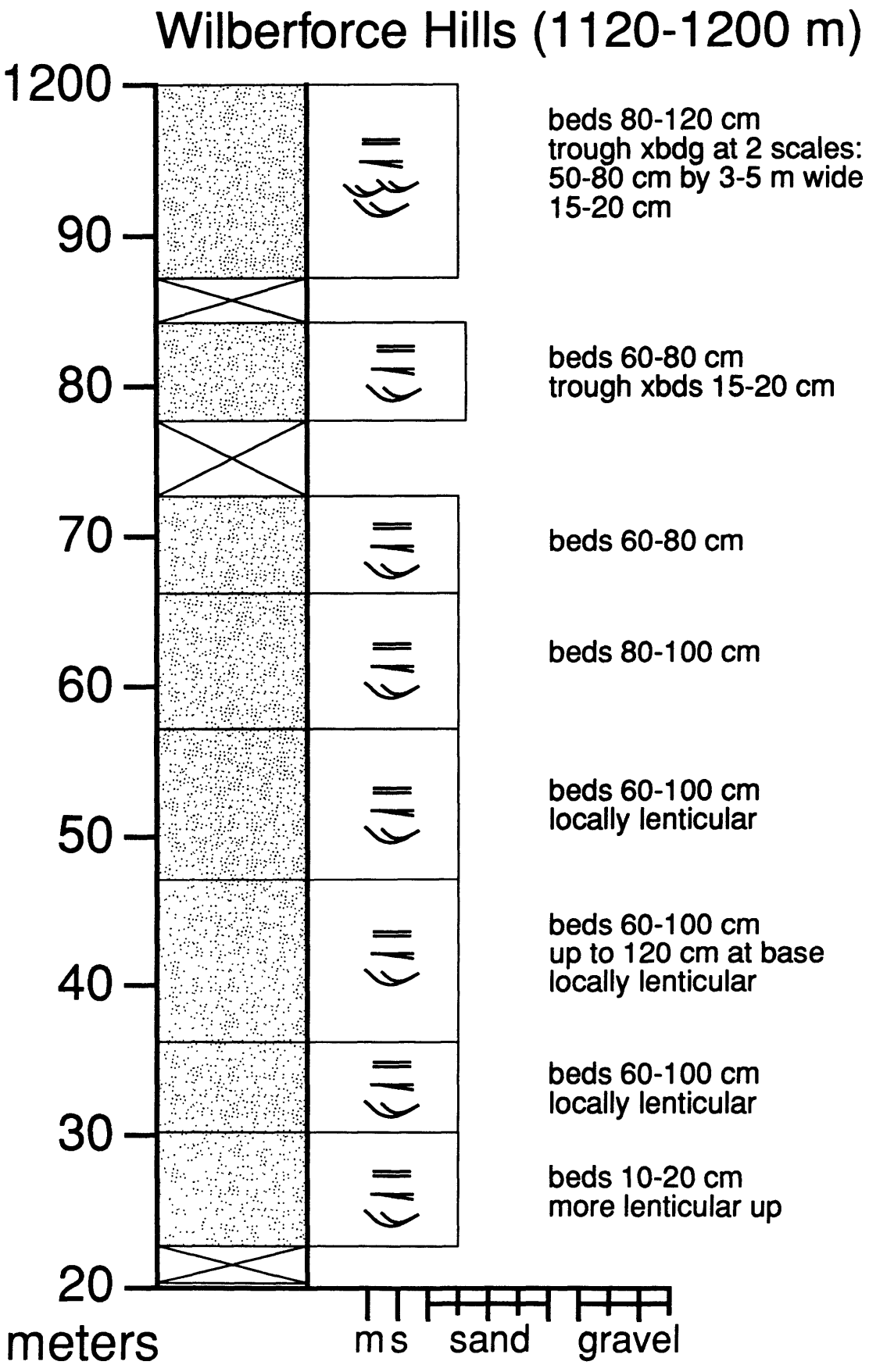
Wilberforce Hills (1120-1200 m)
1200
90
80
70
60
50
40
30
20
meters
beds 80-120 cm
trough xbdg at 2 scales:
50-80 cm by 3-5 m wide
15-20 cm
beds 60-80 cm
trough xbds 15-20 cm
beds 60-80 cm
beds 80-100 cm
beds 60-100 cm
locally lenticular
beds 60-100 cm
up to 120 cm at base
locally lenticular
beds 60-100 cm
locally lenticular
beds 10-20 cm
more lenticular up
m s
sand
gravel

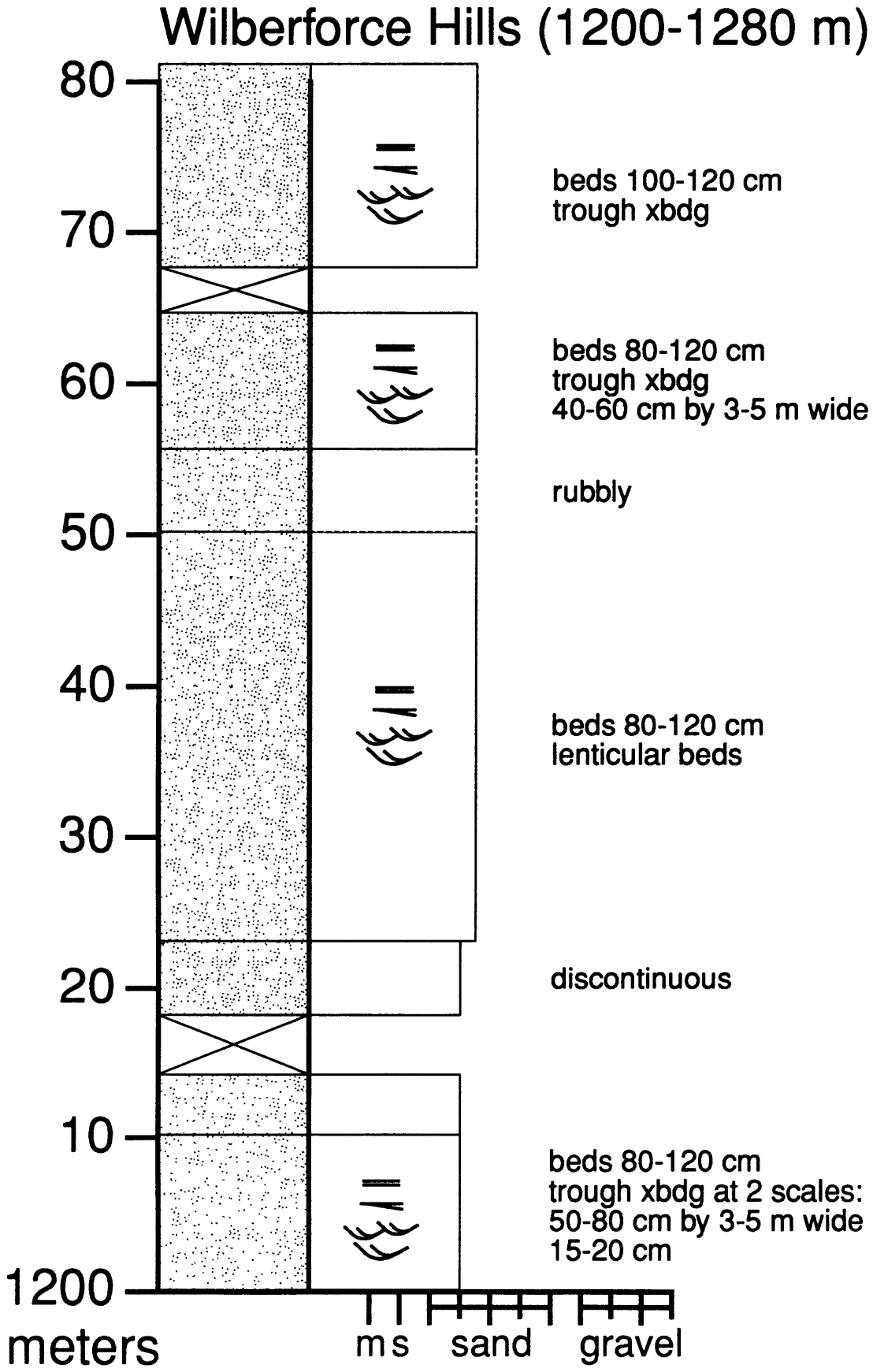
Wilberforce Hills (1200-1280 m)
80
70
60
50
40
30
20
10
1200
meters
beds 100-120 cm
trough xbdg
beds 80-120 cm
trough xbdg
40-60 cm by 3-5 m wide
rubbly
beds 80-120 cm
lenticular beds
discontinuous
beds 80-120 cm
trough xbdg at 2 scales:
50-80 cm by 3-5 m wide
15-20 cm
ms
sand
gravel

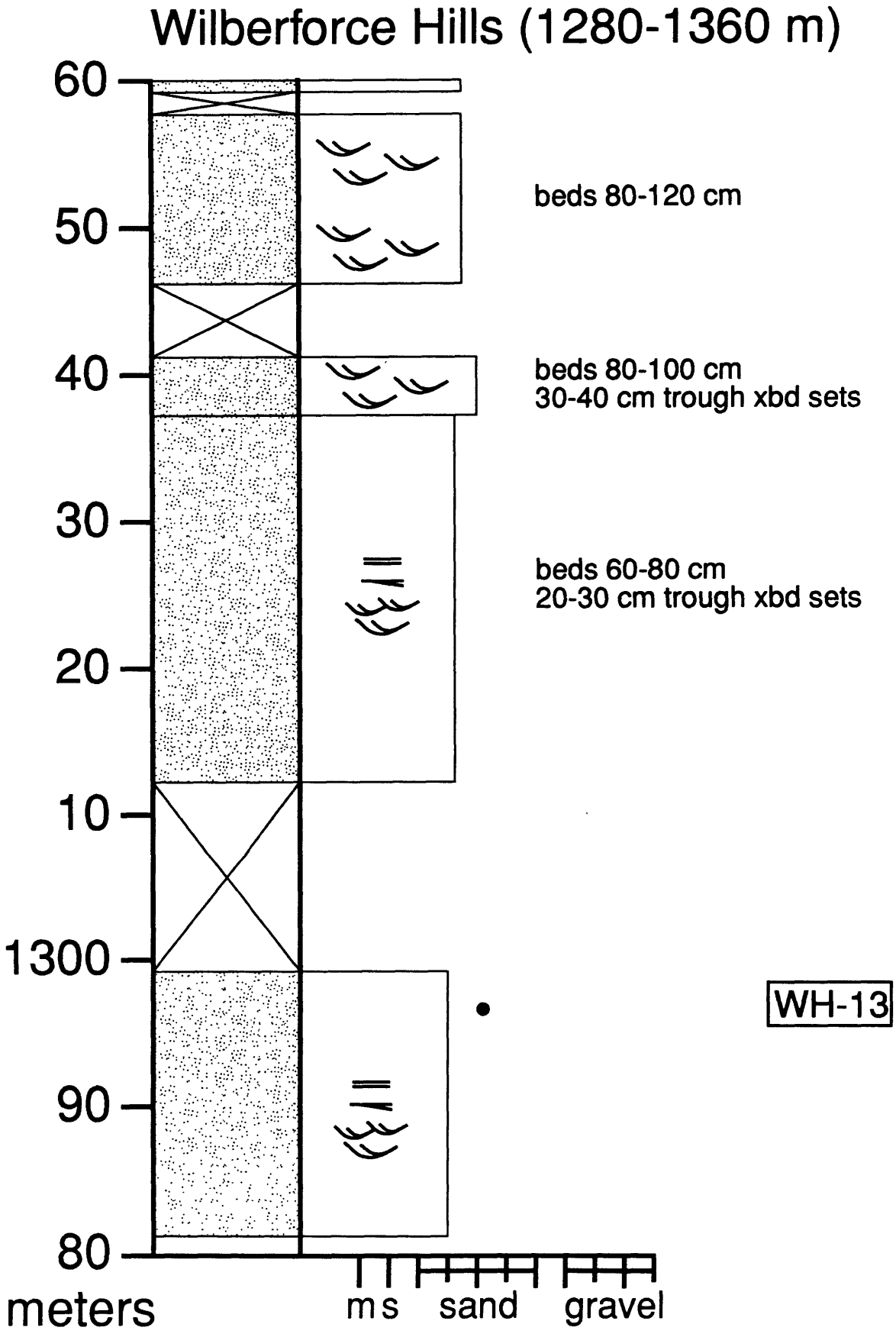
Wilberforce Hills (1280-1360 m)
60
50
40
30
20
10
1300
90
80
meters
beds 80-120 cm
beds 80-100 cm
30-40 cm trough xbd sets
beds 60-80 cm
20-30 cm trough xbd sets
WH-13
ms
sand
gravel

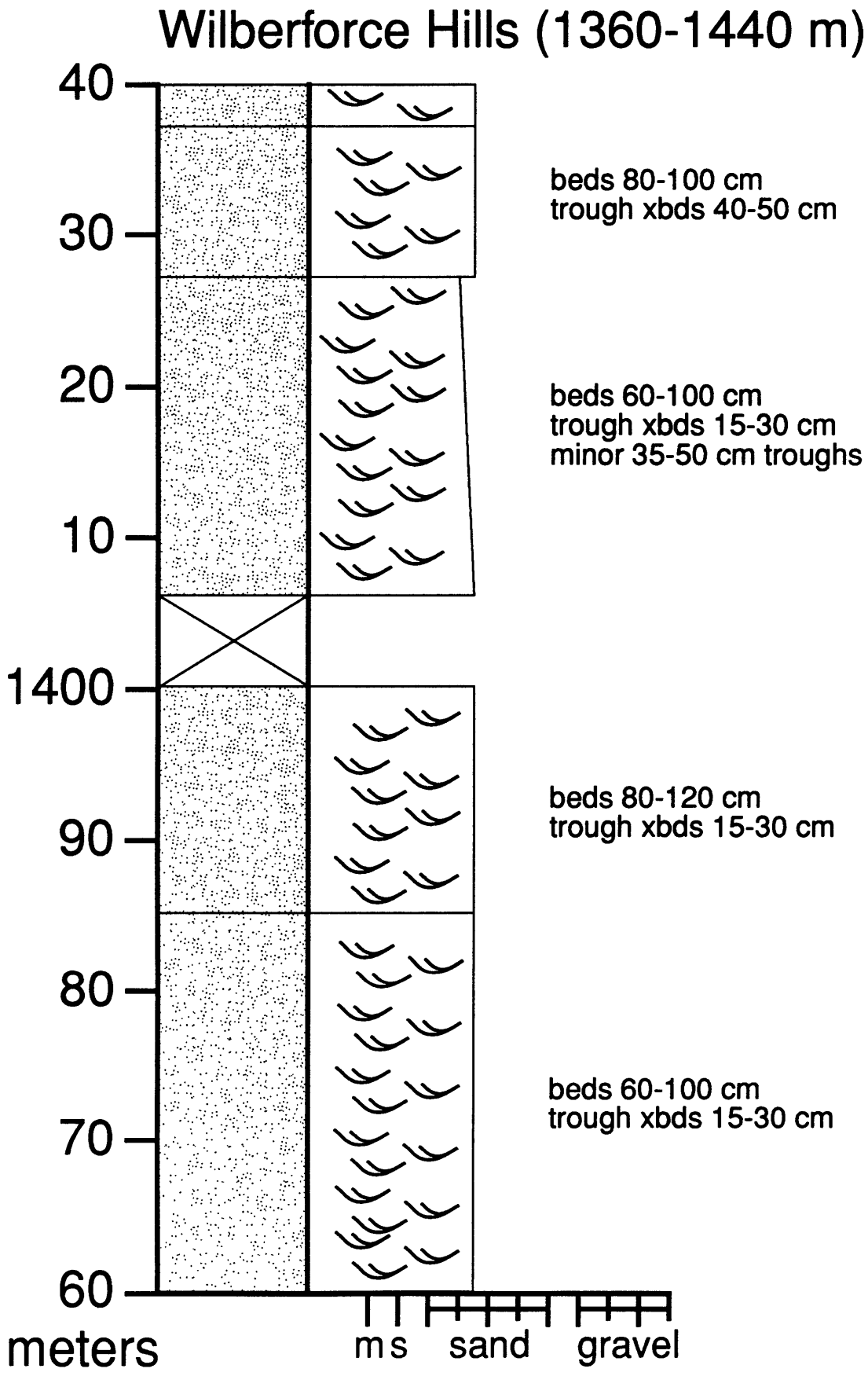
Wilberforce Hills (1360-1440 m)
40
30
20
10
1400
90
80
70
60
meters
beds 80-100 cm
trough xbds 40-50 cm
beds 60-100 cm
trough xbds 15-30 cm
minor 35-50 cm troughs
beds 80-120 cm
trough xbds 15-30 cm
beds 60-100 cm
trough xbds 15-30 cm
m s
sand
gravel

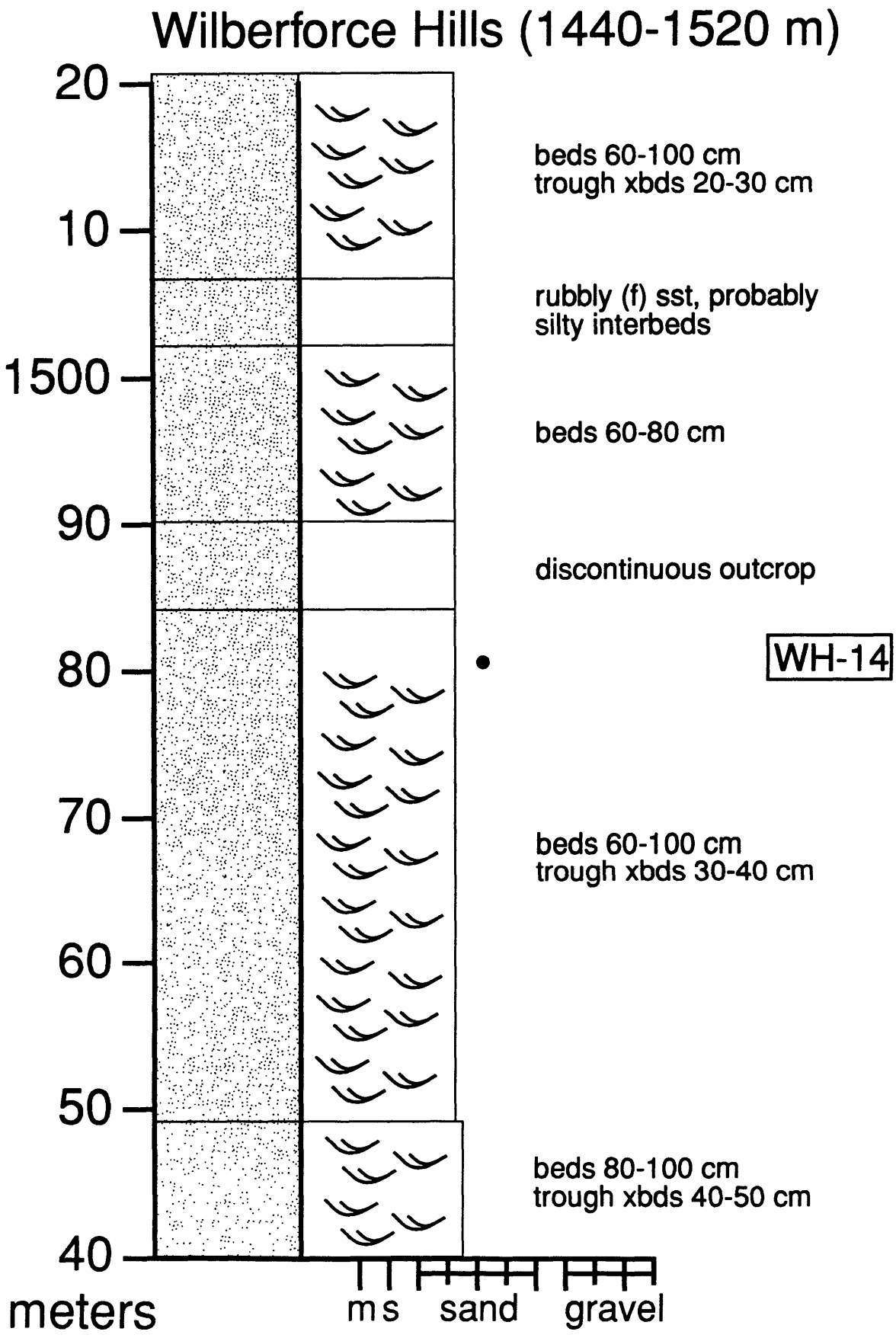
Wilberforce Hills (1440-1520 m)
20
10
1500
90
80
70
60
50
40
meters
beds 60-100 cm
trough xbds 20-30 cm
rubbly (f) sst, probably
silty interbeds
beds 60-80 cm
discontinuous outcrop
WH-14
beds 60-100 cm
trough xbds 30-40 cm
beds 80-100 cm
trough xbds 40-50 cm
m s
sand
gravel

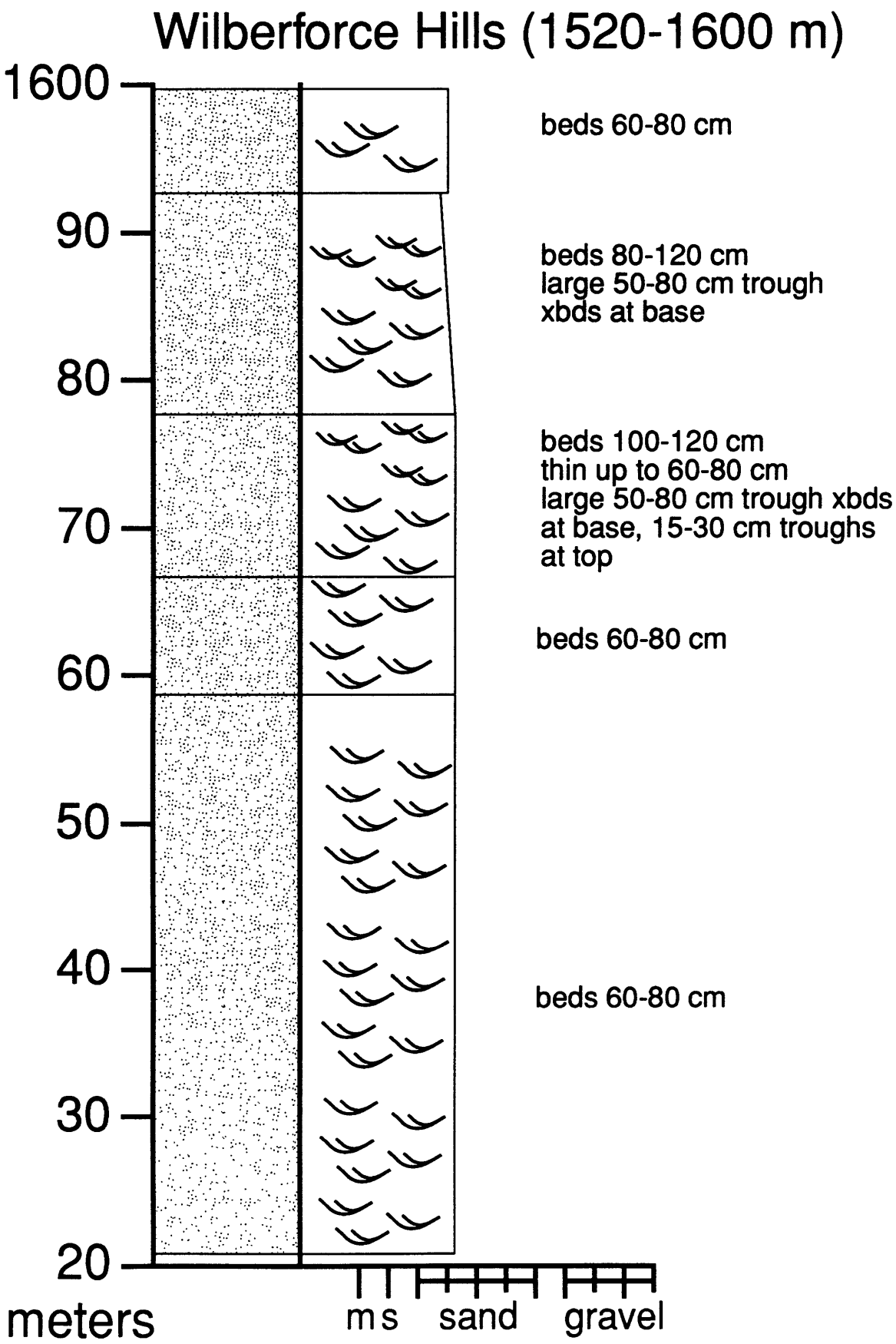
Wilberforce Hills (1520-1600 m)
1600
90
80
70
60
50
40
30
20
meters
beds 60-80 cm
beds 80-120 cm
large 50-80 cm trough
xbds at base
beds 100-120 cm
thin up to 60-80 cm
large 50-80 cm trough xbds
at base, 15-30 cm troughs
at top
beds 60-80 cm
beds 60-80 cm
ms
sand
gravel

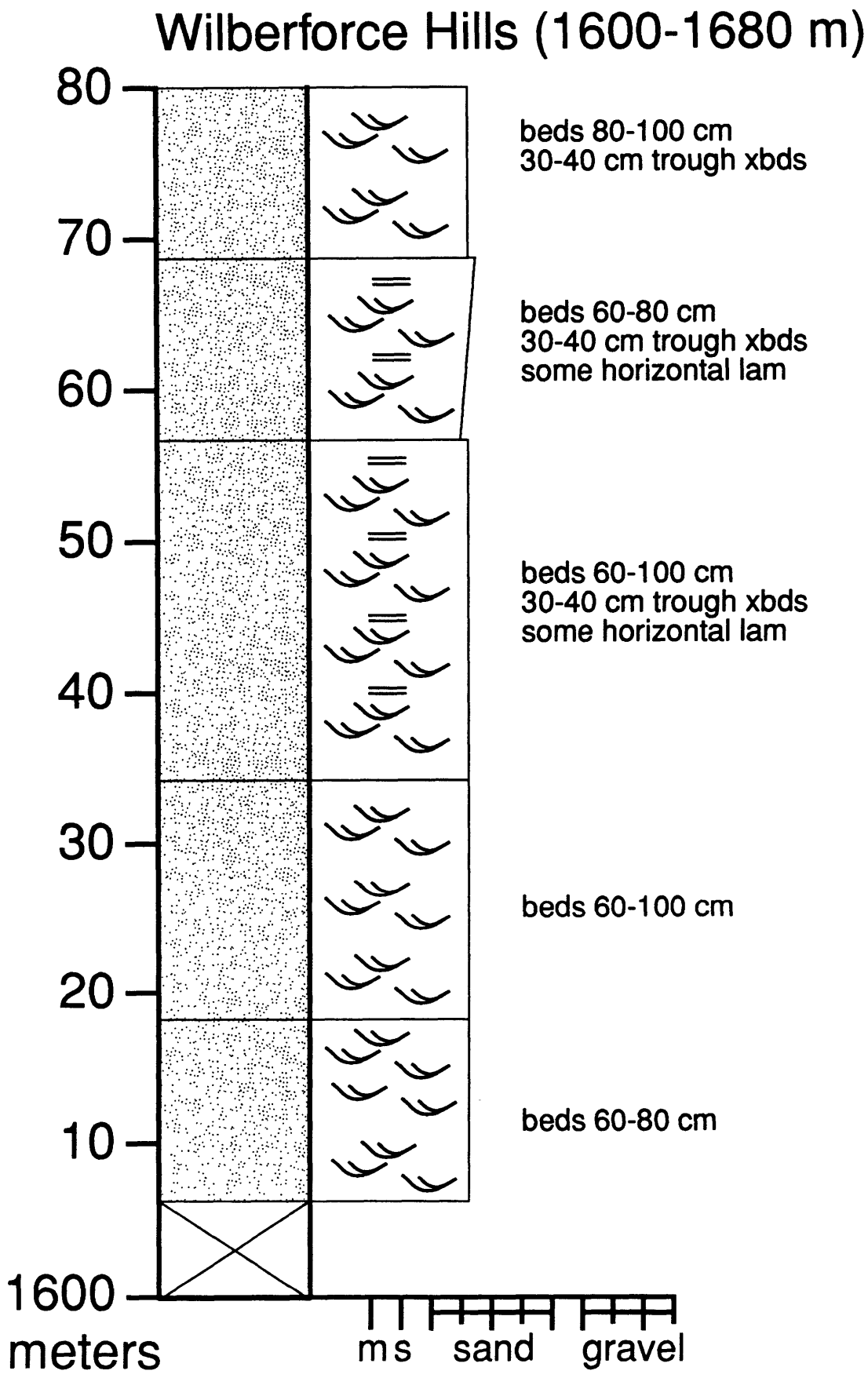
Wilberforce Hills (1600-1680 m)
80
70
60
50
40
30
20
10
1600
meters
beds 80-100 cm
30-40 cm trough xbds
beds 60-80 cm
30-40 cm trough xbds
some horizontal lam
beds 60-100 cm
30-40 cm trough xbds
some horizontal lam
beds 60-100 cm
beds 60-80 cm
ms
sand
gravel

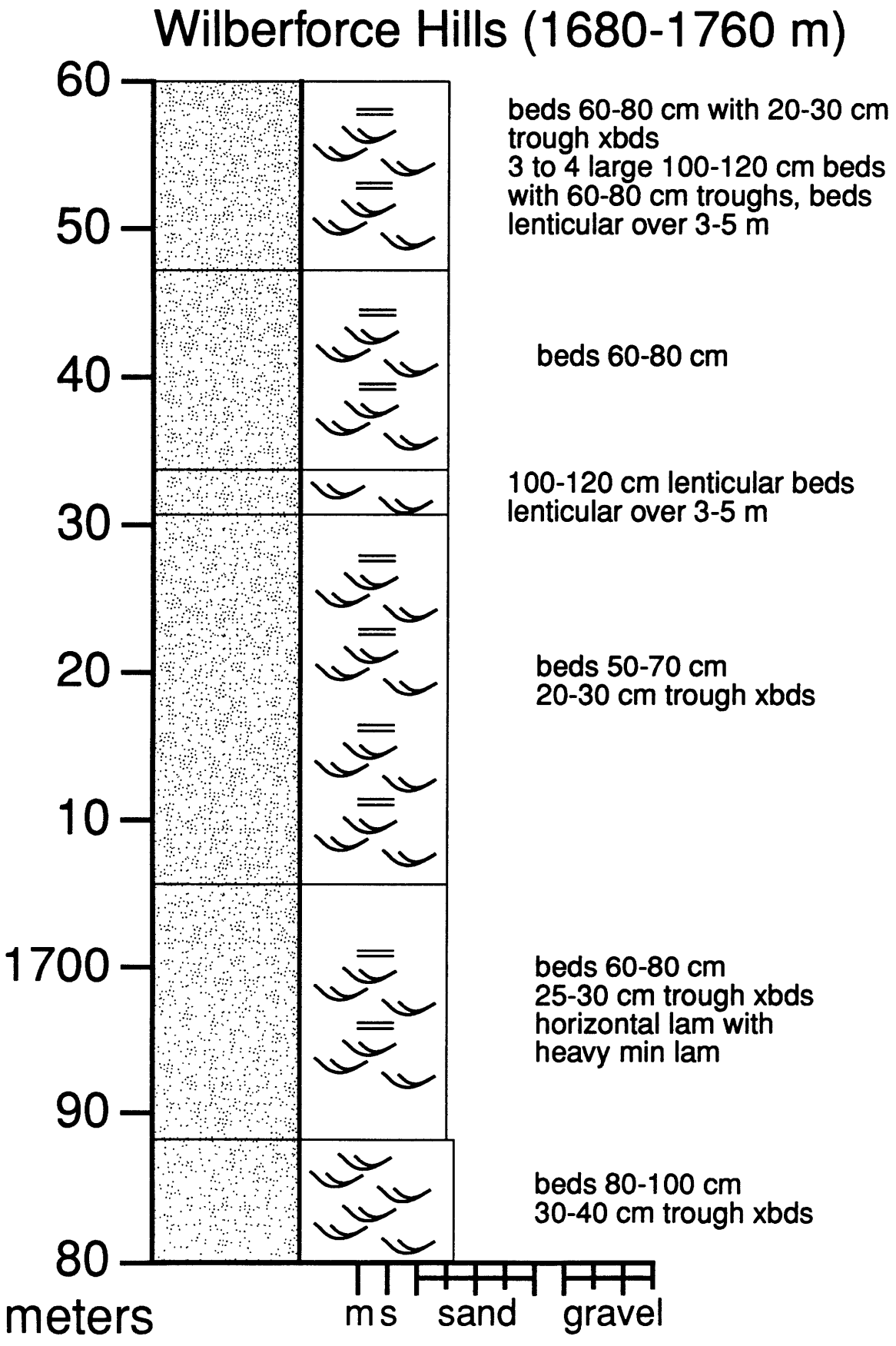
Wilberforce Hills (1680-1760 m)
60
50
40
30
20
10
1700
90
80
meters
beds 60-80 cm with 20-30 cm trough xbds
3 to 4 large 100-120 cm beds with 60-80 cm troughs, beds lenticular over 3-5 m
beds 60-80 cm
100-120 cm lenticular beds
lenticular over 3-5 m
beds 50-70 cm
20-30 cm trough xbds
beds 60-80 cm
25-30 cm trough xbds
horizontal lam with heavy min lam
beds 80-100 cm
30-40 cm trough xbds
m s
sand
gravel

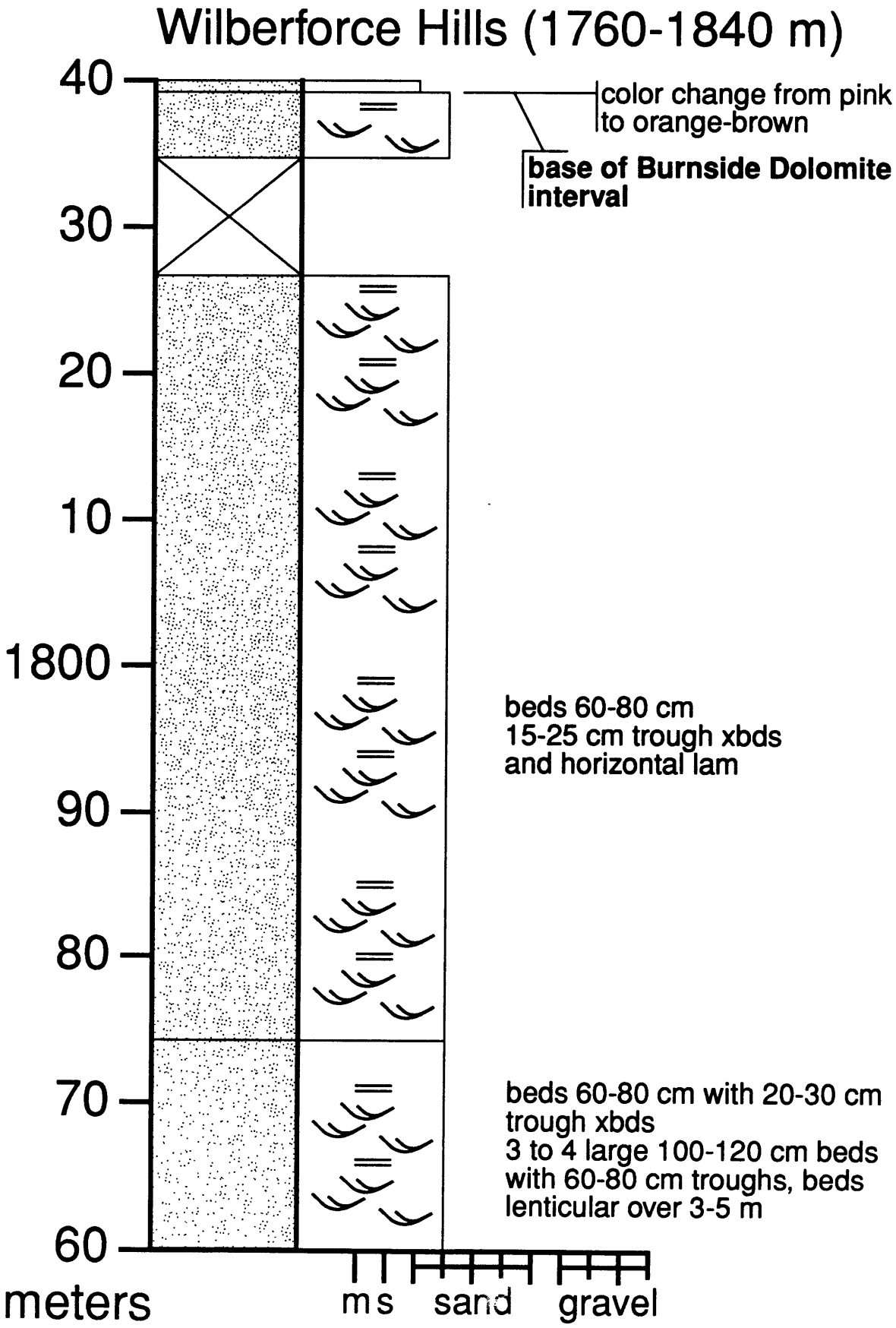
Wilberforce Hills (1760-1840 m)
40
30
20
10
1800
90
80
70
60
meters
color change from pink to orange-brown
base of Burnside Dolomite interval
beds 60-80 cm
15-25 cm trough xbds
and horizontal lam
beds 60-80 cm with 20-30 cm trough xbds
3 to 4 large 100-120 cm beds with 60-80 cm troughs, beds lenticular over 3-5 m
ms
sand
gravel

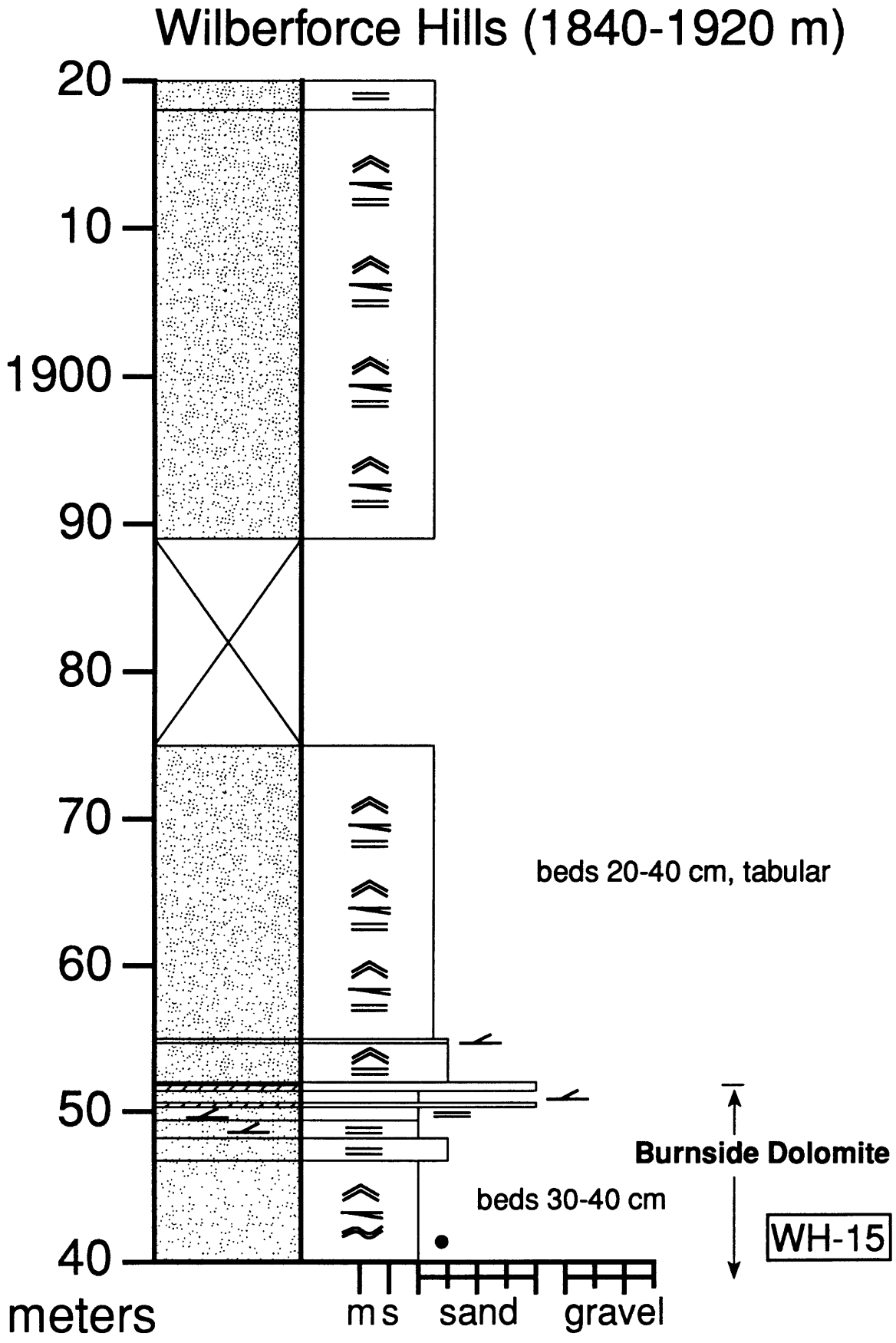
Wilberforce Hills (1840-1920 m)
20
10
1900
90
80
70
60
50
40
meters
beds 20-40 cm, tabular
Burnside Dolomite
beds 30-40 cm
WH-15
ms
sand
gravel

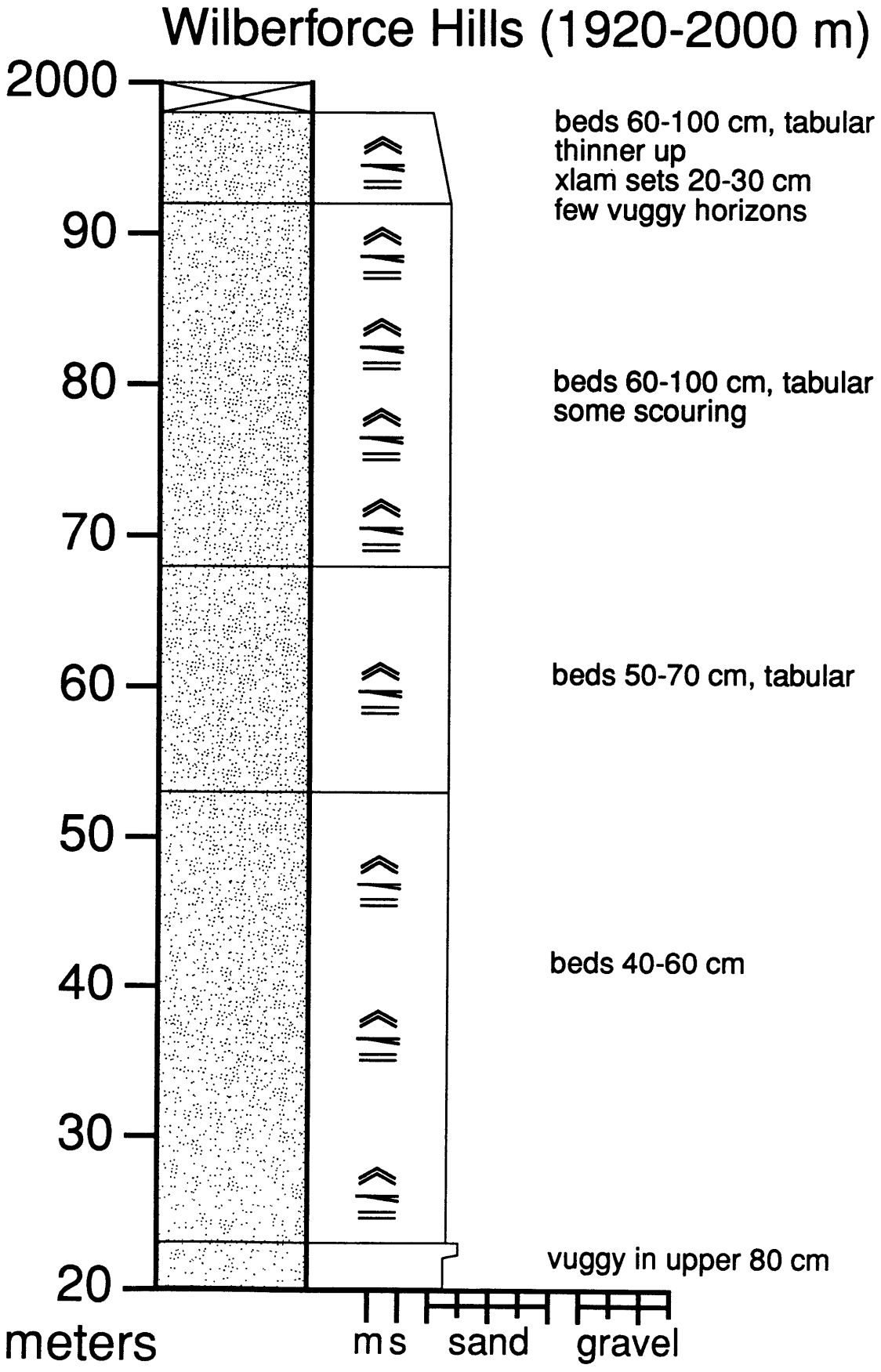
Wilberforce Hills (1920-2000 m)
2000
90
80
70
60
50
40
30
20
meters
beds 60-100 cm, tabular
thinner up
xlam sets 20-30 cm
few vuggy horizons
beds 60-100 cm, tabular
some scouring
beds 50-70 cm, tabular
beds 40-60 cm
vuggy in upper 80 cm
m s
sand
gravel

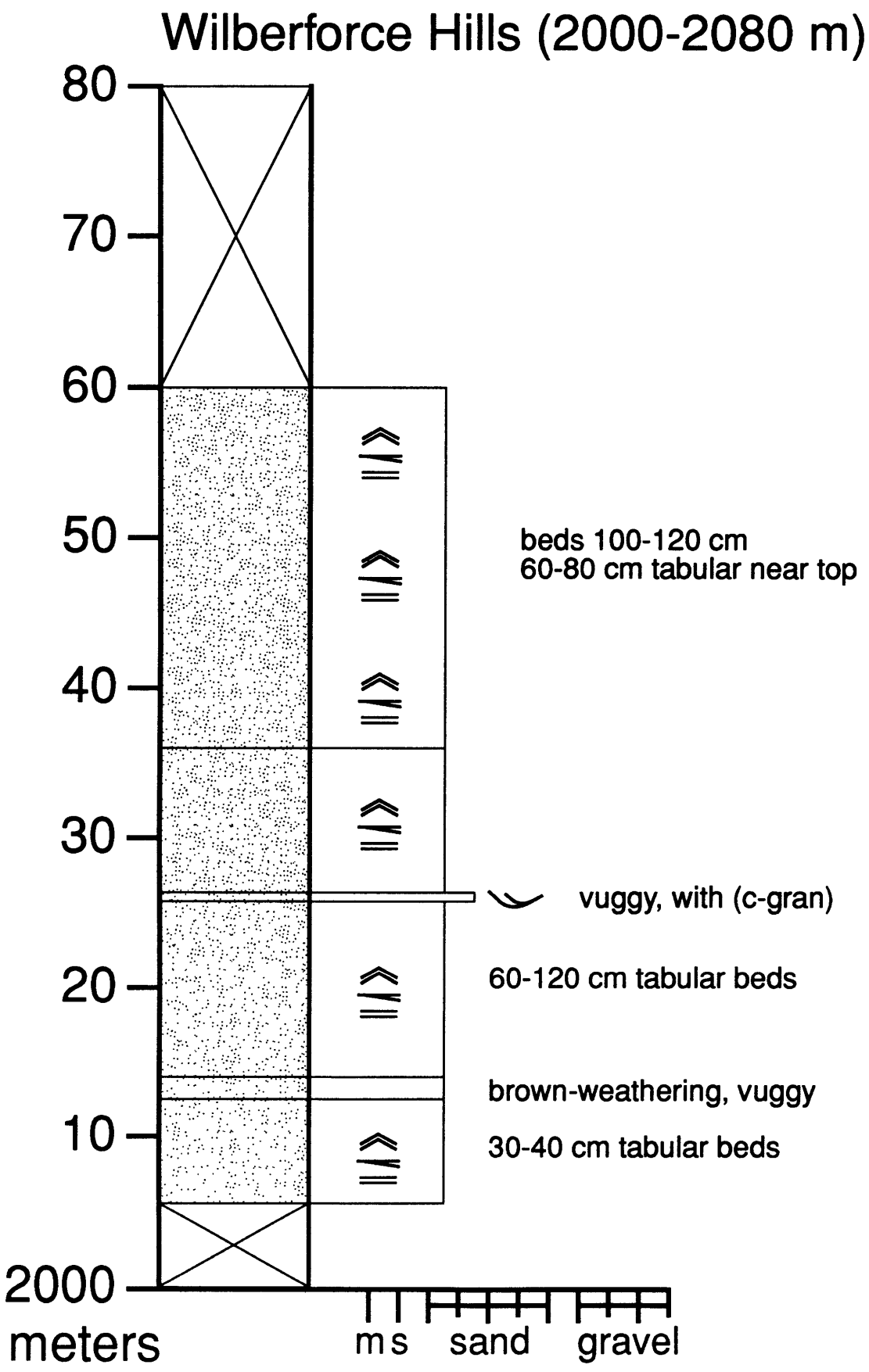
Wilberforce Hills (2000-2080 m)
80
70
60
50
40
30
20
10
2000
meters
beds 100-120 cm
60-80 cm tabular near top
vuggy, with (c-gran)
60-120 cm tabular beds
brown-weathering, vuggy
30-40 cm tabular beds
ms
sand
gravel

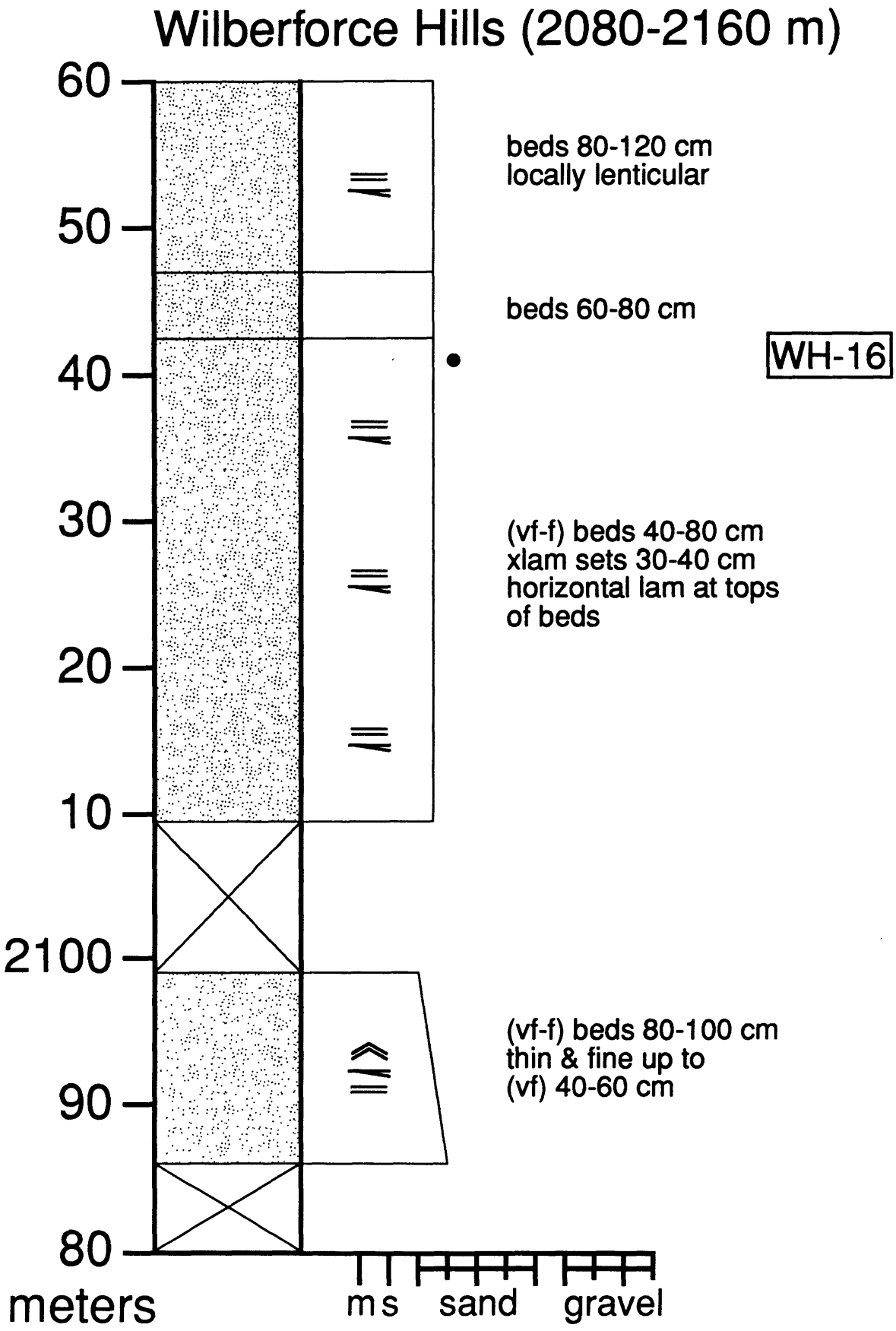
Wilberforce Hills (2080-2160 m)
60
50
40
30
20
10
2100
90
80
meters
beds 80-120 cm
locally lenticular
beds 60-80 cm
WH-16
(vf-f) beds 40-80 cm
xlam sets 30-40 cm
horizontal lam at tops
of beds
(vf-f) beds 80-100 cm
thin & fine up to
(vf) 40-60 cm
m s
sand
gravel

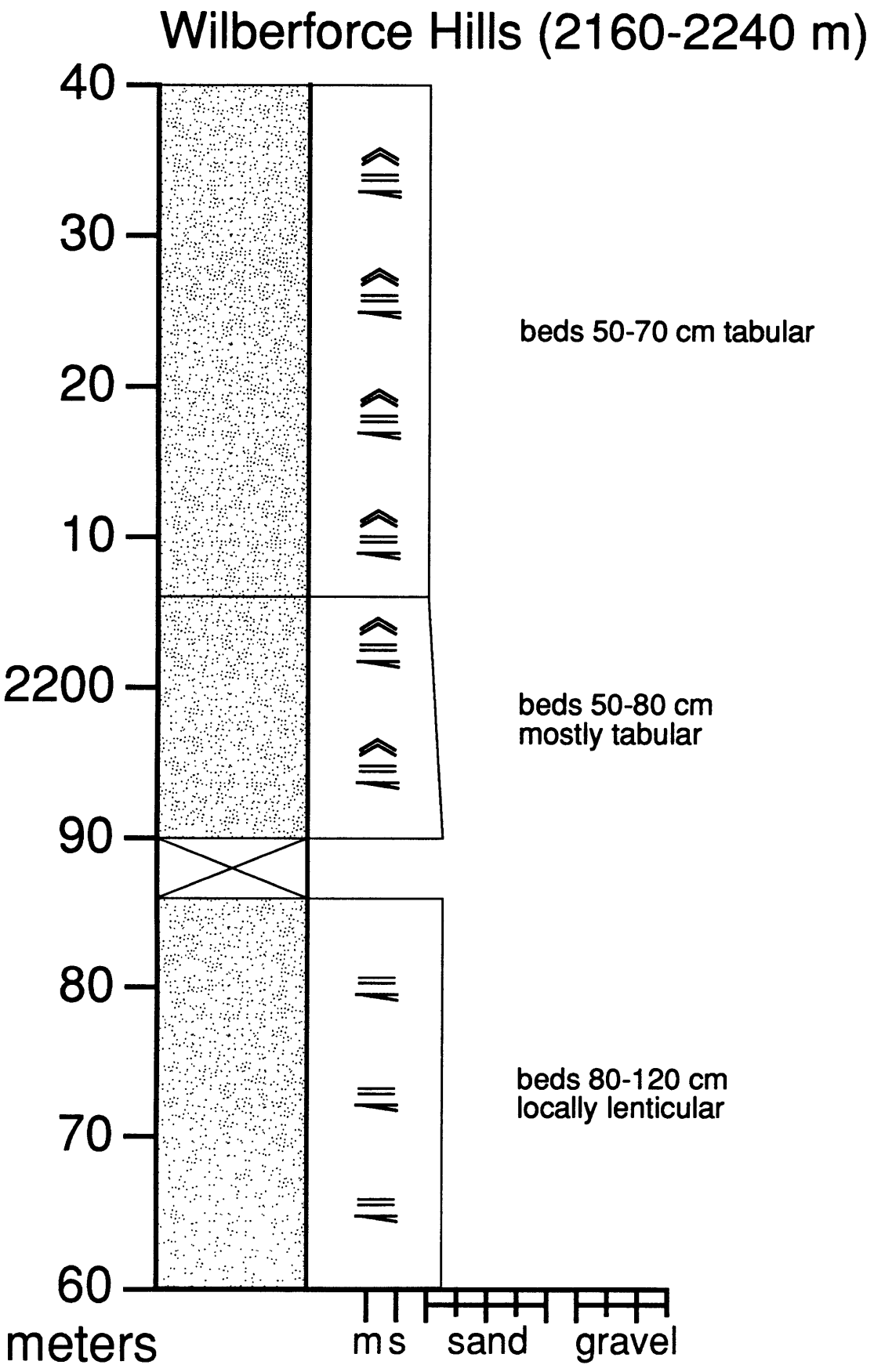
Wilberforce Hills (2160-2240 m)
40
30
20
10
2200
90
80
70
60
meters
beds 50-70 cm tabular
beds 50-80 cm
mostly tabular
beds 80-120 cm
locally lenticular
m s
sand
gravel

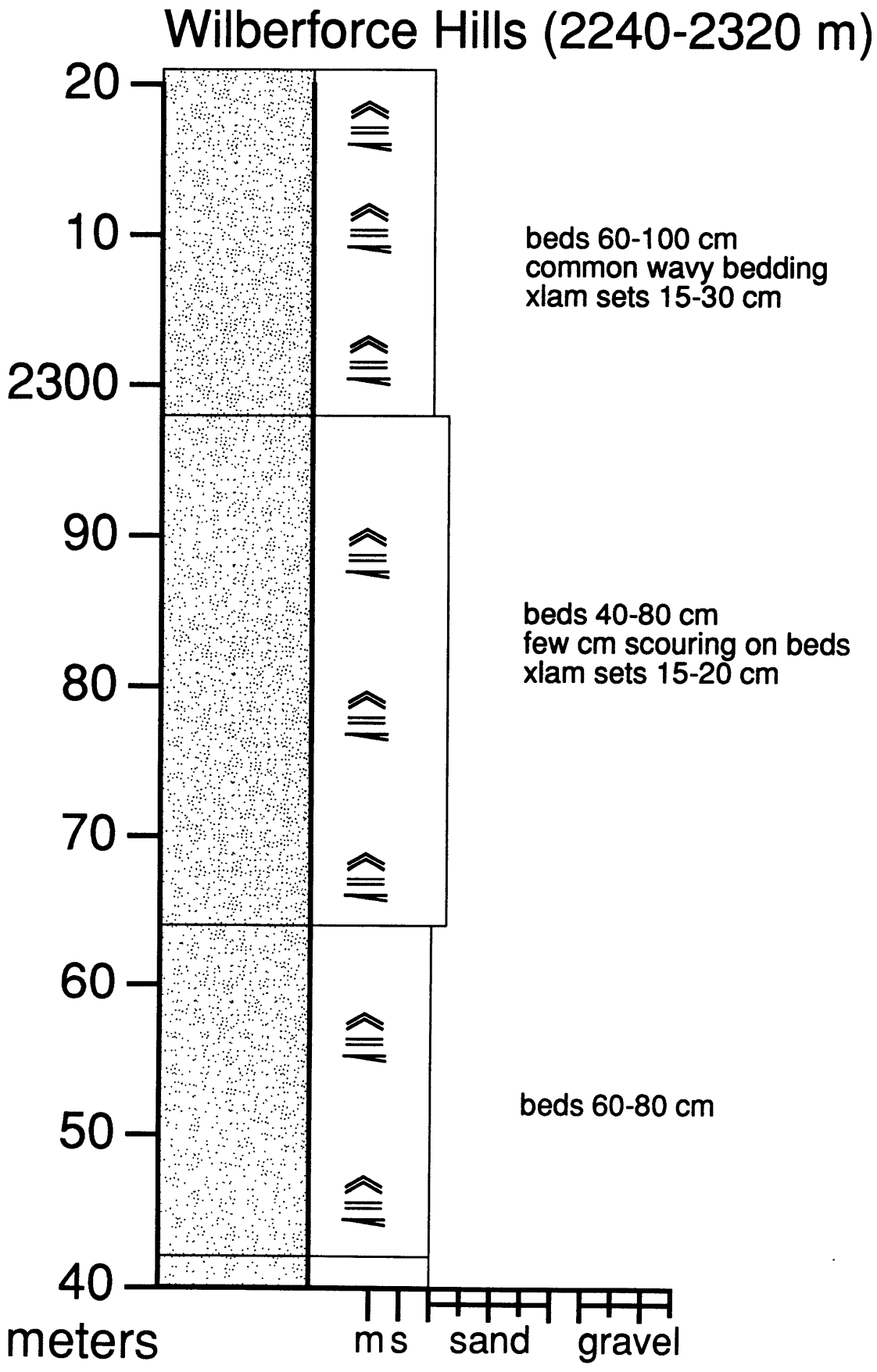
Wilberforce Hills (2240-2320 m)
20
10
2300
90
80
70
60
50
40
meters
beds 60-100 cm
common wavy bedding
xlam sets 15-30 cm
beds 40-80 cm
few cm scouring on beds
xlam sets 15-20 cm
beds 60-80 cm
m s
sand
gravel

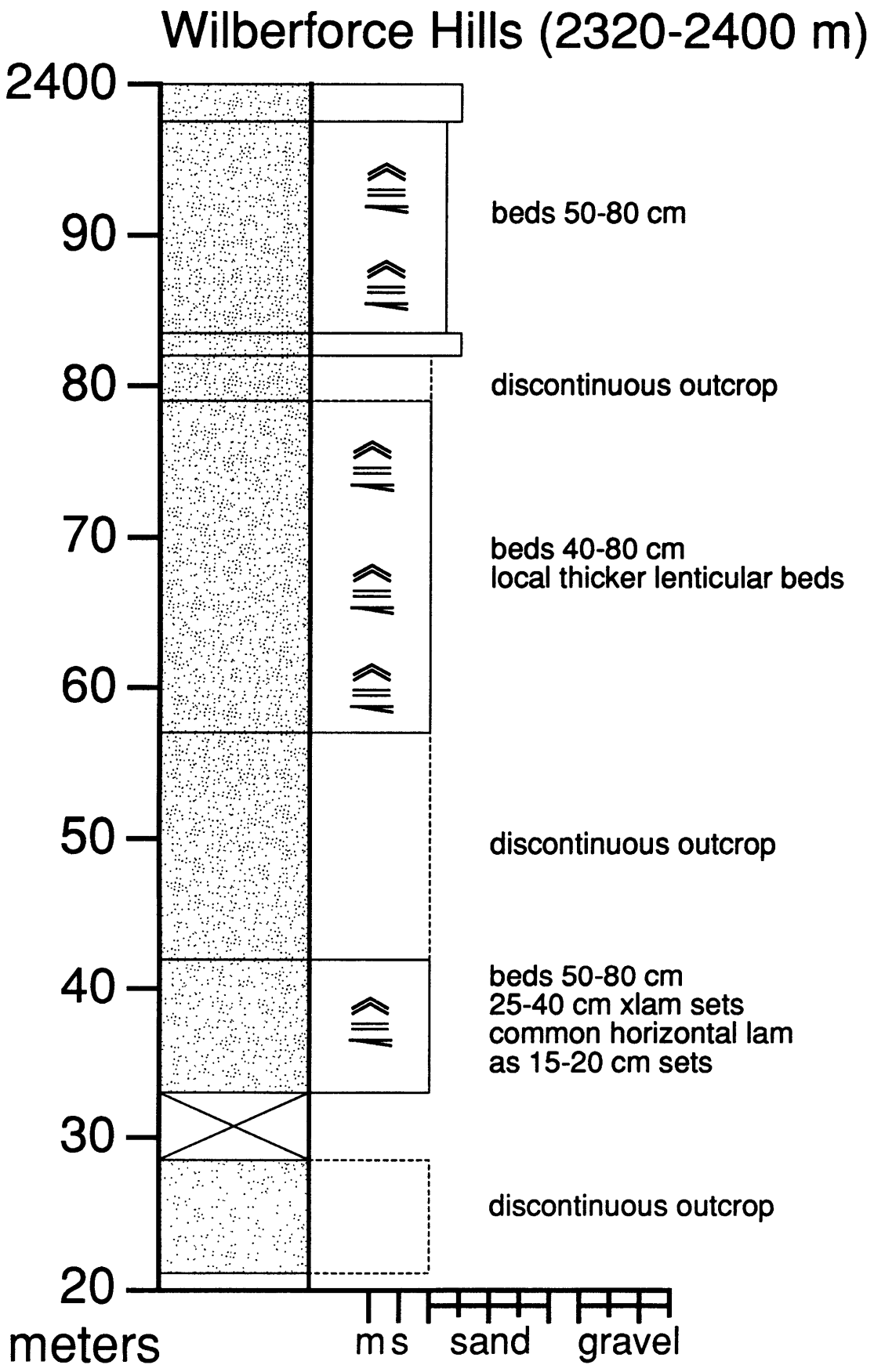
Wilberforce Hills (2320-2400 m)
2400
90
80
70
60
50
40
30
20
meters
beds 50-80 cm
discontinuous outcrop
beds 40-80 cm
local thicker lenticular beds
discontinuous outcrop
beds 50-80 cm
25-40 cm xlam sets
common horizontal lam
as 15-20 cm sets
discontinuous outcrop
m s
sand
gravel

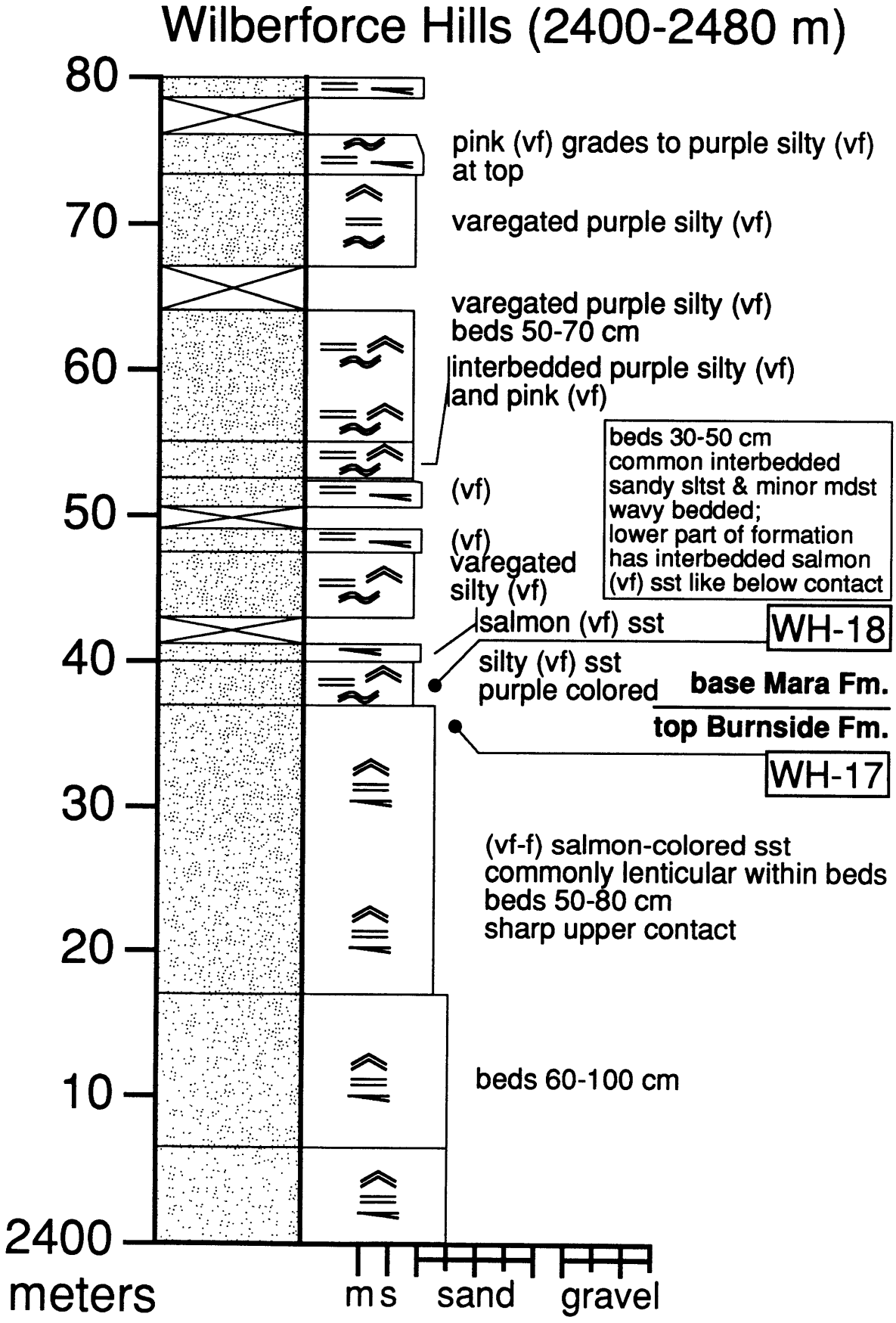
Wilberforce Hills (2400-2480 m)
80
70
60
50
40
30
20
10
2400
meters
m s
sand
gravel
pink (vf) grades to purple silty (vf) at top
varegated purple silty (vf)
varegated purple silty (vf) beds 50-70 cm
interbedded purple silty (vf) and pink (vf)
(vf)
(vf) varegated silty (vf)
beds 30-50 cm common interbedded sandy sltst & minor mdst wavy bedded; lower part of formation has interbedded salmon (vf) sst like below contact
salmon (vf) sst
WH-18
silty (vf) sst purple colored
base Mara Fm.
top Burnside Fm.
WH-17
(vf-f) salmon-colored sst commonly lenticular within beds beds 50-80 cm sharp upper contact
beds 60-100 cm

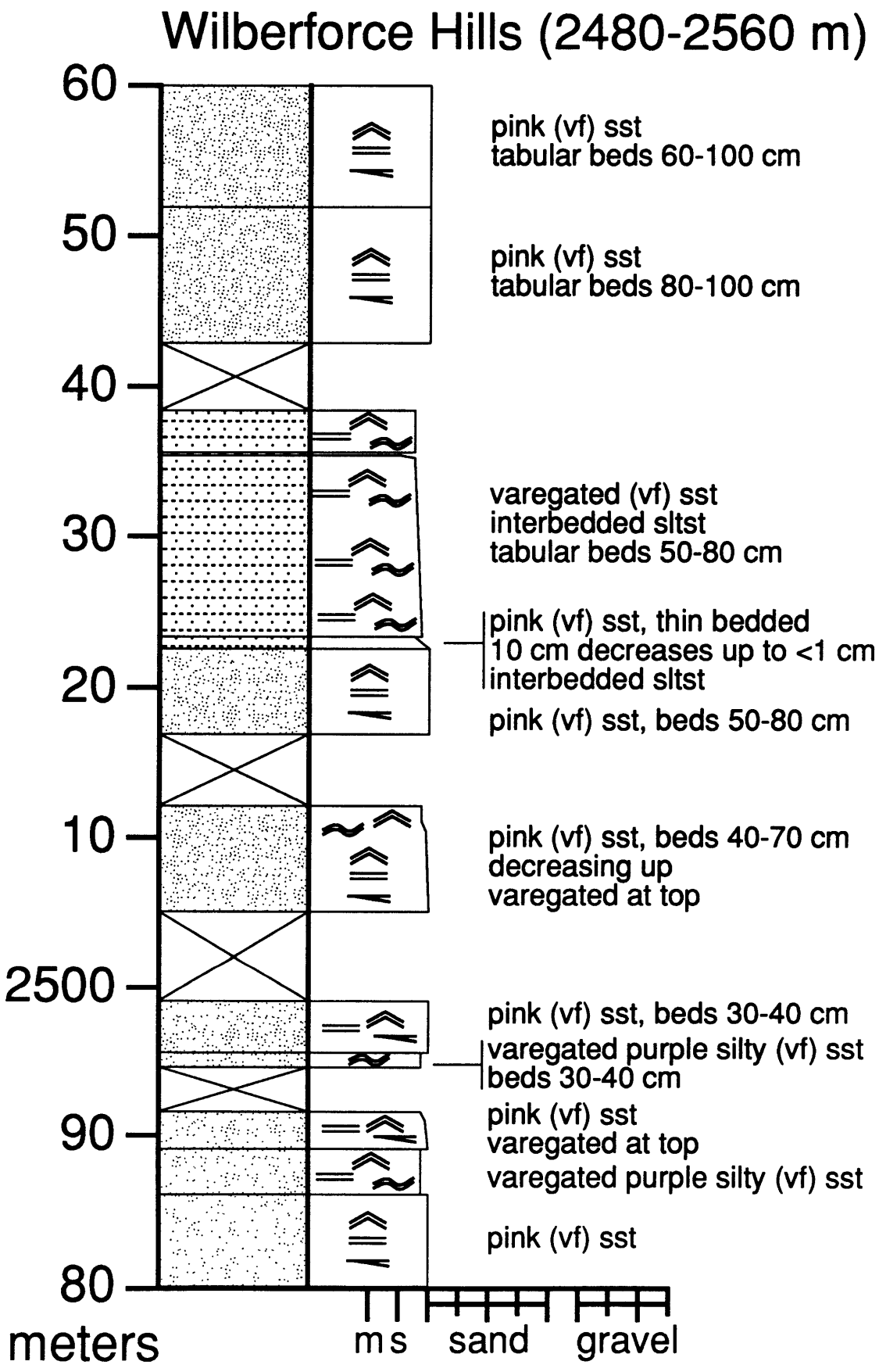
Wilberforce Hills (2480-2560 m)
60
50
40
30
20
10
2500
90
80
meters
pink (vf) sst
tabular beds 60-100 cm
pink (vf) sst
tabular beds 80-100 cm
varegated (vf) sst
interbedded sltst
tabular beds 50-80 cm
pink (vf) sst, thin bedded
10 cm decreases up to <1 cm
interbedded sltst
pink (vf) sst, beds 50-80 cm
pink (vf) sst, beds 40-70 cm
decreasing up
varegated at top
pink (vf) sst, beds 30-40 cm
varegated purple silty (vf) sst
beds 30-40 cm
pink (vf) sst
varegated at top
varegated purple silty (vf) sst
pink (vf) sst
ms
sand
gravel

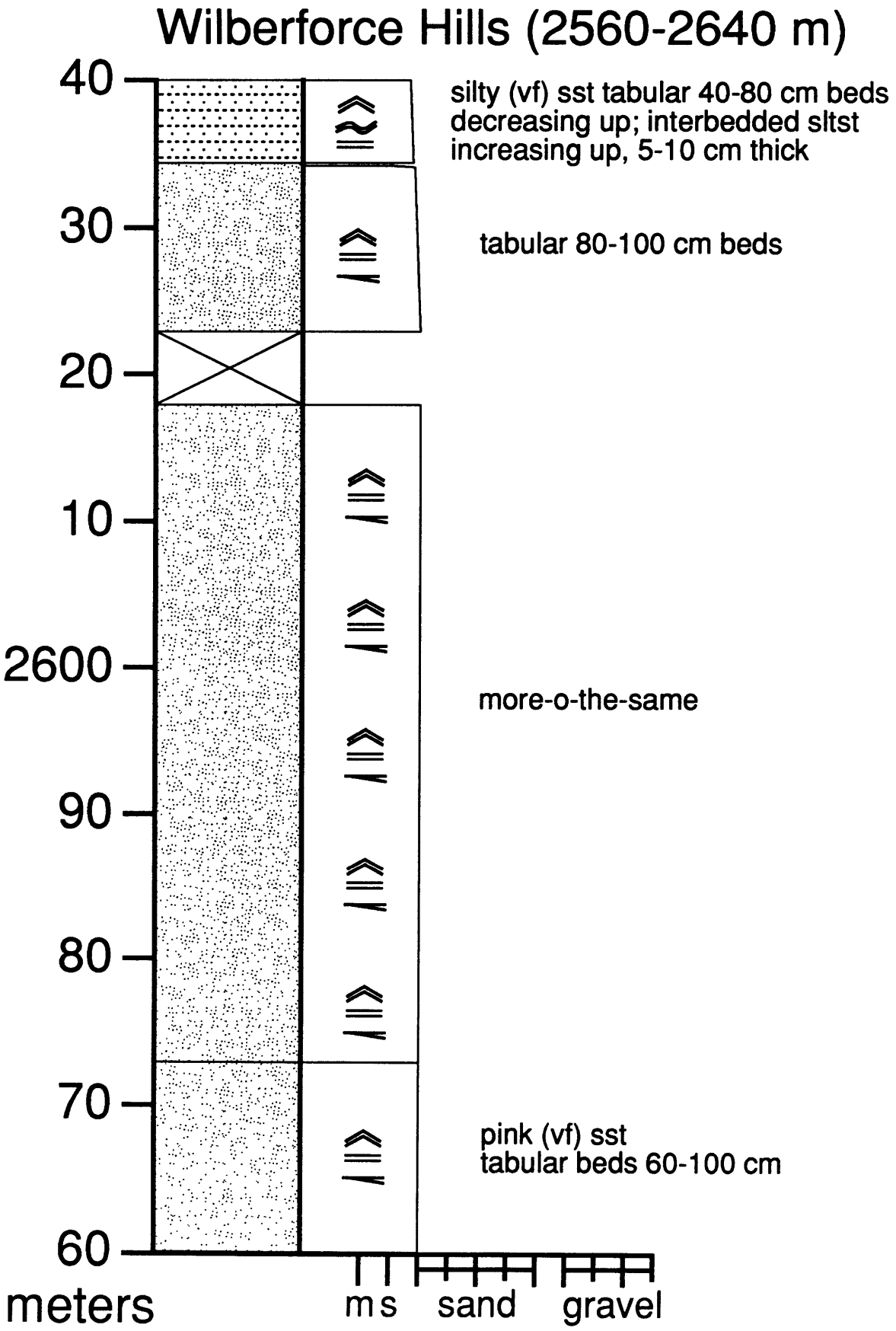
Wilberforce Hills (2560-2640 m)
40
30
20
10
2600
90
80
70
60
meters
silty (vf) sst tabular 40-80 cm beds
decreasing up; interbedded sltst
increasing up, 5-10 cm thick
tabular 80-100 cm beds
more-o-the-same
pink (vf) sst
tabular beds 60-100 cm
m s
sand
gravel

Wilberforce Hills (2640-2670 m)

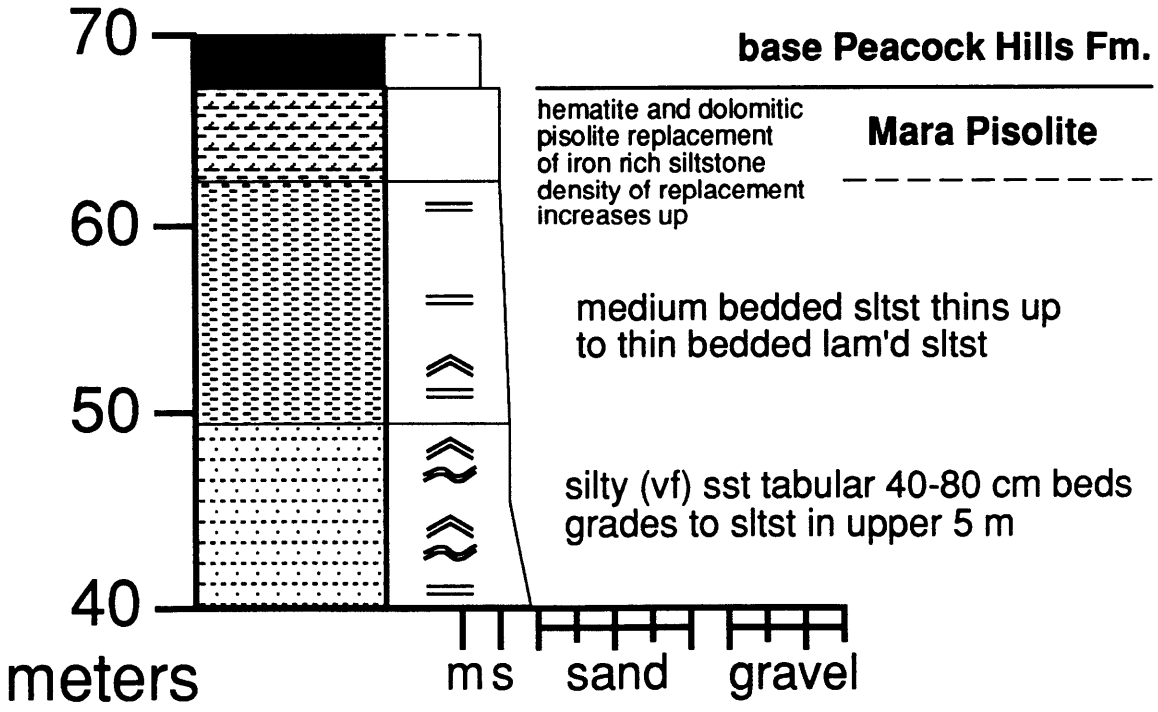

Appendix B:
Petrographic data of the Goulburn Supergroup

sample ID BC-H

location

Hackett Fm., Bear Creek Group, west side of Kathleen Lake., east of Bathurst Inlet.

field relations

Shelf sandstone facies, top of a coarsening up sequence, below the sub-Rifle Fm. sequence boundary.

thin section description

summary

Subarkosic sandstone

texture

(cL-cU), moderately sorted, moderately to well rounded, moderately elongate to spherical. Texturally mature.

mineralogy

quartz

Dominantly monocrystalline. Undulose grains may be due almost entirely to compaction at grain-to-grain point contacts. Polycrystalline grains have predominantly strain free intercrystal boundaries (plutonic/high rank metamorphic). Some polycrystalline grains with crenulated grain boundaries. Minor chert.

feldspar

Common microcline; compositional variations within grains that show variable alteration to mica. Some grains unaltered. Grains angular to well rouneded. Some as inclusions in quartz. Probable preferential replacement of plagioclase by late dolomite. Obvious less altered plagioclase range from angular to moderately rounded.

lithic fragments

Plutonic rock fragments of monocrystalline quartz with subordinate feldspar. Few altered grains with polycrystalline quartz and apprarent mica as alteration or replacement.

accessory minerals

Zircon as both detrital grains and within quartz grains.

intrabasinal grains

None.

cement

Quartz overgrowths occlude all primary porosity. Later euhedral dolomite rhombs preferenctiallly replace intergranular quartz cement, plagioclase, and polycrystalline quartz. Dolomite rhombs locally zoned.

matrix

Minor white mica after clay.

porosity

Completely occluded by quartz overgrowths.

other notes

Sample	BC-H	number	%total	%framework	
raw data	Qmnu	181	37.1	42.3	
	Qmu	136	27.9	31.8	
	Qpq2-3	18	3.7	4.2	
	Qpq>3	55	11.3	12.9	
	P	17	3.5	4.0	
	K	19	3.9	4.4	
	Lv	0	0.0	0.0	
	Lm	0	0.0	0.0	
	Ls	0	0.0	0.0	
	Cht	2	0.4	0.5	
	M	0	0.0	0.0	
	D	0	0.0	0.0	
	other framework	0	0.0	0.0	
	cement	23	4.7	qz overgrowth	
	matrix	0	0.0		
	other non-framework	37	7.6	dolomite replacement	
	U	0	0.0		
	total	488	100.0		
	total framework	428	87.7		
	total non-framework	60	12.3		
recalculated	Qm	317	65.0	74.1	
data	Qpq	73	15.0	17.1	
	Q	392	80.3	91.6	
	F	36	7.4	8.4	
	L	0	0.0	0.0	
	Lm	0	0.0	0.0	
	Lv	0	0.0	0.0	
	Ls	0	0.0	0.0	
	Qp	75	15.4	17.5	
	Lvm	0	0.0	0.0	
	Lsm	0	0.0	0.0	
	Lt	75	15.4	17.5	
		normalized %	normalized total		
ternary	QFL%Q	91.6	428		
data	QFL%F	8.4			
	QFL%L	0.0			
	LmLvLs%Lm	0.0	0		
	LmLvLs%Lv	0.0			
	LmLvLs%Ls	0.0			
	QpLvmLsm%Qp	100.0	75		
	QpLvmLsm%Lvm	0.0			
	QpLvmLsm%Lsm	0.0			
	QmFLt%Qm	74.1	428		
	QmFLt%F	8.4			
	QmFLt%Lt	17.5			
	QmPK%Qm	89.8	353		
	QmPK%P	4.8			
	QmPK%K	5.4			
	QmQpq%Qmnu	46.4	390		
	QmQpq%Qmu	34.9			
	QmQpq%Qpq2-3	4.6			
	QmQpq%Qpq>3	14.1			

sample ID BC-R

location

Rifle Fm., Bear Creek Group, west side of Kathleen Lake., east of Bathurst Inlet

field relations

Shelf sandstone facies, top of a coarsening up sequence, below the sub-Beechey Fm. sequence boundary.

thin section description

summary

Subarkosic sandstone

texture

(cL-cU), moderately sorted, moderately to well rounded, moderately elongate to spherical. Texturally mature.

mineralogy

quartz

Dominantly monocrystalline. Undulose grains may be due almost entirely to compaction at grain-to-grain point contacts. Polycrystalline grains have predominantly strain free intercrystal boundaries (plutonic/high rank metamorphic). Some polycrystalline grains with crenulated grain boundaries.

feldspar

Common microcline; compositional variations within grains that show variable alteration to mica. Common perthite. Some grains unaltered. Grains angular to well rouneded. Some as inclusions in quartz. Probable preferential replacement of plagioclase by late dolomite.

lithic fragments

Quartz-mica phyllite and schist fragments; more micaceous fragments have common chlorite alteration of muscovite.

accessory minerals

Zircon as both detrital grains and within quartz grains.

intrabasinal grains

None.

cement

Quartz overgrowths occlude all primary porosity. Later euhedral dolomite rhombs preferenctiallly replace intergranular quartz cement, plagioclase, and polycrystalline quartz. Dolomite rhombs locally zoned.

matrix

Minor recrystallization of micas next to altered feldspars.

porosity

Completely occluded by quartz overgrowths.

other notes

Sample	BC-R	number	%total	%framework	
raw data	Qmnu	300	56.0	67.9	
	Qmu	55	10.3	12.4	
	Qpq2-3	28	5.2	6.3	
	Qpq>3	17	3.2	3.8	
	P	11	2.1	2.5	
	K	19	3.5	4.3	
	Lv	0	0.0	0.0	
	Lm	3	0.6	0.7	phyllosilicate & qz
	Ls	0	0.0	0.0	
	Cht	0	0.0	0.0	
	M	1	0.2	0.2	
	D	0	0.0	0.0	
	other framework	6	1.1	1.4	
	cement	70	13.1		
	matrix	14	2.6		
	other non-framework	10	1.9		
	U	2	0.4	0.5	
	total	536	100.0		
	total framework	442	82.5		
	total non-framework	94	17.5		
recalculated	Qm	355	66.2	80.3	
data	Qpq	45	8.4	10.2	
	Q	400	74.6	90.5	
	F	30	5.6	6.8	
	L	3	0.6	0.7	
	Lm	3	0.6	0.7	
	Lv	0	0.0	0.0	
	Ls	0	0.0	0.0	
	Qp	45	8.4	10.2	
	Lvm	0	0.0	0.0	
	Lsm	3	0.6	0.7	
	Lt	48	9.0	10.9	

		normalized %	normalized total
ternary	QFL%Q	92.4	433
data	QFL%F	6.9	
	QFL%L	0.7	
	LmLvLs%Lm	100.0	3
	LmLvLs%Lv	0.0	
	LmLvLs%Ls	0.0	
	QpLvmLsm%Qp	93.8	48
	QpLvmLsm%Lvm	0.0	
	QpLvmLsm%Lsm	6.3	
	QmFLt%Qm	82.0	433
	QmFLt%F	6.9	
	QmFLt%Lt	11.1	
	QmPK%Qm	92.2	385
	QmPK%P	2.9	
	QmPK%K	4.9	
	QmQpq%Qmnu	75.0	400
	QmQpq%Qmu	13.8	
	QmQpq%Qpq2-3	7.0	
	QmQpq%Qpq>3	4.3	

sample ID STH-111

location

Burnside Fm., Bear Creek Group, south Tinney Hills section (172 m), east of Bathurst Inlet; coincides with STH-DZ-1 detrital zircon sample.

field relations

Braid delta facies, top of first coarsening up sequence within the Transitional Member of the Burnside Fm. in the proximal (southeastern) part of the basin.

thin section description

summary

Subarkosic sandstone

texture

(vf-m), moderately sorted, bimodal grains size distribution between well rounded (m) and angular to subrounded silt to (vf). Texturally mature.

mineralogy

quartz

Dominantly monocrystalline. Undulose grains may be due almost entirely to compaction at grain-to-grain point contacts. Polycrystalline grains very uncommon. Sparse chert.

feldspar

Common microcline and common plagioclase; more plagioclase than in underlying shelf sandstones (Hackett and Rifle Formations); compositional variations within grains that show variable alteration to mica. Common perthite mostly as stringers, minor exsolution blebs. Some grains unaltered. Grains angular to well rouneded. Some as inclusions in quartz. Probable preferential replacement of plagioclase by late dolomite.

lithic fragments

Quartz-mica schist fragments.

accessory minerals

Sparse muscovite. Possible rounded epidote.

intrabasinal grains

Sandy mudstone clast.

cement

None.

matrix

Quartz silt and clay. Clay is recrystallized to white micas. Local vermicular chlorite.

porosity

Completely occluded by matrix.

other notes

Sample	STH-111	number	%total	%framework	
raw data	Qmnu	217	47.3	50.9	
	Qmu	83	18.1	19.5	
	Qpq2-3	33	7.2	7.7	
	Qpq>3	14	3.1	3.3	
	P	18	3.9	4.2	
	K	46	10.0	10.8	
	Lv	0	0.0	0.0	
	Lm	0	0.0	0.0	
	Ls	1	0.2	0.2	
	Cht	6	1.3	1.4	
	M	0	0.0	0.0	
	D	0	0.0	0.0	
	other framework	0	0.0	0.0	
	cement	0	0.0		
	matrix	32	7.0		qz silt
	other non-framework	1	0.2		
	U	8	1.7	1.9	altered grains
	total	459	100.0		
	total framework	426	92.8		
	total non-framework	33	7.2		
recalculate	Qm	300	65.4	70.4	
data	Qpq	47	10.2	11.0	
	Q	353	76.9	82.9	
	F	64	13.9	15.0	
	L	1	0.2	0.2	
	Lm	0	0.0	0.0	
	Lv	0	0.0	0.0	
	Ls	1	0.2	0.2	
	Qp	53	11.5	12.4	
	Lvm	0	0.0	0.0	
	Lsm	1	0.2	0.2	
	Lt	54	11.8	12.7	
		normalized %	normalized total		
ternary	QFL%Q	84.4	418		
data	QFL%F	15.3			
	QFL%L	0.2			
	LmLvLs%Lm	0.0	1		
	LmLvLs%Lv	0.0			
	LmLvLs%Ls	100.0			
	QpLvmLsm%Qp	98.1	54		
	QpLvmLsm%Lvm	0.0			
	QpLvmLsm%Lsm	1.9			
	QmFLt%Qm	71.8	418		
	QmFLt%F	15.3			
	QmFLt%Lt	12.9			
	QmPK%Qm	82.4	364		
	QmPK%P	4.9			
	QmPK%K	12.6			
	QmQpq%Qmnu	62.5	347		
	QmQpq%Qmu	23.9			
	QmQpq%Qpq2-3	9.5			
	QmQpq%Qpq>3	4.0			

sample ID STH-116

location

Burnside Fm., Bear Creek Group, south Tinney Hills section (378 m), east of Bathurst Inlet.

field relations

Braid delta facies, top of second coarsening up sequence within the Transitional Member of the Burnside Fm. in the proximal (southeastern) part of the basin.

thin section description

summary

Subarkosic sandstone

texture

(fU-mU), ranges from silt to (c), moderately sorted, grains moderatly to well rounded. Texturally submature.

mineralogy

quartz

Dominantly monocrystalline. Undulose grains may be due almost entirely to compaction at grain-to-grain point contacts. Polycrystalline grains very uncommon. Sparse chert.

feldspar

Common microcline but no obvious plagioclase; compositional variations within grains that show variable alteration to mica. Common perthite mostly as stringers, minor exsolution blebs. Some grains unaltered. Grains angular to well rouneded.

lithic fragments

Elongate polycrystalline quartz with mica. Chert and jasper (jasper), plutonic fragments of quartz and K-feldspar. Chalcedony.

accessory minerals

Sparse muscovite. Possible rounded epidote.

intrabasinal grains

None.

cement

Appears to be micro- to cryptocrystalline quartz intergranular cement that is altered by micas.

matrix

Quartz silt and clay. Clay is recrystallized to white micas.

porosity

Completely occluded by cement and matrix.

other notes

Sample	STH-116	number	%total	%framework	
raw data	Qmnu	265	52.0	60.0	
	Qmu	50	9.8	11.3	
	Qpq2-3	21	4.1	4.8	
	Qpq>3	20	3.9	4.5	
	P	0	0.0	0.0	
	K	58	11.4	13.1	
	Lv	0	0.0	0.0	
	Lm	2	0.4	0.5	
	Ls	0	0.0	0.0	
	Cht	6	1.2	1.4	
	M	0	0.0	0.0	
	D	1	0.2	0.2	
	other framework	19	3.7	4.3	*see next page
	cement	11	2.2		
	matrix	56	11.0		
	other non-framework	1	0.2		
	U	0	0.0	0.0	
	total	510	100.0		
	total framework	442	86.7		
	total non-framework	68	13.3		
recalculated data	Qm	315	61.8	71.3	
	Qpq	41	8.0	9.3	
	Q	362	71.0	81.9	
	F	58	11.4	13.1	
	L	2	0.4	0.5	
	Lm	2	0.4	0.5	
	Lv	0	0.0	0.0	
	Ls	0	0.0	0.0	
	Qp	47	9.2	10.6	
	Lvm	0	0.0	0.0	
	Lsm	2	0.4	0.5	
	Lt	49	9.6	11.1	

		normalized %	normalized total
ternary data	QFL%Q	85.8	422
	QFL%F	13.7	
	QFL%L	0.5	
	LmLvLs%Lm	100.0	2
	LmLvLs%Lv	0.0	
	LmLvLs%Ls	0.0	
	QpLvmLsm%Qp	95.9	49
	QpLvmLsm%Lvm	0.0	
	QpLvmLsm%Lsm	4.1	
	QmFLt%Qm	74.6	422
	QmFLt%F	13.7	
	QmFLt%Lt	11.6	
	QmPK%Qm	84.5	373
	QmPK%P	0.0	
	QmPK%K	15.5	
	QmQpq%Qmnu	74.4	356
	QmQpq%Qmu	14.0	
	QmQpq%Qpq2-3	5.9	
	QmQpq%Qpq>3	5.6	

STH-116

other framework grains

6	chert & hematite
3	Fe oxide & chert
10	altered phyllosilicate & chert
19	total other framework grains

sample ID STH-120
location
Burnside Fm., Bear Creek Group, south Tinney Hills section (648 m), east of Bathurst Inlet.
field relations
Sandy braid plain facies, base of the Buff Sandstone Member of the Burnside Fm. in the proximal (southeastern) part of the basin. Corresponds with detrital zircon sample STH-DZ-2.
thin section description
summary
quartz arenite
texture
Bimodal grain size distribution of (vf) and (m-c), ranges from silt to (c), moderately sorted, grains moderatly to well rounded. Sutured grain boundaries between quartz grains. Texturally submature.
mineralogy
quartz
Dominantly monocrystalline. Undulose grains may be due almost entirely to compaction at grain-to-grain point contacts. Polycrystalline grains common; common grains with straight subgrains boundaries, minor grains with serrate and variably sized subgrains. Sparse chert.
feldspar
Felspar entirely absent.
lithic fragments
Almost entirely absent. Trace chalcedony.
accessory minerals
None.
intrabasinal grains
None.
cement
Extensive quartz overgrowths that occlude all primary porosity.
Minor conspicuous high relief cement that is probably clinozoisite-epidote (colorless to very pale green, high relief, high birefringence, single perfect cleavage, parallel extinction). Epidote cement may replace dolomite psuedomorphously and perhaps plagioclase. It occurs preferentially in intergranular pore space replacing matrix and certain framework grains (possibly feldspar). This cement appears only within the Buff Sandstone Member and this quarz arenite facies.
Minor Fe oxide recrytallized that overgrows framework grains. Minor recrystallized white mica matrix.
matrix
Quartz silt and clay. Clay is recrystallized to white micas.
porosity
Completely occluded by cement and matrix.
other notes
Feldspar and lithic fragments conspicuously absent. Most of the monocrystalline and polycrystalline quartz suggests a plutonic/high-grade

metamorphic source. The polycrystalline quartz textures are indicative of strained metamorphic source (e.g., deformation under greenschist to amphibolite facies).

Sample	STH-120	number	%total	%framework	
raw data	Qmnu	251	55.2	60.3	
	Qmu	54	11.9	13.0	
	Qpq2-3	53	11.6	12.7	
	Qpq>3	44	9.7	10.6	
	P	1	0.2	0.2	
	K	6	1.3	1.4	
	Lv	0	0.0	0.0	
	Lm	0	0.0	0.0	
	Ls	0	0.0	0.0	
	Cht	5	1.1	1.2	
	M	0	0.0	0.0	
	D	0	0.0	0.0	
	other framework	0	0.0	0.0	
	cement	26	5.7		high relief cement
	matrix	8	1.8		
	other non-framework	5	1.1		
	U	2	0.4	0.5	
	total	455	100.0		
	total framework	416	91.4		
	total non-framework	39	8.6		
recalculated data	Qm	305	67.0	73.3	
	Qpq	97	21.3	23.3	
	Q	407	89.5	97.8	
	F	7	1.5	1.7	
	L	0	0.0	0.0	
	Lm	0	0.0	0.0	
	Lv	0	0.0	0.0	
	Ls	0	0.0	0.0	
	Qp	102	22.4	24.5	
	Lvm	0	0.0	0.0	
	Lsm	0	0.0	0.0	
	Lt	102	22.4	24.5	

		normalized %	normalized total
ternary data	QFL%Q	98.3	414
	QFL%F	1.7	
	QFL%L	0.0	
	LmLvLs%Lm	0.0	0
	LmLvLs%Lv	0.0	
	LmLvLs%Ls	0.0	
	QpLvmLsm%Qp	100.0	102
	QpLvmLsm%Lvm	0.0	
	QpLvmLsm%Lsm	0.0	
	QmFLt%Qm	73.7	414
	QmFLt%F	1.7	
	QmFLt%Lt	24.6	
	QmPK%Qm	97.8	312
	QmPK%P	0.3	
	QmPK%K	1.9	
	QmQpq%Qmnu	62.4	402
	QmQpq%Qmu	13.4	
	QmQpq%Qpq2-3	13.2	
	QmQpq%Qpq>3	10.9	

sample ID STH-126p

location

Burnside Fm., Bear Creek Group, south Tinney Hills section (970 m), east of Bathurst Inlet.

field relations

Gravelly and sandy braid plain facies within the Buff Sandstone Member of the Burnside Fm. in the proximal (southeastern) part of the basin. Corresponds with detrital zircon sample STH-DZ-7.

thin section description

summary

quartz arenite or sublitharenite

texture

(m-c), ranges from (vf) to (c), moderately sorted, grains moderatly to well rounded. Straight to concavo-convex grain boundaries between quartz grains. Texturally submature.

mineralogy

quartz

Dominantly monocrystalline. Common polygonized undulose monocrystalline quartz grains; some undulosity is due to compaction at grain-to-grain point contacts. Polycrystalline grains present; common grains with straight subgrains boundaries and common grains with serrate and variably sized subgrains. Polycrystalline grains with >3 subgrains are preferentially altered by tiny white mica. Common chert, with abundant alteration to chert + white mica ± Fe oxide which gives a brown diffuse appearance.

feldspar

Sparse K-feldspar, plagioclase absent.

lithic fragments

Almost entirely absent.

accessory minerals

Sparse muscovite.

intrabasinal grains

None.

cement

Extensive quartz overgrowths that occlude all primary porosity.
Minor Fe oxide recrytallized that overgrows framework grains, both hematite and rutile. Fe oxide has a very patchy distribution with some chert grains having 15-20% Minor recrystallized white mica matrix.

matrix

Quartz silt and clay. Clay is recrystallized to white micas.

porosity

Completely occluded by cement and matrix.

other notes

Fe oxide within chert grains suggest an origin of chert-Fe oxide "iron formation" that is commonly associated with Archean greenstone belt metasediments in this area. This makes the proper classification of these grains ambiguous: they could be classified as either chert or metamorphic

rock fragments. Regardless of choice, they will be accurately reflected in QmFLt diagrams as part of Lt field; otherwise chert will end up in the Qp field and "iron formation" would end up in the Lm field. Feldspar and other lithic fragments conspicuously absent. Most of the monocrystalline and polycrystalline quartz suggests a plutonic/high-grade metamorphic source. The polycrystalline quartz textures are indicative of strained metamorphic source (e.g., deformation under greenschist to amphibolite facies).

Sample	STH-126p	number	%total	%framework	
raw data	Qmnu	237	47.5	51.3	
	Qmu	49	9.8	10.6	
	Qpq2-3	31	6.2	6.7	
	Qpq>3	49	9.8	10.6	
	P	0	0.0	0.0	
	K	8	1.6	1.7	
	Lv	0	0.0	0.0	
	Lm	5	1.0	1.1	
	Ls	0	0.0	0.0	
	Cht	81	16.2	17.5	*see next page
	M	1	0.2	0.2	
	D	0	0.0	0.0	
	other framework	0	0.0	0.0	
	cement	19	3.8		
	matrix	18	3.6		
	other non-framework	0	0.0		
	U	1	0.2	0.2	
	total	499	100.0		
	total framework	462	92.6		
	total non-framework	37	7.4		
recalculate	Qm	286	57.3	61.9	
data	Qpq	80	16.0	17.3	
	Q	447	89.6	96.8	
	F	8	1.6	1.7	
	L	5	1.0	1.1	
	Lm	5	1.0	1.1	
	Lv	0	0.0	0.0	
	Ls	0	0.0	0.0	
	Qp	161	32.3	34.8	
	Lvm	0	0.0	0.0	
	Lsm	5	1.0	1.1	
	Lt	166	33.3	35.9	

		normalized %	normalized total
ternary	QFL%Q	97.2	460
data	QFL%F	1.7	
	QFL%L	1.1	
	LmLvLs%Lm	100.0	5
	LmLvLs%Lv	0.0	
	LmLvLs%Ls	0.0	
	QpLvmLsm%Qp	97.0	166
	QpLvmLsm%Lvm	0.0	
	QpLvmLsm%Lsm	3.0	
	QmFLt%Qm	62.2	460
	QmFLt%F	1.7	
	QmFLt%Lt	36.1	
	QmPK%Qm	97.3	294
	QmPK%P	0.0	
	QmPK%K	2.7	
	QmQpq%Qmnu	64.8	366
	QmQpq%Qmu	13.4	
	QmQpq%Qpq2-3	8.5	
	QmQpq%Qpq>3	13.4	

STH-126p

*chert

17	chert
64	chert with extensive mica replacement
81	total chert

sample ID STH-127

location

Burnside Fm., Bear Creek Group, south Tinney Hills section (970 m), east of Bathurst Inlet.

field relations

Cobble conglomerate and sandy braid plain facies within the Buff Sandstone Member of the Burnside Fm. in the proximal (southeastern) part of the basin. Corresponds with detrital zircon sample STH-DZ-3.

thin section description

summary

quartz arenite

texture

(mU-vcL), ranges from (fU) to (vcU), moderately sorted, grains moderatly to well rounded. Straight to concavo-convex grain boundaries between quartz grains. Texturally submature.

mineralogy

quartz

Dominantly monocrystalline. Common polygonized undulose monocrystalline quartz grains; some undulosity is due to compaction at grain-to-grain point contacts. Polycrystalline grains present; common grains with straight subgrains boundaries and common grains with serrate and variably sized subgrains. Polycrystalline grains with >3 subgrains are preferentially altered by tiny white mica. Common microcrystalline (Qp>3) and cryptocrystalline (chert) polycrystalline quartz, with abundant alteration to chert + white mica ± Fe oxide which gives a brown diffuse appearance.

feldspar

Almost entirely absent, trace of both K-feldspar and plagioclase.

lithic fragments

Trace quartz-mica aggregates (schistose quartzite or schist).

accessory minerals

None.

intrabasinal grains

None.

cement

Extensive quartz overgrowths that occlude all primary porosity.
Minor Fe oxide recrytallized that overgrows framework grains, both hematite and rutile. Fe oxide has a very patchy distribution. Minor recrystallized white mica matrix. High relief epidote cement locally replaces intergranular quartz cement.

matrix

Quartz silt and clay. Clay is recrystallized to white micas.

porosity

Completely occluded by cement and matrix.

other notes

Feldspar and other lithic fragments conspicuously absent. Most of the monocrystalline and polycrystalline quartz suggests a plutonic/high-grade metamorphic source. The polycrystalline quartz textures are indicative of

strained metamorphic source (e.g., deformation under greenschist to amphibolite facies).
Late fractures show quartz grain size reduction along fractures and authigenic white mica lining the fractures then Fe oxide growing across mica grains.

Sample	**STH-127**	number	%total	%framework	
raw data	Qmnu	246	52.0	58.7	
	Qmu	54	11.4	12.9	
	Qpq2-3	31	6.6	7.4	
	Qpq>3	70	14.8	16.7	
	P	1	0.2	0.2	
	K	0	0.0	0.0	
	Lv	0	0.0	0.0	
	Lm	1	0.2	0.2	
	Ls	0	0.0	0.0	
	Cht	12	2.5	2.9	
	M	0	0.0	0.0	
	D	0	0.0	0.0	
	other framework	0	0.0	0.0	
	cement	16	3.4	qz overgrowths	
	matrix	24	5.1	phyllosilicate	
	other non-framework	14	3.0	4 hematite, 10 hi relief	
	U	4	0.8	1.0	
	total	473	100.0		
	total framework	419	88.6		
	total non-framework	54	11.4		
recalculated	Qm	300	63.4	71.6	
data	Qpq	101	21.4	24.1	
	Q	413	87.3	98.6	
	F	1	0.2	0.2	
	L	1	0.2	0.2	
	Lm	1	0.2	0.2	
	Lv	0	0.0	0.0	
	Ls	0	0.0	0.0	
	Qp	113	23.9	27.0	
	Lvm	0	0.0	0.0	
	Lsm	1	0.2	0.2	
	Lt	114	24.1	27.2	

		normalized %	normalized total
ternary	QFL%Q	99.5	415
data	QFL%F	0.2	
	QFL%L	0.2	
	LmLvLs%Lm	100.0	1
	LmLvLs%Lv	0.0	
	LmLvLs%Ls	0.0	
	QpLvmLsm%Qp	99.1	114
	QpLvmLsm%Lvm	0.0	
	QpLvmLsm%Lsm	0.9	
	QmFLt%Qm	72.3	415
	QmFLt%F	0.2	
	QmFLt%Lt	27.5	
	QmPK%Qm	99.7	301
	QmPK%P	0.3	
	QmPK%K	0.0	
	QmQpq%Qmnu	61.3	401
	QmQpq%Qmu	13.5	
	QmQpq%Qpq2-3	7.7	
	QmQpq%Qpq>3	17.5	

sample ID STH-128

location

Burnside Fm., Bear Creek Group, south Tinney Hills section (1342 m), east of Bathurst Inlet.

field relations

Cobble conglomerate and sandy braid plain facies within the Buff Sandstone Member of the Burnside Fm., between the 1st and 4th cobble conglomerate horizons in the proximal (southeastern) part of the basin.

thin section description

summary

quartz arenite

texture

(fU-cL), ranges from (fU) to (granule (2.45mm)), moderately to poorly sorted, grains angular to rounded. Straight to concavo-convex grain boundaries between quartz grains. Texturally submature.

mineralogy

quartz

Dominantly monocrystalline. Minor undulose monocrystalline quartz grains. Polycrystalline grains common; common grains with straight subgrains boundaries and some grains with serrate and variably sized subgrains. Polycrystalline grains with >3 subgrains are preferentially altered by tiny white mica. Common microcrystalline (Qp>3) polycrystalline quartz, with abundant alteration to white mica ± Fe oxide which gives a brown diffuse appearance. Minor chert.

feldspar

Almost entirely absent, trace of K-feldspar.

lithic fragments

Minor quartz-mica aggregates (schistose quartzite or schist).

accessory minerals

Trace zircon and rutile. Several zircon within quartz grains. Several large (1-2 mm) muscovite grains showing compactional strain, flexure, and breakage.

intrabasinal grains

None.

cement

Very little quartz overgrowths.

matrix

Extensive white mica matrix of clay and from alteration of grains.

porosity

Completely occluded by matrix.

other notes

The lower incidence of undulose quartz probaby due to presence of matrix that inhibits point to point strain buildup. Feldspar and other lithic fragments conspicuously absent. Most of the monocrystalline and polycrystalline quartz suggests a plutonic/high-grade metamorphic source. The polycrystalline quartz textures are indicative of strained metamorphic source (e.g., deformation under greenschist to amphibolite facies).

Sample	STH-128	number	%total	%framework	
raw data	Qmnu	314	59.6	68.9	
	Qmu	25	4.7	5.5	
	Qpq2-3	17	3.2	3.7	
	Qpq>3	78	14.8	17.1	see next page*
	P	0	0.0	0.0	
	K	2	0.4	0.4	
	Lv	0	0.0	0.0	
	Lm	7	1.3	1.5	
	Ls	0	0.0	0.0	
	Cht	0	0.0	0.0	
	M	6	1.1	1.3	
	D	1	0.2	0.2	
	other framework	6	1.1	1.3	see next page**
	cement	4	0.8		Fe oxide
	matrix	67	12.7		
	other non-framework	0	0.0		
	U	0	0.0	0.0	
	total	527	100.0		
	total framework	456	86.5		
	total non-framework	71	13.5		
recalculated	Qm	339	64.3	74.3	
data	Qpq	95	18.0	20.8	
	Q	434	82.4	95.2	
	F	2	0.4	0.4	
	L	7	1.3	1.5	
	Lm	7	1.3	1.5	
	Lv	0	0.0	0.0	
	Ls	0	0.0	0.0	
	Qp	95	18.0	20.8	
	Lvm	0	0.0	0.0	
	Lsm	7	1.3	1.5	
	Lt	102	19.4	22.4	

		normalized %	normalized total
ternary	QFL%Q	98.0	443
data	QFL%F	0.5	
	QFL%L	1.6	
	LmLvLs%Lm	100.0	7
	LmLvLs%Lv	0.0	
	LmLvLs%Ls	0.0	
	QpLvmLsm%Qp	93.1	102
	QpLvmLsm%Lvm	0.0	
	QpLvmLsm%Lsm	6.9	
	QmFLt%Qm	76.5	443
	QmFLt%F	0.5	
	QmFLt%Lt	23.0	
	QmPK%Qm	99.4	341
	QmPK%P	0.0	
	QmPK%K	0.6	
	QmQpq%Qmnu	72.4	434
	QmQpq%Qmu	5.8	
	QmQpq%Qpq2-3	3.9	
	QmQpq%Qpq>3	18.0	

STH-128

*Qpq>3

30	Qpq>3
48	altered polycrystalline quartz grains
78	total Qpq>3

**other framework

3	highly altered polyxtal qz with Fe oxide
3	chert & Fe oxide
6	total other framework

sample ID STH-130

location

Burnside Fm., Bear Creek Group, south Tinney Hills section (1410 m), east of Bathurst Inlet.

field relations

Cobble conglomerate facies at the base of the Conglomerate Member of the Burnside Fm. (the 4th cobble conglomerate horizon), in the proximal (southeastern) part of the basin. Corresponds with detrital zircon sample STH-DZ-4.

thin section description

summary

sublitharenite

texture

(mU-granule (2.3mm)), very poorly sorted, grains angular to rounded. Straight to concavo-convex grain boundaries between quartz grains. Texturally submature.

mineralogy

quartz

Dominantly monocrystalline, but high polycrystalline content. Minor undulose monocrystalline quartz grains. Polycrystalline grains common; common grains with straight subgrains boundaries and common grains with serrate and variably sized subgrains. Polycrystalline grains with >3 subgrains are preferentially altered by tiny white mica. Common microcrystalline (Qp>3) polycrystalline quartz, with abundant alteration to white mica ± Fe oxide which gives a brown diffuse appearance. Minor chert.

feldspar

No obvious feldspar.

lithic fragments

Common quartz-mica aggregates (schistose quartzite or schist), plus minor Fe oxide ± quartz ± phyllosilicate ("iron formation") and chert + Fe oxide ± phyllosilicate (chert). Some of the phyllosilicate-chert-Fe oxide grains may be volcanic lithic fragments.

accessory minerals

Several large (1-2 mm) muscovite grains showing compactional strain, flexure, and breakage.

intrabasinal grains

None.

cement

Authigenic Fe oxide.

matrix

Extensive white mica matrix of clay and from alteration of grains. Some may be psudomatrix of compacted altered fine grained clasts.

porosity

Completely occluded by matrix.

other notes

The lower incidence of undulose quartz probaby due to presence of matrix that inhibits point to point strain buildup. Feldspar and other lithic fragments

conspicuously absent. Most of the monocrystalline and polycrystalline quartz suggests a plutonic/high-grade metamorphic source. The polycrystalline quartz textures are indicative of strained metamorphic source (e.g., deformation under greenschist to amphibolite facies).
The interpretation of the highly altered grains is difficult; I have erred on the side of a metamorphic interpretation given the results of conglomerate clast counts that show common meta-siltstone and schist.

Sample	STH-130	number	%total	%framework	
raw data	Qmnu	213	45.1	52.9	
	Qmu	30	6.4	7.4	
	Qpq2-3	43	9.1	10.7	
	Qpq>3	79	16.7	19.6	see next page*
	P	0	0.0	0.0	
	K	0	0.0	0.0	
	Lv	0	0.0	0.0	
	Lm	34	7.2	8.4	see next page**
	Ls	0	0.0	0.0	
	Cht	2	0.4	0.5	
	M	2	0.4	0.5	
	D	0	0.0	0.0	
	other framework	0	0.0	0.0	
	cement	0	0.0		
	matrix	62	13.1		
	other non-framework	7	1.5		see next page***
	U	0	0.0	0.0	
	total	472	100.0		
	total framework	403	85.4		
	total non-framework	69	14.6		
recalculated data	Qm	243	51.5	60.3	
	Qpq	122	25.8	30.3	
	Q	367	77.8	91.1	
	F	0	0.0	0.0	
	L	34	7.2	8.4	
	Lm	34	7.2	8.4	
	Lv	0	0.0	0.0	
	Ls	0	0.0	0.0	
	Qp	124	26.3	30.8	
	Lvm	0	0.0	0.0	
	Lsm	34	7.2	8.4	
	Lt	158	33.5	39.2	

		normalized %	normalized total
ternary data	QFL%Q	91.5	401
	QFL%F	0.0	
	QFL%L	8.5	
	LmLvLs%Lm	100.0	34
	LmLvLs%Lv	0.0	
	LmLvLs%Ls	0.0	
	QpLvmLsm%Qp	78.5	158
	QpLvmLsm%Lvm	0.0	
	QpLvmLsm%Lsm	21.5	
	QmFLt%Qm	60.6	401
	QmFLt%F	0.0	
	QmFLt%Lt	39.4	
	QmPK%Qm	100.0	243
	QmPK%P	0.0	
	QmPK%K	0.0	
	QmQpq%Qmnu	58.4	365
	QmQpq%Qmu	8.2	
	QmQpq%Qpq2-3	11.8	
	QmQpq%Qpq>3	21.6	

STH-130

*polycrystalline quartz

46 polycrystalline quartz
4 polyxtal qz with phyllosilicate flecks
27 highly altered chert & phyllo + minor Fe oxide
2 highly altered phyllosilicate & Fe oxide & qz
79 total polycrystalline qz

**Lm

14 low-rank metasediment (qz & mica)

"iron formation"

6 Fe oxide + minor phyllo & qz

chert and qz as Lm

1 chert + minor phyllo & Fe oxide
4 chert & Fe oxide
5 microxtaline qz & Fe oxide
4 chert & Fe oxide + minor phyllosilicate
14 total chert ± Fe oxide ± phyllosilicate (Lm)

34 total Lm

***authigenic Fe oxide

7 Fe oxide

NB: the assignment of many of these grains to modal catagories is uncertain, but the important conclusion to draw is that many of the grains derive from a low- to moderate-grade metasedimentary source

some of the grains could be reclassified from Qpq to Lm

sample ID STH-131
location
Burnside Fm., Bear Creek Group, south Tinney Hills section (1492 m), east of Bathurst Inlet.
field relations
Cobble conglomerate facies within the Conglomerate Member of the Burnside Fm. (the 4th cobble conglomerate horizon), in the proximal (southeastern) part of the basin.
thin section description
summary
sublitharenite
texture
(mL-granule (2.1mm)), poorly sorted, grains angular to rounded. Straight to concavo-convex grain boundaries between quartz grains. Texturally submature.
mineralogy
quartz
Dominantly monocrystalline, but high polycrystalline content. Minor undulose monocrystalline quartz grains. Polycrystalline grains common; common grains with straight subgrains boundaries and common grains with serrate and variably sized subgrains. Polycrystalline grains with >3 subgrains are preferentially altered by tiny white mica. Common microcrystalline (Qp>3) polycrystalline quartz, with abundant alteration to white mica ± Fe oxide which gives a brown diffuse appearance. Minor chert variably altered to to fine white micas.
feldspar
No obvious feldspar.
lithic fragments
Very common quartz-mica aggregates (schistose quartzite or schist), and chert + Fe oxide ("iron formation"). Some of the phyllosilicate-chert-Fe oxide grains could be volcanic lithic fragments. Probable plutonic fragments of quartz with internal grains completely altered to mica and chert that were probably feldspar.
accessory minerals
Several large (1-2 mm) muscovite grains showing compactional strain, flexure, and breakage. Local concentrations of zircon and rutile.
intrabasinal grains
None.
cement
Minor quartz overgrowths at quartz-quartz grain contacts.
matrix
Extensive white mica matrix of clay and from alteration of grains. Some large micas may be pseudomorphous after diagenetic vermicular clays. Some may be psudomatrix of compacted altered fine grained clasts.
porosity
Completely occluded by matrix.
other notes

The lower incidence of undulose quartz probaby due to presence of matrix that inhibits point to point strain buildup. Feldspar and other lithic fragments conspicuously absent. Most of the monocrystalline and polycrystalline quartz suggests a plutonic/high-grade metamorphic source. The polycrystalline quartz textures are indicative of strained metamorphic source (e.g., deformation under greenschist to amphibolite facies).
The interpretation of the highly altered grains is difficult; I have erred on the side of a metamorphic interpretation given the results of conglomerate clast counts that show common meta-siltstone and schist.

Sample	**STH-131**	number	%total	%framework	
raw data	Qmnu	167	39.2	42.1	
	Qmu	29	6.8	7.3	
	Qpq2-3	37	8.7	9.3	
	Qpq>3	113	26.5	28.5	see next page*
	P	0	0.0	0.0	
	K	0	0.0	0.0	
	Lv	0	0.0	0.0	
	Lm	45	10.6	11.3	see next page**
	Ls	2	0.5	0.5	
	Cht	2	0.5	0.5	
	M	2	0.5	0.5	
	D	0	0.0	0.0	
	other framework	0	0.0	0.0	
	cement	4	0.9		
	matrix	25	5.9		
	other non-framework	0	0.0		
	U	0	0.0	0.0	
	total	426	100.0		
	total framework	397	93.2		
	total non-framework	29	6.8		
recalculated	Qm	196	46.0	49.4	
data	Qpq	150	35.2	37.8	
	Q	348	81.7	87.7	
	F	0	0.0	0.0	
	L	47	11.0	11.8	
	Lm	45	10.6	11.3	
	Lv	0	0.0	0.0	
	Ls	2	0.5	0.5	
	Qp	152	35.7	38.3	
	Lvm	0	0.0	0.0	
	Lsm	47	11.0	11.8	
	Lt	199	46.7	50.1	

		normalized %	normalized total
ternary	QFL%Q	88.1	395
data	QFL%F	0.0	
	QFL%L	11.9	
	LmLvLs%Lm	95.7	47
	LmLvLs%Lv	0.0	
	LmLvLs%Ls	4.3	
	QpLvmLsm%Qp	76.4	199
	QpLvmLsm%Lvm	0.0	
	QpLvmLsm%Lsm	23.6	
	QmFLt%Qm	49.6	395
	QmFLt%F	0.0	
	QmFLt%Lt	50.4	
	QmPK%Qm	100.0	196
	QmPK%P	0.0	
	QmPK%K	0.0	
	QmQpq%Qmnu	48.3	346
	QmQpq%Qmu	8.4	
	QmQpq%Qpq2-3	10.7	
	QmQpq%Qpq>3	32.7	

STH-131

*polycrystalline qz

73	polycrystalline qz
40	highly altered phyllosilicate & chert
113	total polycrystalline qz

**Lm

26	strained qz + mica ± Fe oxide
12	banded Fe oxide + chert
7	chert + Fe oxide
45	total Lm

sample ID STH-132

location

Burnside Fm., Bear Creek Group, south Tinney Hills section (1684 m), east of Bathurst Inlet.

field relations

Very coarse cobble conglomerate horizon at the top of the Conglomerate Member of the Burnside Fm. in the proximal (southeastern) part of the basin. Corresponds with detrital zircon sample STH-DZ-5.

thin section description

summary

quartz arenite

texture

(f-m), moderately sorted, grains subrounded to well rounded. Straight to concavo-convex grain boundaries between quartz grains. Texturally submature.

mineralogy

quartz

Dominantly monocrystalline, but high polycrystalline content. Minor undulose monocrystalline quartz grains. Polycrystalline grains common; common grains with serrate and variably sized subgrains. Minor chert.

feldspar

No obvious feldspar.

lithic fragments

Common grains that are entirely altered to radiating white mica and crypto- to microcrystalline quartz. Some of phyllosilicate-chert-Fe oxide grains could be volcanic lithic fragments. Probable plutonic fragments of quartz with internal grains completely altered to mica and chert that were probably feldspar.

accessory minerals

Hematite, opaque authigenic Fe oxide that form thin radiating crystal bunches. Zircon.

intrabasinal grains

Altered grains that may be mudstone clasts.

cement

Common quartz overgrowths at quartz-quartz grain contacts and away from grains that have been altered to micas. Thin Fe oxide coatings on grains make it distinction of rounded quartz from overgrowths. Common white mica growth as radiating crystals from grain boundaries.

matrix

Extensive white mica matrix of clay and from alteration of grains. Some may be psudomatrix of compacted altered fine grained clasts.

porosity

Completely occluded by matrix and cement.

other notes

The lower incidence of undulose quartz probaby due to presence of matrix that inhibits point to point strain buildup. Feldspar and other lithic fragments conspicuously absent. Most of the monocrystalline and polycrystalline quartz

suggests a plutonic/high-grade metamorphic source. The polycrystalline quartz textures are indicative of strained metamorphic source (e.g., deformation under greenschist to amphibolite facies).

Sample	STH-132	number	%total	%framework	
raw data	Qmnu	265	55.4	61.9	
	Qmu	33	6.9	7.7	
	Qpq2-3	36	7.5	8.4	
	Qpq>3	63	13.2	14.7	
	P	0	0.0	0.0	
	K	0	0.0	0.0	
	Lv	0	0.0	0.0	
	Lm	0	0.0	0.0	
	Ls	0	0.0	0.0	
	Cht	10	2.1	2.3	
	M	1	0.2	0.2	
	D	0	0.0	0.0	
	other framework	20	4.2	4.7	intrabasinal Ls
	cement	8	1.7		
	matrix	28	5.9		
	other non-framework	14	2.9	authigenic Fe oxide	
	U	0	0.0	0.0	
	total	478	100.0		
	total framework	428	89.5		
	total non-framework	50	10.5		
recalculated data	Qm	298	62.3	69.6	
	Qpq	99	20.7	23.1	
	Q	407	85.1	95.1	
	F	0	0.0	0.0	
	L	0	0.0	0.0	
	Lm	0	0.0	0.0	
	Lv	0	0.0	0.0	
	Ls	0	0.0	0.0	
	Qp	109	22.8	25.5	
	Lvm	0	0.0	0.0	
	Lsm	0	0.0	0.0	
	Lt	109	22.8	25.5	

		normalized %	normalized total
ternary data	QFL%Q	100.0	407
	QFL%F	0.0	
	QFL%L	0.0	
	LmLvLs%Lm	0.0	0
	LmLvLs%Lv	0.0	
	LmLvLs%Ls	0.0	
	QpLvmLsm%Qp	100.0	109
	QpLvmLsm%Lvm	0.0	
	QpLvmLsm%Lsm	0.0	
	QmFLt%Qm	73.2	407
	QmFLt%F	0.0	
	QmFLt%Lt	26.8	
	QmPK%Qm	100.0	298
	QmPK%P	0.0	
	QmPK%K	0.0	
	QmQpq%Qmnu	66.8	397
	QmQpq%Qmu	8.3	
	QmQpq%Qpq2-3	9.1	
	QmQpq%Qpq>3	15.9	

sample ID STH-139

location

Burnside Fm., Bear Creek Group, south Tinney Hills section (1975 m), east of Bathurst Inlet.

field relations

Gravelly sandstone and conglomerate within the Gravelly Sandstone Member of the Burnside Fm. in the proximal (southeastern) part of the basin.

thin section description

summary

subarkose-sublitharenite

texture

(mL-cU), moderately sorted, grains angular to rounded. Straight to concavo-convex grain boundaries between quartz grains. Texturally submature.

mineralogy

quartz

Dominantly monocrystalline, but high polycrystalline content. Minor undulose monocrystalline quartz grains. Polycrystalline grains common; common grains with serrate and variably sized subgrains. Minor chert.

feldspar

Minor K-feldspar including microcline, perthite, and orthoclase. Trace plagioclase. Feldspars are commonly very fresh.

lithic fragments

Probable silicic volcanic clasts that are cherty with definite flow fabric. Plutonic fragments of quartz with feldspar inclusions.

accessory minerals

Hematite, opaque authigenic Fe oxide that form thin radiating crystal bunches. Zircon.

intrabasinal grains

Altered grains that may be mudstone clasts.

cement

Minor quartz overgrowths at quartz-quartz grain contacts and away from grains that have been altered to micas. Common white mica growth as radiating crystals from grain boundaries.

matrix

Extensive white mica matrix of clay and from alteration of grains. Some may be psudomatrix of compacted altered fine grained clasts.

porosity

Completely occluded by matrix and cement.

other notes

The lower incidence of undulose quartz probaby due to presence of matrix that inhibits point to point strain buildup. Feldspar and other lithic fragments conspicuously present. Most of the monocrystalline and polycrystalline quartz suggests a plutonic/high-grade metamorphic source. The polycrystalline quartz textures are indicative of strained metamorphic source (e.g., deformation under greenschist to amphibolite facies). The common feldspar suggests plutonic source.

Sample	STH-139	number	%total	%framework	
raw data	Qmnu	247	43.6	49.4	
	Qmu	68	12.0	13.6	
	Qpq2-3	40	7.1	8.0	
	Qpq>3	81	14.3	16.2	see next page*
	P	0	0.0	0.0	
	K	32	5.6	6.4	
	Lv	1	0.2	0.2	
	Lm	13	2.3	2.6	see next page**
	Ls	7	1.2	1.4	
	Cht	11	1.9	2.2	
	M	0	0.0	0.0	
	D	0	0.0	0.0	
	other framework	0	0.0	0.0	
	cement	1	0.2		
	matrix	60	10.6		
	other non-framework	6	1.1		Fe oxide
	U	0	0.0	0.0	
	total	567	100.0		
	total framework	500	88.2		
	total non-framework	67	11.8		
recalculated	Qm	315	55.6	63.0	
data	Qpq	121	21.3	24.2	
	Q	447	78.8	89.4	
	F	32	5.6	6.4	
	L	21	3.7	4.2	
	Lm	13	2.3	2.6	
	Lv	1	0.2	0.2	
	Ls	7	1.2	1.4	
	Qp	132	23.3	26.4	
	Lvm	1	0.2	0.2	
	Lsm	20	3.5	4.0	
	Lt	153	27.0	30.6	

		normalized %	normalized total
ternary	QFL%Q	89.4	500
data	QFL%F	6.4	
	QFL%L	4.2	
	LmLvLs%Lm	61.9	21
	LmLvLs%Lv	4.8	
	LmLvLs%Ls	33.3	
	QpLvmLsm%Qp	86.3	153
	QpLvmLsm%Lvm	0.7	
	QpLvmLsm%Lsm	13.1	
	QmFLt%Qm	63.0	500
	QmFLt%F	6.4	
	QmFLt%Lt	30.6	
	QmPK%Qm	90.8	347
	QmPK%P	0.0	
	QmPK%K	9.2	
	QmQpq%Qmnu	56.7	436
	QmQpq%Qmu	15.6	
	QmQpq%Qpq2-3	9.2	
	QmQpq%Qpq>3	18.6	

Sample STH-139

*polycrystalline qz	
34	pristine polycrystalline qz
20	polycrystalline qz with phyllo flecks
27	highly altered qz & mica after polyxtal qz
81	total polycrystalline qz
**Lm	
4	strained qz-mica aggregates
5	chert + Fe oxide
4	Fe oxide + chert
13	total Lm

sample ID STH-142

location

Burnside Fm., Bear Creek Group, south Tinney Hills section (2065 m), on east shore of Bathurst Inlet.

field relations

Prominant gravelly sandstone and conglomerate horizon on shoreline that contains red undeformed felsic volcanic clasts near the top of the Gravelly Sandstone Member of the Burnside Fm. in the proximal (southeastern) part of the basin. Corresponds with detrital zircon sample STH-DZ-6.

thin section description

summary

subarkose-sublitharenite

texture

(mU-vcU), poorly sorted, grains angular to rounded. Straight to concavo-convex grain boundaries between quartz grains. Texturally submature.

mineralogy

quartz

Dominantly monocrystalline, but high polycrystalline content. Minor undulose monocrystalline quartz grains. Polycrystalline grains common; most grains show straight subgrain boundaries; minor grains with serrate and variably sized subgrains. Minor chert.

feldspar

Common K-feldspar including microcline, perthite, and orthoclase. Minor plagioclase. Feldspars are commonly very fresh.

lithic fragments

Silicic volcanic clasts that are cherty with definite flow fabric; phenocrysts include beta quartz and completely altered feldspars. Plutonic fragments of quartz with feldspar inclusions and K-feldspar with quartz inclusions. Feldspar lacks zoning. Minor metamorphic clasts of foliated quartzite with muscovite and hematite + chert (jasper, "iron formation"). Minor silststone and (vf) sandstone clasts with quartz and K-feldspar.

accessory minerals

Hematite, opaque authigenic Fe oxide. Zircon.

intrabasinal grains

None.

cement

Minor quartz overgrowths at quartz-quartz grain contacts and away from grains that have been altered to micas. Common white mica growth as radiating crystals from grain boundaries.

matrix

Minor clay altered to mica in muddy-silty laminae.

porosity

Completely occluded by matrix and cement.

other notes

The lower incidence of undulose quartz probaby due to presence of matrix that inhibits point to point strain buildup. Feldspar and other lithic fragments conspicuously present. Fresh feldspar must derive from a plutonic source

because no feldspars show any zoning and all phenocrysts in volcanic clasts that suggest original feldspars have been completely replaced by mica. Most of the monocrystalline and polycrystalline quartz suggests a plutonic/high-grade metamorphic source. The polycrystalline quartz textures are indicative of strained metamorphic source (e.g., deformation under greenschist to amphibolite facies). The common feldspar suggests plutonic source.

Sample	STH-142	number	%total	%framework
raw data	Qmnu	193	36.8	41.1
	Qmu	85	16.2	18.1
	Qpq2-3	34	6.5	7.2
	Qpq>3	62	11.8	13.2
	P	5	1.0	1.1
	K	39	7.4	8.3
	Lv	29	5.5	6.2
	Lm	7	1.3	1.5
	Ls	5	1.0	1.1
	Cht	7	1.3	1.5
	M	0	0.0	0.0
	D	0	0.0	0.0
	other framework	0	0.0	0.0
	cement	0	0.0	
	matrix	55	10.5	
	other non-framework	0	0.0	
	U	4	0.8	0.9
	total	525	100.0	
	total framework	470	89.5	
	total non-framework	55	10.5	
recalculated data	Qm	278	53.0	59.1
	Qpq	96	18.3	20.4
	Q	381	72.6	81.1
	F	44	8.4	9.4
	L	41	7.8	8.7
	Lm	7	1.3	1.5
	Lv	29	5.5	6.2
	Ls	5	1.0	1.1
	Qp	103	19.6	21.9
	Lvm	29	5.5	6.2
	Lsm	12	2.3	2.6
	Lt	144	27.4	30.6
		normalized %	normalized total	
ternary data	QFL%Q	81.8	466	
	QFL%F	9.4		
	QFL%L	8.8		
	LmLvLs%Lm	17.1	41	
	LmLvLs%Lv	70.7		
	LmLvLs%Ls	12.2		
	QpLvmLsm%Qp	71.5	144	
	QpLvmLsm%Lvm	20.1		
	QpLvmLsm%Lsm	8.3		
	QmFLt%Qm	59.7	466	
	QmFLt%F	9.4		
	QmFLt%Lt	30.9		
	QmPK%Qm	86.3	322	
	QmPK%P	1.6		
	QmPK%K	12.1		
	QmQpq%Qmnu	51.6	374	
	QmQpq%Qmu	22.7		
	QmQpq%Qpq2-3	9.1		
	QmQpq%Qpq>3	16.6		

sample ID STH-014

location

Burnside-Mara Fm., Bear Creek Group, south Tinney Hills section, on east shore of Bathurst Inlet, at Tinney Cove. ("2543 m" in the upper section of south Tinney Hills).

field relations

Braid delta facies of Orange Sandstone Member of the Burnside Fm. in the proximal (southeastern) part of the basin.

thin section description

summary

subarkose, nearly arkose

texture

(fU-cL), moderately sorted, grains angular to rounded. Straight to concavo-convex grain boundaries between quartz grains. Texturally submature.

mineralogy

quartz

Dominantly monocrystalline. Minor undulose monocrystalline quartz grains. Minor polycrystalline grains; most grains show straight subgrain boundaries. Trace chert.

feldspar

Abundant K-feldspar including microcline, perthite, and orthoclase. Minor plagioclase. Feldspars are commonly very fresh, but show variable alteration and probable thin K-feldspar overgrowths that are preferentially replaced by late dolomite. Plagioclase preferentially replaced by dolomite.

lithic fragments

Minor quartz-mica schistose grains. Minor silststone and (vf) sandstone clasts with quartz and K-feldspar.

accessory minerals

Opaque authigenic Fe oxide. Zircon.

intrabasinal grains

None.

cement

Quartz overgrowths occlude all primary porosity. Late secondary dolomite preferentially replaces along quartz cemented intergranular pores and plagioclase, but forms euhedral rhombs across quartz grains.

matrix

Extensive white mica matrix of clay and from alteration of grains. Some may be psudomatrix of compacted altered fine grained clasts.

porosity

Completely occluded by cement.

other notes

Feldspar and other lithic fragments conspicuously present. Most of the monocrystalline and polycrystalline quartz suggests a plutonic/high-grade metamorphic source. The common feldspar suggests plutonic source.

Sample	STH-014	number	%total	%framework	
raw data	Qmnu	221	37.4	48.7	
	Qmu	37	6.3	8.1	
	Qpq2-3	23	3.9	5.1	
	Qpq>3	48	8.1	10.6	see next page*
	P	13	2.2	2.9	
	K	93	15.7	20.5	see next page**
	Lv	0	0.0	0.0	
	Lm	3	0.5	0.7	
	Ls	7	1.2	1.5	
	Cht	9	1.5	2.0	
	M	0	0.0	0.0	
	D	0	0.0	0.0	
	other framework	0	0.0	0.0	
	cement	62	10.5		
	matrix	1	0.2		
	other non-framework	74	12.5		dolomite replcmt
	U	0	0.0	0.0	
	total	591	100.0		
	total framework	454	76.8		
	total non-framework	137	23.2		
recalculated	Qm	258	43.7	56.8	
data	Qpq	71	12.0	15.6	
	Q	338	57.2	74.4	
	F	106	17.9	23.3	
	L	10	1.7	2.2	
	Lm	3	0.5	0.7	
	Lv	0	0.0	0.0	
	Ls	7	1.2	1.5	
	Qp	80	13.5	17.6	
	Lvm	0	0.0	0.0	
	Lsm	10	1.7	2.2	
	Lt	90	15.2	19.8	

		normalized %	normalized total
ternary	QFL%Q	74.4	454
data	QFL%F	23.3	
	QFL%L	2.2	
	LmLvLs%Lm	30.0	10
	LmLvLs%Lv	0.0	
	LmLvLs%Ls	70.0	
	QpLvmLsm%Qp	88.9	90
	QpLvmLsm%Lvm	0.0	
	QpLvmLsm%Lsm	11.1	
	QmFLt%Qm	56.8	454
	QmFLt%F	23.3	
	QmFLt%Lt	19.8	
	QmPK%Qm	70.9	364
	QmPK%P	3.6	
	QmPK%K	25.5	
	QmQpq%Qmnu	67.2	329
	QmQpq%Qmu	11.2	
	QmQpq%Qpq2-3	7.0	
	QmQpq%Qpq>3	14.6	

Sample STH-014

* polycrystalline qz

43	pristine polycrystalline qz
3	polycrystalline qz with phyllo flecks
2	highly altered qz & mica after polyxtal qz
48	total polycrystalline qz

**K

82	relatively unaltered
11	common phyllo alteration
93	total K

sample ID STH-021

location

Burnside-Mara Fm., Bear Creek Group, south Tinney Hills section, on east shore of Bathurst Inlet, at Tinney Cove. ("2785 m" in the upper section of south Tinney Hills). Corresponds with detrital zircon sample STH-DZ-8.

field relations

Braid delta facies of Orange Sandstone Member of the Burnside Fm. in the proximal (southeastern) part of the basin.

thin section description

summary

arkose

texture

(fU), moderately to well sorted with sparse (vc-granule), grains angular to rounded. Straight to concavo-convex grain boundaries between quartz grains. Texturally submature.

mineralogy

quartz

Dominantly monocrystalline. Minor undulose monocrystalline quartz grains. Minor Polycrystalline grains; most grains show straight subgrain boundaries. Trace chert.

feldspar

Abundant K-feldspar including microcline, perthite, and orthoclase. Minor plagioclase. Feldspars are commonly very fresh, but show variable alteration and thin K-feldspar overgrowths that are preferentially replaced by late dolomite. Plagioclase preferentially replaced by dolomite.

lithic fragments

Common volcanic fragments, minor plutonic fragments of quartz and feldspar. Minor quartz-mica with annealed quartz grains. Minor silststone and (vf) sandstone clasts with quartz and K-feldspar.

accessory minerals

Muscovite. Opaque authigenic Fe oxide. Zircon.

intrabasinal grains

Platy carbonate clasts with quartz and feldspar silt.

cement

Quartz overgrowths occlude all primary porosity. Late thin feldspar overgrowths. Late secondary dolomite preferentially replaces along quartz cemented intergranular pores and plagioclase, but forms euhedral rhombs across quartz grains.

matrix

Extensive white mica matrix of clay and from alteration of grains. Some may be psudomatrix of compacted altered fine grained clasts.

porosity

Completely occluded by cement.

other notes

Feldspar and other lithic fragments conspicuously present. Most of the monocrystalline and polycrystalline quartz suggests a plutonic/high-grade metamorphic source. The common feldspar suggests plutonic source.

Sample	STH-021	number	%total	%framework	
raw data	Qmnu	139	27.7	30.2	
	Qmu	32	6.4	7.0	
	Qpq2-3	10	2.0	2.2	
	Qpq>3	11	2.2	2.4	
	P	113	22.6	24.6	
	K	123	24.6	26.7	
	Lv	8	1.6	1.7	
	Lm	0	0.0	0.0	
	Ls	2	0.4	0.4	
	Cht	1	0.2	0.2	
	M	4	0.8	0.9	
	D	1	0.2	0.2	
	other framework	12	2.4	2.6	
	cement	22	4.4		qz overgrowths
	matrix	1	0.2		
	other non-framework	18	3.6		dolomite replcmt
	U	4	0.8	0.9	
	total	501	100.0		
	total framework	460	91.8		
	total non-framework	41	8.2		
recalculated	Qm	171	34.1	37.2	
data	Qpq	21	4.2	4.6	
	Q	193	38.5	42.0	
	F	236	47.1	51.3	
	L	10	2.0	2.2	
	Lm	0	0.0	0.0	
	Lv	8	1.6	1.7	
	Ls	2	0.4	0.4	
	Qp	22	4.4	4.8	
	Lvm	8	1.6	1.7	
	Lsm	2	0.4	0.4	
	Lt	32	6.4	7.0	

		normalized %	normalized total
ternary	QFL%Q	44.0	439
data	QFL%F	53.8	
	QFL%L	2.3	
	LmLvLs%Lm	0.0	10
	LmLvLs%Lv	80.0	
	LmLvLs%Ls	20.0	
	QpLvmLsm%Qp	68.8	32
	QpLvmLsm%Lvm	25.0	
	QpLvmLsm%Lsm	6.3	
	QmFLt%Qm	39.0	439
	QmFLt%F	53.8	
	QmFLt%Lt	7.3	
	QmPK%Qm	42.0	407
	QmPK%P	27.8	
	QmPK%K	30.2	
	QmQpq%Qmnu	72.4	192
	QmQpq%Qmu	16.7	
	QmQpq%Qpq2-3	5.2	
	QmQpq%Qpq>3	5.7	

sample ID WC-01A

location

Base of Burnside Fm., Bear Creek Group, Wolverine Canyon section west of Mara River, southeast of Kuuvik Lake.

field relations

Mixed sandstone-siltstone marine shelf facies in the distal (northwestern) part of the basin.

thin section description

summary

quartz arenite

texture

(cL-vcU), moderately to well sorted, grains rounded to well-rounded. Straight, concavo-convex grain, and sutured boundaries between quartz grains. Texturally submature.

mineralogy

quartz

Dominantly monocrystalline. Undulose grains may be due almost entirely to compaction at grain-to-grain point contacts. Common polycrystalline grains; most grains show straight subgrain boundaries. Trace chert.

feldspar

Trace K-feldspar.

lithic fragments

Minor metamorphic chert + white mica ± chlorite.

accessory minerals

Muscovite broken by compaction. Opaque authigenic Fe oxide. Zircon.

intrabasinal grains

Mudstone-siltstone and (vf) sandstone with chlorite, dolomite, and Fe oxide.

cement

Partial fill by syntaxial quartz overgrowths. Fe-rich dolomite fills remaining primary porosity; this may be a late phase.

matrix

Chlorite replacement of clay and from alteration of grains, especially polycrystalline quartz and intrabasinal sedimentary grains. Fe oxide. Some may be psudomatrix of compacted altered fine grained clasts.

porosity

Completely occluded by cement and matrix.

other notes

Feldspar and other lithic fragments conspicuously absent. Most of the monocrystalline and polycrystalline quartz suggests a plutonic/high-grade metamorphic source.

Sample	WC-1A	number	%total	%framework	
raw data	Qmnu	231	40.5	45.7	
	Qmu	95	16.7	18.8	
	Qpq2-3	28	4.9	5.5	
	Qpq>3	42	7.4	8.3	
	P	0	0.0	0.0	
	K	1	0.2	0.2	
	Lv	0	0.0	0.0	
	Lm	9	1.6	1.8	see next page*
	Ls	0	0.0	0.0	
	Cht	4	0.7	0.8	
	M	0	0.0	0.0	
	D	0	0.0	0.0	
	other framework	96	16.8	19.0	see next page**
	cement	19	3.3		
	matrix	45	7.9		
	other non-framework	0	0.0		
	U	0	0.0	0.0	
	total	570	100.0		
	total framework	506	88.8		
	total non-framework	64	11.2		
recalculated data	Qm	326	57.2	64.4	
	Qpq	70	12.3	13.8	
	Q	400	70.2	79.1	
	F	1	0.2	0.2	
	L	9	1.6	1.8	
	Lm	9	1.6	1.8	
	Lv	0	0.0	0.0	
	Ls	0	0.0	0.0	
	Qp	74	13.0	14.6	
	Lvm	0	0.0	0.0	
	Lsm	9	1.6	1.8	
	Lt	83	14.6	16.4	

		normalized %	normalized total
ternary data	QFL%Q	97.6	410
	QFL%F	0.2	
	QFL%L	2.2	
	LmLvLs%Lm	100.0	9
	LmLvLs%Lv	0.0	
	LmLvLs%Ls	0.0	
	QpLvmLsm%Qp	89.2	83
	QpLvmLsm%Lvm	0.0	
	QpLvmLsm%Lsm	10.8	
	QmFLt%Qm	79.5	410
	QmFLt%F	0.2	
	QmFLt%Lt	20.2	
	QmPK%Qm	99.7	327
	QmPK%P	0.0	
	QmPK%K	0.3	
	QmQpq%Qmnu	58.3	396
	QmQpq%Qmu	24.0	
	QmQpq%Qpq2-3	7.1	
	QmQpq%Qpq>3	10.6	

Sample **WC-1A**

*Lm

2	chert + phyllo
7	chert + phyllo + chlorite
9	total Lm

**intrabasinal clasts

44	(vf) qz sandstone with dolomite replacement
52	chloritic, Fe oxide altered mudstone
96	total intrabasinal clasts

sample ID WC-14

location

Burnside Fm., Bear Creek Group, Wolverine Canyon section (280 m) west of Mara River, southeast of Kuuvik Lake. Corresponds with detrital zircon sample WC-DZ-1.

field relations

Coarse lower braid plain facies in the distal (northwestern) part of the basin.

thin section description

summary

subarkose

texture

Bimodal grain size (fL-fU) and (cL-cU), moderately to well sorted, large grains grains rounded to well-rounded, (f) grains more angular. Straight, concavo-convex grain, and sutured boundaries between quartz grains. Texturally submature. Thin (few mm) laminae of sandy mudstone-siltstone.

mineralogy

quartz

Dominantly monocrystalline. Undulose grains may be due almost entirely to compaction at grain-to-grain point contacts. Common polycrystalline grains; grains show both straight subgrain boundaries and crenulated boundaries with variable subgrain size. Trace chert. Few quartz grains contain inclusions of zircon or vermicular chlorite.

feldspar

Common K-feldspar, trace plagioclase. Feldspars are commonly very fresh, some quite altered to mica.

lithic fragments

Minor metamorphic Fe oxide + chert or foliated polycrystalline quartz + mica grains.

accessory minerals

Muscovite broken by compaction.

intrabasinal grains

Trace mudstone.

cement

Minor syntaxial quartz overgrowths.

matrix

Extensive sericite and chert pore fills; probably replacement of clay matrix. Fe oxide. Some may be psudomatrix of compacted altered fine grained clasts.

porosity

Completely occluded by cement and matrix.

other notes

Feldspar and other lithic fragments conspicuously present. Most of the monocrystalline and polycrystalline quartz suggests a plutonic/high-grade metamorphic source. Common feldspar suggests plutonic source.

Sample	WC-14	number	%total	%framework	
raw data	Qmnu	234	47.0	54.2	
	Qmu	46	9.2	10.6	
	Qpq2-3	44	8.8	10.2	
	Qpq>3	53	10.6	12.3	
	P	2	0.4	0.5	
	K	36	7.2	8.3	see next page*
	Lv	0	0.0	0.0	
	Lm	6	1.2	1.4	see next page**
	Ls	1	0.2	0.2	
	Cht	6	1.2	1.4	
	M	1	0.2	0.2	
	D	0	0.0	0.0	
	other framework	1	0.2	0.2	intrabasinal mdst
	cement	8	1.6		
	matrix	58	11.6		
	other non-framework	0	0.0		
	U	2	0.4	0.5	
	total	498	100.0		
	total framework	432	86.7		
	total non-framework	66	13.3		
recalculated	Qm	280	56.2	64.8	
data	Qpq	97	19.5	22.5	
	Q	383	76.9	88.7	
	F	38	7.6	8.8	
	L	7	1.4	1.6	
	Lm	6	1.2	1.4	
	Lv	0	0.0	0.0	
	Ls	1	0.2	0.2	
	Qp	103	20.7	23.8	
	Lvm	0	0.0	0.0	
	Lsm	7	1.4	1.6	
	Lt	110	22.1	25.5	
		normalized %	normalized total		
ternary	QFL%Q	89.5	428		
data	QFL%F	8.9			
	QFL%L	1.6			
	LmLvLs%Lm	85.7	7		
	LmLvLs%Lv	0.0			
	LmLvLs%Ls	14.3			
	QpLvmLsm%Qp	93.6	110		
	QpLvmLsm%Lvm	0.0			
	QpLvmLsm%Lsm	6.4			
	QmFLt%Qm	65.4	428		
	QmFLt%F	8.9			
	QmFLt%Lt	25.7			
	QmPK%Qm	88.1	318		
	QmPK%P	0.6			
	QmPK%K	11.3			
	QmQpq%Qmnu	62.1	377		
	QmQpq%Qmu	12.2			
	QmQpq%Qpq2-3	11.7			
	QmQpq%Qpq>3	14.1			

Sample **WC-14**

*K

25 relatively unaltered K
11 phyllo replacement of K
36 total K

*Lm

1 strained qz-mica aggregates
5 Fe oxide + chert
6 total Lm

sample ID WC-27

location

Burnside Fm., Bear Creek Group, Wolverine Canyon section (712 m) west of Mara River, southeast of Kuuvik Lake. Corresponds with detrital zircon sample WC-DZ-2.

field relations

Coarse lower braid plain facies in the distal (northwestern) part of the basin.

thin section description

summary

quartz arenite

texture

(mL-cU), some (vc), moderately to well sorted, large grains grains rounded to well-rounded, (f) grains more angular. Straight, concavo-convex grain, and sutured boundaries between quartz grains. Texturally submature.

mineralogy

quartz

Dominantly monocrystalline. Undulose grains may be due almost entirely to compaction at grain-to-grain point contacts. Common polycrystalline grains; grains show both straight subgrain boundaries and crenulated boundaries with variable subgrain size. Trace chert. Few quartz grains contain inclusions of zircon.

feldspar

Common K-feldspar, though less than in lower samples; trace plagioclase. Feldspars are commonly very fresh, some quite altered to mica. Large K-feldspar are commonly well rounded; other sizes are more angular.

lithic fragments

Minor strained polycrystalline quartz + mica grains, Fe oxide + recrystallized polycrystalline quartz. Minor plutonic rock fragments of polycrystalline quartz with subordinate feldspar.

accessory minerals

Muscovite.

intrabasinal grains

None.

cement

All primary porosity occluded by syntaxial quartz overgrowths. Minor locally distributed Fe oxide around few grains. Thin syntaxial feldspar overgrowths on feldspar.

matrix

Trace sericite and chert pore fills; probably replacement of clay matrix. Fe oxide. Some may be psudomatrix of compacted altered fine grained clasts.

porosity

Completely occluded by cement and matrix.

other notes

Feldspar and other lithic fragments conspicuously present. Most of the monocrystalline and polycrystalline quartz suggests a plutonic/high-grade metamorphic source. Common feldspar suggests plutonic source.

Sample	WC-27	number	%total	%framework	
raw data	Qmnu	253	51.7	59.7	
	Qmu	71	14.5	16.7	
	Qpq2-3	26	5.3	6.1	
	Qpq>3	49	10.0	11.6	
	P	0	0.0	0.0	
	K	18	3.7	4.2	
	Lv	0	0.0	0.0	
	Lm	3	0.6	0.7	2qz-mica,1Fe-chert
	Ls	0	0.0	0.0	
	Cht	1	0.2	0.2	
	M	3	0.6	0.7	
	D	0	0.0	0.0	
	other framework	0	0.0	0.0	
	cement	60	12.3		qz overgrowths
	matrix	3	0.6		
	other non-framework	2	0.4		Fe oxide cement
	U	0	0.0	0.0	
	total	489	100.0		
	total framework	424	86.7		
	total non-framework	65	13.3		
recalculated data	Qm	324	66.3	76.4	
	Qpq	75	15.3	17.7	
	Q	400	81.8	94.3	
	F	18	3.7	4.2	
	L	3	0.6	0.7	
	Lm	3	0.6	0.7	
	Lv	0	0.0	0.0	
	Ls	0	0.0	0.0	
	Qp	76	15.5	17.9	
	Lvm	0	0.0	0.0	
	Lsm	3	0.6	0.7	
	Lt	79	16.2	18.6	

		normalized %	normalized total
ternary data	QFL%Q	95.0	421
	QFL%F	4.3	
	QFL%L	0.7	
	LmLvLs%Lm	100.0	3
	LmLvLs%Lv	0.0	
	LmLvLs%Ls	0.0	
	QpLvmLsm%Qp	96.2	79
	QpLvmLsm%Lvm	0.0	
	QpLvmLsm%Lsm	3.8	
	QmFLt%Qm	77.0	421
	QmFLt%F	4.3	
	QmFLt%Lt	18.8	
	QmPK%Qm	94.7	342
	QmPK%P	0.0	
	QmPK%K	5.3	
	QmQpq%Qmnu	63.4	399
	QmQpq%Qmu	17.8	
	QmQpq%Qpq2-3	6.5	
	QmQpq%Qpq>3	12.3	

sample ID WC-33

location

Burnside Fm., Bear Creek Group, Wolverine Canyon section (1220 m) west of Mara River, southeast of Kuuvik Lake.

field relations

Braid delta to lower braid plain facies in the distal (northwestern) part of the basin. Sample is about ~100 m below the marine shelf Burnside Dolomite interval.

thin section description

summary

arkose

texture

(vfU-mL), well sorted, angular to rounded. Straight to sutured boundaries between framework grains. Texturally mature.

mineralogy

quartz

Dominantly monocrystalline; this sample has the most of any sample but this may be partly an artifact of the relatively fine grain size of the sample compared to others. Undulose grains may be due almost entirely to compaction at grain-to-grain point contacts. Minor polycrystalline grains; grains show only straight subgrain boundaries. Trace chert.

feldspar

Abundant K-feldspar; common plagioclase. Feldspars are commonly very fresh, some quite altered to mica. Some plagioclases do not take the feldspar stain, but are obvious due to albite twinning.

lithic fragments

None seen.

accessory minerals

Muscovite.

intrabasinal grains

None.

cement

Minor sytaxial quartz overgrowths. Late euhedral dolomite rhombs replace intergranular pores and adjacent grains.

matrix

Recrystallized white mica after clay. Appears to impart a fabric on the rock (incipient cleavage).

porosity

Completely occluded by cement and matrix.

other notes

Feldspar conspicuously present. Most of the monocrystalline and polycrystalline quartz suggests a plutonic/high-grade metamorphic source. Common feldspar suggests plutonic source. High percentage of unstrained monocrystalline quartz may be partly an artifact of fine grain size.

Sample	WC-33	number	%total	%framework	
raw data	Qmnu	214	50.1	52.7	
	Qmu	34	8.0	8.4	
	Qpq2-3	2	0.5	0.5	
	Qpq>3	11	2.6	2.7	
	P	29	6.8	7.1	
	K	113	26.5	27.8	
	Lv	0	0.0	0.0	
	Lm	0	0.0	0.0	
	Ls	0	0.0	0.0	
	Cht	1	0.2	0.2	
	M	2	0.5	0.5	
	D	0	0.0	0.0	
	other framework	0	0.0	0.0	
	cement	0	0.0		
	matrix	16	3.7		
	other non-framework	5	1.2		dolomite replcmt
	U	0	0.0	0.0	
	total	427	100.0		
	total framework	406	95.1		
	total non-framework	21	4.9		
recalculated data	Qm	248	58.1	61.1	
	Qpq	13	3.0	3.2	
	Q	262	61.4	64.5	
	F	142	33.3	35.0	
	L	0	0.0	0.0	
	Lm	0	0.0	0.0	
	Lv	0	0.0	0.0	
	Ls	0	0.0	0.0	
	Qp	14	3.3	3.4	
	Lvm	0	0.0	0.0	
	Lsm	0	0.0	0.0	
	Lt	14	3.3	3.4	

		normalized %	normalized total
ternary data	QFL%Q	64.9	404
	QFL%F	35.1	
	QFL%L	0.0	
	LmLvLs%Lm	0.0	0
	LmLvLs%Lv	0.0	
	LmLvLs%Ls	0.0	
	QpLvmLsm%Qp	100.0	14
	QpLvmLsm%Lvm	0.0	
	QpLvmLsm%Lsm	0.0	
	QmFLt%Qm	61.4	404
	QmFLt%F	35.1	
	QmFLt%Lt	3.5	
	QmPK%Qm	63.6	390
	QmPK%P	7.4	
	QmPK%K	29.0	
	QmQpq%Qmnu	82.0	261
	QmQpq%Qmu	13.0	
	QmQpq%Qpq2-3	0.8	
	QmQpq%Qpq>3	4.2	

sample ID WC-58

location

Burnside Fm., Bear Creek Group, Wolverine Canyon section (1485 m) west of Mara River, southeast of Kuuvik Lake. Corresponds with detrital zircon sample WC-DZ-3.

field relations

Lower braid plain facies in the distal (northwestern) part of the basin.

thin section description

summary

subarkose

texture

(vfU-fU), moderately to well sorted, angular to rounded. Straight to sutured boundaries between framework grains. Texturally mature.

mineralogy

quartz

Dominantly monocrystalline; this sample has the most of any sample but this may be partly an artifact of the relatively fine grain size of the sample compared to others. Undulose grains may be due almost entirely to compaction at grain-to-grain point contacts. Minor polycrystalline grains; grains show only straight subgrain boundaries. Trace chert.

feldspar

Abundant K-feldspar; trace plagioclase. Microcline and perthite. Feldspars are commonly very fresh, some quite altered to mica; plagioclase alters to mica ± Fe oxide. Common thin late syntaxial overgrowths on feldspars; composition differs between grain and overgrowth; overgrowths commonly more altered; cuts across quartz grains and overgrowths.

lithic fragments

None seen.

accessory minerals

Muscovite and trace biotite.

intrabasinal grains

Trace mudstone.

cement

Sytaxial quartz overgrowths occlude all primary porosity. Late sytaxial feldspar on feldspar.

matrix

Sparse recrystallized white mica after clay.

porosity

Completely occluded by cement and matrix.

other notes

Feldspar conspicuously present. Most of the monocrystalline and polycrystalline quartz suggests a plutonic/high-grade metamorphic source. Common feldspar suggests plutonic source. Higher percentage of monocrystalline quartz may be partly an artifact of fine grain size.

Sample	WC-58	number	%total	%framework	
raw data	Qmnu	214	45.8	51.9	
	Qmu	72	15.4	17.5	
	Qpq2-3	21	4.5	5.1	
	Qpq>3	22	4.7	5.3	
	P	2	0.4	0.5	
	K	76	16.3	18.4	
	Lv	0	0.0	0.0	
	Lm	0	0.0	0.0	
	Ls	0	0.0	0.0	
	Cht	0	0.0	0.0	
	M	1	0.2	0.2	
	D	0	0.0	0.0	
	other framework	1	0.2	0.2	intrabasinal
	cement	53	11.3		qz overgrowths
	matrix	1	0.2		
	other non-framework	1	0.2		Fe oxide cmt
	U	3	0.6	0.7	
	total	467	100.0		
	total framework	412	88.2		
	total non-framework	55	11.8		
recalculated data	Qm	286	61.2	69.4	
	Qpq	43	9.2	10.4	
	Q	329	70.4	79.9	
	F	78	16.7	18.9	
	L	0	0.0	0.0	
	Lm	0	0.0	0.0	
	Lv	0	0.0	0.0	
	Ls	0	0.0	0.0	
	Qp	43	9.2	10.4	
	Lvm	0	0.0	0.0	
	Lsm	0	0.0	0.0	
	Lt	43	9.2	10.4	

		normalized %	normalized total
ternary data	QFL%Q	80.8	407
	QFL%F	19.2	
	QFL%L	0.0	
	LmLvLs%Lm	0.0	0
	LmLvLs%Lv	0.0	
	LmLvLs%Ls	0.0	
	QpLvmLsm%Qp	100.0	43
	QpLvmLsm%Lvm	0.0	
	QpLvmLsm%Lsm	0.0	
	QmFLt%Qm	70.3	407
	QmFLt%F	19.2	
	QmFLt%Lt	10.6	
	QmPK%Qm	78.6	364
	QmPK%P	0.5	
	QmPK%K	20.9	
	QmQpq%Qmnu	65.0	329
	QmQpq%Qmu	21.9	
	QmQpq%Qpq2-3	6.4	
	QmQpq%Qpq>3	6.7	

sample ID WC-66

location

Burnside Fm., Bear Creek Group, Wolverine Canyon section (1875 m) west of Mara River, southeast of Kuuvik Lake. Corresponds with detrital zircon sample WC-DZ-4.

field relations

Lower braid plain facies in the distal (northwestern) part of the basin.

thin section description

summary

subarkose

texture

(fL-mL), moderately to well sorted, angular to rounded. Straight to sutured boundaries between framework grains. Texturally mature.

mineralogy

quartz

Dominantly monocrystalline; this sample has the most of any sample but this may be partly an artifact of the relatively fine grain size of the sample compared to others. Undulose grains may be due almost entirely to compaction at grain-to-grain point contacts. Minor polycrystalline grains; grains show only straight subgrain boundaries. Trace chert.

feldspar

Abundant K-feldspar; minor plagioclase. Microcline and perthite. Feldspars are commonly very fresh. Plagioclases preferentially alter to sericite along twin planes. Common thin late syntaxial overgrowths on feldspars; composition differs between grain and overgrowth; overgrowths commonly more altered; cuts across quartz grains and overgrowths.

lithic fragments

Fe oxide + mica. Polycrystalline quartz + muscovite.

accessory minerals

Layers with dense minerals common; opaque Fe oxide, zircon, epidote (?). Muscovite broken in compaction.

intrabasinal grains

Trace mudstone.

cement

Sytaxial quartz overgrowths occlude all primary porosity. Late sytaxial feldspar on feldspar.

matrix

Sparse recrystallized white mica after clay.

porosity

Completely occluded by cement and matrix.

other notes

Feldspar conspicuously present. Most of the monocrystalline and polycrystalline quartz suggests a plutonic/high-grade metamorphic source. Common feldspar suggests plutonic source. Higher percentage of monocrystalline quartz may be partly an artifact of fine grain size.

Sample	WC-66	number	%total	%framework	
raw data	Qmnu	242	44.9	54.1	
	Qmu	36	6.7	8.1	
	Qpq2-3	9	1.7	2.0	
	Qpq>3	15	2.8	3.4	
	P	14	2.6	3.1	
	K	116	21.5	26.0	
	Lv	0	0.0	0.0	
	Lm	4	0.7	0.9	Fe oxide & mica
	Ls	0	0.0	0.0	
	Cht	6	1.1	1.3	
	M	0	0.0	0.0	
	D	0	0.0	0.0	
	other framework	3	0.6	0.7	intrabasinal
	cement	79	14.7		qz overgrowths
	matrix	9	1.7		
	other non-framework	4	0.7		Fe oxide cmt
	U	2	0.4	0.4	
	total	539	100.0		
	total framework	447	82.9		
	total non-framework	92	17.1		
recalculated data	Qm	278	51.6	62.2	
	Qpq	24	4.5	5.4	
	Q	308	57.1	68.9	
	F	130	24.1	29.1	
	L	4	0.7	0.9	
	Lm	4	0.7	0.9	
	Lv	0	0.0	0.0	
	Ls	0	0.0	0.0	
	Qp	30	5.6	6.7	
	Lvm	0	0.0	0.0	
	Lsm	4	0.7	0.9	
	Lt	34	6.3	7.6	

		normalized %	normalized total
ternary data	QFL%Q	69.7	442
	QFL%F	29.4	
	QFL%L	0.9	
	LmLvLs%Lm	100.0	4
	LmLvLs%Lv	0.0	
	LmLvLs%Ls	0.0	
	QpLvmLsm%Qp	88.2	34
	QpLvmLsm%Lvm	0.0	
	QpLvmLsm%Lsm	11.8	
	QmFLt%Qm	62.9	442
	QmFLt%F	29.4	
	QmFLt%Lt	7.7	
	QmPK%Qm	68.1	408
	QmPK%P	3.4	
	QmPK%K	28.4	
	QmQpq%Qmnu	80.1	302
	QmQpq%Qmu	11.9	
	QmQpq%Qpq2-3	3.0	
	QmQpq%Qpq>3	5.0	

sample ID WC-68

location

Top of the Burnside Fm., Bear Creek Group, Wolverine Canyon section (1935 m), just below the Burnside-Mara Formation contact, west of Mara River, southeast of Kuuvik Lake.

field relations

Lower braid plain facies in the distal (northwestern) part of the basin.

thin section description

summary

arkose

texture

(fU-cL), moderately sorted, angular to rounded. Straight to sutured boundaries between framework grains. Texturally submature.

mineralogy

quartz

Dominantly monocrystalline. Undulose grains may be due almost entirely to compaction at grain-to-grain point contacts. Minor polycrystalline grains; grains show only straight subgrain boundaries. Trace chert.

feldspar

Abundant K-feldspar; minor plagioclase. Microcline and perthite. Feldspars are variably altered, some very fresh, others highly altered to phyllosilicate. Plagioclases preferentially alter to sericite along twin planes. Common thin late syntaxial overgrowths on feldspars; composition differs between grain and overgrowth; overgrowths commonly more altered; cuts across quartz grains and overgrowths.

lithic fragments

Chert + mica ± Fe oxide.

accessory minerals

Layers with dense minerals common; opaque Fe oxide, zircon, epidote (?). Muscovite broken in compaction.

intrabasinal grains

Trace mudstone, siltstone, (vf) sandstone with dolomite.

cement

Sytaxial quartz overgrowths occlude all primary porosity. Sparese later euhedral dolomite in intergranular pores. Late sytaxial feldspar on feldspar.

matrix

Sparse recrystallized white mica after clay.

porosity

Completely occluded by cement and matrix.

other notes

Feldspar conspicuously present. Most of the monocrystalline and polycrystalline quartz suggests a plutonic/high-grade metamorphic source. Common feldspar suggests plutonic source.

Sample	**WC-68**	number	%total	%framework	
raw data	Qmnu	234	44.2	52.7	
	Qmu	40	7.6	9.0	
	Qpq2-3	16	3.0	3.6	
	Qpq>3	23	4.3	5.2	
	P	8	1.5	1.8	
	K	117	22.1	26.4	see next page*
	Lv	0	0.0	0.0	
	Lm	0	0.0	0.0	see next page**
	Ls	0	0.0	0.0	
	Cht	2	0.4	0.5	
	M	0	0.0	0.0	
	D	0	0.0	0.0	
	other framework	4	0.8	0.9	
	cement	51	9.6		qz overgrowth
	matrix	2	0.4		
	other non-framework	32	6.0		see next page***
	U	0	0.0	0.0	
	total	529	100.0		
	total framework	444	83.9		
	total non-framework	85	16.1		
recalculated	Qm	274	51.8	61.7	
data	Qpq	39	7.4	8.8	
	Q	315	59.5	70.9	
	F	125	23.6	28.2	
	L	0	0.0	0.0	
	Lm	0	0.0	0.0	
	Lv	0	0.0	0.0	
	Ls	0	0.0	0.0	
	Qp	41	7.8	9.2	
	Lvm	0	0.0	0.0	
	Lsm	0	0.0	0.0	
	Lt	41	7.8	9.2	

		normalized %	normalized total
ternary	QFL%Q	71.6	440
data	QFL%F	28.4	
	QFL%L	0.0	
	LmLvLs%Lm	0.0	0
	LmLvLs%Lv	0.0	
	LmLvLs%Ls	0.0	
	QpLvmLsm%Qp	100.0	41
	QpLvmLsm%Lvm	0.0	
	QpLvmLsm%Lsm	0.0	
	QmFLt%Qm	62.3	440
	QmFLt%F	28.4	
	QmFLt%Lt	9.3	
	QmPK%Qm	68.7	399
	QmPK%P	2.0	
	QmPK%K	29.3	
	QmQpq%Qmnu	74.8	313
	QmQpq%Qmu	12.8	
	QmQpq%Qpq2-3	5.1	
	QmQpq%Qpq>3	7.3	

Sample **WC-68**

*K

107	relatively unaltered K
10	phyllo replacement of K
117	total K

**Lm

6	chert + phyllo ± Fe oxide
6	total Lm

***other non-framework

10	Kspar cement
7	felspar overgrowths
15	dolomite replacement
32	total other non-framework

sample ID WC-70

location

Base of Mara Fm., Bear Creek Group, Wolverine Canyon section (1937 m), just above the Burnside-Mara Formation contact, west of Mara River, southeast of Kuuvik Lake.

field relations

Braid plain facies in the distal (northwestern) part of the basin.

thin section description

summary

feruginous arkose

texture

(vfU-fL), moderately sorted, angular to rounded. Straight to sutured boundaries between framework grains. Texturally submature. Grains reoriented obliquely to bedding due to rock cleavage that elongates grains and their syntaxial overgrowths.

mineralogy

quartz

Dominantly monocrystalline. Undulose grains may be due almost entirely to compaction at grain-to-grain point contacts and cleavage formation. Minor polycrystalline grains; grains show only straight subgrain boundaries. Trace chert.

feldspar

Abundant K-feldspar; minor plagioclase. Microcline and perthite. Feldspars are variably altered, some very fresh, others highly altered to phyllosilicate. Plagioclases preferentially alter to sericite along twin planes. Common thin late syntaxial overgrowths on feldspars; composition differs between grain and overgrowth; overgrowths commonly more altered; cuts across quartz grains and overgrowths.

lithic fragments

Chert + mica ± Fe oxide. Plutonic fragments of quartz and feldspar.

accessory minerals

Layers with dense minerals common; opaque Fe oxide, zircon, epidote (?). Common muscovite broken in compaction, regrown in cleavage formation.

intrabasinal grains

Trace mudstone, (vf) sandstone.

cement

Ubiquitous Fe oxide as recrystallized cement after grain coatings. Sytaxial quartz overgrowths occlude all primary porosity. Late sytaxial feldspar on feldspar.

matrix

Mica growth along grain boundaries that partly defines cleavage.

porosity

Completely occluded by cement and matrix.

other notes

The Fe oxide grain coating is the signature of the Mara Formation. Feldspar conspicuously present. Most of the monocrystalline and polycrystalline quartz

suggests a plutonic/high-grade metamorphic source. Common feldspar ad quartz-feldspar rock fragments suggest plutonic source.

Sample	WC-70	number	%total	%framework	
raw data	Qmnu	205	32.0	46.5	
	Qmu	53	8.3	12.0	
	Qpq2-3	9	1.4	2.0	
	Qpq>3	15	2.3	3.4	
	P	8	1.2	1.8	
	K	124	19.3	28.1	see next page*
	Lv	0	0.0	0.0	
	Lm	0	0.0	0.0	
	Ls	0	0.0	0.0	
	Cht	10	1.6	2.3	
	M	0	0.0	0.0	
	D	0	0.0	0.0	
	other framework	17	2.7	3.9	see next page**
	cement	65	10.1		
	matrix	107	16.7		
	other non-framework	28	4.4		
	U	0	0.0	0.0	
	total	641	100.0		
	total framework	441	68.8		
	total non-framework	200	31.2		
recalculated data	Qm	258	40.2	58.5	
	Qpq	24	3.7	5.4	
	Q	292	45.6	66.2	
	F	132	20.6	29.9	
	L	0	0.0	0.0	
	Lm	0	0.0	0.0	
	Lv	0	0.0	0.0	
	Ls	0	0.0	0.0	
	Qp	34	5.3	7.7	
	Lvm	0	0.0	0.0	
	Lsm	0	0.0	0.0	
	Lt	34	5.3	7.7	

		normalized %	normalized total
ternary data	QFL%Q	68.9	424
	QFL%F	31.1	
	QFL%L	0.0	
	LmLvLs%Lm	0.0	0
	LmLvLs%Lv	0.0	
	LmLvLs%Ls	0.0	
	QpLvmLsm%Qp	100.0	34
	QpLvmLsm%Lvm	0.0	
	QpLvmLsm%Lsm	0.0	
	QmFLt%Qm	60.8	424
	QmFLt%F	31.1	
	QmFLt%Lt	8.0	
	QmPK%Qm	66.2	390
	QmPK%P	2.1	
	QmPK%K	31.8	
	QmQpq%Qmnu	72.7	282
	QmQpq%Qmu	18.8	
	QmQpq%Qpq2-3	3.2	
	QmQpq%Qpq>3	5.3	

Sample WC-70

*K

120	relatively unaltered K
4	phyllo replacement of K
124	total K

**other framework

10	intrabasinal sst
7	intrabasinal mudstone
17	total other non-framework

sample ID BSA-1

location

Brown Sound Fm., Bathurst Group, base section on the southeast shore of Bathurst Lake, west of southern Bathurst Inlet. Coincides with detrial zircon sample BSA-DZ-1.

field relations

Lower braid plain facies in the proximal (southeastern) part of the basin.

thin section description

summary

arkose

texture

(vfU-mL), moderately sorted, angular to rounded. Straight to sutured boundaries between framework grains. Texturally submature.

mineralogy

quartz

Dominantly monocrystalline. Undulose grains may be due almost entirely to compaction at grain-to-grain point contacts and cleavage formation. Minor polycrystalline grains; grains show only straight subgrain boundaries. Trace chert.

feldspar

Abundant K-feldspar; minor plagioclase. Microcline and perthite. Feldspars are variably altered, some very fresh, others highly altered to phyllosilicate. Plagioclases preferentially alter to sericite along twin planes. Common thin late syntaxial overgrowths on feldspars; composition differs between grain and overgrowth; overgrowths commonly more altered; cuts across quartz grains and overgrowths.

lithic fragments

Minor foliated polycrystalline quartz-mica grains. Chert ± mica ± Fe oxide.

accessory minerals

Common muscovite, minor biotite. Muscovites are bent from compaction.

intrabasinal grains

Trace mudstone, (vf) sandstone.

cement

Minor Fe oxide as recrystallized cement after grain coatings. Sytaxial quartz overgrowths occlude all primary porosity. Late dolomite replacement of intergranular pore-filling cement. Late sytaxial feldspar on feldspar.

matrix

Mica recrystallization.

porosity

Completely occluded by cement and matrix.

other notes

Feldspar conspicuously abundant; this sample has the most feldspar of any Goulburn Supergroup sample. Most of the monocrystalline and polycrystalline quartz suggests a plutonic/high-grade metamorphic source. Common feldspar suggests plutonic source.

Sample	**BSA-1**	number	%total	%framework	
raw data	Qmnu	166	30.7	35.6	
	Qmu	21	3.9	4.5	
	Qpq2-3	11	2.0	2.4	
	Qpq>3	14	2.6	3.0	see next page*
	P	34	6.3	7.3	
	K	187	34.6	40.1	see next page**
	Lv	0	0.0	0.0	
	Lm	18	3.3	3.9	see next page***
	Ls	0	0.0	0.0	
	Cht	2	0.4	0.4	
	M	10	1.9	2.1	
	D	2	0.4	0.4	
	other framework	0	0.0	0.0	
	cement	30	5.6		
	matrix	19	3.5		
	other non-framework	25	4.6		see next page****
	U	1	0.2	0.2	
	total	540	100.0		
	total framework	466	86.3		
	total non-framework	74	13.7		
recalculated	Qm	187	34.6	40.1	
data	Qpq	25	4.6	5.4	
	Q	214	39.6	45.9	
	F	221	40.9	47.4	
	L	18	3.3	3.9	
	Lm	18	3.3	3.9	
	Lv	0	0.0	0.0	
	Ls	0	0.0	0.0	
	Qp	27	5.0	5.8	
	Lvm	0	0.0	0.0	
	Lsm	18	3.3	3.9	
	Lt	45	8.3	9.7	

		normalized %	normalized total
ternary	QFL%Q	47.2	453
data	QFL%F	48.8	
	QFL%L	4.0	
	LmLvLs%Lm	100.0	18
	LmLvLs%Lv	0.0	
	LmLvLs%Ls	0.0	
	QpLvmLsm%Qp	60.0	45
	QpLvmLsm%Lvm	0.0	
	QpLvmLsm%Lsm	40.0	
	QmFLt%Qm	41.3	453
	QmFLt%F	48.8	
	QmFLt%Lt	9.9	
	QmPK%Qm	45.8	408
	QmPK%P	8.3	
	QmPK%K	45.8	
	QmQpq%Qmnu	78.3	212
	QmQpq%Qmu	9.9	
	QmQpq%Qpq2-3	5.2	
	QmQpq%Qpq>3	6.6	

Sample	**BSA-1**
*polycrystalline qz	
11	pristine polycrystalline qz
3	polycrystalline qz with phyllo flecks
14	total polycrystalline qz
**K	
180	relatively unaltered K
7	phyllo replacement of K
187	total K
***Lm	
7	strained qz-mica aggregates
1	phyllo + Fe oxide
4	chert + Fe oxide
6	chert + phyllo
18	total Lm
****other non-framework	
12	authigenic Fe oxide
13	dolomite replacement
25	total other non-framework.

sample ID BSA-2

location

Brown Sound Fm., Bathurst Group, top of exposed section on the southeast shore of Bathurst Lake, west of southern Bathurst Inlet. Coincides with detrial zircon sample BSA-DZ-2.

field relations

Braid plain facies in the proximal (southeastern) part of the basin.

thin section description

summary

arkose

texture

(mL-vcU), some grains to 3.5 mm, poorly sorted, angular to rounded. Straight to sutured boundaries between framework grains. Texturally submature.

mineralogy

quartz

Dominantly monocrystalline. Undulose grains may be due almost entirely to compaction at grain-to-grain point contacts and cleavage formation. Minor polycrystalline grains; grains show only straight subgrain boundaries. Trace chert.

feldspar

Abundant K-feldspar; minor plagioclase. Microcline and perthite. Feldspars are variably altered, some very fresh, others highly altered to phyllosilicate. Compositional variation seen by variable alteration within single grains. Plagioclases preferentially alter to sericite along twin planes. Common thin late syntaxial overgrowths on feldspars; composition differs between grain and overgrowth; overgrowths commonly more altered; cuts across quartz grains and overgrowths.

lithic fragments

Minor foliated polycrystalline quartz-mica grains. Chert ± mica ± Fe oxide. Altered felsic volcanic clasts that appear as chert phyllosilicate with flow banding with phyllosilicate rich ghosts after feldspar (totally hosed over). Plutonic rock fragments of quartz with subordinate feldspar. Trace mymerkitic plutonic fragment.

accessory minerals

Common muscovite, minor biotite. Muscovites are bent from compaction.

intrabasinal grains

Trace mudstone, (vf) sandstone.

cement

Minor Fe oxide as recrystallized cement after grain coatings. Sytaxial quartz overgrowths occlude all primary porosity. Late dolomite replacement of intergranular pore-filling cement. Late sytaxial feldspar on feldspar.

matrix

Mica recrystallization.

porosity

Completely occluded by cement and matrix.

other notes

Feldspar conspicuously abundant. Most of the monocrystalline and polycrystalline quartz suggests a plutonic/high-grade metamorphic source. Common feldspar suggests plutonic source.

Sample	BSA-2	number	%total	%framework	
raw data	Qmnu	174	30.3	33.6	
	Qmu	23	4.0	4.4	
	Qpq2-3	38	6.6	7.3	
	Qpq>3	80	13.9	15.4	see next page*
	P	16	2.8	3.1	
	K	159	27.7	30.7	see next page**
	Lv	4	0.7	0.8	
	Lm	12	2.1	2.3	see next page***
	Ls	9	1.6	1.7	
	Cht	0	0.0	0.0	
	M	2	0.3	0.4	
	D	0	0.0	0.0	
	other framework	0	0.0	0.0	
	cement	37	6.4		
	matrix	19	3.3		
	other non-framework	0	0.0		
	U	1	0.2	0.2	
	total	574	100.0		
	total framework	518	90.2		
	total non-framework	56	9.8		
recalculated	Qm	197	34.3	38.0	
data	Qpq	118	20.6	22.8	
	Q	315	54.9	60.8	
	F	175	30.5	33.8	
	L	25	4.4	4.8	
	Lm	12	2.1	2.3	
	Lv	4	0.7	0.8	
	Ls	9	1.6	1.7	
	Qp	118	20.6	22.8	
	Lvm	4	0.7	0.8	
	Lsm	21	3.7	4.1	
	Lt	143	24.9	27.6	

		normalized %	normalized total
ternary	QFL%Q	61.2	515
data	QFL%F	34.0	
	QFL%L	4.9	
	LmLvLs%Lm	48.0	25
	LmLvLs%Lv	16.0	
	LmLvLs%Ls	36.0	
	QpLvmLsm%Qp	82.5	143
	QpLvmLsm%Lvm	2.8	
	QpLvmLsm%Lsm	14.7	
	QmFLt%Qm	38.3	515
	QmFLt%F	34.0	
	QmFLt%Lt	27.8	
	QmPK%Qm	53.0	372
	QmPK%P	4.3	
	QmPK%K	42.7	
	QmQpq%Qmnu	55.2	315
	QmQpq%Qmu	7.3	
	QmQpq%Qpq2-3	12.1	
	QmQpq%Qpq>3	25.4	

Sample **BSA-2**

*polycrystalline qz

78	pristine polycrystalline qz
2	polycrystalline qz with phyllo flecks
80	total polycrystalline qz

**K

148	relatively unaltered K
11	phyllo replacement of K
159	total K

***Lm

2	strained qz-mica aggregates
8	chert + Fe oxide
2	chert + phyllo
12	total Lm

Appendix C:
Zircon sample locations

samples analysed		Sample Name	position within measured section (m)	latitude N	longitude W	comments
		detrital zircons from Goulburn Supergroup, Kilohigok Basin				
		Kenyon Fm. (Kimerot Group) alluvial sandstone				
1		WR1a		66° 44'	107° 22'	Starvin Lake
		lower Bear Creek Group turbidites				
2		WR2e		66° 32'	107° 20'	Meat Cleaver Lake
		Hackett Fm. (lower Bear Creek Group) shelf sandstone				
3, 4, 5		BCH		66° 49'	107° 33'	W of N end of Kathleen Lake
		Rifle Fm. (lower Bear Creek Group) shelf sandstone				
6		BCR		66° 49'	107° 35'	W of N end of Kathleen Lake
		Burnside Formation in proximal foredeep (section 2)				
7, 8		STH-1	172			
		STH-2	648			
		STH-7	971			
		STH-3	1248			
9		STH-4	1411			
10		STH-5	1684			
11		STH-6	2066			
12, 13		STH-8	"2772 m" in upper section			
		felsic volcanic clasts in Gravelly Sst. Mbr. of Burnside Fm. (= STH-6)				
14, 15		Ryolite g-1 mag2				
		Burnside Formation in distal foredeep (section 12)				
16, 17		WC-1	265			
18		WC-2	714			
19		WC-3	1492			
20		WC-4	1880			
		Burnside Fm. in distal foredeep (section 13)				
21		BC-CL	498			coarsest interval
		Brown Sound Fm. (Bathurst Group)				
		BSA-1		66° 13'	107° 03'	base of section at Bathurst Lake
22, 23, 24		BSA-2		66° 12'	107° 05'	top of section at Bathurst Lake
		detrital zircons from Coronation Supergroup, Wopmay Orogen				
		Tree River Fm. (Recluse Group)				
		CS-Eo1		65° 59' 10"	133° 06'	Takiyuak Lake
25, 26		CS-Rtr-1		65° 59' 20"	133° 10'	Takiyuak Lake
		CS-tak				Takiyuak Lake
		CS-Eo2		67° 28' 10"	112° 19' 30"	Eokuk Uplift
		CS-Rtr-2		67° 29' 50"	112° 16' 30"	Eokuk Uplift, "716 Lake"
		Asiak Fm. greywacke (Recluse Group)				
27		greywacke d-3				
		zircons from Queen Maud basement rocks (Queen Maud block)				
28		QM1		103° 12'	66° 47'	NW of Macalpine Lake
29		QM2		101° 12'	66° 56'	Pitok River
30		QM3		100° 01'	66° 48'	SW of Simpson River
31		QM4		98° 43'	67° 28'	NW of McNaughton Lake
				547		